PERIMETRY UPDATE 1990/1991

edited by Richard P. Mills and Anders Heijl

Navigation Menu

kugler & ghedini

Library of Congress Cataloging-in-Publication Data

Perimetry update 1990/1991 / edited by Richard P. Mills and Anders Heijl.
p. cm.
Selected papers presented at the Ninth International Visual Field Symposium, held in Malmö, Sweden, June 17-20, 1990 and organized by the International Perimetric Society.
Includes bibliographical references.
ISBN 9062990754 : $175.00
1, Perimetry--Congresses. I. Mills, Richard P., 1945- ,
II. Heijl, A. (Anders) III. International Visual Field Symposium (9th : 1990 : Malmö, Sweden) IV. International Perimetric Society.
RE79.P4P48 1991
617.7'075--dc20 91-14629
CIP

ISBN 09-6299-075-4

Distributors:
For the U.S.A. and Canada:
Kugler Publications
P.O. Box 1498
New York, NY 10009-9998

For Italy:
Ghedini Editore
Via della Signora, 6
20122 Milano
Telefax (02) 781150

For all other countries:
Kugler Publications bv
P.O. Box 516
1180 AM Amstelveen, The Netherlands
Telefax (+31.20) 380524

TABLE OF CONTENTS

Preface

This volume contains a selection of papers and posters presented at the Ninth International Visual Field symposium. The symposium was organized by the International Perimetric Society (IPS) and was held in Malmö, Sweden, June 17-20, 1990.

The IPS meeting was larger than ever before with approximately 310 participants. Increased interest in perimetric research accounts for the growth in the meeting and in the dues-paying membership of the IPS, which now numbers 265 representing 24 countries worldwide. Of 140 abstracts submitted for the meeting, 48 read papers and 56 posters were selected for presentation.

The read papers were given seven 90-minute sessions devoted to neuro-ophthalmology, ophthalmic imaging, computer-assisted interpretation, variability, color perimetry, and other topics. The posters were on display during the entire meeting, authors were asked to be present at their posters at specific times, and they were asked to defend their findings during two 90-minute general sessions devoted exclusively to public poster discussion.

Because of a burgeoning interest in ophthalmic imaging, and because perimetry and imaging share much common ground, especially in relation to progression of glaucomatous optic nerve damage, a special invitation to attend the meeting was extended to the international imaging community. They were encouraged to submit abstracts of their work, especially correlations of visual field results to topographical image analysis. The success of that invitation is proven by the 18 submissions in chapter 1 of this volume, by the revitalization of the IPS group on optic disc and retina with Bernard Schwartz, M.D. as chairman, and by the decision of many "imagers" to become members and adopt the IPS meetings as a forum for their future work.

Several papers dealt with the correlation of various optic disc and nerve fiber layer topographical parameters and visual field data. Unfortunately, while often statistically significant, the correlation levels did not approach the expectations of many who believe that form and function in glaucoma ought to be more intimately related.

The evolution of visual field defects in pseudotumor cerebri was reported during a strong neuro-ophthalmology paper session. The early results from the optic neuritis treatment trial indicate the importance of technician training and feedback even in totally "automated" perimetry, and two papers indicated a surprisingly high incidence of "atypical" defects, such as altitudinal or hemianopic, in the initial visual fields of optic neuritis patients.

In glaucoma, there was further study of the usefulness of color, resolution, and flicker perimetry. The mode of progression of field defects in glaucoma and in low tension glaucoma was contrasted. Defects appearing very close to fixation were studied over time using a fine matrix macular program. The importance of peripheral field data in glaucoma was also examined by several authors.

Variability in perimetric data has been an ongoing topic of interest for many years. Different ways of measuring variability were found to correlate with visual field abnormality and patient unreliability in different degrees. The effect of depressed thresholds on the estimates of variability and the consequent effect on confidence limits for abnormality was reported. Long-term fluctuation is at last receiving greater attention as attention is being turned to detecting change in serial fields in patients with glaucoma.

New methods of analysis of perimetric data were reported in several papers and posters. Extremely sophisticated mathematical models and neural networks were devised. As at previous meetings of the society, new devices for testing the field were described. Some represented totally new instrumentation, and others were modifications of previously available hardware.

While the presentations highlighted above were of particular interest to me, other readers will have a different bias. This volume, reflecting the great breadth of current research in perimetry and related areas, has something for everyone. It is our hope that this and

past proceedings of the IPS will remain important and convenient references for those who seek up-to-date information and current opinion in the field.

The organization of the meeting was superb in all respects, and we owe a great debt to the hard work of Anders and Agneta Heijl and the local organizing committee.

On behalf of the editorial committee, I want to thank the authors for their timeliness, their attention to detail, and their expertise with the English language, especially those for whom English is not a native tongue. My heartfelt thanks also to the previous editor, Dr. Heijl, who agreed to co-edit this volume instead of enjoying a well-deserved retirement.

We are all looking forward to the next meeting, scheduled for October 20-23, 1992, in Kyoto, Japan, hosted by Yoshiaki Kitazawa, M.D. and his colleagues. It promises to be a stimulating meeting, as the previous nine IPS symposia have been.

Richard P. Mills, M.D.
IPS Secretary and Editor

Obituary

Professor Edward M. Brussell (1964-1988)

Professor Edward M. Brussell was born in New York City on January 18, 1946. He received his B.A. from Hobart College, his M.A. from DePauw University, and his Ph.D. from the new School for Social Research in New York City. After two years as Lecturer and Research Associate at York University, he moved to Concordia University in 1974, where he was promoted to Associate Professor of Psychology in 1977 and to full Professor in 1985. His main research interest was in the field of vision and vision perception, for which he received many grants from agencies including the Natural Sciences and Engineering Research Council of Canada and the Medical Research Council of Canada. He published more than 40 papers in scientific journals.

Professor Brussell was especially interested in the psychophysical assessment of visual disorders. When we first met in 1983, his chief interest was in the study of the temporal response of the visual system, using his new technique which he called multi-flash campimetry. The natural spin-off was the investigation of glaucoma patients. I pursuaded him to join the IPS and he presented a review of his technique at our symposium in Amsterdam in 1986. Ed was very excited that he was finally with a Society which "spoke his language".

Our work was interrupted in early 1988 when back pains were diagnosed as a very large renal carcinoma. This was excised and Ed made a miraculous recovery, back in the lab within a few weeks, leaner but working even harder towards the next IPS meeting. Unfortunately, the tumor recurred. The night before my flight to Vancouver, I visited him in hospital, where he was at once directing the hospital staff, scribbling notes – on papers spread over his hospital bed – to those presenting posters at the meeting, and discussing with me where the next stage of our investigations should take us. Unfortunately, while we were in Vancouver, Ed slipped into a coma and passed away on May 25, 1988.

Professor Brussell was an active contributor to the body of knowledge in psychophysics and the driving force in our investigations. His energy, enthusiasm and friendship will be sorely missed by all those who worked with him.

Gordon Balazsi, M.D.

Obituary

Professor Elfriede Aulhorn (1923-1991)

Regrettably on March 14th the International Perimetric Society lost one of its founders and its first president. Ophthalmology in Germany lost one of its most prominent researchers, the University of Tübingen one of its academic pillars and many of us, a very warm and engaging friend. I had the good fortune of working with her when static perimetry had not yet been generally accepted. I recall when she taught me the method in her beautiful Tübingen which could be seen in all its splendor from her home on the hill. She was persuaded to spend three undisturbed weeks in Vancouver teaching the new method to our technicians. She was relaxed, and fell in love with our city and also with the visual performance of our patients when she compared them with her own. She spoke halting English at that time and some of the literal translations from German into English have remained with us. She was such a keen hiker that when offered a ride she would prefer to "go by the feet" which of course is the literal translation from German. She endeared herself in no time to all our technicians and patients and we were sad to see her leave.

Elfriede was truly a giant in the area of visual psychophysics and her careful collaboration with Professor Harms led to the popularization of static perimetry, which revolutionized all perimetry and provided a new dimension to the understanding of the visual field. This was one of the precursors and prerequisites for the subsequent explosion of computerized perimetry. She kept an interest in computerized perimetry to the end, and her method of screening on a video screen may yet be another big advance. Elfriede had other ophthalmological interests including amblyopia and the visual requirements for driving safety, but all of these were dwarfed by her human qualities. She was kind, selfless, warm and generous with her time. She loved young people and their vitality and was a mentor and sponsor for many bright colleagues and a role model for many technicians. She oozed charm and was also very courageous. She loved the International Perimetric Society and even when she was first disabled, by what finally turned out to be her terminal illness, she fought back and only missed one of the IPS Meetings, in Amsterdam. She returned for the Vancouver meeting and contributed again for the benefit of her colleagues.

When Elfriede relinquished the presidency of the International Perimetric Society, Professor Dubois Poulsen, who was such an accomplished wordsmith, coined the term "the Queen of Perimetry". There is no doubt that this was a deserved title and we in the Society will always remember her graceful and successful reign. It will be a long time before her accomplishments are equalled. We were all proud and privileged to have known her.

Stephen M. Drance, O.C., M.D.

Fundus imaging

Correlation of the optic disc and visual field in glaucoma

Fritz Dannheim, Thomas Damms and Susann Obrecht

University of Hamburg, Department of Ophthalmology, Martinistrasse 52, D-2000 Hamburg 20, Germany

Abstract

The authors performed computer perimetry (Octopus program G1), random masked manual planimetry, and computerized optic disc topometry (ONHA) on 93 eyes of 53 subjects with chronic glaucoma, low tension glaucoma, ocular hypertension, pseudo-glaucomatous large discs, or normal findings They correlated multiple disc parameters with visual field indices MD and CLV This was least with computerized topometry (no correlation), better for planimetric C/D ratio, even better for planimetric rim area, and best for temporal rim planimetry (r^2=0.57 when correlated with MD within 10°). The degree of correlation reversed when separation of glaucomatous from normal subjects was considered. Thus, vertical C/D ratio separated better than temporal rim area. Computerized topometric cup volume decreased with age It neither correlated with field defects nor helped distinguish normal from glaucomatous subjects

Introduction

A quantitative correlation of optic disc morphology with perimetry is of special interest in the early stages of glaucoma. Automated optic disc topometry requires complex instrumentation and a trained technician, however, and manual planimetry is dependent on an experienced observer. We compared the two topometric techniques and correlated their findings with visual field indices.

Material and methods

Ninety-three eyes of 53 subjects with chronic glaucoma (n=74), low tension glaucoma (n=5), ocular hypertension (n=37), pseudo-glaucomatous large discs (n=17) and of normal subjects (n=10) were examined with program G1 of the Octopus perimeter and with computerized optic disc topometry using the Rodenstock Optic Nerve Head Analyzer (ONHA). Manual planimetry, masked and in random order, was carried out under stereoscopic observation of projected Topcon stereo slides with a 13-fold magnification[1] For both techniques, we obtained C/D ratio and absolute values of rim area for disc quadrants and the entire disc using refraction and axial length[1,2]. Two independent measurements with the same test modality were available for both methods in 78 of the 93 eyes. The mean values of all disc parameters were used in these eyes for the correlation with perimetric indices. Cup volume could be obtained only with the ONHA and maximum C/D ratio for one of 360 radii only with manual planimetry.

Results

The intertest reliability of the two topometric techniques calculated from the double determinations is presented in Table 1. The mean ±1 SD and maximum absolute and relative difference between the two independently repeated recordings was significantly smaller using manual planimetry than with ONHA, both for vertical C/D ratio and rim area. The correlation coefficients between the first and second examinations indicate greater reliability from manual planimetry. Values of the disc area correspond for the two methods, since the manual marking of the disc edge was repeated with the ONHA, if necessary, to obtain disc areas within a 10%

Perimetry Update 1990/91, pp. 3-8
Proceedings of the IXth International Perimetric Society Meeting,
Malmö, Sweden, June 17-20, 1990
edited by Richard P. Mills and Anders Heijl

Table 1 Mean and maximum absolute (D) and relative difference (V) and correlation coefficient (R) between 78 double determinations of vertical C/D ratio, rim area and disc area, both with planimetry and ONHA, and of cup volume. V=D/2 · 100/mean value (%)

	C/D vertical		*Rim area*		*Disc area*		*Volume*
	Planimetry	*ONHA*	*Planimetry*	*ONHA*	*Planimetry*	*ONHA*	*ONHA*
D	0.03±0.03	0.07±0.06	0.08±0.07	0.12±0.10	0.07±0 07	0.07±0.06	0.08±0.07
D_{max}	0.16	0.31	0.29	0.44	0.25	0.32	0.3
V %	2.5 ±2.6	5.9 ±6.4	2.8 ±2.5	5.3 ±4.8	1 3 ±1.1	1.5 ±1.1	7.6 ±8.1
V_{max} %	15.8	34 1	11.9	22.8	4.5	5.6	34.6
R	0.96	0.82	0.98	0.84	0.99	0.98	0.95

Table 2 Coefficient of determination (r^2) and p values of optic disc parameters, vertical C/D ratio and rim area with visual field indices MD and CLV, and of temporal rim area with MD within 10°, for all 93 eyes and for 29 glaucomatous eyes (planimetry and ONHA)

	C/D^v/MD		*C/D^v/CLV*		*rim/MD*		*rim/CLV*		*rim^t/MD 10°*	
	r^2	p	r^2	p	r^2	p	r^2	p	r^2	p
Planimetry										
all	0 30	0.0000	0 31	0.0000	0.37	0.0000	0.31	0.0000	0.32	0.0000
glaucoma	0 17	0 0272	0.14	0.0473	0.48	0.0000	0.18	0.0230	0.57	0.0000
ONHA										
all	0.05	0.0412	0.03	0 0752	0.07	0.0131	0.03	0.0994	0.01	0.2498
glaucoma	0.01	0.5804	0.00	0 9446	0.05	0.2492	0 00	0.7630	0.01	0.6154

tolerance range for an individual eye, whereas the planimetric plots were truly masked and randomized. Cup volume, measured with the ONHA, revealed a relatively high reliability. The high maximum relative difference was due to moderate differences in very small values of volume.

Correlation data of vertical C/D ratio and rim area with mean defect (MD) and corrected loss variance (CLV) and of rim area of the temporal disc quadrant with MD within 10° can be seen in Table 2. A graphic display of the correlation of vertical C/D ratio with MD and CLV is given in Fig. 1. Two values of the glaucoma group, marked with circles, belonged to the eyes of a patient with very small discs and progressive field loss despite seemingly physiological cupping. Apart from these two, the values of glaucomatous and non-glaucomatous eyes are clearly separated with only some overlap.

The values for rim area (Fig. 2a) of the two striking eyes in Fig. 1 are well within the typical glaucomatous range due to the small size of these discs. Values for the glaucoma group (filled symbols) considerably overlap those of the non-glaucomatous eyes.

Correlation of quadrants of the disc with MD values of corresponding hemifields or nasal quadrants slightly improved the coefficient of determination. The best observed correlation was found for the rim area of the temporal disc quadrant with MD of the central field within 10° for the glaucoma group (Table 2, Fig. 2b). The overlap of values of glaucomatous and non-glaucomatous eyes is even broader for this disc parameter than for total rim area, however.

Separation of affected and unaffected eyes, expressed by percent overlap of values of these two groups, is depicted in Fig. 3 for a number of optic disc parameters on the y-axis, correlation of glaucomatous disc damage with perimetric MD on the x-axis. The two glaucomatous eyes with outlying values of C/D ratio have been excluded for a more clear-cut impression.

By and large, vertical C/D ratio allows a reasonably precise separation of glaucomatous eyes, but limited correlation with perimetric damage. Temporal rim area, in contrast, correlates well with the functional deficit without distinctly separating glaucomatous eyes. All the other disc parameters including maximum C/D ratio lie between these two extremes. Cup volume did not correlate with visual field indices and allowed no separation of glaucomatous from normal eyes, and it significantly decreased with age in glaucomatous eyes (r^2=0.6, p=0.0000).

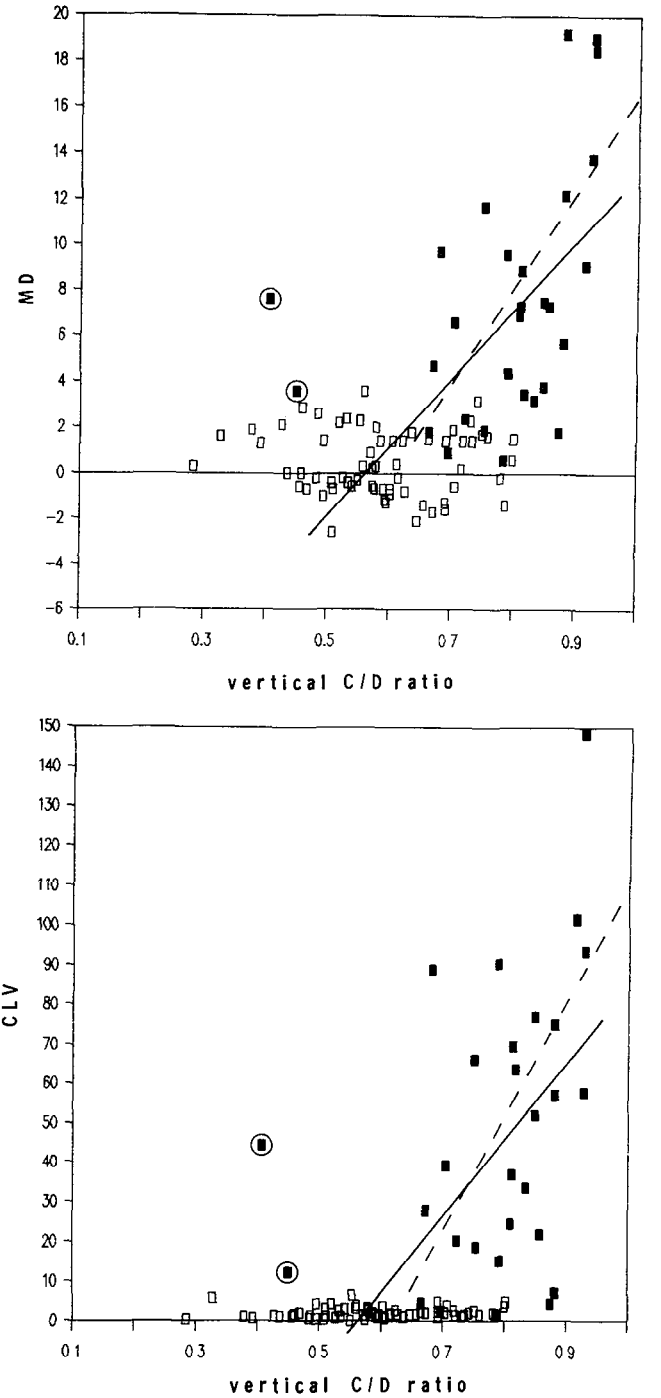

Fig 1 Correlation of vertical C/D ratio of planimetry with MD (a) and CLV (b) for all 93 eyes. Values for 29 glaucomatous eyes (filled symbols) contain two eyes far outside the typical glaucomatous range (circles, see text). Independent regression line for all (solid) and 29 glaucomatous eyes (broken).

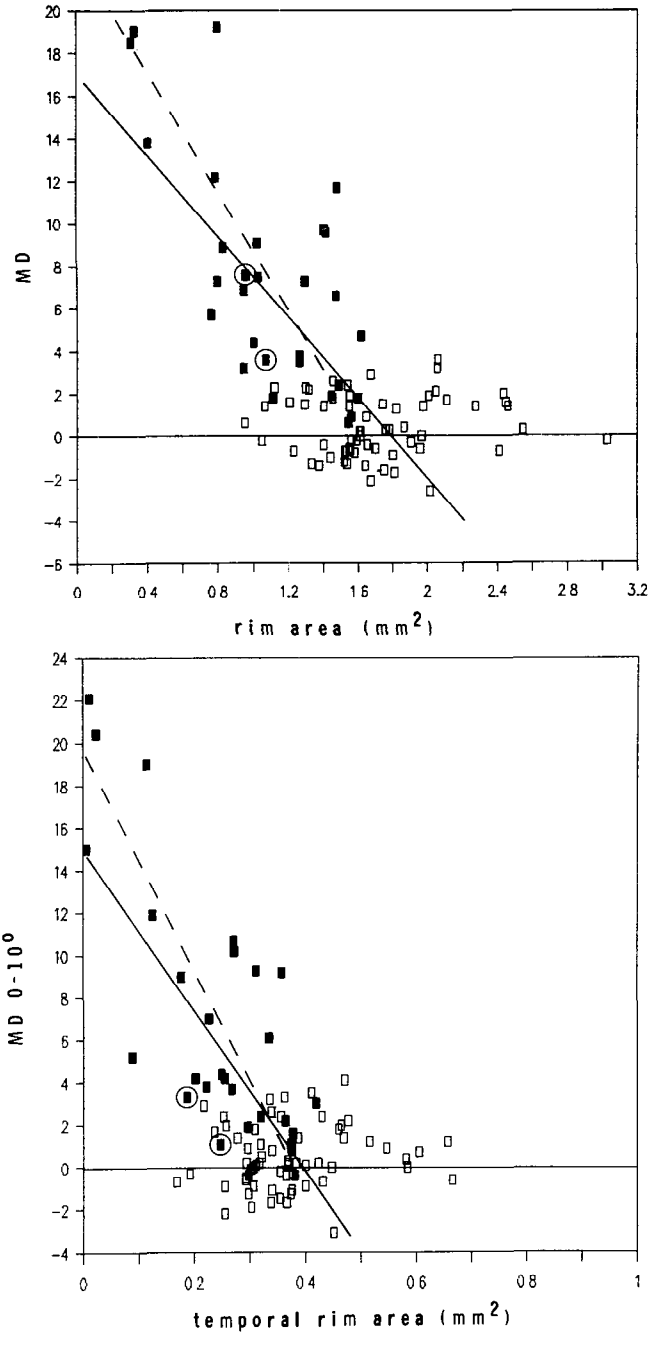

Fig. 2 Correlation of rim area with MD (a) and of temporal rim area with MD within 10° (b), depicted as in Fig. 1 Values for the two "stray shots" of Fig 1 now in glaucomatous range.

Comment

Automated optic disc topometry is highly desirable for the diagnosis of glaucoma since it allows independence from a skilled planimetrist. Our correlation coefficient for values of total and vertical C/D ratio for both methods was just below 0.6[1], thus lying in the lower range of

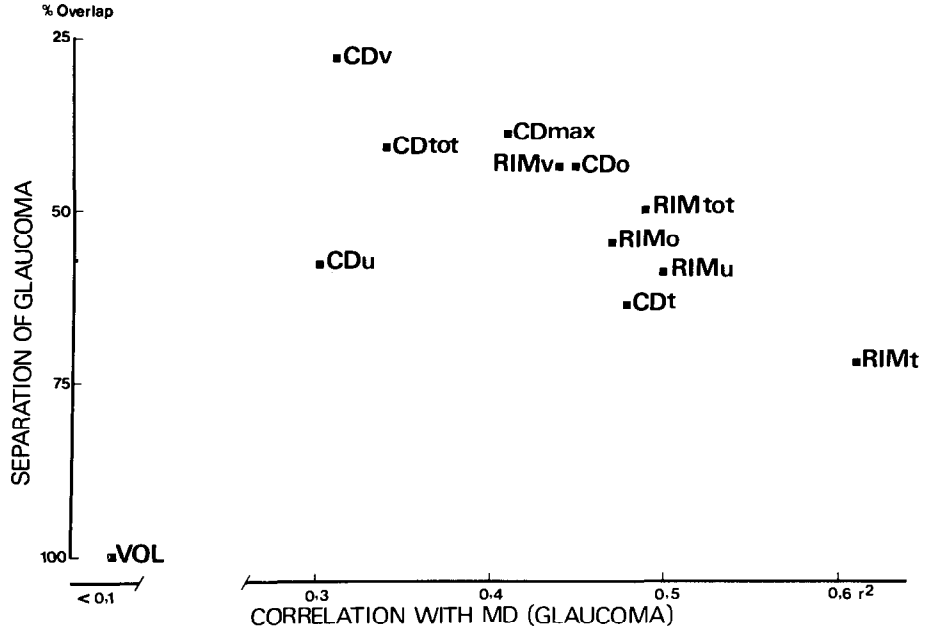

Fig 3 Correlation of coefficient of determination (r^2) of optic disc parameters with MD in glaucomatous eyes (x-axis) with separation of glaucomatous and non-glaucomatous eyes, evaluated as percentage overlap of values of the two groups (y-axis). Index "tot" for total disc, "v" for vertical, "t" for temporal, "u" for inferior, "o" for superior quadrants, "max" for maximal C/D ratio.

comparable studies[3]. Correlation for C/D ratio in disc quadrants and for rim area was much weaker, however, being as low as r=0.28 for the temporal rim area[4]. Multiple measurements of individual eyes indicate that the reproducibility of the automated device is significantly lower than that of manual planimetry[1,3]. Our results in a series of double determinations with both methods agree with this (Table 1).

The absence of any significant correlation of automatically recorded disc data with visual field indices, as opposed to the manual planimetric data, is additional evidence of the limited accuracy of automated data acquisition, since at least a moderate correlation is to be expected. Some investigators have found a weak correlation between such automatically recorded data and visual field indices[3], others not[5]. New evaluation software for the ONHA might improve validity.

Even the correlation of manual planimetric disc data with perimetry is limited, though. Admittedly, a normal disc corresponds to an unaffected field, and a totally cupped disc to definite functional damage. The transition reveals a wide range of variation resulting in a limited linear correlation. Therefore, the assessment of glaucomatous alterations must include a thorough analysis both of the optic disc and the visual field.

The correlation between C/D ratio and MD and CLV, and between rim area and CLV seemed, at first, paradoxical. When viewing the glaucomatous group, very limited correlation was present while the non-glaucomatous group demonstrated no correlation at all. These populations taken as a whole, though, revealed a significantly higher correlation. This high correlation is obviously caused by the two distinctly different subgroups. Linear regression is depicted as independent regression lines (Figs. 1 and 2), as both parameters have an inherent variability. Calculation of non-linear correlation[6] did not improve our data.

Correlation improves by using sectors of the disc and corresponding parts of the field. A further step towards better correlation is the calculation of a complex index including focal characteristics[7] and a topographical comparison of focal disc damage with perimetric nerve fiber bundle zones[8]. The correlation may also benefit from the application of additional visual field indices[9]. It must be noted that pallor of the disc was not used for our calculations.

The size of the optic disc influences the likelihood of the presence of a glaucomatous visual

field defect[10]. Indeed, the two eyes of one of our glaucoma subjects (Fig. 1, circles) had field defects even though the discs were only centrally cupped. From the masked inspection of the discs we had erroneously anticipated a normal field in these two discs, the smallest in the entire population (disc area 2 SD below the mean). The 17 eyes with pseudo-glaucomatous cupping looked suspect with a C/D ratio over 0.7. The rim area of these large discs was even greater than that of the normal subjects or of the ocular hypertensives, and all had a perfectly normal visual field.

Separation of glaucomatous from normal eyes may be specified by the overlap of values of a parameter found in affected and unaffected eyes (Figs. 1 and 2). Calculation of "ROC curves"[9] confirmed our observations. The planimetric parameter with best separation characteristics, vertical C/D ratio, had the poorest correlation with glaucomatous field damage, however (Fig. 3). Temporal rim area, in contrast, was most limited in its separation ability, but it correlated well with glaucomatous field depression. Thus, individual diagnostic parameters using optic disc data seem to allow only one of the two important conclusions. The optic disc in glaucoma obviously cannot be described by a single parameter.

Cup volume correlated neither with field defects nor helped distinguish normal from glaucomatous subjects, and it decreased significantly with age[5,11]. This must be due to a progressing atrophy of the peripapillary choroid and retina. The "top" of the cup will thus shift down towards the lamina cribrosa. Volume measurements might be inadequate even for the follow-up of individual cases.

Acknowledgements

This study was supported by a grant of the German Federal Department of Research and Technology The programs for the special visual field analysis and for the computer-assisted planimetry were provided by D. Dannheim Jr. David Maslen revised the manuscript. The authors have no financial affiliation with the companies which produce the instruments used in this study.

References

1. Dannheim F: Vergleich manueller und computer-gestützter Papillenanalyse beim primär-chronischen Glaukom Fortschr Ophthalmol 85:445-447, 1988
2 Wilms KH: Zur Struktur einfacher Programme zur Berechnung von absoluten Grössen des Augenhintergrundes Optometrie 4:204-206, 1986
3 Klingbeil U: Fundus geometry measured with the analyzing stereo video ophthalmoscope. In: Masters B (ed) Non-Invasive Diagnostic Techniques in Ophthalmology. Heidelberg: Springer 1990 (in press)
4. Wagner M: Vergleich computergestützter und manueller Papillenanalyse beim primär-chronischen Glaukom Thesis, University of Hamburg, Faculty of Medicine 1991
5. Stürmer J, Schaer-Stoller F, Gloor B: Papillenausmessung mit Planimetrie und "Optic Nerve Head Analyzer" bei Glaukom und Glaukomverdacht Klin Mbl Augenheilk (in press)
6. Airaksinen PJ, Drance SM, Douglas GR, Schulzer M: Neuroretinal rim areas and visual field indices in glaucoma Am J Ophthalmol 99:107-110, 1985
7. Drance SM, Wijsman K, Schulzer M, Douglas GR: The correlation between neuroretinal rim and visual field indices. In: Heijl A (ed) Perimetry Update 1988/89, pp 285-287. Amsterdam/Berkeley/Milan: Kugler & Ghedini Publications 1989
8. Weber J, Dannheim F, Dannheim D: The topographical relationship between the optic disc and visual field in glaucoma. Acta Ophthalmol 68:568-574, 1990
9 Chauhan BC, Drance SM, Douglas GR: The use of visual field indices in detecting changes in the visual field in glaucoma. Invest Ophthalmol Vis Sci 31:512-520, 1990
10 Jonas J: Biomorphometrie des Nervus opticus. Stuttgart: Enke, Bücherei des Augenarztes Vol 120, 1989
11 Tuulonen A: Kriterien und Nützlichkeit der Exkavationsvolumenbestimmung Presented at the Meeting "Biomorphometrie des Nervus optikus", Erlangen 23 January 1988

The relationship of optic nerve and nerve fiber layer parameters with visual field loss in glaucoma

Joseph Caprioli and Mario Zulauf

Glaucoma Service, Department of Ophthalmology and Visual Science, Yale University School of Medicine, 330 Cedar Street, New Haven, Connecticut 06510-8061, USA

Abstract

The authors investigated the relationships between optic nerve head and nerve fiber layer (NFL) structural parameters and indices of visual field loss in normals (53), glaucoma suspects (87), and glaucoma patients (112). Structural parameters were derived from computerized digital analysis of simultaneous stereoscopic video images acquired with the Rodenstock Analyzer and included cup-disc ratio, disc rim area, cup volume, average nerve fiber layer height, and nerve fiber layer height at the superior and inferior poles of the disc (polar NFL height). The correlation coefficients between these and the visual field indices mean defect, corrected loss variance, and short term fluctuation were all statistically significant. The strongest correlation was between polar NFL height and visual field mean defect (r=0.45, p=0.000). Multivariate analyses were used to combine functional parameters and to test the relationship with combined structural parameters. Structure and function expressed in this way had a linear correlation coefficient of r=0.55 (p=0.000). The authors conclude that (1) quantitative relationships between the visual field and the optic disc/nerve fiber layer are not constant between subjects; and (2) that there is a need to improve the parameters with which to describe the visual field and optic nerve/nerve fiber layer in glaucoma Additional structural parameters may be found which are more sensitive and more specific indicators of glaucomatous optic nerve damage.

Introduction

Careful clinical correlation of optic disc appearance with the visual field is an important part of the evaluation of glaucoma patients, Automated threshold perimetry has made it possible to routinely obtain standardized, quantitative threshold measurements of the visual field. In contradistinction, routine clinical evaluation of the optic nerve head remains largely subjective and qualitative. There is little information available about the relationships between quantitative measurements of optic disc topography and quantitative measurements of the visual field.

The purpose of this work is to investigate the relationships between structural parameters of the optic nerve head and newly developed measurements of the peripapillary nerve fiber layer surface contour with functional abnormalities of glaucoma as measured by automated static threshold perimetry.

Methods

Image analysis

A system for computerized image analysis (Rodenstock Instruments, Munich, Germany) was used to acquire fundus images and perform preliminary topographic analyses, Measurements of disc area, cup-disc ratio, disc rim area, and cup volume were made with the software supplied by the manufacturer; the methodology and reproducibility of these measurements have been reported[1-3]. The methods used to measure the relative height of the nerve fiber layer (NFL) at

This study is supported in part by grants from the Robert Leet and Clara Guthrie Patterson Trust, Connecticut Lions Eye Research Foundation, Inc , Research to Prevent Blindness, Inc , and the National Eye Institute (EY-00785 and EY-073533).

Perimetry Update 1990/91, pp. 9-14
Proceedings of the IXth International Perimetric Society Meeting,
Malmö, Sweden, June 17-20, 1990
edited by Richard P Mills and Anders Heijl

the edge of the optic disc have been previously described[4]. Measurements of the height of the NFL surface relative to a standardized reference plane are made 100 μm outside the disc edge, at 64 separate locations around the disc. These measurements are corrected for the optical magnification of the eye and are in units of microns, Correction to absolute measurements are made with ultrasonic measurements of axial length (in most cases), or with refractive and keratometric measurements[5]. The set of 64 individual measurements of relative NFL height are summarized by the following arbitrarily defined parameters:

1. NFL height: the average of all 64 individual relative NFL height measurements;
2. superior polar NFL height: the average of eight individual relative NFL height measurements which are included in a 45 degree sector at the superior pole of the disc, centered at the vertical axis;
3. inferior polar NFL height: the average of eight individual relative NFL height measurements which are included in a 45 degree sector at the inferior pole of the disc, centered at the vertical axis;
4. polar NFL height: the average of all relative NFL height measurements within the two polar sectors defined in 2 and 3 above.

The variability of the individual measurements of relative NFL height has been reported[6].

Subjects

Normal subjects had no history of eye disease and were recruited from hospital staff and spouses or friends of patients; none had presented for medical evaluation. All those older than 40 years of age with normal eye history and examination and with normal visual fields tested with automated threshold perimetry (Octopus or Humphrey) were included. The eye examination included slit lamp biomicroscopy, tonometry, gonioscopy, dilated indirect ophthalmoscopy, stereoscopic optic disc photography, and computerized image analysis of the optic nerve head. Normal subjects had no family history of glaucoma.

All glaucoma patients over 40 years of age who had automated threshold perimetry (Octopus program 32 or G1), stereoscopic optic disc photographs, and computerized image analysis were included. Computerized image analysis was performed in patients with reasonably clear media (20/50 or better) who could be dilated to 5 mm or more.

Patients were considered glaucomatous if they had elevated intraocular pressure (or a history of elevated intraocular pressure before treatment) and typical glaucomatous visual field defects. Glaucoma suspects met all of the same criteria as glaucoma patients, except that the visual fields were clinically normal. The vast majority of glaucoma suspects and glaucoma patients have had previous experience with automated perimetry. Typical glaucomatous visual field defects were defined, in a reliably performed visual field test, as at least:

1. two contiguous points with 10 decibel loss or greater in the superior or inferior Bjerrum areas, compared with perimeter defined age-matched controls;
2. three contiguous points with 5 decibel loss or greater in the superior or inferior Bjerrum areas; or
3. a 10 decibel difference across the nasal horizontal midline in two or more adjacent locations.

Pupils were dilated for perimetry only in eyes with a pupil size of ≤ 2.0 mm. The most superior and inferior rows of threshold measurements were excluded from these criteria to eliminate the inclusion of rim artifacts. Visual field indices mean defect, corrected loss variance, and short term fluctuation were recorded or calculated for each visual field. One eye of each patient was used in the study, and was chosen randomly if both eyes were eligible. Informed consent was obtained from each subject after the nature of the procedure was fully explained.

Statistics

The distributions for age and refractive error of the groups were compared with the Kolmogorov-Smirnov test[7]. Data are reported as the mean ± the standard error of the mean. The level of statistical significance used was $p<0.05$. This was adjusted downward with the Bonferroni correction when multiple simultaneous comparisons were made. Linear approximations

were used to model individual relationships between structure and function. Multivariate models were used to evaluate several parameters simultaneously and to test the relationships of combined parameters.

Results

Summary data for age, sex, eye, refractive error, visual field indices, and standard optic disc parameters are given in Table 1. The groups did not differ significantly for age or refractive error. The visual field indices did not differ significantly between the normals and the glaucoma suspects. The values in the glaucoma group reflected the selection criteria of visual field loss; most patients had early to moderate visual field loss. There were no significant differences among the groups for disc area. The cup-disc ratio of the normals differed significantly from the glaucoma patients (p=0.000) but not from the glaucoma suspects (p=0.26). Likewise, disc rim area differed significantly between normals and glaucomas (p=0.000), but not between normals and suspects (p=0.18). Cup volume was significantly different among all three groups (p<0.006; $p_{critical}$=0.016).

Table 1 Summary statistics for age, sex, eye, refractive error, visual field and optic nerve head*

	Normal (*n*=53)	*Glaucoma suspect* (*n*=87)	*Glaucoma* (*n*=112)
Age (years)	63 0±1 1	58.2±1.1	61 5±0 9
Male (*n*)	18	42	56
Right eye (*n*)	27	47	60
Refractive error (spherical equivalent, diopters)	0.8±0.3	–0 1±0 3	–0 6±0 3
Visual field			
mean defect (dB)	0.0±0.2	–0.1±0.2	7 2±0 5
corrected loss variance (dB^2)	4 0±1 0	2 7±0.4	34 5±3 3
short term fluctuation (dB)	1.6±0.1	1.7±0 1	3.6±0.4
Optic disc			
disc area (mm^2)	1 70±0 04	1.73±0.05	1 73±0 04
cup-disc	0 52±0 02	0 56±0 02	0.64±0.02
rim area (mm^2)	1.08±0.03	1 02±0 03	0.84±0.03
cup volume (mm^3)	0.36±0.02	0 48±0 04	0 62±0.03

*data are given, where applicable, as mean ± SEM

Table 2 Correlation coefficients for optic nerve/nerve fiber layer and visual field relationships

	Visual field		
	MD	*CLV*	*STF*
Optic nerve			
cup-disc	0.29	0.27	0 17
rim area	0.36	0.31	0.23
polar rim area	0.35	0.32	0 25
cup volume	0.28	0.26	0 12
Nerve fiber layer			
NFL height	0 33	0.22	0 20
polar NFL height	0.45	0.37	0 19

There were statistically significant correlations between NFL height measurements and visual field indices (see Table 2). The best correlations were found for polar NFL height with mean defect (r=0.45, p=0.000) (Fig. 1) and with corrected loss variance (r=0.37, p=0.000). The best correlations among the standard disc parameters were for disc rim area and mean defect (r=0.36, p=0.000) (Fig. 2) and with corrected loss variance (r=0.31, p=0.000).

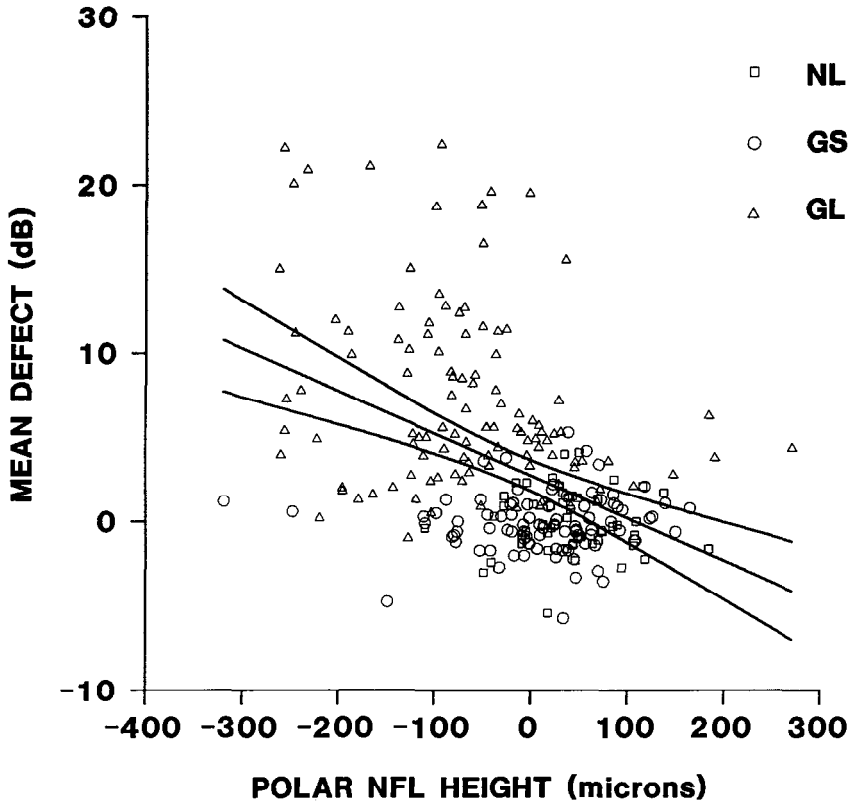

Fig 1 The relationship between polar NFL height (see text) and visual field mean defect (y = - (0.025)× + 2.7; r=0.45; p=0 000) The 99% confidence limits for the linear regression are shown.

When structural parameters and functional parameters were combined in a multivariate model, the following statistically significant relationship was obtained:

$$.18(MD/dB) + .017(CLV/dB^2) + .087(STF/dB) =$$
$$10.14 - 6.5(CD) - 6.0(RA/mm^2) + 2.9(CV/mm^3) + .015(NFL/u) - .27(POLAR\ NFL/u),$$

where r=0.54 and p=0.000 (Fig. 3), and MD = mean defect, CLV = corrected loss variance, STF = short term fluctuation, CD = cup-disc ratio, RA = disc rim area, CV = cup volume, NFL = average nerve fiber layer height, and polar NFL = average polar nerve fiber layer height.

Discussion

The advent of computerized analysis of digitized fundus images has revived interest in the quantification of optic disc structure, especially as it relates to the study of glaucomatous damage. New structural parameters have been recently introduced which appear to make better use of the quantitative information obtained with image analysis and provide more sensitive and specific measures of early glaucomatous damage[4,6]. We were interested in testing the ability of these new parameters, especially as it compared to that of more standard quantitative disc parameters, to correlate with visual function measured with automated threshold perimetry in glaucoma patients.

Airaksinen and co-workers investigated the relationship between manual measurements of disc rim area and visual field loss in glaucoma[8]. Statistically significant correlations existed for optic disc rim area with visual field mean defect and corrected loss variance. The strongest

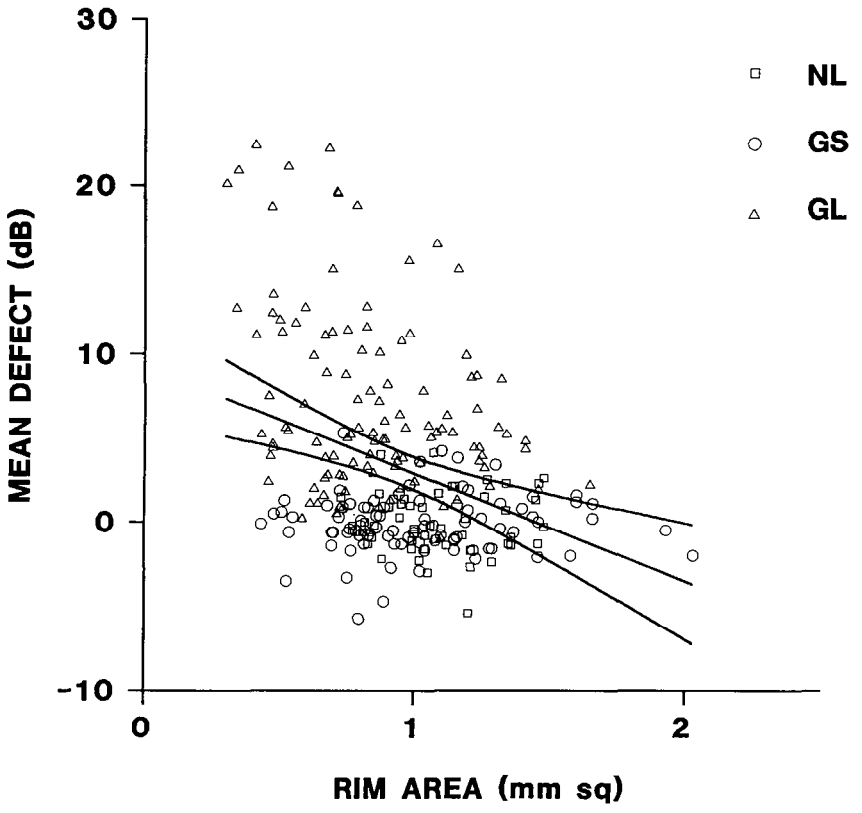

Fig 2 The relationship between disc rim area and visual field mean defect (y = - (6 4)× + 9 2; r=0 36; p=0.000). The 99% confidence limits for the linear regression are shown

correlation was between rim area and the measure for overall sensitivity loss, mean defect. Drance *et al* [9] further reported correlations for measurements of diffuse structural abnormalities of the optic nerve and nerve fiber layer with visual field mean defect, while localized abnormalities seemed more closely related to visual field corrected loss variance.

We previously reported significant correlations for quantitative optic nerve head parameters with indices of visual field loss[10]. We predicted that closer correlations with function might be uncovered if structural parameters could be identified which more closely reflected the number of retinal ganglion cell axons in the optic nerve head. We have described a technique to measure the relative height of the peripapillary nerve fiber layer surface, and have provided clinical correlations which demonstrate the resolution of the methods[4,6]. These measurements were more sensitive and more specific in their ability to discriminate between normal and glaucomatous subjects than were cup-disc ratio, disc rim area, or cup volume. Such measurements of nerve fiber layer height correlated better with the visual field indices than did the other structural parameters. The strength of the structure-function relationship was further increased by combining parameters in a multivariate model. Still, only 25% of the variance of visual field measurements (as expressed by the currently used indices) could be explained by the variance of the structural parameters. We conclude that (1) quantitative relationships between the visual field and the optic disc/nerve fiber layer are not constant between subjects; and (2) that there is a need to improve the parameters with which to describe the visual field and optic nerve/nerve fiber layer in glaucoma. Additional structural parameters may be found which are more sensitive and more specific indicators of glaucomatous optic nerve damage.

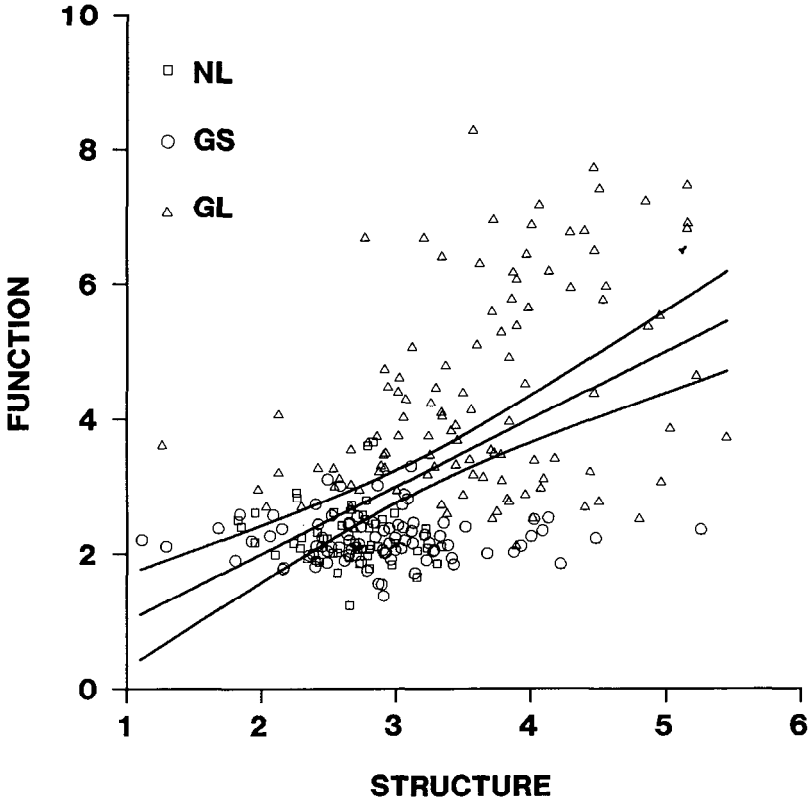

Fig 3 The relationship between combined optic nerve/nerve fiber layer structural parameters and combined visual field indices (see text) (y = (29)× + 2 2; r=0.55; p=0.000) The 99% confidence limits for the linear regression are shown.

References

1 Caprioli J, Klingbeil U, Sears M, Pope B: Reproducibility of the optic disc measurements with computerized analysis of stereoscopic video images Arch Ophthalmol 104:1035-1039, 1986
2 Shields MB, Martone JF, Shelton AR, Ollie AR, MacMillan J: Reproducibility of topographic measurements with the optic nerve head analyzer Am J Ophthalmol 104:581-586, 1987
3 Bishop KI, Werner EB, Krupin T, Kozart DM, Beck SR, Nunan BS, Wax MB: Variability and reproducibility of optic disk topographic measurements with the Rodenstock optic nerve head analyzer. Am J Ophthalmol 106:696-702, 1988
4. Caprioli J, Ortiz-Colberg R, Miller JM, Tressler C: Measurements of peripapillary nerve fiber layer contour in glaucoma Am J Ophthalmol 108:404-413, 1989
5. Littman H: Zur Bestimmung der wahren Grosse eines Objektes auf dem Hintergrund eines lebenden Auges Klin Mbl Augenheilk 192:66-67, 1988
6 Caprioli J: The contour of the juxtapapillary nerve fiber layer in glaucoma Ophthalmology 97:358-366, 1990
7 Sokal RR, Rohlf FJ: Biometry: The Principles and Practice of Statistics in Biological Research, 2nd edn, pp 440-445 San Francisco: WH Freeman Co 1981
8 Airaksinen PJ, Drance SM, Schulzer M: Neuroretinal rim areas and visual field indices in glaucoma. Am J Ophthalmol 99:107-110, 1985
9. Drance SM, Airaksinen PJ, Price M et al: The correlation of functional and structural measurements in glaucoma patients and normal subjects Am J Ophthalmol 102:612-616, 1986
10. Caprioli J, Miller JM: Correlation of structure and function in glaucoma Ophthalmology 95:723-727, 1988

Correlation of optic disc cupping, pallor and retinal nerve fiber layer thickness with visual field loss in chronic open angle glaucoma

Colm O'Brien*, Bernard Schwartz and Takenori Takamoto

Department of Ophthalmology, New England Medical Center and Tufts University School of Medicine, Boston, MA, USA

Abstract

The authors have developed quantitative methods for measurement of optic disc cup volume, depth, area at surface of retina and slope (by photogrammetry), retinal nerve fiber layer thickness (RNFLT) at the disc rim (by photogrammetry) and optic disc pallor (by computerized image analysis) They correlated these measurements with measurements of visual field thresholds (Octopus perimeter 2000R) in 33 patients with open angle glaucoma For the total disc, a significant Spearman correlation was obtained for cup area (r_s -0.4875; p = 0.004) but not for the other parameters of the cup, pallor or RNFLT Quadrant analysis of the optic disc showed significant correlations of thresholds for the corresponding quadrant of the visual field with cup area for all quadrants, with cup volume for the inferior quadrant, with area of pallor for the nasal quadrant and for RNFLT for the temporal quadrant. Intercorrelations between disc parameters were also significant especially for pallor and cup parameters The authors conclude that the most consistent and significant correlation between functional visual field loss and structural damage occurs at the surface of the disc, namely cup area Even this correlation was not as large as a previously obtained correlation for 59 glaucomatous eyes between fluorescein angiography filling defects of the optic disc and visual field loss (r_s = -0.8013; p - 0 0001) New methods for measuring functional loss in glaucoma that more closely reflect structural damage, require development

Introduction

The use of measurements of the optic disc and the retinal nerve fiber layer in the management of patients with glaucoma requires the identification of those parameters of structural damage that accurately reflect visual field loss[1]. To address this issue, we examined the relationship between structure, using reproducible computer and photogrammetric assisted methods of measuring optic disc and retinal nerve fiber layer thickness (RNFLT), and function as measured by automated perimetry in a group of patients with chronic open angle glaucoma. In addition to determining correlation for the total disc and field, we also examined the relationships between corresponding quadrants of the discs and field, as well as intercorrelations between the various measurements of the optic disc and RNFLT.

Methods

We studied 33 primary open angle glaucoma patients whose intraocular pressures were greater than or equal to 21 mmHg on at least two independent examinations, with characteristic optic disc damage and visual field loss. One eye of each patient was randomly selected. The visual field loss was either localized or localized with some general depression of the visual field. Patients with pigmentary dispersion and exfoliation syndrome were excluded. All patients

Supported in part by grants from the Ainsworth Scholarship, The International Glaucoma Association, and Alcon Research Institute, Forth Worth, Texas

*This study was carried out while Dr O'Brien was a Glaucoma Fellow at Tufts-New England Medical Center. Dr. O'Brien is currently at St. Paul's Eye Hospital, Liverpool, UK

Address for correspondence Bernard Schwartz, M D , Ph D , Ophthalmology Department, Tufts-New England Medical Center, NEMC #450, 750 Washington Street, Boston, MA 02111, USA

Perimetry Update 1990/91, pp. 15-22
Proceedings of the IXth International Perimetric Society Meeting,
Malmö, Sweden, June 17-20, 1990
edited by Richard P Mills and Anders Heijl

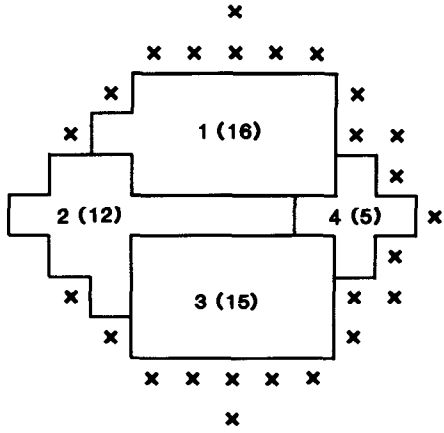

Fig 1 Data points of right eye used on visual field program 31 to obtain corresponding superior, inferior, nasal and temporal quadrants of optic disc The numbers identify the quadrants. The numbers in brackets indicate the number of points used to obtain mean threshold values for each quadrant The "X" indicated points that were excluded

had a corrected visual acuity of 20/40 or better. Six patients were emmetropic, seven had myopia of less than 5 diopters, two had myopia of 5 diopters or greater, 15 had hyperopia of less than 5 diopters and two had hyperopia greater than 5 diopters. The refractive error was unknown for one patient.

Optic disc photographs and visual field examinations were taken within two months of each other. Optic disc cupping and RNFLT thickness at the optic disc margin were measured by photogrammetry from simultaneous stereophotographs[2,3]. For measurements of cup area, the cup edge was defined as a topographic edge that is a change of slope from cup wall to neuroretinal rim[2]. Optic disc pallor was measured by computerized image analysis with manually applied plan points from single color disc photographs[4]. Measurements of quadrants of the optic disc were obtained by the use of a St. Andrew's Cross[4]. The reproducibility of our measurements was determined as percent coefficient of variation (standard deviation/mean x 100) for duplicate measurements. For optic disc cup volume/(mm^3)/disc area (mm^2)% the mean percent coefficient variation ± standard deviation was 4.7 ± 3.3%; for optic disc area of pallor (mm^2)/disc area (mm^2)%, it was 2.6 ± 1.8% and for retinal nerve fiber layer thickness (mm)/vertical disc radius (mm) it was 4.2 ± 3.2.%

Visual field threshold values were measured with the Octopus 2000R perimeter using program 31. Fig. 1 shows the division of the central 30° field into quadrants to correspond with the appropriate optic disc quadrants. The values of mean defect and correlated loss standard deviation were also determined[5,6]. Non-parametric tests were used to test the significance of the Spearman rank order correlations[7].

Table 1 Ocular and systemic characteristics of open angle glaucoma patients

	Mean ±standard deviation (n=33)
Age (years)	62 9 ±12.8
Race white/black	24/ 9
Sex male/female	19/14
Ocular pressure (mmHg) at time of photograph	18.67± 5 89
Average ocular pressure (mmHg)	19 36± 5 46
Maximum ocular pressure (mmHg)	31.00± 8.57
Mean threshold value (dB)	13.32± 5 90
Mean defect (dB)	11 02± 0 578
Corrected loss standard deviation (dB)	7.03± 2.10

Table 2. Measurements for total disc for open angle glaucoma patients

	Mean ±standard deviation (n=33)
Cup volume (mm^3)/disc area (mm^2) %	28.17 ± 8.01
Cup area (mm^2)/disc area (mm^2) %	59.22 ± 9.47
Cup depth (mm)/disc area (mm^2) %	19.40 ± 5.08
Cup slope (degrees)	47 97 ± 9.68
Area pallor (mm^2)/disc area (mm^2) %	44.00 ±11.20
Retinal nerve fiber layer thickness (mm)/ vertical disc radius (mm)	0 258± 0.063

Table 3 Spearman rank correlations (r_s) of optic disc and retinal nerve fiber layer thickness (RNFLT), measurements of total disc with visual field indices (n=33)

	Mean threshold value (dB)		*Mean defect (dB)*		*Correlated loss standard deviation*	
	r_s	p	r_s	p	r_s	p
Total disc cup volume (mm^2)/ disc area (mm^2) %	–0.2012	NS	0.3021	0.0875*	0.1687	NS
Cup area (mm^2)/ disc area (mm^2) %	–0.4875	0.0040	0.4855	0 0042	–0.0104	NS
Cup depth (mm)/ disc area (mm^2) %	–0.1490	NS	0.2355	NS	0.1191	NS
Cup slope (degrees)	–0.1109	NS	0.2185	NS	0.3213	0 0683*
Area pallor (mm^2)/ area disc (mm^2) %	0.2197	NS	0.2936	0 0972	0 2166	NS
RNFLT (mm)/vertical disc radius (mm)	0.2248	NS	–0.2995	0.0904*	–0.2622	NS

*borderline in significance $p>0.05$ $p<0.10$
NS: non-significant $p\geq 0.10$

Table 4. Significant ($p<0.05$) Spearman correlations (r_s) for corresponding mean threshold values (dB) of quadrant of visual field ($n=29$)

	r_s	p
Optic disc		
Cup volume (mm^3)/disc area (mm^2) %		
inferior	–0 3711	0 0475
Cup area (mm^2)/disc area (mm^2) %		
inferior	–0.4563	0.0128
nasal	–0.4798	0.0084
superior	–0.4114	0 0266
temporal	–0 4205	0 0231
Area pallor (mm^2)/disc area (mm^2) %		
nasal	–0 4217	0 0227
Retinal nerve fiber layer thickness (mm)/vertical disc radius (mm)		
temporal	0 4424	0.0163

Results

Table 1 presents the ocular and systemic characteristics of the 33 patients with open angle glaucoma. Table 2 presents the measurements of the optic disc and the RNFLT for the total disc of these patients. Table 3 shows the Spearman rank correlations of the various optic disc measurements as well as the RNFLT with indices of measurements of the visual fields. The largest and most significant correlations were obtained between measurements of cup area in relation to disc area for mean threshold values as well as mean defect values. None of the other measurements of the optic disc or RNFLT were significant in relation to mean threshold value or mean defect value. No significant correlations were obtained with the corrected loss standard

Table 5 Spearman (r_s) correlations of retinal nerve fiber layer thickness and pallor measurement with optic disc cup measurements for total disc (n=33)

	Retinal nerve fiber layer thickness (mm)/vertical disc radius (mm)		*Area pallor (mm²)/ disc area (mm²) %*	
	r_s	p	r_s	p
Cup volume (mm³)/disc area (mm²) %	–0.3258	0.0643	0.5161	0.0021
Cup area (mm²)/disc area (mm²) %	–0 3129	0.0762	0.3958	0.0226
Cup depth (mm)/disc area (mm²) %	–0 2943	0.0964	0.4423	0.001
Cup slope (degrees)	–0 2626	>0.10	0 5680	0.006
Retinal nerve fiber layer thickness (mm)/ vertical disc radius (mm)	–	–	–0.5304	0.0015

deviation.

Table 4 shows the significant Spearman correlations obtained for analysis by quadrant. For the cup area all four quadrants showed significant correlations. In addition, cup volume for the inferior quadrant, pallor area for the nasal quadrant and RNFLT for the temporal quadrant showed significant correlations with mean threshold values.

Analysis of the inter-correlations of the optic disc cupping parameters showed significant correlations of cup area with volume (r_s = 0.4278; p = 0.0130), cup depth with volume (r_s = 0.8435; p<0.0001) and cup slope with volume (r_s = 0.6932; p<0.0001). However, there was no significant correlation of cup area with depth, but a highly significant correlation of cup slope with depth (r_s = 0.7822; p<0.0001).

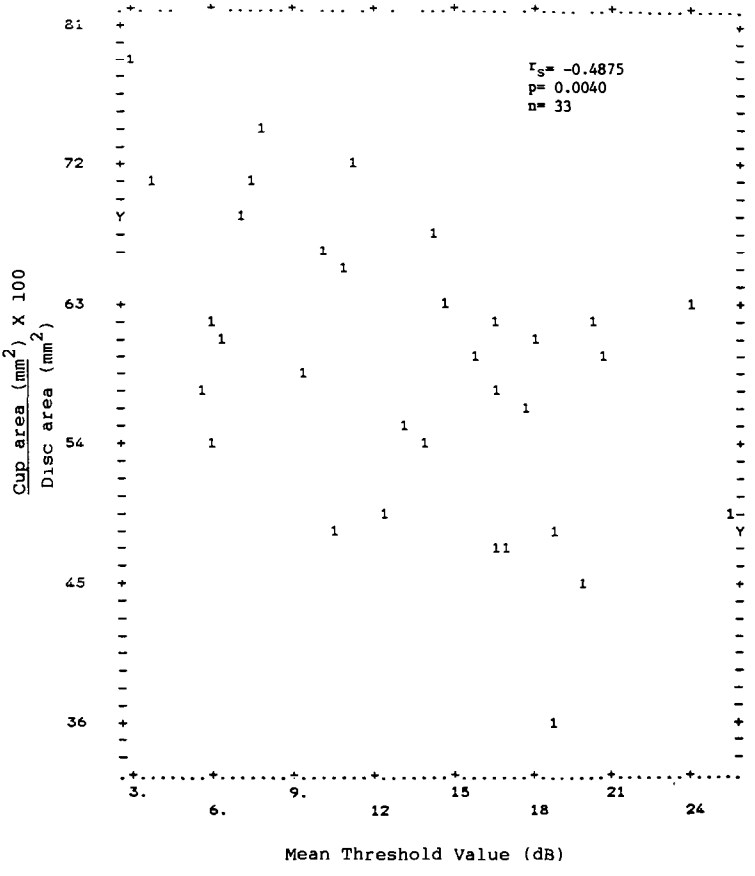

Fig 2 Spearman correlations (r_s) between optic disc cup area (mm²)/disc area (mm²) × 100 with mean visual field threshold (dB).

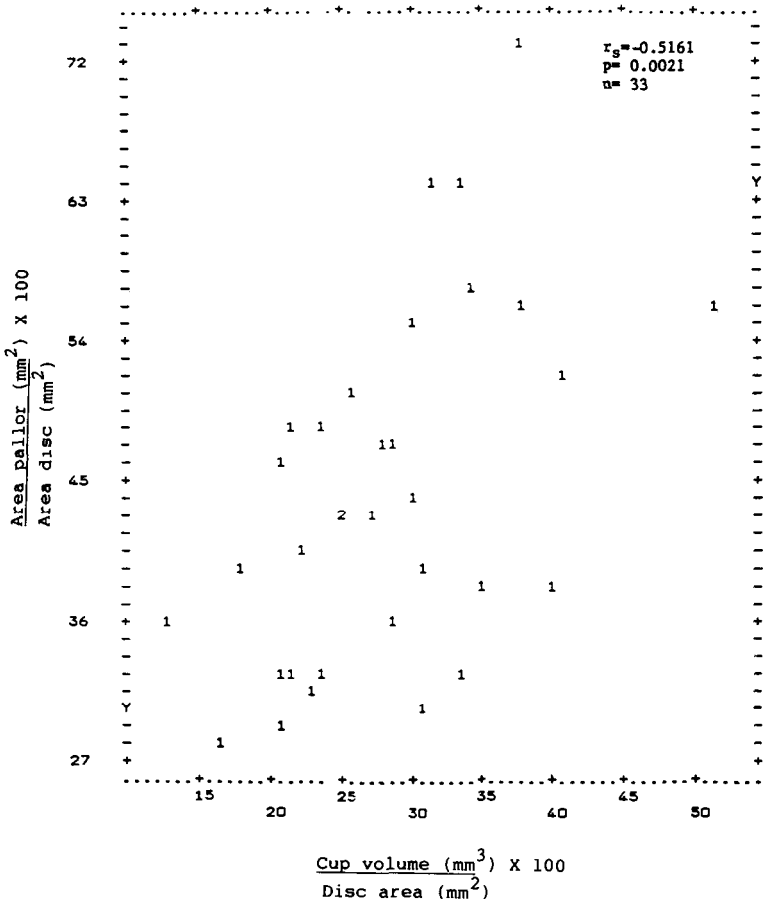

Fig 3 Spearman correlations (r_s) between optic disc area pallor (mm^2)/area disc (mm^2) × 100 with optic disc cup volume (mm^3)/disc area (mm^2) × 100.

Inter-correlations of the retinal nerve fiber layer thickness and pallor measurements with the optic disc cup measurements are shown in Table 5 for the total disc. No significant correlations were obtained with RNFLT and cup parameters. The correlations with pallor are generally somewhat larger than the correlations obtained between optic disc and RNFLT measurements with visual field indices as shown in Table 3. The correlation of RNFLT or pallor with cupping measurements for corresponding quadrants, superior, inferior, temporal or nasal, showed some increased enhancement of the correlation coefficients with the largest correlation of $r_s = 0.6296$ for area of pallor in the nasal quadrant with cup depth in the nasal quadrant.

Discussion

In the clinical setting, the appearance of glaucomatous optic nerve damage is generally associated with the extent of visual field loss. A patient presenting with a field defect not compatible with the appearance of the optic disc is often referred for neurological evaluation to rule out an extraocular cause for the field loss. The strength of this relationship between disc and field has been explored both qualitatively and quantitatively in previous studies[8-20].

Our measurements of mean visual thresholds on open angle glaucoma eyes range widely from about 3 to 25 dB, as do optic disc and RNFLT measurements. For the total disc and field and their corresponding quadrants, significant correlations for mean threshold were obtained

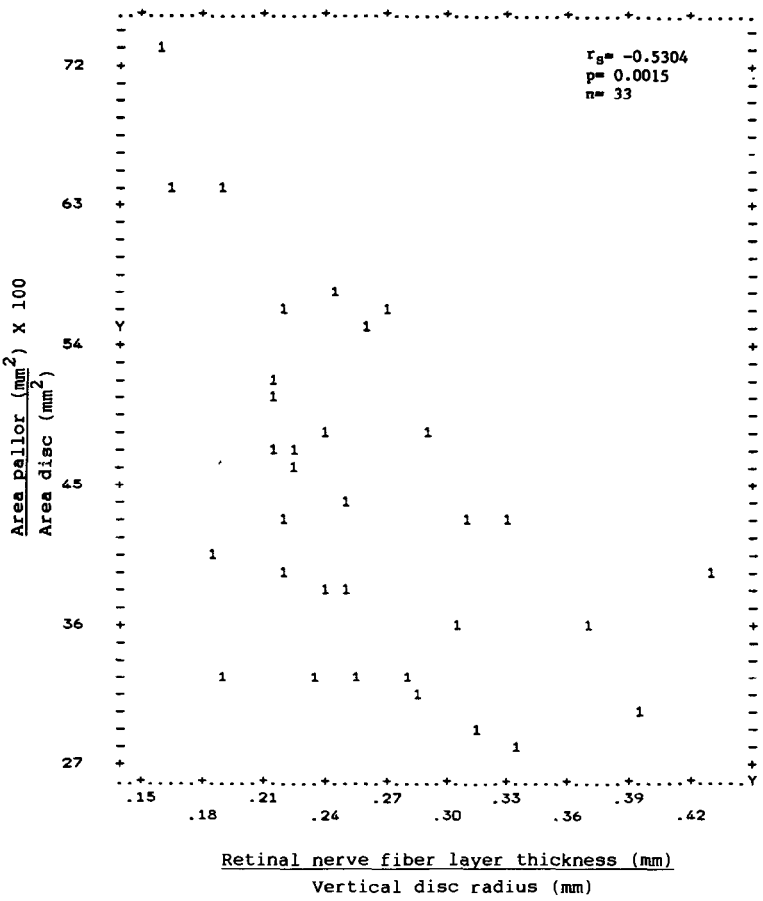

Fig 4 Spearman correlations (r_s) between optic disc area pallor (mm^2)/area disc (mm^2) × 100 with retinal nerve fiber layer thickness (mm)/vertical disc radius (mm)

for the cup area. For corresponding quadrants, but not for the total disc, significant correlations were also obtained for the cup volume in the inferior quadrant, area of pallor for the nasal quadrant and RNFLT for the temporal quadrant. No significant correlations were obtained with the corrected loss standard deviation for the total disc.

Several reports have described how the disc appearance may be used to predict qualitatively the presence and location of visual field loss[8-10]. Quantitative measurements (including planimetry and computerized image analysis techniques) have repeatedly shown that of the different parameters of optic nerve topography, neuro-retinal rim area has the strongest correlation with visual field loss[11-18], despite the fact that different authors have used different definitions of the neuro-retinal rim area. Some have based their definition on contour changes of the cup[11-13,17,18] and other have used the pallor cup[14]. Those using the Rodenstock Optic Nerve Head Analyzer have defined the cup at 150 microns below the disc surface[16,18]. In our study, cup area had the strongest correlation with mean threshold value (r_s = -0.4875) and mean defect (r_s = 0.4885). Cup area, as measured by photogrammetry is based on contour changes, that is a change of slope from cup wall to neuro-retinal rim[2] and is an indirect measurement of neuro-retinal rim area.

Most of the previous studies correlating disc measurements and visual field loss included normals and glaucoma suspects in their study groups. Both these groups have normal or almost normal visual field data and including them with glaucomatous patients with field loss will therefore bias or weigh any correlation, especially at or near normal visual field values. Fur-

thermore, some previous studies used both eyes of the same subject when analyzing correlations. Since both eyes of the same subject are usually significantly correlated, the use of both eyes increases the sample size and therefore artefactually increases the correlation towards a more significant level[21].

We analyzed only primary open angle glaucoma patients and identified that parameter of structural damage which best reflects visual field loss. Caprioli and Miller[16] did examine their glaucoma patients separately and obtained similar results to the observations presented in this study. They found in 37 glaucoma eyes that disc rim area correlated significantly with mean defect (r_s = -0.46; p = -0.004) but not with corrected loss standard deviation similar to our findings. They also determined that mean defect correlated significantly with cup to disc ratio (r = 0.38; p = 0.015), but was not significant for cup volume (r_s = 0.33) (personal communication, J Caprioli). Of the other disc parameters in our study, cup volume in the inferior quadrant (r_s = -0.4213) had significant correlations with mean threshold values.

Airaksinen *et al.* found a strong quadratic relationship between a semi-quantitative method of scoring the retinal nerve fiber layer (RNFL) and mean retinal sensitivity[19]. Recently, Caprioli *et al.*[20] have shown that the contour of the peripapillary RNFL, particularly that of the superior and inferior quadrants, correlates better with the visual field indices than the standard parameters of optic nerve damage. Both these studies used normals and glaucoma suspects in their methodology and did not analyze the open angle glaucoma patients separately. We found a significant correlation between RNFLT and mean visual field thresholds only in the temporal quadrant (r_s = 0.4224). The absence of a stronger correlation may indicate that a considerable loss of the RNFL has occurred prior to the detection of the earliest field defects by automated perimetry, a concept previously suggested by Airaksinen *et al* [19].

The lack of correlation coefficients of higher magnitude when functional and structural measurements of the same optic nerve are measured, is surprising. There are probably several reasons for this discrepancy. First the optic disc measurements are generally highly reproducible[2,3], but the visual field measurements are probably less reproducible[5,22,23]. The correlation coefficients obtained for pallor measurements with optic disc cup measurements for the total disc (Table 5) are generally larger than those correlations obtained between the disc and visual field measurements. However, some of these correlations are still probably not significantly different from the correlations obtained between the optic disc and visual field measurements.

A second reason for the relative lack of high correlations between structural and functional measurements is that these measurements reflect changes in the optic disc and visual field occurring at different rates in time. It is assumed, in our present model of development of open angle glaucoma, that changes in the optic disc and RNFLT occur prior to visual field loss. Therefore, the optic disc and RNFLT parameters are probably increased to a greater extent than the visual field loss. This suggests that some other functional measurement of optic nerve function that occurs prior to visual field loss would probably be more correlated with the optic disc measurements.

The third reason for the lack of a large correlation between the disc and visual field loss is that visual field loss may not be as sensitive a measurement of optic nerve damage as the optic disc measurements.

Finally, not all structural change may represent functional change and, therefore, the correlation will not be exact.

In spite of the above reasons, one still has to explain the relatively large correlation of cup area with visual field threshold. Perhaps this is the first disc parameter to enlarge with the progression of optic disc cupping. Therefore, early in the disease, it may show the greatest change over time.

We have previously shown that there are significant correlations between the area of optic disc fluorescein filling defect and the area of the isopter of the visual field in glaucomatous changes, as determined with the Goldmann perimeter[24]. All but five of the glaucomatous eyes had a diagnosis of chronic open angle glaucoma. For the II4e isopter, for 59 eyes with only one eye chosen per individual, the Spearman correlation coefficient was large (r_s = -0.8013) with a p value of less than 0.0001. This correlation is larger than the correlations obtained with any of the optic disc or RNFLT measurements in this study, and strongly suggests that the vascular defect of the optic disc, as shown by fluorescein angiography, is closely correlated with visual field loss.

We conclude that, in order to obtain larger correlations of structural changes of the optic disc

and RNFLT with functional loss, we require functional methods of high reproducibility and great sensitivity, especially if they are to be applied in an early stage of the disease.

References

1. Shields MB: The future of computerized image analysis in the management of glaucoma (Editorial) Am J Ophthalmol 108:319-323, 1989
2. Takamoto T, Schwartz B: Reproducibility of photogrammetric optic disc cup measurements. Invest Ophthalmol Vis Sci 26:814-817, 1985
3. Takamoto T, Schwartz B: Photogrammetric measurement of nerve fiber layer thickness. Ophthalmology 96:1315-1319, 1989
4. Nagin P, Schwartz B, Nanba K: The reproducibility of computerized boundary analysis for measuring optic disc pallor in the normal optic disc Ophthalmology 92:248-251, 1985
5. Flammer J, Drance SM, Zulauf M: Differential light threshold, short and long-term fluctuations in patients with glaucoma, normal controls and patients with suspected glaucoma. Arch Ophthalmol 102:704-706, 1984
6 Flammer J, Drance SM, Augustiny L, Funkhauser A: Quantification of glaucomatous visual field defects with automated perimetry. Invest Ophthalmol Vis Sci 26:176-181, 1985
7. Siegel S, Castellan NJ Jr: Nonparametric Statistics for the Behavioral Sciences, 2nd edn New York: McGraw-Hill 1988
8 Hoskins HD, Gelbar EC: Optic disc topography and visual field defects in patients with increased intraocular pressure. Am J Ophthalmol 80:284-290, 1975
9 Hitchings RA, Spaeth GL: The optic disc in glaucoma. II. Correlation of the appearance of the optic disc with the visual field. Br J Ophthalmol 61:107-113, 1977
10 Holmin C: Optic disc evaluation versus the visual field in chronic glaucoma Acta Ophthalmol 60:275-283, 1982
11. Balazsi AG, Drance SM, Schulzer M, Douglas GR: Neuro-retinal rim area in suspected glaucoma and early chronic open-angle glaucoma: correlation with parameters of visual function. Arch Ophthalmol 102:1011-1014, 1984
12. Airaksinen PJ, Drance SM, Douglas GR, Schulzer M: Neuro-retinal rim areas and visual field indices in glaucoma Am J Ophthalmol 99:107-110, 1985
13 Drance SM, Airaksinen PJ, Price M, Schulzer M, Douglas GR, Tansley BW: The correlation of functional and structural measurements in glaucoma patients and normal subjects. Am J Ophthalmol 102:612-616, 1986
14 Guthauser U, Flammer J, Niesel P: The relationship between the visual field and the optic nerve in glaucomas Graefe's Arch Clin Exp Ophthalmol 225:129-132, 1987
15 Funk J, Bornscheur C, Grehn F: Neuroretinal rim area and visual field in glaucoma Graefe's Arch Clin Exp Ophthalmol 226:431-434, 1988
16. Caprioli J, Miller JM: Correlation of structure and function in glaucoma: quantitative measurements of disc and field. Ophthalmology 95:723-727, 1988
17 Jonas JB, Gusek GL, Neumann GOH: Optic disc morphometry in chronic primary open-angle glaucoma II Correlation of the intrapapillary morphometric data to visual field indices Graefe's Arch Clin Exp Ophthalmol 226:531-538, 1988
18. Stürmer J, Schaer-Stoller F, Gloor B: Papillenausmessung mit Planimetrie und "Optic Nerve Head Analyzer" bei Glaukom und Glaukomverdacht II. Korrelation der Resultate der beiden Methoden mit Veränderungen des Gesichtsfeldes untersueht mit dem automatischen Perimeter Octopus Klin Mbl Augenheilk 196:132-142, 1990
19. Airaksinen PJ, Drance SM, Douglas GR, Schulzer M, Wijsman K: Visual field and retinal nerve fiber layer comparisons in glaucoma Arch Ophthalmol 103:205-207, 1985
20 Caprioli J, Ortiz-Colberg R, Miller JM, Tressler C: Measurements of peripapillary nerve fiber layer contour in glaucoma. Am J Ophthalmol 108:404-413, 1989
21. Ederer F: Shall we count number of eyes or number of subjects? Arch Ophthalmol 89:1-2, 1973
22 Bebie H, Fankhauser F, Spahr J: Static perimetry: accuracy and fluctuation. Acta Ophthalmol 54:339-344, 1976
23. Brenton RS, Argus WA: Fluctuations on the Humphrey and Octopus perimeters Invest Ophthalmol Vis Sci 28:767-772, 1988
24. Nanba K, Schwartz B: Fluorescein angiographic defects of the optic disc in glaucomatous visual field loss Proceedings of the Fifth International Visual Field Symposium, Sacramento. Doc Ophthalmol Proc Ser 35:67-73, 1983

The correlation between retinal nerve fiber layer defect and visual field defect in glaucoma

Yoshio Yamazaki[1], Toshio Miyazawa[2] and Hiroaki Yamada[2]

Departments of Ophthalmology[1] and Industrial Technology[2], Nihon University, Tokyo, Japan

Abstract

Twenty eyes of 20 normal-tension glaucoma patients and 20 eyes of high-tension glaucoma patients matched for similar visual field defects had retinal nerve fiber layer (RNFL) analysis with a computerized digital image analysis system Patients with low-tension glaucoma showed more localized RNFL loss than diffuse loss when compared with high-tension glaucoma patients The results support the hypothesis that there may be different mechanisms of damage in glaucoma

Introduction

The association between elevated intraocular pressure and glaucoma is well known, however, the exact role of intraocular pressure in producing optic nerve damage is not clear. Although most glaucoma patients exhibit elevated intraocular pressure, there are many patients with typical glaucomatous damage with normal intraocular pressure. The occurrence of glaucomatous damage without elevated intraocular pressure raises the question in these patients of the mechanism of their damage. Differences in the pattern of visual field loss in patients with normal tension glaucoma (NTG) and high-tension glaucoma (HTG) have been observed by some investigators[1-3], whereas others have found no significant differences between the two groups[4-6].

Examination of the optic nerve for evidence of glaucomatous damage is an important aspect of the evaluation of all patients and is especially important in those at risk for glaucoma Histologic studies and clinical observations suggest that the optic nerve may undergo significant structural alteration in the retinal nerve fiber layer (RNFL) before visual field loss is manifest[7,8], and that RNFL changes correspond to visual field defects in terms of the depth and location[9]. If the pattern of RNFL loss is different in NTG and HTG, it would imply different mechanisms of optic nerve damage

Using updated computer technology, an attempt has been made to further sophisticate the microdensitometric analyses of RNFL in red-free fundus photographs[10] This computerized digital image analysis of RNFL provides a reproducible measurement of RNFL topography, and can correctly identify 95% of patients with glaucoma.

The purpose of this study is to determine the relationship between the qualitative evaluation of RNFL changes and retinal sensitivity measured with the Humphrey program 30-2 in NTG and HTG patients matched for similar visual field defects.

Material and methods

This study was performed on one randomly selected eye of 20 NTG patients and 20 HTG patients matched for visual field defects (NTG: MD= -8 3±6.8 dB, HTG: MD= -8.1±8.3 dB). The mean ages of the two groups were not statistically significantly different, but the individual

This study was supported by Grand-in-Aid for Scientific Research No 01771445, Ministry of Education and Culture, Japan.

Address for correspondence Yoshio Yamazaki, M D , Department of Ophthalmology, Nihon University, 30-1, Oyaguchikami-machi, Itabashi, Tokyo, 173, Japan

Perimetry Update 1990/91, pp. 23-26
Proceedings of the IXth International Perimetric Society Meeting,
Malmö, Sweden, June 17-20, 1990
edited by Richard P Mills and Anders Heijl

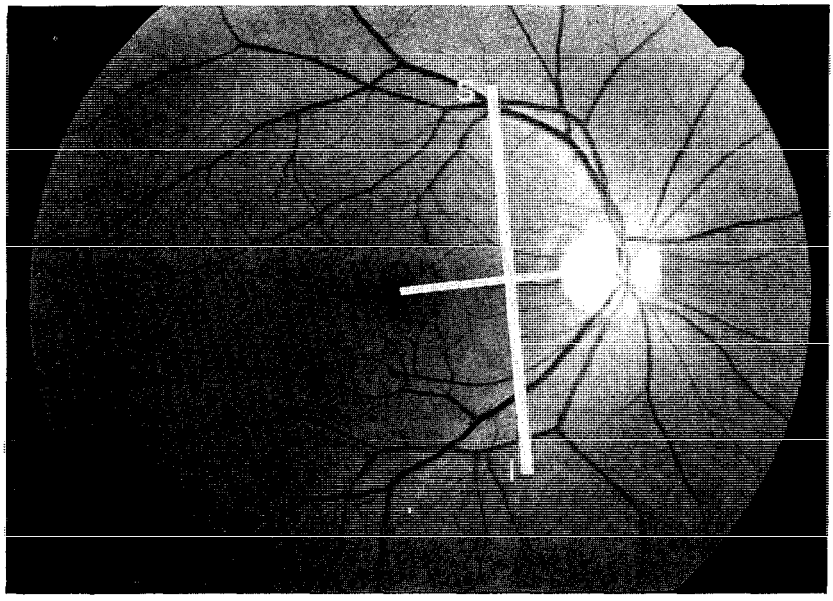

Fig 1 Example of red-free fundus photograph: S-I line shows a scanned line which perpendicularly bisected an imaginary line between disc and fovea for 30 degrees of visual angle S: superior 15 degrees on the scanned line; I: inferior 15 degrees on the scanned line

patients were not age-matched (NTG: 58.1±7.3 years, HTG: 58.9±5.8 years). All patients had visual acuity of 20/20 or better and no history of ophthalmic surgery. All of them had a visual field examination with program 30-2 on the Humphrey Field Analyzer and red-free RNFL photography with a 60-degree wide-angle fundus camera.

A system for computerized digital image analysis was used to acquire the original red-free fundus photographs. A detailed description of the analysis methods has been given previously[10]. The positives of red-free photographs were converted into the digital image, ready to be analyzed or stored on an optical disc recorder with a CCD camera and a digital image processor. The digital image processor stores the digital presentation of the red-free fundus photographs in an on-board memory with resolution of 500×375 picture elements for 60×45 degrees. The image intensity of RNFL was then computed into 256 levels along a scanned line which perpendicularly bisected an imaginary line between the disc and macula (fovea) and covering 30-degrees of visual angle (Fig 1).

Two parameters were calculated for the RNFL evaluation from each photograph. They were derived from the image intensities obtained along the scanned line. Fig 2 shows the mathematical formulas for calculating the two parameters. The intensity decrease is the arithmetic mean of the difference between actual measured intensity values and normal intensity values stored in the analysis system. It is sensitive to all kinds of diffuse RNFL loss. Zero means no intensity loss (seen in normals) and a positive number expresses directly the extent of RNFL loss. The intensity variance represents the local non-uniformity of the RNFL loss. It is small if the RNFL loss is more or less even. On the other hand, it is very large in the presence of deep RNFL loss.

All patients had their visual field examined with the Humphrey Field Analyzer using program 30-2. Using formulas adapted from Flammer[11], the visual field indices MD and CPSD were calculated.

Regression analyses were carried out correlating MD and CPSD with the intensity decrease and the intensity variance for the 20 NTG patients and 20 HTG patients. Statistical analysis was carried out with the Student's *t*-test.

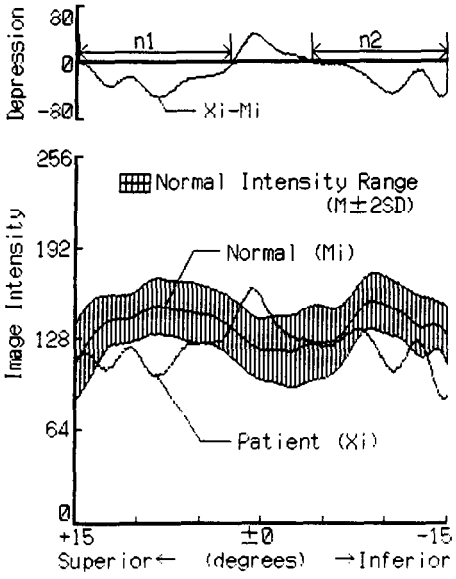

$$Di = Xi-Mi \quad \begin{cases} Xi-Mi <= 0 \\ Xi-Mi > 0 \end{cases}$$
$$= 0 \qquad \begin{cases} Xi-Mi <= 0 \\ Xi-Mi > 0 \end{cases}$$

$$ni = 1 \quad \begin{cases} Xi-Mi <= 0 \\ Xi-Mi > 0 \end{cases}$$
$$= 0 \qquad \begin{cases} Xi-Mi <= 0 \\ Xi-Mi > 0 \end{cases}$$

$$n = \sum ni$$
$$= n1+n2$$

Intensity Decrease (ID)

$$ID = \frac{\sum Di}{n}$$

Intensity Variance (IV)

$$IV = \sqrt{\frac{\sum (Di-ID)^2}{n-1}}$$

Fig. 2. Mathematical formulas for calculating the RNFL parameters: Xi is the actual image intensity of measured pixel; Mi is the age corrected mean normal intensity of that measured pixel; Di is the image intensity decrease in each pixel; n is the number of measured pixels which have image intensity decreases compared with the age corrected mean normal intensity The shaded zone is the 95th percentile confidence interval of the age-corrected normal subjects

Results

In the 40 eyes, the linear relationship between the intensity decrease and the intensity variance of RNFL analysis on the one hand, and MD and CPSD on the other was examined by the use of regression techniques. The linear regression of intensity decrease on MD index was statistically very significant (gamma= 0.407, $p<0.01$). The linear regression of intensity variance on CPSD index was also very significant (gamma 0.620, $p<0.005$).

The relationship between the intensity decrease and the intensity variance was examined to determine the pattern difference of RNFL loss in 20 NTG patients and 20 HTG patients. Both regression lines demonstrate good correlation coefficients and significance levels (NTG: gamma = 0.894, $p<0.005$; HTG: gamma = 0.723, $p<0.005$). When comparing the slope of regression lines of the intensity variance on the intensity decrease, the patients with NTG show a significantly larger slope than those with HTG ($p<0.05$).

Discussion

This study shows a statistically highly significant correlation between the neural structure of the retina as evaluated using the new parameters calculated from our computerized digital image analysis system and visual function measured with the visual field indices calculated with the Humphrey program 30-2.

The index which expressed the intensity decrease was related to diffuse retinal damage whereas the index expressing the intensity variance was related to the estimates of localized retinal damage. The RNFL evaluation which mathematically expressed structural alterations which attempted to distinguish between generalized and localized loss of RNFL were in excellent agreement with the quantitative assessment of generalized and localized visual functional changes in the retina.

In this study we analyzed the characteristics of RNFL loss in patients with NTG and HTG in whom the visual field defects were matched. A significantly larger slope of the intensity variance on the intensity decrease was found in the patients in the NTG group. RNFL loss

tended to be localized in the LTG group, while in the HTG group, RNFL loss was generalized. These findings support the hypothesis that different mechanisms may be responsible for optic nerve damage in NTG and HTG.

References

1. Levene RZ: Low tension glaucoma: a critical review and new material. Surv Ophthalmol 24:621-664, 1980
2. Anderton S, Hitchings RA: A comparative study of visual fields of patients with low-tension glaucoma and those with chronic simple glaucoma Doc Ophthalmol Proc Ser 35:97-99, 1983
3 Caprioli J, Spaeth GL: Comparison of visual field defects in the low-tension glaucomas with those in the high-tension glaucomas. Am J Ophthalmol 97:730-737, 1984
4. Phelps CD, Hayreh SS, Montague PR: Visual field in low-tension glaucoma, primary open-angle glaucoma, and anterior ischemic optic neuropathy Doc Ophthalmol Proc Ser 35:113-124, 1983
5 Motolko M, Drance SM, Douglas GR: The visual field defects of low-tension glaucoma Doc Ophthalmol Proc Ser 35:107-113, 1983
6 King D, Drance SM, Douglas GR et al: Comparison of visual field defects in normal-tension glaucoma and high-tension glaucoma. Am J Ophthalmol 101:204-207, 1986
7 Sommer A, Miller HR, Pollack I et al: The nerve fiber layer in the diagnosis of glaucoma Arch Ophthalmol 95:2149-2156, 1984
8. Quigley HA, Addicks EM, Green WR: Optic nerve damage in human glaucoma. III. Quantitative correlation of nerve fiber loss and visual field defect in glaucoma, ischemic neuropathy, papilledema, and toxic neuropathy Arch Ophthalmol 100:135-146, 1982
9. Iwata K: The earliest finding of POAG and the mode of progression In: Krieglstein GK (ed) Glaucoma Update II Berlin/Heidelberg/New York: Springer Verlag, 1983
10 Yamazaki Y, Miyazawa T, Yamada Y: Retinal nerve fiber layer analysis by a computerized digital image analysis system Jpn J Ophthalmol 34:173-180, 1990
11 Flammer J, Drance SM, Augustiny L et al: Quantification of glaucomatous visual field defects with automated perimetry. Invest Ophthalmol Vis Sci 26:176-181, 1985

Correlation of retinal nerve fiber layer loss, changes at the optic nerve head and various psychophysical criteria in glaucoma

Bernhard J. Lachenmayr[1], P. Juhani Airaksinen[2], Stephen M. Drance and Kees Wijsman

Department of Ophthalmology, University of British Columbia, Vancouver, BC, Canada

Abstract

In 61 eyes of 61 patients with glaucoma semi-quantitative assessment of retinal nerve fiber layer loss and neuroretinal rim measurement of the optic nerve head by means of the Optic Nerve Head Analyzer were correlated to the outcome of automated light-sense, flicker and resolution perimetry and FM 100-Hue test. A significant influence of age on total RNFL and total diffuse RNFL scores was found but there was no measurable effect of age on neuroretinal rim area Total RNFL score and total diffuse RNFL score show a good correlation to the various visual field indices: for total RNFL score *versus* mean flicker frequency in flicker perimetry r=-0 606, p<0 0001, *versus* mean sensitivity in light-sense perimetry r=-0 385, p=0.002, and *versus* mean ring score in resolution perimetry r=0.341, p=0 007. There is no significant correlation between RNFL scores and FM 100-Hue score Correlation between neuroretinal rim area and the various psychophysical indices is poor and mostly not statistically significant. The high correlation of flicker scores with retinal nerve fiber layer loss provides interest for future applications of this perimetric technique.

Introduction

Glaucomatous damage causes morphological changes at the optic nerve head, the retinal nerve fiber layer, and psychophysical deficits detected by perimetry or other functional tests. The question, however, of to what extent morphological changes correlate with functional deficits is controversial. There are quite a number of reports finding a moderate to fairly good correlation between optic disc parameters, such as the area of the neuroretinal rim, and visual field indices in light-sense perimetry[1-6], or between retinal fiber layer loss, assessed in a semi-quantitative way, and visual field indices[7,8] and color vision[9]. Other investigators, however, find only a poor or no correlation at all[10,11] All studies exploring the correlation between morphological changes and visual field damage hitherto have been restricted to static light-sense perimetry. In recent times more sophisticated perimetric techniques using complex temporal and/or spatial threshold criteria were developed[12-20]. Some of these methods seem to provide information about early functional glaucomatous damage[12-16,19,20] or are claimed to correlate to local retinal ganglion cell density[17,18].

The purpose of the present study was to provide a direct comparison of changes at the retinal fiber layer, the optic nerve head and functional deficits with light-sense perimetry, color vision and more complex perimetric techniques. We decided to use two perimetric methods, one tests a temporal threshold criterion, the automated flicker perimetry described by Lachenmayr[19,20], and the other tests a spatial threshold criterion, the resolution perimetry of Frisén[17,18]. Foveal color vision was tested with the Farnsworth-Munsell 100-Hue test. Assessment of retinal nerve fiber layer was achieved by the semi-quantitative scoring described by Airaksinen *et al* [21]. Morphometric analysis of the optic nerve head was done with the Optic Nerve Head Analyzer

This study was supported by the German Research Foundation Grant La517/2-1 (B J Lachenmayr), by the Sigrid Juselius Foundation (P J Airaksinen) and by the Medical Research Council of Canada Grant 1578 (S.M. Drance)

[1]*Present address/requests for reprints* Bernhard J Lachenmayr, M D , Ph D , University Eye Hospital, Mathildenstrasse 8, D-8000 Munich 2, Germany; [2]Department of Ophthalmology, University of Oulu, Finland.

Perimetry Update 1990/91, pp 27-34
Proceedings of the IXth International Perimetric Society Meeting,
Malmö, Sweden, June 17-20, 1990
edited by Richard P. Mills and Anders Heijl

ONHA (Rodenstock). The question of whether there is a correlation between retinal nerve fiber layer loss, morphometric disc parameters as calculated by the Optic Nerve Head Analyzer and functional changes detected by light-sense, flicker and resolution perimetry and color vision was studied. In addition the correlation between nerve fiber layer loss, neuroretinal rim changes and age was analyzed.

Material and methods

Patients

Sixty-one eyes of 61 patients with glaucoma were included in the present study. Thirty-three eyes had primary open angle glaucoma, 20 eyes had normal tension glaucoma and eight eyes had other types of glaucoma with currently or previously very high pressures (four eyes with pigmentary glaucoma, three with chronic angle closure glaucoma, one with secondary glaucoma due to heterochromic cyclitis). In all cases the diagnosis of glaucoma was established if there was either a visual field loss in light-sense perimetry and/or if there were glaucomatous disc changes. For this purpose all visual fields were classified in masked fashion into being normal, having a localized defect, having a diffuse loss or both a localized defect and diffuse loss using quantitative statistical criteria described elsewhere*. Forty-seven eyes had both disc and field changes, ten eyes had an abnormal disc with a normal field, four eyes had a field loss and normal discs. The patients were unselected but presented as they came, providing they were willing to participate in the study and they met the following selection criteria: best corrected visual acuity $\geq$ 6/9 (0.7); pupil diameter $\geq$ 2.0 mm; refractive error $\leq$ 6.5 dpt. sph. $\leq$ 3 dpt. cyl.; clear optical media; no relevant ocular pathology. One patient with secondary glaucoma due to heterochromic cyclitis was deliberately included because of the high intraocular pressures. The age distribution showed a minimum of 31 years, a maximum of 80 years, a mean of 59.6 $\pm$ 11.4 years and a median of 61 years. Retinal nerve fiber layer photography and morphometry of the optic nerve head with the Optic Nerve Head Analyzer ONHA (Rodenstock) were performed in all cases. All patients were tested with light-sense, flicker and resolution perimetry and the Farnsworth-Munsell 100-Hue test.

Retinal nerve fiber layer

The assessment of retinal nerve fiber layer loss was done according to the semi-quantitative scoring developed by Airaksinen *et al* and which is described elsewhere in detail[21,22]. The scoring was done by one of the authors (JPA) in completely masked fashion. For ten sectors (Nos. 1-10 in[21]) a score describing a localized nerve fiber layer loss and for six segments (A=1+2+3, B=4, C=5, D=6+7+8, E=9, F=10 in[21]) a score describing a diffuse nerve fiber layer loss were determined. A diffuse loss was also accepted when it was restricted to only one or several of these segments with other segments being normal; this is a modification of the original scoring technique[21]. From these data a total localized score, a total diffuse score and a total overall score were calculated. The total localized score is the sum of the localized scores in each of the ten sectors. The total diffuse score is the sum of the diffuse scores in each of the six segments taking into account that segments A and D comprise three sectors; if $D_{A\text{-}F}$ are the diffuse scores for the segments, the total diffuse score is thus calculated as follows: total diffuse score = $3\times D_A + D_B + D_C + 3\times D_D + D_E + D_F$. The total overall score is equal to the sum of the total localized score plus the total diffuse score.

Optic nerve head

For the morphometry of the optic nerve head the Optic Nerve Head Analyzer ONHA (Rodenstock)[23] was used. For the subsequent analysis the total disc area, the total rim area and the rim area of the temporal sector were used because the visual functions were estimated in the inner 30° of the visual field which corresponded to that part of the rim.

*Lachenmayr B et al: Diffuse and localized glaucomatous field loss in light-sense, flicker and resolution perimetry: evidence for pressure-induced damage. 1990 (submitted to Invest Ophthalmol Vis Sci)

Light-sense perimetry

Static light-sense perimetry was performed with a Humphrey Field Analyzer using program 30-2 testing 77 points (76 plus fovea) on a rectangular 6 degree-grid with a two-fold bracketing procedure. For each field a STATPAC single field analysis was performed.

Flicker perimetry

Flicker perimetry using critical flicker fusion frequency as threshold criterion was performed with a setup developed by Lachenmayr which is described elsewhere in detail[19,20]. The system examines 77 points with a two-fold bracketing procedure in the central 40°, 69 of the points are within 30°.

Resolution perimetry

Resolution perimetry was performed with the Ophthimus System according to Frisén using high-pass spatial frequency ring targets[17,18]. The standard program which was used for the present study examined 50 locations in the central 30° of the visual field.

Color vision

The Farnsworth-Munsell 100-Hue test was used for the assessment of central color vision.

For all three perimetric techniques mean sensitivities over the tested visual field area were calculated, *i.e.*, mean light difference sensitivity MS for the Humphrey Field Analyzer (HFA) in decibels (dB), mean flicker frequency MF in cycles/sec (cps) and mean ring score MR in decibels (dB).

Results

Total and total diffuse RNFL scores decrease significantly with increasing mean sensitivity MS of the Humphrey Field Analyzer (Fig. 1), whereas the total localized RNFL score is independent of MS (Table 1). The correlation between total RNFL score and the mean frequency MF of flicker perimetry is much better (Fig. 2) There is also a good correlation between total diffuse RNFL score and MF. The total localized RNFL score again is independent of MF (Table 1). For resolution perimetry the correlation between total RNFL score and mean ring score MR is shown in Fig. 3. The correlation is not as good as the correlation between total RNFL score

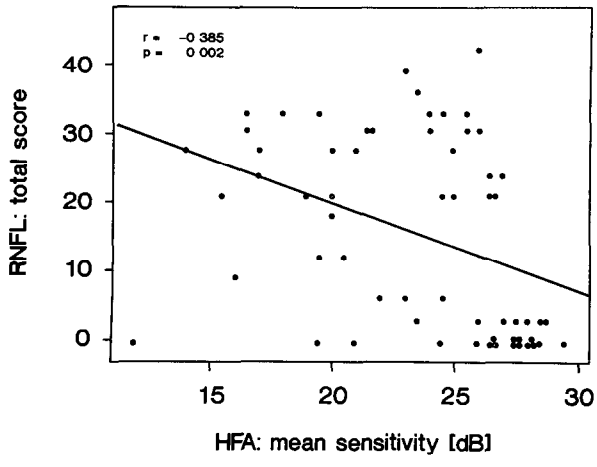

Fig 1 Linear regression of total RNFL score on mean sensitivity MS of the Humphrey Field Analyzer.

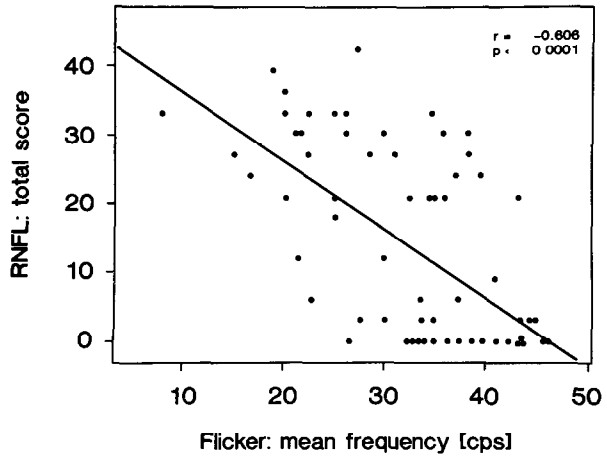

Fig 2 Linear regression of total RNFL score on mean flicker frequency MF in flicker perimetry

and MS but still statistically significant. There is also a significant increase of total diffuse and total localized RNFL scores with mean ring score (Table 1). The RNFL scores are not significantly correlated with the Farnsworth-Munsell 100-Hue score (Table 1). Limiting of the RNFL scores to the temporal 110°- and 40°-sectors does not provide a better correlation to the functional parameters, in the majority of instances the correlation coefficients tend to be smaller.

Correlation of total rim area with the various psychophysical parameters is poor and mostly not statistically significant (Table 2). The situation is similar when correlating temporal rim area and total disc area with the various functional parameters.

Total and total diffuse RNFL scores are independent from total rim area, whereas the total localized RNFL score decreases significantly with total rim area (Table 3). The situation is similar when limiting rim area to the temporal 90°-sector and the RNFL scores to the temporal 110°- (Table 3) and 40°-sectors as described above.

Total and total diffuse RNFL scores show a significant increase with age (Table 4). The total

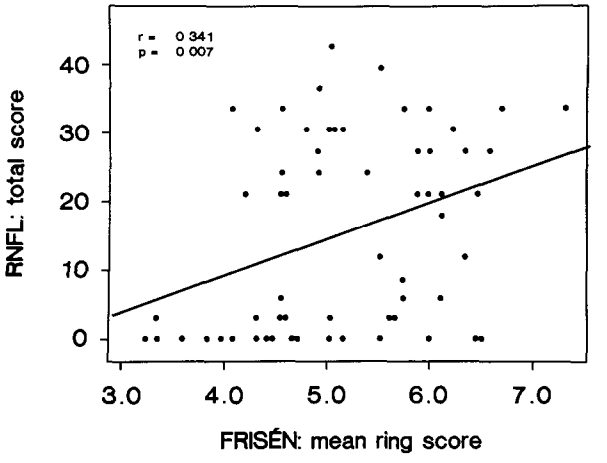

Fig 3 Linear regression of total RNFL score on mean ring score MR in resolution perimetry

Table 1 Regression of RNFL scores on functional parameters

	r	*p*
Total RNFL score/		
Mean sensitivity MS	–0 385	0.002
Mean frequency MF	–0.606	< 0.0001
Mean ring score MR	0 341	0.007
FM 100-Hue score	0.105	0 423
Total diffuse RNFL score/		
Mean sensitivity MS	–0 356	0.005
Mean frequency MF	–0.581	< 0 0001
Mean ring score MR	0 293	0.022
FM 100-Hue score	0 091	0.487
Total localized RNFL score/		
Mean sensitivity MS	–0.189	0.145
Mean frequency MF	–0.213	0.099
Mean ring score MR	0.260	0.043
FM 100-Hue score	0.077	0.557

Table 2 Regression of ONHA parameters on functional parameters

	r	*p*
Total rim area/		
Mean sensitivity MS	0 243	0.059
Mean frequency MF	0 137	0 293
Mean ring score MR	–0.255	0 048
FM 100-Hue score	–0.194	0.135
Temporal rim area/		
Mean sensitivity MS	0 225	0 081
Mean frequency MF	0.197	0.129
Mean ring score MR	–0 069	0 599
FM 100-Hue score	–0.134	0 303

Table 3 Regression of RNFL scores on ONHA parameters

	r	*p*
Total RNFL score/Total rim area	0 011	0 936
Total diffuse RNFL score/Total rim area	0 106	0.418
Total localized RNFL score/Total rim area	–0 389	0 002
Total RNFL score (110°)/Temporal rim area	–0 104	0 425
Total diffuse RNFL score (110°)/Temporal rim area	–0 077	0 556
Total localized RNFL score (110°)/Temporal rim area	–0.104	0.423

Table 4 Regression of RNFL scores and ONHA parameters on age

	r	*p*
Total RNFL score	0.365	0.004
Total diffuse RNFL score	0 390	0.002
Total localized RNFL score	–0.035	0 789
Total rim area	–0.052	0.692
Temporal rim area	–0 296	0.021
Total disc area	–0 063	0 629

localized RNFL score, however, is independent of age. There is no significant influence of age on total disc area and total rim area as calculated by the ONHA. The situation is quite similar when limiting the RNFL scores to the 110° temporal sector which includes the sector 55° above and below the connecting line between the center of the disc and of the fovea (this corresponds to the sectors 3+4+5+6 in[21]) or to the 40° temporal sector which includes the sector of 20° above and below the horizontal (this corresponds to the sectors 4+5 in[21]). The temporal rim area, namely the area of the neuroretinal rim calculated by the ONHA in a 90°-sector 45° above and below the connecting line between the center of the disc and the fovea, shows a small but significant decrease with age.

Discussion

For all three perimetric modalities we found a fairly good correlation between total RNFL score and total diffuse RNFL score and the mean visual field indices (mean sensitivity MS for HFA, mean flicker frequency MF for flicker perimetry and mean ring score MR for resolution perimetry). The flicker data show the best correlation, followed by light-sense perimetry and resolution perimetry. The fact that flicker perimetry in the present setup[19,20] is better related to the appearance of the retinal nerve fiber layer than light-sense or resolution perimetry provides interest for future applications of this perimetric technique. The correlation between total localized RNFL score and the various field indices, however, is poor and not significant in most cases. Our observation that there is no statistically significant correlation between the various ~L scores and the Farnsworth-Munsell 100-Hue score confirms previous results of Airaksinen and coworkers[9].

The correlation of total rim area and temporal rim area as calculated by the ONHA with the various functional parameters is poor and in most cases not statistically significant. Our data tend to support the reports which find a poor correlation between neuroretinal rim area and visual field indices[10,11]. A possible reason for this could be the fact that the ONHA calculates rim area automatically and defines the edge of the rim as a level 150 µm below retinal surface[23].

In this population total RNFL score and total diffuse RNFL score were not statistically related to total rim area and temporal rim area. These findings are contrary to the results published by Airaksinen and Drance[24] who found a good correlation between the diffuse RNFL score and the area of the neuroretinal rim (r=0.721, p=0.000) and between the localized RNFL score and the area of the neuroretinal rim (r=0.508, p=0.000). Possible reasons for this discrepancy are:

1. The definition of a diffuse retinal nerve fiber layer loss which they used was slightly different from that used in the present study. They accepted a diffuse loss only when such a loss was present in all ten sectors whereas in the present study a diffuse loss could be confined to only one or several of the six segments A to F.
2. The neuroretinal rim area in this study was derived from the calculations of the ONHA whereas in the study of Airaksinen and Drance[24] the borders of the rim were manually plotted and the measurement of the rim was made with a computerized planimeter.

The number of axons in the human optic nerve decreases with age. The presence of an age-related nerve fiber loss was demonstrated for normal human eyes[25,26] and is also to be expected in abnormal eyes, such as in our glaucoma study population. We found a significant increase of total RNFL score and total diffuse RNFL score with age, whereas the total localized RNFL score was unaffected by age. Part of this age-effect is probably due to the normal aging process. We did not find a statistically significant decrease of total neuroretinal rim area with age except for a slight decrease of the rim area in the temporal sector. This finding is consistent with the results of Funk *et al.*[27] and Britton *et al* [28].

The results of the present study suggest that further efforts in the development of automated analysis of morphological glaucomatous changes should be directed to the assessment of the retinal nerve fiber layer. This approach could provide the possibility to assess the age-related nerve fiber loss and to find a better correlation with functional deficits. Among the various psychophysical methods compared in the present study flicker perimetry showed the best correlation to the overall and diffuse nerve fiber loss. At the moment the reason for this is unclear. One possible explanation could be the fact that flicker thresholds are much more resistant to optical image degradation by such factors as slight media opacities or refractive defocus[19], than

threshold criteria using spatial information, such as in light-sense or resolution perimetry. In order to answer this question further research is necessary.

Acknowledgements

The authors are grateful to G R. Douglas, M.D. and F S Mikelberg, M D for providing part of the patients. We are especially grateful to S. Lalani, O D. and to all members of the staff for performing and arranging the examinations.

References

1. Airaksinen PJ, Drance SM, Douglas GR, Schulzer M: Neuroretinal rim area and visual field indices in glaucoma. Am J Ophthalmol 99:107-110, 1985
2. Balazsi AG, Drance SM, Schulzer M, Douglas GR: Neuroretinal rim area in suspected glaucoma and early open-angle glaucoma Arch Ophthalmol 102:1011-1014, 1984
3 Dannheim F: First experiences with the new Octopus G1-program in chronic simple glaucoma Doc Ophthalmol Proc Series 49:321-328, 1987
4. Drance SM, Airaksinen PJ, Price M, Schulzer M, Douglas GR, Tansley BW: The correlation of functional and structural measurements in glaucoma patients and normal subjects Am J Ophthalmol 102:612-616, 1986
5. Guthauser U, Flammer J, Niesel P: The relationship between the visual field and the optic nerve head in glaucomas. Graefe's Arch Clin Exp Ophthalmol 225:129-132, 1987
6. Jonas JB, Gusek GC, Naumann GOH: Optic disc morphometry in chronic open-angle glaucoma II Correlations of the intrapapillary parameters to visual field indices. Graefe's Arch Clin Exp Ophthalmol 226:531-538, 1988
7. Airaksinen PJ, Heijl A: Visual field and retinal nerve fiber layer in early glaucoma after optic disc haemorrhage. Acta Ophthalmol 61:186-194, 1983
8 Airaksinen PJ, Drance SM, Douglas GR, Schulzer M, Wijsman K: Visual field and retinal nerve fiber layer comparisons in glaucoma. Arch Ophthalmol 103:205-207, 1985
9. Airaksinen PJ, Lakowski R, Drance SM, Price M: Color vision and retinal nerve fiber layer in early glaucoma Am J Ophthalmol 101:208-213, 1986
10. Cloux-Fey U, Gloor B, Jäggi P, Hendrickson P: Papille und Gesichtsfeld beim Glaukom Klin Mbl Augenheilk 189:92-103, 1986
11 Dimitracos SA, Frey W, Gloor B, Jaeggi P: Correlation or non-correlation between glaucomatous field loss as determined by automated perimetry and changes in the surface of the optic disc? Doc Ophthalmol Proc Series 32:23-33, 1985
12 Drum B, Breton M, Massof R, Quigley H, Krupin T, Leight J, Mangat-Rai J, O'Leary D: Pattern discrimination perimetry: a new concept in visual field testing Doc Ophthalmol Proc Series 49:433-440, 1987
13. Drum B, Severns M, O'Leary D, Massof R, Quigley H, Breton M, Krupin T: Pattern discrimination and light detection test different types of glaucomatous damage In: Heijl A (ed) Perimetry Update 1988/1989. Proceedings of the International Perimetric Society Meeting Vancouver 1988, pp 341-347. Amsterdam/Berkeley/Milan: Kugler & Ghedini Publications 1989
14. Faubert J, Balazsi AG, Overbury O, Brussel EM: Multi-flash campimetry and other psychophysical tests in chronic open angle glaucoma. Doc Ophthalmol Proc Series 49:425-432, 1987
15. Faubert J, Balazsi AG, Muermans M, Brussel EM, Kasner OP: Multi-flash campimetry and optic nerve structure in early chronic open angle glaucoma. In: Heijl A (ed) Perimetry Update 1988/1989. Proceedings of the International Perimetric Society Meeting Vancouver 1988, pp 349-358. Amsterdam/Berkeley/Milan: Kugler & Ghedini Publications 1989
16. Fitzke PW, Poinoosawmy D, Nagasubramanian S, Hitchings RA: Peripheral displacement thresholds in glaucoma and ocular hypertension In: Heijl A (ed) Perimetry Update 1988/1989. Proceedings of the International Perimetric Society Meeting Vancouver 1988, pp 399-405. Amsterdam/Berkeley/Milan: Kugler & Ghedini Publications 1989
17. Frisén L: A computer-graphics visual field screener using high-pass spatial frequency resolution targets and multiple feedback devices Doc Ophthalmol Proc Series 49:441-446, 1987
18. Frisén L: High pass resolution perimetry. In: Heijl A (ed) Perimetry Update 1988/1989. Proceedings of the International Perimetric Society Meeting Vancouver 1988, pp 369-375 Amsterdam/Berkeley/Milan: Kugler & Ghedini Publications 1989
19. Lachenmayr B: Analyse der zeitlich-raumlichen Übertragungseigenschaften des visuellen Systems: Ein neuer Weg zur Frühdiagnose von Netzhaut- und Sehnerverkrankungen? Thesis (Habilitationsschrift) 1988

20. Lachenmayr B, Rothbacher H, Gleissner M: Automated flicker perimetry versus quantitative static perimetry in early glaucoma. In: Heijl A (ed) Perimetry Update 1988/1989. Proceedings of the International Perimetric Society Meeting Vancouver 1988, pp 361-368. Amsterdam/Berkeley/Milan: Kugler & Ghedini Publications 1989
21. Airaksinen P, Drance SM, Douglas GR, Mawson DK, Nieminen H: Diffuse and localized nerve fiber loss in glaucoma. Am J Ophthalmol 98:566-571, 1984
22. Mawson DK, Nieminen H: Retinal nerve fiber layer photography. J Ophthalm Photogr 8:8-10, 1985
23. Cornsweet TN, Hersh S, Humphries JC, Beesmer RJ, Cornsweet DW: Quantification of the shape and color of the optic nerve head. In: Breinin GM, Siegel IM (eds) Advances in Diagnostic Visual Optics, pp 141-149. New York: Springer 1983
24. Airaksinen PJ, Drance SM: Neuroretinal rim area and retinal nerve fiber layer in glaucoma. Arch Ophthalmol 103:203-204, 1985
25. Balazsi AG, Rootman J, Drance SM, Schulzer M, Douglas GR: The effect of age on the nerve fiber population of the human optic nerve. Am J Ophthalmol 97:760-766, 1984
26 Mikelberg FS, Drance SM, Schulzer M, Yidegiligne HM, Weis MM: The normal human optic nerve: axon count and axon diameter distribution. Ophthalmology 96:1325-1328, 1989
27 Funk J, Dieringer T, Grehn F: Correlation between neuroretinal rim area and age in normal subjects. Graefe's Arch Clin Exp Ophthalmol 227:544-548, 1989
28 Britton RJ, Drance SM, Schulzer M, Douglas GR, Mawson DK: The area of the neuroretinal rim of the optic nerve in normal eyes. Am J Ophthalmol 103:497-504, 1987

Comparison of optic disc image analysis with automated perimetry in the detection of glaucomatous progression

Mark B. Sherwood[1] and Steven T. Simmons[2]

[1]*University of Florida, Gainesville, Florida,* [2]*Albany Medical College, Albany, New York, USA*

Abstract

Eighty-eight eyes of 55 patients at two centers were followed with serial automated visual field examinations and Topcon simultaneous stereoscopic disc photographs for a mean of 12 months (range six to 24 months). Analysis of disc photographs was performed with the Imagenet "change program" using slide input. Standard parameters for visual field or disc progression were selected. Twenty-one percent of glaucomatous eyes showed progression in both field and disc, 49% were stable for both field and disc and 30% demonstrated a stable field but disc progression. In no case was visual field progression seen with stable disc topography. For those eyes with both visual field and disc change there was a 100% correlation between the area of topographic change in the disc and the area of progressive field loss. The predictive value of the change program was significantly better than standard generated disc indices (C/D ratio, neuroretinal rim area, cup volume) in the eyes with visual field progression Eleven glaucoma suspect eyes were examined. The visual fields remained within normal limits for age in all cases but 55% showed progressive disc change with the change program. This study suggests that the Imagenet change program may be helpful in early detection of glaucoma and in follow-up of glaucoma patients to determine progression, but much larger, longer term studies are needed to elucidate its exact clinical role Future improvements in image registration may decrease variability and increase accuracy of the change program

Introduction

Examination of the optic disc is one of the key elements for detection and following of patients with glaucoma. Recent advances in computerized image analysis have provided more objective quantitation of optic disc topography but significant variability still exists, largely associated with operator input[1-7] Attention has initially been focussed on reproducing human observer parameters, such as vertical and horizontal cup/disc ratio, rim area and cup volume. These parameters, however, suffer from being difficult to define because of the frequent vagueness of the cup margin and also are global indices of disc topography Localized areas of change can therefore be lost in the overall quantitation.

The Topcon Imagenet "change program" compares approximately 800 conjugate points on two topographical maps derived from stereometric image analysis of an optic disc It is therefore independent of user defined terms such as cup edge and theoretically, as it compares individual points, should be more sensitive to localized changes in disc topography, which might be associated with visual field progression. The purpose of this ongoing study is to compare the Imagenet change program with serial automated visual fields and to determine its possible role in the clinical detection of progressive optic nerve damage in patients with glaucoma.

Subjects and methods

Eighty-eight eyes of 55 patients at two centers have been enrolled in the study to date Exclusion criteria include patient inability to perform accurate automated visual fields or those subjects for whom at least fair quality disc photographs cannot be obtained, because of poor pupillary dilation or hazy media. Seventy-seven eyes of 44 patients had confirmed visual field defects consistent with glaucoma and 11 eyes of 11 patients were graded as glaucoma suspects,

This research was sponsored in part by grants from the Research to Prevent Blindness Foundation.

Perimetry Update 1990/91, pp. 35-38
Proceedings of the IXth International Perimetric Society Meeting,
Malmö, Sweden, June 17-20, 1990
edited by Richard P. Mills and Anders Heijl

having fields within normal limits for age at study entry. The patient demographics and diagnoses are shown in Table 1.

Table 1 Patient demographics and diagnoses

Mean age of patients	55 years
Race W:B	52:3
Sex M:F	32:23
Diagnosis	*Number of eyes*
Primary open angle glaucoma	65
Pigmentary glaucoma	9
Inflammatory glaucoma	2
Angle closure glaucoma	1
Glaucoma suspect	11

All patient were followed, for a minimum of six months (mean 12 months), with serial automated visual field using the Octopus G1 or 32 programs or the Humphrey 30-2, and with simultaneous stereo disc photographs using the Topcon Imagenet 100 System. A single visual field program was used for each individual. Indirect slide acquisition was employed for disc analysis throughout the study and a single, highly experienced, masked technician at each center registered each pair of images, by marking four identical points at the disc margin. The same registration points were used for the pairs of disc images at different dates. The slides of 11 patients (20%) were transferred between centers and repeat registration and analyses performed to determine inter-center result variability.

Standard criteria for progression were chosen to prevent observer bias. Visual field progression was defined as three or more adjacent points, excluding peripheral points, with 6 dB or greater depression. Progressive disc topographical change was defined as five or more adjacent points with a greater than 200 μm change[8] in the positive direction, using the Topcon Imagenet change program. If progression occurred in either the visual field or in disc topography, the quadrant or quadrants of progression were noted.

Results

With a mean of 12 months between examinations (range six to 24 months), 16 of 77 eyes of patients with glaucoma demonstrated progression in both field and disc topography, 37 eyes had stable field and disc parameters, and 24 eyes demonstrated a stable field but showed progressive disc change. In no case was there visual field progression with stable disc topography (see Table 2). For the 16 eyes with both visual field and disc change there was a 100% correlation between the area of topographical change in the disc and the area of progressive visual field loss.

Table 2 Comparison of progression in automated visual field and disc topography by Imagenet change program

	Percentage of eyes	
	Glaucoma group (77 eyes)	*Glaucoma suspect group (11 eyes)*
Progression in field and disc	21	0
Stable field and disc	49	45
Stable field – progression in disc	30	55
Progression in field – stable disc	0	0

None of the 11 glaucoma suspect eyes showed progression to visual field defect. However, six of these eyes (55%) demonstrated progressive disc topographical change by our parameters, despite retaining a normal field (Table 2). The mean baseline vertical cup/disc ratio was 0.66 for the glaucoma suspect group, using a cup drop of 120 μm for Imagenet analysis, compared

to 0.72 for eyes in the glaucoma group.

Comparison disc analyses of 8 of the 11 glaucoma and glaucoma suspect patient slides swapped between the two centers (73%) showed agreement regarding progression or stability of disc topography In one of the eight cases there was disagreement regarding the quadrant of worsening.

The predictive value of the standard Imagenet disc analysis indices (vertical and horizontal cup/disc ratio, neuroretinal rim area and cup volume) were examined for the 39 glaucomatous eyes which demonstrated progression with the Imagenet change program. Using a confidence interval of twice the coefficient of variability previously described by Varma *et al.*[4] for each of these parameters, 49% of eyes had one of the four indices above confidence interval and 21% had two or more of the indices suggesting progression. If the 16 eyes with demonstrated visual field progression alone are considered, then 44% had one and 6% two or more indices above confidence interval, respectively (Table 3).

Table 3. Predictive value of standard indices (vertical and horizontal cup/disc ratio, neural rim area, cup volume)

	Progressive field/ progressive disc change	*Stable field/ progressive disc change*
One of four indices above confidence interval (2×COV)	7/16 (44%)	12/23 (52%)
Two or more of four indices above confidence interval	1/16 (6%)	7/21 (30%)

Discussion

It has long been the hope of ophthalmologists to detect early glaucoma before any visual field loss occurs and to detect the most minimal signs of progression for those patients with established field loss. Disc quantitation has been helpful but because of wide variation and overlap of standard indices (such as cup/disc ratio, neuroretinal rim area and cup volume) between the normal population and patients with early glaucoma, single quantitative measurements of these parameters have proved disappointing in distinguishing normal from glaucomatous eyes[9-11].

It is well recognized that serial visual field examinations provide more useful information for the management of the individual patient with glaucoma than a single examination comparing that patient to age matched normals. Likewise, comparison of sequential retinal sensitivities at specific points in a visual field is more useful than an overall single mean index of sensitivity.

The Imagenet change program, like the delta change program of automated field analyzers, compares individual points, located in a grid pattern, from two examinations separated by time. Previous work[8] has shown that with a single trained observer marking the registration points, depth changes of 200 μm or greater in disc topography fall outside the 95% confidence interval. Using these parameters, this study demonstrated a 100% sensitivity for detecting progressive field change and further, there was correlation between the quadrant of disc topographical progression and the area of field worsening. Comparison with the standard indices of vertical and horizontal cup/disc ratio, neuroretinal rim area and cup volume show these to have a lower sensitivity for delineating those eyes with field change. The specificity of the change program is more difficult to determine. The mean follow-up in this study is relatively short and continued longitudinal review of the 24 glaucomatous eyes which demonstrated disc change but no visual field progression is needed to see if field loss will later occur.

It has been demonstrated histologically that considerable nerve fiber loss occurs in eyes with glaucoma before any visual field defect is detectable by perimetry[12]. Several clinical studies have also suggested that structural changes of the optic nerve head may precede perimetric abnormalities[13-15]. With a mean of 12 months' follow-up, six of our 11 glaucoma suspects showed localized areas of disc topographical change, although none progressed to visual field defect. There is no gold standard to detect change and it is impossible to say at this time whether the Imagenet change program is more sensitive to slight progression than routine automated

visual field examinations, or is merely recording artefact. Long-term follow-up of these and other patients is required to determine the clinical importance of disc analysis in general and the change program in particular in the early detection of glaucoma.

It is important to note that this study was performed with patients who had clear media and dilated well, which provided good quality photographs. A highly trained technician was available to register the images, which is critical to obtain low variability of the change program data. Future planned alterations in image registration may decrease the current need for highly accurate placement of points by the technician.

References

1. Mikelberg FS, Douglas GR, Schulzer M et al: Reliability of optic disc topographic measurements recorded with a video-ophthalmograph Am J Ophthalmol 98:98-102, 1984
2. Caprioli J, Klingbeil U, Sears M et al: Reproducibility of optic disc measurements with computerized analysis of stereoscopic video images Arch Ophthalmol 104:1035-1039, 1986
3 Shields MB, Martone JF, Shelton AR et al: Reproducibility of topographic measurements with the Optic Nerve Head Analyzer. Am J Ophthalmol 104:581-586 1987
4 Varma R, Steinmann WC, Spaeth GL et al: Variability in digital analysis of optic disc topography Graefe's Arch Clin Exp Ophthalmol 226:435-442, 1988
5 Bishop KI, Werner EB, Krupin T et al: Variability and reproducibility of optic disc topographic measurements with the Rodenstock optic nerve head analyzer Am J Ophthalmol 106:696-702, 1988
6. Dandona L, Quigley HA, Jampel HD: Reliability of optic nerve head topographic measurements with computerized image analysis Am J Ophthalmol 108:414-421, 1989
7. Kruse FE, Burk ROW, Volcker HE et al: Reproducibility of topographic measurements of the optic nerve head with laser tomographic scanning. Ophthalmology 96:1320-1324, 1989
8. Lim ES, Taylor S, Simmons ST: Variability of an optic disc change program Invest Ophthalmol Vis Sci (Suppl) 30:174, 1989
9. Balazsi GA, Drance SM. Schulzer M et al: Neuroretinal rim area in suspected glaucoma and early chronic open-angle glaucoma Arch Ophthalmol 102:1011-1014, 1984
10 Airaksinen PJ, Drance SM, Schulzer M: Neuroretinal rim area in early glaucoma Am J Ophthalmol 99:1-4, 1985
11 Caprioli J, Miller JM: Videographic measurements of optic nerve topography in glaucoma. Invest Ophthalmol Vis Sci 29:1294, 1988
12 Quigley HA, Addicks EM, Green WR: Optic nerve damage in human glaucoma III Quantitative correlation of nerve fiber loss and visual field defect in glaucoma ischemic neuropathy, papilledema and toxic neuropathy Arch Ophthalmol 100:135-146, 1982
13 Armaly MF: Cup/disc ratio in early open-angle glaucoma Doc Ophthalmol 26:526-533, 1969
14 Pederson JE, Anderson DR: The mode of progressive disk cupping in ocular hypertension and glaucoma Arch Ophthalmol 98:490-495, 1980
15 Caprioli J, Miller JM, Sears M: Quantitative evaluation of the optic nerve head in patients with unilateral visual field loss from primary open-angle glaucoma Ophthalmology 94:1484-1487, 1987

Computerized image analysis in the optic disc color changes with the progression of visual field defects in glaucoma

Miki Ito, Kazuaki Tetsumoto, Hiroyuki Miyazawa and Kuniyoshi Mizokami

Department of Ophthalmology, School of Medicine, Kobe University, 7-5-2, Kusunoki-cho, Chuo-ku, Kobe, 650 Japan

Abstract

The rim color changes in 20 eyes with glaucoma, eight eyes at an early stage and 12 eyes at a middle stage, with documented progression of visual field defects, were studied using the authors' modified computerized color analyzer. Optic disc photographs subdivided into 16 by 8 pixels were analyzed respectively in red, green, and blue components. The reproducibility of this system showed an 1.8% intraphotographic and a 1.9% interphotographic coefficient of variation The cup area to disc area ratios (C/D.A) were also measured The correlation among the changes in disc color, visual field and C/D A ratios was evaluated In two eyes at an early stage of glaucoma the rim color changed with the cup enlargement In four eyes at a middle stage of glaucoma the rim color also changed, in three eyes the cup also enlarged but in one eye there was no enlargement of the cup It is suggested that the rim color changes not only in the middle stage but also in the early stages of glaucoma

Introduction

In the diagnosis and management of glaucoma, the assessment of optic disc cupping and the disc rim color related to progression of visual field damage plays an important role. The relation between optic disc cupping and the progression of visual field defects has been quantitatively studied[1,2].

However, previous reports on rim color change were based chiefly on ophthalmoscopic findings. Therefore a quantitative analysis of the correlation between rim color changes and progression of visual field defects is desirable. In this study, a modified computerized color analyzer was used on optic disc photographs. Quantitative analysis of both the cup area to disc area ratio and disc rim color related to the progression of visual field defects in glaucoma was carried out.

Material and methods

Twenty eyes of primary open angle glaucoma (POAG) patients followed from two to five years were studied Visual fields were followed using the Octopus 201 program 31 All cases showed significant progression of visual field defects using program Delta The rim color in these 20 eyes (eight eyes with early damage, 12 eyes with moderate damage) was analyzed using the color analyzer.

Each optic disc photograph was entered into the computerized image analyzer (Toshiba TOSPIX-U) with a digital video camera (Sony XC-711). The color is composed of red, green, and blue components. The intensities of each component were measured with the analyzer. It is possible to subdivide the picture into as many as 256 by 256 pixels. In this study 16 by 8 (128 pixels) divisions were used and each color intensity was divided into 100 levels. The color changes in each pixel of the optic disc photograph were analyzed respectively in red, green, and blue components. To determine the reliability of the data, we analyzed one photograph five times and also five different photographs of the same eye. The intraphotographic and interphotographic coefficients of variation were 1.8% and 1.9%, respectively[3,4]. Digital counts of color intensity were superimposed on the original photograph. The intensity of the optic disc rim colors before and after the progression of visual field defects were evaluated. In addition the

Perimetry Update 1990/91, pp. 39-44
Proceedings of the IXth International Perimetric Society Meeting,
Malmö, Sweden, June 17-20, 1990
edited by Richard P. Mills and Anders Heijl

temporal upper and temporal lower disc sectors were each divided into two areas named F1 and F2 according to the retinal nerve fiber pathway (Fig. 1). The optic disc at F2 was analyzed in this study. The cup area/disc area ratio (C/D.A) was also measured and the correlation among the changes in color, visual field defects and C/D.A ratio was evaluated. Visual field defects were divided into two groups. Group 1 showed focal progressive damage. Group 2 showed generalized progressive damage.

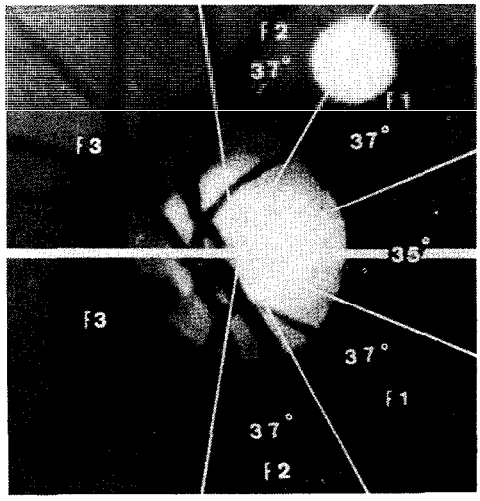

Fig 1 Division of optic disc according to the retinal nerve fiber pathway

Results

Table 1 Case 1: Octopus program delta

Program/date	*Summary A 31/09 11 84*	*Summary B 31/07 02 86*	*Difference (B min A)*
Total loss (whole field)	45	118	+73
Mean sensitivity			
Whole field	27.3	25.1	–2.2
Quad upper nasal	28 6	26 3	–2 3
lower nasal	23.7	18 9	–4 8
upper temporal	27 8	27 1	–0 8
lower temporal	28 7	27 0	–1 7
Confidence interval for mean difference/*t*-test			
1 Pathological area	–2.3±1.5 (*t*-test: alternation is indicated)		
2 Whole field	–2.2±0.7 (*t*-test: alternation is indicated)		

Case 1 was a 41-year-old man whose total loss of visual field sensitivity increased from 45 to 118 dB over two years. The sensitivity decreased focally, showing 2.3 dB depression in the upper nasal area and 4.8 dB depression in the lower nasal area respectively (Table 1). C/D.A at the temporal upper and lower disc increased by 5.4% and 4.9%. But the changes of the rim color could not be detected clearly by ophthalmoscopy. Fig 2 shows the analysis of the disc photographs before and after progression of the damage The intensity of the red component on the areas of the retinal vein, the upper temporal rim, and the lower temporal rim changed from 29, 58, 63 to 34, 66, 67, those of the green component from 14, 34, 38 to 18, 44, 45, and the blue component from 11, 18, 18 to 12, 22, 22. In order to reduce the influence of brightness in the photographs, the relative ratio of the intensity of the three components was calculated (total value of 1):

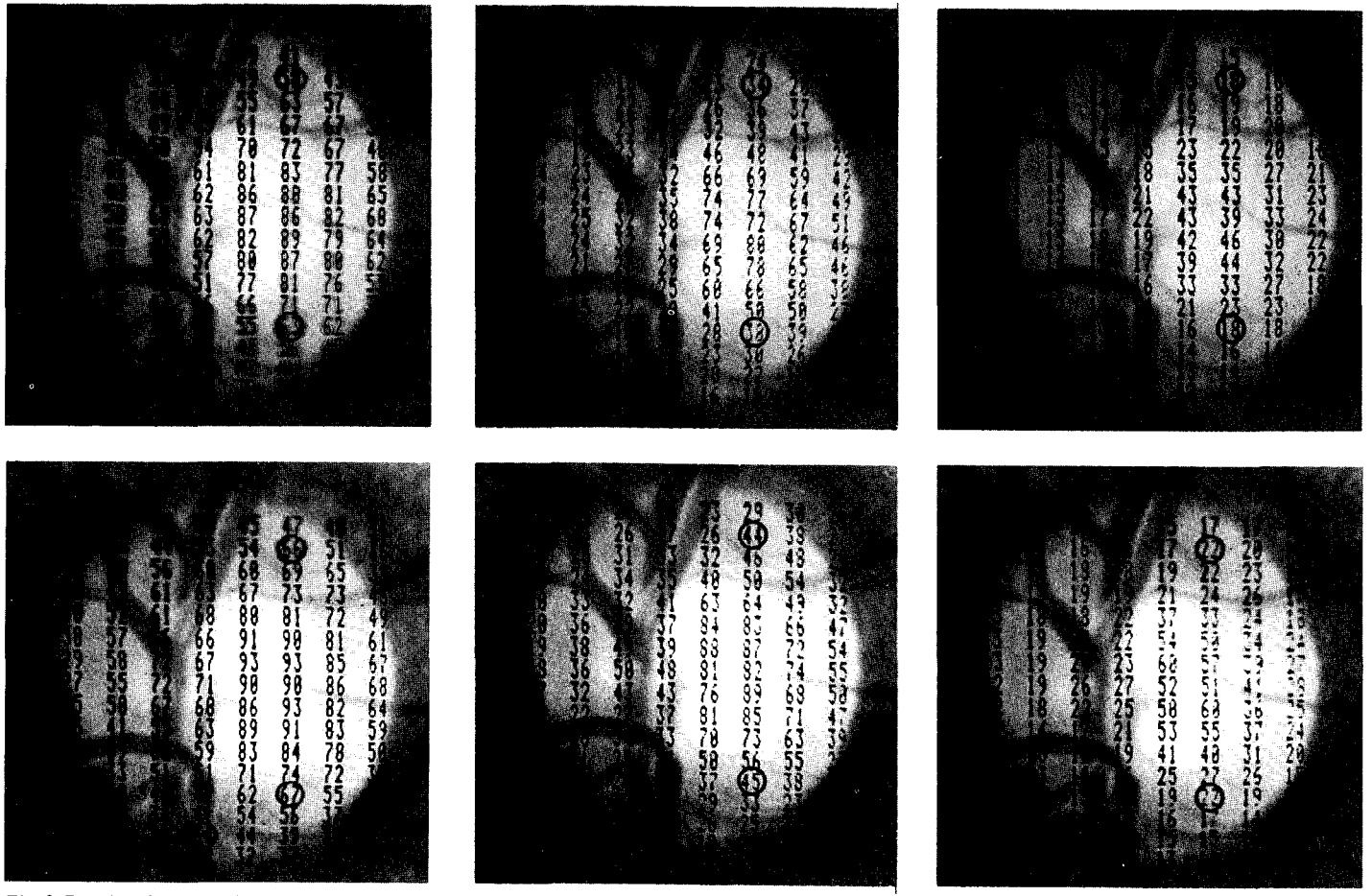

Fig. 2. Results of color analysis in case 1. Top: color intensities in red (left), green (middle), and blue components (right) before progression. Bottom: color intensities in red (left), green (middle), and blue components (right) after progression.

	Before progression			After progression		
	R	G	B	R	G	B
Vein	0 54	0.26	0 24	0.53	0.28	0 19
Temporal upper	0.53	0.31	0 16	0.50	0.33	0 17
Temporal lower	0.53	0 32	0 15	0.50	0 33	0 17

After this revision, the RGB ratio on the vein was unchanged, while the ratio was changed on upper and lower disc rim with progression of the damage. This result shows good reliability of the system. For the purpose of quantification of the color change, the change in the ratio of the red component (dR) was calculated as follows: dR=R2-R1/R1×100. R1 and R2 are the ratios of the red component before and after progression of visual field damage. In case 1 dR at the upper and lower temporal rim both decreased by -5.7%.

Table 2 Case 2: Octopus program delta

Program/date	*Summary A 31/08 31 84*	*Summary B 31/08 06 86*	*Difference (B min A)*
Total loss (whole field)	580	647	+73
Mean sensitivity			
Whole field	17 1	15 1	–2 0
Quad upper nasal	17 0	12 6	–4.4
lower nasal	13.2	13 7	+0.5
upper temporal	20 0	16 9	–3 1
lower temporal	20 3	20.0	–0 3
Confidence interval for mean difference/*t*-test			
1. Pathological area	–2 6±2 0 (*t*-test: alternation is indicated)		
2. Whole field	–2 1±1 1 (*t*-test: alternation is indicated)		

Case 2 was a 56-year-old man, whose total visual field loss increased from 580 to 647 dB over four years. The sensitivity of the upper nasal sector deteriorated by 4.4 dB, in spite of that the lower nasal sector improved by 0.5 dB, as shown in Table 2. C/D.A at the upper and lower temporal disc enlarged 1.3% and 5.8%, respectively. RGB relative ratios were as follows:

	Before progression			After progression		
	R	G	B	R	G	B
Vein	0.49	0 31	0 20	0.49	0 32	0 19
Temporal upper	0.48	0 35	0 17	0.47	0 34	0 18
Temporal lower	0.51	0 30	0 19	0.47	0 33	0 20

The RGB ratio on the retinal vein and upper temporal rim demonstrated no change, but the RGB ratio at the lower temporal rim changed. dR at this location was -7.8%. These results mean that the rim color corresponding to the damaged disc sector has changed.

The results of all cases are shown in Table 3. The values of dR on veins were within 2% in all cases. In eight eyes with under 100 dB total loss (seven eyes generalized and one focal), C/D.A showed enlargement of the optic disc cupping by 5.9+1.8%. dR showed relatively large values in two eyes, one of each type of field loss In twelve eyes with over 100 dB total loss (five generalized and seven focal), C/D.A increased, except for one eye. dR showed significant change in four eyes with focal defects.

Discussion

It is important to detect optic disc change objectively and quantitatively in both the early diagnosis and ongoing management of glaucoma. Previously it has been reported that C/D.A increases significantly, correlated with progression of visual field damage, especially in the early stage of the disease. By the time visual field defects were detectable by Goldmann perimetry, a 20% enlargement of the C/D.A had occurred. In the early stages of glaucoma, the disc cup enlarges without changes in rim color, whereas in the end stage of glaucoma the rim color becomes pale as the cup enlarges.

Table 3. Results of all cases

		dMS (dB)	*dC/D A*	*dR (rim)*	*dR (vein)*
Total loss <100					
General type	1	−1.2	3.2	−2 2	0 0
	2	−0 8	5.9	0 0	0 0
	3	−0.7	6 4	+2.0	+1 7
	4	−0 5	6 0	0.0	0 0
	5	−0 8	2 5	0 0	−1 9
	6	−1.4	7.0	−4 2	0 0
	7	−1.0	4.5	0 0	0.0
Local type	1	−4.8	4 9	−5 7	−1 8
Total loss ≥100					
General type	1	−0.8	3.7	0 0	0.0
	2	−2 7	3 7	0 0	0.0
	3	−1 5	3.0	−2 0	+1 7
	4	−1 6	2 7	−1 9	0 0
	5	−2 1	3 3	0 0	0 0
Local type	1	−3.0	7 3	−7 3	−1 9
	2	10.1	9.0	−11 6	0.0
	3	−2 6	5 8	−7.8	0 0
	4	−2 3	7 4	0.0	0 0
	5	−2.5	6.2	0 0	−1.8
	6	−5 1	7 1	0 0	0 0
	7	−4 4	0 7	−4 2	0 0

These reports were based on non-quantitative ophthalmoscopic examination. Recently, computerized image analysis of the optic nerve head has made quantitative analysis possible. For example, the optic nerve head analyzer (ONHA, Rodenstock), records the topography of optic disc with the help of a microcomputer which calculates the vertical cup-disc ratio, the vertical optic disc diameter, the cup volume and neuroretinal rim area. It has been reported that these parameters have good reproducibility[5-7]. It is also possible to measure the color density and generate a pallor map from separate recordings using red and green illuminations with ONHA, but its reproducibility has not been adequate[7].

We modified a commercially available computerized color analyzer. Disc cup enlargement and changes in disc rim color were correlated to the progression of visual field defects. The TV camera (Sony, XC-711) used in this study has an RGB digital signal output system. This system does not require a decoder circuit which is necessary to convert a composite video signal into an RGB digital signal. As a result, it can put more accurate image color density information into the computer. In the middle stages of glaucoma, the optic disc has a rather narrow neuroretinal rim associated with disc cup enlargement So in this study a relatively fine division, 16 by 8 pixels was employed. To evaluate color change the theory of the three primary colors was employed. To decrease the influences of uneven brightness in photographs due to opacity of the media and variabilities in the process of taking pictures, the RGB ratio was calculated as the relative intensity of red, green, and blue components whose sum was adjusted to 1.0. The color analysis thus became more reliable.

To evaluate the color change quantitatively, the changing rate of the ratio of the red component (dR) was calculated as a percentage in each case studied. The RGB intensities measured with this system were based on the RGB signal of the video camera, and so there are some differences between the color measured with this system and that which is usually viewed ophthalmoscopically. That is to say, even if the red ratio decreased, it is not possible to state that the rim became pale. It is only possible to say the rim color has changed.

The absolute values of dR in all cases were within 2%. This shows the good reliability of this system. On the other hand, the absolute value of dR over 2% can point to a significant color change. In eight eyes with early glaucoma (under 100 dB total visual field loss), two eyes showed dR change. These results suggest that even in the early stages of glaucoma with progression of visual field defects, neuroretinal rim color changes along with enlargement of the

disc cup. Four out of 12 eyes in the middle stages of glaucoma demonstrated changes of absolute values of dR. This quantitatively shows that the neuroretinal rim color often changes with the cup enlargement. In one eye the rim color density changed without enlargement of the cup. This suggests that in cases with severe visual field damage and enlargement of the cup, to some extent the rim color changes without any cup enlargement. Color changes in the rim area were detected more often in eyes with focal visual field defects than in those with generalized loss.

References

1 Okubo K, Mizokami K: Correlation between glaucomatous optic disc and visual field defects I. Early glaucomatous stage. Jpn J Clin Ophthalmol 37:607-612, 1983
2 Okubo K, Katsumori N, Mizokami K: Correlation between glaucomatous optic disc and visual field defects I Early glaucomatous stage. Acta Soc Ophthalmol Jpn 88:332-337, 1984
3 Miyazawa H et al: Digital analysis of optic disc with computerized color analyzer. Neuro-Ophthalmol Jpn 6:222-227, 1989
4. Tetsumoto K et al: Evaluation of glaucomatous disc by computerized digital color analyzer. Jpn J Clin Ophthalmol 43:1921-1924, 1989
5 Mikelberg FG, Douglas GR et al: Reliability of optic disc topographic record with a videoophthalmograph. Am J Ophthalmol 98:98-102, 1984
6 Caprioli J et al: Reproducibility of optic disc measurements with computerized analysis of stereoscopic video images Arch Ophthalmol 104:1035-1039, 1986
7 Shields MB: The feature of computerized image analysis in the management of glaucoma. Am J Ophthalmol 108:319-323, 1989

The predictive value of computerized visual field/disc pallor as an indicator of future glaucoma development

Erik Linnér[1], Bernard Schwartz[2] and Daniel Araujo[2]

[1]*University of Göteborg, Göteborg, Sweden,* [2]*Tufts University, Boston, MA, USA*

Abstract

In a prospective study of untreated ocular hypertension, 59 individuals were selected: 48 of them were non-exfoliative and 11 exfoliative One eye only from each individual was included in the study The initial values showed that the area of disc pallor was larger among those who developed glaucoma during the time of observation than among those who did not These main results indicate that a larger area of disc pallor may have a predictive value for future development of glaucoma.

Introduction

Ocular hypertension has an increased risk of developing glaucomatous lesions[1]. In a previous study the association between the changes in the optic disc and in the visual field in untreated ocular hypertensives with and without the exfoliation syndrome was reported[2].

In this study the same group of hypertensive individuals was used, and a comparison was made between those who developed glaucoma and those who did not during the time of observation. The purpose was to evaluate the predictive value for future glaucoma development of the disc and visual field parameters used in this study and to investigate the association between them. Pedersen and Anderson found that changes in the optic disc may precede changes in the visual field[3].

Material

In a long-term study of untreated ocular hypertension, 91 individuals were initially selected. They showed moderately elevated IOP, but no evidence of glaucomatous damage of visual field or of optic nerve head. The angle of the anterior chamber was open A slit-lamp examination after dilating the pupil was performed initially In this study 59 individuals were selected, in whom perimetry as well as optic disc photographs were performed serially over time Of these individuals 48 were non-exfoliative and 11 exfoliative. The time of observation was at least 1000 days and for the regression analysis with time (days) the number of examinations was at least four.

One eye only from each individual was included in the study. In 27 of the non-exfoliative individuals, both the right and the left eye could be used and in this group the right eye was selected. A comparison between the right and the left eye was carried out separately. The left eye was included only in those subjects in whom the right eye did not meet the criteria.

In subjects showing unilateral exfoliation syndrome the eye without exfoliation was excluded.

Supported in part (EL) by grants from the National Eye Institute, Bethesda, MD (RO1 EY 03035), from the Society "De Blindas Vänner" and from Volvo Medical Advisory Board, Göteborg, Sweden, and in part (BS) by a grant from Research to Prevent Blindness, Inc , New York, NY

Address for correspondence Erik Linnér, M D., Lilla Danska Vägen 6, S-412 74 Göteborg, Sweden

Perimetry Update 1990/91, pp 45-49
Proceedings of the IXth International Perimetric Society Meeting,
Malmö, Sweden, June 17-20, 1990
edited by Richard P. Mills and Anders Heijl

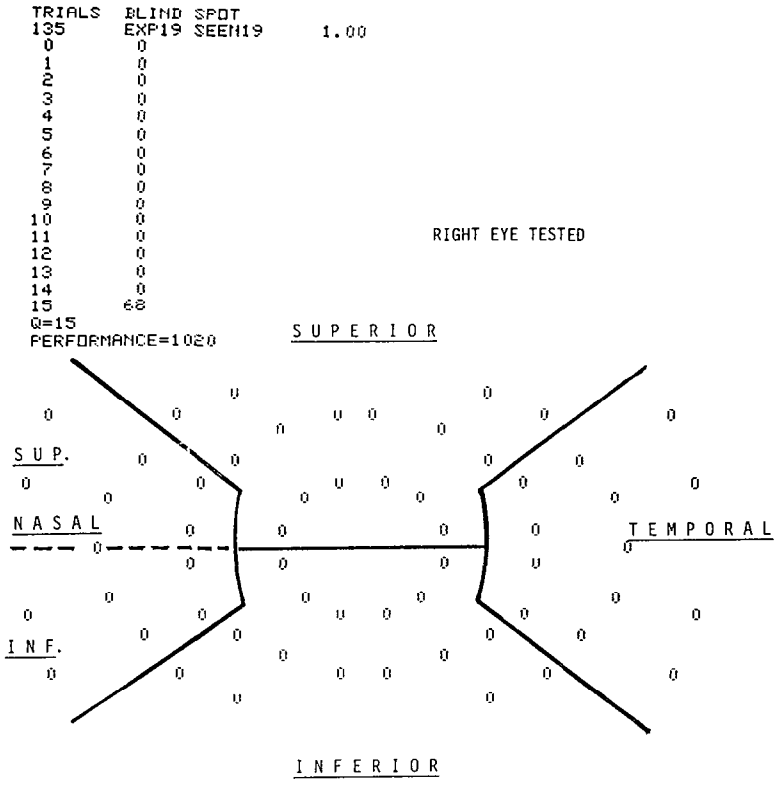

Fig 1 Competer: Automated, static perimeter[6]

Methods

Optic disc pallor was measured from disc photographs with the technique of computerized image analysis using multiple plan points Pallor was measured as percentage area of pallor, that is the ratio of the area of pallor to the area of the optic disc for the whole disc and for the superior, temporal, inferior and nasal quadrants The quadrants were delineated by means of a St. Andrew's Cross.

All photographs were of 35 mm size and taken with the standard Zeiss fundus camera and with the 2× lens converter. Pallor was measured by one individual (DA). The photographs were numbered and masked for patient's name, diagnosis, presence of exfoliation, ocular pressure, visual field results and time of photographs All photographs were measured in duplicate by an independent remeasurement. If for any pair of duplicates the percentage error was greater than 10%, these pairs of photographs were remeasured again in duplicate in a randomly masked manner[4,5].

The central visual field out to 20° was examined using an automated, static threshold perimeter called Competer[6]. The background illumination was 3.14 asb. The intensity of the test object could vary in 16 steps by a factor of 1:2, each step corresponding to approximately 3 dB from about 1000 to 0.03 asb Intensity level 0 denoted no response to maximum stimulus and 15 the highest retinal sensitivity. The circles of test points corresponded to 5°, 10°, 15° and 20° of eccentricity The visual field was divided into quadrants in the same way as the disc photographs. The temporal quadrant with the blind spot was not included in the analysis. The nasal quadrant was in addition divided into one upper and one lower part (Fig. 1).

The statistical analysis was carried out as a two-tail t-test between each parameter of the two groups separately without the use of any multiple test correction.

Results

Table 1 shows the basic characteristics of the initial observations for the patients without the exfoliation syndrome. One eye only per patient is selected. The patients are divided into one group without and another group with glaucoma development during the period of observation of at least 1000 days.

The nasal quadrant of the visual field shows significantly lower values in the glaucoma group. The percentage of disc pallor is significantly larger in the total disc as well as in all its quadrants of the glaucoma group.

Table 2 demonstrates no significant differences between 27 right eyes included in the main study (Table 1) and the left eyes from the same non-exfoliative individuals.

Table 3 shows the regression coefficients with time (days) for the patients without the exfoliation syndrome, in whom at least four observations exist. There are no significant differences between the group without and the group with glaucoma development.

Table 4 demonstrates the basic characteristics of the initial observations for the patients with the exfoliation syndrome. One eye only per patient is selected. The patients are divided into one group without and another group with glaucoma development during the period of observation of at least 1000 days. There are no significant differences between the group without and the group with glaucoma development.

Table 1 Characteristics of non-exfoliative OH-eyes (one eye/individual, preferably right eye)

	Glaucoma development		
	Negative (40) Mean ±SD	*Positive (8)* Mean ±SD	*Difference* p
Age	60 1± 8 42	60 3± 8 70	NS
Initial IOP	23.2± 2 31	23 8± 2 71	NS
Initial VF, total	10 9± 0 54	10 5± 0 72	NS
1. superior	11 0± 0 65	10 6± 0 81	NS
3 inferior	11 0± 0 55	10 6± 0 59	NS
4 nasal	10 7± 0 56	10 0± 0 97	<0.01
Difference 1-3	0 34± 0.30	0 34± 0 20	NS
Difference nasal superior/ nasal inferior	0.45± 0 30	0 75± 1 02	NS
Initial disc pallor total	19.9± 9 93	29 9±11 27	<0 05
1 superior	18 8±11 48	27 8±10 26	<0 05
2 temporal	27 9±15 40	41.2±18 52	<0 05
3 inferior	15 1± 8 69	22 2±13 61	<0.05
4 nasal	18 1±12 51	29 2±15 76	<0 05
Difference 1-3	7.0± 5.25	7 6± 7 29	NS

Table 2 Characteristics of non-exfoliative OH-eyes (pairs of right and left eyes from individuals without glaucoma development)

	Right eye (27) Mean ±SD	*Left eye (27)* Mean ±SD
Age	55 4± 8 82	55.4± 8 82
Initial IOP	23 3± 2 77	22.6± 2 44
Initial VF, total	10 9± 0 52	10 9± 0 45
1 superior	11 0± 0 62	11 0± 0.46
3. inferior	11 1± 0 51	11 0± 0 53
4 nasal	10 7± 0 53	10 7± 0 59
Difference 1-3	0 31± 0 32	0 31± 0 27
Difference nasal superior/ nasal inferior	0 39± 0 25	0 47± 0 55
Initial disc pallor total	18 0± 9.32	20 4±10 00
1. superior	17 6±11.30	17 4±11 83
2. temporal	27 3±17 03	30.9±15 20
3. inferior	12 4± 7 47	16.2± 8 30
4. nasal	14 8±11.21	18.0±10 97
Difference 1-3	7 7± 5 50	7 5± 6 07

Table 3. Regression coefficient with time, days (b) of non-exfoliative OH-eyes (one eye/individual, preferably right eye)

	Glaucoma development		
	Negative Mean ±SD b (×10⁻⁴)	*Positive Mean ±SD b (×10⁻⁴)*	*Difference p*
	(38)	(8)	
IOP	−8 91±21.55	5 54±25 42	NS
VF, total	−2 13± 2.71	−4 67± 7 61	NS
1 superior	−3 76± 3.41	−6 98± 8 97	NS
3 inferior	−0 65± 2.77	−2 15± 4 76	NS
4 nasal	−1 94± 4.39	−4 92±10 93	NS
Difference 1-3	1.12± 3.23	3 30± 5 64	NS
Difference nasal superior/ nasal inferior	0 58± 4 71	0 30± 5 18	NS
	(29)	(6)	
Disc pallor, total	1 30± 7 62	0.74±11.33	NS
1. superior	99 28±73 77	40.30±58.11	NS
2. temporal	−3 58±22 58	−5.03±28.94	NS
3. inferior	0 81±23 05	−18.50±40 44	NS
4. nasal	10 90±35 13	−11.69±47 21	NS
Difference 1-3	16 57±78.55	62 85±90 95	NS

Table 4 Characteristics of exfoliative OH-eyes (one eye/individual, preferably right eye)

	Glaucoma development		
	Negative (8) Mean ±SD	*Positive (3) Mean ±SD*	*Difference p*
Age	63 1± 6 60	63 3±12.74	NS
Initial IOP	22.4± 3.07	24 7± 5 03	NS
Initial VF, total	10.9± 0.43	10 6± 0.67	NS
1 superior	10.8± 0.71	10 6± 0 81	NS
3. inferior	11.2± 0 30	10 7± 0.81	NS
4 nasal	10.6± 0.50	10 5± 0 33	NS
Difference 1-3	0 42± 0.61	0 15± 0 14	NS
Difference nasal superior/ nasal inferior	0 65± 0.57	0 61± 0 51	NS
Initial disc pallor, total	31 2±16 00	27.1±15.63	NS
1 superior	29 7±18 78	27.6±15.95	NS
2 temporal	39 1±18 78	33.2±17.08	NS
3 inferior	25 7±13 68	19.9±14.06	NS
4 nasal	30 6±19 13	28.4±18.76	NS
Difference 1-3	6 4± 5 58	11.8± 7.00	NS

Table 5 shows the regression coefficients with time (days) for the patients with the exfoliation syndrome, in whom at least four observations exist. The nasal quadrant of the visual field shows a significantly lower value and the inferior quadrant of the disc shows a significantly larger percentage of pallor in the group developing glaucoma.

Discussion

The initial values in the non-exfoliative group showed a significantly larger percentage of disc pallor in the total area, as well as in the different quadrants, and lower perimetric values in the nasal quadrant among patients developing glaucoma than among the remaining group who did not.

In the exfoliative group the area of disc pallor was large as previously reported[2]. The initial values did not demonstrate significant differences between those patients who developed glaucoma and those who did not. The regression coefficients with time showed a lower perimetric value in the nasal quadrant and a higher disc pallor percentage in the inferior quadrant of those

Table 5 Regression coefficient with time, days (b) of exfoliative OH-eyes (one eye/individual, preferably right eye)

	Glaucoma development		
	Negative Mean ±SD b (×10⁻⁴)	*Positive Mean ±SD b (×10⁻⁴)*	*Difference p*
	(8)	(3)	
IOP	−3 45±28 94	−11.57±60 54	NS
VF, total	−3 07± 5 63	−17 32±17.95	NS
1. superior	−5.52± 4.40	−14 84±10 44	NS
3. inferior	−2 99± 5.28	−20.30±26 49	NS
4. nasal	−2.42± 2 95	−16 72±17.09	<0.05
Difference 1-3	2.61± 2.56	8 68±12.24	NS
Difference nasal superior/ nasal inferior	−0 37± 1.57	4.27± 6.10	NS
	(7)	(3)	
Disc pallor, total	5 51± 8.61	27.98±37 74	NS
1. superior	7.88±19 89	46.82±84.10	NS
2 temporal	−3.43±19 27	−20 26±19 19	NS
3. inferior	4.25±21.81	56.61±45 62	<0 05
4 .nasal	6 87±13 53	22 66± 5.67	NS
Difference 1-3	4.11±30.91	35 45±38 61	NS

who developed glaucoma. A similar but not significant trend was found in the non-exfoliative group, where the percentage of disc pallor in the inferior quadrant was higher among those developing glaucoma.

Tomita *et al* reported a significantly larger cupping and pallor in the inferior quadrant of a glaucoma group, as compared to a group of patients showing glaucoma-like discs[7].

The number of exfoliative patients in our study was small and does not warrant further conclusions. Our main results show that a larger area of disc pallor might have a predictive value for future development of glaucoma in a group of non-exfoliative, ocular hypertensive subjects. There is, however, a large variability, which limits our ability to predict accurately in an individual patient.

Comparative studies of the optic disc and of the visual field with the use of different analysis techniques will be of great interest.

Acknowledgement

The computer and statistical work (EL) was carried out by Axel Linnér, Grafax Data AB and by Göteborgs Datacentral, Göteborg, Sweden

References

1 Lundberg L, Wettrell K, Linner E: Ocular hypertension Acta Ophthalmol 65:705-708, 1987
2 Linnér E, Schwartz B, Araujo D: Optic disc pallor and visual field defect in exfoliative and non-exfoliative, untreated ocular hypertension Int Ophthalmol 13:21-24, 1989
3 Pedersen JE, Andersen DR: The mode of progressive disc cupping in ocular hypertension and glaucoma Arch Ophthalmol 98:490-495, 1980
4 Nagin P, Schwartz B: Detection of increased pallor over time using computerized image analysis in untreated ocular hypertension. Ophthalmology 92:252-261, 1985
5 Nagin P, Schwartz B, Namba K: The reproducibility of computerized boundary analysis for measuring optic disc pallor in the normal disc Ophthalmology 92:243-251, 1985
6 Heijl A, Krakau CET: An automatic perimeter for glaucoma visual field screening and control: construction and clinical cases. Graefe's Arch Clin Exp Ophthalmol 197:13-23, 1975
7. Tomita G, Takamoto T, Schwartz B: Glaucoma-like disks without increased intraocular pressure or visual field loss Am J Ophthalmol 108:496-504, 1989
8. Quigley HA, Hohmann RM, Addicks EM, Green WR: Blood vessels of the glaucomatous optic disc in experimental primate and human eyes Invest Ophthalmol Vis Sci 25:918-931, 1984

Relationship between optic disc damage and visual field defects in glaucoma

Katsuhiko Nanba, Kazuo Iwata and Kyoko Nagata

Department of Ophthalmology, Niigata University School of Medicine, Asahimachidori-1, Niigata City, Japan 951

Abstract

Quantitative optic disc measurements were performed by computerized image analysis for rim area, cup area, cup volume and cup-disc ratio of 35 asymmetric glaucoma patients who showed normal rim area and normal visual field, as determined by Humphrey program 30-2 in one eye. There was a significant correlation between differences in cup area and cup volume and difference in mean deviation. The difference in rim area showed a borderline significant correlation to mean deviation. These results may indicate that optic disc changes precede visual field defects up to a loss of 0.37 mm^2 in rim area, 0 38 mm^2 in cup area and 0.16 mm^2 in cup volume.

Introduction

A number of studies confirm that changes in the optic disc usually precede visual field changes in early glaucoma[1-3]. With computerized image analysis, quantitative optic disc measurements can be performed for optic disc parameters such as rim area, cup area and cup volume. Automated static perimetry can provide quantitative measurements of visual field. Optic disc parameters were found not to be constant but to be correlated with disc size in normal eyes[4,5]. Their wide range of values showed large overlaps with those of glaucomatous eyes[6,7]. Although a significant correlation was reported between optic disc parameters and statistical indices of automated perimetry in glaucoma, wide distributions of these parameters were observed[8,9]. To estimate how quantitatively measured optic disc changes can precede visual field defects, we studied the relationship between the difference in optic disc parameters and visual field parameters of both eyes of patients with glaucoma.

Material and methods

Patients with chronic open-angle glaucoma were selected who satisfied the following criteria:

1. optic discs of both eyes of each patient were almost the same size;
2. one eye of each patient had normal rim area related to the disc area without glaucomatous visual field defect;
3. the other eye showed damage in the optic disc and visual field;
4. the difference in refractive error between both eyes was within 2.0 diopters.

Thirty-five patients were analyzed; 18 patients were male and 17 were female. The age distribution was between 17 and 69 years (average 42.8 years). Twenty-three cases had POAG, nine cases juvenile glaucoma, two cases unilateral secondary OAG and one case unilateral capsular glaucoma. Seven patients were not on medical treatment. Three patients used pilocarpine for one eye only. Other patients used pilocarpine, beta-blockers, epinephrine, or combinations of them in both eyes.

Optic disc measurements were performed by computerized image analysis (Rodenstock Optic Nerve Head Analyzer) for rim area, cup area, cup volume and cup-disc ratio. The margin

This study was supported by a Grant-in-Aid for General Scientific Research (A) from the Ministry of Education, Science and Culture.

Perimetry Update 1990/91, pp. 51-55
Proceedings of the IXth International Perimetric Society Meeting,
Malmö, Sweden, June 17-20, 1990
edited by Richard P. Mills and Anders Heijl

of the cup was defined by the points which lie 150 μm below the retinal surface of the disc edge. Refraction keratometry and axial length measurements were used for magnification-correction of optic disc parameters. In this study, parameters for the total disc were used.

Visual fields were examined by automated perimetry (STATPAC program 30-2 on a Humphrey Visual Field Analyzer). Mean deviation was used as a statistical index. Computerized image analysis of the optic disc and automated perimetry were performed within a month of each other.

Differences in mean deviation and in optic disc parameters between the two eyes of each patient were calculated. The difference in mean deviation was shown as a negative number. The difference in optic disc parameters was presented as a positive number if rim area was larger and other parameters were smaller in the eye without visual field defect compared to those in the other eye.

To compare the difference in optic disc parameters in glaucoma patients, 21 ocular hypertensives with optic disc area of almost the same size in both eyes were measured by computerized image analysis. For statistical analyses, a Student's *t*-test was used. Linear regression analysis was used for the correlation coefficient. A p level of ≤ 0.05 was chosen as significant.

Results

The data for the optic disc parameters and visual field parameters are given in Table 1. There were no significant differences in pupil diameter, refractive error, axial length or disc area between the two eyes. The difference in disc area between the eyes was 0.19±0.14 mm^2. Eighty percent of the patients had a larger optic disc in the eyes with a visual field defect than in the eyes without a visual field defect. In three patients, rim area was larger in eyes with a visual field defect than in eyes without a visual field defect. One patient showed larger cup area, cup volume and cup-disc ratio in the eye without a visual field defect than in the eye with visual field abnormality.

Table 1 Data for optic disc parameters and visual field parameters of 35 patients (mean ±standard deviation)

Parameter	*Eye without visual field defect*	*Eye with visual field defect*
Optic disc parameters		
Disc area (mm^2)	2.22±0.34	2.28±0.36
Rim area (mm^2)	1.27±0.32	0 81±0 30
Cup area (mm^2)	0.95±0.43	1 48±0.47
Cup volume (mm^3)	0 37±0 19	0.60±0 24
Cup-disc ratio	0 54±0 22	0.74±0.17
Visual field parameters		
Pupil diameter (mm)	3.00±0.80	3.10±0.70
Refraction (diopters)	−1.00±2.75	−1 12±2.61
Axial length (mm)	23.33±1 33	23.64±1.28
Mean deviation (dB)	−1.45±2.11	−10.91±9.00

In eyes with a visual field defect, a significant correlation was found between cup volume and mean deviation (r=0.35). There was a borderline significant correlation between cup area and mean deviation (r=0.34) and between rim area and mean deviation (r=-0.33). No significant correlation was found between cup-disc ratio and mean deviation (r=0.25).

A borderline significant relationship was found between difference in rim area and difference in mean deviation. Linear regression analysis showed a regression equation of $y=0.011x+0.37$ (Fig. 1). There was a significant correlation between the difference in cup area and the difference in mean deviation. A regression equation was obtained of $y=0.017x+0.38$ (r=0.45) (Fig. 2). The difference in cup volume showed a significant correlation to the difference in mean deviation. The regression equation was $y=0.008x+0.16$ (r=0.44) (Fig. 3). No significant correlation was observed between the difference in cup-disc ratio and the difference in mean deviation. The regression equation was $y=0.004x+0.17$ (r=0.21) (Fig. 4).

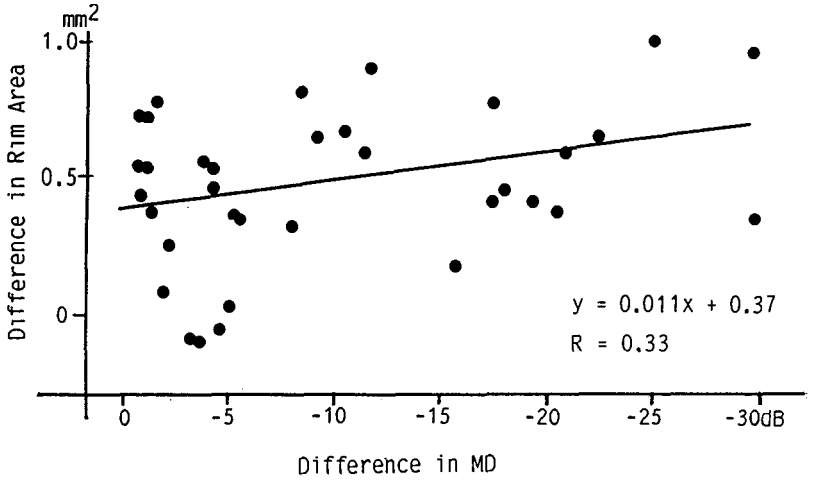

Fig 1 Scatterplot diagram of values of difference in rim area between the eyes of each of 35 patients to values of difference in mean deviation between the eyes of each patient.

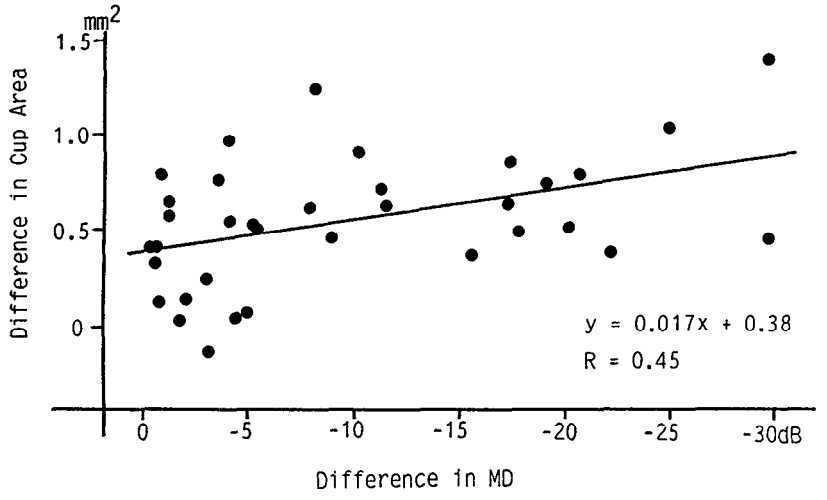

Fig. 2. Scatterplot diagram of values of difference in cup area between the eyes of each of 35 patients to values of difference in mean deviation between the eyes of each patient.

The ocular hypertensive patients showed a rim area difference of 0.31±0.17 mm^2 (mean ±SD) between the two eyes, the cup area difference was 0.31±0.19 mm^2, the cup volume difference was 0.16±0.11 mm^2, and the cup-disc ratio difference was 0.12±0.08.

Comment

We found significant correlations between the difference in optic disc cup area and cup volume and the difference in mean deviation of the visual field, and a borderline significant correlation between the difference in rim area and the difference in mean deviation. Linear regression analysis suggests that optic disc changes may precede visual field loss. For the optic disc parameters, we can estimate that cup area may increase by 0.38 mm^2, rim area may decrease by 0.37 mm^2, and cup volume may increase by 0.16 mm^2, before visual field abnormality is detected by automated perimetry. The values of difference in optic disc parameters

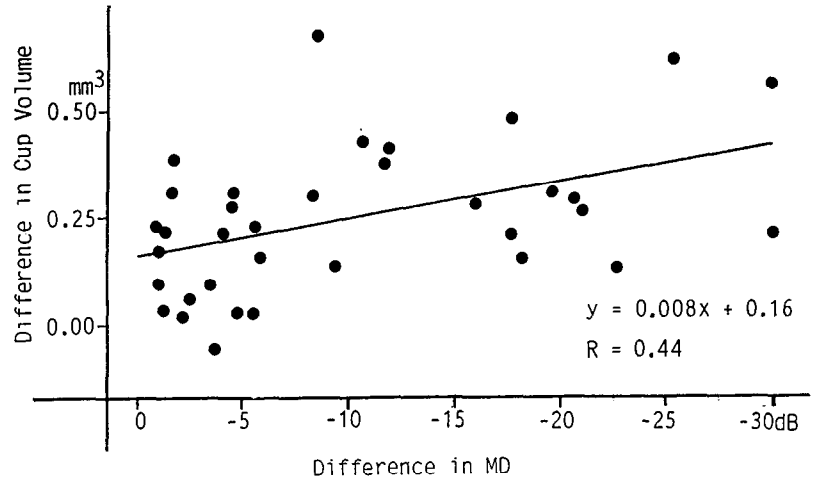

Fig 3 Scatterplot diagram of values of difference in cup volume between the eyes of each of 35 patients to values in mean deviation between the eyes of each patient.

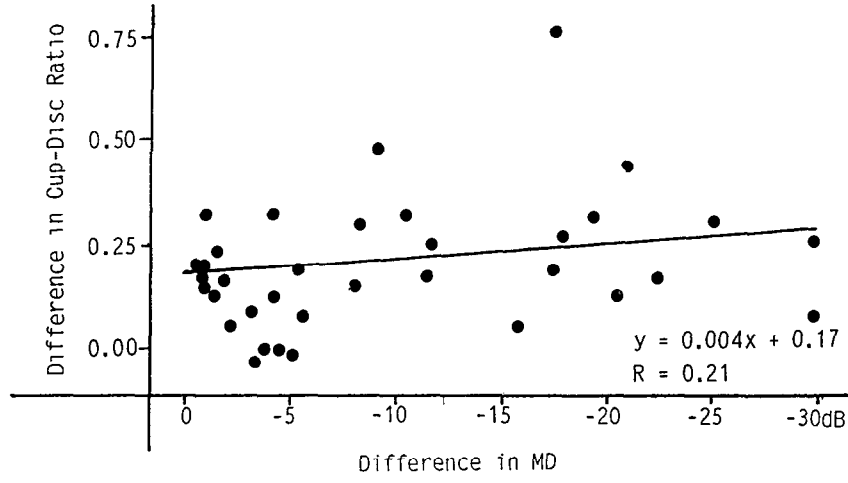

Fig 4 Scatterplot diagram of values of difference in cup-disc ratio between the eyes of each of 35 patients to values of difference in mean deviation between the eyes of each patient.

in ocular hypertensives approach these estimates. To confirm this, we compared these values with the difference in optic disc parameters between normals and patients with early glaucoma[7]. Between these two groups, rim area was 0.55 mm^2 different, cup area was 0.62 mm^2 different, and cup volume 0.26 mm^2. The values of difference in optic disc parameters between normals and early glaucoma patients are larger than those observed in this study. In this study, 91% of patients had at some time an IOP higher than 21 mmHg in both eyes, although one eye of each patient showed a rim area within normal limits and a normal visual field. It is possible that optic disc damage had occurred in the eye with normal rim area. For this reason, the differences between normals and glaucoma patients seem to be larger than the values obtained in this study.

There was still a wide scatter of values of difference in optic disc parameters plotted against the values of difference in mean deviation. One of the main causes of this wide distribution of the values may be based on the fact that we included only the data from the central 30 degrees of the visual field, while optic disc parameters covered the entire disc. Another possible cause

is that the optic disc of the eye without visual field defect may actually have been damaged. Further study will be necessary to evaluate more accurately values of optic disc parameters, which were affected at a time before visual field defects could be detected.

References

1. Armaly MF: The correlation between appearance of the optic cup and visual function. Trans Am Acad Ophthalmol Otolaryngol 73:898-913, 1969
2. Read RM, Spaeth GL: The practical clinical appraisal of the optic disc in glaucoma: the natural history of cup progression and some specific disc-field correlations Trans Am Acad Ophthalmol Otolaryngol 78:255-274, 1974
3. Hart WM, Yablonski M, Kass MA et al: Quantitative visual field and optic disc correlates early in glaucoma. Arch Ophthalmol 96:2209-2211, 1978
4. Caprioli J, Miller MJ: Optic disc rim is related to disc size in normal subjects. Arch Ophthalmol 105:1683-1685, 1987
5 Nanba K, Iwata K: Optic disc measurements in normal subjects by computerized image analysis. Acta Soc Ophthalmol Jpn 92:1889-1895, 1988
6. Caprioli J, Miller MJ: Videographic measurements of optic nerve topography in glaucoma. Invest Ophthalmol Vis Sci 29:1294-1298, 1988
7 Nanba K, Iwata K: Optic disc measurements by computerized image analysis: the difference between normals, ocular hypertensives and early glaucomas Acta Soc Ophthalmol Jpn (in press)
8. Caprioli J, Miller MJ: Correlation of structure and function in glaucoma: quantitative measurements of disc and field Ophthalmology 95:723-727, 1988
9 Matsubara K, Yamada T, Shirai H et al: Correlation of visual field changes and optic disc measurements with computerized videographic image analyzer in glaucoma. Acta Soc Ophthalmol Jpn 92:1414-1418, 1988

Long-term effect of reduction of intraocular pressure on reversal of glaucomatous optic disc cupping

Keiko Matsubara, Goji Tomita and Yoshiaki Kitazawa

Department of Ophthalmology, Gifu University School of Medicine, 40 Tsukasa-Machi, Gifu 500, Japan

Abstract

The authors prospectively studied topographic changes induced by intraocular pressure (IOP) reduction in 14 primary open-angle glaucoma eyes after trabeculectomy. Topographic parameters including cup-disc ratio, rim area, and cup volume were determined by the Optic Nerve Head Analyzer (Rodenstock) before, and three or six months and one year after surgery The 30-2 central threshold field was obtained with a Humphrey Field Analyzer at the same time. The authors evaluated the value of the mean deviation and total deviation as indices of visual field changes. Significant improvement of cup parameters were noted one year after surgery with significant IOP reduction (24.2±5.5 mmHg *versus* 12.2±3.6 mmHg). Significant improvement of the absolute value of the mean deviation was also observed one year post-surgery (18.7±9.5 dB *versus* 16.6±10.8 dB). There was significant negative correlation between the preoperative mean deviation and the percentage change of the mean deviation one year post-surgery (r=-0 80, $p<0.01$) The authors' results seem to suggest that lasting cup reversal induced by IOP reduction might lead to the improvement of visual function in early stage glaucoma.

Introduction

The reversal of the glaucomatous optic disc cupping associated with intraocular pressure (IOP) reduction has been well described in young and adult patients with glaucoma since Von Graefe's first description in the Nineteenth Century[1-11].

However, most studies relied on subject evaluation of the optic disc only. Recent development of computerized image analysis systems and automated perimetry has enabled the quantitative estimation of the amount of changes in the optic disc and visual fields. This has led to some prospective studies which aimed at quantitatively investigating the reversal of optic disc cupping following IOP reduction in adults with chronic open-angle glaucoma[12,13]. However, all previous studies addressed a rather acute effect of IOP reduction on the topographic features of the disc and visual field. Hence, it still remains to be clarified whether or not this phenomenon is directly associated with the improvement of visual function in the long run. Furthermore, whether reversal of cupping brought about by the prolonged IOP reduction persists over a long period still remains to be elucidated. We prospectively studied the topographic changes of optic discs and the visual field changes of primary open-angle glaucoma (POAG) eyes after trabeculectomy over one year, in an effort to clarify the long-term effect of IOP reduction on glaucomatous optic disc cupping and visual field defects.

Patients and methods

Fourteen eyes of nine patients with POAG were enrolled in the study. The patients underwent trabeculectomy because of elevated IOP despite maximum tolerable medication. They were followed up at the Glaucoma Clinic of the Department of Ophthalmology, Gifu University School of Medicine.

The topographic changes of optic discs were determined using a Rodenstock Optic Nerve Head Analyzer before trabeculectomy, and three or six months and one year after surgery. We selected cup to disc ratio (C/D ratio), rim area, and cup volume as disc parameters for evaluation of optic disc changes. All measurements of optic discs used for the study were corrected for

Perimetry Update 1990/91, pp 57-61
Proceedings of the IXth International Perimetric Society Meeting,
Malmö, Sweden, June 17-20, 1990
edited by Richard P. Mills and Anders Heijl

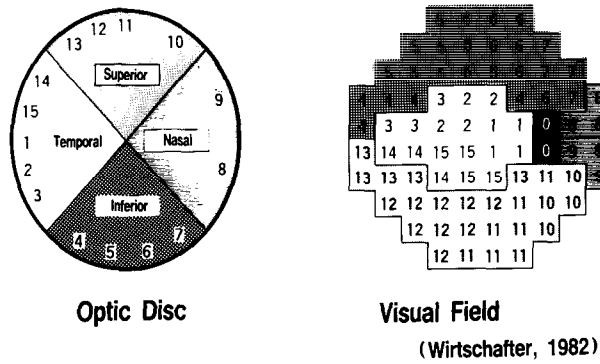

Fig 1 Division of the visual field and corresponding area to the optic disc.

optical magnification with refractive error, corneal curvature and axial length using Littman's formula[14], and were the average of two analyses of the same image performed by one of the authors (KM) at an interval of at least seven days. We analyzed disc parameters for the entire disc and for each quadrant, *i.e.*, superior, inferior, temporal, and nasal.

The 30-2 central threshold fields were obtained with a Humphrey Field Analyzer 630. To evaluate the visual field changes, we adopted the mean deviation and the total deviation calculated using the statistical program STATPAC 1. The minus signs of both indices were omitted to simplify the analyses. Visual acuity of each eye was better than or equal to 0.5, and pupil diameter of each eye was larger than or equal to 2.0 mm during visual field testing. Only visual fields with high reliability as follows were adopted: fixation loss: <20%; false positive: <20%; false negative: <20%. One far advanced POAG eye with poorly reliable visual field testing was excluded from the analyses. Therefore, visual field analyses were carried out in the remaining 13 eyes of eight patients. Based on the retinotopic projection of visual fields onto the optic disc proposed by Wirtschafter[15], we tried to classify the visual field into four sectors, so as to have each sector correspond to one quadrant of the optic disc (Fig. 1). We represented visual field defects as the values of total deviation which were added up for each sector.

All IOP measurements were performed with a Goldmann applanation tonometer. The mean IOP before surgery was the average of all pressure readings within one month before surgery. The mean IOP after surgery was the average of all postoperative pressure readings until the time of the disc measurements.

The clinical characteristics of patients are shown in Table 1. The mean age was 37.1 years. Four males and five females were studied. The mean preoperative spherical equivalent refractive error was -2.8 diopters. The mean preoperative visual acuity was 0.9. The preoperative mean deviation of the visual field ranged from 3.7 to 31.5 dB.

For statistical analysis, the Wilcoxon signed rank test was used for paired comparisons. Linear regression analysis was used to calculate correlation coefficients. We considered $p<0.05$ to be statistically significant.

Table 1 Clinical background

Age (years)	37 1±16 6	(18 –66)
Male/female	4/5	
Refractive error (D)	–2.8± 3 3	(–11.8– 1.4)
Visual acuity	0 9± 0.3	(0 5– 1.2)

Fourteen eyes of nine patients; mean ±SD; ( ): range

Results

Associated with a significant IOP reduction of from 24.5±5.5 mmHg to 11.0±4.8 mmHg, the total C/D ratio and total cup volume significantly decreased, and the total rim area significantly increased at three or six months after trabeculectomy. There was no statistically significant

difference between the pre- and postoperative mean deviation of the visual field three or six months after surgery (Table 2). One year after surgery, a significant reduction of IOP (from 24.2±5.5 mmHg to 12.2±3.6 mmHg) was still associated with significant decreases of the total C/D ratio and the total cup volume, a significant increase of the total rim area, and a significant improvement in the mean deviation was now observed (Table 3).

Table 2. Measurements before and three or six months after surgery

	Before		*After*		*p-value*
C/D ratio	0.85±0 10	(14)	0.76±0.19	(14)	<0.01
Rim area (mm^2)	0.54±0 40	(14)	0.79±0 57	(14)	<0 01
Cup volume (mm^3)	0.81±0 37	(14)	0.61±0.31	(14)	<0.01
Mean deviation (dB)	18.7±9.5	(13)	16 6±9 9	(13)	NS
Mean IOP (mmHg)	24 2±5 5	(14)	11.0±4.8	(14)	<0 01

mean ±SD; ( ): number of eyes; Wilcoxon signed rank test

Table 3. Measurements before and one year after surgery

	Before		*After*		*p-value*
C/D ratio	0.85±0.10	(14)	0.78±0.15	(14)	<0 01
Rim area (mm^2)	0 54±0 40	(14)	0 68±0.50	(14)	<0.05
Cup volume (mm^3)	0.81±0.37	(14)	0 62±0 28	(14)	<0 05
Mean deviation (dB)	18.7±9 5	(13)	16 6±10.8	(13)	<0.05
Mean IOP (mmHg)	24 2±5.5	(14)	12.2±3 6	(14)	<0 01

mean ±SD; ( ): number of eyes; Wilcoxon signed rank test

In 13 of the 14 eyes, a decrease of the total cup volume was observed one year after surgery. In the remaining eye, the total cup volume had increased postoperatively at both three or six months and one year after surgery. Hence, for 13 eyes of eight patients with decreased cup volume after surgery, we assessed cup changes in each quadrant of the disc as well as in the whole disc. Changes in the total deviation were also evaluated in each sector and the whole field for 12 eyes of seven patients with decreased total cup volume and reliable visual field data. Cup volume significantly decreased in all quadrants at both three or six months and one year after surgery (Tables 4 and 5). There was no statistically significant difference between pre- and postoperative total deviation in the whole field or each quadrant three or six months after surgery (Table 6). However, one year after surgery, the global total deviation and the total deviation sectors corresponding to the inferior and nasal quadrants of the optic disc were significantly improved (Table 7). The scattergram of preoperative mean deviation and the percentage reduction of mean deviation three or six months after surgery are shown in Fig. 2. There was no statistically significant correlation between the two. However, one year after surgery there was statistically significant negative correlation between both ($r=-0.80$, $p=<0.01$) (Fig. 3). That is, the earlier the visual field changes, the larger the percentage mean deviation reduction.

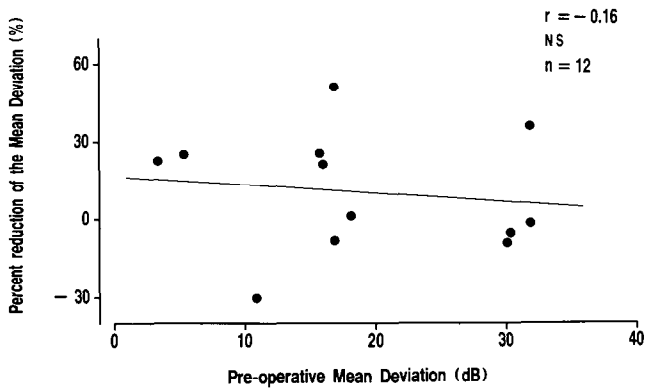

Fig 2 Mean deviation: preoperative *versus* percentage reduction (three or six months).

Table 4 Changes of cup volume (mm^3) between before and three or six months after surgery

	Before	*After*	*% reduction*	*p-value*
Quadrants				
superior	0 19±0 09	0 13±0.08	32.2±27.6	<0.01
inferior	0.23±0 12	0 17±0 10	28.2±22.6	<0.01
temporal	0.22±0.08	0 18±0.07	18.0±18.3	<0.01
nasal	0.17±0.10	0.12±0.08	31.7±32.6	<0.01
Total	0.82±0.38	0.60±0.32	33.9±34 1	<0.01

mean ±SD; n=13; Wilcoxon signed rank test

Table 5 Changes of cup volume (mm^3) between before and one year after surgery

	Before	*After*	*% reduction*	*p-value*
Quadrants				
superior	0 19±0.09	0.14±0 06	21.1±29.4	<0 01
inferior	0 23±0 12	0 16±0 09	29 2±21.3	<0.01
temporal	0 22±0 08	0.17±0.06	22 6±11.0	<0.01
nasal	0.17±0 10	0.11±0.07	38.1±17.7	<0 01
Total	0.82±0.38	0.59±0 26	32 4±45 1	<0.01

mean ±SD; n=13; Wilcoxon signed rank test

Table 6 Changes of total deviation (dB) between before and three or six months after surgery

Projected area on the disc	*Before*	*After*	*% reduction*	*p-value*
Quadrants				
superior	503.5±235.0	432.5±242.6	12.7±29.3	NS
inferior	486.5±237.2	428.8±266.3	16 8±23 8	NS
temporal	330.4±190.3	307.0±199.0	10.4±24 1	NS
nasal	87.4± 65 6	71.8± 66.6	18 1±34 5	NS
Total	1407.8±698.6	1240.1±746.4	13 9±23 4	NS

mean ±SD; n=12; Wilcoxon signed rank test

Table 7 Changes of total deviation (dB) between before and one year after surgery

Projected area on the disc	*Before*	*After*	*% reduction*	*p-value*
Quadrants				
superior	503 5±235.0	441 8±265 6	16 2±27.6	NS
inferior	486 5±237 2	416.8±269 7	22 7±32.6	<0.05
temporal	330.4±190.3	307.0±216.6	17.0±33.7	NS
nasal	87.4± 65.6	76.0± 71.0	24.1±36 4	<0 05
Total	1407 8±698 6	1241.5±803.0	19 9±24.8	<0.05

mean ±SD; n=12; Wilcoxon signed rank test

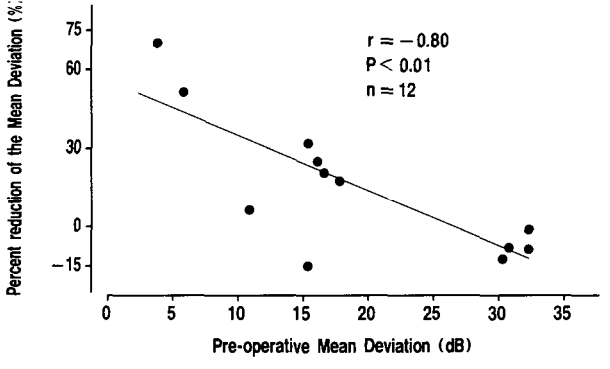

Fig 3 Mean deviation: preoperative *versus* percentage reduction (one year).

Discussion

We carried out a prospective study to investigate, using quantitative methods, topographic changes of the optic discs and changes in the visual fields of POAG eyes after trabeculectomy for one year. The results of our study show that the reversal of cupping persists for at least one year, if adequate reduction of IOP is obtained. Furthermore, the lasting reversal of cupping following IOP reduction can be associated with improvement of the visual field particularly in early glaucoma. These results seem to suggest that adequate IOP reduction for early stage glaucoma does not only maintain visual function but improves it gradually. Therefore, we should aim at lowering IOP for as long as possible in the management of POAG.

References

1. Von Graefe A: Weitere klinische Bemerkungen über Glaukom, glaukomatöse Krankheiten und über die Heilwirkungen der Iridektomie. Arch Ophthalmol 4:127-162, 1858
2. Jaeger E: Ophthalmoskopischer Hand-Atlas. Vienna: Druck und Verlag der KK Hofund Staatsdruckerei 1869
3. Schaffer RN: New concepts in infantile glaucoma. Can J Ophthalmol 2:243, 1967
4. Neumann E, Hyams SW: Intermittent glaucomatous excavation. Arch Ophthalmol 90:64-66, 1973
5. Spaeth GL, Fernandes E, Hitchings RA: The pathogenesis of transient or permanent improvement in the appearance of the optic disc following glaucoma surgery. Doc Ophthalmol Proc Ser 22:111-126, 1980
6. Iwata K, Sobue K, Imai A et al: On the reversibility of the glaucomatous disc cupping and the visual field. Jpn J Clin Ophthalmol 31:759-765
7. Shaffer RN, Hetherington J: The glaucomatous disc in infants: a suggested hypothesis for disc cupping. Ophthalmology 73:929-935, 1969
8. Hetherington J, Shaffer RN, Hoskins HD: The disc in congenital glaucoma. In: Etienne R, Paterson GD (eds) XXII Congrès International d'Ophtalmologie, pp 127-143 International Glaucoma Symposium, Albi, France 1974 Marseille: Diffusion Générale de Librairie 1975
9. Quigley HA: The pathogenesis of reversible cupping in congenital glaucoma. Am J Ophthalmol 84:358-370, 1977
10. Spaeth GL, Fellman RL, Starita RL et al: A new management system for glaucoma based on improvement of the appearance of the optic disc or visual field. Trans Am Ophthalmol Soc 83:268-284, 1985
11. Yassure Y, Lusky M, Grunewald E et al: Regression of optic disc excavation and visual field damage following glaucoma surgery in eyes with long-standing glaucoma. Glaucoma 6:202-207, 1984
12 Tomita G, Matsubara K, Kitazawa Y: Optic disc changes studied by means of image analysis: an example for application. Presented at Symposium of Normotensive Glaucoma, Angers, France 1989
13. Shin DH, Bielik M, Hong YJ et al: Reversal of glaucomatous optic disc cupping in adult patients. Arch Ophthalmol 107:1599-1603, 1989
14. Littman H: Zur Bestimmung der wahren Grösse eines Objektes auf dem Hintergrund des lebenden Auges. Klin Mbl Augenheilk 180:286-289, 1982
15. Wirtschafter JD, Becker W, Howe J, Younge B: Glaucoma visual field analysis by computed profile of nerve fiber function in optic disc sectors Ophthalmology 89:255-267, 1982

Visual field global indices improve following IOP reduction in adult COAG patients

Clark S. Tsai and Dong H. Shin

The Kresge Eye Institute, Wayne State University, School of Medicine, Detroit, MI, USA

Abstract

The authors studied visual field change in adult patients with early to moderate chronic open-angle glaucoma (COAG) associated with reversal of glaucomatous disc cupping following a prolonged reduction of chronically elevated IOP. The mean of each of the three global indices [mean deviation (MD), pattern standard deviation (PSD), and corrected pattern standard deviation (CPSD)] improved in the patients with an IOP reduction of ≥40%, in statistically significant contrast to no improvement of the mean global indices in those with an IOP reduction of <40% ($p<0.05$). This study underscores the beneficial effect of a greater magnitude of IOP reduction.

Introduction

A strong correlation exists between visual field (VF) defect and optic disc cupping *in vivo*[1] and between visual field sensitivity and number of remaining retinal ganglion cells *in vitro*[2]. When glaucoma is uncontrolled, progressive disc cupping is usually accompanied or followed by increasing VF loss. Conversely, reversal of optic disc cupping in adult glaucoma patients has been demonstrated following IOP reduction with therapies[3-5]. In addition, an improvement of VF associated with an improvement of IOP control has been observed in some (but not all) adult glaucoma patients, while a deterioration of VF has been found with a deterioration of IOP control[6]. A higher percentage of patients with IOP reduction of ≥30% had qualitative evidence of VF improvement when compared to patients with IOP reduction of <20%; the magnitude of IOP reduction was suggested as an important factor in VF improvement[7].

Our present study attempted to quantitatively correlate the magnitude of IOP reduction to improvement of VF global indices in adult COAG patients who demonstrated reversal of disc cupping following IOP reduction. We also considered such variables as age, duration of IOP reduction, perimetric test-taking experience, reliability indices, and short-term fluctuation.

Patients and methods

Improvement of Humphrey (Humphrey Instruments, Palo Alto, CA) VF global indices was investigated in 28 eyes of 28 adult patients with early to moderate COAG (Aulhorn's stages 1 to 3)[8]. These patients had documented reversal of optic disc cupping by Rodenstock Optic Nerve Head Analyzer (RONA, Rodenstock Instrumente, GMBH, Munich, Germany) following IOP reduction. The 24-2 central threshold program of the Humphrey visual field analyzer was utilized.

None of the patients included had peripheral visual field constriction, which might suggest either "inexperienced" VF[9] or lens rim artifact[10]. When more than one Humphrey VF test was available at either high or low IOP, the one with the best reliability indices was chosen.

"Change" of data was defined as post-IOP reduction data less pre-IOP reduction data (Δ = data 2 - data 1). "Negative change" of data referred to pre-IOP reduction data less post-IOP reduction data ([-]Δ = data 1 - data 2). The sign designation is to keep all of the improvements of the global indices moving in a positive direction.

Learning effect was explored by comparing age, IOP reduction, duration of IOP reduction, and changes of global indices between inexperienced subjects (who never had a VF test) and

Perimetry Update 1990/91, pp. 63-66
Proceedings of the IXth International Perimetric Society Meeting,
Malmö, Sweden, June 17-20, 1990
edited by Richard P. Mills and Anders Heijl

experienced subjects (who had at least one VF test) using the unpaired *t*-test.

The effect of magnitude of IOP reduction on the improvement of VF global indices was probed by comparing the global indices along with other factors between patients with percent IOP reduction ≥40% and those with percent IOP reduction <40% using the unpaired *t*-test.

Results

The mean (±SD) age of the 28 patients was 55.1 (±14.7) years (range: 31 to 78 years). IOP was reduced from 29.3 (±5.9) to 19.4 (±4.3) mm Hg for 34.8 (±24.8) weeks (range: five to 98 weeks) with medical therapy, argon laser trabeculoplasty, or filtering surgery. The mean IOP reduction and percent IOP reduction were 9.9 (±5.4) mm Hg and 32.6 (±13.4) percent, respectively.

No significant differences were found between inexperienced and experienced perimetric test takers in changes of global indices, changes of IOP, age, and duration of IOP reduction (unpaired *t*-test, $p>0.05$ for each).

Among the three reliability indices [fixation loss (FL), false positive (FP) and false negative (FN)], only the change of FN between the post- and pre-IOP reduction VF tests (ΔFN = FN2 - FN1) demonstrated significant correlation with the change of PSD (simple linear regression, $r = -0.452$ $p = 0.0157$) and on the change of CPSD ($r=-0.34$, $p=0.08$). MD and short-term fluctuation (SF) did not appear to be affected by the changes of any of the three reliability indices (simple linear regression, $p>0.05$).

Patients were divided into two groups according to IOP reduction (<40% *vs* ≥40%), and comparisons were made between them. Both groups had compatible age, VF experience, duration of IOP reduction, SF (Table 1), and reliability indices (unpaired *t*-test, $p>0.05$ for each). However, the patients with IOP reduction ≥40% had improvement of mean MD, PSD, and CPSD indices, in statistically significant contrast to no improvement of these indices in patients who had IOP reduction <40% (unpaired *t*-test, $p<0.05$ for each index) (Table 1).

Table 1 Comparison between two groups with IOP reduction ≥40% ($n=11$) and <40% ($n=17$)

	≥40%[a] ($n=11$) (mean ±SD)	<40%[a] ($n=17$) (mean ±SD)	p[b]
VF experience (n)[c]	0.6± 1 2	1.7± 2.0	NS[d]
Age (years)	49.5±13.8	58.8±14.5	NS
Duration (weeks)[e]	32.8±21.7	36.1±27.2	NS
ΔMD (dB)[f]	1.79±1.69	–0.15±1.55	<0 05
(-)ΔPSD (dB)[g]	0.92±1.51	–0.30±1 28	<0 05
(-)ΔCPSD (dB)[h]	1 29±1.73	–0.25±1.49	<0.05
(-)ΔSF (dB)[i]	–0 36±1 48	0.02±0.65	NS

a: ≥40%: IOP reduction ≥40%; <40%: IOP reduction <40%. b: two-tailed unpaired *t*-test c: VF experience: number (n) of previous visual tests. d: NS: statistically not significant. e: duration of IOP reduction (weeks). f: Δ = measurement 2 - measurement 1; MD: mean deviation in decibels (dB). g: (-)Δ = measurement 1 - measurement 2; PSD: pattern standard deviation (dB). h: CPSD: corrected pattern standard deviation (dB). i: SF: short-term fluctuation (dB)

Discussion

Reversal of optic disc cupping in direct proportion to the magnitude of IOP reduction has been demonstrated following a prolonged reduction of chronically elevated IOP in patients with early to moderate COAG[5]. The reversal of the backward bowing of the lamina cribrosa associated with optic disc cupping reversal[11] may bring about a secondary relief of stretching, compression, strangulation, and/or hypoxia on axons. Subsequently, those compromised but not atrophied axons may become rehabilitated or revitalized by the re-establishment of normal blood and/or axoplasmic flow and the resumption of normal metabolism. Indeed, after medical or surgical IOP reduction therapies, improvement of visual function as well as optic disc cupping has been observed in adult glaucoma patients[5-7,12-13]. Katz and coworkers reported a higher percentage of patients with qualitative evidence of VF improvement in the group with IOP reduction ≥30% than in that of patients with IOP reduction <20%[7]. Our present study demon-

strated quantitative evidence of IOP-dependent improvement of VF global indices in patients with documented reversal of optic disc cupping following IOP reduction. The mean global indices in patients with IOP reduction ≥40% improved, in contrast to no improvement of the mean indices in patients with IOP reduction <40%. Thus the beneficial effect of a greater IOP reduction is underscored.

Our study included 11 inexperienced and 17 experienced perimetric test takers. None of the 28 patients had concentrically constricted VF. With similar magnitude of IOP reduction and age, the inexperienced and experienced groups had no significant differences in the changes of VF global indices. Nor did the VF experience correlate to change of global indices in simple or multiple linear regression analysis. Therefore the learning effect[9,14,15] should have been minimal and could not be responsible for the improvement of global indices in our study. In our present study, the FN but not the FP index influenced the PSD and CPSD significantly. Furthermore, SF correlated to CPSD. The finding was similar to that of Heijl *et al.*, who also noted the influence of FN and SF on global indices[16]. Therefore, FN and SF were controlled (multiple regression analysis) in our study.

It has been suggested that both short-term and long-term fluctuations are increased in glaucoma patients[17]. It would be very difficult to isolate the VF change from the fluctuation of threshold sensitivity when a single best pre- and post-IOP reduction VF is used. However, as suggested by Spaeth, the "noise" (fluctuation) would serve only to lessen the apparent significance of the results[6]. The correlation between IOP reduction and the change of VF global indices in the present study must have been strong enough to withstand any influence of "noise".

We are not recommending using a single VF change as a therapeutic guideline. When more than one reliable VF is available, averages of both pre- and post-IOP reduction VFs should be derived and compared. We suspect that the inclusion of unreliable VFs either in comparison of mean VF values or linear regression analysis will lead to unreliable study outcome.

Our study demonstrates a quantitative evidence of improvement of VF as well as reversal of optic disc cupping dependent on IOP reduction in patients with early to moderate glaucoma, and underscores the beneficial effect of a large magnitude of IOP reduction.

References

1 Guthauser U, Flammer J, Niesel P: The relationship between the visual field and the optic nerve head in glaucomas. Graefe's Arch Clin Exp Ophthalmol 225:129-132, 1987
2. Quigley HA, Dunkelberger GR, Green WR: Retinal ganglion cell atrophy correlated with automated perimetry in human eyes with glaucoma. Am J Ophthalmol 107:453-464, 1989
3. Pederson JE, Herschler J: Reversal of glaucomatous cupping in adults Arch Ophthalmol 100:426-431, 1982
4. Greenidge KC, Spaeth GL, Traverso CE: Change in appearance of the optic disc associated with lowering of intraocular pressure. Ophthalmology 92:897-903, 1985
5. Shin DH, Bielik M, Hong YJ, Briggs KS, Shi DX: Reversal of glaucomatous optic disc cupping in adult patients Arch Ophthalmol 107:1599-1603, 1989
6. Spaeth GL: The effect of change in intraocular pressure on the natural history of glaucoma: lowering intraocular pressure in glaucoma can result in improvement of visual fields Trans Ophthalmol Soc UK 104:256-264, 1985
7. Katz LJ, Spaeth GL, Cantor LB, Poryzees EM, Steinmann WC: Reversible optic disk cupping and visual field improvement in adults with glaucoma. Am J Ophthalmol 107:485-492, 1989
8. Aulhorn E: Visual field defects in chronic glaucoma. In: Heilman K, Richardson KT (eds) Glaucoma, Conceptions of a Disease: Pathogenesis, Diagnosis, Therapy. Philadelphia: WB Saunders Co 1978
9. Heijl A, Lindgren G, Olsson J: The effect of perimetric experience in normal subjects. Arch Ophthalmol 107:81-86, 1989
10. Zalta AH: Lens rim artifact in automated threshold perimetry. Ophthalmology 96:1302-1311, 1989
11. Briggs K, Shin D, Rho S, Hong Y, Shi D, Kim C: Reversal of optic nerve cup depth following intraocular pressure reduction in chronic open-angle glaucoma and ocular hypertensive patients. Invest Ophthalmol Vis Sci (Suppl) 30:429, 1989
12. Greve EL, Furuno F, Verduin WM: The clinical significance of reversibility of glaucomatous visual field defects. Doc Ophthalmol 19:197-203, 1979
13. Tsai CS, Shin DH, Hong YJ, Rho S, Bielik M, Shi DX: Improvement of visual field following IOP reduction in adult COAG patients. Invest Ophthalmol Vis Sci (Suppl) 31:16, 1990

14. Wood JM, Wild JM, Hussey MK, Crews SJ: Serial examination of the normal visual field using Octopus automated projection perimetry: evidence for a learning effect. Acta Ophthalmol 65:326-333, 1987
15. Werner EB, Adelson A, Krupin T: Effect of patients experience on the results of automated perimetry in clinical stable glaucoma patients. Ophthalmology 95:764-767, 1988
16. Heijl A, Lindgren G, Olsson J: Reliability parameters in computerized perimetry. In: Greve EL, Heijl A (eds) Proceedings of the Seventh International Visual Field Symposium, September 1986. Dordrecht: Dr W Junk Publishers 1987
17 Flammer J, Drance SM, Zulauf M: Differential light threshold: short- and long-term fluctuation in patients with glaucoma, normal controls and patients with suspected glaucoma. Arch Ophthalmol 102:704-705, 1984

Choroidal plerometry: an approach to the dynamics of choriocapillaris perfusion by digital analysis of fluorescein angiograms

G.N. Lambrou, T.J.T.P. van den Berg, F. Temporelli and E.L. Greve

Academic Medical Center, Amsterdam, The Netherlands

The interpretation of fluorescein angiography is, to this day, essentially qualitative. However, rapid sequences of early angiographic frames contain data on the hemodynamics of the choriocapillaris, which should allow quantitative analysis, given an adequate algorithm. For that purpose, we developed a computerized system (Fig. 1) based on a model of the choriocapillaris filling process.

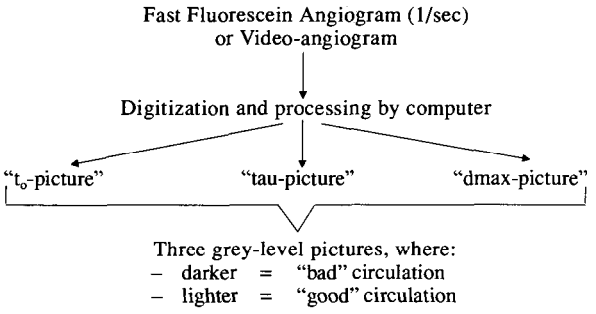

Fig 1 General diagram of the system. The computer "grabs" the early angiographic frames, processes the data, and produces three "pictures", which are actually gray-scale maps of the distribution of three hemodynamic parameters: appearance time of fluorescein in seconds after cubital vein injection (t_o), maximum fluorescence measured as density on the negatives (d_{max}), and perfusion rate or blood refresh rate expressed in terms of the time necessary for refreshing approximately two-thirds of the blood content of a choriocapillaris elementary area (tau)

The principle of the method, which we termed "plerometry"*, is explained in a prior publication[1]. In short, angiographic frames starting before the arrival of fluorescein in the eye, and extending approximately 10 to 15 seconds after the end of the arterial phase, are adjusted so as to neutralize eye movements, and are stored in the computer memory. The system then computes, for each location of the fundus, the *fluorescein appearance time* (t_o, in seconds from injection), the *maximum fluorescence* (d_{max}, as density on the negatives) and the *blood refreshing rate* (tau, in seconds; tau is a measure of the time it takes to refresh approximately two-thirds of the blood content of a given area of the choriocapillaris). From this data, the system produces three "gray-scale maps" of the fundus, each showing the distribution of one of the three hemodynamic parameters. The gray-scale is designed with the convention that "darker" indicates "worse circulation" (*i.e., lower* maximal fluorescence, *later* appearance time, *slower* refreshing rate) and, respectively, "lighter" indicates "better circulation".

The "maximum fluorescence" map is not very different from a late angiographic frame. The other two maps, however, display essentially new information. If it is argued that a very careful examination of the early angiographic frames can give a good idea of the distribution of the appearance times, it does not provide any real insight into the perfusion rates, except in the

*from the Greek root "plero-", meaning "to fill".

Perimetry Update 1990/91, pp. 67-69
Proceedings of the IXth International Perimetric Society Meeting,
Malmö, Sweden, June 17-20, 1990
edited by Richard P. Mills and Anders Heijl

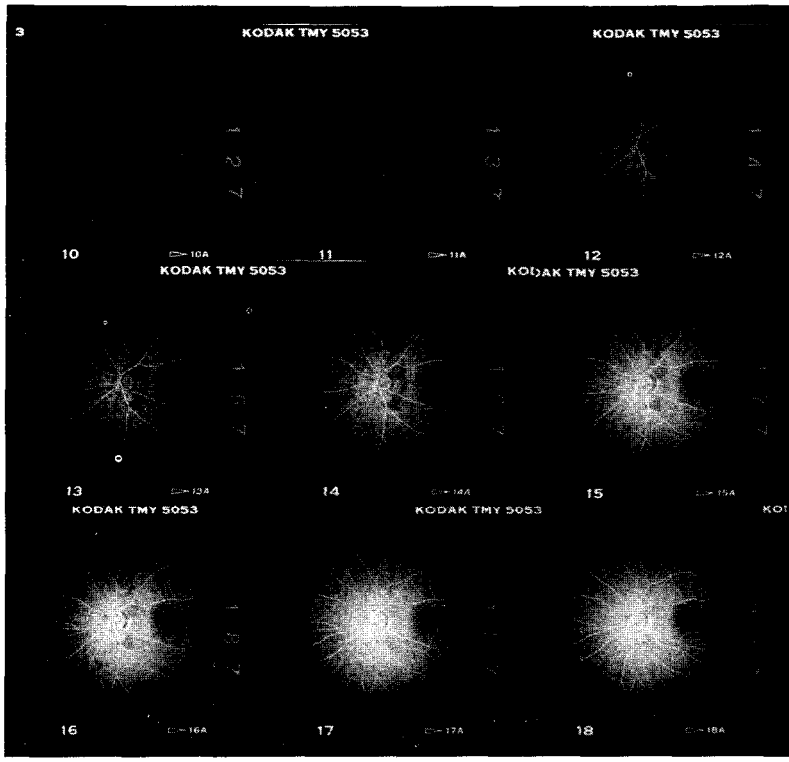

Fig 2a

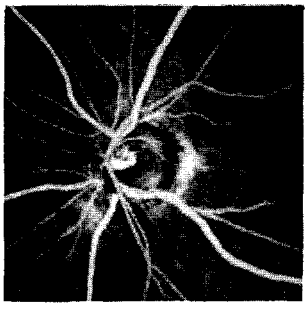

Fig 2b

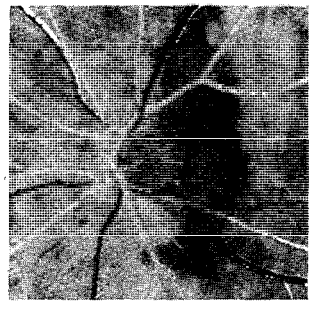

Fig 2c

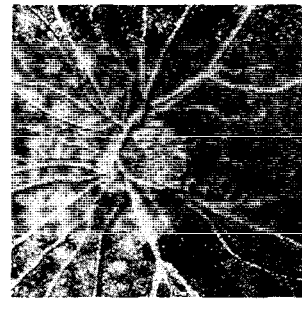

Fig 2d

Fig 2 Example of an angiographic sequence (a) and the resulting "gray-scale maps" (b: maximum fluorescence picture; c: appearance time picture; d: perfusion rate picture). Note that the maximum fluorescence picture is not very different from a late angiographic frame, and that from the angiographic sequence it is possible to predict the general aspect of the appearance time picture However, the information presented in the perfusion rate picture, although present in the angiographic sequence, is very hard to extract mentally, even by experienced examiners.

most severe cases. In the example shown in Fig. 2, the highly delayed appearance in the territory temporal to the optic nerve head is evident from the angiographic sequence, but the lower perfusion rate of the temporal half of the choriocapillaris is not.

Based on the assumption that the prelaminar region of the optic nerve head shares a common arterial supply with the peripapillary choroid[2], we expect that analysis of the perfusion rates of the latter may provide a useful tool for the prognostic assessment of glaucoma patients and ocular hypertensives. This expectation is enforced by the results of a previous investigation[3], as well as by literature data[4-6] indicating that the choroidal blood flow is reduced in low-tension glaucoma.

References

1. Lambrou GN, van den Berg TJTP, Greve EL: Vascular plerometry of the choroid: an approach to the quantification of choroidal blood flow using computer-assisted processing of fluorescein angiograms. In: Lambrou GN Greve EL (eds) Ocular Blood Flow in Glaucoma, pp 287-294. Amsterdam/Berkeley/Milano: Kugler & Ghedini Publ 1989
2. Hayreh SS: Structure and blood supply of the optic nerve. In: Heilmann K, Richardson KT (eds) Glaucoma, Conceptions of a Disease, pp 78-96. Stuttgart: Thieme Publ 1978
3. Lambrou GN, Sindhunata P, van den Berg TJTP, Geijssen HC, Vyborny P, Greve EL: Ocular pulse measurements in low-tension glaucoma. In: Lambrou GN, Greve EL (eds) Ocular Blood Flow in Glaucoma, pp 115-120. Amsterdam/Berkeley/Milano: Kugler & Ghedini Publ 1989
4. Ulrich WD, Ulrich A, Petzschmann Ä, Ulrich Ch: Okuläre Autoregulation und Ziliarer Perfusionsdruck beim Niedrigdruckglaukom. Fol Ophthalmol 13:333-337, 1988
5. Spaeth GL: The Pathogenesis of Optic Nerve Damage in Glaucoma: Contributions of Fluorescein Angiography. New York: Grune & Stratton Publ 1977
6. Laatikainen L: Fluorescein angiographic studies of the peripapillary and perilimbal regions in simple, capsular and low-tension glaucoma. Acta Ophthalmol (Suppl) 111:9-83, 1971

Infrared camera for glaucoma screening

P. Juhani Airaksinen, Anja Tuulonen, Antonio Montagna and Heikki Nieminen

Department of Ophthalmology, University of Oulu, SF-90220 Oulu, Finland

Abstract

One hundred and eighty-three first degree relatives of glaucoma patients were photographed by a technician with a non-mydriatic fundus camera in order to study the suitability of wide angle black-and-white fundus photographs for glaucoma screening The success rate of photography was 92% The optic disc and retinal nerve fiber layer abnormalities were evaluated by an ophthalmologist. Thirty-one subjects (17%) were referred for a full ophthalmological examination Fifteen new cases of glaucoma (8%) were found. In six of them retinal nerve fiber layer defect was the only abnormality. Only one of the 15 patients (7%) with glaucoma had an elevated IOP The results of this study indicate that a non-mydriatic retinal camera is a useful tool in screening for glaucoma

Introduction

A number of different techniques have been used for glaucoma screening including tonometry, visual field testing and ophthalmoscopy[1-3] With tonometry one can detect patients with abnormally high intraocular pressure. However, patients with "normal pressure" and glaucoma will remain undetected[4-6]. Testing of visual fields is more time consuming and definite standards for mass visual field screening with automated perimetry have not been fully provided[7,8]. Ophthalmoscopy has been under-utilized for glaucoma screening[2]. Optic disc viewers or grids on the photographs have been used successfully to identify glaucomatous disc changes also by non-medically qualified observers[5,9].

The purpose of this study was to assess the usefulness of a wide angle non-mydriatic fundus camera in glaucoma screening.

Material and methods

We used a Canon CR3-45NM non-mydriatic 45 degree retinal camera. With this picture angle one can observe the optic disc and obtain a good overview of the retinal nerve fiber layer The photographs were taken in a dark room with no mydriatics. The pupils should dilate to 4 mm or more. The fundus was focused with infrared light and viewed on a monitor. A split-lines focusing device and alignment side-marks are used. The photographs were taken on high sensitivity black-and-white Kodak Panatomic-X film with a green filter (Wratten No. 58). Enlarged paper-prints (13 × 18 cm) were made for the analysis.

Three health care centers in northern Finland participated in this study. A technician or a nurse from each health care center was trained for two days in the eye clinic and then took the camera to their respective centers.

As positive family history of glaucoma may increase the risk of glaucoma[1-3], we decided to photograph the first degree relatives of previously known glaucoma patients registered at the eye clinic. There were 208 glaucoma patients of the three communes registered in the eye clinic glaucoma registry. At least one relative of 119 (57%) glaucoma patients was photographed. As this was not an epidemiologic study we did not try to trace all relatives.

The photographs were evaluated by two observers (PJA and AT) independently. The signs that we looked for were: abnormal or suspicious optic disc or RNFL, disc hemorrhages, and venous collaterals as a sign of asymptomatic stasis. Patients with such findings were invited to the eye clinic for full ophthalmological examination including automated visual field testing, optic disc stereophotography and retinal nerve fiber layer photography.

Perimetry Update 1990/91, pp 71-73
Proceedings of the IXth International Perimetric Society Meeting,
Malmö, Sweden, June 17-20, 1990
edited by Richard P. Mills and Anders Heijl

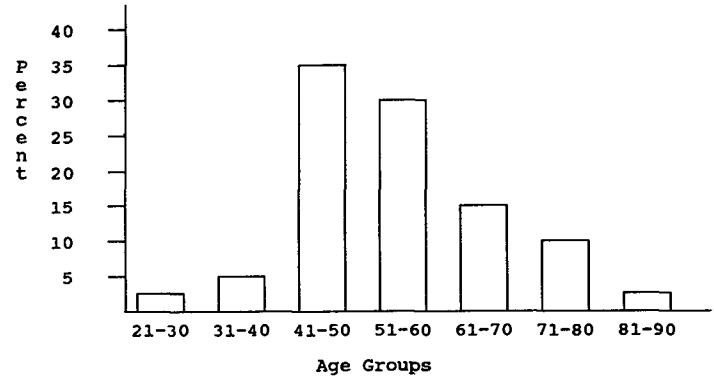

Fig 1 Age distribution of the 183 subjects photographed.

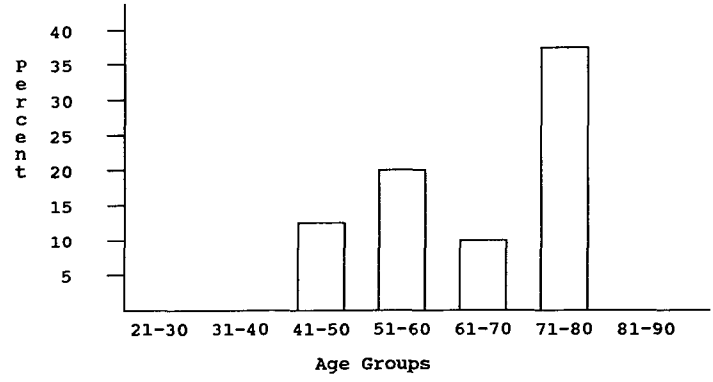

Fig 2 Age distribution of the 31 subjects referred to full eye examination.

Results

Three hundred and forty-six of 366 photographs (95%) were assessable. Picture quality was good or excellent in 328 of 366 photographs (90%), and fair or poor but assessable in 18 of 366 (5%) photographs. In 15 of 183 subjects (8%) photography of one or both eyes was unsuccessful. The time the ophthalmologist used for picture analysis was about ten minutes for 100 photographs.

A total of 31 subjects (17%) were referred for further ophthalmological examinations. Agreement of the referred cases between the two observers was 92%. The age distribution of the total material and the referred group is presented in Figs. 1 and 2. In 21 of the 31 cases (68%) the findings in the photographs were confirmed in the clinical examination. In 15 cases (8%) a glaucoma diagnosis could be made. Definition of glaucoma was: abnormal optic disc and/or abnormal RNFL with or without visual field abnormalities. Four patients had only an optic disc hemorrhage or asymptomatic venous stasis changes. Two patients had an eye disease other than glaucoma: pale optic disc after retrobulbar neuritis and anterior ischemic optic neuropathy.

Six of the 15 glaucoma patients had typical glaucomatous changes at the optic disc, in the retinal nerve fiber layer and visual fields. Nine of the 15 patients had nerve fiber layer abnormalities with normal looking optic discs. Three of these nine patients had abnormal visual fields. There were four pairs of siblings among the 15 patients with glaucoma.

Two eyes had collateral vessels as a sign of asymptomatic venous stasis change at the optic disc[10]. One of them had diffuse retinal nerve fiber layer atrophy and normal Humphrey 30-2 visual field. In the other a collateral vessel loop was the only abnormal finding.

Three of the 31 referred cases (10%) had an intraocular pressure >20 mmHg. One of them had glaucoma, two had suspicious looking optic discs but normal nerve fiber layer and normal

visual fields. Mean IOP of the glaucoma patients was 17.8±4.1 mmHg and of the non-glaucoma cases 16.2±3.0 mmHg. The difference was not statistically significant.

Discussion

Our findings are in agreement with previous studies[5] indicating that the non-mydriatic retinal camera with a 45-degree picture angle is a useful tool in screening for glaucoma. Shiose[5] found that optic disc and nerve fiber layer abnormalities were the most specific parameters for detection of glaucoma and correctly predicted visual field loss in 68% of the glaucomatous eyes.

In the present study we used black-and-white paper prints. Green filter was chosen because it enhances the visibility of the nerve fibers[11]. The 92% success rate of photography performed by a technician after a two-day training period, and 92% agreement of the findings between the two observers may be regarded as very good.

In this screening study new patients with glaucoma were found, some of them in a very early phase of the disease. The percentage of new cases (8%) was quite high compared to some previous reports (0.33%)[5]. We want to emphasize, however, that this study was not planned as an epidemiologic analysis but merely to test the suitability of non-mydriatic black-and-white photography as a method of screening for glaucoma.

It has been demonstrated how knowing the intraocular pressure level and visual fields causes significant bias in the evaluation of optic disc photographs[12]. In the present study tonometry was not a part of the screening procedure and only one of 15 newly detected glaucomas had increased intraocular pressure at the first clinic visit.

With the combination of optic disc and RNFL evaluation new glaucoma patients can be found in very early stages of the disease. Photography using an infrared camera is quicker and safer since mydriatics are not needed and it is independent of the subject's response. Analysis of the photographs takes but a few minutes of the ophthalmologist's time

Acknowledgements

This study was supported by the University Central Hospital of Oulu and the Sigrid Juselius Foundation

References

1. Becker B, Kolker AE, Roth FD: Glaucoma family study Am J Ophthalmol 50:557-567, 1960
2. Levi L, Schwartz B: Glaucoma screening in the health care setting. Surv Ophthalmol 28:164-174, 1983
3. Rosenthal AR, Perkins ES: Family studies in glaucoma. Br J Ophthalmol 69:664-667, 1985
4. Bengtsson B: The prevalence of glaucoma. Br J Ophthalmol 65:46-49, 1981
5. Shiose Y, Komuro K, Itoh T, Amano M, Kawase Y: New system of mass screening of glaucoma as part of automated multiphasic health testing services. Jpn J Ophthalmol 35:160-177, 1981
6. Eddy DM, Sanders LE, Eddy JF: The value of screening for glaucoma with tonometry. Surv Ophthalmol 28:194-205, 1983
7. Bengtsson B, Krakau CET: Automatic perimetry in a population survey. Acta Ophthalmol 57:929-937, 1979
8. Keltner JL, Johnson CA: Screening for visual field abnormalities with automated perimetry. Surv Ophthalmol 28:175-183, 1983
9. Hitchings RA, Brown DB, Anderton SA: Glaucoma screening by means of an optic disc grid Br J Ophthalmol 67:352-355, 1983
10. Tuulonen A: Asymptomatic miniocclusions of the optic disc veins in glaucoma. Arch Ophthalmol 107:1475-1480, 1989
11. Airaksinen PJ, Nieminen H, Mustonen E: Retinal nerve fibre layer photography with a wide angle fundus camera. Acta Ophthalmol 60:362-368, 1982
12. Shrader RR, Pistoia OA, Nicholl JE, Steinmann WC: The effect of clinical information on optic disc assessment. 1989 Annual meeting of the American Academy of Ophthalmology. Ophthalmology (Suppl) 96:125, 1989

Tonometry, fundus photography and automated perimetry in glaucoma screening

Kuniyoshi Mizokami, Yoshihiko Shiose, Yoshiaki Kitazawa, Shigeo Tsukahara, Tsunehiko Akamatsu, Ryusuke Futa, Harumi Katsuchima and Hiroshi Kosaki

Japan Glaucoma Society, Kobe, Japan

Introduction

Efficient methods for glaucoma screening have been evaluated[1-3], but the results are still inconclusive. Perimetry may be the most effective procedure[1], but it is both time-consuming and expensive for primary screening[2].

We organized a collaborative glaucoma survey examining populations in seven regions in Japan[4]. Twelve thousand three hundred and seventy eyes were examined in patients over 40 years of age, using two stages of screening: tonometry and fundus photography as the first stage, and automated perimetry as the second stage.

The efficiency of each screening process for glaucomatous visual field damage (VFD) was analyzed.

Material and methods

The survey was organized in 1988: 6186 persons (12,370 eyes) of 40 years or older were examined.

Tonometry and non-mydriatic fundus photography were used in the first stage of screening, and automated perimetry was used in the second. Intraocular pressure (IOP) was measured using a non-contact tonometer (Canon T-1). Cases with over 18 mmHg IOP were re-examined using a Goldmann applanation tonometer. Abnormal IOP was defined as pressures greater than or equal to 21 mmHg.

Fundus photographs were taken using a non-mydriatic camera set to a wide angle on ASA 200 color transparency film. Exposed rolls of film were delivered to the control center for evaluation according to standardized criteria[5].

Major features noted included disc signs; cupping and pallor of the disc and retinal signs, nerve fiber layer defect and splinter hemorrhages at the disc margin.

After evaluating the fundus photographs, result tables indicating the subjects to be examined in the second stage of screening were transferred back to the districts.

In the second stage screening, visual field testing was performed with a Humphrey Field Analyzer with the Armaly central 30-degree, three-zone program. Abnormal points found during this screening were retested using a custom program.

Glaucomatous VFD were divided into four patterns (Fig. 1), as follows:

1. nasal, *i.e.*, defects among 12 test points located 20-25° nasally;
2. Bjerrum, those among 48 test points at 10° and 15° eccentricity;
3. paracentral, 28 points within the central 5°;
4. arcuate means that defects were found in all of these three zones.

Results

Of the 886 eyes screened at the first stage (Table 1), 818 were subjected to second-stage visual field screening. Of these, glaucomatous VFD were detected in 290 eyes (35.5%). Other

Address for correspondence Kuniyoshi Mizokami, M D , Department of Ophthalmology, School of Medicine, Kobe University, Kusunoki-cho, 7-chome, Chuo-ku, Kobe, Japan 650

Perimetry Update 1990/91, pp 75-78
Proceedings of the IXth International Perimetric Society Meeting,
Malmö, Sweden, June 17-20, 1990
edited by Richard P. Mills and Anders Heijl

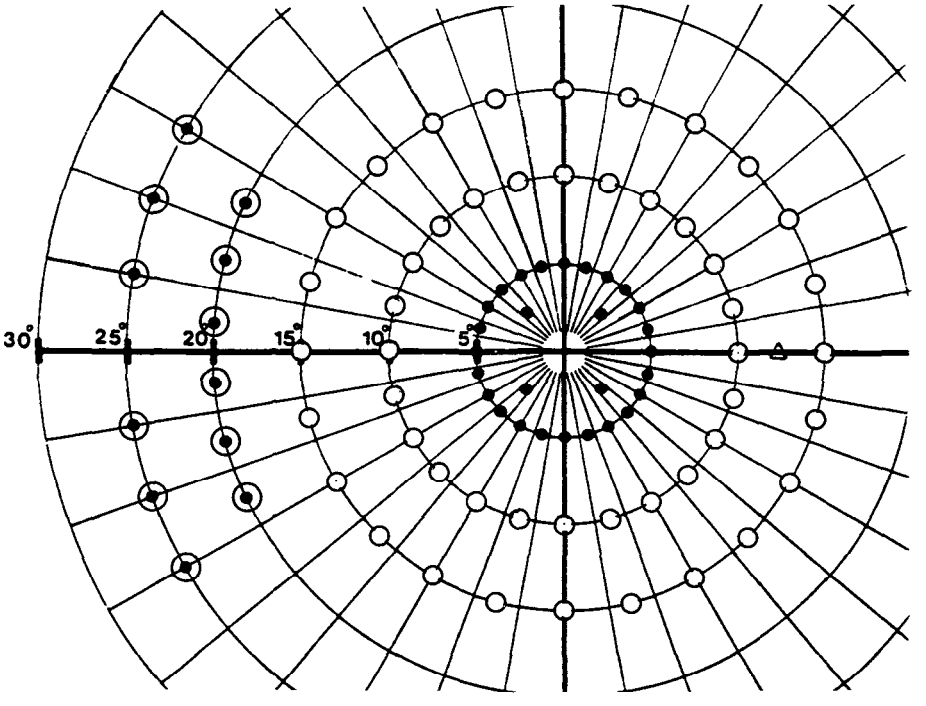

Fig 1 Classification of defect patterns in Armaly central screening test points, nasal (⊙), Bjerrum (○), paracentral (●). Arcuate means that defects were found in all three zones.

defects were found in 105 eyes. Four hundred and twenty-three were normal (Table 2). Specificity for various screening modes are shown in Table 3. 94.5% of eyes with glaucomatous VFD had abnormal fundus findings, but abnormal IOP was found only in 19% (Table 4). The defect patterns are classified in Table 5. The efficiency of fundus screening differed with different visual field patterns (Table 6). Fundus examination picked up 100% of eyes with paracentral scotomas alone, and 83% of those with Bjerrum scotomas. But only 68% of eyes with hemifield nasal step were picked up by the fundus screening.

Table 1 Results of first stage screening

Fundus screening			
Normal	10,217	(82 6%) eyes	
Glaucoma	339	(2 7%)	5 3%
Suspect	317	(2 6%)	5 3%
	461	(11 8%) eyes could not be checked	
Tonometry	210	(1.7%) eyes over 21 mmHg	

Table 2 Results of visual field screening (818 eyes)

Normal	423	(51 7%)
GLVFD	290	(35 5%)
Other VFD	105	(12 8%)
including cataract macular diseases		

Table 3. Specificity for tonometry and fundus inspection (818 eyes)

	Eyes	*GLVFD*
IOP and fundus	44	39 (88.6%)
IOP alone	163	16 (9.8%)
Fundus alone	611	235 (38.5%)
IOP	207	55 (26.6%)
Fundus	655	274 (41.8%)

Table 4 Positive screening in 290 eyes with GLVFD

Fundus	274 eyes (94.5%)
IOP	55 eyes (19.0%)

Table 5 Patterns of defects

Defect type	*No of eyes*
1. Arcuate	128
2. Nasal	50
3. Bjerrum	12
4. Paracentral	13
5. Nasal and Bjerrum	88
6. Nasal and Paracentral	9
Total	290

Table 6. Defect patterns and fundus findings (these steps and scotomas were only in one hemifield)

	Nasal step	*Bjerrum scotoma*	*Paracentral scotoma*
Total	22 eyes	12	13
Abnormal fundus	15 (68%)*	10 (83%)	13 (100%)*
Normal fundus	7	2	0

*$p<0.05$

Discussion

Visual field testing is a time-consuming procedure and frequently slows down the handling of patients during glaucoma screening. Automated perimetry is also time-consuming, expensive, and physically demanding for the patient. For this reason, the number of subjects undergoing visual field examination in this study was limited by using IOP measurements and disc evaluations in the first-stage screening procedure.

In the current screening survey, intraocular pressure proved to be almost useless: it missed 81% of eyes with glaucomatous VFD. Fundus photography with a non-mydriatic camera was effective. Of the eyes with glaucomatous VFD, 94.5% were recognized on fundus screening. A non-mydriatic camera greatly facilitates fundus photography and avoids hazards associated with mydriatic drops. With the exception of photographs of miotic eyes and eyes with hazy media, the images obtained in this survey were amazingly clear, even in the elderly.

Detection rates with various screening processes depended on the pattern of glaucomatous visual fields. The efficacy of fundus screening was lowest in eyes with nasal steps, even though it was highest in paracentral scotoma.

The results suggest that functional damage at sites proximal to the optic disc tend to exert a larger influence of the formation of fundus abnormalities, but that functional damage at the distal side may exert only slight influence on fundus appearance. When fibers are more proximal to the optic disc, they travel in the inner layer of the nerve fiber layer, that is the retinal surface, and enter into the center of the optic disc[6,7]. The results thus also suggest that nerve fiber drop-out occurring nearer to the optic disc is often clinically evident and exerts a strong influence on cupping.

Acknowledgements

We are grateful to Allergan SKB Co , Chibret International Ophthalmic Group of Merck Sharp & Dohme International, Banyu Pharmaceutical Co. Ltd , and Santen Pharmaceutical Co , Cannon Co. for their significant contributions to this survey This survey was supported in part by a grant from the Japan National Association for the Prevention of Blindness

References

1. Mundorf TK, Zimmerman TJ et al: Automated perimetry, tonometry, and questionnaire in glaucoma screening Am J Ophthalmol 108:505-508, 1989
2. Henson DB: An optimized visual field screening method (summary). Surv Ophthalmol 33:443-444, 1989
3. Eddy DM, Sanders LE, Eddy JF: The value of screening for glaucoma with tonometry Surv Ophthalmol 28:194-205, 1983
4. Shiose Y, Kitazawa et al: A collaborative glaucoma survey for 1988 in Japan Jpn J Clin Ophthalmol 44:653-659, 1990
5. Shiose Y, Komuro K, Itoh T, Amano M: A new system for mass screening of glaucoma. Jpn J Clin Ophthalmol 34:509-517, 1980
6. Minckler DS: The organization of nerve fiber bundle in the primate optic nerve head Arch Ophthalmol 98:1630-1636, 1980
7 Radius R, Anderson DR: The course of axons through the retina and optic nerve head Arch Ophthalmol 97:1154-1158, 1979

Longitudinal monitoring of glaucoma suspects by means of computerized disc analysis and Octopus perimetry

J. Funk

Universitäts-Augenklinik, Killianstrasse 5, D-78 Freiburg, Germany

Abstract

Computerized disc analysis and automated perimetry were used for the longitudinal monitoring of glaucoma suspects with moderate intraocular pressure elevation <25 mm Hg and without visual field defects. A statistically significant decrease in the neuroretinal rim area (p = 0 004 - 0 1) was found in seven of 29 eyes monitored >18 months and in one monitored for 15 months Since a decrease in neuroretinal rim area is non-physiological, it has to be interpreted as an important sign of ongoing glaucoma damage. Only one eye developed glaucomatous visual field loss during the follow-up period Even in this case the first sign of ongoing glaucoma was a decrease in neuroretinal rim area, the visual field defect developed subsequently This is in accordance with previous findings showing that a decrease in neuroretinal rim area commonly precedes the onset of visual field defects

Introduction

Computerized disc analysis[1,2] was developed to enable objective and accurate measurement of the neuroretinal rim area. Objective and accurate measurement of the neuroretinal rim area was thought to facilitate the diagnosis of glaucoma. However, it was found that a *single* computerized disc analysis is obviously inadequate to distinguish between healthy subjects, those suspected of having glaucoma and those with definite glaucoma[3]. This induced us to study whether *longitudinal* monitoring of the optic disc by means of computerized disc analysis is more adequate to detect early glaucoma damage.

Patients and methods

Patient selection

We monitored glaucoma suspects with moderate intraocular pressure elevation. The study entry criteria were:

- intraocular pressure <24 mm Hg in untreated eyes
- intraocular pressure ≤25 mm Hg after medical treatment

Exclusion criteria were:

- visual field defects detectable by routine automated perimetry
- improper fundus image caused by considerable cataract, corneal opacity, poor fixation or missing compliance
- inadequate pupil dilatation <5.3 mm
- any systemic or ocular diseases that may interfere with follow-up examinations

Nerve head analysis

The structure of the optic disc was examined using the Optic Nerve Head Analyzer (Rodenstock). This equipment automatically computes the three-dimensional topography of the optic disc. After manual selection of the disc edge by the investigator the border of the excavation and several disc parameters are calculated. More details about the Optic Nerve Head Analyzer including its accuracy and reproducibility have already been published[2,4-7]. Nerve head analysis was repeated every three to six months.

Perimetry Update 1990/91, pp. 79-83
Proceedings of the IXth International Perimetric Society Meeting,
Malmö, Sweden, June 17-20, 1990
edited by Richard P Mills and Anders Heijl

Visual field testing

Automated perimetry (Octopus 2000R, program G1[8]) was used for visual field analysis. Usually visual field testing was repeated every six to 12 months.

Statistics

The neuroretinal rim area of each eye was plotted as a function of the observation time. Linear regression analysis was then performed to determine the mean change of neuroretinal rim area during the follow-up period. The 67% confidence interval was used to define the standard deviation of the initial neuroretinal rim area and the neuroretinal rim area after 18 months.

Results

Eighty-two eyes (45 patients) were monitored for at least six months, 51 eyes (27 patients) were monitored for at least 12 months, 29 eyes (15 patients) were monitored for at least 18 months. Fig. 1 gives the neuroretinal rim area after 18 months as a function of the initial value. Only those eyes monitored >18 months were plotted in the diagram. Both the 18 months value and the initial value were calculated from a linear regression analysis of the measured data. The standard deviation bars indicate the 67% confidence interval of the 18 months value. The standard deviation of the initial value is of the same order. For purposes of clarity it is not plotted in the diagram. Apparently, there are seven eyes with marked decrease in neuroretinal rim area during the follow-up period. Table 1 gives the amount of decrease in neuroretinal rim area together with its significance level in these seven cases.

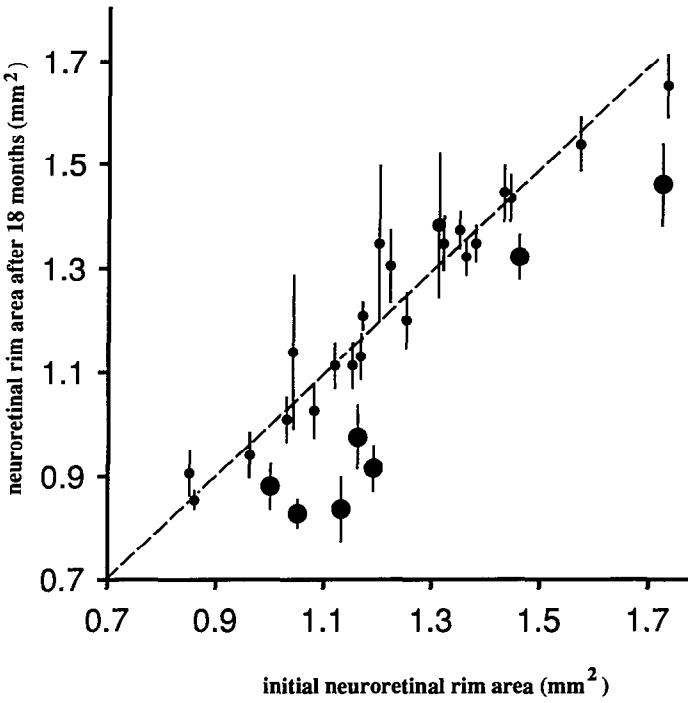

Fig 1 Neuroretinal rim area after 18 months versus initial neuroretinal rim area. Both the 18 months' value and the initial value were extrapolated from a linear regression analysis of the measured data. Seven eyes with marked decrease in neuroretinal rim area are given as large black circles.

Table 1. Amount of decrease in neuroretinal rim area and error probability of the corresponding linear regression analysis. All eyes with marked decrease in neuroretinal rim area and follow-up time >18 months were listed (*cf* Fig. 1).

Patient	*Age (years)*	*Δ neuroretinal rim area (mm^2)*	*p*
MJ	80	–0.29	0.033
IZ	61	–0.27	0.077
CN r	60	–0.27	0.004
CN l	60	–0.13	0 044
CJ r	51	–0.11	0.100
CJ l	51	–0.25	0 023
TD	35	–0.18	0 027

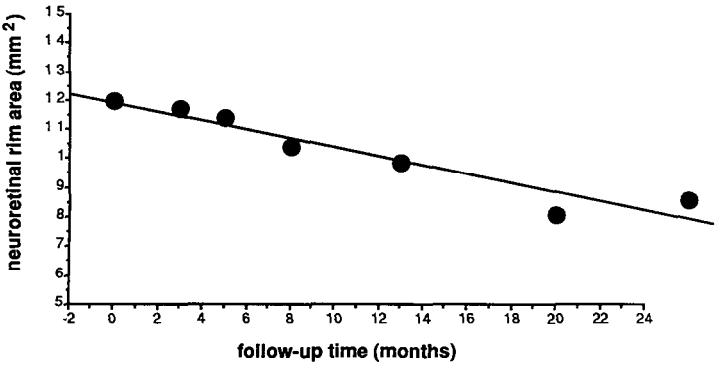

Fig 2 Neuroretinal rim area as a function of the observation time, patient CN (*cf* Table 1). The measured values are given as black circles together with the regression line

A marginally significant decrease in neuroretinal rim area ($p = 0.062$) was found in only one out of 22 eyes monitored >12 but <18 months and in none of 31 eyes monitored >6 but <12 months. No changes in the total disc area were found during the follow-up period.

Fig. 2 gives an example of a marked decrease in neuroretinal rim area (patient CN, see Table 1). The measured values of the neuroretinal rim area are plotted as a function of the observation time together with the regression line.

Up until now only one eye has developed glaucomatous visual field loss. Even in this case the first sign of ongoing glaucoma was a decrease in neuroretinal rim area. Fig. 3a shows the excavation border at the first examination (inner line, dark) and 14 months later (outer line, light). As can be seen in Fig. 3b, the change in neuroretinal rim area preceded the onset of visual field defects. During the first 14 months the mean deviation remained <-0.8, but the neuroretinal rim area decreased. After 14 months the visual field began to deteriorate resulting in an increase of the mean deviation from -2.0 to +2.5.

Conclusions

Longitudinal monitoring of glaucoma suspects by means of computerized disc analysis proved to be an adequate method to detect changes in the disc structure. Despite the limited accuracy of the device the detected decrease in neuroretinal rim area was significant in seven out of 29 cases monitored for at least 18 months, the error probability being <0.05 in five cases and <0.1 in two additional cases. Since a significant decrease in neuroretinal rim area is non-physiological[9], it has to be interpreted as an important sign of ongoing glaucoma damage. The decrease in neuroretinal rim area found by computerized disc analysis obviously precedes the appearance of visual field defects. This had already been concluded from an earlier study[10] of the correlation between the neuroretinal rim area and the corresponding threshold sensitivity. The study showed that eyes with defects in the central part of the visual field usually have a

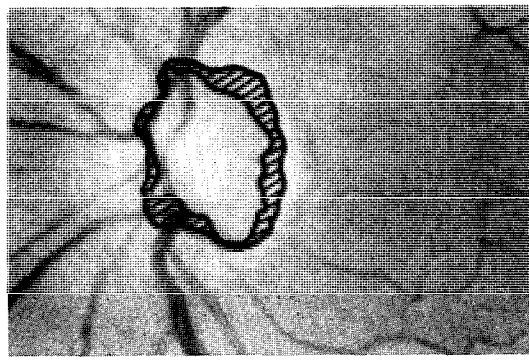

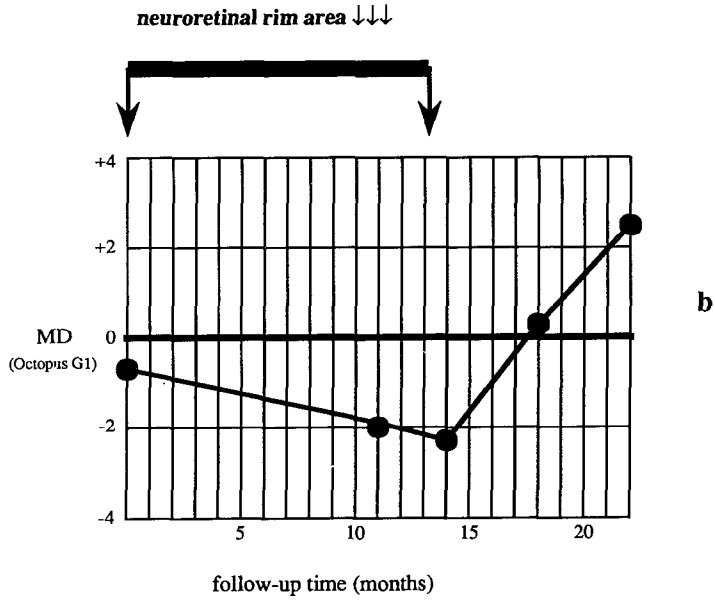

Fig 3a Excavation border found by the Optic Nerve Head Analyzer at the first examination (inner line, dark) and 14 months later (outer line, light), patient TD (*cf* Table 1) *b* Time course of the visual field index "mean deviation", same patient as in Fig 3a; as indicated by the bar top left the decrease in neuroretinal rim area preceded deterioration of the visual field

small neuroretinal rim area in the corresponding temporal disc quadrant. A large neuroretinal rim area therefore must drop before a visual field defect occurs. In addition to this study many observers have already described that changes in the disc structure found by clinical examination appear earlier than visual field defects[11]. In the present study, only one eye developed glaucomatous visual field loss. In accordance with the findings mentioned above, the first sign of ongoing glaucoma in this case was a decrease in neuroretinal rim area found by computerized disc analysis. Apparently at least 18 months of follow-up are necessary to obtain reliable results. This is presumably caused by the limited accuracy of the equipment. In the present study only one eye monitored 15 months, but seven eyes monitored >18 months, showed a significant decrease in neuroretinal rim area. Perhaps further improvements of the technique will enable more rapid detection of glaucomatous nerve head changes.

References

1. Cornsweet TN, Hersh S, Humphries JC, Beesmer RJ, Cornsweet DW: Quantification of the shape and color of the optic nerve head. In: Brenin GM, Siegel IM (eds) Advances in Diagnostic Visual Optics, pp 141-149. New York: Springer 1983
2. Caprioli J, Klingbeil U, Sears M, Bryony P: Reproducibility of optic disc measurements with computerized analysis of stereoscopic video images Arch Ophthalmol 104:1035-1039, 1986
3. Caprioli MD, Miller JM: Videographic measurements of optic nerve topography in glaucoma. Invest Ophthalmol Vis Sci 29:1294-1298, 1988
4. Bishop KI, Werner EB, Krupin T, Kozart DM, Beck SR, Nunan FA, Wax MB: Variability and reproducibility of optic disc topographic measurements with the Rodenstock optic nerve head analyzer Am J Ophthalmol 106:696-702, 1988
5. Mikelberg FS, Douglas GR, Schulzer M, Cornsweet TN, Wijsman K: Reliability of optic disc topographic measurements recorded with a video-ophthalmograph Am J Ophthalmol 98:98-102, 1984
6. Shields MB, Martone JF, Shelton AR, Ollie AR, MacMillan J: Reproducibility of topographic measurements with the optic nerve head analyzer. Am J Ophthalmol 104:581-586, 1987
7. Shields MB, Tiedeman JS, Miller KN, Hickingbotham D, Ollie AR: Accuracy of topographic measurements with the Optic Nerve Head Analyzer. Am J Ophthalmol 107:273-279,1989
8. Flammer J, Jenni F, Bebie H, Keller B: The Octopus glaucoma G1 program. Glaucoma 9:67-72, 1987
9. Funk J, Grehn F: Correlation between neuroretinal rim area and age in normal subjects Graefe's Arch Clin Exp Ophthalmol 227:544-548, 1989
10. Funk J, Bornscheuer C, Grehn F: Neuroretinal rim area and visual field in glaucoma Graefe's Arch Clin Exp Ophthalmol 226:431-434, 1988
11 Anderson DR: The optic nerve in glaucoma. In: Duane TD, Jaeger EA (eds) Clinical Ophthalmology, Ch 48, Vol 3. Philadelphia: Harper & Row 1985

Scanning laser ophthalmoscope for static fundus perimetry in glaucomatous nerve-fiber-bundle defects

Joerg Stuermer[1], Carsten Schroedel[2] and Wolfgang Rappl[2]

[1]*Ophthalmology Department, University Hospital, CH-8091 Zurich, Switzerland;*
[2]*G. Rodenstock Instruments Ltd., D-8012 Ottobrunn, Germany*

Abstract

The advantage of fundus perimetry is an exact, direct correspondence between fundus image and simultaneous perimetric result. For static fundus perimetry, the authors modified the tightly confocal Rodenstock scanning laser ophthalmoscope by installing an infrared diode laser for fundus imaging, providing a background brightness at the same level as that of conventional hemispheric perimeters The originally installed HeNe laser is still used for generating the stimuli, background, and fixation aid by computer-controlled acousto-optic modulation Software was developed to change stimulus size and intensity as well as to place the stimulus at any desired point in the 18° × 13° field. For correction of fixation shifts, manual fundus tracking was incorporated The first clinical experience in 56 eyes of 43 glaucoma patients with perimetrically (Octopus) or photographically (red-free fundus photography) proven nerve fiber layer defects is reported. Despite the unfavorable increase in wavelength, a high rate of detection of these defects could be determined. Fundus perimetry was seen to provide a more exact description of scotomata relative to their morphological location

Introduction

Exact correlations between observable morphological changes and psychophysical alterations in different ocular pathologies are difficult to obtain with conventional clinical investigative methods. Indirect correspondence can be obtained by simply overlaying results of projection perimetry onto fundus photographs, but the exactitude of such indirect correlations is limited mostly by the fixation ability of the subject[1].

Fundus perimetry, by definition, is the direct combination of simultaneous fundus imaging and visual field testing in one device. This allows direct visualization of the test location and therefore yields the desired point-to-point correspondence between fundus image and perimetric result. Since exact fixation is guaranteed by instant control, exact follow-up of the margins of deep scotomata, such as glaucomatous nerve-fiber-bundle defects (NFBD) becomes possible.

Since the simple direct ophthalmoscope which Trantas[2] used to perform the first fundus perimetry, the development of fundus perimetric devices has come a long way, including several modified Japanese fundus cameras with[3-5] and without[6,7] infrared illumination, to the presently used Scanning Laser Ophthalmoscope (SLO)[8,9]. The normal version of the latter allows real-time fundus observation under light intensities one hundred times less than those in conventional fundus photography, but, nevertheless, still much higher than those in conventional perimetry and, therefore, for our purposes, had to be further reduced.

Material and methods

Device

For the presently used[10,11] low background brightness, static fundus perimetry, an infrared laser for fundus imaging has been installed in the tightly confocal, prototype SLO from Roden-

Supported by the Swiss National Fund for Scientific Research Grant No 3200-02583

Address for correspondence Joerg Stuermer, M.D , Glaucoma Department, Moorfields Eye Hospital, City Road, London EC1V 2PD, UK.

Perimetry Update 1990/91, pp. 85-92
Proceedings of the IXth International Perimetric Society Meeting,
Malmö, Sweden, June 17-20, 1990
edited by Richard P. Mills and Anders Heijl

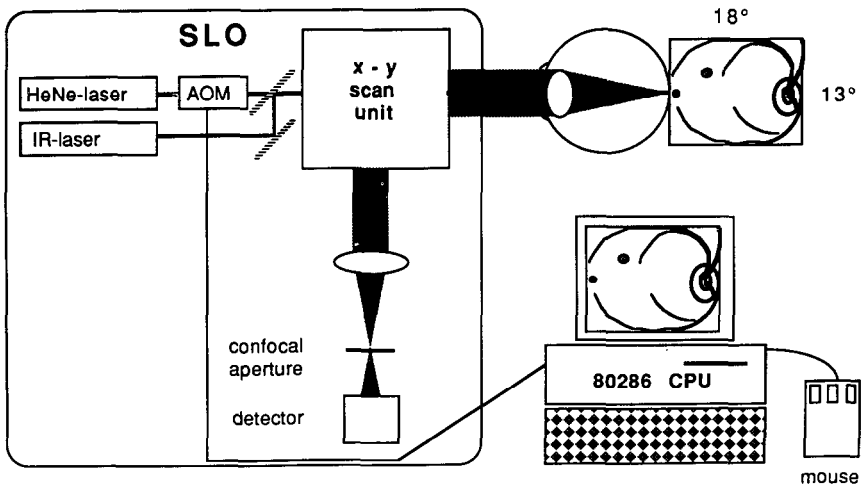

Fig 1 Principal setup of the SLO foı low background brightness, static fundus perimetry On the left side, the measuring head of the SLO contains the two lasers, of which the HeNe laser is modulated (AOM) for background, stimuli, and fixation aid generation Then the two lasers are united in a semitransparent mirror and deflected in synchrony in the x and y directions to create the scanning field Detection is done after scanning the light collected back through the same optics (confocal arrangement) On the right side is the fundus image, which can be seen at the monitor The computer controls the modulation. Perimetry is performed by the movements and the three keys of the mouse

stock (Table 1). This diode laser is scanned in synchrony (Fig. 1) with the originally installed HeNe laser, still used for generation of stimuli, fixation aid, and background illumination by acousto-optic modulation. This allows the scanning laser beam intensity to be briefly increased or decreased at a fixed point on the raster, appearing to the subject as a small brightened point flashed on the raster for stimulus or seen as a constant point or cross as a fixation aid. The background is dimmed to the same level as that in conventional perimetry, *i.e* , about 8 asb, allowing non-mydriatic fundus observation. The whole test procedure is controlled by an IBM AT clonc.

Table 1 Configuration of the SLO for low-background brightness, static fundus perimetry

Rodenstock prototype confocal SLO
18° × 13° scanning field
High resolution of 2 arc-min/pixel
Infrared (780 nm) diode laser for permanent high quality fundus imaging
Background brightness 8 asb (non-mydriatic fundoscopy)
HeNe laser (633 nm) for generation of stimuli, background illumination and fixation aid by acousto-optic modulation
Manual fundus tracking

Software has been developed to change the different examination parameters, such as stimulus form, size and intensity and to place it at any desired point in the 18° × 13° scanning field. Manual fundus tracking is incorporated, but no staircase threshold strategy, such as "static isoptometry"[12] or hybrid technique[13] with a Goldmann III stimulus of 0.1 sec duration, is performed.

Patients

Fifty-six eyes of 43 glaucoma patients (Table 2) with photographically or perimetrically proved NFBD were investigated by static fundus perimetry. Twenty-nine of these patients had primary open-angle glaucoma, and 12 normal tension glaucoma. The mean age of this group was almost 64 years, and visual acuity was mostly intact.

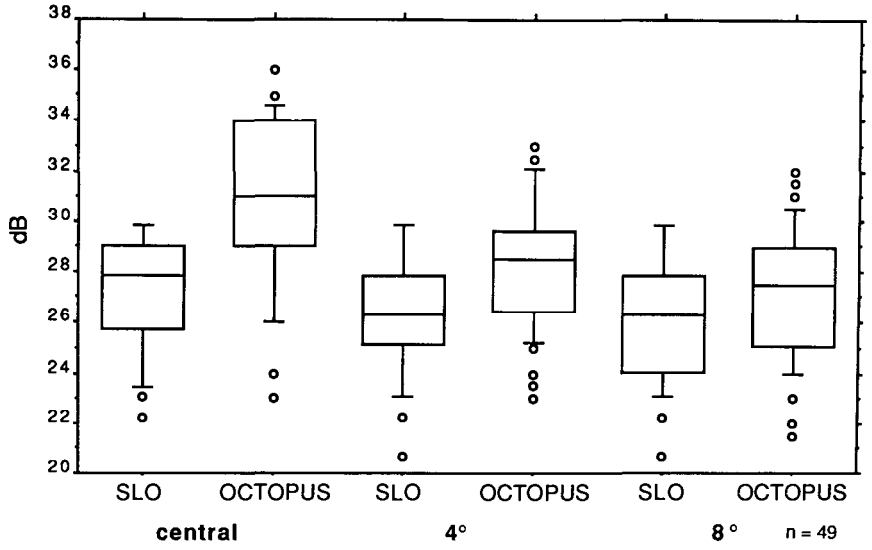

Fig 2 Sensitivity in low background brightness, static fundus perimetry *versus* Octopus Box-and-whisker plot; y-axis sensitivity in dB (corrected for Octopus dB units). Mean sensitivity for fundus perimetry (SLO) and Octopus in three different eccentricities (central, 4° and 8°) Mean sensitivity central is 27.2±2 2 dB for fundus perimetry and 31 0±3 4 dB for Octopus (at 4°: 26.5±2 6 dB *versus* 28 3±2 5 dB; at 8°: 26.1±2 4 *versus* 27 3±2 5 dB). The difference becomes less from central to peripheral points (central: 3.82±4 5 dB; paired-t = 5 887; p<0 0001; at 4°: 1.76±3 68 dB; paired-t = 3 343; p<0 005; at 8°: 1 14±3.88 dB; paired-t = 2 047; p<0.05).

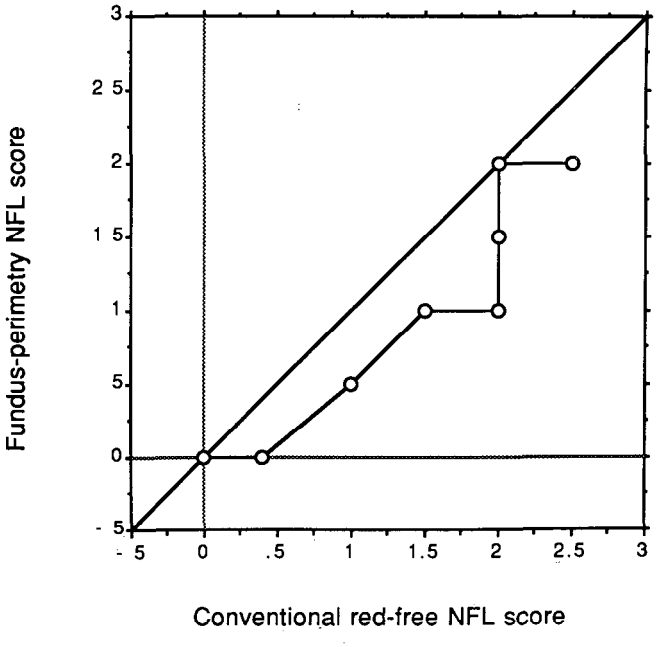

Fig 3 Nerve fiber layer score in low background brightness, static fundus perimetry *versus* conventional red-free photography Percentile comparison of subjective scoring from 0 (invisible) to 3 (excellent); x-axis: red-free fundus photography score; y-axis: fundus perimetry under infrared illumination score (conventional mean score 1 50±0.90 *versus* fundus perimetry 0.95±0 68; paired-t = -5 88; p<0 001).

Table 2. Glaucoma patients

Number	43 patients
Sex	28 women/15 men
Age	mean 63.9±9 3 years (40-82)
Diagnosis	29 primary open-angle glaucoma
	12 normal tension glaucoma
	1 juvenile glaucoma
	1 chronic angle-closure glaucoma (after filtering surgery)
Side	17 right/13 left/13 both eyes
Visual acuity	mean 20/23 (20/100-150/100)

Results

In ten normal subjects and in the still normal retinal areas of 39 eyes of the glaucoma patients, quantitative comparability to conventional perimetry was tested. In the center of the visual field, the mean sensitivity threshold was significantly lower than that in Octopus perimetry (Fig. 2), due to the monochromatic red of the light source (633 nm) and the slightly increased background brightness (Octopus 4 asb, SLO 8 asb). This difference decreased in the more peripheral points, indicating a flatter contour of the hill of vision under these conditions.

Visibility of the nerve fiber layer was still slightly inferior to that in conventional red-free fundus photography (Fig. 3), but the unfavorable effect of the increase in wavelength of the illuminating light is at least partly compensated for by the confocal detection mode. In a subjective scoring, the visibility of the nerve fiber layer in fundus perimetry proved to be slightly less effective than in conventional red-free photography. This difference seems to be more

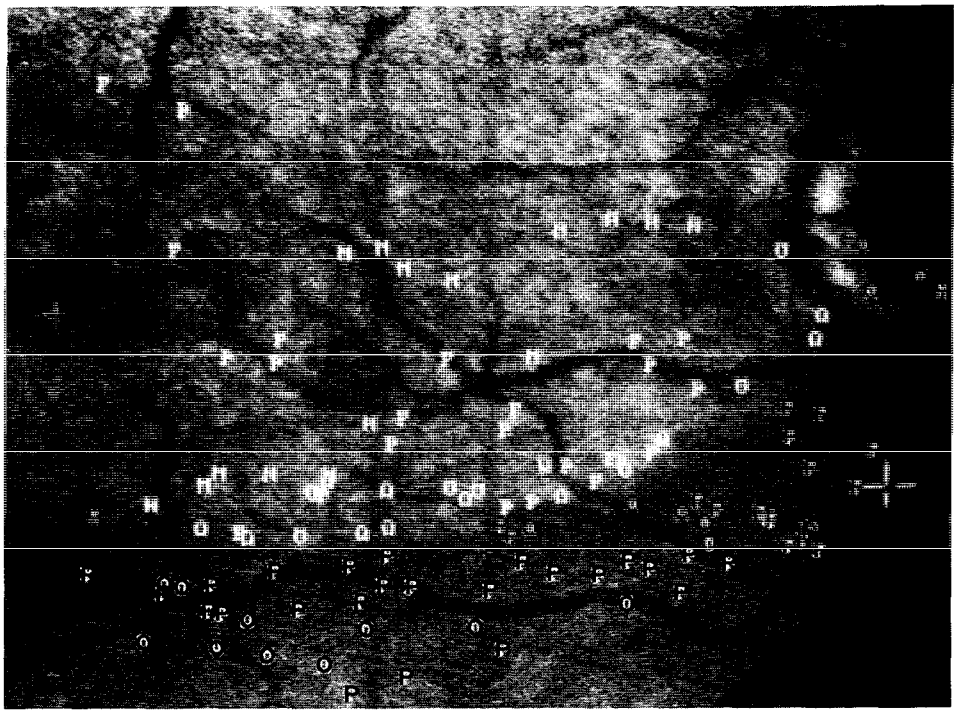

Fig 4 Example 1: left eye of a 55-year-old patient with primary open-angle glaucoma. In the fundus perimetry picture (reversed), a broad NFBD can easily be seen in the lower half. All white letters mean stimuli seen; all black ones, stimuli not seen. The fixation cross is seen on the left side at the margin of the picture The other cross on the vascular branching is the reference cross used for manual fundus tracking.

pronounced in patients with diffuse atrophy of the remaining nerve-fiber layer, which is more easily detectable in a panoramic view of the fundus. Nevertheless, in 33 of 56 eyes (58.9%), the NFBD were clearly detectable by fundus perimetry. In 20 further eyes (35.7%), NFBD at the upper and lower pole and at the nasal side of the optic nerve head were visible but, due to the limited measuring field, could not be evaluated.

In the detectable NFBD, the following facts could be demonstrated:

1. Borders of deep relative or absolute scotoma are sharp and well defined, at least at the macular side, and correspond exactly to the underlying NFBD (Fig. 4). When there was no general reduction of sensitivity, we could not see any sensitivity loss over the normal nerve fiber layer adjacent to the borders of these scotomata. On the peripheral side of the nerve fiber layer defect, which could only be evaluated in a few, small slit-like defects, the border of the scotoma also seems to be steep and not gradual.
2. A periphery *versus* central sensitivity gradient in relative scotomata could not be proven.
3. Some nerve fiber bundle defects are clearly visible at the margin of the optic nerve head, but no sensitivity alterations could be detected corresponding to these defects (Fig. 5).
4. The limited size of the scanning field only permits perimetry of the posterior pole between optic nerve head and foveola. This small field gives the false impression of broad, more centrally beginning visual field defects when compared to the results of conventional perimetry (program G-1 of the Octopus), where these defects seem to be smaller and often more peripheral.

We also performed fundus perimetry on glaucomatous parapapillary changes. Over the zone with almost total chorio-pigment-epithelio-retinal atrophy, characterized by whitish color, visible large choroidal vessels and visible sclera (zone "Beta" according to Jonas[14,15]), an absolute scotoma could be detected (Fig. 6). The modulation cut-off of our device at 20 dB does not

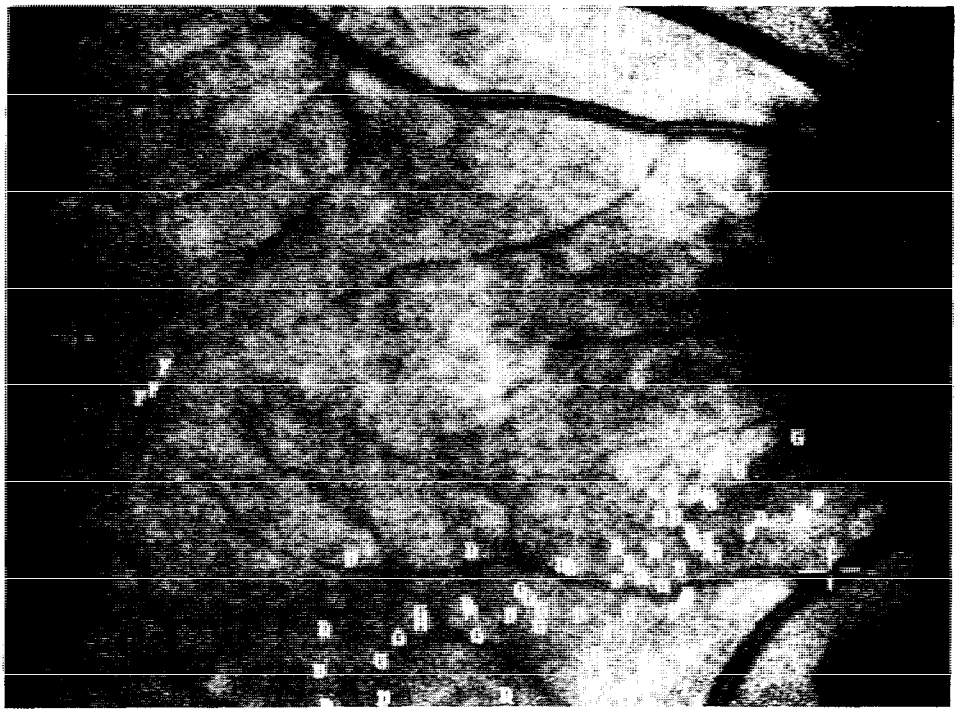

Fig 5 Example 2: left eye of a 67-year-old patient with normal-tension glaucoma In the fundus perimetry picture (reversed), the defect can easily be seen in the lower half All white stimuli could be seen even over the NFBD, thus proving that it is not absolute and probably could be better detected in the mid-periphery of the visual field. Central visual fields with computerized static perimetry were normal throughout.

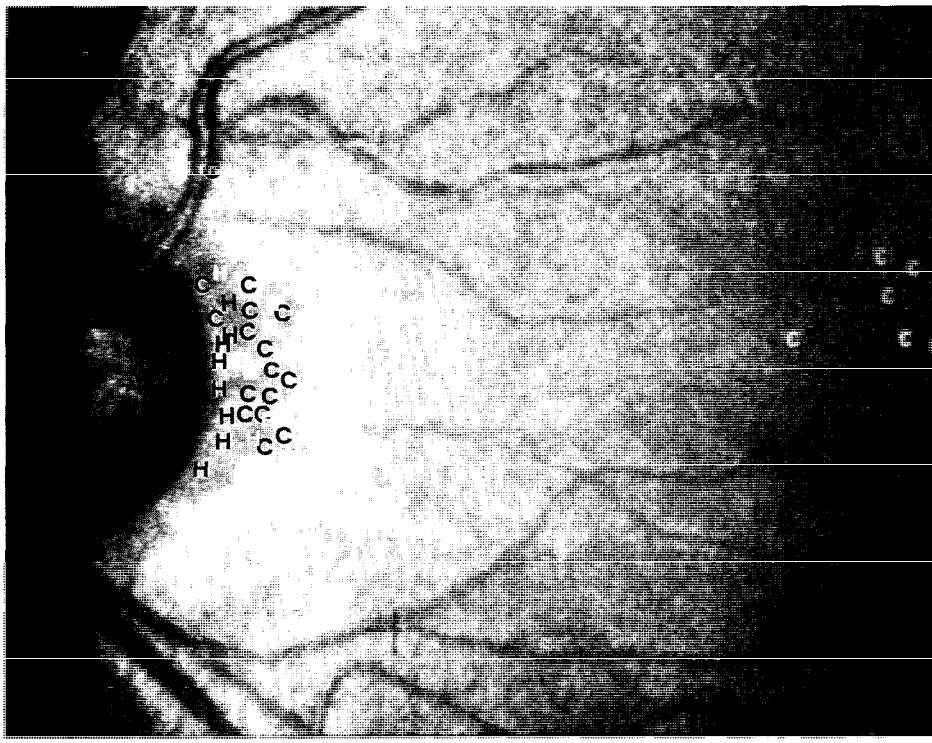

Fig 6 Example 3: right eye of a 40-year-old patient with primary open angle glaucoma. Fundus perimetry over the parapapillary atrophy shows two different zones: one on the inner side with an absolute scotoma (no stimulus seen) and one on the outer side with a relative scotoma, where the more intense stimuli could be detected These two different scotomata are congruent with the zone of total respectively relative parapapillary atrophy

allow exact assessment of the depth of these scotomata. The more peripheral zone "Alpha", with irregular hyper- and hypo-pigmentation, proved to show mild to moderate sensitivity reduction. The extent of the relative scotoma corresponds well with the visible parapapillary changes, but these changes are – in comparison to conventional fundus photography – more pronounced and larger under the infrared illumination used in our device.

Discussion

By installing an infrared laser for permanent, high-quality fundus imaging, background illumination for static fundus perimetry in the scanning laser ophthalmoscope could be reduced to the same level as that in conventional perimetry. This allows not only non-mydriatic fundoscopy but also comparable results. Exact correlation between observable morphological changes and psychophysical alteration for glaucomatous NFBD are a demanding challenge for fundus perimetry. This is especially difficult because, in almost all available fundus perimetry devices, high wavelength illumination is used for fundoscopy, unfavorable in the detection of superficial retinal structures and their alterations. Nevertheless, it could be demonstrated by kinetic fundus perimetry (in addition to conventional methods) that visual field defects in juvenile glaucoma patients are only reversible after lowering intraocular pressure, when no nerve fiber layer defect could be seen[16]. The same Japanese group[17] proved that early foveal dysfunction in glaucoma patients is correlated to diffuse atrophy or slit-like defects in the papillo-macular bundle of the nerve fiber layer. In these cases, a good correspondence between small paracentral scotomata and nerve fiber layer defects could be demonstrated by a combi-

nation of static and kinetic fundus perimetry.

Typical, small arcuate nerve fiber bundle defects often cause scotomata which are only detectable at the nasal periphery of these defects[18], therefore known for a long time as the "nasal step". If only the central part of this nerve fiber bundle defect is visible (or only the central visual field is tested), no visual field defect (Fig. 5) or only a slight increase in short-term fluctuations[11] could be detected.

In wedge-shaped nerve fiber layer defects, either a shallower or no depression could be detected near the blind spot by kinetic fundus perimetry[18], while deeper depressions were detected further away from the blind spot. As we did not detect such sensitivity gradients in static fundus perimetry, this could either be due to the very bright stimulus used for kinetic testing or to the limited dynamic range of our device. The exact correspondence between scotomata and visible nerve fiber layer alterations is subject to discussion: in kinetic fundus perimetry, either the scotoma seems to be broader[19] throughout or, while there was exact congruence at the distal portion, near the blind spot, the sensitivity depression was smaller[18] than the discernible nerve fiber layer defect. While one of these groups[19] postulated a gradual border of these scotomata, the other[18] admitted a sharp, well-defined border at least at the macular side. But these gradual borders of deep scotoma, inherent in kinetic perimetry, are also seen in conventional static perimetry[20]. This scattering of responses at the borders of deep scotomata is most probably due to small saccadic fixation shifts, as their extent of 0.5 to 1.0 degree[21] is exactly the same as the width of this uncertain area[18]. If an exact correlation for these fixation movements is performed, as it could only be done by static fundus perimetry with careful, either manual – as in our device – or automatic[21,22] fundus tracking, this uncertainty is excluded, and borders of wedge-shaped scotomata caused by glaucomatous nerve fiber bundle defects are well defined and congruent[10,11,22] (Fig. 4).

The exact assessment of the blind spot in normals and in the presence of parapapillary changes, has been another interesting field for fundus perimetry since the very beginning[2,23]. On the one side, parapapillary alterations in glaucoma are seen very often, and their extent correlates well to the stage of the glaucoma[14,15]. On the other side, the increase of blind spot size in conventional kinetic perimetry has been known for a long time as a sign of progression of glaucoma. While it is obvious that a total parapapillary atrophy, where we can almost see the bare sclera from inside, causes a corresponding absolute scotoma, the sensitivity depression caused by the relative chorio-pigment-epithelio-retinal atrophy characterized by irregular hyper- and hypo-pigmentation are mild to moderate (Fig 6) Due to limitations in dynamic range and measuring field size, these findings are only preliminary.

In summary, the scanning laser ophthalmoscope is a superb tool for psychophysical examination in different ocular pathologies. The configuration for static fundus perimetry used allows direct comparison of results with conventional perimetry. A more exact description of visual field abnormalities induced by morphological changes, such as NFBD and peripapillary atrophy in glaucoma, is now possible.

The fundus perimetry version of the now available, first production version scanning laser ophthalmoscope from Rodenstock offers two-fold enlargement of the scanning field and a dynamic range of more than 30 dB. Automatic fundus tracking and staircase threshold determination, soon to be incorporated, will improve static fundus perimetry considerably and allow semi-automatic testing of a previously selected region of interest

Acknowledgement

The authors thank Phillip Hendrickson of the Ophthalmology Department in Zurich for proofreading the manuscript

References

1. Bek T, Lund-Andersen H: Accurate superimposition of perimetry data onto fundus photographs. Acta Ophthalmol 68:11-18, 1990
2 Trantas NG: Applications et résultats d'un moyen simple d'examen de la photosensibilité de la rétine Bull Soc Ophtalmol Fr 55:499-513, 1955

3. Kani K, Eno N, Abe K, Ono T: Perimetry under television ophthalmoscopy Doc Ophthalmol Proc Ser 14:231-236, 1977
4. Kani K, Ogita Y: Fundus controlled perimetry. Doc Ophthalmol Proc Ser 19:341-350, 1979
5. Ohta Y, Miyamoto T, Harasawa K: Experimental fundus photo perimeter and its application Doc Ophthalmol Proc Ser 19:351-358, 1979
6 Inatomi A: A simple fundus perimetry with fundus camera Doc Ophthalmol Proc Ser 19:359-362, 1979
7. Isayama Y, Tagami Y: Quantitative maculometry using a new instrument in cases of optic neuropathies. Doc Ophthalmol Proc Ser 14:237-242, 1977
8. Timberlake GT, Webb RH, Mainster MA: Direct retinal localization of scotomata. Invest Ophthalmol Vis Sci (ARVO Suppl) 92: 1980
9. Timberlake GT, Mainster MA, Webb RH, Hughes GW, Trempe CL: Retinal localization of scotomata by scanning laser ophthalmology Invest Ophthalmol Vis Sci 22:91-97, 1982
10. Stuermer J, Schroedel C, Rappl W: Low-background-brightness, static SLO fundus-perimetry. Invest Ophthalmol Vis Sci (ARVO Suppl) 31/4:504, 1990
11 Stuermer J, Schroedel C, Rappl W: Scanning laser ophthalmoscope for static fundus-controlled perimetry. In: Nasemann JE, Burk ROW (eds) Scanning Laser Ophthalmoscopy and Tomography Berlin: Quintessenz Verlag 1990
12. Ogita Y, Sotani T, Kani K, Imachi J: Fundus controlled perimetry in optic neuropathy. Doc Ophthalmol Proc Ser 26:279-285, 1981
13 Van de Velde FJ, Jalkh AE, Katsumi O, Hirose T, Timberlake GT, Schepens CL: Clinical scanning laser ophthalmoscope applications. In: Nasemann JE, Burk ROW (eds) Scanning Laser Ophthalmoscopy and Tomography. Berlin: Quintessenz Verlag 1990
14 Jonas JB, Nguyen XN, Gusek GC, Naumann GOH: Parapapillary chorioretinal atrophy in normal and glaucoma eyes I. Morphometric data. Invest Ophthalmol Vis Sci 30:908-918, 1989
15. Jonas JB, Naumann GOH: Parapapillary chorioretinal atrophy in normal and glaucoma eyes. II. Correlations. Invest Ophthalmol Vis Sci 30:919-926, 1989
16. Mizokami K, Tagami Y, Isayama Y: The reversibility of visual field defects in the juvenile glaucoma cases. Doc Ophthalmol Proc Ser 19:241-246, 1979
17 Mizokami K, Katsumori N, Miyazawa H: Early foveal dysfunction in glaucoma. Doc Ophthalmol Proc Ser 49:469-474, 1987
18. Okubo K, Mizokami K: Fundus perimetry and Octopus perimetry for the evaluation of nerve fiber layer defects. Doc Ophthalmol Proc Ser 42:457-466, 1985
19 Ogawa T, Furuno F, Seki A, Miyamoto T, Ohta Y: Kinetic quantitative perimetry of retinal nerve fiber layer defects in glaucoma by fundus photo-perimeter. Doc Ophthalmol Proc Ser 35:27-34, 1983
20 Haefliger IO, Flammer J: Increase of the short-term fluctuation of the differential light threshold around a physiologic scotoma. Am J Ophthalmol 107:417-420, 1989
21. Chapero-Rueda V: Hochauflösende fundusstabilisierte Perimetrie – Ein System aus Eye-tracker und Laser Scan Ophthalmoskop zur Erzeugung und Nachführung von Mustern am Augenhintergrund Inaugural dissertation Physik Universität Heidelberg 1988
22 Chapero-Rueda V, Bille J, Dreher A, Reiter K, Weinreb RN: Fundus stabilized high resolution perimetry. Invest Ophthalmol Vis Sci (ARVO Suppl) 29/4:357, 1988
23. Masukagami H, Furuno F, Matsuo H: Blind spot of normal and high myopic eyes measured by fundus photo-perimetry. Doc Ophthalmol Proc Ser 49:489-493, 1987

Microperimetry with the scanning laser ophthalmoscope

Frans J. Van de Velde, Alex E. Jalkh and Ann E. Elsner

Eye Research Institute of Retina Foundation, 20 Staniford Street, Boston, MA 02114, USA

Abstract

Psychophysical stimuli are generated by computer controlled acousto-optic modulation of the laser beam in scanning laser ophthalmoscopy The retina with stimuli is observed on a monitor. Perimetry is performed using 256 potential stimulus intensity levels and a combination of 633 nm and 780 or 830 nm background illumination Linear or logarithmic interval, incremental or decremental stimuli relative to a low or high photopic background are therefore possible. A fundamental advantage for the examiner is the ability to see psychophysical stimuli presented on the retina in real-time Accurate monitoring of fixation and localization of the stimulus is a major advantage. A static technique eliminates reaction time artifacts. The term microperimetry refers to the high resolution typically obtained (<1 degree) in the posterior pole Three psychophysical static microperimetry techniques have been described before. Microperimetry with the SLO is quite different from conventional field testing. Potential light scatter, Maxwellian viewing and bleaching are factors that influence the outcome of clinical results To prove the reliability of quantitative perimetry and to derive optimal testing parameters, the authors evaluated the Weber-Fechner relation under various testing conditions in normals

Introduction

Algorithms for three psychophysical techniques with the scanning laser ophthalmoscope (SLO) have already been described: (1) automated microperimetry with a precise user predefined configuration of test locations on the retina and a new reliability index, the bivariate area of fixation. Certain test locations can also be designated as a reference to normalize data; (2) manual (or hybrid) microperimetry, in which the static stimulus is placed on the retina under visual feedback by the examiner during testing, effectively combining the flexibility of a kinetic procedure with the rigor of static techniques; and (3) a threshold (or static) microperimetry using a staircase procedure to measure the retinal sensitivity at a single locus on the retina[1-9].

Microperimetry with the SLO, however, is quite different from conventional field testing. A scanning laser beam (RS-170 interlaced 60 Hz video) is used to illuminate the retina and to create the stimuli. Background illumination and stimuli are therefore spatially and temporally "quantitized" and are subject to small variations in space and time. Furthermore, illumination is Maxwellian view and monochromatic (633 nm). All of this in contrast to the homogeneous Ganzfeld background of traditional perimeters, *i e* , Newtonian, stable and white (3000°K). Until recently, stimuli were decrementally relative to a monochromatic (633 nm) and high background retinal irradiance (100-300 $\mu W/cm^2$) (but see[3]) which was necessary to generate a SLO video image. The recent addition of a second diode 780 or 830 nm laser allows a substantial reduction in 633 nm light, and therefore perimetry under low photopic background conditions with incremental stimuli can also be performed.

To demonstrate the reliability of quantitative perimetry, we evaluated the Weber-Fechner relationship under various testing conditions in three normal observers. At lower background light levels, the law of Weber-Fechner, $\log \Delta I/I = c$ prevailed. The failure of this law, due to bleaching of photopigment or saturation of neural response, became evident at higher light levels and $\Delta I/I$ increased moderately. Other problems with high illumination perimetry were

This work was supported by an NIH-NEI grant EY07624 to AE

Address for correspondence Dr. Frans J. Van de Velde, Betsberg, Geraardsbergsestw 38, 9860 Oosterzele, Belgium

Perimetry Update 1990/91, pp. 93-101
Proceedings of the IXth International Perimetric Society Meeting,
Malmö, Sweden, June 17-20, 1990
edited by Richard P. Mills and Anders Heijl

identified during clinical trials of the hybrid microperimetry technique. From these experiments, we derived optimal examination parameters for our clinical microperimetry algorithms. We were also able to identify the factors that may influence the outcome of clinical results. Some of the problems identified are potential light scatter, and bleaching. Maxwellian viewing has important theoretical and practical clinical consequences.

Material and methods

The instrument used for the Weber-Fechner studies was a confocal scanning laser ophthalmoscope, described before[5,8,9], capable of viewing the entire posterior pole 28×28 degrees). At present five wavelengths can be used for psychophysical testing or imaging. We combined visible 633 nm and invisible 830 nm background illumination for our experiments.

Psychophysical stimuli are generated by computer controlled acousto-optic modulation of the laser beam in scanning laser ophthalmoscopy. The graphics board has a resolution of 8 bits. Perimetry is performed using 256 potential stimulus intensity levels. This matches the dynamic range of the AOM (max 30 dB) which is carefully calibrated.

The Weber-Fechner relation was verified under various testing conditions in three normal young adults ranging in age between 23 and 32 years. We used a single staircase procedure to measure the retinal sensitivity along the horizontal meridian at 0, 1, 2, 4, 8, and 16 degrees of eccentricity. The background irradiance for all points in a meridian measurement was a constant level. Target locations were selected to avoid blood vessels and the optic disc. The light levels used were 1.74, 3.74, 4.05, 4.35, 4.65, 4.95 and 5.03 log Td. Target size was 21 minarc on a side. Stimulus duration was 200 ms. In one subject a smaller test size was also used, 7 minarc on a side.

A fixed number of reversals was taken into consideration after the first valid reversal. Threshold was operationally defined as the mean of these reversals. We also calculated the standard deviation of the reversals and the mean amplitude of the reversals in the staircases. Staircases were plotted graphically to verify slope and general correlation of samples. The ideal staircase produced two, three, or four like responses before reversal.

Experience obtained in light scatter and consequences of Maxwellian viewing were obtained from our extensive clinical studies (1200 hybrid microperimetry examinations to date)[1,2,4].

Results

Weber-Fechner relation

Weber-Fechner behavior does not hold as the retinal illuminance increases above about 1.74 log Td, which is shown as an increase in the mean amplitude of the reversals with retinal illuminance (Fig. 1). This is particularly true for peripheral targets, as seen in Fig. 2, which shows that the Weber fraction has a flatter shape across eccentricities for the low retinal illuminance. The failure of the curves to change systematically with increasing retinal illuminance may be due to more variable performance for both increasing retinal illuminance and increasing eccentricity, *i.e.*, there is a striking increase in the width of the psychometric function. This is demonstrated by plotting the standard deviation of the reversals (Fig. 3). The increase in the width of the psychometric function may indicate that we were at the end of the dynamic range of the visual system. The increase in standard deviation is also striking with the smaller targets (Fig. 4). The Weber-Fechner fraction is much more peaked for the smaller stimulus size (Fig. 5). Using the larger size, we obtained fairly flat response curves for photopic light levels.

Light scatter experiments

If not taken into account, light scatter will not only influence the characteristics of the SLO image but even more so the psychophysical results. Some examples will illustrate the importance of this phenomenon. So far we have approached this problem in an empirical way. A patch of chorioretinal atrophy, caused by a laser treatment, is visualized in Fig. 6. It can be considered an absolute scotoma. Fixation was foveal (F). A 20 dB incremental stimulus or

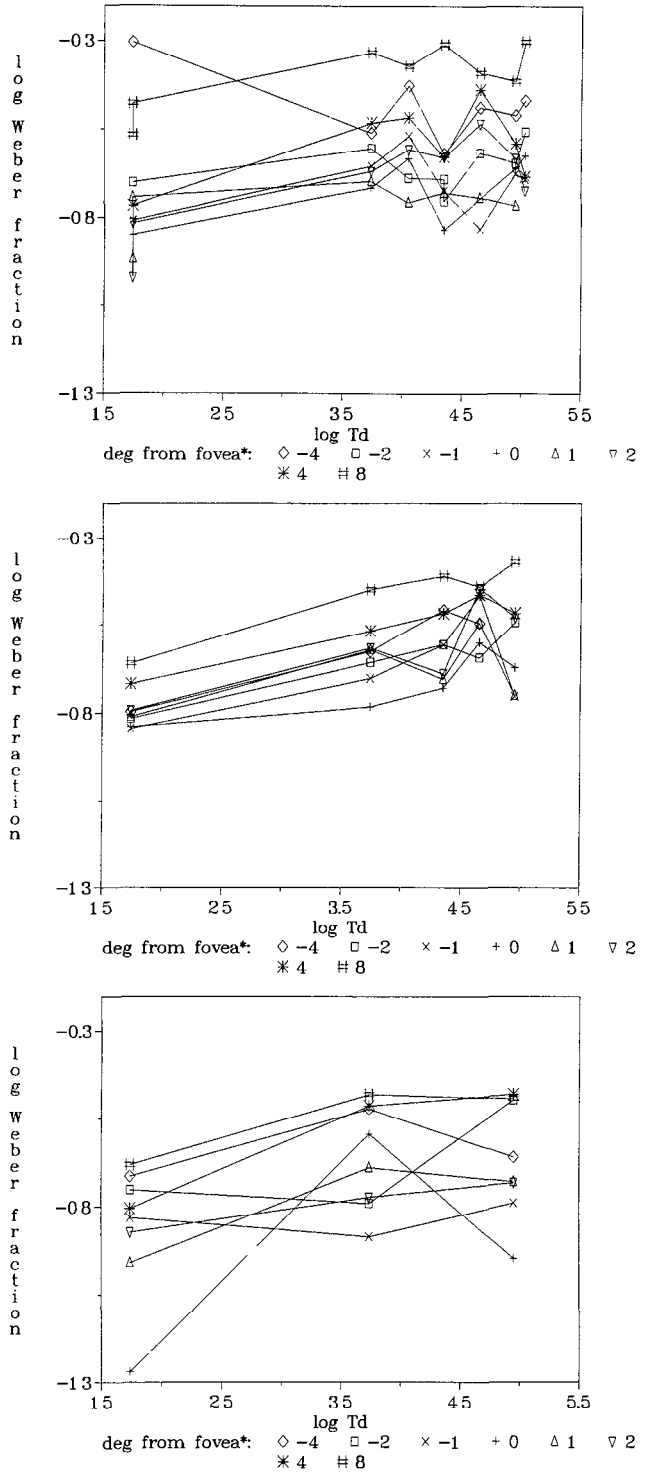

Fig. 1 The log Weber-Fechner fraction plotted in function of background illuminance in log Td for various eccentricities.

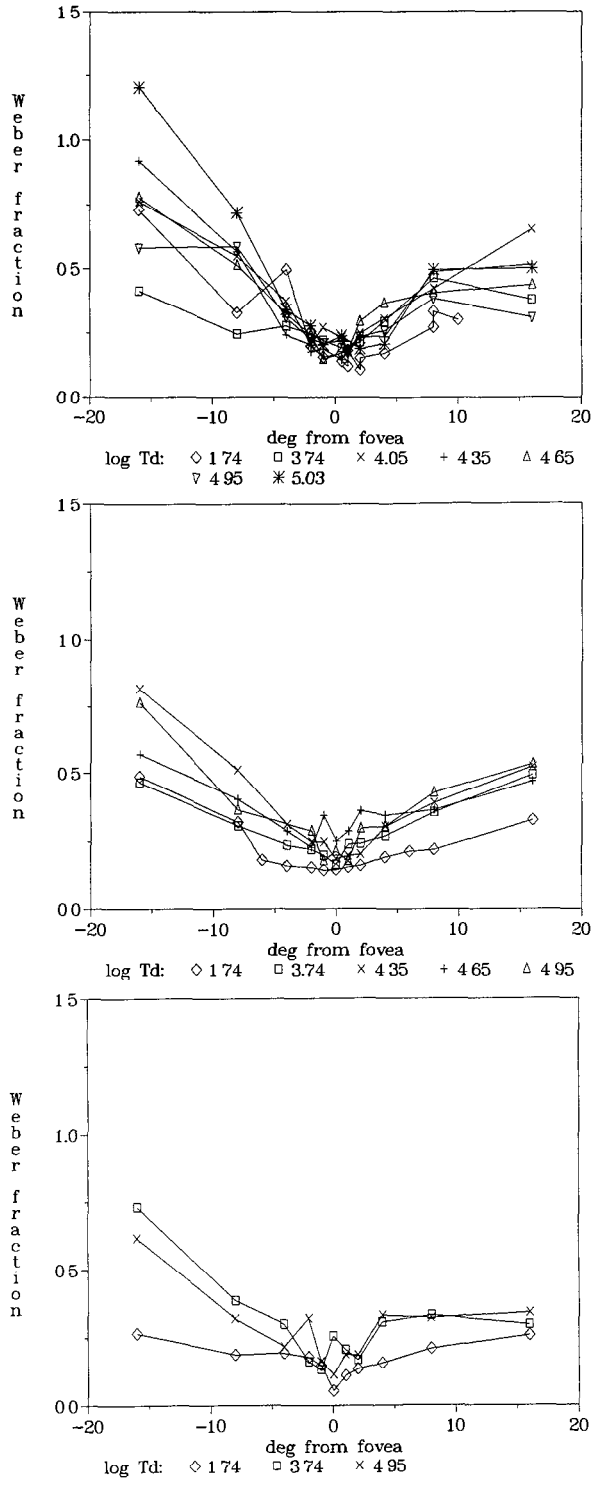

Fig 2 The Weber-Fechner fraction plotted as a function of eccentricity for various background retinal illuminances.

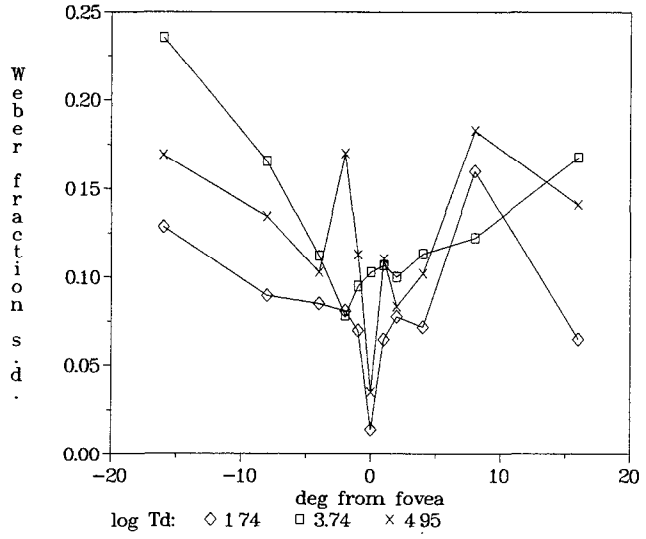

Fig 3. The standard deviation (SD) of reversals plotted as a function of log Td for various background retinal illuminances

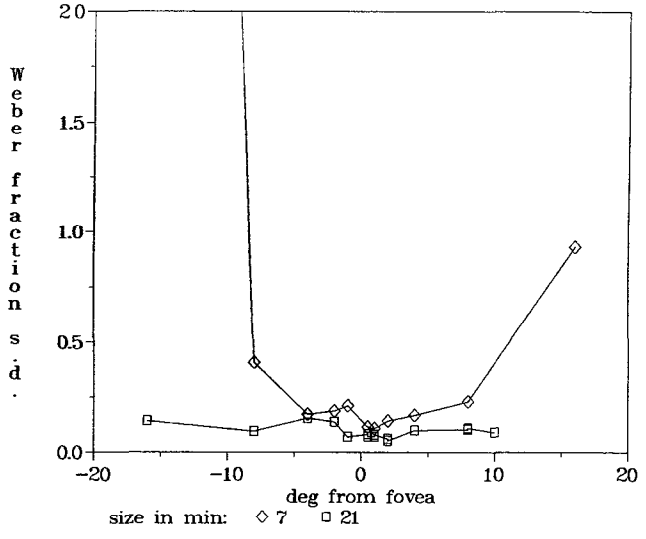

Fig 4. The standard deviation (SD) of reversals for 21 *versus* 7 minarc targets plotted as a function of degree from the fovea

100% contrast decremental stimulus was seen only on healthy adjacent retina, a + 30 dB test stimulus could be noticed within the scar.

Fig. 6. also illustrates a case of hard exudates in diabetic retinopathy. Fixation was foveal (F). A dense scotoma could be demonstrated on the hard exudates using a relatively large 100% contrast decremental stimulus. It was impossible to detect the same dense scotoma with a much smaller incremental stimulus of +30 dB. The light scatter was particularly evident in the indirect viewing modality of the SLO.

Light scatter can also be caused by focal pre-retinal opacities, such as floaters (Fig. 7) or lens opacities. The opacities will either "wash out" a decremental stimulus or produce a false positive response when using a strong incremental stimulus.

The best way to avoid light scatter is to limit the dynamic range and background light intensity to levels comparable to traditional Goldmann testing and to use careful clinical judgement.

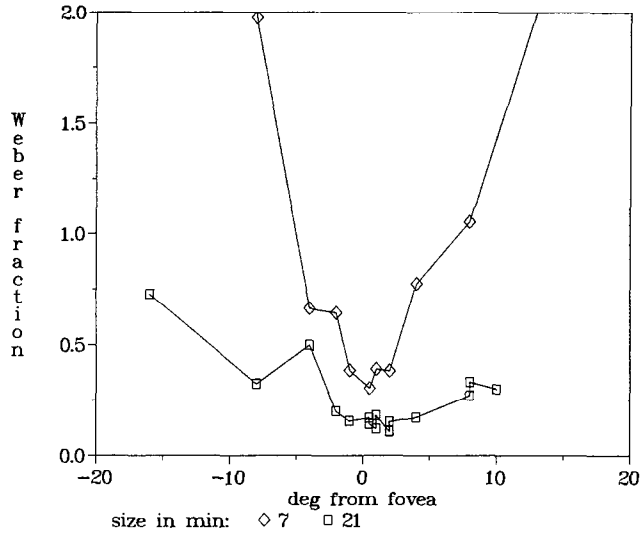

Fig 5 The Weber fraction plotted as a function of retinal eccentricity for small (7 min) and large (21 min) targets.

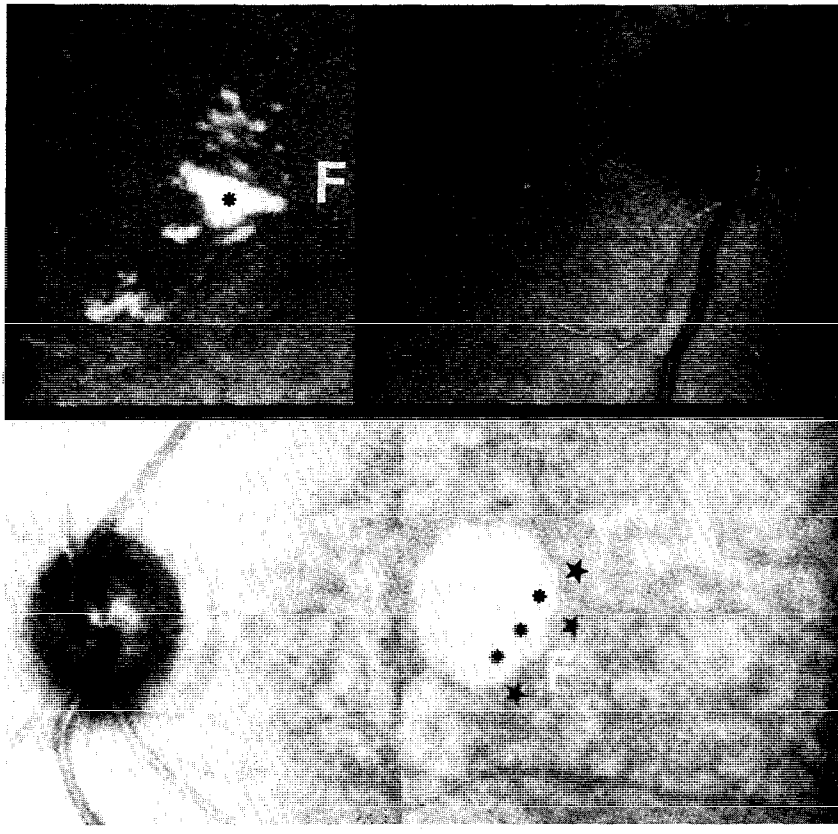

Fig 6 Composite picture illustrating retinal (hard exudates) and choroid (atrophy) lesions in the perifoveal area

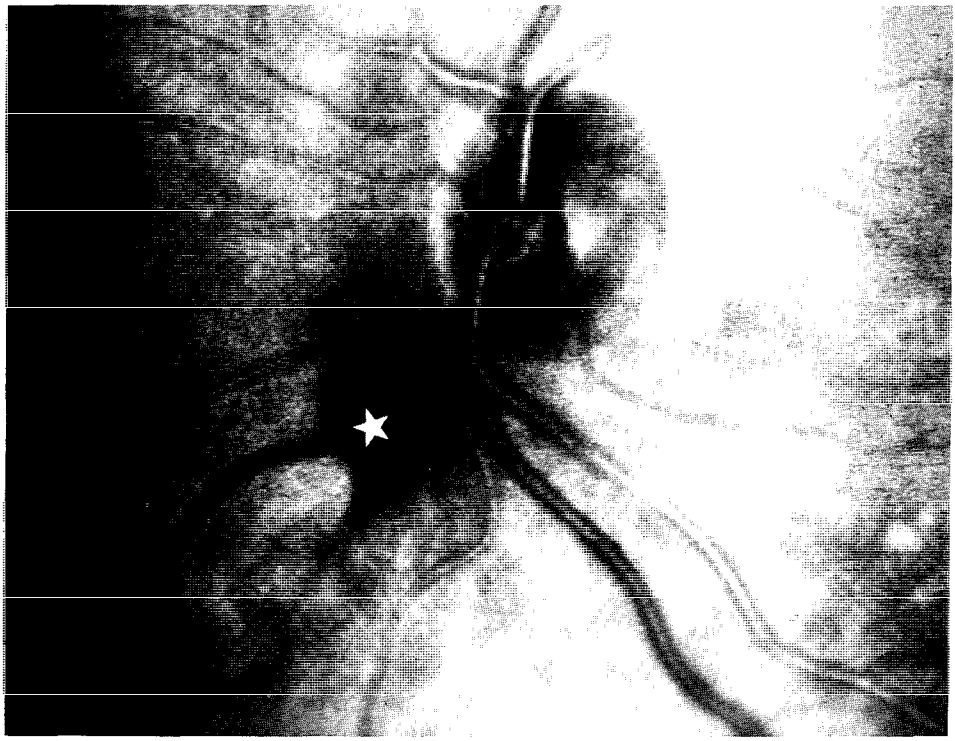

Fig 7 Dense pre-retinal opacity (floater), cause of light scatter

Consequences of Maxwellian viewing

It is easily understood that a constant retinal irradiance is possible with Maxwellian viewing if the entrance pupil remains within the pupillary diameter. Otherwise the problem of vignetting will occur. This was often the case when examining under high illumination and using no dilatation, or in patients using miotics.

Maxwellian viewing is more difficult to maintain for patient (and examiner) during prolonged psychophysical testing. This should be taken into consideration when designing algorithms for automated microperimetry. This is also evident from our clinical experience. On the other hand, Maxwellian viewing as opposed to Newtonian viewing allows us to work around some lens and vitreous opacities.

It seems that it should be possible to demonstrate a Stiles-Crawford I (SCI) effect because the entrance pupil of the SLO optics can move within the pupillary area. We believe that the psychophysical Stiles-Crawford effect is unimportant here because the relative effectiveness of ΔI and I (background) will vary together. This was demonstrated in one normal observer. Of course we assume that $\Delta I/I$ is a constant, as the change is probably less than 0.3 log unit. At most, the careful observer will notice a non-disturbing Stiles-Crawford II (SCII) effect.

Discussion

We can derive optimal microperimetry parameters and observations from previous experiments and well-known psychophysical laws. Automated, manual (or hybrid) and staircase (or static) algorithms and results have been discussed before. The parameters discussed below are size and duration of static stimulus, background characteristics, intensity scale and dynamic range.

Size

Most often SLO size III, corresponding to approximately Goldmann III (400 minarc^2 or 100 μm stimulus diameter on the retina in the standard observer) should be used. SLO size II (approximately 100 minarc^2) is reserved for testing within the perifoveal area, small lesions identified in the SLO image (*e.g.*, small cysts). The same is true for SLO size I (similar to Goldmann size I) which potentially could be used for evaluation of small receptive fields around the foveal area. This would certainly necessitate a real-time 60 Hz eye tracker. Also this small size is not available in the 40 degree field of view because of the limited resolution of the laser raster. Goldmann sizes IV or V are traditionally used for medico-legal evaluation. The sizes of targets are calibrated for the standard observer (nodal point at 16.7 nm) and are subject to distortion of the laser beam raster (±10%) and deviation from the exact theoretical size because of the use of discrete pixels which can be considered size quanta. Because of spatial summation properties of the retina, differences are irrelevant to clinical perimetry measurements.

Duration

Static stimuli exclude reaction time artifacts, the confusion with "motion" perception and the complex interaction between temporal and spatial summation. They are essential for "micro" perimetry in the posterior pole and make on-line analysis of results possible with a fundus tracker. Duration is limited to 200 ms, preventing optomotor reflex (saccade after perception of stimulus which destabilizes fixation). Generally 200 ms is thought to be equal to or larger than the duration of maximal temporal summation.

Background characteristics

Traditionally, perimetry with the SLO was performed using a high background monochromatic illumination and decremental stimuli. The combination of diode IR and visible wavelengths allow much lower backgrounds to be used with incremental stimuli.

Low background 633 nm (red) illumination corresponding to about ±50 Td or 0.1 μW/cm^2 irradiance at the retina with incremental stimuli is used in combination with the IR light source for generating the background image. It results in a fairly flat ΔI/I (cone) response curve in the posterior pole when using SLO III stimuli. This is ideal for quantitation of retinal sensitivity. The flat response makes interpretation of comparison thresholds and suprathreshold estimates, between symmetrical areas equidistant from the fovea or areas immediately adjacent to areas on the retina, easier and more accurate.

High background illumination, typically 100,000 Td or 200 μW/cm^2 is used with incremental or decremental stimuli. One laser source only is necessary to generate both psychophysical stimuli and background image on the SLO monitor. There is however an important potential psychophysical problem. Pigment is bleached when background illumination is sufficiently high, and we have to avoid transition levels between bleached and unbleached status of the retina. Also a coarser intensity scale is necessary for quantitation (dB or 2 dB) as the psychometric function widens, as shown by the increase in SD of reversals in staircase. The Weber-Fechner relation does not remain constant, but increases. This response curve is peaked for all sizes. Blinking and other artifacts can interfere with threshold judgments. These phenomena may be even more pronounced in pathology.

A constant relationship between ΔI and I is necessary to exclude certain variables: change in laser output, variable media opacities, potential SCI effect, etc. This is possible because of the hardware configuration: ΔI and I are changing together in the traditional Goldmann perimeter where an ND filter is used, as well as in the SLO where an AOM is used. This considerable benefit would be lost if the Weber-Fechner relationship was no longer valid.

Dynamic range

Light scatter, as illustrated above, is a problem when the difference between background and stimulus intensity is large This is not the case with the differential incremental or decremental light intensities that we used in normals for the purpose of characterizing the Weber-Fechner relation. However, it is a serious problem with pathology in which stimuli must be made much

brighter (or dimmer) from the background so that the patient can detect them. This can result in false positive responses for small lesions, false negative responses in the case of focal media opacities, and a lower than calculated contrast of a decremental stimulus.

Because of potential light scatter problems in microperimetry and the specific dynamic range and resolution of the FG100AT imaging board and AOM, we adopted a +20 dB dynamic range maximum. This is identical to the traditional Goldmann perimeter dynamic range.

Intensity scales

Fechner integrated the observation made by Weber: a differential increment (decrement) of light intensity *di* results in a differential increment (decrement) of sensation *ds* according to the law $c \times di/i = ds$. This integration results in "the amount of sensation" in normal observers:

$$S = \int ds = c \times \int di/i = c \times \log i$$

This derivation can be criticized when dealing with pathology where "sensation" is diminished. This is obvious when using decremental stimuli different from background by more than a mere "*di*" for detection. We therefore use linear intensity scales in the case of decremental perimetry and reserve the "natural" logarithmic scales for incremental perimetry In automated microperimetry, because of algorithmic design, we prefer to use a low background, 50 Td at 633 nm with incremental stimuli using a 1 dB scale. Full bracketing is done with 2 dB interval strategies.

In hybrid microperimetry, which shares many features with classic static/kinetic field testing on a Goldmann perimeter, we like to use: (a) a low visible background and obligatory IR imaging with incremental stimuli and a 1 dB log scale; or (b) a relatively high background with optional IR illumination (not necessary in 40 degree field viewing) and decremental stimuli. We use an empirically fixed 5% linear contrast bracketing of the intensity scale to circumvent problems mentioned above, *e g* , light scatter, contrast lowering of stimulus, and failure of the Weber-Fechner relation.

In staircase microperimetry, because of algorithmic design, we opt for a low background with 1, 2 or 4 dB logarithmic intervals using incremental stimuli. Which one to use depends essentially on the shape of the resultant staircase and the SD of the reversals. Three to four steps between reversals are optimal to derive thresholds. This is, of course, still not the best way to get an impression of the slope of the psychometric function, but it can give some idea.

References

1. Van de Velde FJ, Timberlake GT, Jalkh AE, Schepens CL: La micropérimétrie statique avec l'ophtalmoscope à balayage laser. Ophtalmologie 4:291-294, 1990
2. Van de Velde FJ, Jalkh AE, Katusmi O, Hirose T, Timberlake GT, Schepens CL: Clinical scanning laser ophthalmoscope applications: an overview In: Nasemann J, Burk R (eds) Scanning Laser Ophthalmoscopy and Tomography Berlin: Quintessenz Verlag 1990
3. Elsner AE, Timberlake GT, Burns SA, Kreitz MR: High illuminance perimetry: photopigment mechanisms. Noninvasive assessment of the visual system technical digest. Opt Soc Am 1989
4. Van de Velde FJ, Timberlake GT, Jalkh AE, Acosta F, Nasrallah F: Static SLO microperimetry in macular disease. Invest Ophthalmol Vis Sci (Suppl) 30:367, 1989
5. Elsner AE, Burns SA, Hughes GW, Webb RH: Evaluating the photoreceptor/rpe complex with the SLO: Noninvasive assessment of the visual system, technical digest. Opt Soc Am 1990
6. Van de Velde FJ, Jalkh AE, Laskari K, Chedid N: Evaluation of the Weber-Fechner relationship in SLO microperimetry. Invest Ophthalmol Vis Sci (Suppl) 31:190, 1990
7. Elsner AE, Burns SA, Kreitz MR, Webb RH: Sensitivity maps vs cone pigment density distribution Invest Ophthalmol Vis Sci (suppl) 31:109, 1990
8. Webb RH, Hughes GW, Delori FC: Confocal scanning laser ophthalmoscope Appl Opt 26:1492-1499, 1987
9. Plesch A, Klingbeil U, Rappl W, Schrodel C: Scanning ophthalmic imaging. In: Nasemann J, Burk R (eds) Scanning Laser Ophthalmoscopy and Tomography Berlin: Quintessenz Verlag 1990
10. Elsner AE, Burns SA, Delori FC, Webb RH: Quantitative reflectometry with the SLO In: Nasemann J, Burk R (eds) Scanning Laser Ophthalmology and Tomography Berlin Quintessenz Verlag 1990

Localized scotomas and vascular impairment in diabetic maculopathy

Toke Bek

Department of Ophthalmology, University of Copenhagen, Gentofte Hospital, DK-2900 Hellerup, Denmark

Abstract

A technique for accurate superimposition of visual field data onto corresponding fundus morphology as seen on fundus photography and fluorescein angiograms was developed, and a systematic study of diabetic maculopathy was undertaken employing this technique. The present paper reviews the findings from a correlation of retinal light sensitivity with corresponding morphology displaying signs of vascular impairment, such as vascular occlusion and break-down of the blood-retina barrier. Localized scotomas could be correlated with focal areas of non-perfusion in the macular area, but no correlation was found between retinal light sensitivity and break-down of the blood-retina barrier as evidenced by angiographical leakage of fluorescein. In some cases with pronounced signs of maculopathy, including macular edema, scotomas occurred which could neither be related to areas of distribution from the central retinal artery nor to focal areas of fluorescein leakage The findings indicate that other factors than retinal vascular impairment may be co-involved in producing visual loss in diabetic maculopathy.

Introduction

Diabetic retinopathy is the most frequent cause of blindness among young adults in the western world. It is therefore of major importance to obtain access to new ways of treating this disease, and to improve existing methods of treatment. In order to achieve these goals it is necessary to gain new knowledge about the pathophysiological mechanisms underlying the disease, possibly by including new approaches for the study of retinal pathology.

The findings described in the present paper are based on such a new approach. A technique for accurate superimposition of visual field data onto corresponding fundus morphology as seen on fundus photographs and fluorescein angiograms was developed, and a systematic study of patients with diabetic retinopathy was undertaken employing this technique. Since it is generally believed that disturbance of retinal vascular supply is a major factor in the pathogenesis of diabetic retinopathy, visual field data were correlated with funduscopic and angiographical signs of vascular impairment, such as occlusion of the retinal vessels and break-down of the blood-retina barrier. The present paper reviews the findings of this comparative study.

Material and methods

Subjects

The findings of the present paper are based on 30 patients with diabetic retinopathy. The patients were subjected to routine ophthalmological examination including fundus photography, fluorescein angiography and computerized perimetry, and the visual field data were accurately correlated with the corresponding retinal morphology as seen on fundus photographs and fluorescein angiograms according to the technique described below. Informed consent was obtained.

Photography

Photography was performed with a Canon CF-60Z fundus camera employing Ektachrome 64 (EPR 135-36) film for fundus photography, and Ilford HP-5 black-and-white film for

Perimetry Update 1990/91, pp. 103-108
Proceedings of the IXth International Perimetric Society Meeting,
Malmö, Sweden, June 17-20, 1990
edited by Richard P. Mills and Anders Heijl

fluorescein angiography. 5 ml 10% fluorescein sodium was injected into an antecubital vein for fluorescein angiography. Angiograms were taken of the central fundus in fast sequence during the filling phase of the vessels, and with regular intervals until 15 minutes after injection. Prior to photography, cycloplegia and mydriasis were induced with metaoxedrine 10% and tropicamid 1% eyedrops.

Perimetry

Perimetry was carried out with a Humphrey Field Analyzer (HFA). Full-threshold examinations were performed employing Goldmann stimulus size I in stimulus grids with a density of one degree. The stimulus grids were placed in areas of the visual field which corresponded to retinal lesions observed by prior funduscopic examination. Since the minimum density of customized programs of the HFA is two degrees, four intersecting patterns with a displacement of one degree in the horizontal and the vertical plane were subsequently tested, and finally merged. The blind spot was delimited with Goldmann stimulus size II with a single intensity of 10 dB in two special point patterns located in the area of the blind spot, one (pattern A) extending from degree coordinates (x,y) = (11,-7) to (19,3) and one (pattern B) from degree coordinates (x,y) = (12,-8) to (18,2). By merging these two patterns, a spatial resolution of 1.4 degrees could be obtained in this area. Corrective lenses were added when necessary for the patient to fixate the perimeter screen sharply. Fixation was continuously checked on the fixation monitor supplied on the HFA, and was found stable in the patients included.

Superimposition technique

The superimposition of visual field data onto fundus pictures was carried out according to a technique described previously[1]. This technique is applicable to a fundus photograph (subtending approximately 60 degrees with the camera employed here) with the foveal region in center, and the accuracy of the overlay of visual field data onto the corresponding fundus photograph is better than one degree. Briefly, with knowledge of the optical imaging in the fundus camera, the visual field printout is reduced to match the size of the corresponding fundus photograph. The visual field is inverted about a horizontal axis, and the overlay is subsequently performed on the basis of two points of reference. One, the fixation point in the visual field is laid over the foveola on the fundus picture, and the other, the blind spot in the visual field is laid over the optic nerve head on the fundus picture.

Data analysis

The visual fields obtained with the HFA were transmitted in hexadecimal code from the perimeter to a personal computer via an RS-232 serial interface. Programs were developed in Turbo C (Borland Inc.) for data transmission and subsequent translation into readable format. The translation program automatically created an input data file for the topographical program Surfer (Golden Software) for creation of contour lines, and edited a command file for Surfer with information to perform the correct scaling of visual field data according to the algorithm[1].

Results

Localized scotomas in the visual field were found to correspond with focal areas of nonperfusion in the macular area (*e g* , Fig. 1).

No correlation was found between retinal light sensitivity and break-down of the blood-retina barrier as studied on fluorescein angiograms. In most cases there was normal light sensitivity in retinal areas with even pronounced leakage of fluorescein (*e.g.*, Fig. 2). In cases where scotomas occurred, there were pronounced signs of maculopathy, including retinal edema, but there was no topographical correlation between the sensitivity loss and fluorescein leakage, and the scotomas could not be correlated to areas of distribution from the central retinal artery (*e.g.*, Fig. 3).

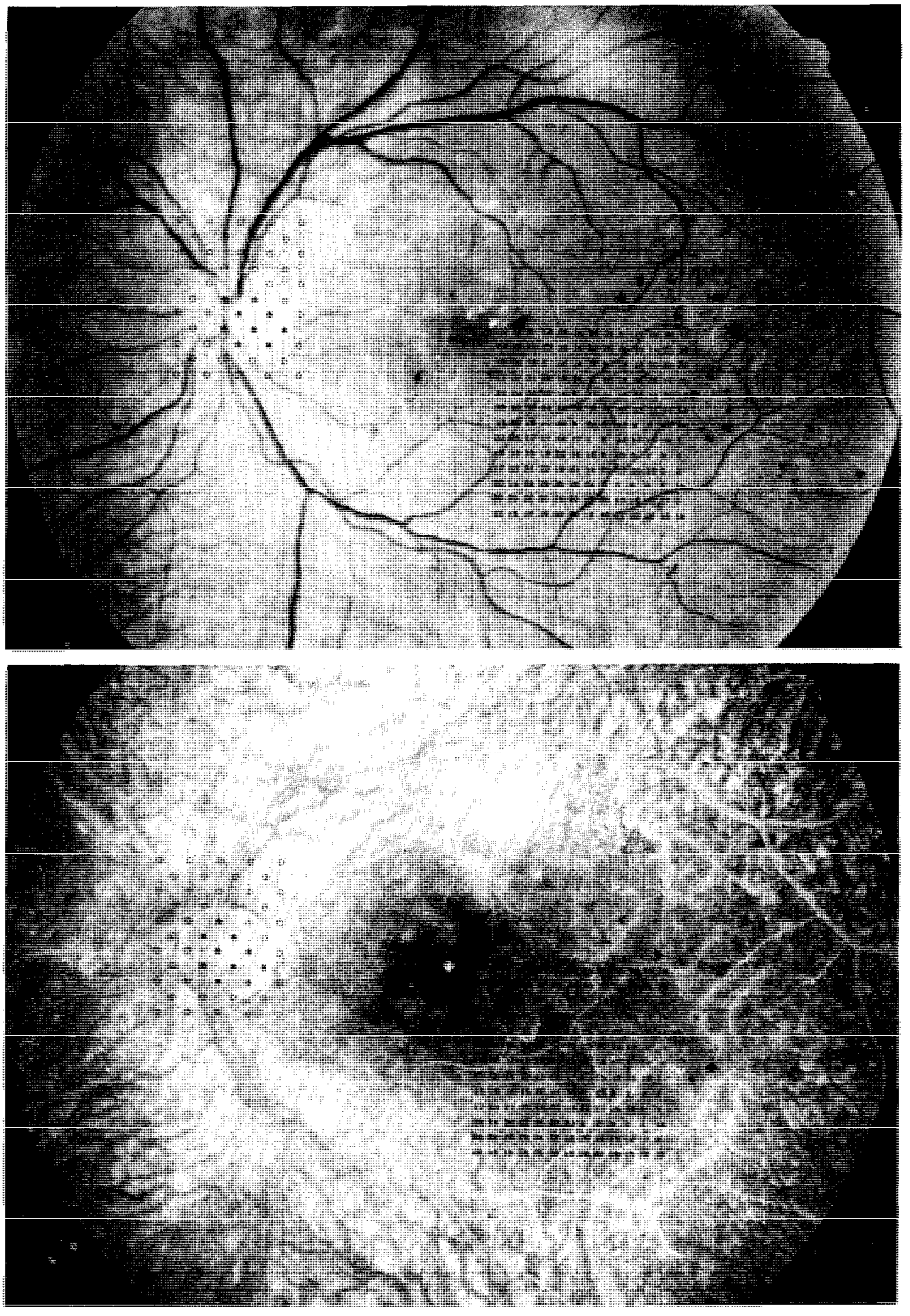

Fig 1a A left eye fundus photograph of a patient with diabetic maculopathy, mainly consisting of small hemorrhages. Visual field data have been accurately superimposed onto corresponding fundus morphology. Stimulus pattern extended from degree coordinates (x,y) = (2,0) to (14,12). Focal areas with low decibel values are seen scattered in stimulus pattern with no apparent relation to fundus morphology. *b* A fluorescein of the same eye 281 seconds after intravenous injection of fluorescein. Low decibel values correspond to focal areas of retinal non-perfusion Visual acuity was 6/6

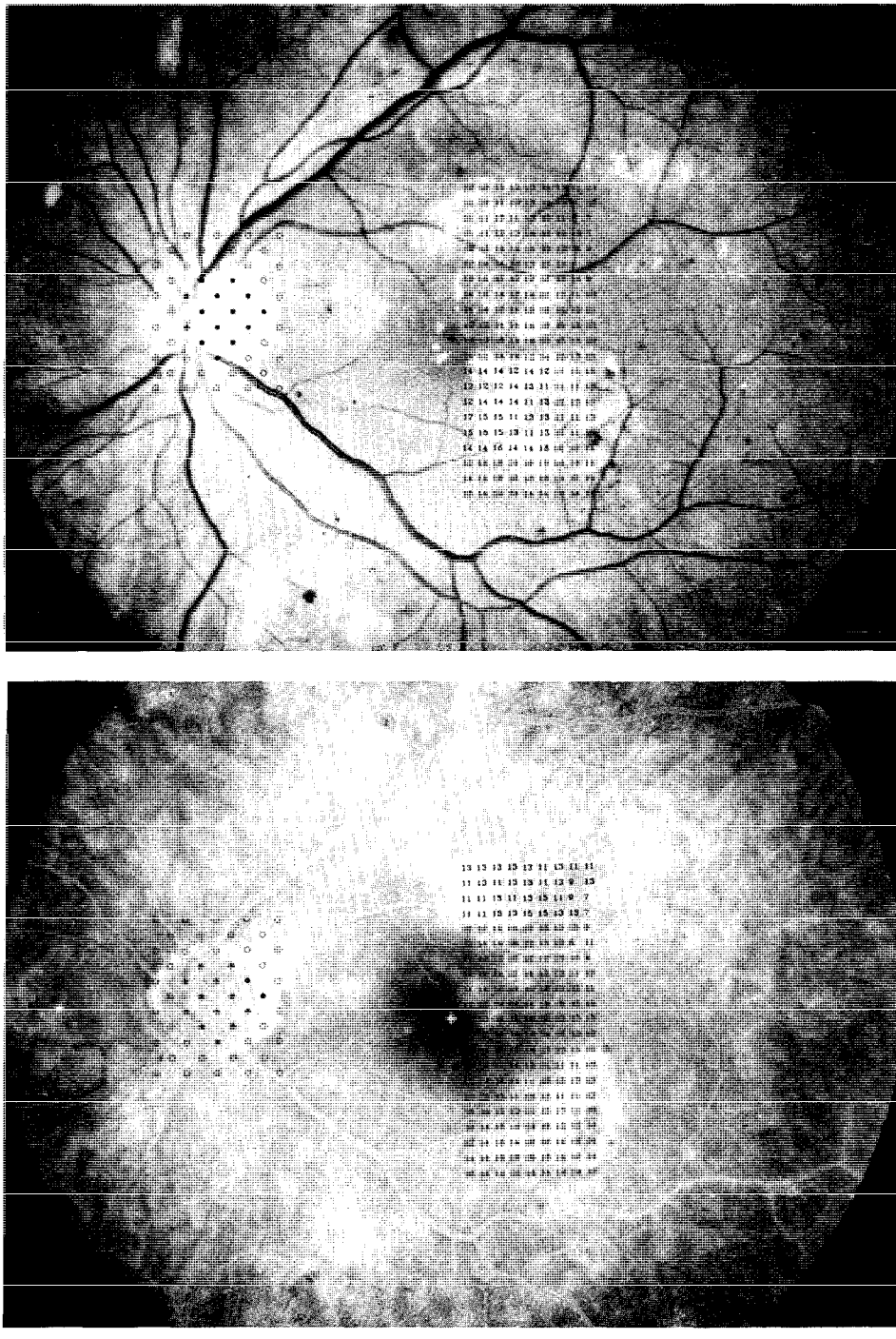

Fig 2a A left eye fundus photograph of a patient with diabetic maculopathy, mainly consisting of hard exudates. Stimulus pattern extended from degree coordinates (x,y) = (1,-10) to (9,10). Possible visual field defects caused by hard exudates have not been resolved with the stimulus parameters employed. *b* A fluorescein angiogram of the same patient 404 seconds after intravenous injection of fluorescein Focal areas with leakage of fluorescein display normal light sensitivity. Visual acuity was 6/6

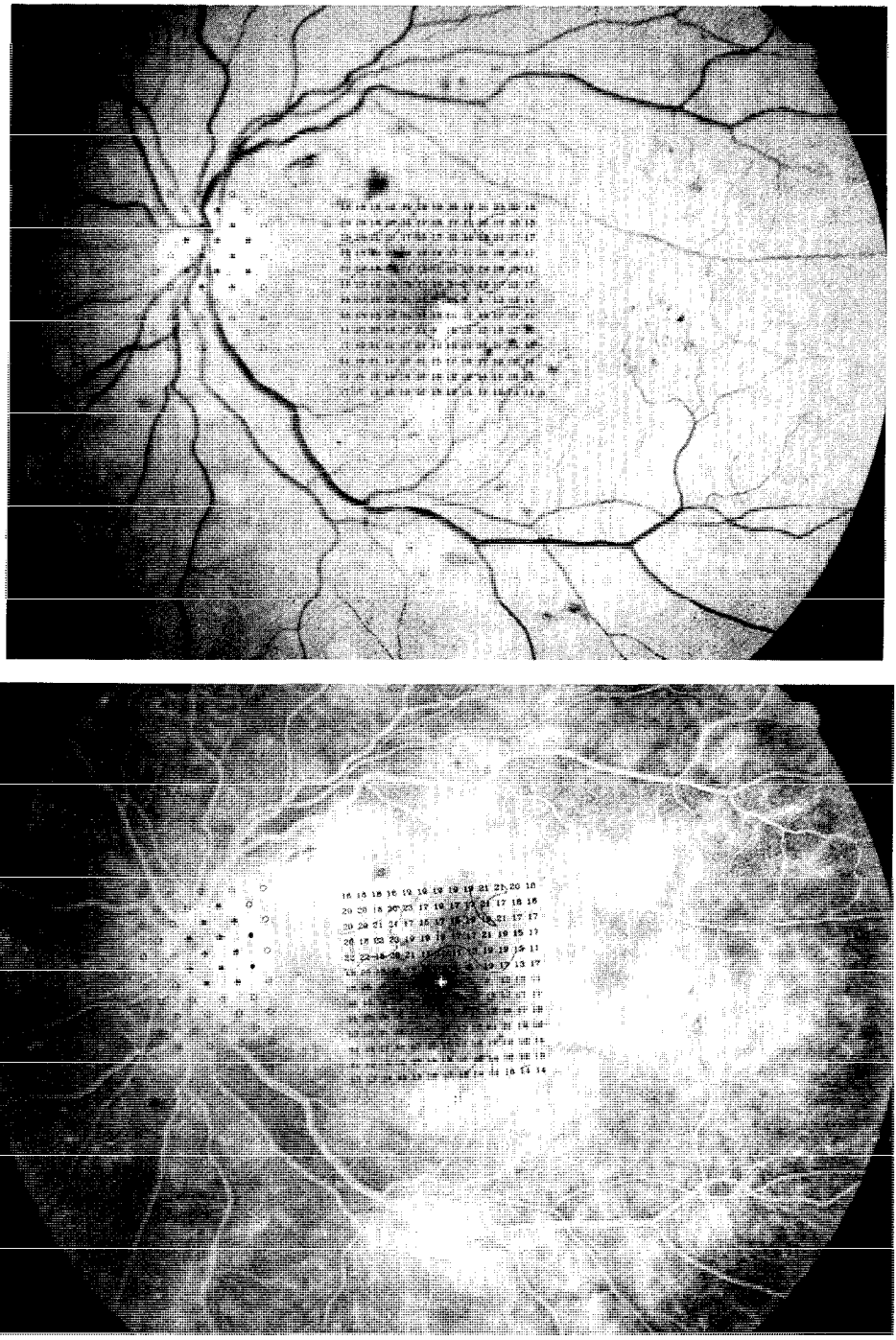

Fig 3a A left eye fundus photograph of a patient with pronounced signs of diabetic maculopathy including retinal edema. Stimulus pattern extended from degree coordinates (x,y) = (-6,-6) to (6,6). Contour lines have been plotted at borders of 4 dB sensitivity shifts in threshold values of the stimulus pattern A scotoma includes foveola extending temporally. Visual acuity was 6/18. *b* A fluorescein angiogram of the same eye 244 seconds after intravenous injection of fluorescein. Pronounced leakage of fluorescein is seen in the macular area, but this leakage shows no apparent topographical relation to retinal areas with impaired light sensitivity, and the scotoma does not correspond with an area of retinal non-perfusion

Discussion

The results presented in the present paper confirm the general belief that retinal vascular impairment is an important factor in producing visual loss in diabetic retinopathy. Moreover, it seems that this visual loss mainly is due to occlusion of the retinal vessels, and to a smaller degree, or perhaps not at all, due to break-down of the blood-retina barrier as studied with fluorescein. Furthermore, some visual loss occurs which does not correlate topographically with areas of blood-retina barrier leakage or with areas of distribution from the central retinal artery.

Diabetes mellitus is characterized by widespread disturbances of vascular function which may lead to functional impairment of a multitude of organ systems. In the eye, vascular impairment is a prominent feature of diabetic retinopathy, and is therefore assumed to be a major cause of visual loss in this disease. Retinal vascular impairment is seen morphologically as closure of retinal capillaries and break-down of the barrier integrity of the vessel walls.

In the present study some localized scotomas have been shown to correlate with focal areas of angiographical non-perfusion. This finding supports the assumption that the morphological entity described as non-perfusion represents retinal capillary closure, and consequently supports the hypothesis that retinal vascular occlusion may be an important factor in producing visual loss in diabetic retinopathy[2].

The findings of the present study show no correlation between retinal light sensitivity and blood-retina barrier leakage as seen on fluorescein angiograms. In most cases, retinal light sensitivity was normal in retinal areas with breakdown of the blood-retina barrier displaying even pronounced leakage of fluorescein. Where scotomas occurred, there were pronounced signs of maculopathy including retinal edema, but there was no topographical correlation between barrier leakage and the sensitivity loss[3]. The findings may perhaps indicate that breakdown of the blood-retina barrier in itself has no significant impact on visual function. This may be important since diabetic retinopathy in some cases is treated with photocoagulation at sites of barrier leakage on purely empirical basis since these locations are assumed to represent areas where visual function is threatened.

The fact that some patients with pronounced signs of maculopathy, including macular edema, had localized scotomas which could neither be related to areas of distribution from the central retinal artery nor to breakdown of the blood-retina barrier, may perhaps indicate that pathophysiological factors other than retinal vascular impairment, are responsible for the visual loss in these cases. Such alternative factors could for example be choroidal vascular insufficiency or pigment epithelium dysfunction. Impairment of these structures could directly affect the nutrition of outer retinal layers, including the photoreceptors, or could be responsible for the formation of macular edema with consequent impairment of retinal function.

In conclusion, the results presented in this paper confirm that retinal vascular impairment is a significant contributing factor to visual loss in diabetic retinopathy. Moreover, the results indicate that this impairment is mainly due to closure of retinal vessels, but probably not due to breakdown of the blood-retina barrier as studied with fluorescein. The findings also indicate, however, that other factors, such as choroidal vascular impairment or pigment epithelial dysfunction may be involved in causing visual loss in diabetic maculopathy.

Acknowledgements

The skillful assistance of photographer Hans Henrik Petersen is gratefully acknowledged.

References

1. Bek T: Accurate superimposition of visual field data onto fundus photographs. Acta Ophthalmol 68:11-18, 1990
2 Bek T: Localised scotomata and types of vascular occlusion in diabetic maculopathy. Acta Ophthalmol 69:11-18, 1991
3 Bek T, Lund-Andersen H: Localised blood-retina barrier leakage and retinal light sensitivity in diabetic retinopathy. Br J Ophthalmol 74: 388-392, 1990

Neuro-ophthalmology

The morphology of visual field damage in idiopathic intracranial hypertension: an anatomic region analysis

Michael Wall

Departments of Neurology & Psychiatry and Ophthalmology, Tulane University School of Medicine, 1430 Tulane Avenue, New Orleans, LA 70112, USA

Abstract

Fifty patients with idiopathic intracranial hypertension (pseudotumor cerebri) had automated perimetry of the central 30° and Goldmann perimetry on the same day The right eyes of 49 patients with adequate vision for automated perimetry were analyzed The visual fields were graded with a modified glaucoma system and numerical anatomic region analysis was performed The earliest defects with Goldmann perimetry were usually an inferior nasal step defect and enlargement of the blind spot; loss in the nasal hemifield or a mild generalized depression was usually concomitant with automated perimetry The stages of loss usually evolved from a nasal step to nasal loss to a generalized depression of the visual field with relative sparing of the cecocentral and inferior Bjerrum areas The morphology of visual loss of idiopathic intracranial hypertension is similar to glaucoma

Introduction

Idiopathic intracranial hypertension (IIH, pseudotumor cerebri) is a disorder of increased intracranial pressure of unknown cause. The only major morbidity from the disease is visual loss that occurs in over 90% of patients[1]. The purposes of the study were to describe the stages of visual field damage in IIH, to correlate manual with automated perimetry and to determine whether visual field loss correlated with papilledema grade.

Subjects and methods

Fifty patients who met the modified Dandy criteria for IIH[2] (Table 1) who returned for follow-up and were reliable perimetry subjects were studied. The patients were evaluated in the neuro-ophthalmology clinic at Tulane University Hospital from 1982 through 1989. The degree of papilledema was graded using Frisén's scheme[3]. Grade 0 defines an optic nerve head without swelling; grade 5 denotes marked papilledema.

The same perimetrist performed Goldmann perimetry at all visits, using the same strategy[1]. This is a modification of the Armaly-Drance strategy for glaucoma that concentrates test loci where disc-related field defects occur[1].

Table 1 Modified Dandy criteria for IIH[2]

1.	Signs and symptoms of increased intracranial pressure
2.	Absence of localizing findings on neurologic examination
3.	Absence of deformity, displacement or obstruction of the ventricular system and otherwise normal neurodiagnostic studies, except for increased cerebrospinal fluid pressure
4.	Awake and alert patient
5.	No other cause of increased intracranial pressure present

Automated perimetry during the first four years of the study was performed with the Octopus 201 perimeter; for the last three years the Humphrey perimeter was employed. Regardless of the perimeter, we performed all visual fields with a full threshold program testing 72 points in the central 30 degrees of the visual field with six-degree spacing, offset from the vertical and

Perimetry Update 1990/91, pp. 111-117
Proceedings of the IXth International Perimetric Society Meeting,
Malmö, Sweden, June 17-20, 1990
edited by Richard P. Mills and Anders Heijl

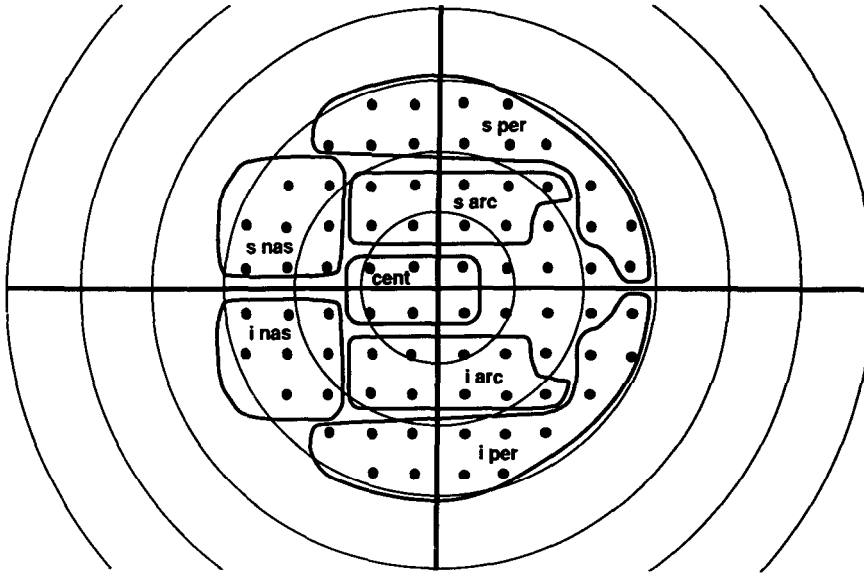

Fig 1 Regions of automated perimetry analysis of the central 30° of a right eye based on nerve fiber bundle anatomy[6]. cent: cecocentral region; s: superior; i: inferior; arc: arcuate or Bjerrum region; nas: nasal; temp: temporal; per: periphery.

horizontal meridians. The visual fields were graded for both types of perimetry using published criteria[1].

The numerical values for the thresholds obtained with these two perimeters are not directly comparable because of differences in background illumination (Octopus, 4 asb, Humphrey, 31.5 asb) and other factors. As an approximation, the Octopus perimetry data was converted to the Humphrey equivalent using the JAWS statistic of Johnson *et al* [4]. Data of the 72 threshold points was then compacted by summing the scores of anatomic regions of the field. The tem-

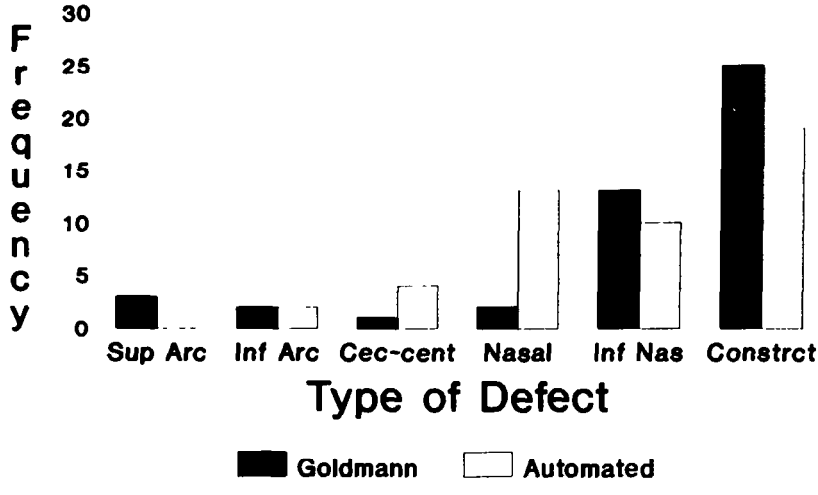

Fig 2 Goldmann perimetry results compared with automated perimetry at the initial examination. Sup Arc: superior arcuate scotoma; Inf Arc: inferior arcuate scotoma; Cec-cent: cecocentral scotoma; Inf nasal: inferior nasal defect; Constrct: visual field constriction.

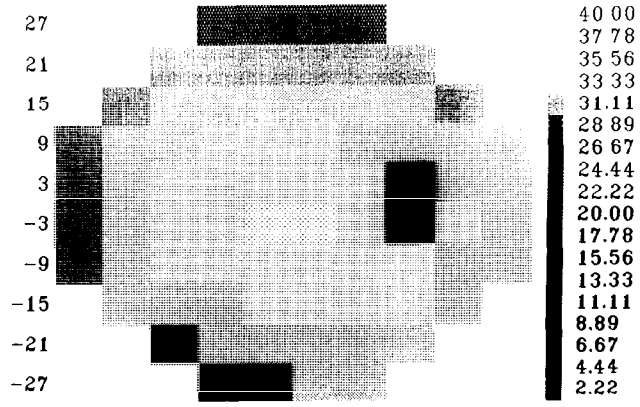

Fig 3a

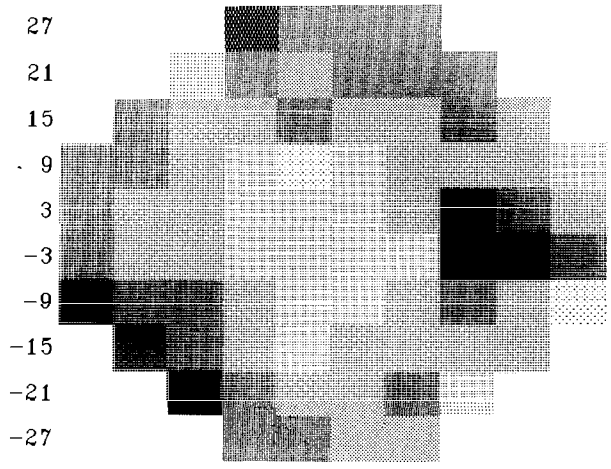

Fig 3b

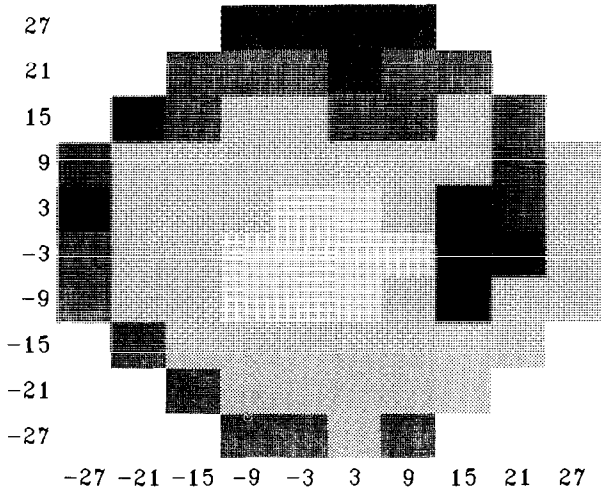

Fig. 3c

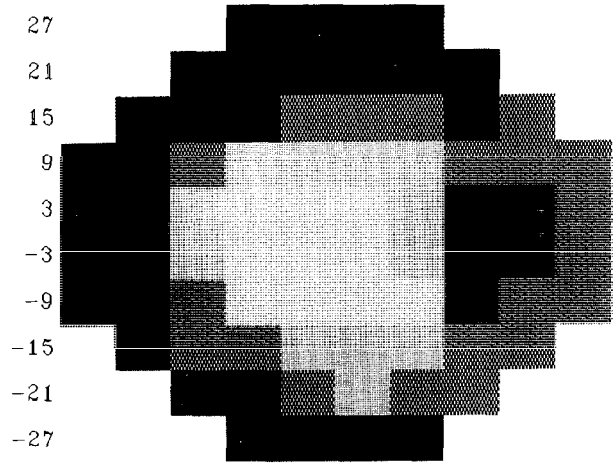

Fig 3d

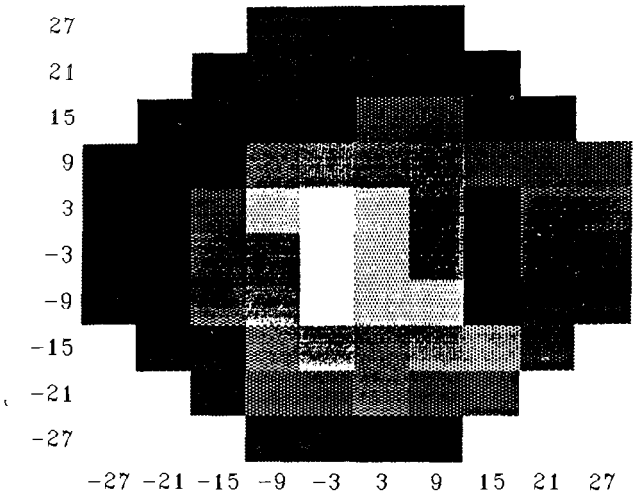

Fig 3e

Fig 3 Gray scale plots of (a) normal visual field; (b-e) results of grades 0-3. Note the inferior nasal depression that appears early (c - grade 1); a generalized depression especially nasally follows (d - grade 2); and with progression, relatively spares the central 10 degrees (e - grade 3) The gray scale key (in decibels) is found on the right margin of the normal field The X and Y axes represent visual field position in degrees from fixation.

plate used (Fig. 1) is based on the patterns of defects commonly in IIH (nerve fiber bundle defects)[5,6]. Quadrant, nasal and temporal hemifield and total visual field scores were also calculated.

A Spearman rank correlation coefficient was calculated using SAS/STAT software for the correlation of papilledema grade and mean automated perimetry score. The value found was interpreted as a significant correlation if the probability of its occurrence was less than 0.05.

Results

Fig. 2 shows the types of visual field defects found with Goldmann perimetry and automated perimetry and their frequency. Of note is the common finding of inferior nasal loss with Goldmann perimetry. With automated perimetry, these defects usually appeared as a depression on

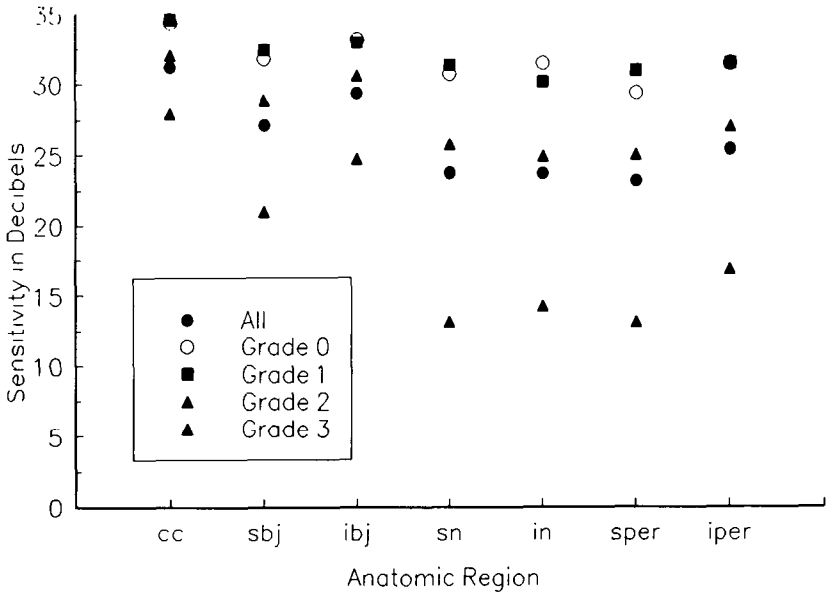

Fig 4 Nerve fiber bundle analysis showing predominant involvement of the superior and nasal regions and the superior and inferior periphery. There is relative sparing of the cecocentral and inferior Bjerrum regions See Fig. 1 for regions. cc: cecocentral; sbj, ibj: superior, inferior Bjerrum; sn, in: superior, inferior nasal; sper, iper: superior, inferior peripheral.

the nasal side of the visual field. Fig. 3 shows the two-dimensional gray scale plots of a normal visual field and the various automated perimetry visual field grades. Note the progression from peripheral inferior nasal loss (Grade I) extending to the superior nasal field (Grade 2) followed by a generalized depression with relative sparing of the cecocentral and inferior Bjerrum areas (Grade 3). Nine patients had a grade 0 Visual field (no loss except possibly a mildly enlarged blind spot), four had grade 1, 24 grade 2 and 11 grade 3

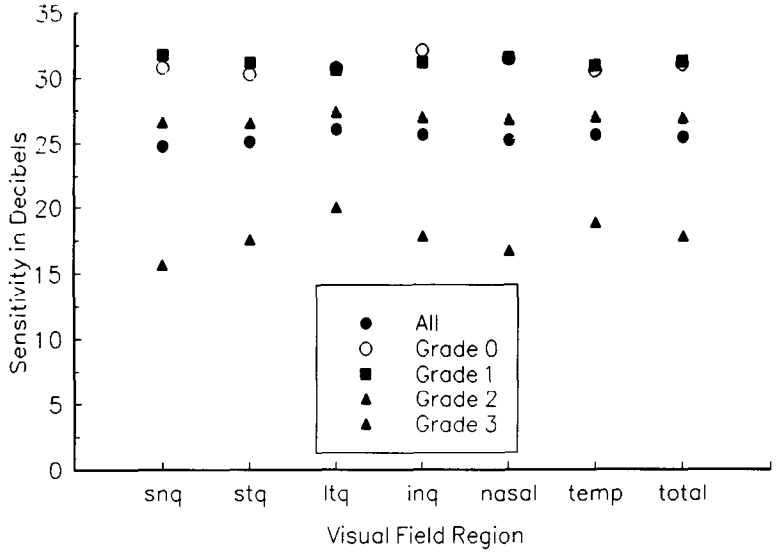

Fig 5. Quadrant and hemifield analysis showing more loss on the nasal side of the visual field than the temporal. snq, inq: superior, inferior nasal quadrants; stq, itq: superior, inferior temporal quadrants; temp: temporal hemifield.

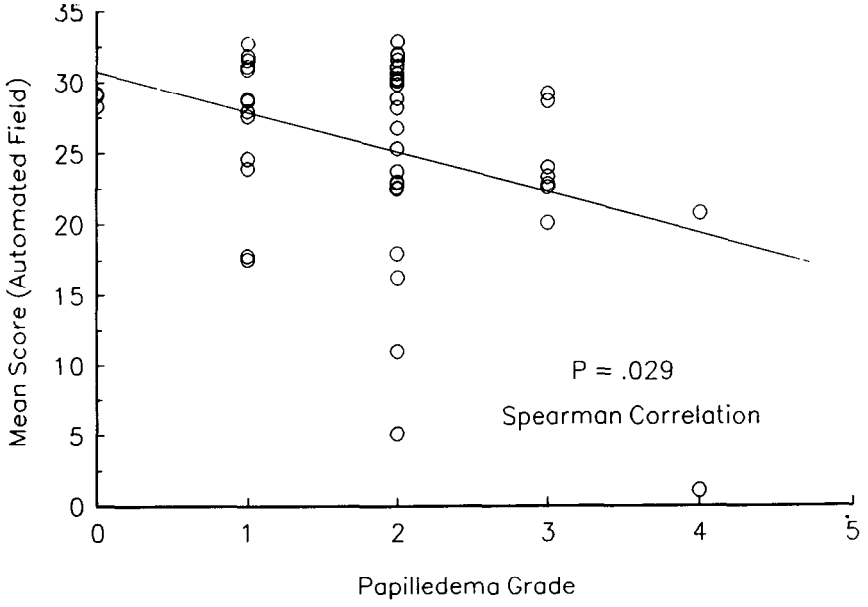

Fig 6 Scatter plot of mean score (automated perimetry) versus papilledema grade with regression line. Spearman rank correlation shows the two variables to be correlated ($p = 0.029$).

Fig. 4 shows a nerve fiber bundle analysis of the visual field in the IIH patients. Note the greatest loss occurs in the nasal and peripheral regions. Fig. 5 shows a quadrant and hemifield analysis. Again, more nasal than temporal involvement is apparent.

Fig. 6 is a regression of mean visual field score plotted against papilledema grade. The correlation coefficient was -0.32 which was significant at a $p = 0.029$ level. The graph also shows that, for some patients, the amount of visual loss cannot be predicted by the papilledema grade.

Discussion

The types of visual field defects that occur in IIH have been reported by many authors[1,7-10]. This study extends the previous work by comparing the defects of Goldmann perimetry and automated perimetry and analyzing the numerical thresholds of automated perimetry of 50 patients by anatomic region.

We had many instances of defects appearing larger and denser using automated perimetry and more defects were present using automated perimetry. Others have also noted this in comparison studies[11].

We found the pattern of loss in IIH similar to glaucoma as first described by Grehn[12]. Excluding blind spot enlargement, the earliest defect with Goldmann perimetry is usually an inferior nasal step. With automated perimetry a small inferior nasal step or a mild nasal depression often is the first defect. With increasing severity of visual loss, the hill of vision begins to sink with relative preservation of the central 10-15° (Fig. 3b-e). These stages are similar to glaucoma[13]. This has major implications on the visual field strategy used to test IIH patients.

We also found the higher the grade of papilledema, the greater the mean deviation ($p= 0.029$, Fig. 6). However, in individual patients, this may not be the case. This finding is expected as most of the visual loss occurs from dysfunction at the level of the optic nerve head.

In conclusion, the visual loss of IIH is of the disk-related type with defect morphology and stages of severity similar to glaucoma. This implies that kinetic screening strategies should be of the Armaly-Drance "keyhole" type to increase the sensitivity of the test. If the patient is a reliable subject for automated perimetry, a threshold strategy covering the central 24 to 30 degrees can be used. Although the visual loss found is often mild and unnoticed by the patient, it serves as a marker for guiding therapeutic intervention.

Acknowledgement

The author thanks Donna George for her excellent perimetry assistance

References

1. Wall M, George D: Idiopathic intracranial hypertension: a prospective study of 50 patients Brain (in press)
2. Smith JL: Whence pseudotumor cerebri? J Clin Neuro Ophthalmol 5:55-56, 1985
3 Frisén L: Swelling of the optic nerve head: a staging scheme J Neurol Neurosurg Psychiat 45:13-18, 1982
4. Johnson CA, Keltner JL, Lewis RA: JAWS (joint automated weighting statistic): a method of converting results between automated perimeters Doc Ophthalmol Proc Ser 42:563-568, 1987
5 Wall M, George D: Visual loss in pseudotumor cerebri: incidence and defects related to visual field strategy. Arch Neurol 44:170-175, 1987
6. Wirtschafter JD, Becker WL, Howe JB, Younge BR: Glaucoma visual field analysis by computed profile of nerve fiber bundle function in optic disc sectors. Ophthalmology 89:255-267, 1982
7 Corbett JJ, Savino PJ, Thompson HS et al: Visual loss in pseudotumor cerebri: follow-up of 57 patients from 5 to 41 years and a profile of 14 patients with permanent severe visual loss Arch Neurol 39:461-474, 1982
8 Wall M, Hart WM Jr, Burde RM: Visual field defects in idiopathic intracranial hypertension (pseudotumor cerebri) Am J Ophthalmol 96:654-669, 1983
9. Orcutt JC, Page NG, Sanders MD: Factors affecting visual loss in benign intracranial hypertension Ophthalmology 91:1303-1312, 1984
10 Smith TJ, Baker RS: Perimetric findings in pseudotumor cerebri using automated techniques Ophthalmology 93:887-894, 1986
11 Beck RB, Bergstrom TJ, Lichter PR: A clinical comparison of visual field testing with a new automated perimeter, the Humphrey field analyzer, and the Goldmann perimeter Ophthalmology 92:77-82, 1985
12. Grehn F, Knorr-Held S, Kommerell G: Glaucomatous like visual field defects in chronic papilledema Graefe's Arch Clin Exp Ophthalmol 217:99-109, 1981
13. Aulhorn E, Karmeyer H: Frequency distribution in early glaucomatous visual field defects Doc Ophthalmol Proc Ser 14:75-83, 1977

Atypical field defects in optic neuritis and the significance of the Tübingen flicker test in its diagnosis

Susanne Trauzettel-Klosinski and Elfriede Aulhorn

Department of Pathophysiology of Vision and Neuro-Ophthalmology, University Eye Clinic, D-7400 Tübingen, Germany

Abstract

This report deals with 50 patients suffering from optic neuritis (ON), who do not show the typical absolute central scotoma, but instead show atypical field defects, such as arcuate scotomas, reduction of light difference sensitivity, paracentral scotomas and other defects, when examined with the Tübingen manual perimeter. In these cases which imply quite a few problems in differential diagnosis, the Tübingen flicker test is of special diagnostic value, as this test gives pathological results only in active ON and is highly specific. Using this method, a reliable diagnosis of ON can be made in most of these cases.

Introduction

The typical field defect in optic neuritis (ON) is a sudden absolute central scotoma However, atypical field defects are not so rare and they raise quite a few problems in differential diagnosis.

This paper describes the different types of atypical field defects that we found in ON, and further, it discusses the significance of the Tübingen flicker test in these often difficult cases.

The Tübingen flicker test, also called the Aulhorn flicker test, is a simple and highly specific test in the diagnosis of active ON, as we have demonstrated in more than 1000 eyes[1-5]. The Aulhorn flicker test gives pathological values only in active ON and gives normal results after the inflammation has subsided[6].

Visual evoked potentials (VEPs), in contrast, remain pathological in subsided ON, so that the diagnosis of a recurrent attack is often ambiguous. Furthermore, the results of VEPs are not so specific and can give pathological latencies also in other optic nerve diseases[7].

The cases presented here are all eyes with acute ON of unknown etiology, which occurred isolated or combined with multiple sclerosis.

Patients

In a total cohort of 169 eyes with acute ON, 50 eyes exhibited an atypical field defect. Seven of them showed this atypical defect only at the onset and developed a typical absolute central scotoma during follow-up. All but two cases had had no previous episode of ON in the involved eye

Methods

Perimetry

All 50 patients were examined with the Tübingen manual perimeter in the 30° area. First kinetic perimetry, then profile perimetry, was performed. In profile perimetry, for determination of the light difference sensitivity curve (LDS) the 45° or 135° meridian was examined in cases without circumscribed scotomas, in the others it was chosen according to the localization of the scotomas.

In some patients 30° automatic grid perimetry with the Tübingen automatic perimeter (TAP 2000) was also carried out, and sometimes 90° perimetry, either Goldmann or TAP 2000, were performed, but these results are not the subject of this presentation.

Perimetry Update 1990/91, pp. 119-125
Proceedings of the IXth International Perimetric Society Meeting,
Malmö, Sweden, June 17-20, 1990
edited by Richard P Mills and Anders Heijl

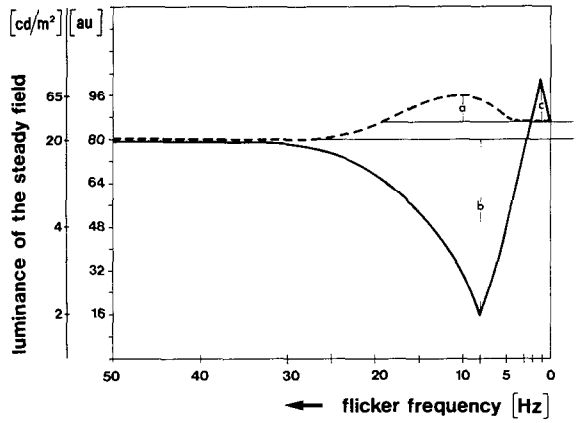

Fig 1 Schematic diagram of brightness sensation dependent on flicker frequency (abscissa). Ordinate: subjective brightness (corresponding to the luminance of the steady field which matches the brightness of the flickering field in arbitrary units (au) and in luminance values (cd/m²) Normal persons (broken line): increase of subjective brightness with decreasing frequency with a brightness enhancement (a) at 8-10 Hz (Brücke-Bartley effect) and return to the luminance at 0 Hz (non-intermittent steady light, line 1) Optic neuritis (ON: thick solid line), decrease of subjective brightness with decreasing frequency below Talbot level (luminance above critical fusion frequency, line 2) with a minimum at 8 Hz (b) and a brightness enhancement (c) at 1-3 Hz (late maximum) and return to line 1. (Reprinted from Trauzettel-Klosinski and Aulhorn[3] with permission)

Tübingen flicker test

In addition, all patients underwent the Tübingen flicker test, which measures the subjective brightness of a flickering light.

A double projector projects onto a screen two half-fields (with a diameter of 7°7'). The ray-path of one half-field is interrupted by a rotating sector disc, resulting in approximately rectangular flicker stimuli, the frequency of which can be varied between 0 and 50 Hz by the investigator.

The luminance of the non-intermittent, steady half-field can be varied by the patient. The patient is given the task of adjusting the subjective brightness of the steady field to that of the flickering field. The test is performed under photopic and suprathreshold conditions. It is performed *monocularly*, beginning with 50 Hz, with decreasing frequencies to 0 Hz.

In normal persons (Fig. 1, broken line), brightness sensation increases with decreasing flicker frequency. At 8-10 Hz subjective brightness of the flickering light is enhanced above the brightness of the steady stimulus at 0 Hz, known as the Brücke-Bartley effect[8,9]. Then the curve returns to the luminance at 0 Hz (line 1).

In ON (Fig. 1, thick solid line) by contrast, subjective brightness decreases to a minimum (b) when flicker frequency is lowered. Then the curve either returns to the luminance at 0 Hz or exhibits a brightness enhancement at 1-3 Hz, which we call "late maximum" (c). These two pathological phenomena (b,c) can appear in combination or isolated according to the stage of the disease[6]. In the diminishing stage of ON, only a late maximum is to be found. As a few patients were not examined at frequencies below 10 Hz, in these cases this second criterion for a pathological result was not judgeable.

Verification of the diagnosis

The clinical diagnosis was supported by the sudden onset of the field defect, and additional symptoms such as afferent pupil defect, painful eye-movement, Uhthoff phenomenon, spontaneous recovery and partial optic atrophy during follow-up, as well as by delayed latencies of the VEPs. Further, in some patients there were additional signs of multiple sclerosis.

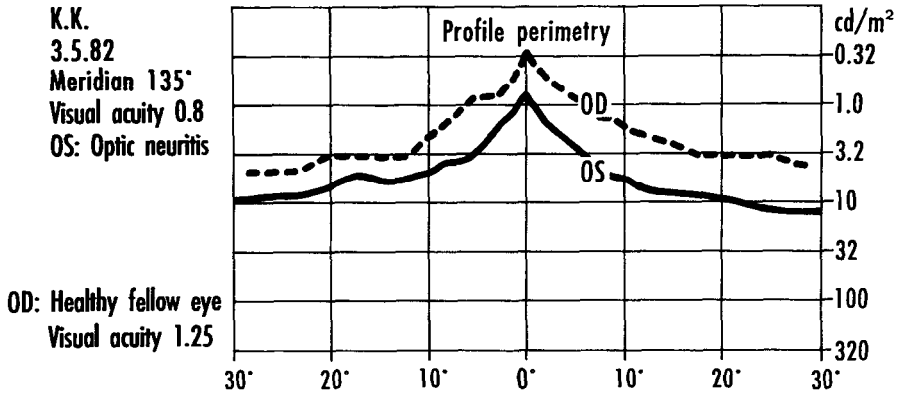

Fig 2 Decreased light difference sensitivity in ON compared to the healthy fellow eye (Tübingen manual profile perimetry).

Results

Thirteen of the 50 eyes with atypical field defects had nothing but a *decreased light difference sensitivity (LDS)* without circumscribed scotomas. Fig. 2 shows an example compared to the curve of the healthy fellow eye. Visual acuity was 0.4-1.0. The flicker test result was pathological in eight eyes, false-negative in one eye, and in four eyes the second criterion was not judgeable (Table 1).

Table 1. Atypical field defects in ON: (n=50) types and flicker test results

Type	*No of eyes*	*Frequency in the total cohort (n=169) in %*	*Flicker test result (No of eyes)*		
			pathological	*false negative*	*unjudgeable*
Decreased LDS without circumscribed scotoma	13	7.6	8	1	4
Arcuate scotoma	13	7 6	10	1	2
Circumscribed paracentral scotoma	10	5 9	7	1	2
Enlarged blind spot	3	1 7	3	–	–
Other types (see Table 2)	11	6 5	9	2	–
Total	50	29 3	37 (74%)	5 (10%)	8 (16%)

Arcuate scotomas, i.e., nerve fiber bundle defects, were found in 13 eyes, five relative (one example is shown in Fig. 3, left side), and eight absolute (Fig. 3, right side). In two eyes the scotoma later changed to an absolute central scotoma. Visual acuity ranged from 0.2-1.0. All defects in this group, as well as in the following one, extended to at least 7° to the center. From the 13 eyes, ten eyes had a pathological flicker test result, one eye had a false negative, and in two eyes the second criterion was not judgeable (Table 1)

A circumscribed, roughly circular *paracentral scotoma* was found in ten eyes, in eight eyes relative (Fig. 4), in two eyes absolute (Fig. 5). The diameter was 3-10°. Visual acuity ranged from 0.3-0.8. The flicker test result was pathological in seven eyes, false negative in one eye and not judgeable in two eyes (Table 1).

In three eyes there was only an *enlargement of the blind spot* with more or less decreased LDS. All three eyes showed a pathological flicker test result (Table 1).

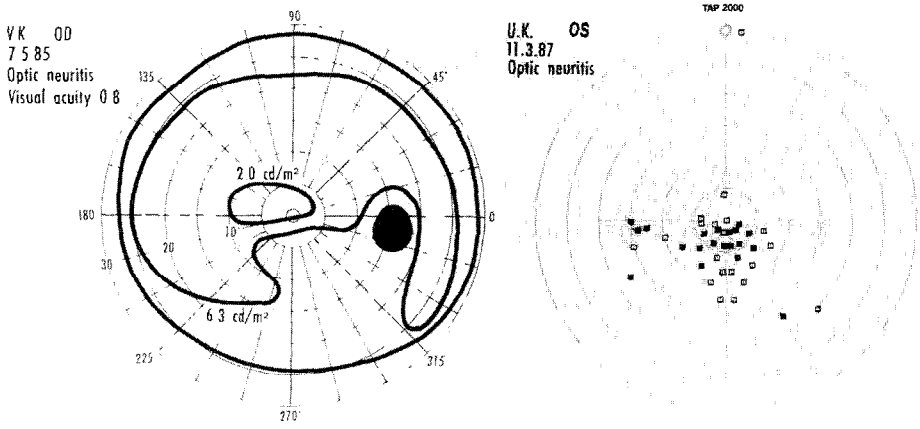

Fig 3 Arcuate scotoma in ON: relative scotoma in patient VK (left, Tübingen manual kinetic perimetry), mainly absolute scotoma in patient UK (right, TAP 2000)

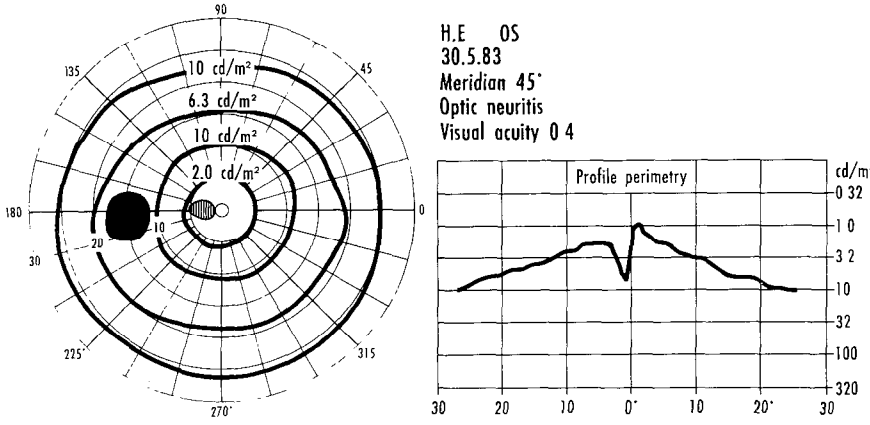

Fig 4 Relative circumscribed paracentral scotoma in ON, kinetic (left) and profile (right) perimetry (Tübingen manual perimeter)

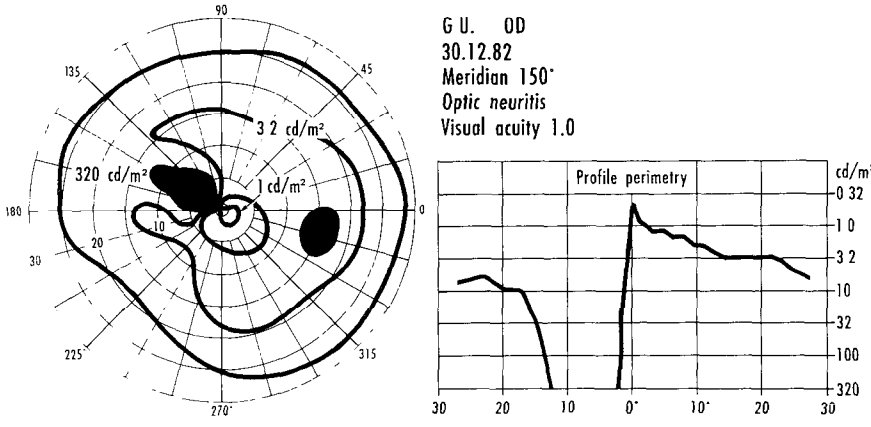

Fig 5 Absolute circumscribed paracentral scotoma in ON.

Table 2 Flicker test results in 11 eyes with various types of atypical field defects

Type	*No of eyes*	*Flicker test result (No of eyes)*	
		pathological	*false negative*
Large irregularly shaped scotomas			
extending over one quadrant	2	–	2
extending over two quadrants (nasal, temporal or altitudinal)	7	7	–
Diffuse, patchy defects	2	2	–

Eleven eyes showed *various types of atypical field defects* (Table 2). In nine eyes there was a *large irregularly shaped defect* extending over one or two quadrants, which was absolute in all but one case. In the two eyes with a scotoma covering approximately one quadrant (one absolute, one relative), the defect was located outside the 10° area, thus outside the flicker test field. The flicker test results in these two eyes were false negative. The other seven eyes showed irregularly shaped absolute defects extending over two quadrants, four eyes with nasal, one eye with temporal, two eyes with altitudinal involvement. Three of them changed to an absolute central scotoma during follow-up. All flicker test results were pathological. None of the nine eyes in this group was suspicious of eccentric fixation. Two eyes exhibited *diffuse patchy scotomas* (absolute and relative), which were not concentrated towards the center. One of them started with diffuse patchy defects, then developed an arcuate scotoma, followed by an absolute central scotoma after one week. The other one changed to a paracentral scotoma after one week. Both had a pathological flicker test result.

Discussion

Atypical field defects in ON, which do not show the characteristic absolute central scotoma, are not very rare[10,11]. In our cohort of 169 eyes with acute ON, 50 eyes produced an atypical field defect. When the seven eyes, which showed the atypical field defect only at the onset and later changed to an absolute central scotoma, are subtracted, the frequency is 25.4%.

Due to different systems of classification of the visual field defects and various perimetric methods, the comparison of the results between different authors is limited. Furthermore, verification of the diagnosis ON in some reports is not certain. Thus, reports of the frequency of atypical field defects of ON vary widely

Similar rates for some types of atypical field defects are reported by Keltner *et al* [11]: arcuate 8.9% (referred to cases with localized visual field loss) and 2.7% with enlarged blind spot (compared to 7.6% and 1.7%, respectively, in our series). Chamlin[12] even found 44% of arcuate defects. However, it is presumed that some of them might be shifted central scotomas (see below). Perkin and Rose[13] described various types of field defects in ON. When we apply our classification system to their cohort - as far as possible - and include their cases with "altitudinal, sectorial, hemianopic" defects, which do not spare the center, the total rate of atypical field defects in their series is approximately 18%. The results of Nikoskelainen[14] are similar to those of Perkin and Rose. She described 68% of central defects (with and without peripheral extension).

Some types of field defects are especially vulnerable to misinterpretation. Large absolute scotomas getting near to the center and covering one or two quadrants can easily be mistaken as an atypical field defect, whereas in reality they are shifted central scotomas due to eccentric fixation. Attention to the location of the blind spot is very important. The cases presented here (see Table 2, first group) are not suspicious for eccentric fixation.

Some problems of interpretation can arise in the cases with diffuse patchy scotomas. In our two cases (see Table 2, group 2), the defects were not concentrated towards the center. When such defects are accentuated to the center, they are not really atypical cases, because there are only gradual differences to an incomplete central scotoma.

Fig. 6 shows a large absolute scotoma with preserved central fixation. During follow-up first the central scotoma becomes smaller, but later less dense. It is evident that at this stage the defects can be especially well detected using automatic grid perimetry and this method is more suitable in these cases. Using a moving target, no exact isopter can be found.

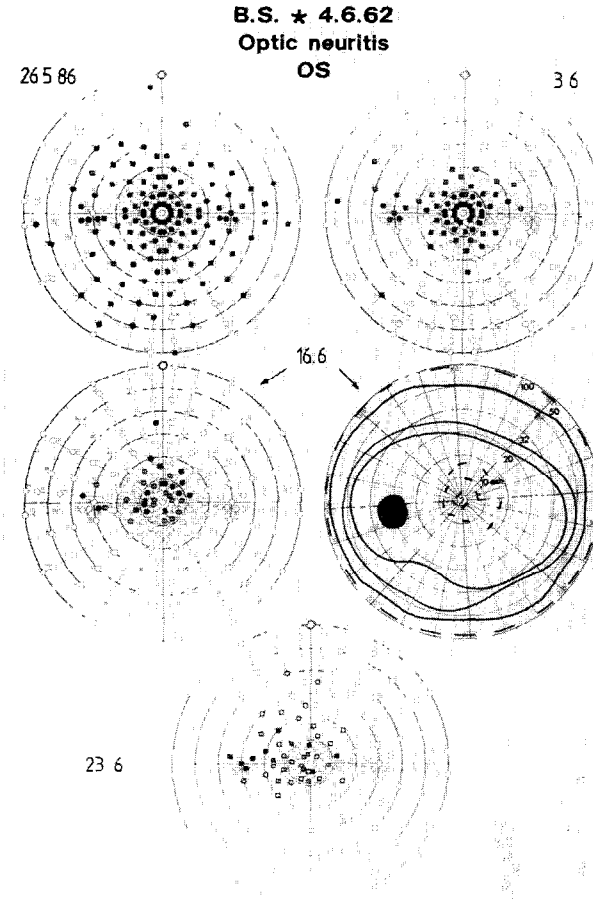

Fig 6 Absolute central scotoma sparing the center, during follow-up first becoming smaller (3/6/86), then less dense Note that these patchy defects are detected far better by automatic grid perimetry (TAP 2000) than by a moving target (16/6/86)

Atypical field defects in ON raise quite a few problems in differential diagnosis. In patients who exhibit a decreased LDS only without circumscribed scotomas, the differential diagnosis often includes the total palette of unexplained visual loss. In patients with a previous episode of ON it can be difficult to differentiate a recurrent attack from other visual disturbances, for example accommodation disorders. Here it is very helpful that the flicker test gives pathological values only in active ON and normalizes after the inflammation has subsided[6]. The diagnosis of a recurrent attack is easy by means of the flicker test, but is often ambiguous by means of the VEPs, because the latencies mostly remain pathological in subsided ON.

A sudden arcuate field defect is primarily suspicious of a vascular origin, such as an anterior ischemic optic neuropathy. A circumscribed paracentral scotoma is often the first sign of a beginning central retinopathy. In patients with ON who show only an enlargement of the blind spot, the differential diagnosis concerning papilledema due to optic nerve compression can be difficult.

In all these cases it is of special value that pathological flicker test results occur only in active inflammation of the optic nerve, not in papilledema due to compression or vascular disease, nor in visual loss of other origin. Previously, in a cohort of 527 eyes, we found a specificity of 98%[4]. The results of VEPs, by contrast, are not so specific and can give pathological latencies in other optic nerve diseases as well (for detailed references, see[7]).

Table 3. Sensitivity of the flicker test in ON

	Actual group with only atypical field defects (n=50)	*Former group with both typical and atypical field defects (n=138)*
Pathological	74%	85 5%
False negative	10%	8 7%
Unjudgeable	16%	5.8%

Table 3 summarizes the flicker test results of the 50 eyes with atypical field defects: in 37 eyes, *i.e.*, 74%, the flicker test result was pathological. False-negative results were found in only five eyes (10%). In two of these there was a very rapid recovery - within a few days - so that the active stage had nearly subsided and the case was examined too late, as it were. In two of the false-negative cases, the scotoma was localized outside the test field. In one eye there was no follow-up. As we have shown previously[5], the pathological result does not depend on the severity of visual loss, but on the activity of the inflammation.

In eight eyes (16%) the late maximum (see Fig. 1) was not judgeable, because the eyes were not examined at 1-3 Hz. As most of them were already in the recovery stage, a late maximum could have been expected. Sensitivity could be improved by consequent examination of all patients at low frequencies. Compared with our former patient group[3,5] of 138 eyes with both typical and atypical field defects, the false-negative results are in about the same range (see Table 3), and the slightly lower sensitivity in the cohort actually presented is due to the higher rate of unjudgeable cases.

Summarizing, we can state that in patients with atypical field defects in ON, the flicker test is of special value and in most of these difficult cases it enables certain diagnosis.

References

1. Aulhorn E, Trauzettel-Klosinski S: Der Flimmertest: Ein neues, einfaches Verfahren zur Diagnostik der Neuritis nervi optici. Fortschr Ophthalmol 80:398-400, 1983
2. Trauzettel-Klosinski S, Honegger J: Helligkeitsempfindung für Flimmerlicht bei Patienten mit Neuritis nervi optici. In: Herzau V (ed) Pathophysiologie des Sehens, pp 79-86 Stuttgart: Enke 1984
3. Trauzettel-Klosinski S, Aulhorn E: Measurement of brightness sensation caused by flickering light: a simple and highly specific test for assessing the florid stage of optic neuritis Clin Vis Sci 2:63-82, 1987
4 Trauzettel-Klosinski S, Aulhorn E: Die Bedeutung des Tübingen Flimmertests in der Differentialdiagnose der Neuritis nervi optici Fortschr Ophthalmol 85:557-561, 1988
5. Trauzettel-Klosinski S, Schüpbach M, Aulhorn E: Standardization of the Tübingen flicker test Graefe's Arch Clin Exp Ophthalmol 227:221-229, 1989
6. Trauzettel-Klosinski S: Various stages of optic neuritis assessed by subjective brightness of flicker. Arch Ophthalmol 107:63-68, 1989
7 Trauzettel-Klosinski S, Diener HC, Fahle M: Vergleich des Flimmertests nach Aulhorn mit den visuell evozierten Potentialen in der Diagnostik der Neuritis nervi optici Fortschr Ophthalmol 87:171-177, 1990
8. Brücke E: Ueber den Nutzeffekt intermittierender Netzhautreizungen. Sitzungsber K Akad Wissensch Math-Naturwiss Klasse Wien 49:128-153, 1864
9. Bartley SH: Subjective brightness in relation to flash rate and the light-dark ratio J Exp Psychol 23:313-319, 1938
10 Miller NR: Walsh and Hoyt's Clinical Neuro-Ophthalmology, Vol 1 Baltimore: Williams and Wilkins 1982
11. Keltner JL, Johnson CA, Spurr JO et al: Optic neuritis treatment trial: initial visual field defects IX IPS Meeting 1990 (this volume, p 135)
12. Chamlin M: Visual field changes in optic neuritis Arch Ophthalmol 50:699-713, 1953
13. Perkin GB, Rose FC: Optic Neuritis and its Differential Diagnosis, pp 74-93 Cambridge: Oxford University Press 1979
14. Nikoskelainen E: Symptoms, signs and early course of optic neuritis Acta Ophthalmol 53:254-272, 1975

Evaluation of the visual fields in patients with clinically-diagnosed transient ischemic attacks and minor stroke from the carotid artery territory

Benjamin M. Abela Jr[1], Pia Falke[2], C.E. Torsten Krakau[1] and Folke Lindgarde[2]

Departments of Experimental Ophthalmology[1] and Internal Medicine[2], University of Lund, Malmö General Hospital, S-214 01, Malmö, Sweden

The higher incidence of cardiovascular mortality and morbidity among carotid artery TIA patients compared to minor stroke patients from the carotid territory has prompted investigators to suggest that these two disease entities differ in vascular pathophysiology, the former being associated with generalized atherosclerosis and the latter with cerebral arteriolosclerosis or other mechanisms. The clinical definitions of TIA and minor stroke differ mainly by the duration of neurological symptoms. It is the aim of several investigations to assess other differences between these two groups, particularly regarding the cerebral circulation.

Computerized perimetry provides a non-invasive and sensitive documentation of ischemic insults involving the optical pathway. Therefore, we proceeded to evaluate the central visual fields of TIA and minor stroke patients.

Seventeen carotid artery TIAs and 14 minor stroke patients from the carotid artery territory were tested using the screening program of the Competer 750. Six patients (five TIA, one minor stroke) had symptoms of amaurosis fugax Only male patients were studied, to exclude differences in atherosclerotic manifestations due to sex and age. Average age in the TIA group was 66 years and in the minor stroke group 72 years. Doppler ultrasound of the carotid arteries and CT scan findings during the time of cerebral insult were taken from the patients' files. All patients were cleared of fundus lesions by ophthalmoscopy and none had had previous experience with the computerized perimetry.

Five TIA patients (29%) manifested visual field defects. The predominant finding was that of relative, paracentral scotomas in a patchy distribution across the binocular visual fields Eight minor stroke patients (57%) had visual field defects. These were mainly absolute defects, confluent with adjacent relative scotomas, found in localized areas Half the cases had a monocular presentation. Only one (TIA) of the six patients with amaurosis fugax had a field defect.

There were no significant differences in the TIA or minor stroke groups with regard to the frequency of visual field defects. In addition, there was no correlation of the degree of stenosis and the presence of CT scan findings with the presence of these defects.

These findings support the well-accepted tenet of an embolic pathogenesis of TIA A dissemination of multiple micro-emboli giving rise to small and discrete areas of infarction involving any part of the visual pathway is suspected in this syndrome. Minor strokes, on the other hand, are speculated to be due to solitary episodes of cerebral ischemia, probably thrombotic in origin, as a result of a diseased intra-cerebral vascular network.

This study is part of a comprehensive investigation directed at assessing differences between carotid TIA and minor stroke patients with regard to the occurrence of cerebral defects The clinical correlations of the visual fields, ocular blood flow using the Langham Ocular Blood Flow System, CT scan results, Doppler ultrasound findings, and cerebral blood flow results, are found in a separate report.

The full article will be published elsewhere.

Address for correspondence Dr. B Abela, Room E-6, C.P1 Manahan Annex Building, Makati Medical Center, 2 Amorsolo Street, Legaspi Village, Makati, Metro Manila, Philippines

Perimetry Update 1990/91, p 127
Proceedings of the IXth International Perimetric Society Meeting,
Malmö, Sweden, June 17-20, 1990
edited by Richard P. Mills and Anders Heijl

Statokinetic dissociation: analysis of spatial and temporal characteristics by perimetry*

Masahiro Osako, Evanne J. Casson, Chris A. Johnson, Peter Huang and John L. Keltner

Optics and Visual Assessment Laboratory (OVAL), Department of Ophthalmology, University of California, Davis, CA 95616, USA

Abstract

Statokinetic dissociation (SKD) refers to a greater reduction in sensitivity to stationary visual stimuli relative to similar targets in motion The authors evaluated SKD in nine optic neuritis (ON) patients and in nine normals by measuring the difference between static and 4°/sec kinetic thresholds for a size I target along the four oblique meridians (31 5 asb background) To assess temporal response characteristics, they used flicker perimetry to measure sensitivity of 2, 8 and 20 Hz sinusoidal flicker at 5° intervals along the same oblique meridians The patients' flicker sensitivity to all three frequencies was reduced at all eccentricities. In a number of cases, flicker sensitivity was unmeasurable to one or more frequencies within the region where kinetic targets were detectable. Sixty percent of the flicker thresholds for tests presented between 20 and 25° were unmeasurable even if a moving target could be seen These results indicate that SKD in these patients may not be due to a selective loss of mechanisms sensitive to low frequency temporal modulation with a relative sparing of mechanisms sensitive to high frequency temporal modulation as has been previously suggested The authors hypothesize that SKD may be due to differences in spatial summation in these patients, making a moving target, which has a greater spatial extent, more detectable than a stationary target. Therefore ON patients exhibiting SKD might be expected to show great improvement in static perimetry thresholds as target size is increased. The authors tested this by comparing the results of standard 30-2 Humphrey perimetry for size III and size V targets for normals and ON patients The patients showed a larger sensitivity gain for using the size V targets, in accordance with the authors' predictions.

Introduction

Statokinetic dissociation (SKD) was described by Riddoch in 1917 for patients with occipital lobe injuries. Since then, SKD has been associated with pathology at a number of other locations in the visual pathway, particularly in optic neuritis (ON)[1-4]. To explain the underlying mechanism, Safran and Glaser postulated a selective loss of mechanisms responding to low frequency temporal modulation or flicker (P-cell type, sustained or tonic mechanisms)[1]. This type of loss would presumably result in decreased sensitivity to slowly-moving or long-duration, stationary targets relative to rapidly-moving or abruptly-presented, short duration targets To assess this hypothesis, we investigated the temporal and spatial components of SKD. This was done by performing flicker perimetry and static perimetry with various target sizes on ON patients exhibiting SKD.

Experiment 1: analysis of temporal characteristics of SKD

In SKD, detectability of a moving target relative to a stationary target may be based on either the differences in the temporal components or the spatial components of the two types of targets. We investigated possible differences in sensitivity to the temporal components of stationary and moving targets by performing static, kinetic and flicker perimetry in the same areas of visual field in both ON patients and normals.

*Supported in part by National Eye Institute Grant No EY03424 (to CAJ) and an Unrestricted Research grant from Research to Prevent Blindness, Inc

Perimetry Update 1990/91, pp 129-134
Proceedings of the IXth International Perimetric Society Meeting,
Malmö, Sweden, June 17-20, 1990
edited by Richard P Mills and Anders Heijl

Method

Static, kinetic and flicker perimetry were performed on nine normal observers (mean age: 27.1 years) and nine ON patients with SKD (mean age: 48.5 years). Patients were selected for the study on the basis of clinical evidence of SKD, as revealed by greater sensitivity losses present in automated static perimetry than in manual kinetic perimetry (Goldmann perimetry).

Static and kinetic perimetry were performed on the SQUID automated perimeter[5,6], using a background luminance of 31.5 asb (10 cd/m^2) and a Goldmann size I (0.11° diameter) target. Preliminary studies revealed that a small target was most effective for demonstrating SKD. In normals, four oblique meridians were tested: 45°, 135°, 225° and 315°. In patients, only one or two meridians were tested because of the limited time available for the evaluation. Kinetic perimetry was performed using a 1000 asb (317.5 cd/m^2) moving at 4°/sec. In the static perimetry tests, thresholds for a 800 ms, size I target were obtained at 5° intervals. A 15 minute of arc diameter red fixation stimulus was provided, and fixation was monitored by an infrared video camera system. Normal observers and patients were tested without a refractive correction in place. This was done to maintain consistent test conditions for both static and kinetic visual field testing. Furthermore, all participants had low refractive errors, and most kinetic responses occurred outside the central 30 degrees where a lens rim might interfere with vision. Other details of the procedures may be found in Wedemeyer *et al* [2].

Flicker perimetry (31.5 asb or 10 cd/m^2 yellow background) was performed with a custom-made, automated perimeter which used 1° diameter yellow LEDs (315 asb or 100 cd/m^2) as stimuli. The temporal characteristics of the stimuli consisted of a square-wave onset and offset of sinusoidal modulation at either 2, 8 or 20 Hz for 2 seconds. Due to the nature of the background, maximum contrast was limited to 91%. Flicker modulation (contrast) thresholds were determined by a staircase procedure (yes/no response) for each of the temporal frequencies along the four oblique meridians (45°, 135°, 225° and 315°) at 5° intervals out to a 25° radius. A 1° diameter fixation point was provided, and fixation was monitored by means of an infrared video camera. A complete set of measurements was obtained from all normal observers and patients.

Results

The static equivalent to the kinetic isopter position value along each meridian was determined by interpolating between the static threshold values to determine the location at which a size I target of 1000 asb would be just detectable The difference between the static and kinetic values was then taken as an estimate of SKD for each meridian tested. When the SKD data are collapsed across meridians, ON patients show a mean magnitude of 17.0° (SD 11.3), considerably larger and more variable than normals (mean 4.5°, SD 1.25°).

Fig. 1 shows the results for Experiment 1. Panels (a) through (e) present the averaged sensitivity (10 × log reciprocal contrast threshold) for 2, 8, and 20 Hz temporal frequencies at each eccentricity (5°, 10°, 15°, 20°, and 25°) in normal subjects and ON patients. Data have been collapsed across meridians, excluding the meridians on which scotomata were located. In the patients, the mean flicker sensitivities were depressed for all of the temporal frequencies compared to the normal subjects.

In a number of individual cases, we found that flicker sensitivity to some or all of the frequencies was so depressed that we were unable to measure it; that is, patients appeared unable to see even very high contrast flicker. This totally depressed flicker sensitivity often occurred within the boundaries of the area where patients indicated they could see the moving stimulus in the kinetic perimetry and sometimes also within regions where patients indicated they could see the static stimulus. The bottom right panel of Fig. 1 summarizes this finding by showing the frequency with which this phenomenon was observed within the region where the moving target was detectable. Each bar represents the cumulative frequency for all three flicker rates at each eccentricity. The bar on the far right indicates the sum total percentage of cases of unmeasurable flicker thresholds within the kinetic boundary Forty-four percent of all flicker thresholds within the kinetic boundary were below measurable limit (91% contrast), with about 60% of all flickering targets at 20 and 25° being undetectable The numbers above each bar on the graph indicate the number of times no measurable sensitivity to any of the three flicker frequencies was found at that location. In 30% of the cases, patients were unable to detect

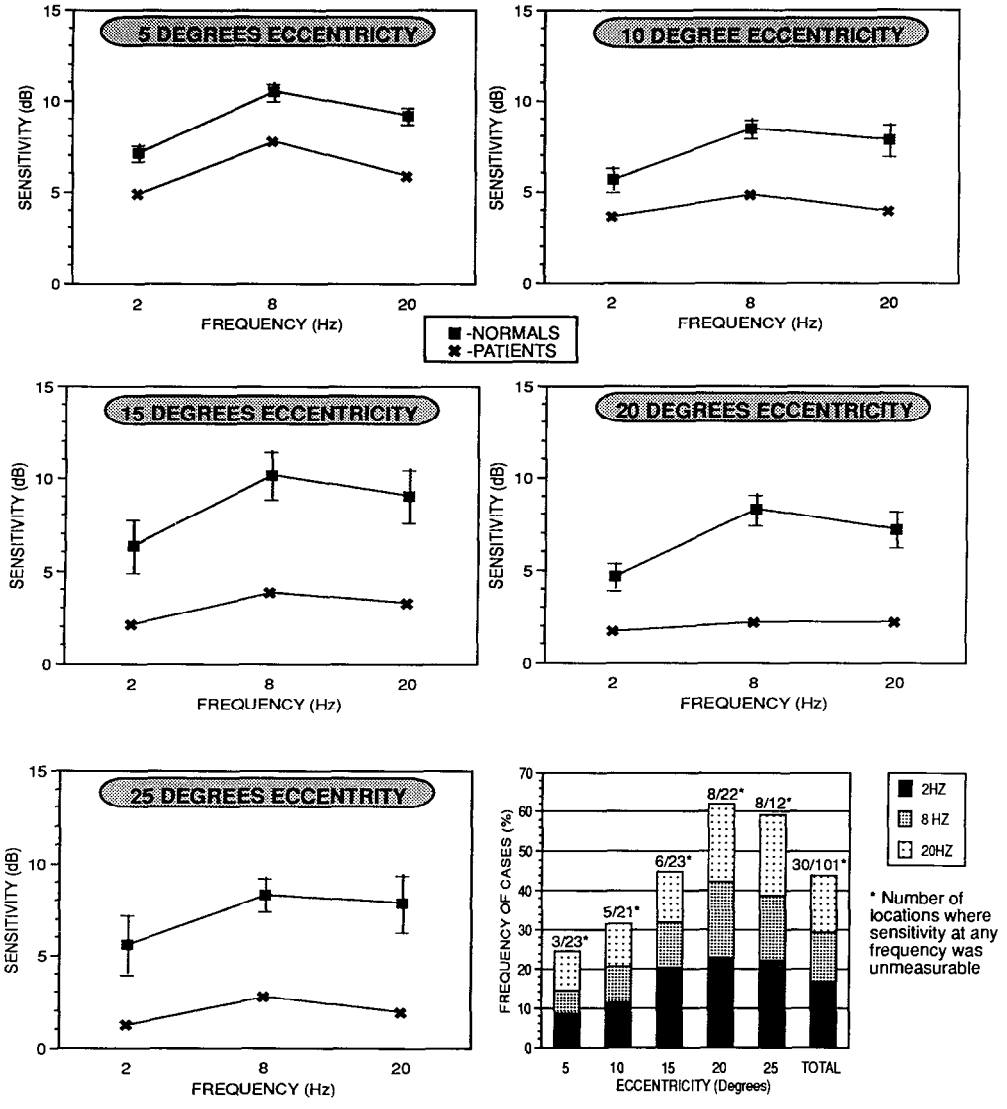

Fig 1 Panels are labelled (a) through (f) from left to right, top to bottom Average sensitivity to temporal frequencies (2, 8, and 20 Hz) at each eccentricity are shown in panel (a) through (e) Standard error bars are shown for the normal subjects' data Histogram of the frequency of unmeasurable thresholds at each eccentricity and in total are shown in panel (f) Accumulated values for each temporal frequency are plotted in each bar The numbers on top of each bar indicate number of locations where sensitivity at all three frequencies was unmeasurable.

flicker at any of the three frequencies presented at that location even though a moving target presumably would have been detectable. This indicates that sensitivity to the temporal component of the moving target is not an important factor underlying SKD.

Experiment 2: analysis of spatial characteristics of SKD

Another important difference between a moving and a stationary target is the spatial characteristics of the target: a moving target activates a much larger area than a similarly-sized, stationary target. If the superiority for detecting moving targets seen in these ON patients is a

(a) Mean difference of thresholds at each location
Normal subjects (10 eyes)

Mean (S.D.)									
			5.8 (2.7)	4.6 (2.5)	5.8 (2.7)	5.4 (3.0)			
		5.8 (2.4)	5.8 (2.2)	6.0 (2.5)	5.6 (1.3)	5.4 (2.1)	6.0 (2.1)		
	6.4 (2.6)	4.6 (2.3)	4.6 (1.3)	4.6 (1.0)	4.8 (1.4)	5.2 (1.9)	5.8 (2.4)	5.2 (1.4)	
5.4 (1.9)	5.8 (2.0)	4.6 (2.3)	4.6 (1.3)	4.6 (1.6)	5.0 (1.4)	5.0 (1.1)	4.4 (1.3)	6.2 (1.8)	5.6 (2.1)
6.6 (1.9)	5.2 (2.7)	4.4 (1.6)	5.4 (1.9)	4.2 (1.1)	4.8 (1.0)	4.6 (1.6)		4.4 (2.6)	4.2 (3.3)
5.4 (3.0)	4.6 (2.7)	5.6 (1.8)	4.2 (1.5)	4.0 (1.3)	4.4 (1.3)	4.2 (1.8)		4.8 (1.0)	4.8 (1.0)
6.8 (1.9)	5.8 (2.2)	4.8 (1.7)	4.4 (2.3)	4.2 (1.8)	4.8 (1.0)	4.8 (1.4)	4.8 (1.7)	4.4 (1.8)	5.6 (1.6)
	5.8 (2.7)	5.2 (2.1)	4.4 (1.3)	4.0 (1.6)	5.4 (2.1)	4.6 (1.9)	4.0 (3.3)	5.6 (1.6)	
		6.6 (1.9)	6.0 (2.7)	5.2 (2.3)	4.8 (1.4)	6.0 (1.6)	5.0 (1.9)		
			7.0 (1.7)	6.0 (2.5)	4.8 (2.9)	4.8 (1.7)			

(b) Topography of frequencies of locations above normal limit (Mean+2SD)
Four patients (5 eyes)

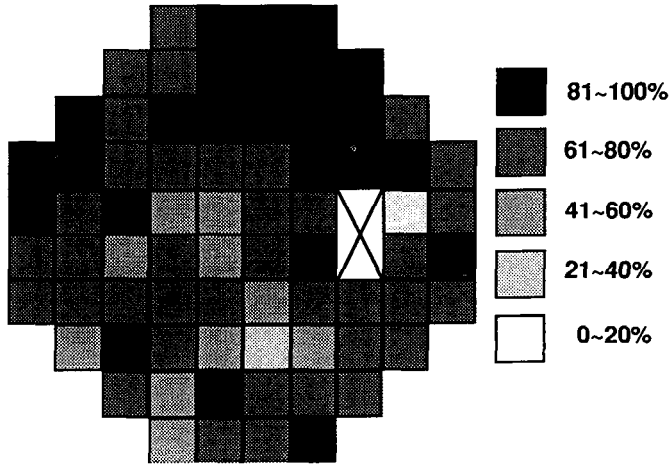

Fig 2 Panel (a) shows average threshold difference between size III and size V for normals at each location and panel (b) shows the frequency (in percent) with which ON patients exceeded upper limit of 95% confidence interval at each location in visual field

result of the spatial differences between moving and stationary targets, one might expect that increasing target size would improve performance on static perimetry dramatically for ON patients exhibiting SKD. We tested this hypothesis by performing static perimetry on ON patients and normals with size III and size V targets.

Method

Humphrey 30-2 static perimetry was performed on two ON patients with SKD (three eyes) and ten normal subjects (ten eyes, 27 to 55 years old) size III (0.43° diameter) and size V (1.72° diameter) stimuli on the same day. All subjects were optimally corrected with near refractive corrections appropriate to their age. Mean difference between thresholds for size III and size

V was calculated at each location. The normal data was used to define a 95% confidence interval for normal threshold differences between these two target sizes. Threshold differences at each location for the ON patients were compared to upper limit of the 95% confidence interval Retrospectively, we also reviewed the visual fields for two patients (two eyes) who had the 30-2 test for both size III and size V stimuli in our clinic within a short time (maximum lag of two weeks with size V tested before size III) and evaluated the resulting size V-III threshold differences in the same way.

Results

Fig. 2a shows normal averages (also SD) of the size V-III threshold differences at each spot. The confidence interval for the threshold differences averaged over the full field (mean ±2 SD) was 18.0 dB. These differences become larger with increasing eccentricity. Fig. 2b shows the frequency with which thresholds at each location within the visual fields of ON patients exceeded the upper limit of the 95% confidence interval. Abnormally large improvements were seen at all visual field locations, but the frequency was highest in the superior mid-periphery. These results clearly indicate that pathologic spatial summation is a factor in ON patients exhibiting SKD and may explain how the patients can be more sensitive to a moving target than a stationary one in spite of having no measurable flicker perception between 2 and 20 Hz.

Discussion

Our results show that ON patients can exhibit severely reduced sensitivity to flickering or temporally modulated targets, and yet can detect a moving target of roughly the same luminance better than a stationary target. This result is inconsistent with previous theories suggesting that following an attack of optic neuritis, more residual dysfunction of P-cells remains than M-cells[7,8]. If the hypothesis that SKD is caused by selective loss of P-cells were true, a selective loss of sensitivity to low temporal frequencies should be detected in flicker perimetry. In our study, mean flicker sensitivities to all temporal frequencies were generally depressed compared with normal subjects and no clear relationship between any particular loss of flicker sensitivities and SKD is apparent in individual patient data. Furthermore, in some patients, the ability to detect moving targets was preserved while the ability to detect flicker was not, further emphasizing the lack of correlation between SKD and flicker sensitivity These results suggests that temporal characteristics of two mechanisms (P- and M-cells) are not related to statokinetic dissociation.

Without the sensitivity to the temporal modulation, how can a moving stimulus be detected better than a stationary stimulus? Greve has noted that physiological SKD in normals could be due to "successive lateral spatial summation" of the moving target[9]. While spatial and temporal summation occur at the same time for a moving target, in ON patients, it appears that spatial summation is the most likely mechanism underlying SKD. In our studies of spatial characteristics of SKD, ON patients showed remarkable improvement of sensitivity by the increase of stimulus size. This kind of pathologic summation has been reported previously in other circumstances. For example, Wilson reported "photometric disharmony" in patients with various lesions of the visual pathways[10]. Others have also reported that SKD decreases when larger target sizes are used, due to a substantial improvement in static thresholds with large target size[11]. This evidence from earlier studies, combined with the results here, suggest that SKD is a result of altered spatial summation in the recovering visual field, rather than a selective loss of P-cell mechanisms.

References

1. Safran A, Glaser J: Statokinetic dissociation in lesions of anterior visual pathways Arch Ophthalmol 98:291-295, 1980
2. Wedemeyer L, Johnson C, Keltner J: Statokinetic dissociation in optic nerve disease In: Heijl A (ed) Perimetry Update 1988/89, Proceedings of the VIIIth International Perimetric Society Meeting. Amsterdam/Berkeley/Milan: Kugler & Ghedini Publ 1988/89

3 Yabuki K, Sakal M, Suzumura H, Endo N, Matsuo H: A comparison of kinetic and static perimetry for lesions in the visual pathway. In: Heijl A (ed) Perimetry Update 1988/89, Proceedings of the VIIIth International Perimetric Society Meeting Amsterdam/Berkeley/Milano: Kugler & Ghedini Publ 1988/89
4. Zappia R, Enoch J, Stamper R, Winkelman J: The Riddoch phenomenon revealed in non-occipital lobe lesions. Br J Ophthalmol 55:416-420, 1971
5. Keltner JL, Johnson C: The Synemed "Fieldmaster" perimeters In: Drance SM (ed) Automated Perimetry in Glaucoma. Orlando: Grune and Stratton 1985
6. Keltner JL, Johnson C: Preliminary examination of the SQUID automated perimeter Doc Ophthalmol Proc Series (V Int Visual Field Symp) 35:371-377, 1983
7. Alvarez S, King-Smith P: Dichotomy of psychophysical responses in retrobulbar neuritis. Ophthalm Physiol Opt 4:101-105, 1984
8. Russell M, Murray I, Metcalfe R: Variation in spectral sensitivity following optic neuritis. Invest Ophthalmol Vis Sci 31:609, 1990
9 Greve E: Single and multiple stimulus static perimetry in glaucoma Doc Ophthalm 36:1-335, 1973
10. Wilson M: Spatial and temporal summation in impaired regions of the visual field. J Physiol 189:189-208, 1967
11 Wood J, Wild J, Crews S: Stimulus investigative range in the perimetry of retinitis pigmentosa: some preliminary findings Doc Ophthalmol 63:287-302, 1986

Optic neuritis treatment trial: initial visual field defects

John L. Keltner, Chris A. Johnson, John O. Spurr and Optic Neuritis Group

Optic Neuritis Study Group, Department of Ophthalmology, University of California, Davis, CA 95616, USA

The Visual Field Reading Center (VFRC) at the University of California, Davis, Department of Ophthalmology, has reviewed over 5000 Goldmann and Humphrey visual fields in the 17 months since the Optic Neuritis Treatment Trial began. We have classified the initial visual field defects in 223 ONTT tests through October 1989 The initial Goldmann peripheral fields showed 45.3% diffuse and 41.7% localized visual field loss; 13% showed no defect. The initial Humphrey visual fields showed 49.8% diffuse and 50.2% localized visual field loss.

The frequency distribution of the 112 local Humphrey defects were as follows· altitudinal 30.4%; three quadrant 17.0%; hemianopic 10.7%; quadrant 9 8%; arcuate 8.9%; centrocecal 8.9%; peripheral rim 6.3%; central 5.4%; and enlarged blind spot 2.7%

The frequency of abnormality in the fellow eye was much higher than expected Of the 223 initial Humphrey fellow eye visual fields, 47.5% had an abnormal mean deviation with a p value of <0.05.

The full article will be published elsewhere

Supported in part by national Eye Institute Research Grant No EY07461 (JLK), and an Unrestricted Research Grant from Research to Prevent Blindness, Inc.

Perimetry Update 1990/91, p 135
Proceedings of the IXth International Perimetric Society Meeting,
Malmö, Sweden, June 17-20, 1990
edited by Richard P. Mills and Anders Heijl

Time variation of step-like field defects in Gilles de la Tourette syndrome

Jay M. Enoch, Vasudevan Lakshminarayanan and Bakulesh M. Khamar*

School of Optometry, University of California, Berkeley, CA 94720, USA

Abstract

Unique step-like defects are seen in people exhibiting Tourette syndrome (TS) and many of their blood relatives. These step-like field defects fluctuate, *i e* , appear and disappear when visual fields are examined repeatedly on the same or different days These changes in visual field do not follow a fixed pattern. The pathogenesis of such changes is not known

Introduction

Gilles de la Tourette syndrome (TS), a neuropsychiatric disorder, is thought to be an anomaly of the dopaminergic system. Step-like visual field defects have been described in Gilles de la Tourette syndrome[1,2]. Unlike step-like field defects seen in other conditions nasal and temporal steps have been found with almost equal frequency[3,4]. This finding makes this condition unique and important to study. We have also shown that this step-like field defect is largely (but not wholly) due to changes in sensitivity near the horizontal meridian[3-5]. Analyzing the data on visual fields plotted in persons exhibiting Gilles de la Tourette syndrome, we have found that step manifestations are associated with an alteration in prechiasmal sensitivity (*i.e.*, decrease or increase in sensitivity at a given location as revealed by a measured isopter or difference in static threshold assessed above or below the horizontal meridian)[5].

When the field examination is repeated at the interval of approximately one year, it is found that only 50% of steps are found at the same site[6]. There were new steps appearing and old ones disappearing with nearly equal frequency. No evidence of exacerbation of the condition was seen

We have sought to understand this unusual, but important finding. We thought it useful to look for changes taking place in the visual field of TS individuals when examined sequentially on the same day. In a pilot study involving three eyes of two individuals, we found unexpectedly that step-like field defects, though always present, kept on changing their site and orientation Because of this unanticipated finding we felt it critical to further explore these evanescent phenomena in some detail. In this brief report we present illustrative cases; further detailed reports will be published elsewhere[7].

Material and methods

Persons exhibiting TS and their parents were included in this research Similarly, using the same protocol, we examined a number of normal individuals in the same age range. Informed consent was obtained from all individuals.

All persons were given a thorough eye examination which included a manifest refraction, slit lamp examination, keratometry, fundus examination, fundus photographs and measurement of intraocular tensions. Each individual was sharply focussed on the cupola located 30 cm from the entrance pupil of the eye. This correction was always used in order to optimize response sensitivity in the central field[8].

*On leave from M&J Institute of Ophthalmology, BJ Medical College, Ahmedabad 380015, India

This research was supported in part by Grant No EY 03674 (to JME) from the National Eye Institute, NIH, Bethesda, Maryland

Perimetry Update 1990/91, pp 137-141
Proceedings of the IXth International Perimetric Society Meeting,
Malmö, Sweden, June 17-20, 1990
edited by Richard P. Mills and Anders Heijl

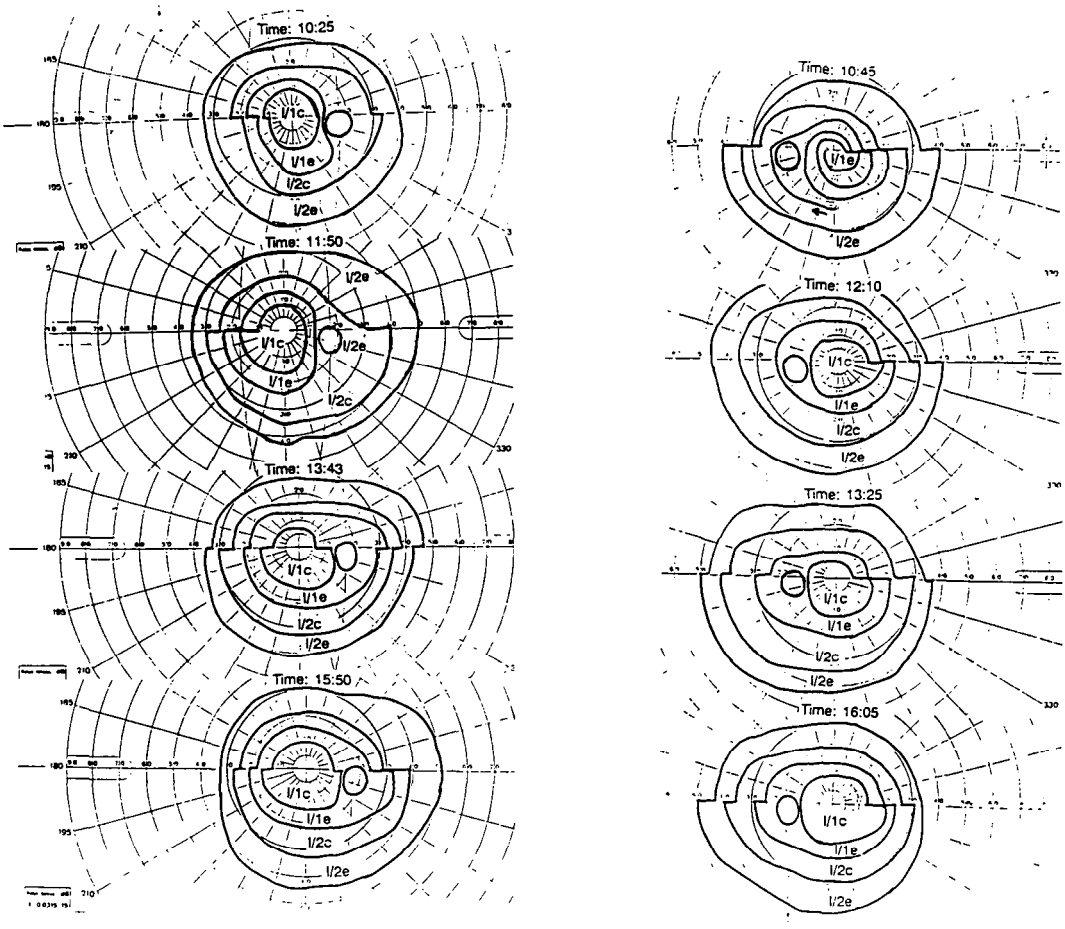

Fig 1 Illustration showing change in step-like field defect in a person exhibiting TS when examined at four different times of the day.

Perimetry was performed on the Goldmann Haag-Streit perimeter equipped with special voltage stabilizer. Perimetry was performed repeatedly using four or more isopters. Tests were repeated a minimum of three times within five hours on the same day under identical conditions. One hour was the minimum time separation between two subsequent examinations Perimetric records of the previous examination were not available to the perimetrist, and records were not analyzed until completion of the entire test sequence. These procedures were taken to minimize bias. Perimetry was performed using the same isopters at each examination.

Results

There were 11 persons exhibiting TS, five parents of TS patients known to manifest field anomalies and four normal individuals. With the exception of normal control subjects, all other subjects had previously exhibited step-like defects Analysis is restricted to step manifestations since this is the most robust finding of all (*i e* , each step area was sampled ten times or more). Since one person (TS) constantly exhibited marked and generalized loss of sensitivity over time, his data could not be properly interpreted in the analysis for steps.

Illustrative cases: KS is a 27-year-old white male exhibiting TS. Both his eyes were examined

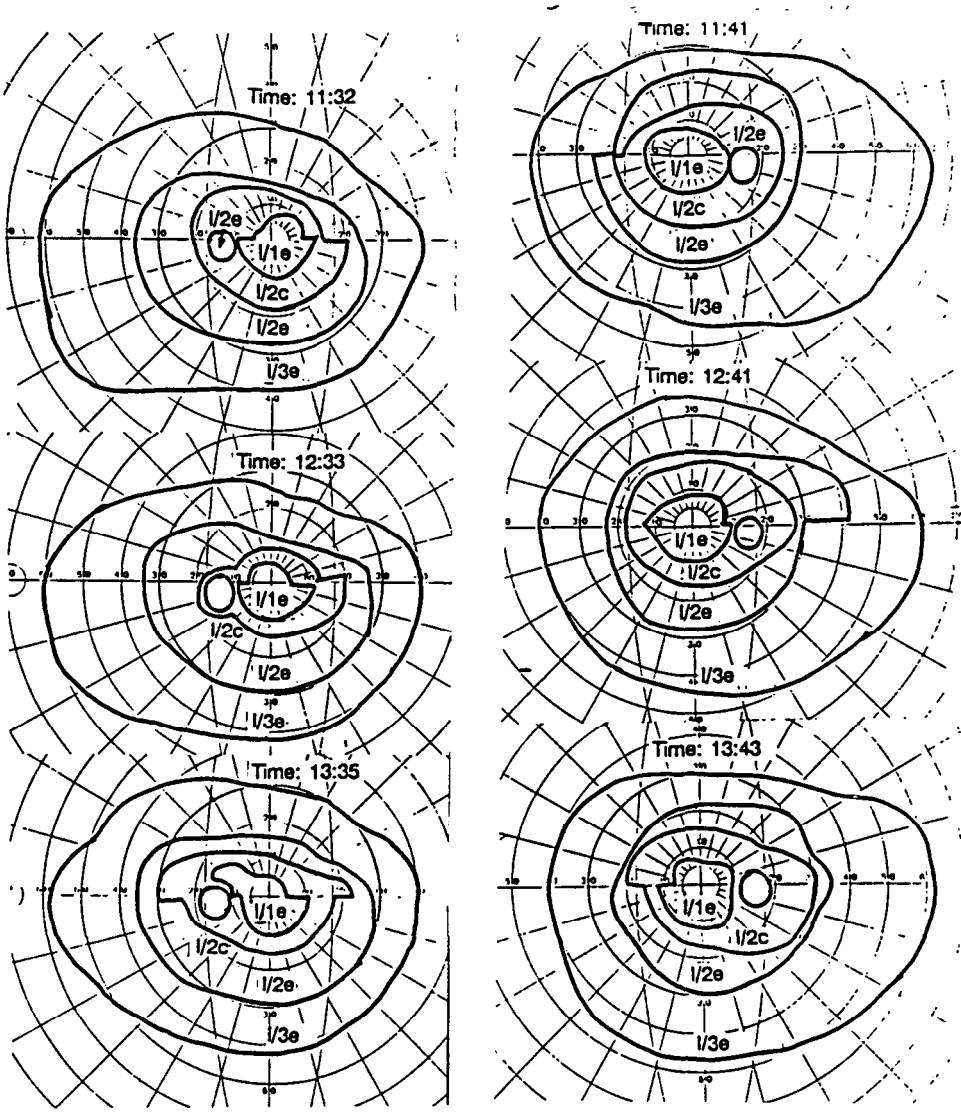

Fig 2 Illustration showing change in step-like field defects in the father of a person exhibiting TS when examined at different times of the day

four times on the same day. The results are shown in Fig. 1. Please compare individual isopters on the data sets. Data from a father of a TS patient is displayed in Fig 2

The number of steps detected differed for all examinations performed on the eyes tested. Not only the number of steps in individual isopters detected changes, but also the isopter with which they were detected was often altered. Identical changes in the visual field were found in five parents of TS patients. All patients had shown visual fields comparable to their TS children on previous occasions.

An important observation is the absence of steps in one eye of one TS individual and in one eye in each of two parents during one of the three or more examinations. In each case, the second eye showed step-like field defects when examined

No correlation was found between the number of steps detected and the time of day of the test, or the order of the examination in the series (*i e* , 1st, 2nd, 3rd, etc).

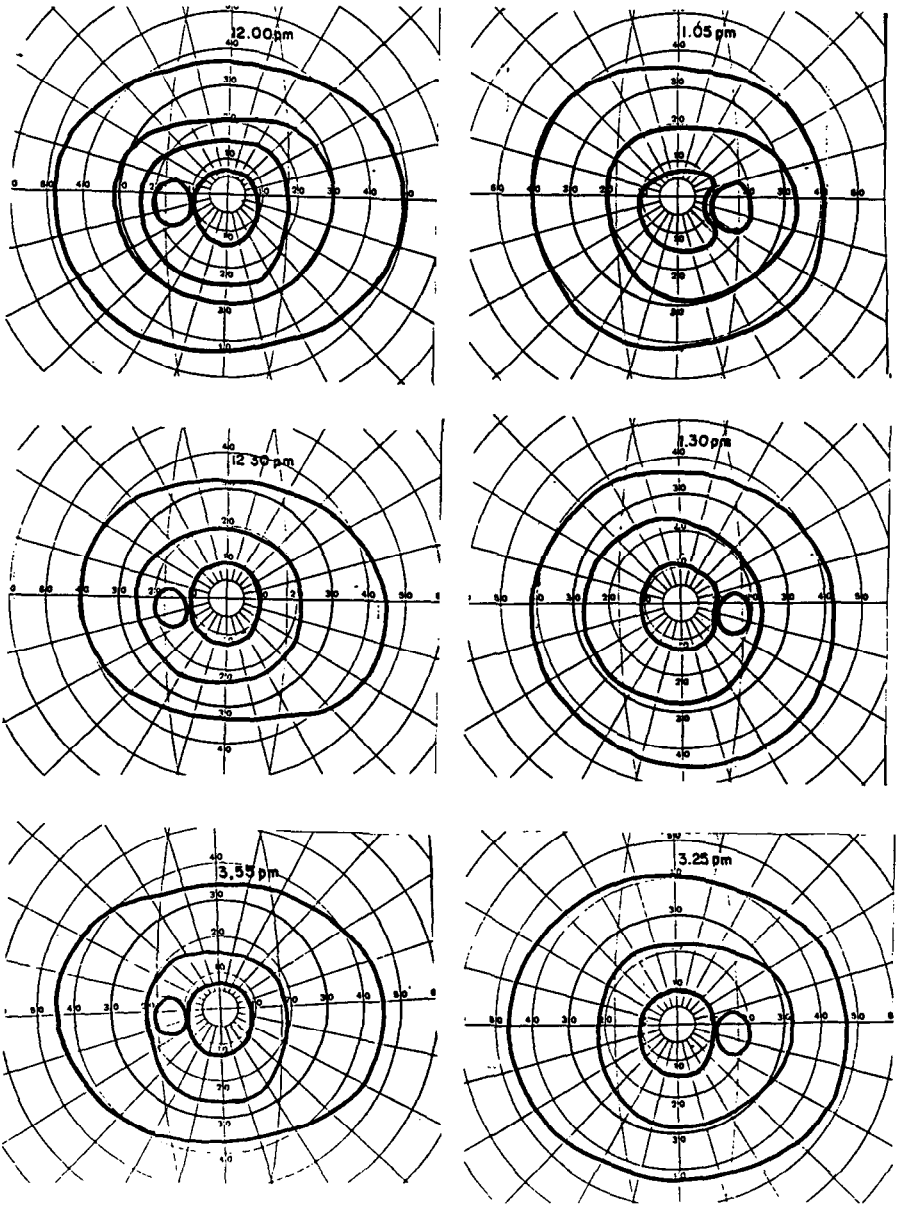

Fig 3 Visual fields from a normal control subject

Loss of sensitivity over time (generalized contraction of field or helical spiralling of the field)

Although appropriate, data of the one subject with extreme loss of sensitivity over time are not included for consistency in the analysis. In perimetric examinations of 11 individuals exhibiting TS, eight persons showed this phenomenon 18 times in 12 of 22 eyes. In four persons, loss of sensitivity over time was seen in both eyes. This loss of sensitivity over time was seen during the first examination ten times, and eight times during both the second and third examinations. Since the majority of the first examinations began in the morning, it was not possible to define a meaningful relationship between the presence of this phenomenon and time of the

day. Further, since this manifestation appeared more commonly early in the day, our use of the term "fatigue" is probably a misnomer. What is meant by this term is a loss of sensitivity over time during the individual test procedure.

Loss of sensitivity over time was seen in one parent (mother of a TS child) during the second examination in both eyes

Normals· in none of the normals, during any examination, were steps, a loss of sensitivity over time, or gross sensitivity changes seen However, some isopter area changes were seen. These could be attributed most probably to changes in eye pupil size, some accommodation during the test, adaptation state, or criterion of threshold at the time of the test (Fig 3).

Discussion

Step-like field defects and attendant loss of sensitivity over time are seen to appear and disappear in an unpredictable manner in this study These remarkable changes are therefore transient or evanescent alterations in sensitivity. Virtually all fields were taken by the senior author, a highly experienced perimetrist He has never encountered anything quite like the reported findings. Further detailed analyses including relevant statistical data will be published elsewhere[7].

We do not understand how this activity occurs. Additional work is currently being carried out in order to further elucidate this unique phenomenon These are small effects revealed by careful study in a well-controlled test situation (small target, subject carefully refracted to the cupola, rest periods, etc.). The subjects are often difficult individuals to study Automated perimetric examinations are not suitable for this patient population[2] because randomized trials would only obfuscate the outcome.

Clearly we need to conduct further studies on this and other conditions known to have dopaminergic anomalies in order to assess if this is a characteristic finding in all dopamine anomalies or is manifested in TS alone Most importantly, these transient changes may offer valuable insights into neurotransmitter anomalies

References

1. Enoch JM, Itzhaki A, Lakshminarayanan V, Comerford JP, Lieberman M, Lowe T: Gilles de la Tourette syndrome: visual effects. Neuro-Ophthalmology (Amsterdam) 8:251-257, 1988
2. Enoch JM, Itzhaki A, Lakshminarayanan V, Comerford P, Lieberman M: Visual field defects detected in patients with Gilles de la Tourette syndrome: preliminary report Int Ophthalmol 13:331-344, 1989
3 Enoch JM, Khamar BM, Lakshminarayanan V: An analysis of step-like visual field defects in Gilles de la Tourette syndrome Neuro-Ophthalmology (Amsterdam) 10:299-309, 1990
4. Enoch JM, Khamar BM, Lakshminarayanan V: Static and kinetic perimetric field defects in Gilles de la Tourette syndrome: quantifying step-like visual field defects Clin Vis Sci 1990 (in revision)
5 Khamar BM, Enoch JM, Lakshminarayanan V: Step manifestations and sensitivity changes in Gilles de la Tourette syndrome Neuro-Ophthalmology (Amsterdam) 10:293-298, 1990
6 Enoch JM, Khamar BM, Lakshminarayanan V: Step-like visual field defects in Gilles de la Tourette's syndrome: effect of duration (one year). Clin Vis Sci 1990 (in revision)
7 Enoch JM, Lakshminarayanan V, Khamar BM: Step-like field defects in Gilles de la Tourette syndrome: changes during a day Neuro-ophthalmology 1991 (in press)
8. Fankhauser F, Enoch JM: The effects of blur upon perimetric thresholds Arch Ophthalmol 68:240-251, 1962

Evaluation of high-pass resolution perimetry in neuro-ophthalmology

H. Bynke

Department of Neuro-Ophthalmology, University Eye Clinic, S-221 85 Lund, Sweden

Abstract

In 22 visual fields of 14 patients with CNS disorders, high-pass resolution perimetry (HRP) was compared with the conventional automated perimeter Competer 750 (Digilab), using that instrument's central neuro-grid and threshold program HRP was confirmed to have two practical advantages, namely, that the testing procedure was greatly facilitated by the feedback system, and that the test time was shorter. The latter was an effect of the relatively small number of test points Because HRP does not explore the blind spot area, does not test large hemianoptic defects in detail, and uses larger targets than the Competer, some information was lost However, HRP did not miss any diagnostically important defects That the threshold zone of HRP is particularly narrow and that the targets are more distinctive than conventional perimetric targets, could not be confirmed

Introduction

High-pass resolution perimetry (HRP), also called Ring perimetry, uses high-pass spatial frequency filtered resolution targets, which are generated by a personal computer and presented on a video monitor as rings of various sizes at constant contrast[1] Because these targets measure peripheral visual acuity rather than differential light sensitivity, HRP was said to give a more direct insight into the structural properties of the visual system than other perimetric methods, including conventional automated perimetry[2,3]. This is certainly not much more than a hypothesis. Further, the targets were said to be more distinctive at threshold and the threshold zone much narrower than is the case with conventional targets[1,2] Even these statements remain to be proved. More probable advantages over conventional automated perimetry are that the attention and motivation of the examinee are enhanced and that the test time is shorter[1]. Accordingly, most of the learning effects take place between the first and second examination[4] Disadvantages are that the large targets tend to prevent exact definition of the borders of the field defects and precise measurements of the depth of circumscribed defects[1,2]. In addition, a recent investigation showed that the results are much affected by refractive blur[5]

In order to evaluate the sensitivity and other properties of HRP, this method was compared with conventional automated perimetry at examinations of clinical cases As regards the loss of mean sensitivity, there was no great discrepancy between HRP and Octopus computed perimetry in chiasmal lesions[6] or glaucoma[7], but it was emphasized that HRP provides no detailed test of large hemianoptic defects[6] The test of time of HRP was much shorter than that of the Octopus[6,7] HRP was reported to be more sensitive than the computed perimeter Competer (Digilab) in early glaucoma[8], but a more comprehensive study demonstrated that it was markedly less sensitive than the Humphrey Field Analyzer in the detection of this kind of defects – no less than 24% of the glaucoma defects were missed with HRP[9]

The present study compares HRP and Competer perimetry in a small group of patients with disorders of the central nervous system (CNS)

Material and methods

Twenty-seven visual fields (VFs) of 15 patients with CNS disorders were tested with Competer 750 (C), using this perimeter's central neuro-grid, threshold program, and a target exposure time of 0.50 sec[10]. After a rest of about 30 minutes, the same VFs were tested with the

Perimetry Update 1990/91, pp 143-149
Proceedings of the IXth International Perimetric Society Meeting,
Malmö, Sweden, June 17-20, 1990
edited by Richard P Mills and Anders Heijl

Ring perimeter (R). Five VFs of four subjects were rejected because of malfixation, *i e.*, a fixation quotient of C surmounting 0.30. The present study was carried out on the remaining 22 VFs of 14 subjects. In these eyes, the fixation quotient of C ranged between 0 and 0.30 (mean 0.09). The refraction was between -2.00 and +3.00 sph with slight additional astigmatism in some eyes. Essentials of the material are listed in Table 1.

The short target exposure time of R (0.165 sec), which is below the reaction time for changing fixation, the contraction movements of the fixation mark, and the feedback system, were assumed to prevent malfixation of these eyes, which had already been checked with C. Therefore, fixation was also checked with R in only three eyes, in which it was confirmed to be adequate.

Six of the 14 subjects had been tested with C on previous occasions, and one single subject with R.

The results of R and C were compared by inspection of the VF charts and calculations on mean threshold values, test times, numbers of points tested, and numbers of presentations.

The mean threshold values constitute the sum of all threshold values divided by the numbers of points tested. Since R covers a larger portion of the periphery (as far as 30°) than the central grid of C (as far as 20°), but does not explore the blind spot and its surroundings, some corrections were introduced in order to optimize this comparison of the instruments. Thus, the values of 21 peripheral test points on the R-charts and those of eight test points in the blind spot area on the C-charts were excluded.

Table 1 Essentials of the material

Case No	*Sex*	*Age*	*Diagnosis*	*Eye*	*Visual field*	
					Ring test	*Competer test*
1	M	58	Dysthyroid orbitopathy	R	Normal	Normal
2	M	56	Op pituitary adenoma	L	Temp hemidysopia	Temp hemidysopia
3	F	48	Op pituitary adenoma	R	Temp hemidysopia	Temp hemidysopia
				L	Temp hemidysopia	Temp hemidysopia
4	F	46	Parasellar meningioma	R	Temp hemidysopia	Temp hemidysopia
				L	Upper altitud dep:s	Upper altitud dep:s
5	F	40	Optic nerve meningioma	R	Pericentral dep:s	Pericentral dep:s
6	F	50	Migraine	R	Normal	Normal
				L	Normal	Normal
7	M	27	Skull trauma	R	Normal	Multiple dep:s
				L	Normal	Multiple dep:s
8	F	61	Op basilar a aneurysm	R	Nasal total hemianopia	Nasal subtotal hemianopia
				L	Temp hemidysopia	Temp hemidysopia
9	M	68	Pseudotumor cerebri	R	Normal	Normal
				L	Normal	Enlarged blind spot
10	F	24	Occip lobe infarction	R	Upper temp quad-dysopia	Upper temp quad-dysopia
11	F	9	Op craniopharyngioma	R	Nasal total hemianopia	Nasal subtotal hemianopia
				L	Temp subtotal hemianopia	Temp subtotal hemianopia
12	F	57	AION	R	Upper altitud dep:s	Upper altitud dep:s
13	F	41	Op sphenoid meningioma	R	Central dep:s	Central dep:s
				L	Normal	Normal
14	F	19	Headache	L	Normal	Normal

Results

Inspection of charts

In the majority of examined VFs, there was no great discrepancy between the results of R and C (Table 1). Six of the 22 VFs were normal and 13 were pathological according to both perimeters. The results were similar but not completely consistent, as exemplified by the following cases:

Case 8· in a 61-year-old woman, an isolated homonymous hemianopia developed at the ligation of a basilar artery aneurysm. The lesion of the visual pathway could not be identified on a postoperative CT scan, but was probably suprageniculate since no optic atrophy developed

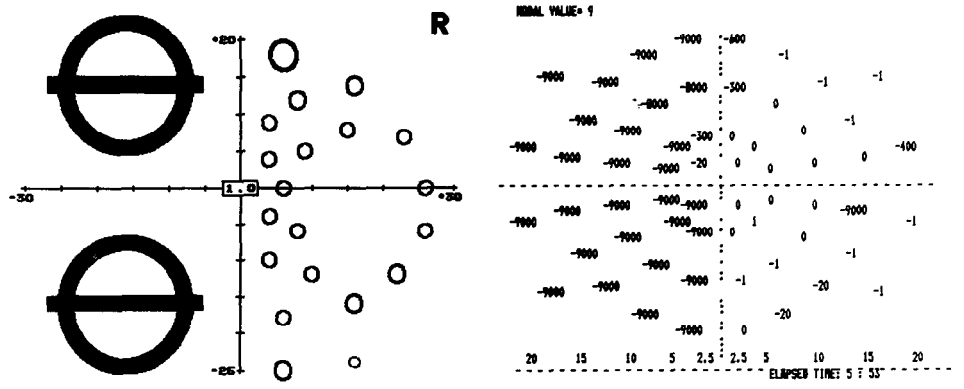

Fig 1 Case 8, right field Ring chart (left): total nasal hemianopia. Competer chart (right): subtotal nasal hemianopia

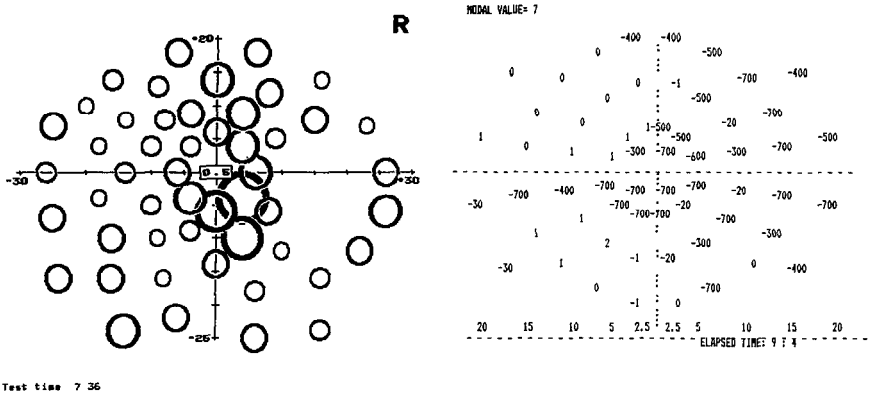

Fig 2 Case 13, right field Ring chart (left): relative central depressions (maximum ring size = 10) Competer chart (right): total depressions at several test points (threshold value 7-7 = 0)

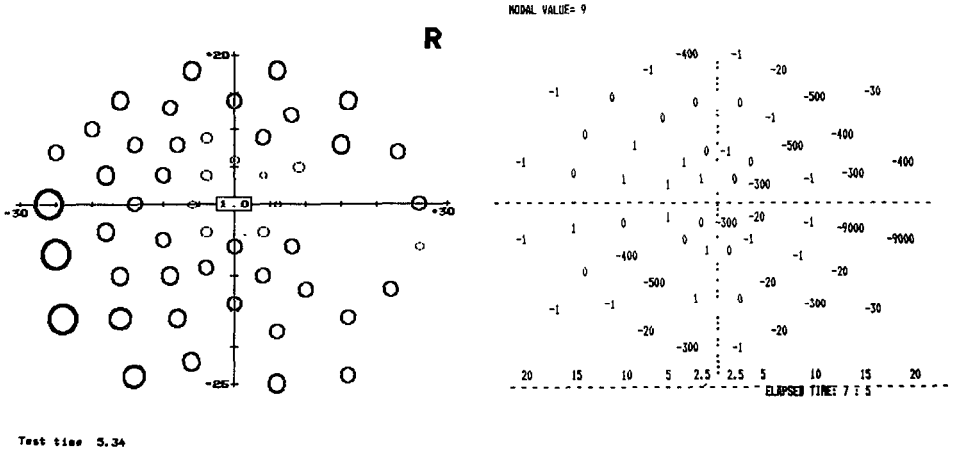

Fig 3 Case 7, right field Ring chart (left): normal results. Competer chart (right): multiple relative depressions.

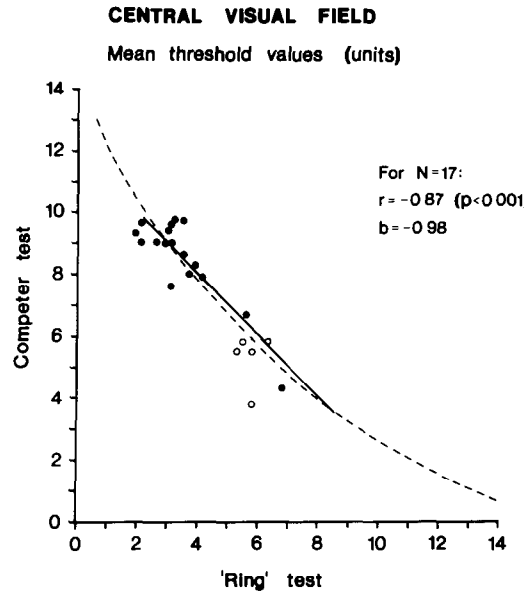

Fig 4 Correlation of the mean threshold values of the instruments

over five months. In the right VF, R recorded a total hemianopia, but according to the detailed C-test, this was subtotal in the upper quadrant (Fig. 1). The test time of R was 60% shorter than that of C.

Case 13 in a 41-year-old woman, a sphenoid meningioma had been partially removed three months earlier. Both perimeters showed multiple deep central depressions in the ipsilateral VF (Fig. 2) These were relative according to R, but several of them were total according to C. The depressions in the blind spot area could not be revealed by R, which does not explore that area. The test time of R was 16% shorter than that of C.

In three VFs of two patients, defects were recorded only by C (Table 1). These were produced by papilledema (three VFs) and retinal folds (two VFs). The discrepancy was obvious in the following case:

Case 7 a 27-year-old man received a hard blow to the head from an iron pole, damaging his superior sagittal sinus. He was immediately operated on but developed intracranial hypertension with transient palsy of the left abducens nerve, longstanding bilateral papilledema and retinal folds. The papilledema gradually subsided but the retinal folds remained. There was no optic atrophy. In both VFs, R gave normal results, including the computed statistics of this instrument, but C revealed enlarged blind spots and multiple small depressions extending into the nasal quadrants Fig 3 shows the right VF seven months after the accident. The test time of R was 21% shorter than that of C The patient had been tested with C on two previous occasions with similar results, so these defects were probably not false positives.

Mean threshold values

Because low values of R (small rings) correspond to high numerical values of C, and *vice versa*, the mean threshold values of the two instruments were negatively correlated (Fig. 4). The correlation of the 22 values was approximately linear. In five VFs with large hemianoptic defects, the mean threshold values of R were inexact (circles) because these VFs were not tested in detail with R As calculated on the remaining 17 VFs (points), the correlation coefficient (r) was -0.87 ($p<0.001$) and the regression coefficient (b) -0.98. Subject to reservations due to the small material, this means that within the measured portion of the correlation curve, the size of the R-steps was almost equal to that of the C-steps This was probably not so outside the measured portion of the curve, since extrapolations suggested that the correlation was actually

non-linear (broken line), as was to be expected because of the widely different kinds of targets. Thus, a blind eye would give a mean R-value of >14 and a C-value of 0, and a supernormal eye a mean R-value of 0 and a C-value of 13-15.

Test time and related parameters

In all 22 VFs, the test time of R was shorter than that of C. The difference ranged between 3 and 60% (mean 25%) and was maximal in two VFs with large hemianoptic defects. The mean test times (Table 2) were found to be proportional to the mean numbers of points tested (5.42/46 = 7.20/60) as well as to the mean numbers of presentations (5.42/184 = 7.20/243). As a consequence, there was no significant difference between the mean numbers of presentations per test point (Table 2). In addition, in individual VFs, the latter quotients were approximately linearly correlated with a correlation coefficient (r) of 0.77 ($p<0.001$) and a regression coefficient (b) of 1.02 (Fig. 5).

Table 2 Test time and related parameters

	Ring test			*Competer test*		
	Mean	*Range*	*SD*	*Mean*	*Range*	*SD*
Test time (min)	5 42	2 35-7 90	1 19	7 20	5.82-9.07	0.98
Test points	46	22-50	–	60	60-60	–
Presentations	184	75-259	40	243	195-309	32
Presentations/test point	3 99	3.41-5 18	0.40	4 05	3 25-5 27	0 53

Patient acceptance

Despite the mentioned fact that six of the 14 patients had been tested with C on previous occasions, no less than 11 preferred R. Two patients preferred C, and one gave no preference for either of the instruments This high acceptance of R was probably mainly due to its excellent feedback system, which facilitated the testing procedure

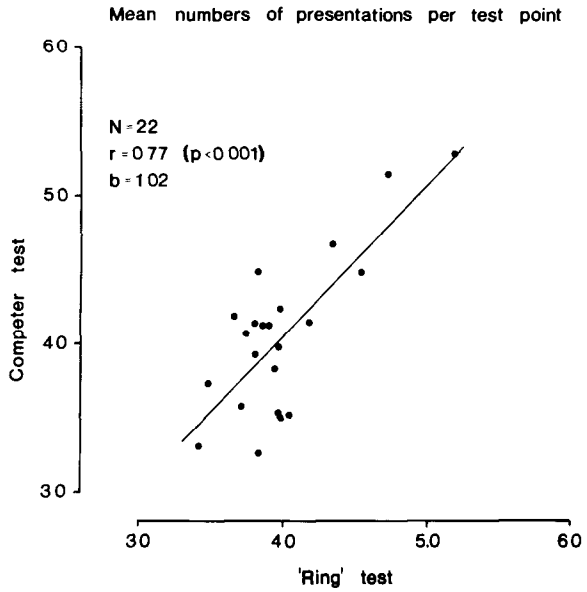

Fig 5 Correlation of the mean numbers of presentations per test point of the instruments

Comments

R was found to have two practical advantages over C, namely that the testing procedure was greatly facilitated by the excellent feedback system and that the test time was shorter. These properties are valuable, particularly in neuro-ophthalmology, because many patients with CNS disorders cannot cooperate adequately with conventional automated perimetry. A prerequisite for the development of the feedback system was the computer graphics of R[1].

As an effect of the relatively small number of test points, the mean test time of R was 25% shorter than it was with the threshold program of C. In two VFs with large hemianopias, the difference amounted to 60% because the number of points tested with R was further reduced. It should be added that the screening program of C, which was not used in this study, is quicker than the threshold program and that C can also test the periphery[10].

For time-saving reasons, R does not test the blind spot area and does not test large hemianopias in detail. Therefore, some information was lost (cases 7, 8, 9, 11 and 13). It may be argued that large hemianopias can be detected by confrontation tests without any substantial further loss of information. In addition, because of the large targets, circumscribed defects were missed (case 7), or their depth was underestimated (cases 10 and 13). It should be emphasized, however, that this loss of information was of minor diagnostic importance. On this point, the author agrees with the inventor[1,2].

As calculated on visual angles, the step between adjacent R targets is 1 dB[1,2]. The targets of C are much smaller and of constant size. In this instrument, the step is calculated on the ratio of light intensity between adjacent levels, which is 1:2[10]. Therefore the C-step is 3 dB. However, the comparison of mean threshold values of the VFs indicated that the steps of both perimeters were almost equal. These statistical calculations should be regarded with some caution because of the small material. Nevertheless, there is reason to doubt the statement that the threshold zone of R is much narrower than that of C[1,2]. The inventor's method of calculating the R-steps on visual angles, *i.e.*, on the width of the rings[1,2], makes the steps too small and consequently leads to an overestimation of the accuracy of the threshold determination. It would certainly be more adequate to base this calculation on the area of the rings, which would give a step of 2 dB.

According to another statement, the appearance at threshold is more distinctive for R targets than for those of conventional perimetry[1,2]. If this means that it is easier to reach the threshold with R than with conventional automated perimetry, *i.e* C, the number of required presentations per test point would probably be less with R than with C. However, these quotients were on an average equal and correlated in individual VFs.

Acknowledgements

Dr. Lars Frisén and HighTech Vision S C I provided me with the Ring test set-up and technical help.

References

1. Frisén L: A computer-graphics visual field screener using high-pass spatial frequency resolution targets and multiple feedback devices. Doc Ophthalmol Proc Ser 49:441-446, 1987
2 Frisén L: High-pass resolution perimetry: recent developments In: Heijl A (ed) Perimetry Update 1988/89, pp 369-375 Amsterdam/Berkeley/Milano: Kugler & Ghedini Publ 1989
3. Frisén L: Acuity perimetry: estimation of neural channels. Int Ophthalmol 12:169-174, 1988
4 Drance SM, Douglas GR, Schulzer M, Wijsman CS: The learning effect of the Frisén high-pass resolution perimeter In: Heijl A (ed) Perimetry Update 1988/89, pp 199-201. Amsterdam/Berkeley/Milano: Kugler & Ghedini Publ 1989
5 House PH, Drance SM, Schulzer M, Wijsman K: The effect of refractive blur on the visual field using the ring perimeter Acta Ophthalmol 68:87-90, 1990
6 Dannheim F, Roggenbuck C: Comparison of automated conventional and spatial resolution perimetry in chiasmal lesions. In: Heijl A (ed) Perimetry Update 1988/89, pp 377-382 Amsterdam/Berkeley/Milano: Kugler & Ghedini Publ 1989
7 Dannheim F, Abramo F, Verlohr D: Comparison of automated conventional and spatial resolution perimetry in glaucoma In: Heijl A (ed) Perimetry Update 1988/89, pp 383-392. Amsterdam/Berkeley/Milano: Kugler & Ghedini Publ 1989

Optic neuritis treatment trial: visual field reading center

John L. Keltner, Chris A. Johnson, John O. Spurr and Optic Neuritis Study Group

Optic Neuritis Study Group, Department of Ophthalmology, University of California, Davis, CA 95616, USA

The Visual Field Reading Center (VFRC) at the University of California, Davis, Department of Ophthalmology, was established to provide high quality and reliable visual field data for the Optic Neuritis Treatment Trial (ONTT). Its major functions include technician training and certification, quality control of ONTT visual field tests, data compression and analysis, and transmission of visual field data to the ONTT Coordinating Center. The VFRC has processed data from over 5000 Goldmann and Humphrey visual fields in the 18 months since the ONTT began.

The VFRC quality control measures provide important feedback to the ONTT clinics and visual field technicians on their performance in both Goldmann and Humphrey visual field testing. The feedback has produced improvement in the quality and reliability of the ONTT visual fields. The average Goldmann quality control score has improved from 2 42 for the first three months of the ONTT to 0.78 for the last three months (where zero is a perfect score on a 0-9 score), and the average Humphrey score has improved from 1.49 to 0.56. The quality control also ensures that the entrance visual field criteria have been followed and that the uniform testing standards are employed by all ONTT clinics. This is the first visual field reading center of this type for clinical trials in ophthalmology

The full article will be published elsewhere.

Supported in part by National Eye Institute Research Grant No EY07461 (JLK), and an Unrestricted Research Grant from Research to Prevent Blindness, Inc

Perimetry Update 1990/91, p. 151
Proceedings of the IXth International Perimetric Society Meeting,
Malmö, Sweden, June 17-20, 1990
edited by Richard P. Mills and Anders Heijl

Study of the influence of target size on the pericentral visual field

Chota Matsumoto, Koji Uyama, Sachiko Okuyama, Yuzo Nakao and Toshifumi Otori

Department of Ophthalmology, Kinki University School of Medicine, 377-2, Ohno-Higashi, Osaka-Sayama City, Osaka 589, Japan

Abstract

The pathophysiology of the pericentral visual field within 10° is not well understood The authors studied the influence of the target size on the sensitivity of this area in normal subjects and patients with various eye diseases Using the SARGON program of the automated perimeter Octopus 201, they examined 49 (7×7) test points on a 2° grid in the pericentral area using target sizes 1, 3 and 5. In many of the patients with optic neuritis and chiasmal syndrome, target size 1 was more sensitive for detecting pericentral scotoma and hemianoptic changes than the standard target size 3 The present results seem to suggest that a small static target, such as target size 1, should be used to examine pericentral visual field abnormalities in neuro-ophthalmological cases.

Introduction

The central visual field around the fixation point is the first to be affected in many neuro-ophthalmological cases and several kinds of retinal disease A detailed analysis of the visual field in this area is important for the early diagnosis of ocular disease and follow-up of cases. On the other hand, the results of visual field examinations are known to be influenced by the target size. Visual field changes resulting from changes in target size are of special and profound interest. However, the influence of target size on the pathological pericentral visual field has not often been studied. We studied the influence of target size on the sensitivity of this area in normal subjects and various eye diseases.

Subjects and methods

We used an automated perimeter Octopus 201, using 1, 3 and 5 or 0 to 5 target sizes Using the SARGON program, we constructed a program M2.0 for the measurement of the square

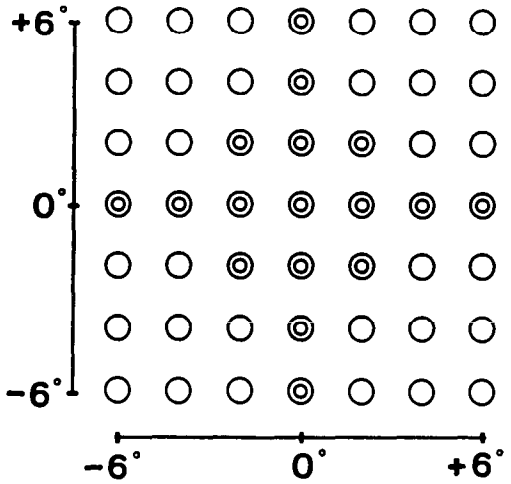

Fig 1 Arrangement of test points in SARGON program M2 0

Perimetry Update 1990/91, pp. 153-159
Proceedings of the IXth International Perimetric Society Meeting,
Malmö, Sweden, June 17-20, 1990
edited by Richard P. Mills and Anders Heijl

visual field within 6° from the center at every 2°[1,2]. Seventeen points were measured twice (Fig. 1).

Normal subjects

The central fields of 63 eyes of 63 normal volunteers (22-68 years of age) were studied. All normal subjects had corrected vision of better than 1.0. The refraction was within ±3.0 D sphere and -2.0 D cylinder. Pupillary diameter was larger than 3.0 mm The optical media and fundus were normal.

In these subjects, measurements were carried out using SARGON program M2.0 with a background luminance of 4 asb using all target sizes from 0 to 5. Initial data were excluded to avoid the learning effect.

Cases

Measurement was carried out in a total of 41 eyes of 37 subjects: seven eyes of seven patients with optic neuritis, nine eyes of six patients with chiasmal syndrome, two eyes of one patient with optic tract damage, six eyes of six patients with glaucoma, seven eyes of seven patients with retinal detachment, and ten eyes of ten patients with central serous chorioretinopathy.

In these patients, measurements were carried out using target sizes 1, 3 and 5. In some cases, all target sizes from 0 to 5 were used Examination of the visual field with targets of various sizes was done within three days of the initial examination.

Results

The slope of the visual field profile was flattened as the target size became larger. At each target size, the visual sensitivity decreased with age. The decrease in visual sensitivity followed a regression line. Table 1 summarizes the rate of decrease in mean sensitivity for each ten years of age at each target size. As seen in Table 1, decrease in visual sensitivity due to aging tended to be more pronounced with smaller targets.

Table 1 Change in mean sensitivity per decade for each stimulus size (dB/decade)

Stimulus size	*0*	*1*	*2*	*3*	*4*	*5*
Mean slope	-1 03	-1 00	-0 85	-0 82	-0 81	-0.56

(ΔdB/decade)

The influence of the target size on the pathological pericentral visual field was then studied.

Case 1 was a 30-year-old male with optic neuritis and suspected Leber disease. The left eye showed a corrected vision of 1.0 with a central critical fusion frequency (CFF) of 48 Hz and Marcus Gunn pupil The value table and gray scale of the central visual field of the left eye using target sizes 0 to 5 are shown at the left side of Fig. 2. The line in the gray scale in the upper right corner of Fig. 2 indicates the horizontal profile Sensitivities on this line using various target sizes are shown in the graph in the center The mean sensitivity of the normal subjects of the same age group on the same line is shown in the lower graph in the bottom right corner. Although the sensitivity was noted to decrease slightly in the upper temporal field when size 3 target was used, the sensitivity decreased down to 0 dB when size 1 target was used.

Case 2 was a 39-year-old male with a pituitary tumor. The left eye was examined. The corrected vision was 1.0 and the central CFF 48 Hz. When the Goldmann perimeter was used, hemianopsia was noted in the internal isopters of the I-1e and I-1a. As the target became smaller in size, the decrease of sensitivity in the nasal field apparently became more pronounced (Fig. 3).

Case 3 was a 27-year-old female who suffered from multiple sclerosis. The corrected vision was 1.0 and the central CFF 38 Hz. Examination of the visual field using the Goldmann perimeter revealed incongruous left homonymous hemianopsia. Marcus Gunn pupil was noted only in the right eye. Sclerotic lesion in the right optic tract was suspected based on the high intensity lesion noted on the MRI T2 image. As shown in Fig. 4, a slight decrease in sensitivity on the temporal side using target size 3 was further reduced with target size 1.

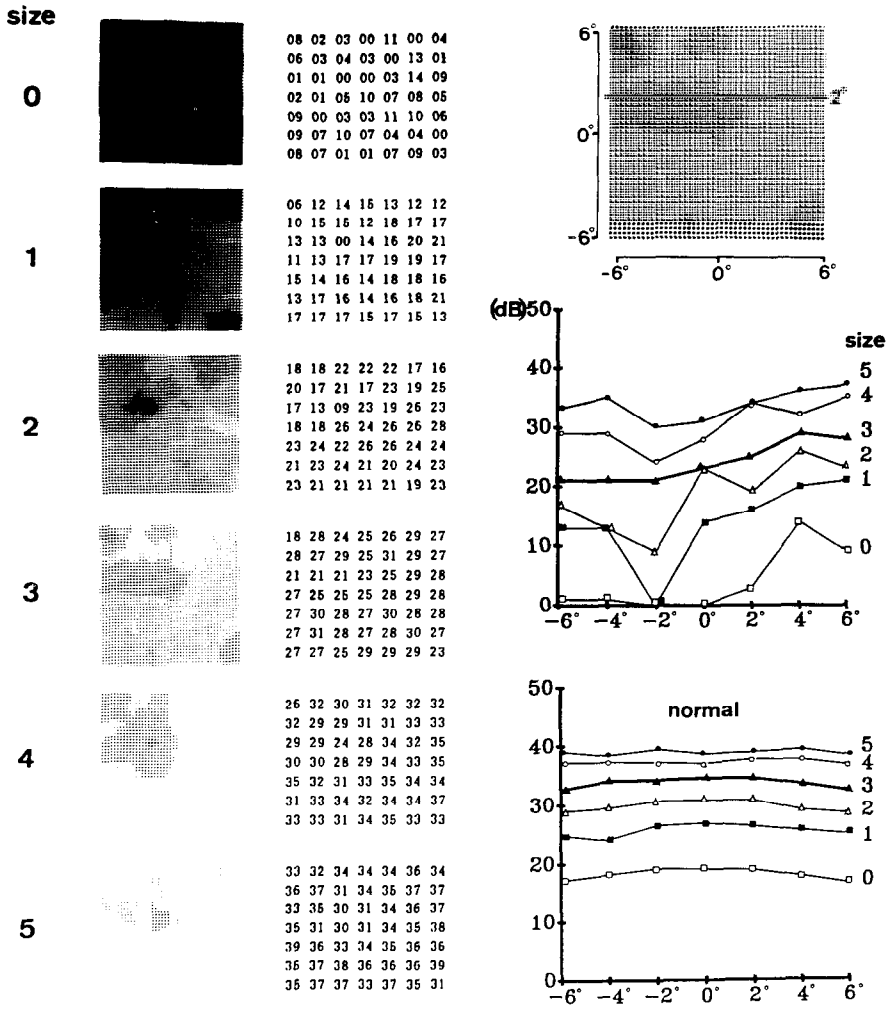

Fig 2 Influence of target size on the pericentral visual field of case 1 The column on the left shows gray scale fields and value tables for various target sizes The column on the right shows a profile of the pericentral visual field The course of the profile is shown in gray scale representation in the upper right corner The middle figure shows profiles for each target size The bottom figure shows mean normal profiles

In order to study the influence of target size in various eye diseases, the difference between target sizes 1 and 3 was studied in all the above mentioned cases Actual measured values beyond the 2 SD range lower than the normal mean sensitivity for each age were judged as abnormal. The difference value at each abnormal point was calculated. The mean of these abnormal difference values was calculated as the mean defect (MD), and the difference of mean defect for target sizes 1 and 3 was obtained (Fig. 5).

In Fig. 6, differences in mean defect using target sizes 1 and 3 at abnormal points were plotted in all cases. In those cases plotted on the right side, the mean defect was greater with target size 1 than with target size 3, indicating the higher sensitivity of target size 1 than target size 3. As seen in Fig 6, the mean defect of the abnormal points tended to be larger with target size 1 than with target size 3 in almost all cases except for retinal detachment This tendency was especially remarkable in cases of optic neuritis, chiasmal syndrome and optic tract damage.

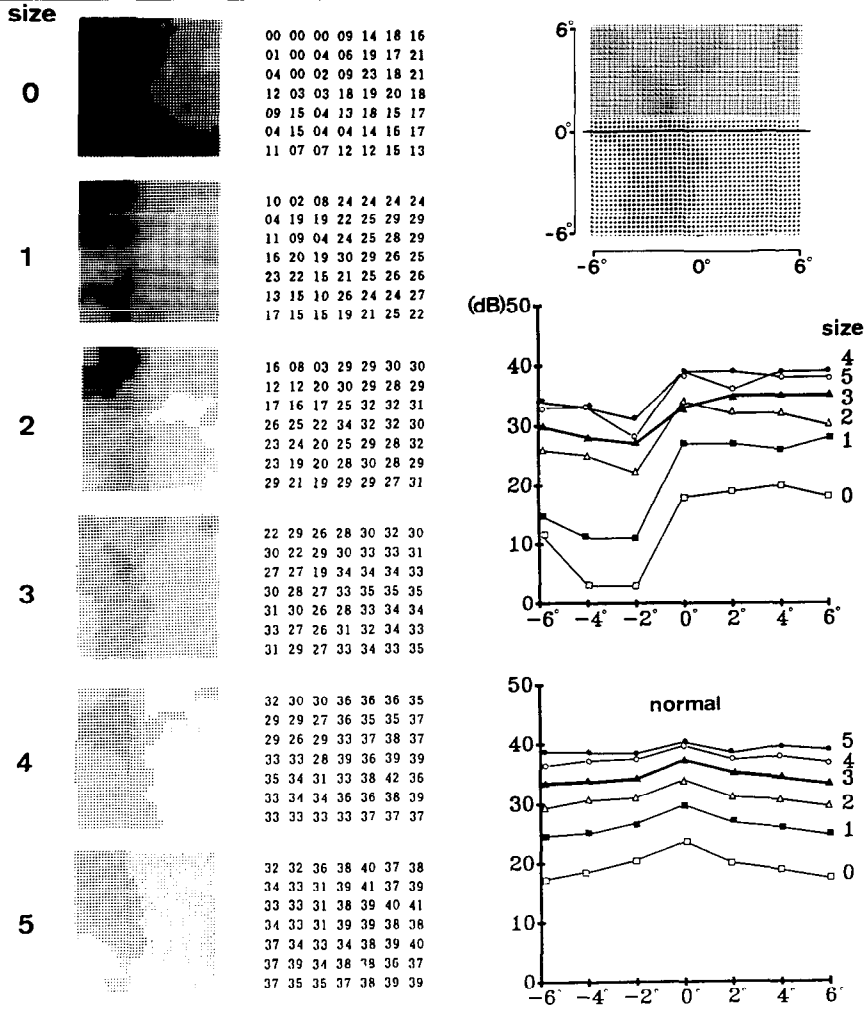

Fig 3 Gray scales, value tables and profiles of case 2

Discussion

In most current automated perimeters, the target size is usually empirically set at size 3 for examination of the visual field within 30°. Whether or not these conditions are suitable for examination of the pericentral visual field near the fixation point has not been well documented.

In normal subjects, the differential light sensitivity decreases with age. It is known that the rate of decrease in visual sensitivity in response to aging takes place approximately rectilinearly with age[3,4]. In our study, decrease in visual sensitivity due to aging became greater as the target size became smaller This may be due to the difference of spatial summation in stimulus sizes 0 to 5 As a point of further consideration, increase in opacity of optic media and decrease in accommodation due to aging should be considered. If the refractive correction is insufficient, the differential light sensitivity measures lower with smaller target sizes[5]. Care must therefore be taken when a small target size is used clinically.

The relationship between target size and target luminance for pathological visual field testing in Goldmann kinetic perimetry has been studied and expressed as a harmonious or disharmonious phenomenon[6]. The influence of target size on pathological visual fields has been studied by static perimetry on the Goldmann instrument[7]. The results obtained in the present study were similar to those obtained by the Goldmann static method.

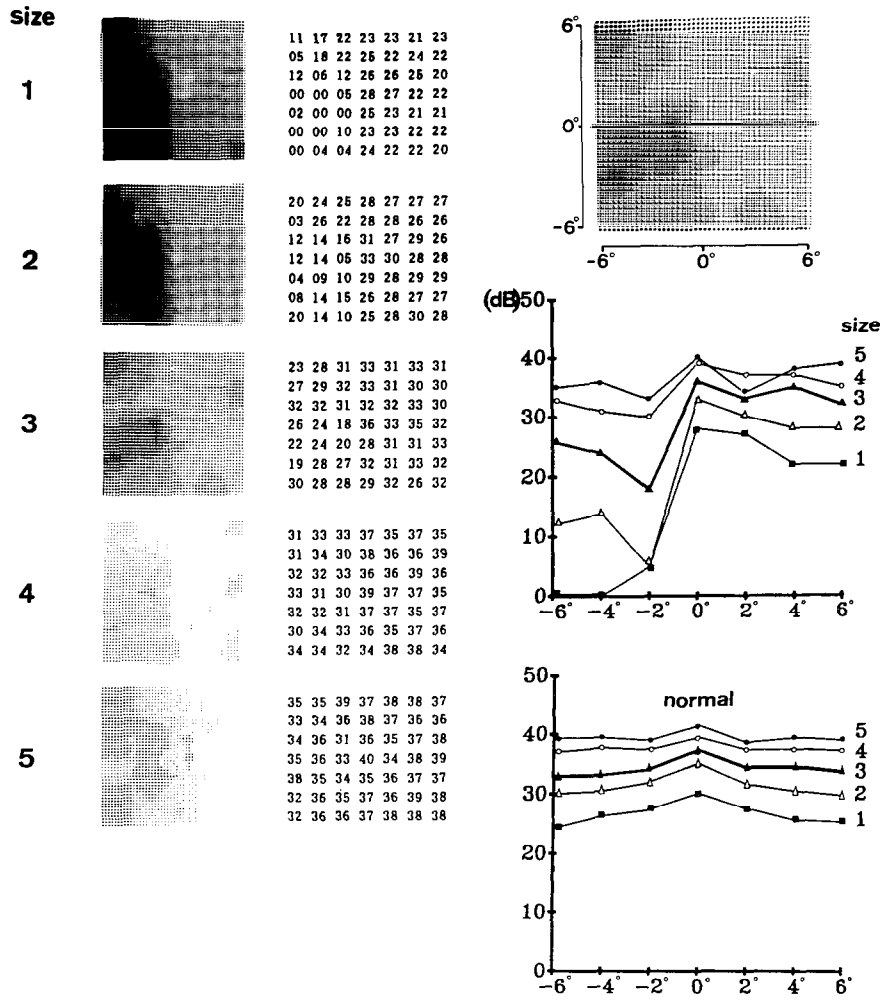

Fig 4 Gray scales, value tables and profiles of case 3

In neuro-ophthalmological diseases, such as optic neuritis, chiasmal syndrome and optic tract damage, the third neuron is mainly damaged The present study seems to suggest that, in many cases of neuro-ophthalmological disease, decrease in differential light sensitivity of the abnormal visual field becomes especially pronounced with the use of small targets The density of retinal ganglion cells, which is the origin of the third neuron, is high in the center of the visual field. When the visual field is examined in the pericentral area, the use of standard target size 3 causes stimulation of many ganglion cells on single presentation of the target. Because of this anatomical fact a small target size may be quite useful for the examination of the pericentral field near the fixation point.

When a small target size is used, the dynamic range of the visual field becomes narrower. However, the visual sensitivity in the vicinity of the fixation point is higher than that in the paracentral or more peripheral visual field. It is therefore possible to maintain a practical dynamic range even with the small target size 1.

In third neuron diseases, such as optic neuritis and chiasmal syndrome, the use of target size 1 revealed a marked fall in the differential light sensitivity of the visual field within 6° of the center. Therefore, the use of the smaller target size 1 in addition to the standard target size 3 in automated perimetry may make it possible to detect field changes with higher sensitivity and allow more effective follow-up to be conducted.

	size 1	size 3
actual value table	00 14 06 22 24 28 22 01 07 05 23 28 25 25 11 03 08 19 25 26 27 15 11 11 27 27 26 28 25 20 18 17 26 28 24 15 19 22 16 25 25 25 19 15 17 22 23 25 27	22 29 26 28 30 32 30 30 22 29 30 33 33 31 27 27 19 34 34 34 33 30 28 27 33 35 35 35 31 30 26 28 33 34 34 33 27 26 31 32 34 33 31 29 27 33 34 33 35
normal value table	22 22 23 23 24 24 22 24 24 24 24 25 25 23 24 25 27 26 26 26 25 24 26 28 30 27 26 25 25 25 26 26 25 25 25 24 25 25 25 24 24 25 23 24 24 24 24 23 23	31 31 32 31 31 32 32 32 33 33 33 32 32 33 33 33 34 34 34 34 33 33 33 34 38 35 34 33 33 33 33 34 34 34 34 33 33 33 33 32 33 32 32 32 33 32 32 32 31
difference value table	22 08 17 + + + + 23 17 19 + + + + 13 22 19 07 + + + 10 15 17 + + + + + 05 08 10 + + + 09 06 + 09 + + + 04 09 07 + + + +	09 + 06 03 + + + + 11 04 + + + + 06 06 15 + + + + 03 05 08 05 + + + + + 07 06 + + + + 06 07 + + + + + + 06 + + + +
mean defect (MD)	12.6 dB	6 6 dB
MD (size 1) - MD (size 3)	6.0 dB	

Fig 5 An example of calculation of mean defect between target sizes 1 and 3

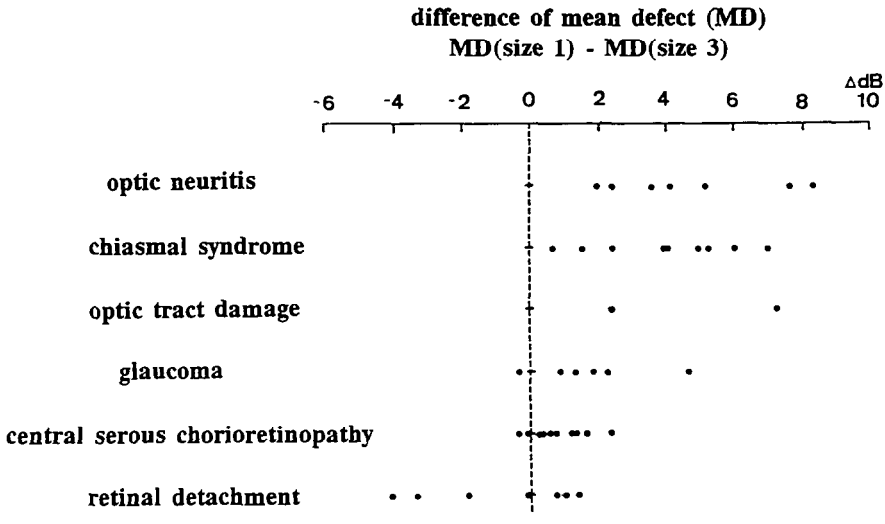

Fig 6 Differences of mean defect between target sizes 1 and 3

References

1. Matsumoto C, Uyama R, Sakamoto H, Nakao Y, Otori T: Evaluation of central visual field with automated perimeter Octopus. Folia Ophthalmol Jpn 39:261-267, 1988
2. Otori T, Nakao Y, Matsumoto C, Fukuda M, Kusube T, Okamura W, Ikeda H: Evaluation of central visual field with automated perimeter (Octopus) Jpn J Clin Ophthalmol 39:715-719, 1985
3. Haas A, Flammer J, Schneider U: Influence of age on the visual field of normal subjects Am J Ophthalmol 101:199-203, 1986
4. Heijl A, Lindgren G, Olsson J: Normal variability of static perimetric threshold values across the central visual field. Arch Ophthalmol 105:1544-1549, 1987
5 Sloan LL: Area and luminance of test object as variables in examination of the visual field by projection perimetry. Vis Res 1:121-138, 1961
6. Dubois-Poulsen A, Magis CL: Les procédés d'examen de la fonction visuelle dans le glaucome chronique. Ophthalmologica 139:155-213, 1960
7 Sloan LL, Brown DJ: Area and luminance of test object as variables in projection perimetry: clinical studies of photometric disharmony Vis Res 2:527-541, 1962

Binocular interaction in normal and amblyopic patients: comparative study using automatic perimetry and visual evoked potentials

M. Fioretto, V. Brezzo, G.P. Fava and E. Gandolfo

University Eye Clinic of Genoa, H San Martino, 16132 Genova, Italy

Abstract

This report describes a study of binocular interaction using VEP and automatic perimetry in patients affected by strabismic amblyopia with suppression or with ARC and in patients with anisometropic amblyopia. The VEP amplitude following binocular stimulation in normal subjects, in patients with strabismic amblyopia with ARC and in those with anisometropic amblyopia was greater than that with stimulation of the dominant eye which in turn was greater than that with stimulation of the amblyopic eye. In the same subjects, computerized perimetry in binocular vision showed a reduction of the foveal threshold compared to the dominant eye which had a threshold lower than that of the amblyopic eye In the patients with strabismic amblyopia and suppression, the results obtained after examining the dominant eye were not significantly different from those obtained binocularly

Introduction

The presence of a heterotropia causes more or less important alterations of binocular vision consisting of suppressive phenomena and anomalous retinal correspondence (ARC)[1-8].

It may be useful to quantify the degree of binocular cooperation and for this we have utilized two methods: computerized perimetry and visual evoked potentials (VEP).

Material and methods

A total of 20 people were examined:

- ten healthy subjects aged from 16 to 78 years (average 31.7±11.6) with a visual acuity of 10/10 in both eyes and a refractive error of between -1.5 and +1 5 D;
- five patients aged from 21 to 36 years (average 21.7±5.8) with strabismic amblyopia (esotropia) with an angle between +4Δ and +20Δ, a visual acuity of between 2/10 and 8/10, and a refractive error of between -3 and +6 D. Orthoptic examination showed three patients to have ARC and two to have suppression;
- five patients aged between 19 and 38 years (average 29.6±8.4) affected by anisometropic amblyopia with a visual acuity of between 2/10 and 8/10, and a refractive error of between -7 and +6.5 D.

All subjects underwent pattern visual evoked potential examination with the following recording parameters:

- active electrodes 0_2 0_1 (10-20 international system)
- ground electrode F_z
- reference electrode F_pz
- time of analysis: 250 msec
- number of epochs: 100
- stimulus: checkerboard pattern reversal of amplitude 60′ – angle subtended from the screen 14° – contrast 75%
- bandpass: 50-200 Hz

The amplitude was measured from peak to peak.

Perimetry Update 1990/91, pp. 161-163
Proceedings of the IXth International Perimetric Society Meeting,
Malmö, Sweden, June 17-20, 1990
edited by Richard P. Mills and Anders Heijl

The subjects then underwent static perimetry using the following method:
- *Perimeter:* Allergan Humphrey Visual Field Analyzer, Model 620.
- *Program:* "Custom" with 16 points within the central 5° and foveal sensitivity determination.
- *Strategy:* Full threshold, size III (4 mm^2) stimulus; background luminance: 31.5 asb.

Both the VEP and visual field examinations were performed first in the dominant eye, then in the amblyopic one and finally with binocular viewing.

Before the definitive perimetric examination, training of the subjects was carried out so as to exclude a possible learning effect. The visual field examination was performed using adequate corrective lenses in the case of ametropia and/or presbyopia.

Results

In the normal subjects, the VEP recorded in binocular vision showed a significant increase in the amplitude of the P100 wave compared to that obtained with monocular stimulation of either eye. No statistically significant differences of latencies were observed. The binocular visual field examination showed a reduction of the central threshold in all cases (mean of the 17 points tested) between 1 and 3 dB.

In the patients affected by strabismic amblyopia, different VEP responses were obtained according to the type of sensory anomaly (ARC or suppression).

In those with ARC, stimulation of the amblyopic eye gave a tracing with a slightly irregular morphology, a significantly reduced amplitude compared to the dominant eye and a latency which was unchanged in one patient and slightly, although not significantly, increased in the other two.

In the tracings recording during binocular vision, the amplitude was significantly increased with respect to the dominant eye alone and the latency of the principal components was essentially unchanged.

In those affected by amblyopia and suppression, the VEP had a considerably reduced amplitude and a significantly increased latency of the principal components compared to the dominant eye. With binocular stimulation, the tracing was not significantly different from that obtained with stimulation of the dominant eye

The perimetric results were analogous with those of the VEP: in the patients with ARC the central threshold in binocular vision was decreased by an averaged of 1-2 dB compared to the dominant eye which had a foveal threshold below that of the amblyopic eye; in those with suppression, the macular threshold in binocular vision was analogous with that of the dominant eye, while in the amblyopic eye the threshold was distinctly higher.

In the patients affected by anisometropic amblyopia, the VEP amplitude was significantly reduced in the amblyopic eye compared to the dominant eye, while the latency was not significantly different With binocular stimulation, the amplitude was significantly increased with respect to that of the dominant eye.

Perimetry showed that the central threshold in binocular vision was reduced compared to the dominant eye (improvement of the average sensitivity of between 1 and 2 dB in the 17 points tested). The threshold of the amblyopic eye was greater, although the difference between the amblyopic and dominant eyes was less than that in patients with strabismic amblyopia.

Discussion

In all the normal subjects, in the patients with anisometropic amblyopia, and in those with strabismic amblyopia with ARC, there was collaboration between the two eyes although to a varying degree[9,10].

The increased VEP amplitude and the decreased threshold with binocular stimulation demonstrate the integration of the visual message originating in the amblyopic eye[11-14]

In the patients with strabismic amblyopia who suppressed the image of the amblyopic eye, this response did not occur and this is indicative of the depth of the anticonfusional scotoma present in this condition

Authors such as Bagolini and Campos, Lennerstrand, and Wanger and Nillson have obtained

analogous results showing the importance of binocular collaboration[3-8,13,15,16]. Others, such as Sokol and Nadler, comparing only the amblyopic eye with the dominant one, conclude that there is a retinal involvement in the amblyopic eye[17-19].

Our results with the perimetric and electrophysiological examinations show how "binocular vision" is possible only in the absence of important suppressive phenomena and with small angles of strabismus. Under these conditions, elicitation of the bipolar cells is possible[20].

Various degrees of binocularity and of the possibility of integration therefore exist. Only when suppression is present should binocular vision be considered to be absent.

References

1 Abram F: Monocular visual field testing under binocular conditions Ann Ophthalmol 20:444-445, 1988
2. Arden GB, Barnard W: Visually evoked responses in amblyopia Br J Ophthalmol 58/3:183-192, 1974
3 Bagolini B: Sensorial anomalies in strabismus (suppression – anomalous correspondence, amblyopia). Doc Ophthalmol 41: 1-22, 1974
4. Bagolini B: Vision binoculaire dans les ésotropies à petit angle (démonstration campimétrique et électrophysiologique) Bull Soc Belg Ophtalmol 196:7-18, 1981
5 Bagolini B, Campos C: Binocular campimetry in small angle: concomitant esotropia Doc Ophthalmol Proc Ser 14:405-409, 1977
6. Campos E: Anomalous retinal correspondence: monocular and binocular visual evoked responses Ophthalmology 98:299-302, 1980
7. Campos E: On the reliability of some tests of binocular sensorial status in strabismic patients J Pediatr Ophthalmol Strabis 15:8-14, 1978
8. Campos E, Castellani T: Perimetria binoculare nell'esotropia concomitante a piccolo angolo Boll Ocul 55:205-220, 1976
9. Capris P, Fava GP, Gandolfo E, Fioretto M: Lo studio della binocularità nella sindrome ambliopica con metodica campimetrica non dissociante Boll Oculist (Suppl) 65/6/2:113-119, 1986
10 Fava GP, Capris P, Fioretto M, Gandolfo E: Binocular threshold campimetry in the amblyopic syndrome. Doc Ophthalmol Proc Ser 49:633-637, 1987
11 Fiorentini A, Maffei L, Pirchio M: An electrophysical correlate of percentual suppression in anisometropia Vis Res 18:1617-1621, 1978
12 Fitzsimons R, White J: Functional scoring of the field of binocular single vision Ophthalmology 97:33-35, 1990
13. Lennerstrand G: Binocular interaction studies with visual evoked responses in humans with normal or impaired binocular vision Acta Ophthalmol 56:628-637, 1978
14. Mahendrastari R, Verriest G: Monocular and binocular visual fields in different types of strabismus Bull Soc Belg Ophtalmol 213:77-81, 1986
15 Philipp W, Mayer W: Investigation of visual field defects in strabismic and anisometropic amblyopes with the Octopus Program G1 Graefe's Arch Clin Exp Ophthalmol 227:448-454, 1989
16. Wanger P, Nilsson B: Visual evoked responses to pattern reversal stimulation in patients with amblyopia and/or defective binocular function Acta Ophthalmol 56:617-627, 1978
17 Mehdorn E: Nasal field defects in strabismic amblyopia Doc Ophthalmol Proc Ser 45: 318-326, 1986
18 Sokol S, Benjamin B: Visually evoked cortical responses of amblyopes to a spatially alternating stimulus Invest Ophthalmol Vis Sci 12/12:936-939, 1973
19 Sokol S, Nadler D: Simultaneous electroretinograms and visually evoked potentials from adult amblyopes in response to a pattern stimulus Invest Ophthalmol Vis Sci (Suppl) 18/8/3:848-855, 1979
20. Bishop PO: Neurophysiology of binocular single vision and stereopsis In: Jung R (ed) Handbook of Sensory Physiology Vol 7/3A, pp 255-301. Berlin: Springer Verlag 1973
21 Sreboro R: The visually evoked response binocular facilitation and failure when binocular vision is disturbed. Arch Ophthalmol 96:839-844, 1978

Symmetry analysis in pituitary adenoma

C. Papoulis and J. Weber

Universitäts-Augenklinik, Joseph-Stelzmann Strasse 9, D-5000 Köln 41, Germany

Abstract

Indices have proven to be a strong instrument for the evaluation of visual fields The authors compared the power of a topographical index (horizontal asymmetry, HA) and a global numerical index (mean deviation, MD) for the detection of pituitary adenoma in 36 clinical cases compared to 28 normals HA and MD gave good discrimination power, which was considerably increased by the combination of both indices. Sensitivity and specificity reached 97% or more in hemifield analysis as well as in quadrant analysis

Introduction

Global visual field indices[1,2] furnish global information about the state of the visual field: the average damage (MD), the homogeneity of the damage (LV, PSD) and the average stability of measured values (SF). They are a powerful instrument for scrutinizing the development of a particular field. The specific topography, however, is not recorded by indices of this type.

Topography, on the other hand, is the basis of diagnosis. The recognition of typical patterns of damage enables different diseases and even different stages of a disease to be distinguished[3].

Topography can also be assessed mathematically. In 1985, Duggan, Sommer and coworkers[4,5] compared sums of threshold values of corresponding groups of test points in the superior and inferior hemispheres of the central 30 degrees. They developed patterns and criteria that, when applied to glaucomatous and control eyes, reached a very good sensitivity and specificity.

Is topographic information of a field superior to global, numeral information as far as diagnosis is concerned?

We assumed that pituitary adenoma would be an easier model than glaucoma for the first approach to this problem, because the topography of its damage is very simple, offering easy quantitative spatial analysis. The hemifield asymmetry can be calculated as the difference of the mean deviation on both sides of the vertical axis We have called this index the "horizontal asymmetry" (HA). We tested the power of this index to discriminate between a group of 36 eyes of pituitary adenoma patients and 28 normal references In comparison, the same was conducted with the global index MD.

Material and methods

All patients (18 subjects, 36 eyes) were outpatients at the Department of Ophthalmology, University of Cologne. The diagnosis of pituitary adenoma was confirmed by histology after operation or by computed tomography In a series of fields, only the first was evaluated for this study. There were no fixed intervals between operation or treatment and the field examination. Some of the patients had been operated on before we saw them on their first visit. The normal references (28 subjects, 28 eyes) were relatives of patients with non-hereditary eye diseases, accompanying persons or staff from the clinic. They all had normal ophthalmological findings and a visual acuity of at least 0.7.

The visual field examination was carried out with the 30-2 program of the Humphrey Field Analyser. HA and MD were calculated for three different areas of analysis: (a) hemifield analysis where HA and MD were calculated from both hemifields; (b) upper quadrant analysis where HA and MD were calculated from both upper quadrants; and (c) lower quadrant analysis where HA and MD were calculated from the lower hemifields.

Perimetry Update 1990/91, pp. 165-171
Proceedings of the IXth International Perimetric Society Meeting,
Malmö, Sweden, June 17-20, 1990
edited by Richard P. Mills and Anders Heijl

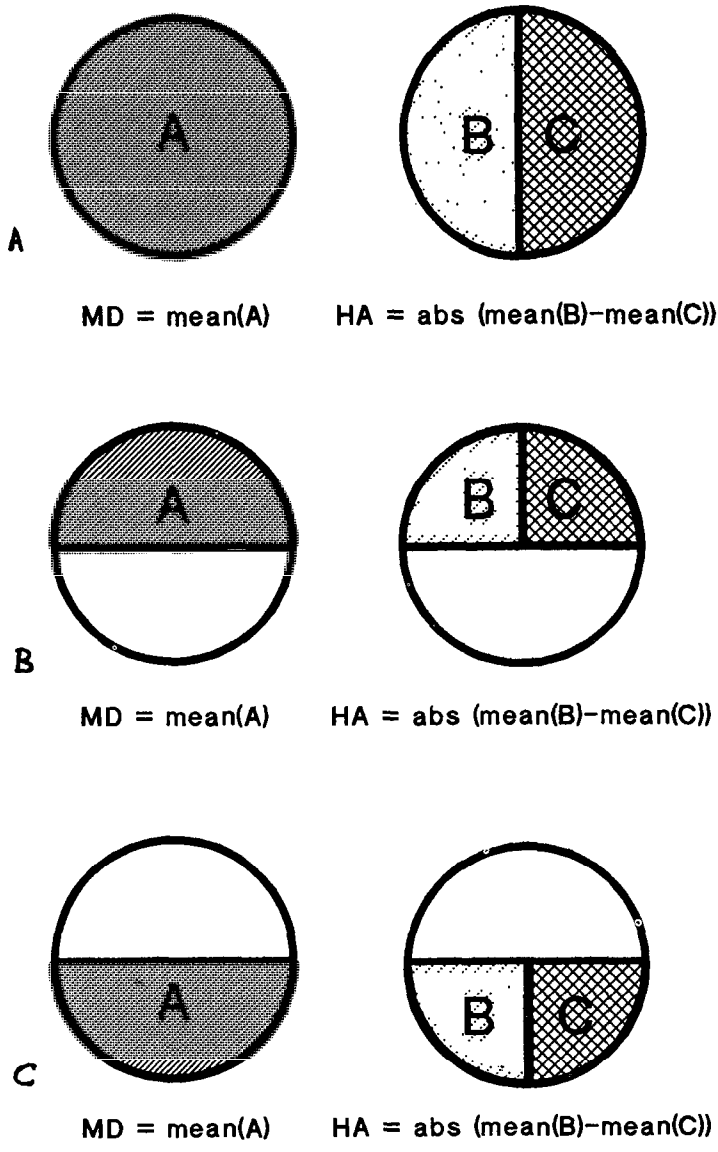

Fig 1a, b and c Calculation mode of mean deviation (MD) and horizontal asymmetry (HA) in hemifield, upper quadrant and lower quadrant analysis

The indices were calculated using the PERIDATA program. The mean deviation (MD) was taken from the "PERIDATA Standard Printout". The "horizontal asymmetry" (HA) is the absolute difference between the mean deviation of corresponding hemifields (Fig. 1a). It was calculated from the mean deviations of the "pattern statistics/hemifield right-left" of the PERIDATA program. The MD and HA for the upper and lower fields were calculated from the mean deviations of the "pattern statistic/quadrants" (Fig. 1b and c).

To obtain perfect symmetry of the evaluated patterns, points in both the blind spot region and the symmetrical corresponding region were excluded from the calculation using the PERIDATA option "delete points/both blind spots" In the next update, the HA index will be included as one of the topographical indices. The border between the normal and pathological index values was determined by choosing iteratively the criterion that served nearly equal

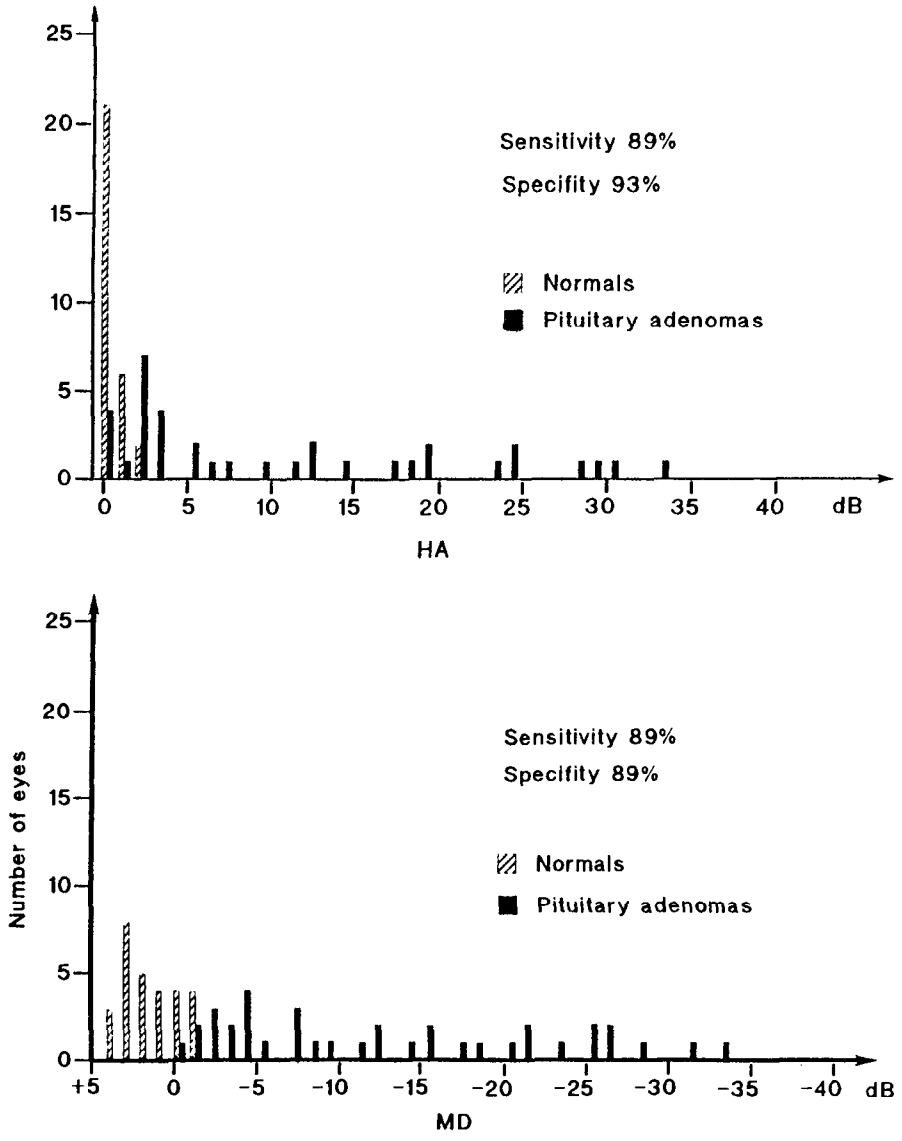

Fig 2a and b Distribution of horizontal asymmetry and mean deviation in hemifield analysis

specificity and sensitivity. This was conducted separately for HA and MD. The discrimination criterion for the two-dimensional analysis was determined graphically in scattergraphs, where HA was plotted against MD for hemifield (Fig. 5a), upper quadrant (Fig 5b) and lower quadrant (Fig. 5c), and a formula was developed.

Results

In the hemifield analysis, the HA criterion was "HA>1.3 dB". It provided a sensitivity of 89% and a specificity of 93%. For MD, the criterion was "MD<-1.1 dB" It provided a sensitivity and a specificity of 89% (Fig. 2a and b) Considering only the upper half fields, which are known to be involved exclusively in cases of slight damage, did not increase the power of

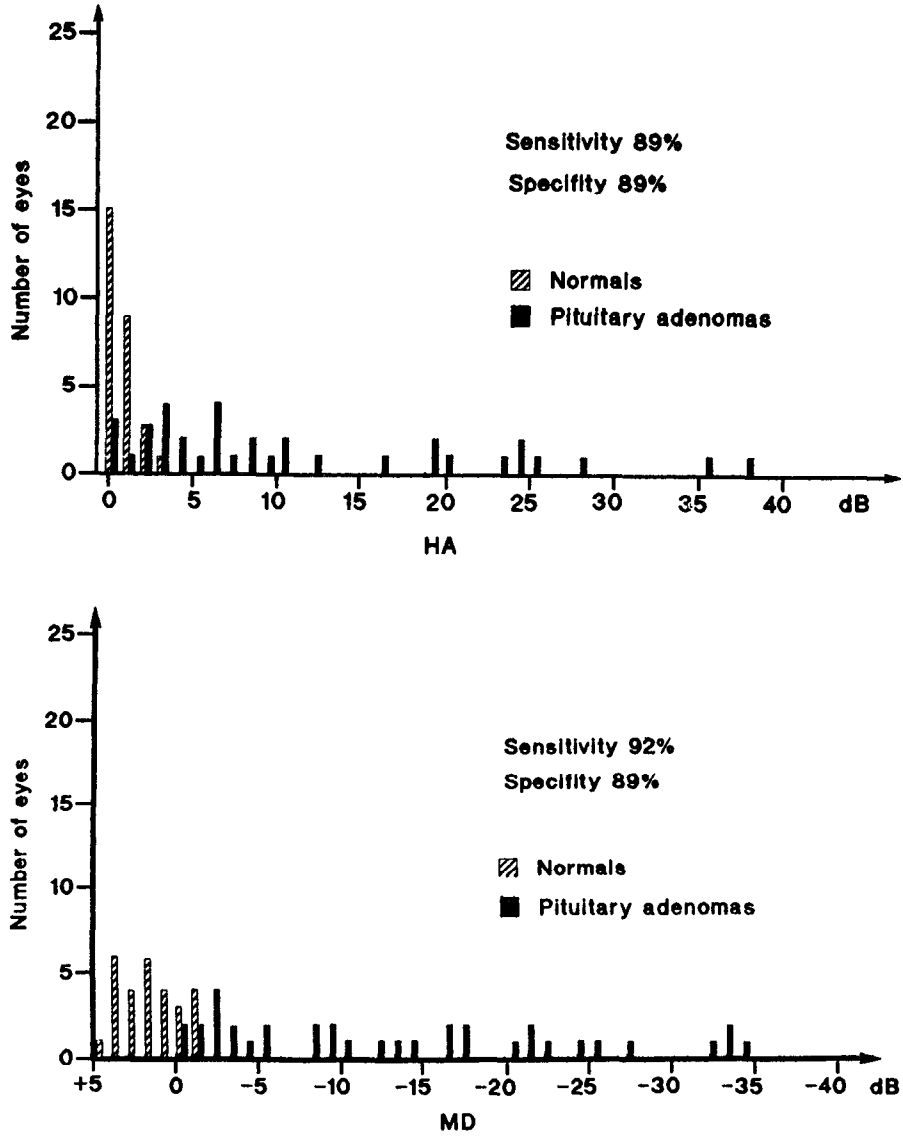

Fig 3a and b Distribution of horizontal asymmetry and mean deviation in upper quadrant analysis

discrimination. In upper quadrant analysis, the HA criterion was "HA>2.3 dB" and provided a sensitivity and specificity of 89% (Fig. 3a), while MD reached a sensitivity of 92% and a specificity of 89% with the criterion "MD<-1.2 dB" (Fig 3b). In lower quadrant analysis, the HA criterion was "HA>0.9 dB" It provided a sensitivity of 86% and a specificity of 89% (Fig. 4a). For MD, the criterion was "MD<-1.3 dB" and provided a sensitivity of 89% and a specificity of 93% (Fig. 4b)

The combination of both indices provided excellent results in all three analyses: the two-dimensional criterion had a sensitivity and a specificity of 100% in the hemifield analysis (formula: HA-0.5MD>2, Fig. 5a) as well as in the upper quadrant analysis (formula: 1.5HA-MD>5, Fig. 5b). In the lower quadrant analysis, it reached 97% sensitivity and 100% specificity (formula: HA-0.66MD>3 33, Fig 5c).

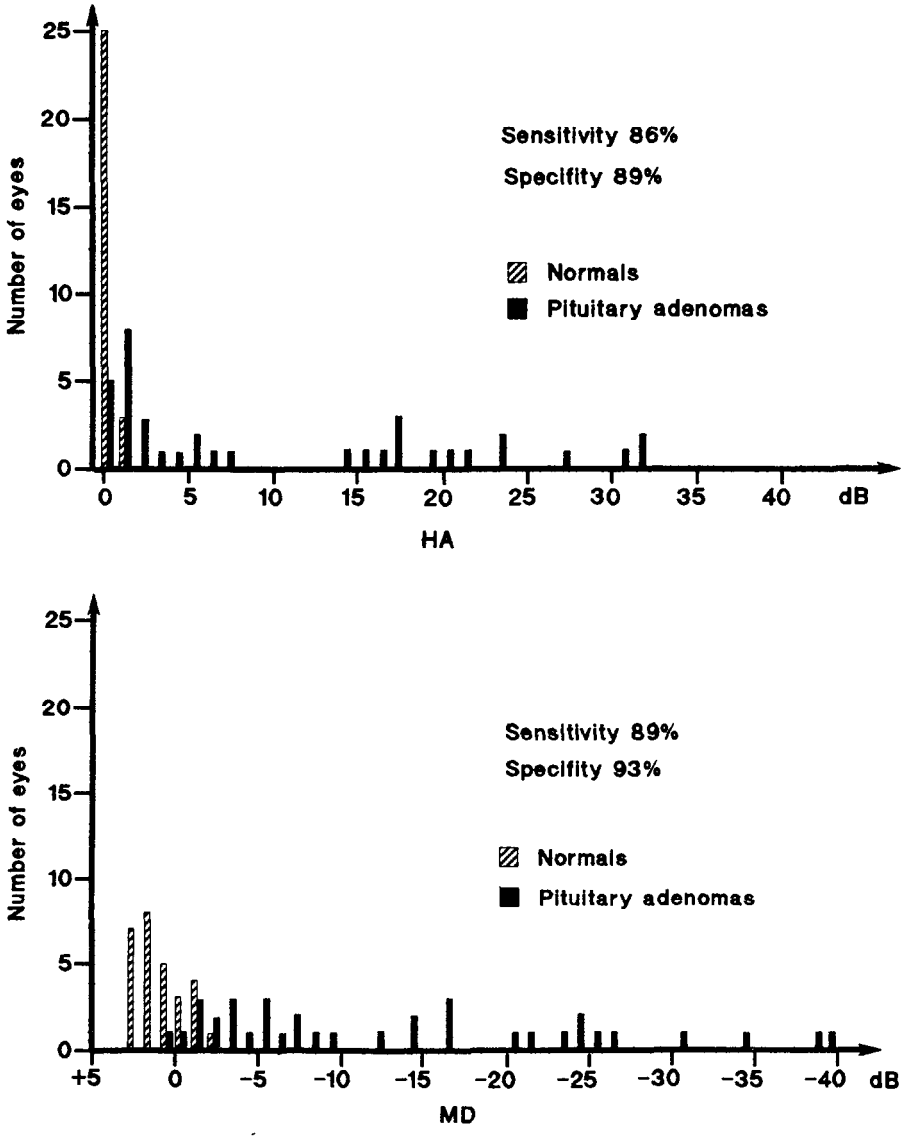

Fig 4a and b Distribution of horizontal asymmetry and mean deviation in lower quadrant analysis

Discussion

The sensitivity and specificity of global, numerical field indices and topographical field indices were compared in cases of pituitary adenoma. The mean deviation (MD) and horizontal asymmetry (HA) furnished almost equal discrimination between normal and pathological fields as measured by sensitivity and specificity. The analysis of quadrants did not improve the results as expected.

A two-dimensional analysis combining both indices, however, increased the sensitivity and specificity to 97% or more. The upper quadrant analysis of MD+HA showed a sensitivity and specificity of 100%.

These figures should be handled with care. As devised by this method, sensitivity and specificity are usually higher than they actually are. An exact determination can only be provided

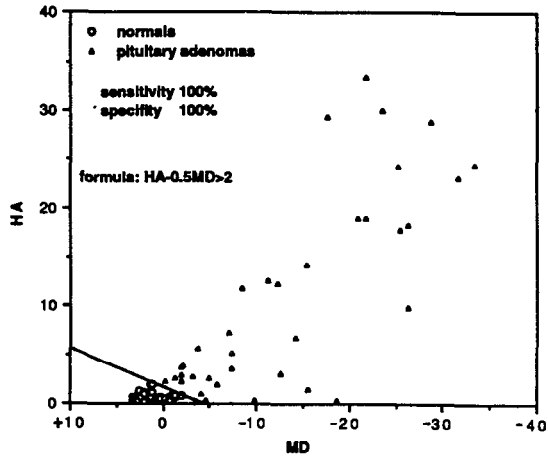

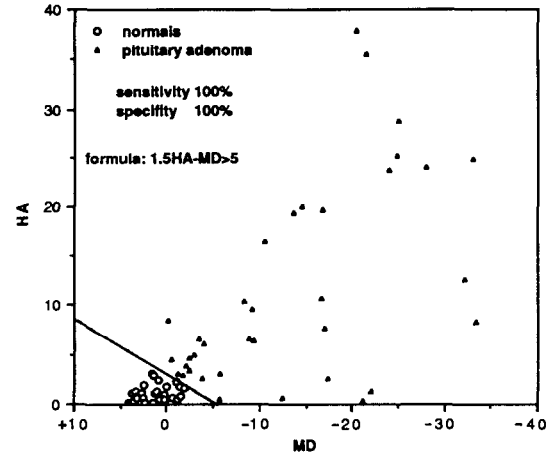

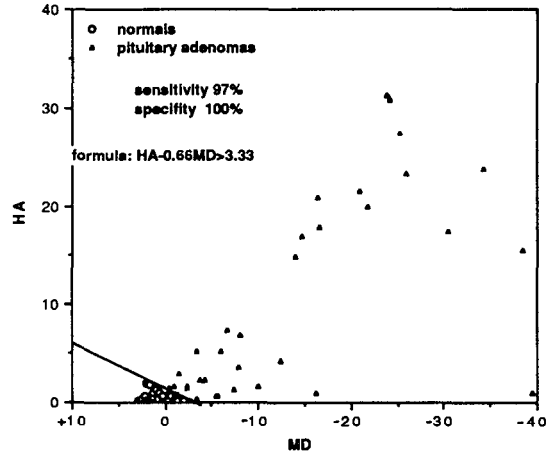

Fig 5a, b and c Scatterplots showing the relationship of normals and pituitary adenomas when horizontal asymmetry and mean deviation are combined

by a prospective study.

However, the major conclusion from this study is the additional effect on the discrimination power using both indices Although the selected model of pituitary adenoma might be different from other diagnoses, it can be expected that combinations of several indices, especially topographical and global numerical indices, increases their diagnostic value considerably. Adaptations of indices to typical patterns of defects[4,5] and readjustment of criteria are certainly necessary.

References

1 Flammer J, Drance SM, Augustiny L, Funkhauser A: Quantification of glaucomatous visual field defects with automated perimetry Invest Ophthalmol Vis Sci 26:176-181, 1985
2. Flammer J: The concept of visual field indices Graefe's Arch Clin Exp Ophthalmol 224:389-392, 1986
3. Aulhorn E, Karmeyer H: Frequency distribution in early glaucomatous visual field defects Doc Ophthalmol Proc Ser 14:75-83, 1977
4. Duggan C, Sommer A, Auer C, Burkhard K: Automated differential threshold perimetry for detecting glaucomatous visual field loss. Am J Ophthalmol 100:420-423, 1985
5. Sommer A, Duggan C, Auer C, Abbey H: Analytical approaches to the interpretation of automated threshold perimetric data for the diagnosis of early glaucoma. Trans Am Ophthalmol Soc 83:250-267, 1985

Normal and abnormal variability

Effect of test point location on the magnitude of threshold fluctuation in glaucoma patients undergoing automated perimetry

Elliot B. Werner[1], Gary Ganiban[1] and A. Gordon Balazsi[2]

[1]*Hahnemann University, Philadelphia, PA 19102, USA,* [2]*McGill University, Montreal, Quebec H3A 1A1, Canada*

Introduction

The presence of large amounts of fluctuation in the visual fields of glaucoma patients has confounded efforts to use automated perimetry to detect progressive visual loss due to glaucoma. The use of standard statistical tests does not appear to be a reliable method to detect true progressive change in the glaucomatous visual field[1,2]. It is now becoming clear that empirical data on the behavior of the visual field in glaucoma patients over time must be acquired in order to develop techniques to detect progressive deterioration in the visual field[3,4].

Recent studies have shown that both intra-subject and inter-subject threshold variation depend on defect depth and test point location[5-8]. In general it has been found that fluctuation is greater in areas of decreased sensitivity and increases with distance from fixation

The purpose of this study was to investigate the relationship between test point location and fluctuation in a sample of patients with glaucomatous visual field defects

Material and methods

Subject selection

The charts of all patients followed on the glaucoma service of the Royal Victoria Hospital, Montreal were reviewed. Sixty-seven patients with primary open-angle glaucoma who met the following criteria were identified and included in the study:

1. 20/30 vision or better;
2. phakic;
3. no surgical or laser treatment during the period encompassed by the four most recent visual field examinations;
4. no change in miotic therapy during the period encompassed by the four most recent visual field examinations;
5. no media opacity, retinal disease, or other ocular or systemic disease likely to affect visual function;
6. at least five available full threshold automated visual fields using program G1 on the Octopus 500 perimeter;
7. presence of an abnormal visual field (*i e* , patients with normal visual fields were eliminated) defined as any one of the following:
   A. mean defect (MD) > 3.5 decibels (dB);
   B. corrected loss variance (CLV) > 5.0 dB;
   C. MD > 2.5 and CLV > 4.0 in the same subject.

Study design

One eye of each subject was studied. If only one eye of a subject met the inclusion criteria, that eye was included. If both eyes met the inclusion criteria, one eye was randomly selected.

Address for correspondence Elliot B Werner, M D , 216 North Broad Street, Mail Stop 209, Philadelphia, PA 19102, USA

Perimetry Update 1990/91, pp 175-181
Proceedings of the IXth International Perimetric Society Meeting,
Malmö, Sweden, June 17-20, 1990
edited by Richard P Mills and Anders Heijl

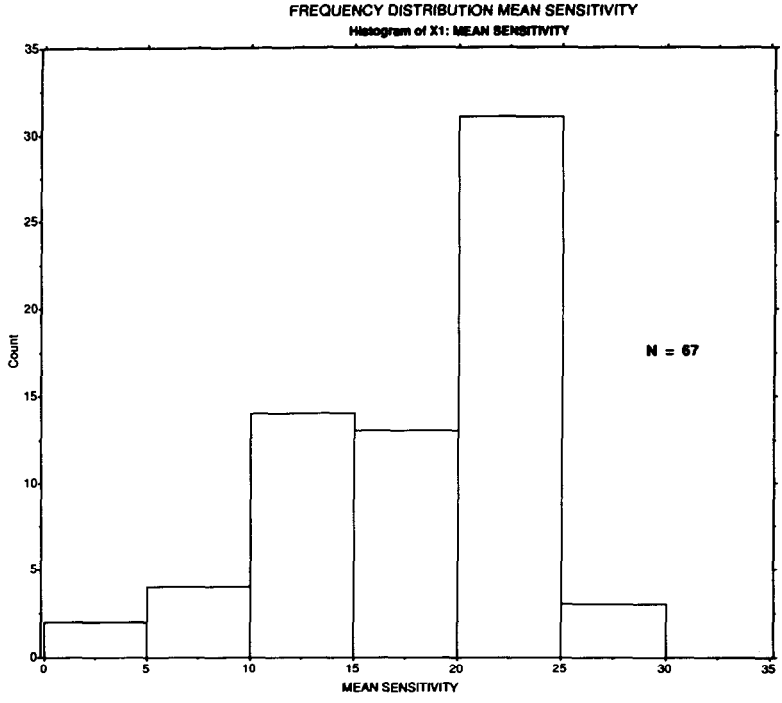

Fig 1 Frequency distribution of the mean sensitivity of the whole visual field of each subject in the study.

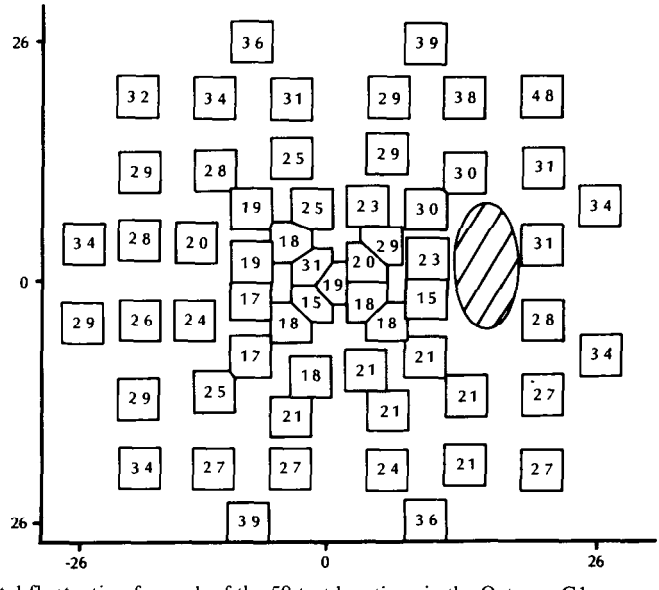

Fig 2 Mean total fluctuation for each of the 59 test locations in the Octopus G1 program over the entire sample of 67 glaucomatous eyes.

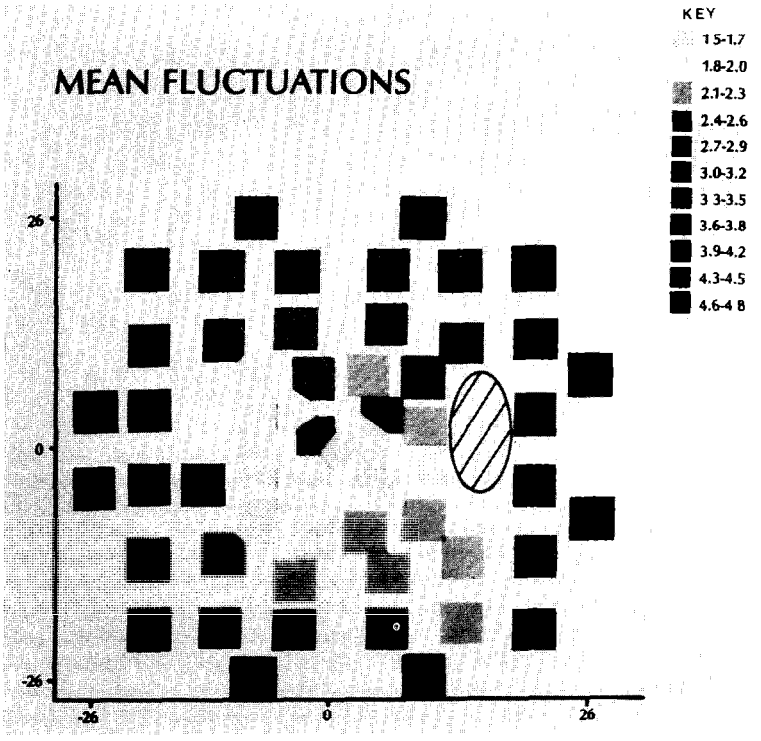

Fig. 3 Gray scale representation of the data in Fig. 2. Darker areas represent larger mean fluctuations Fluctuation appears to be higher in the superior half of the field as well as in the peripheral portions of the field.

The four most recent visual fields available for each eye were retrospectively analyzed. Each of the 59 test locations in the program G1 test pattern were analyzed separately for each of the 67 eyes.

The total fluctuation for each test location was calculated as follows:

1. the four threshold values available for each test location for each subject were regressed against time and the best fit straight line was determined;
2. the root mean square of the residuals was calculated and defined as the total fluctuation of that test location for each individual subject[9];
3. test locations in which a threshold of 0 dB was recorded on all four visual fields were eliminated;
4. the mean total fluctuation for each test location was determined by taking the average of all the subjects' fluctuations for that test location.

The use of the root mean square of the residuals as an index of fluctuation was chosen to eliminate any variability due to progressive change in threshold over time. The root mean square of the residuals measures only random fluctuation even in the presence of a significant trend in a series of values.

Results

Uncorrected fluctuation data

The majority of the subjects had mild to moderate visual field defects (Fig. 1). The mean total fluctuation for individual test locations increased with distance from fixation, and was generally higher in the superior portions of the field (Figs. 2, 3 and 4, Table 1).

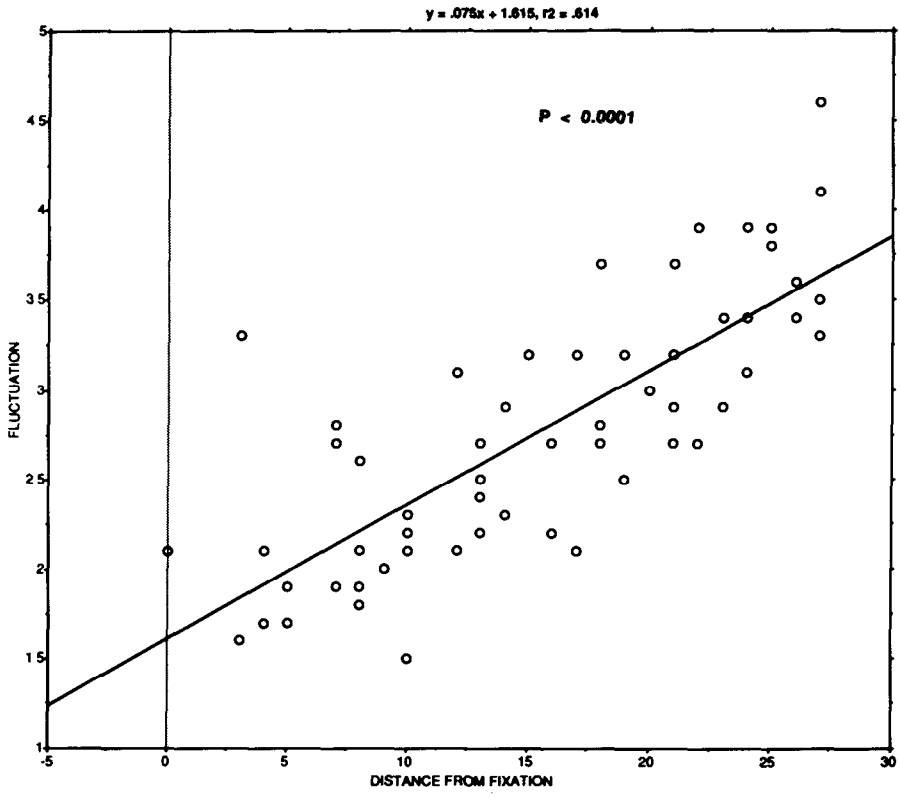

Fig 4 Effect of test point eccentricity on fluctuation The mean fluctuation of each test point location for the sample is shown as a function of distance from fixation There is a highly significant correlation showing that fluctuation increases in the peripheral portions of the field.

Table 1 Average fluctuations values for the superior peripheral, inferior peripheral, superior central and inferior central parts of the visual field for the entire sample

	Average fluctuation	*p*
Peripheral points		
superior	3 2 dB	0 0062
inferior	2 7 dB	
Central points		
superior	2 4 dB	0 0018
inferior	1 8 dB	

Central points were those within 13° of fixation. Peripheral points were outside 13° from fixation For both the peripheral and central portions of the visual field, fluctuation was significantly higher in the superior half of the visual field

Correction of fluctuation data for effect of sensitivity

Like fluctuation, the sensitivity level is strongly dependent on test point location (Fig. 5). It is possible that the relationship between test point location and fluctuation may be due to differences in sensitivity in different parts of the visual field.

In general, the fluctuation for each individual test location increased in subjects with decreased sensitivity at that location until very low levels of sensitivity were reached, at which point fluctuation also decreased (Fig. 6). For most of the test locations in this study, the relationship between fluctuation and sensitivity for the entire sample for each test location was

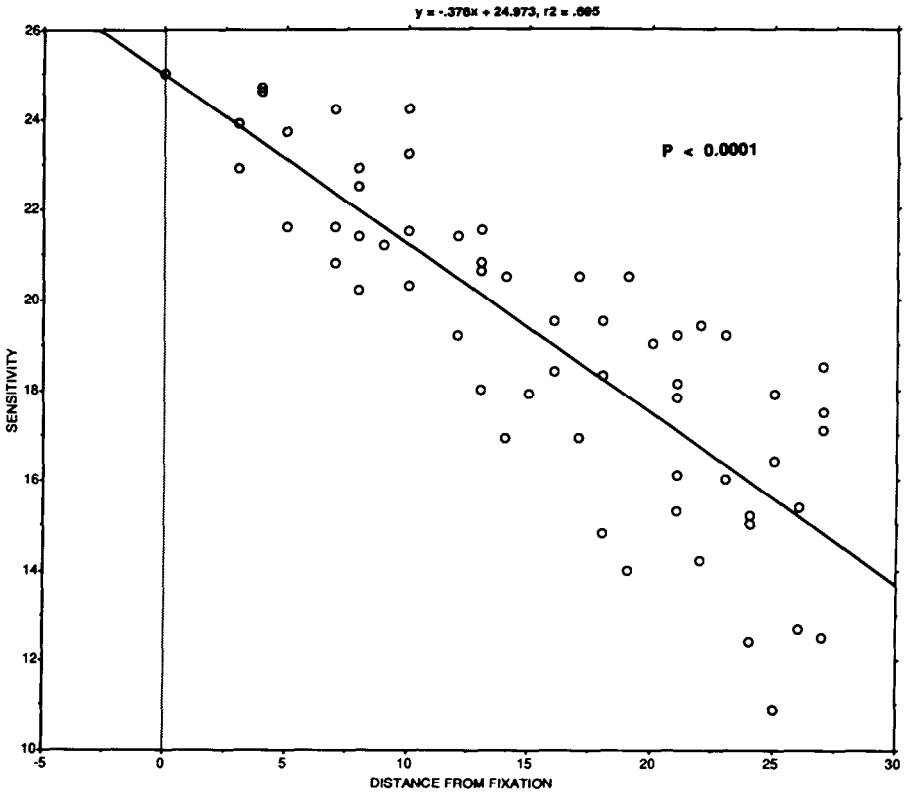

Fig 5 Effect of test point eccentricity on sensitivity The mean sensitivity of each test point location for the sample is shown as a function of distance from fixation There is a highly significant correlation showing that, as expected, sensitivity decreases in the peripheral portions of the field

Table 2 Average corrected fluctuation values for the superior peripheral, inferior peripheral, superior central and inferior central parts of the visual field for the entire sample

	Average corrected fluctuation	*p*
Peripheral points		
superior	2.7 dB	0 10
inferior	3 0 dB	
Central points		
superior	2 9 dB	0 08
inferior	2 2 dB	

When the fluctuation is corrected for differences in sensitivity in different parts of the visual field, the effect of test point location is not significant

best described by a quadratic function.

We calculated the least squares best fit quadratic function for fluctuation versus sensitivity for each test location. The fluctuation of each test location was then corrected to a sensitivity level of 20 decibels. When this was done, the positional effect on fluctuation disappeared (Fig. 7, Table 2).

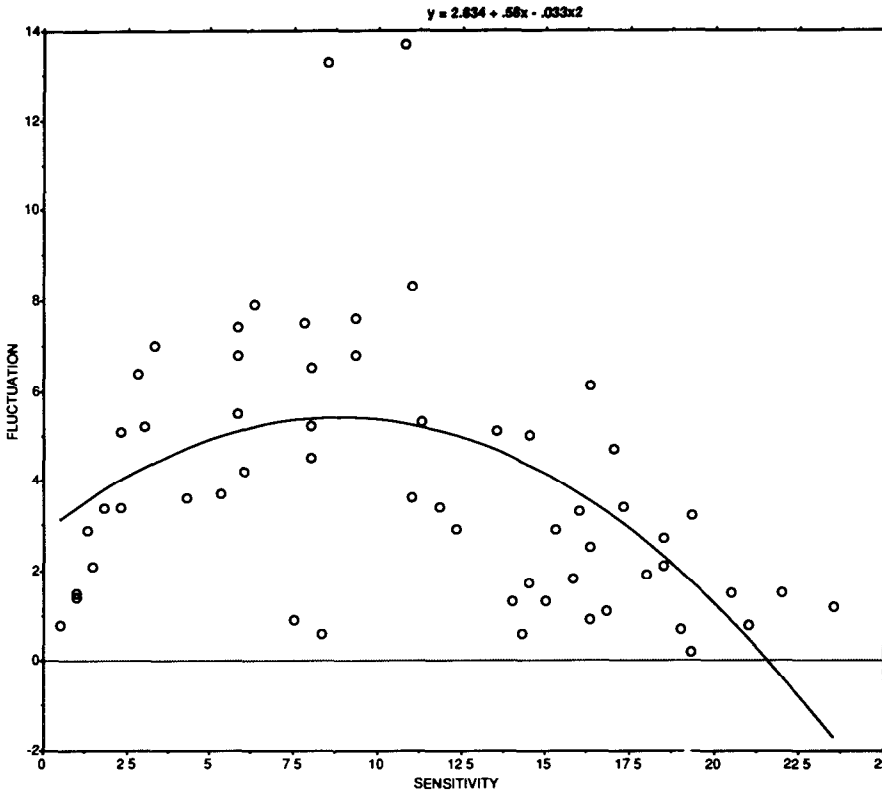

Fig 6 Relationship between fluctuation and sensitivity for a single point in the visual field (10° temporal, 26° superior to fixation). Each open circle in the graph represents the fluctuation and sensitivity for a single patient. The best fit quadratic function shows the tendency for fluctuation to increase as sensitivity decreases until very low levels of sensitivity are reached When the sensitivity is corrected to 20 dB, the corrected fluctuation predicted by the function for this point is 1 2 dB

Conclusions

There is a strong positional effect on the magnitude of point-wise total fluctuation in the visual fields of glaucoma patients within the central 30°. Fluctuation increases with distance from fixation. Fluctuation is also higher in the superior hemifield. This phenomenon, however, seems to be due to the relationship between fluctuation and sensitivity.

In areas of the field where sensitivity is lower, fluctuation is higher. If one corrects for the differences in sensitivity in different parts of the visual field, the effect of test point location on fluctuation largely disappears

References

1 Werner EB, Bishop KI, Koelle J, Douglas GR, LeBlanc R, Mills RP, Schwartz B, Whalen WR, Wilensky JT: A comparison of experienced clinical observers and statistical tests in the detection of progressive visual field loss in glaucoma using automated perimetry Arch Ophthalmol 106:619-623, 1988
2 Chauhan B, Drance SM, Douglas GR: The use of visual field indices in detecting changes in the visual field in glaucoma. Invest Ophthalmol Vis Sci 31:512-519, 1990
3 Werner EB, Petrig B, Krupin T, Bishop KI: Variability of automated visual fields in clinically stable glaucoma patients. Invest Ophthalmol Vis Sci 30:1083-1089, 1989
4 Hoskins HD, Magee SD, Drake MV, Kidd MN: Confidence intervals for change in automated visual fields Br J Ophthalmol 72:591- 597, 1988

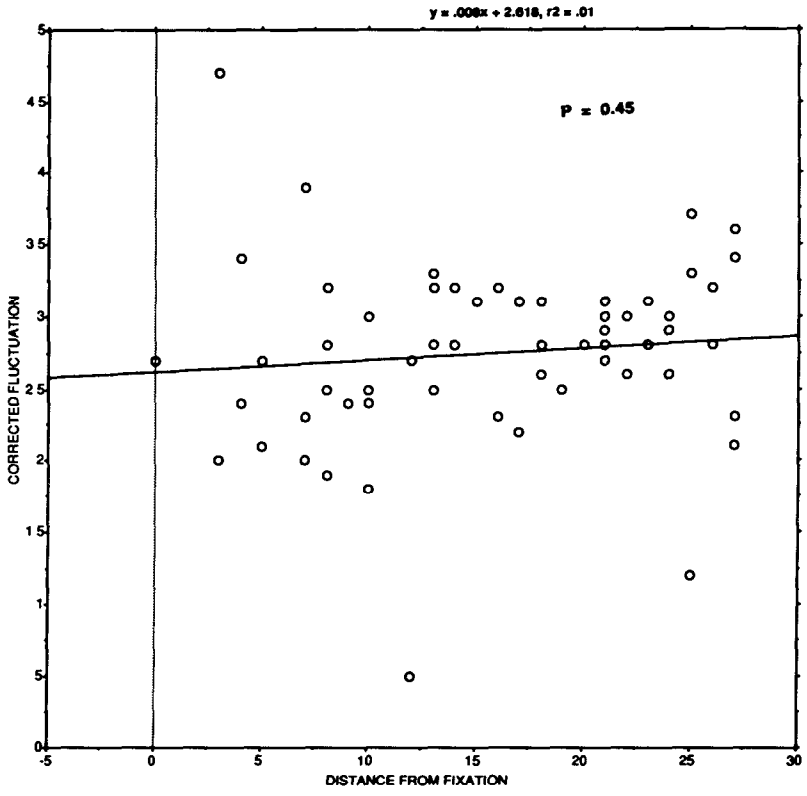

Fig 7 Effect of test point eccentricity on fluctuation corrected for differences in sensitivity in different portions of the field The corrected fluctuation of each test point location for the sample is shown as a function of distance from fixation. The regression line is nearly flat and the slope is not significant, indicating that fluctuation corrected for differences in sensitivity in different parts of the visual field is not affected by test point eccentricity.

5. Katz J, Sommer A: A longitudinal study of age-adjusted variability of automated visual fields Arch Ophthalmol 105:1083-1086, 1987
6. Heijl A, Lindgren G, Olsson J: Normal variability of static perimetric threshold values across the central visual field Arch Ophthalmol 105:1544-15449, 1987
7. Langerhorst CT: Automated Perimetry in Glaucoma: Fluctuation Behavior and General and Local Reduction of Sensitivity. Amsterdam: Kugler Publications 1988
8. Heijl A, Lindgren A, Lindgren G: Test-retest variability in glaucoma Am J Ophthalmol 108:130-135, 1989
9. Feldman Jr DS, Hofmann R, Gagnon J, Simpson J: StatView II Berkeley: Abacus Concepts Inc 1987

Fluctuation of the differential light sensitivity in clinically stable glaucoma patients

Mario Zulauf, Joseph Caprioli, Douglas C. Hoffman and Charles S. Tressler

Glaucoma Service, Yale University School of Medicine, Department of Ophthalmology and Visual Science, New Haven, Connecticut, USA

Abstract

The authors studied the long-term fluctuation of differential light sensitivity in a group of clinically stable glaucoma patients to estimate the magnitude of non-progressive variability of automated static threshold perimetry. We report on 106 visual fields of 29 glaucoma patients performed with Octopus program 32 over an average of 27 9 months (range 11-67), who had no evidence of progressive disease by clinical criteria. Long-term fluctuation was defined as the variance of repeated measurements of differential light sensitivity at individual test locations. The overall mean (±SEM) variance for all test locations in the visual field was 4.25 ± 0 13 dB. Regression analysis revealed an increase of the variance toward the periphery by 0.1 dB^2 per degree (r=0 09, p<0 001). The long-term fluctuation correlated better with defect depth (r=0 32, p<0 001), and best with sensitivity (r=0 35, p<0 001) Long-term fluctuation increased by 0 5 dB^2 for each dB decrease of sensitivity. Fluctuation of visual field thresholds in clinically stable glaucoma patients is a function of differential light sensitivity and location This data may help clinicians distinguish non-progressive fluctuation from progressive damage to the visual field in glaucoma patients

Introduction

Automated static threshold perimetry has provided practitioners with a level of testing standardization which has previously not been readily available It is a sensitive test of glaucomatous visual field loss, is conveniently performed, and the numerical results may be statistically evaluated. The availability of population based age-matched normal values has facilitated the identification of early glaucomatous visual field defects. The comparison of sequential examinations to detect progressive disease remains a difficult and important problem which has received insufficient study[1-7] Physiological fluctuations may mask or falsely suggest a change of the visual field when an insufficient number of examinations are evaluated. Fluctuation is therefore of major interest when considering the follow-up of patients Reliable methods to separate the "signal" of progressive functional loss from variability "noise" still have to be established.

We studied the long-term fluctuation (LF) of differential light sensitivity (dls) in a routine clinical setting in a group of clinically stable glaucoma patients, and examined the relationship of fluctuation with the depth of visual field defect and the eccentricity of the test location.

Material and methods

This retrospective study reports on glaucoma patients attending the Glaucoma Service of the Yale Eye Center who were examined with program 32 of the automated Octopus 201 perimeter. The diagnosis of glaucoma was based on visual field criteria as previously described[8] and optic

This study was supported in part by grants from Research to Prevent Blindness, Inc., the Connecticut Lions Eye Research Foundation, Inc , the National Eye Institute (EY-00785), and the New Haven Foundation Dr Zulauf is a fellow of the Swiss National Fund and the F Verrey Foundation

Address for correspondence Joseph Caprioli, M D , Yale University School of Medicine, Department of Ophthalmology and Visual Science, 330 Cedar Street, P O Box 3333, New Haven, Connecticut 06510-8061, USA

Perimetry Update 1990/91, pp 183-188
Proceedings of the IXth International Perimetric Society Meeting,
Malmö, Sweden, June 17-20, 1990
edited by Richard P. Mills and Anders Heijl

disc appearance. Glaucoma was diagnosed as the only cause of the visual field defects. All patients were phakic. All patients who met the following additional criteria entered the study:

1. a minimum of three visual fields performed with Octopus program 32 over a ten-month period or longer;
2. stable visual fields by clinical criteria during the observation period (see below);
3. previous experience with the automated perimeter Octopus 201;
4. visual acuity of 20/40 or better at each visual field examination;
5. intraocular pressure measurements always <22 mm Hg during the study interval;
6. no changes in medical therapy made during the study interval;
7. a refractive error with spherical equivalent was within -5 to +5 diopters, with less than 2 diopters of astigmatism;
8. a stable refractive error with a change of spherical equivalent between examinations of ≤0.50 diopters;
9. a change in pupillary area of less than a factor of 2 between examinations (*e g* , a change in pupillary diameter of 1.0 mm to 1.5 mm, *i e* , 1 mm^2 to 2.25 mm^2 would disqualify an eye);
10. no laser or surgical intervention during the study interval; and
11. no change in the appearance of the optic nerve with careful inspection of color stereoscopic disc photographs which were obtained at each visual field examination.

A clinically stable visual field was defined as not having >5 dB change at ≥2 adjacent locations or not having a >10 dB change at any location of the visual field when any two examinations of the same eye were compared.

Long-term fluctuation (LF) was defined as the statistical variance of repeated measurements of the differential light sensitivity at each test location. The two test locations which usually include the physiological blind spot were excluded from the calculations to avoid artifactual contributions to fluctuation. All locations with a dls of less than 5 dB in any of the examinations were excluded from the calculations. A loss parameter was calculated for each test location by subtracting the measured threshold value from the normal age-corrected value supplied by the Octopus 201 software. For program 32, an age correction of -0.1 dB per decade of age is applied by the Octopus perimeters.

Table 1 Data for age, refractive error, pupil size, and visual field indices

	Mean	*S D **	*Range*
Age (years)	63 8	11 7	39 0–83.0
Refractive error			
spherical diopters	1 5	2 2	–3.5– 6 5
cylindrical diopters	0.6	0 9	0 0– 3 5
Pupil size	3 9	1 4	1 0– 7.0
Visual field			
mean defect (dB)	6.5	0 9	–1 0–15 3
corrected loss variance (dB^2)	12 5	17 7	0.5–56 1
short-term fluctuation (dB)	1 2	0.8	0.0– 4 5
eccentricity (degrees)	19.9	7 0	4 2–28 5

*standard deviation

Table 2 Linear and quadratic regression analyses of long-term fluctuation with eccentricity, defect depth, and differential light sensitivity (DLS)*

	Correlation coefficient	
	Linear model	*Quadratic model*
LF with eccentricity	0 32	0 34
LF with defect depth	0 32	0 34
LF with DLS	0.35	0.36

*all p=0.000

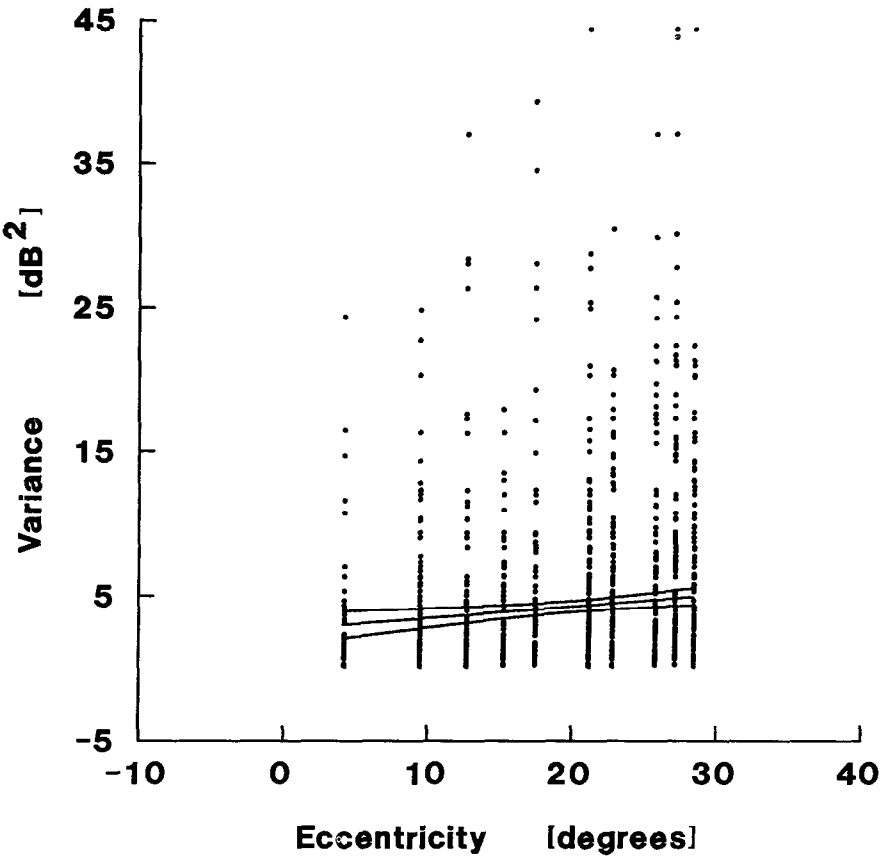

Fig 1 Scatterplot of the long-term fluctuation (variance versus eccentricity) The 99% confidence limits for the linear regression are shown

Results

One hundred and six visual fields of 29 eyes of 29 patients qualified for the study. Patients had an average of 3.6 visual field examinations with a range of 3 to 6 examinations. Data for age, refractive error, pupil size, and visual field indices are given in Table 1 There were 14 males and 15 females in the study.

The mean (± SEM) LF for all test locations was 4.2 ± 0 1 dB^2. Linear regression analysis revealed a statistically significant correlation of the LF with the eccentricity (r=0.093, p<0.001), with defect depth (r=0.32, p<0.001), and with the differential light sensitivity (r=0.35, p<0.001). For a quadratic fit the correlations were only slightly better. The variance increased toward the periphery by an average of approximately 0 1 dB^2 per degree, while the variance increased by approximately 0.5 dB^2 for each dB decrease of sensitivity. Fig. 1 displays the LF as a function of eccentricity, Fig. 2 as a function of the defect depth loss, and Fig 3 as a function of the differential light sensitivity.

Discussion

Short-term and long-term fluctuations of the visual field in normal and glaucomatous subjects have been studied[1-7] Short-term fluctuation is defined as the variability which occurs during the performance of a single test. Long-term fluctuation occurs between tests over days, weeks, months, or longer. Long-term fluctuation increases with age, intraocular pressure, dis-

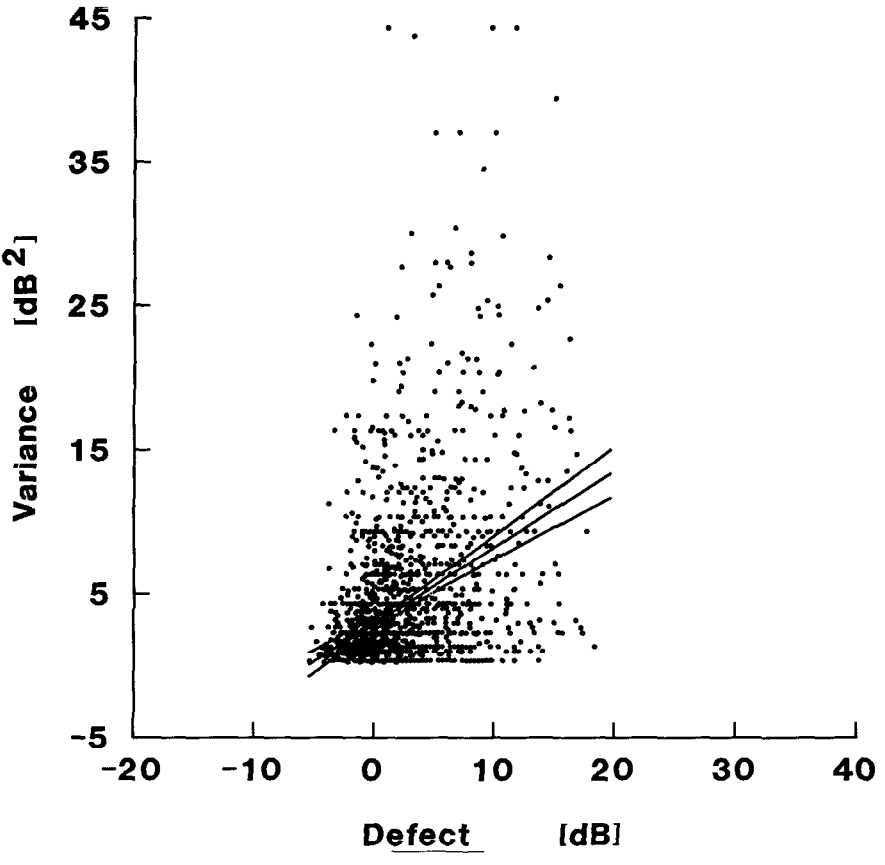

Fig 2 Scatterplot of the long-term fluctuation (variance) versus defect depth (loss). The 99% confidence limits for the linear regression are shown

tance from fixation, and is greater in areas of glaucomatous damage[1-5] Few have attempted to quantify the fluctuation over long periods of time in stable glaucoma patients.

Werner and coworkers studied the total variability in 20 clinically stable open angle glaucoma patients with the Octopus perimeter[6]. The average total variability over four examinations had a variance of 2 8 decibels and a range of 5.1 decibels. The data were not stratified by level of loss or distance from fixation. For purposes of comparison, the average fluctuation in our study expressed as variance was 4 2 dB; the fluctuation rates of these two studies may not be directly comparable because the study populations are not matched for total visual field loss. Heijl and coworkers recently measured the test-retest variation in glaucoma patients with the Humphrey perimeter[7]. Fifty-one subjects were tested four times within a four-week period. Abnormal areas of the visual field showed greater variability than did normal areas, and variability of test locations which were not markedly disturbed increased with distance from fixation. Within normal areas of the visual field, threshold values fluctuated less than 10 dB 90% of the time. In moderately disturbed areas of the visual field, the 90% prediction interval increased to more than 20 dB.

We retrospectively examined serial visual fields of patients previously experienced in perimetry who were tested over a period of 10 months or more. The overall mean (± SEM) fluctuation, defined as the variance of repeated measurements, was 4.2 ± 0.1 dB^2. The fluctuation was significantly greater in depressed areas of the visual field, and approached an estimated value of 20 decibels at a differential light sensitivity of 0 dB on the Octopus perimeter.

There is a statistically significant correlation of fluctuation with distance from fixation, which is about 2 decibels greater in peripheral locations of the 30° visual field compared to

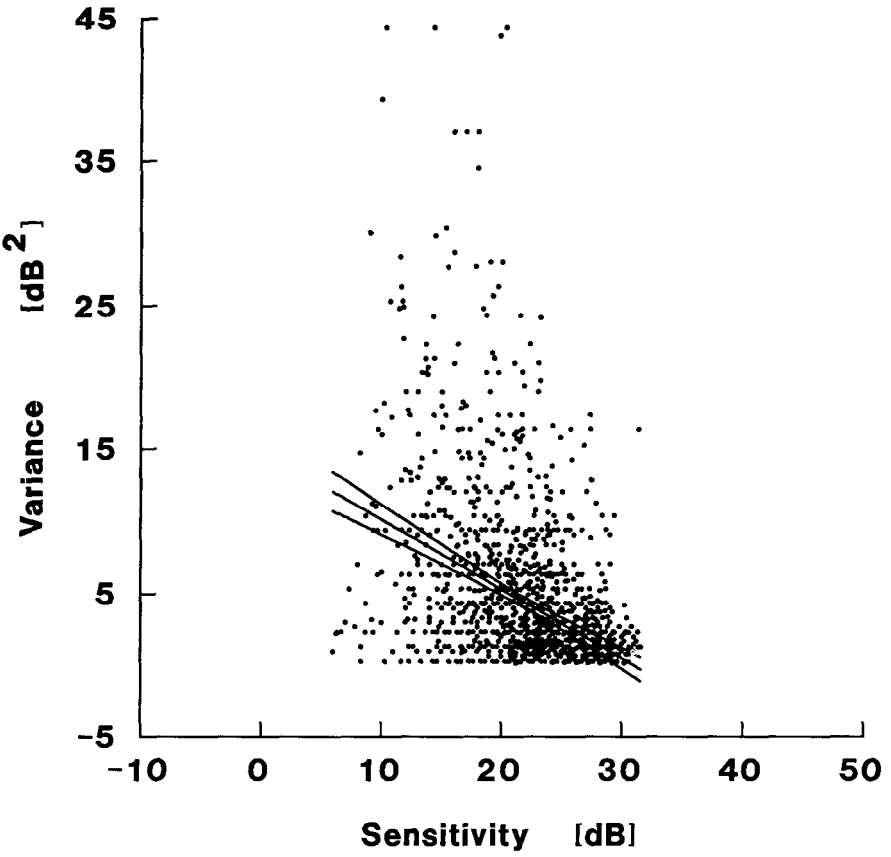

Fig 3 Scatterplot of the long-term fluctuation (variance) versus differential light sensitivity The 99% confidence limits for the linear regression are shown

central locations These estimates demonstrate a wide range of fluctuation of the differential light sensitivity without the apparent implication of progressive damage. There is little quantitative information about the prognostic value of high fluctuation rates of the differential light sensitivity for future visual field loss This and preceding initial studies[5,6] attempt to provide practical guidelines for the evaluation of progressive visual field loss in glaucoma patients Further quantitative studies in carefully defined glaucoma populations and in individuals at risk for glaucomatous visual field loss should provide valuable information to help us separate the "signal" of progressive damage from the "noise" of variability of serial measurements of the visual field.

References

1 Flammer J, Drance S, Schulzer M: Covariates of the long term fluctuation of the differential light threshold Arch Ophthalmol 102:880-882, 1984
2. Flammer J, Drance S, Zulauf M: Differential light threshold: short and long term fluctuation in patients with glaucoma, normal controls, and patients with suspected glaucoma. Arch Ophthalmol 102:704-706, 1984
3 Wilensky JT, Joondeph BC: Variation in visual field measurements with an automated perimeter Am J Ophthalmol 97:328-331, 1984
4 Gloor B, Dimitrakos S, Rabineau P: Long term follow-up of glaucomatous fields by computerized (Octopus) perimetry In: Krieglstein G (ed) Glaucoma Update III, pp 123-138 Berlin: Springer-Verlag 1987

5. Katz J, Sommer A: A longitudinal study of the age-adjusted variability of automated visual fields. Arch Ophthalmol 105:1083-1086, 1987
6 Werner EB, Petrig B, Krupin T et al: Variability of automated visual fields in clinically stable glaucoma patients. Invest Ophthalmol Vis Sci 30:1083-1089, 1989
7. Heijl A, Lindgren A, Lindgren G: Test-retest variability in glaucomatous visual fields. Am J Ophthalmol 108:130-135, 1989
8 Caprioli J, Ortiz-Colberg R, Miller JM, Tressler C: Measurements of peripapillary nerve fiber layer contour in glaucoma. Am J Ophthalmol 108:404-413, 1989

Inter-test threshold variability in glaucoma
Importance of censored observations and general field status

Anders Heijl[1], Anna Lindgren[2], Georg Lindgren[2] and Mike Patella[3]

[1]*Department of Ophthalmology, Malmö General Hospital, Sweden and* [2]*Department of Mathematical Statistics, University of Lund, Sweden,* [3]*Allergan Humphrey, San Leandro, CA, USA*

We tested 51 glaucomatous eyes of 51 patients four times each over a one-month period using the 30-2 program of the Humphrey perimeter. Analysis of these data, reported in Heijl *et al.*[1], showed that the observed threshold variability was small at points with normal sensitivity, became relatively large at moderate defect depths, became smaller again in severely depressed points, and depended on point location.

We now report on two new findings which are important for the interpretation of inter-test variability. Firstly, the observed decrease in variability in severely depressed points is actually an artifact of the limited dynamic range of the instrument; after correction for the resulting censoring of data, we find variability to increase continuously with increasing defect depth.

Secondly, the influence of general field status (as measured by Mean Deviation from age normal sensitivity over the whole field, MD) has been taken into account. Depressed points in generally depressed fields demonstrated inter-test variabilities which were radically different from those observed in similarly depressed points in otherwise normal fields (Fig. 1).

We considered all possible combinations of test results, and grouped the data according to the observed average MD over the four tests. The censoring of data, implied by the limited dynamic range of the perimeter, was corrected for by means of the Kaplan-Meier estimation technique. We calculated and smoothed the 5% and 95% percentile limits for point-to-point inter-test variability within each MD group.

Families of linear functions were then fitted to data extracted from the smoothed curves, in order to define 5% and 95% confidence limits for change as functions of initial defect depth, MD, point location, and number of tests.

These new findings are important additions to our original analysis if applied in clinical practice. Correction for the limited brightness range of the instrument clearly shows that variability increases with increasing defect depth. Without this adjustment, changes in threshold of only a few dB in points with initially large defect depth might have been judged significant. It is now clear that such small changes are within the random variability of threshold measurements in glaucoma patients.

Similarly, it is apparent that deteriorations which are significant in, for instance, fields having nearly normal values of MD, may not be significant when seen in fields with abnormal MDs.

References

1 Heijl A, Lindgren A, Lindgren G: Test-retest variability in glaucomatous visual fields. Am J Ophthalmol 198:130, 1989

Perimetry Update 1990/91, 189-192
Proceedings of the IXth International Perimetric Society Meeting,
Malmö, Sweden, June 17-20, 1990
edited by Richard P. Mills and Anders Heijl

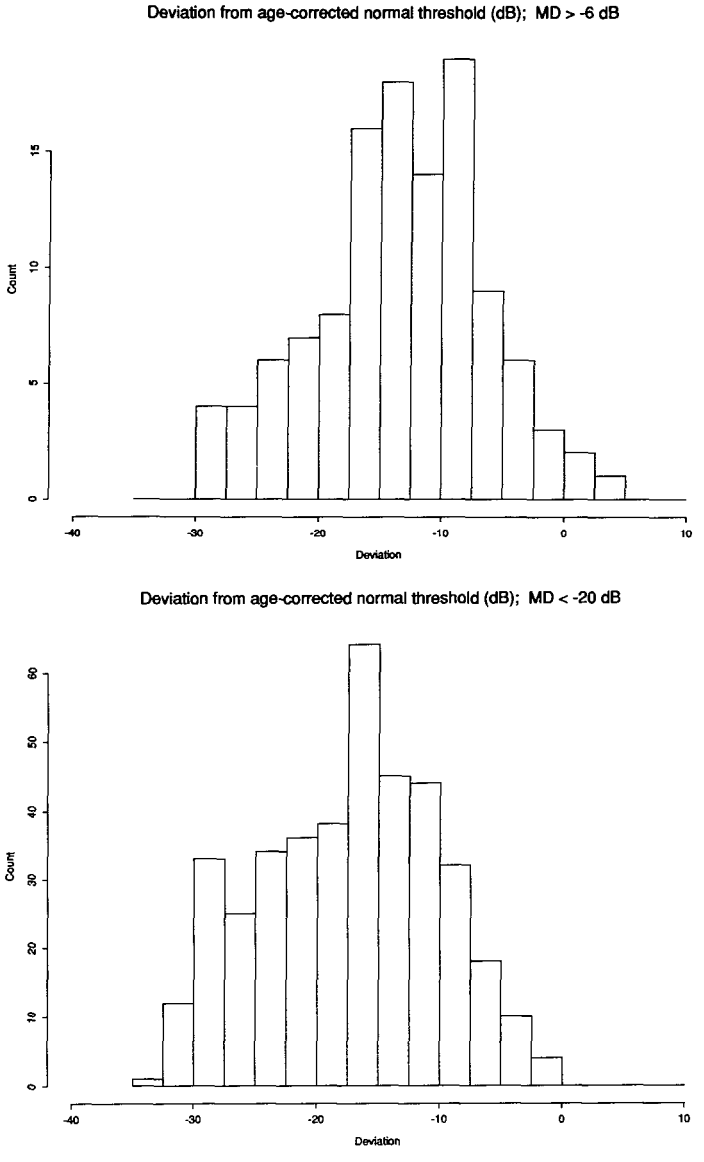

Fig 1 Distributions of deviation from age-corrected normal values at second test for the 22 most central points of the 30-2 test pattern Results shown had initial defect depths of between -15 dB and -17 dB; (a) eyes with MD better than -6 dB, (b) eyes with MD worse than -20 dB

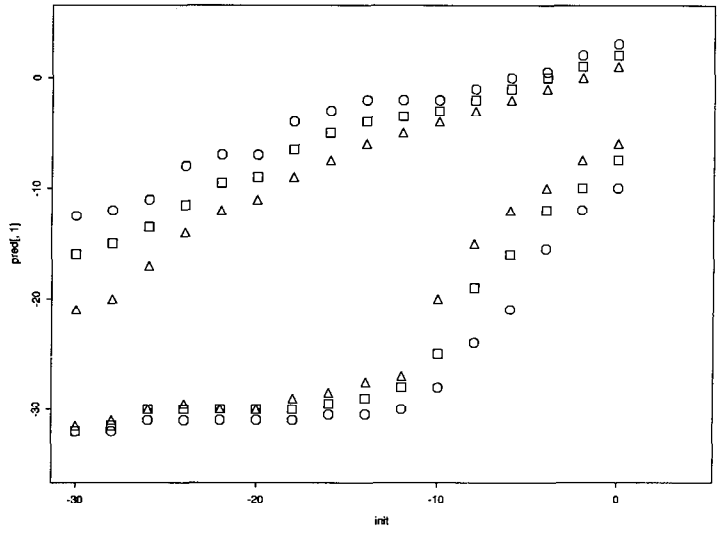

Fig 2 Significance limits for variation from one test to the next as functions of initial defect depth (inner zone) without correction for censoring; O = 2 5% and 97 5%; □ = 5% and 95%; Δ = 10% and 90% limits

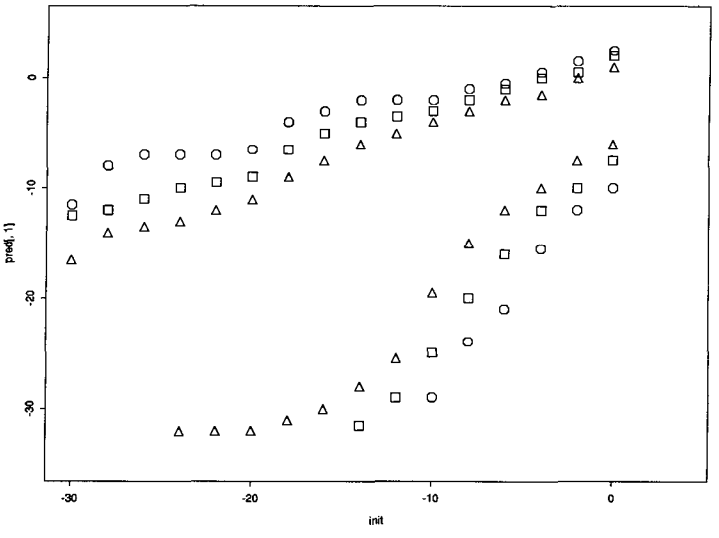

Fig 3 Significance limits for variation from one test to the next as functions of initial defect depth (inner zone) with correction for censoring; O = 2.5% and 97.5%; □ = 5% and 95%; Δ = 10% and 90% limits

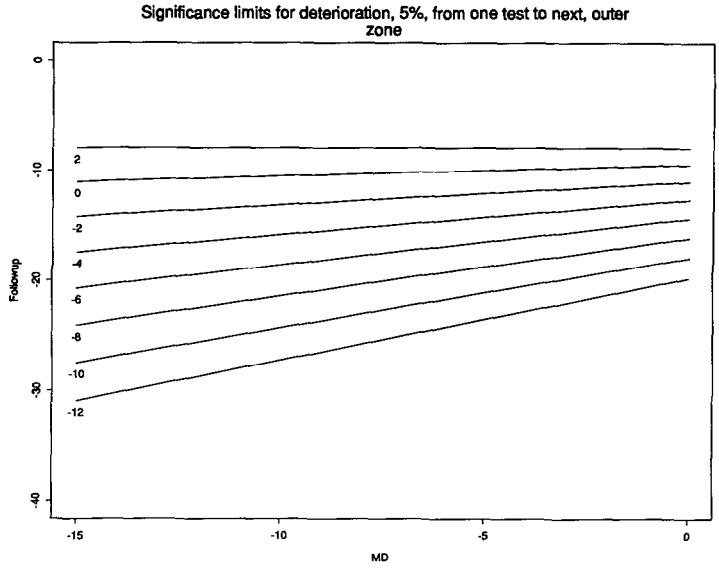

Fig 4 Significance limits for deterioration, 5%, from one test to the next, outer zone.

Pointwise analysis of serial fields in glaucoma

John M. Wild[1], Michael K. Hussey[2], John G. Flanagan[3] and Graham E. Trope[4]

[1]*Department of Vision Sciences and* [2]*Information Management Division, Business School, Aston University, Birmingham, UK;* [3]*School of Optometry, University of Waterloo, Waterloo, Ontario, Canada;* [4]*Toronto General Hospital, University of Toronto, Toronto, Ontario, Canada*

Abstract

The current visual field indices provide summary measures of the data derived from all test locations within the visual field and as a result useful information may be lost concerning the pointwise contribution of sensitivity. When evaluated over time, the indices may not provide a sufficiently sensitive method for detecting the earliest change in the progression of glaucomatous field loss. The study documented the pointwise distribution of sensitivity between serial fields for a given patient using polynomial and multiple regression By comparing the predicted pointwise sensitivity values at any given examination with the measured outcome an index of change might be derived The sample comprised 31 patients from a glaucoma clinic with 7 4 (SD 1.95) Humphrey Field Analyzer 24-2 or 30-2 fields (stimulus size III) examined per patient over 37.6 months (SD 8 4) The goodness of fit between the predicted and the measured sensitivities were found to vary within and between individuals. The degree of fit appeared to be independent of the magnitudes of the mean deviation, pattern standard deviation and short-term fluctuation

Introduction

In static automated perimetry, the threshold values at each test location across a given visual field can be summarized in terms of the data reduction statistics or visual field indices: mean defect or mean deviation and loss variance or pattern standard deviation which describe the height and shape of the visual field respectively[1-3]. The intra- and inter-examination patient variability, or short- and long-term fluctuations[4], can also be calculated.

Increasing empirical clinical opinion and also research findings[5] suggests that when evaluated over time the established visual field indices from serial examinations do not provide a sufficiently sensitive method for detecting the earliest change in the progression of glaucomatous field loss. The lack of precision in detecting change may be attributable to the inadequacy of the indices themselves or to the loss of useful information arising from the data reduction technique itself. Indeed, alternative visual field indices have recently been described by Chauhan *et al*[6].

The aim of the study was to investigate the feasibility of utilizing the sensitivity derived at each test location of a given previous field or fields to predict the measured value for the same location at the next examination. By comparing the expected pointwise distribution of sensitivity with the measured outcome, additional information on change within the visual field may be gained thus independently supplementing the traditional summary measures

Methodology

The visual fields for the study were obtained from 31 patients randomly selected from those attending a glaucoma clinic at Toronto General Hospital. All visual fields were recorded with

This study was funded, in part, by a Wellcome Trust travel grant to JMW and in part by a Canadian Medical Research Council grant.

Address for correspondence Dr J M Wild, Department of Vision Sciences, Aston University, Aston Triangle, Birmingham B4 7ET, UK

Perimetry Update 1990/91, pp 193-199
Proceedings of the IXth International Perimetric Society Meeting,
Malmö, Sweden, June 17-20, 1990
edited by Richard P Mills and Anders Heijl

the Humphrey Field Analyzer. The patients were required to meet certain inclusion criteria: namely a minimum of five visual fields per eye examined with stimulus size III using either programs 24-2 or 30-2 and carried out over a minimum period of two years.

Visual field examination had been undertaken using standard procedures which included use of appropriate refractive correction. The number of fields per patient was governed by conventional clinical considerations, namely adequacy of intraocular pressure control and/or the rate and/or the severity of the field loss. In several cases the visual field at a given examination of a given patient had been determined using the "threshold from prior data" strategy: in such cases, the results were included in the analysis

The data files contained on the Humphrey Field Analyzer formatted diskettes were converted to ASCII files on an IBM compatible personal computer using HDISK, a vehicle for information transfer especially developed for the study. The output files were then interfaced with the commercially available Statistical Graphics Corporation package Statsgraphics, version 2.1.

Where a double determination of sensitivity had been undertaken at a given test location, the value of sensitivity was taken as the mean of the two determinations. Where the examinations for a given patient had been undertaken using both program 30-2 and program 24-2 the peripheral stimulus locations were omitted from data for program 30-2.

Sensitivity was modeled using two components: a topographical model and a longitudinal model The interval between examinations was considered to be ordinal. The topographical model used a polynomial function to describe the pointwise value of sensitivity, z_{jt}, at any general stimulus location (x_{jt}, y_{jt}) at any given period in time, t, in terms of the given x and y stimulus coordinates

$$z_{jt} = {}_tA_{00} + {}_tA_{10}x_j + {}_tA_{01}y_j + {}_tA_{11}x_jy_j + {}_tA_{21}x_j^2y_j + \ldots\ldots\ldots$$

which can be expressed as:

$$z_{jt} = \sum_{r=0}^{\infty}\sum_{s=0}^{\infty} {}_tA_{rs}\, x_j^r\, y_j^s + \tilde{u}_t$$

where ${}_tA_{rs}$ is the coefficient of the term containing $x^r y^s$ at time t and u_t is a stochastic cumulative error term incorporating the short-term fluctuation.

The longitudinal model utilized a linear function to predict the sensitivity z_{jt} at the general stimulus location (x_{jt}, y_{jt}) from a knowledge of the sensitivity at that location determined at one or more previous examinations $z_{j(t-1)}$, $z_{j(t-2)}$, $z_{j(t-3)}$:

$$z_{jt} = B_1 z_{j(t-1)} + B_2 z_{j(e-2)} + B_3 z_{j(t-3)} + \ldots\ldots\ldots$$

which can be expressed as

$$z_{jt} = \sum_{\tau=1}^{k} B_\tau\, z_{j(t-\tau)} + \tilde{v}_t$$

where K is the number of previous examinations included in the model, B is the parameter associated with the value of sensitivity at $(t-\tau)$ and v_t is a stochastic cumulative error term incorporating the short- and long-term fluctuations

Both components of the model can be combined to form a mixed model:

$$z_{jt} = \sum_{r=0}^{\infty}\sum_{s=0}^{\infty} {}_tM_{rs}\, x_j^r\, y_j^s + \sum_{\tau=1}^{k} N_\tau\, z_{j(t-\tau)} + \tilde{u}_t + \tilde{v}_t$$

The polynomial and regression parameters were left unrestricted in the analysis of any given expected sensitivity z_{jt}.

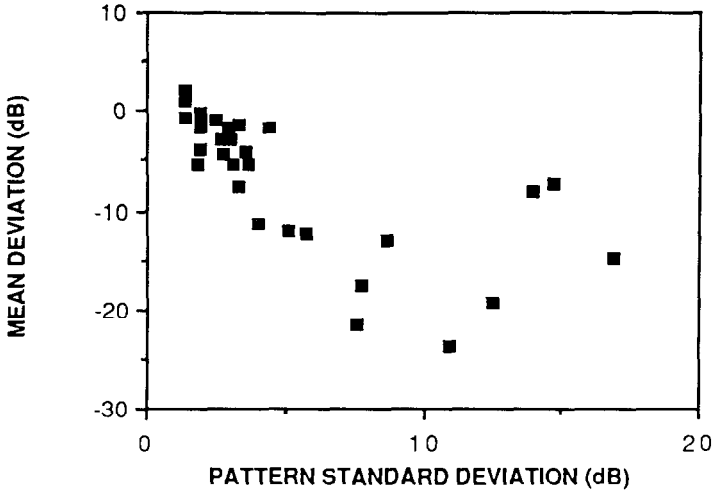

Fig 1 Mean defect against pattern standard deviation illustrating the types of field loss for the 31 patients in the sample

Results

Results were calculated for the fields of the left eye of each patient The mean number of fields examined per patient was 7.4 (SD 1.95) and the mean follow-up period per patient 37.6 months (SD 8.4). The sample comprised 24 primary open angle glaucomas, one chronic open angle glaucoma, one pseudoexfoliation glaucoma and two cases where the diagnosis was unspecified. The depth of field loss within the sample is shown in Fig. 1.

A typical example of the results for one of the 31 patients is illustrated in Fig. 2 The sensitivity at any given test location of the fifth field, z_5, can be predicted by the equation:

$$z_5 = 18.319 + 0.001x - 0.021y - 0.004x^2 - 0.00y^2 + 0\ 457z_4 - 0\ 055z_3 + 0.296z_2 - 0\ 264z_1$$

where x and y are the coordinates of the given stimulus location and z_4, z_3, z_2, z_1 are the values of sensitivity at the given stimulus location recorded at the fourth, third, second and

MODEL FITTING RESULTS

VARIABLE	COEFFICIENT	PROB (>ITI)
CONSTANT	18.319154	.0000
x	0.001033	.9620
x TIMES x	-0.003959	.0058
y TIMES y	-0.002321	.1726
y	-0.020998	.2886
$Z_{j(t-1)}$	0.456828	.0054
$Z_{j(t-2)}$	-0.05467	.7060
$Z_{j(t-3)}$	0.296271	.0591
$Z_{j(t-4)}$	-0.263615	.0689

Fig 2 Example of part of a typical printout illustrating the model fitting results for the estimated pointwise distribution of sensitivity for the fifth field of a given patient derived from a knowledge of the stimulus coordinates (x and y) and of the previous four fields [$z_{j(t-1)}$, $z_{j(t-2)}$, $z_{j(t-3)}$ and $z_{j(t-4)}$]

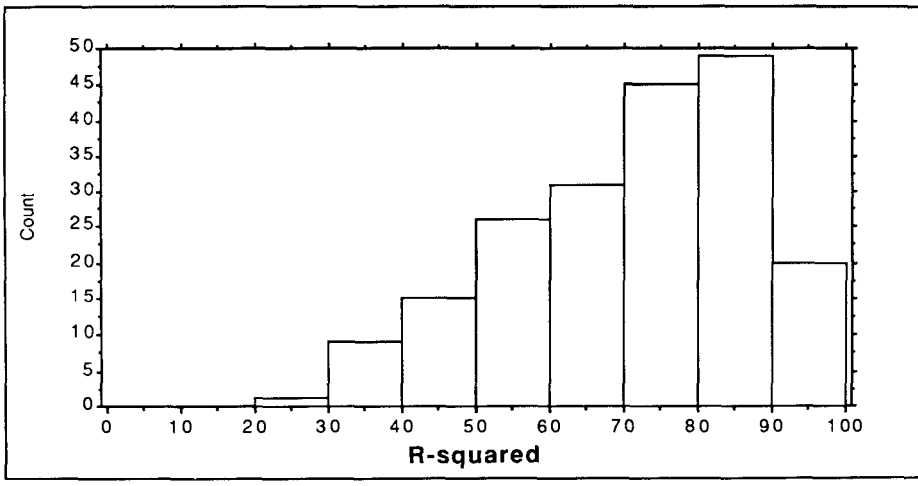

Fig 3 Histogram showing the distribution of the 195 possible R-squared values (%) between the predicted and the measured pointwise distribution of sensitivity for the 31 patients in the sample

first field examinations respectively The results also show that, in this case, only the constant, x^2 and z_4 terms contributed statistically significantly towards the prediction of the sensitivity for the fifth field.

For the sample as a whole, the constant term of the polynomial correlated highly with the mean deviation (r=0.93) and moderately with the pattern standard deviation (r=0.60) and confirmed previous findings[7].

The serial fields for each subject were evaluated in terms of the coefficient of determination R^2 which expressed the goodness of fit relationship between the nth measured field and the nth expected field calculated by the joint topographical and longitudinal model and based upon the t-1, t-2, t-3, etc. previous fields. The distribution of the 195 possible R^2 values for the 31 left eyes in the sample is illustrated in Fig. 3 and shows that approximately 60% of the coefficient of determinations exhibited a value of 70% or more. The magnitude of the largest coefficient of determination for each patient as a function of the depth of field loss is shown in Fig. 4 and would appear to be largely independent of MD, PSD and SF.

Discussion

The topography of the visual field was modelled in terms of a second order polynomial equation since the pointwise age matched normal values for the Humphrey Field Analyzer have been developed using such an approach[3]. The cross-terms were omitted from the model since previous findings[7] suggest that these did not contribute substantially to the overall fit.

The use of multivariate regression assumes that the independent variables are not correlated. The study utilized the classical least squares procedure to fit a multivariate model of the pointwise distribution of sensitivity z_{jt} in terms of the spatial coordinates x and y and in terms of the previous value of sensitivity $z_{j(t-1)}$, $z_{j(t-2)}$, $z_{j(t-3)}$, etc. As such this procedure violates the principle of independence. Nevertheless, the use of such an approach can, however, be justified since the index of determination R^2 was used merely as an overall measure of the goodness of fit of the data. No attempt was made to quantify significant differences in fit between successive fields due to the obvious violations in the classical regression assumption. In addition, both components of the model incorporate an implicit variation due to time. Furthermore, linear regression has been used previously to study visual field decay in glaucomata[8-10].

The interval between examinations was considered as ordinal only since the pointwise structure of the data made consideration of the magnitude of the between examination intervals feasible. Furthermore, the use of the polynomial model restricted the number of available degrees of freedom.

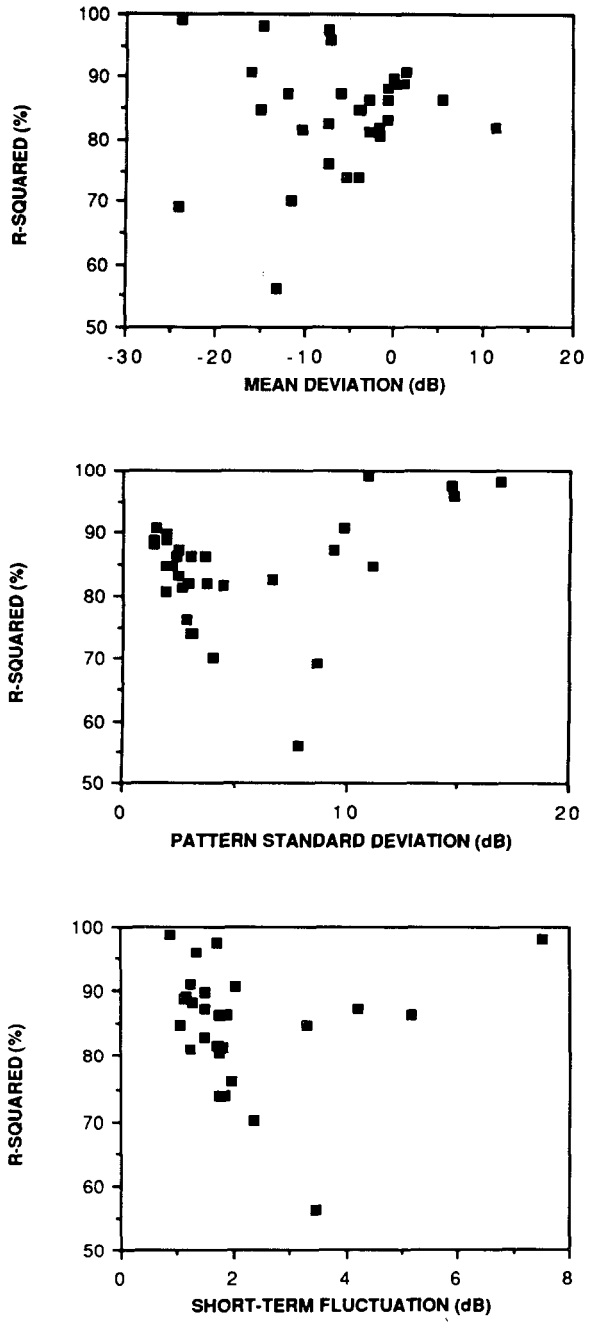

Fig 4 The maximum coefficient of determination, R^2 (%), for each of the 31 patients between the predicted and the measured pointwise distribution of sensitivity for a given field as a function of mean deviation (top), pattern standard deviation (middle) and short-term fluctuation (bottom).

The distribution of the coefficients of determination, R^2, (Fig. 3) suggests that using a criterium for R^2 of ≥70%, the pointwise distribution of sensitivity can be predicted from a knowledge of the previous fields in over half (57%) of the cases in this study. This figure is relatively conservative since, as the number of previous examinations increases, a purely time based model would be expected to produce increasing values of R^2, *i.e* , an increasingly better fit, due to the increased amount of available information. Nevertheless, there would appear to be considerable within and between subject differences in the precision of the model for the pointwise distribution of sensitivity (Fig. 4) Preliminary attempts at developing empirical criteria for the derivation of change for a given patient in terms of the difference between pairs of successive coefficients of determination R^2 have, as perhaps might be expected, correlated poorly with the current indices and with the clinical impression of change.

Conclusions

The results suggest that the pointwise distribution of sensitivity for a given field can in a majority of cases be predicted with a high degree of accuracy from a knowledge of the previously determined pointwise values of sensitivity. The goodness of fit between the measured field and the expected field would seem to be independent of MD, PSD and SF. Apparent change in sensitivity between two successive visual fields as designated by the polynomial and multiple regression technique correlates moderately with the clinical impression of change derived by inspection of the indices and poorly with any clinical intervention. A knowledge of the R^2 value supplements the information derived from the indices and probability plots.

Table 1 Three examples illustrating serial fields with (top) high R^2 values and constant (? minor deterioration in MD) indices, (middle) low R^2 values and changing indices and (bottom) mixed R^2 values and stable indices

Example 1							
	Z1	*Z2*	*Z3*	*Z4*	*Z5*	*Z6*	*Z7*
MD	− 6 08	− 6 20	− 7 19	− 8 84	− 8.03	− 8 14	−
PSD	14 84	14 97	14 75	14.41	13.62	14 01 −	
R^2	−	93.6	95 0	87 7	89 3	94.1	−
Example 2							
	Z1	*Z2*	*Z3*	*Z4*	*Z5*	*Z6*	*Z7*
MD	−12 02	−12 97	− 7 66	− 7 52	− 8 75	− 8 45	−10 98
PSD	8 27	9 06	8 51	7 04	6 96	6 02	7 43
R^2	−	70 1	56 0	45 9	68 3	45 0	69 8
Example 3							
	Z5	*Z6*	*Z7*	*Z8*	*Z9*	*Z10*	*Z11*
MD	−12 02	−12 91	−11 90	−11 36	−11 58	−11.07	−11.30
PSD	13 42	13 65	14 09	13 10	13 77	13 24	13 30
R^2	81 1	85 1	92 1	80 4	92 2	79 6	85 3

References

1 Flammer J, Drance SM, Augustiny L, Funkhauser AT: Quantification of glaucomatous visual field defects with automated perimetry Invest Ophthalmol Vis Sci 26:176-181, 1985
2. Flammer J: The concept of visual field indices Graefe's Arch Clin Exp Ophthalmol 224:389-392, 1986
3 Heijl A, Lindgren G, Olsson J: A package for the statistical analysis of computerized visual fields. Doc Ophthalmol Proc Ser 49:153-168, 1987
4 Bebie H, Fankhauser F, Spahr J: Static perimetry: accuracy and fluctuations Acta Ophthalmol 54:229-348, 1976
5. Chauhan BC, Drance SM, Douglas GR: The use of visual field indices in detecting change in the visual field in glaucoma Invest Ophthalmol Vis Sci 31:512-520, 1990
6 Chauhan BC, Drance SM, Lai C: A cluster analysis for threshold perimetry. Graefe's Arch Clin Exp Ophthalmol 227:216-221, 1989

7. Wild JM, Dengler-Harles M, Hussey MK, Crews SJ, Cole MD, Searle AET, O'Neill EC: Regression techniques in the analysis of visual field loss In: Heijl A (ed) Perimetry Update 1988/89 Amsterdam/Berkeley/Milano: Kugler & Ghedini Publications 1989
8. Holmin C, Krakau CET: Visual field decay in normal subjects and in cases of chronic glaucoma Graefe's Arch Clin Exp Ophthalmol 213:291-298, 1980
9 Holmin C, Krakau CET: Regression analysis of the central visual field in chronic glaucoma cases Acta Ophthalmol 60:267-274, 1982
10 Wu DC, Schwaftt B, Nagin P: Trend analysis of automated visual fields Doc Ophthalmol Proc Ser 49:175-189, 1987

Clinical comparisons of two estimates of short-term fluctuation

Richard P. Mills[1], Wing Lau[2] and Michael Schulzer[2]

[1]*Department of Ophthalmology, University of Washington RJ-10, Seattle, WA 98195, USA,*
[2]*Department of Ophthalmology, University of British Columbia, Vancouver, Canada*

The short-term fluctuation (SF) in threshold static fields can be estimated using a root mean square (RMS) calculation on double threshold determinations at multiple test locations, or using the residuals from a polynomial trend surface based on single determinations of threshold at each point.

It is well known that SF increases as patient unreliability increases, and that SF increases in abnormal areas of the visual field. In a sense, SF can be considered to have two components: that due to patient unreliability and that due to visual field abnormality. This study was carried out to discover if the two components of SF could be separated in clinical testing.

We calculated SF using both methods on Humphrey 24-2 test data from one eye of 173 patients, each of whom performed three replications of the test in one session. Multiple regression and covariance analyses were performed, relating the two estimates of SF to a number of explanatory variables including the mean deviation, reliability indices, and eye examination results.

The trend surface SF correlated best ($p<0.0001$) with the SF estimated by RMS and the mean defect (MD), less strongly ($p<0\ 005$) with normality or abnormality, and less strongly still ($p<0.03$) with age. No correlation was found with unreliability, pattern standard deviation (PSD), corrected pattern standard deviation (CPSD), visual acuity, cataract score, or intraocular pressure (IOP). When the trend surface SF was adjusted for RMS SF and further regressed on unreliability and mean defect, it was not correlated with unreliability but was strongly correlated with MD.

The conventional SF correlated best ($p<0\ 0001$) with the trend surface SF and with the unreliability and less strongly ($p<0.01$) with normality or abnormality No significant correlation was found with age, PSD, CPSD, visual acuity, cataract score, or IOP. When RMS SF was adjusted for trend surface SF and was further regressed on unreliability and MD, it was strongly correlated with unreliability but was not correlated with MD

The finding that trend surface SF correlates better with MD and conventional SF correlates better with unreliability indicates that comparison of the two SF estimates may be helpful in separating the two components of SF – that due to patient unreliability and that related to visual field abnormality. The full article will be published elsewhere.

Supported in part by an award from Research to Prevent Blindness, Inc

Perimetry Update 1990/91, p. 201
Proceedings of the IXth International Perimetric Society Meeting,
Malmö, Sweden, June 17-20, 1990
edited by Richard P. Mills and Anders Heijl

Estimating short-term fluctuation without double threshold determinations Validation of a method

Richard P. Mills[1], Wing Lau[2] and Michael Schulzer[2]

[1]*Department of Ophthalmology, University of Washington RJ-10, Seattle, WA 98195, USA,*
[2]*Department of Ophthalmology, University of British Columbia, Vancouver, Canada*

Abstract

The authors have previously reported a method for estimating short-term fluctuation (SF) from a single determination of threshold at each test location in regular grid visual field examinations Using a technique of trend-surface analysis, the residual variances after detrending the surface correlated very well with the conventional estimates of SF made according to root mean square (RMS) calculations However, since they developed their modification of the trend-surface analysis on an original sample of 65 eyes, they wished to validate the method on a larger independent sample In 113 eyes of 113 patients, excellent correlation (coefficients of log-transforms of 0 8 and better) of the trend surface method with the conventional RMS method was found Since good estimates of SF can be obtained from visual field data using only single threshold determinations, the time-efficiency of double determinations should be reconsidered

Introduction

The short-term fluctuation (SF) defines the "noise" level inherent in visual field data at a given time. In this work, we employed two methods of estimating SF.

Conventional RMS estimate

Threshold determinations are repeated at a number of points in the visual field (*e g* , ten points in the Humphrey 24-2 and 30-2 or all points in the Octopus G1). The variances are calculated at each of these points, then averaged to obtain an estimate of the global variance. The square root of this estimate (root mean square or RMS) is used as a measure of SF. The precision of the RMS estimate of SF improves as the number of replicated points increases, at the cost of increased test time

Trend surface estimate

A polynomial surface is fitted to the grid of single threshold determinations using standard regression techniques (Fig. 1) This fitted surface can be imagined as representing a grid of second determinations of threshold at each point The residual deviations of the measured thresholds from the fitted surface values at the same points are used to calculate the variance of the process, and hence to provide an estimate of SF[1]

Material and methods

One hundred and thirteen unselected patients with a typical mix of diagnoses referred to our visual field service comprised our study group (Fig. 2). None of these patients had been part of our original sample of 65 on whom the trend surface method had been previously tested. On even dates, right eyes were tested with three consecutive repetitions of the 24-2 full threshold program of the Humphrey Field Analyzer; on odd dates, left eyes were tested with the same protocol. All subjects had at least one prior experience with automated perimetry.

Perimetry Update 1990/91, pp. 203-208
Proceedings of the IXth International Perimetric Society Meeting,
Malmö, Sweden, June 17-20, 1990
edited by Richard P Mills and Anders Heijl

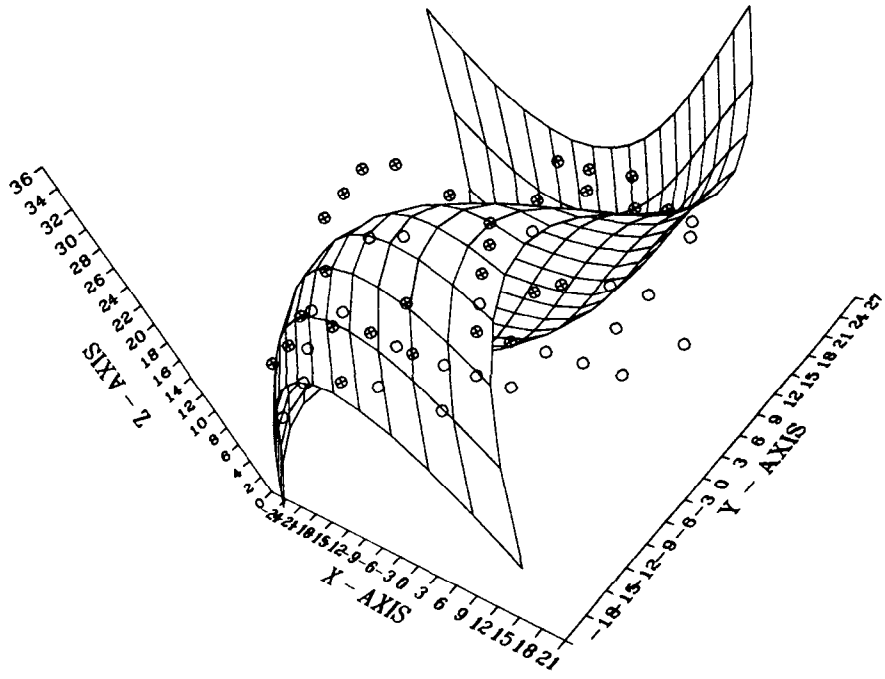

Fig 1 Bicubic trend-surface fitted to 24-2 threshold data from a glaucomatous eye. Open circles: below surface; filled circles: above surface

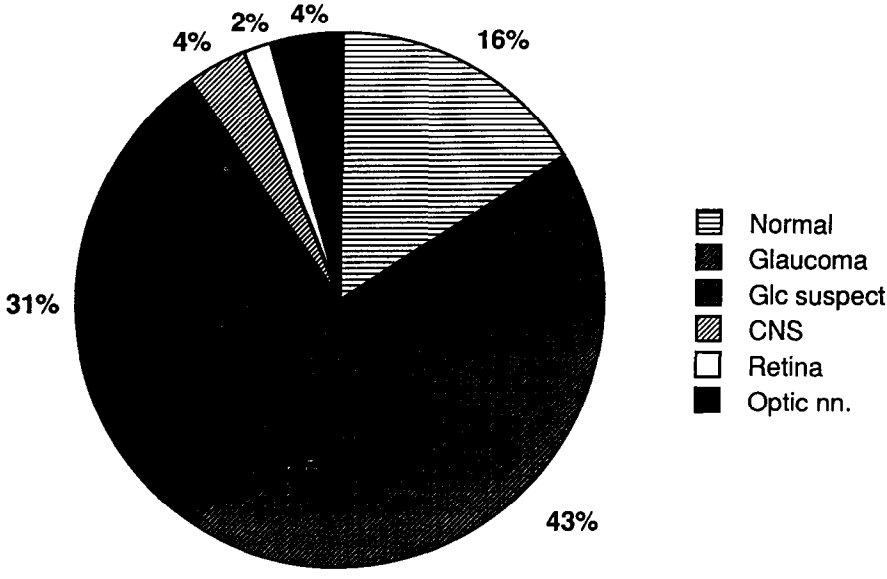

Fig 2 Distribution of patient diagnoses in the study population of 113 patients

Mirror-image reversals of left eye data across the vertical axis were applied to convert all data into right eye format. The two points overlapping the physiologic blind spot were deleted from analysis.

Four SF estimates using the RMS method were calculated:
- S1-2: double determinations using 24-2 repetitions 1 and 2
- S2-3: double determinations using 24-2 repetitions 2 and 3
- S1-3: double determinations using 24-2 repetitions 1 and 3
- S123: triple determinations using 24-2 repetitions 1, 2, and 3

Three SF estimates using the trend surface method (biquartic polynomial) were calculated:
- Q4-1: single determination of threshold, 24-2 repetition 1
- Q4-2: single determination of threshold, 24-2 repetition 2
- Q4-3: single determination of threshold, 24-2 repetition 3

The SF estimates from the RMS method ("S" values) were correlated with those from the corresponding trend surface method ("Q" values) after applying a log transform which brings variance stability and normality to the data.

Results

Representative scatterplots of the log SF estimates in the study eyes (n=113) from the RMS method on the X-axis and trend surface method on the Y-axis are shown in Figs. 3, 4 and 5.

Correlation coefficients between the paired SF estimates from the RMS method and the corresponding trend surface method are shown in Table 1. They show excellent agreement with r values ranging from 0.6677-0.8312.

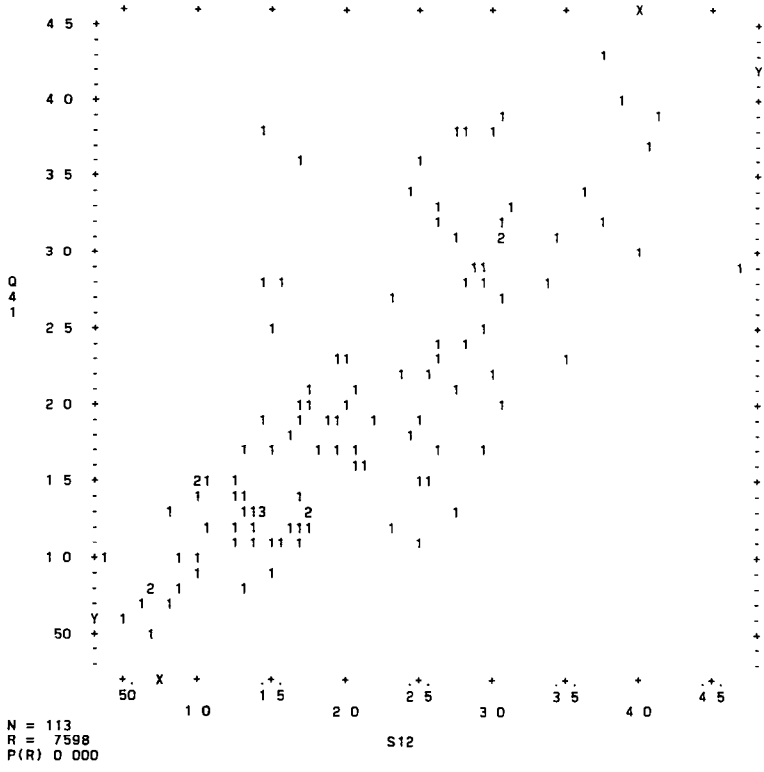

Fig 3 Log SF from RMS method (S12) on abscissa versus log SF from trend surface method (Q41) on ordinate. Correlation coefficient r = 0 7598, p<<0.001

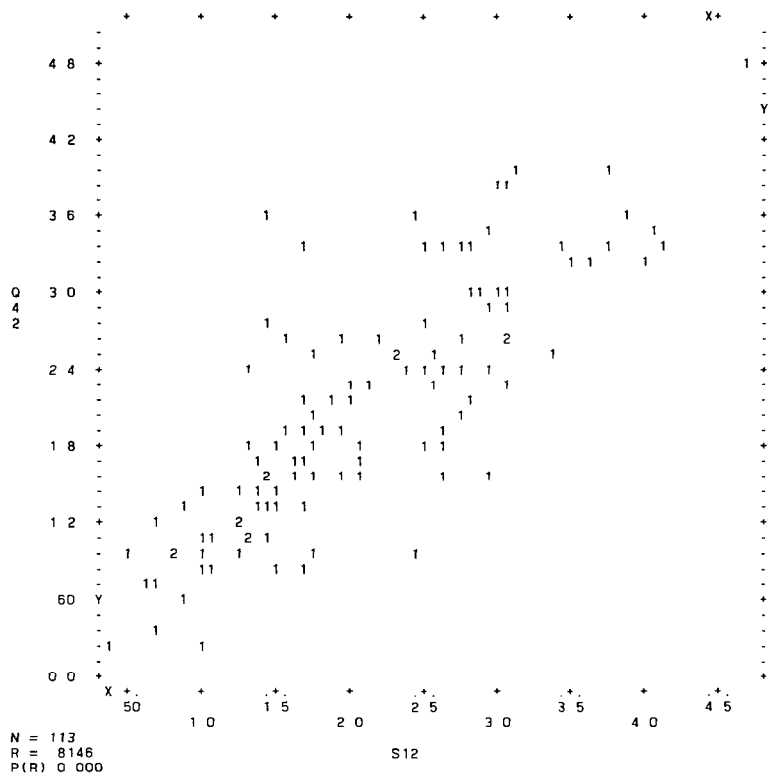

Fig 4 Log SF from RMS method (S12) on abscissa versus log SF from trend surface method (Q42) on ordinate. Correlation coefficient $r = 0\ 8146$, $p<<0\ 001$

Table 1 Correlation coefficients Log SF RMS method versus log SF quartic trend surface method from corresponding pairs and triplets of repeat determinations

SF estimates (see Methods)	*Previous series n=65*	*This series n=113*
Q4-1/S1-2	0 7642	0 7598
Q4-2/S1-2	0 7907	0 8146
Q4-2/S2-3	0 8312	0 6706
Q4-3/S2-3	0 8026	0 7827
Q4-1/S1-3	0 8307	0 6677
Q4-3/S1-3	0 7736	0 7974
Q4-1/S123	0 8060	0.6825
Q4-2/S123	0 8279	0 7260
Q4-3/S123	0 7971	0 7995
Median	0 8026	0 7598
	$P<<0\ 001$	$P<<0\ 001$

Discussion

The problem of estimation of SF from a single determination of the visual field is complicated by the presence of the underlying "hill of vision" which implies correlation between values at neighboring points[2]. By fitting a polynomial regression surface of biquartic degree and subtracting it from the observed data, the field data is reduced to a roughly stationary process, with negligible correlation between adjacent data points[1]. The square root of the residual mean square error provides a very good estimate of the SF.

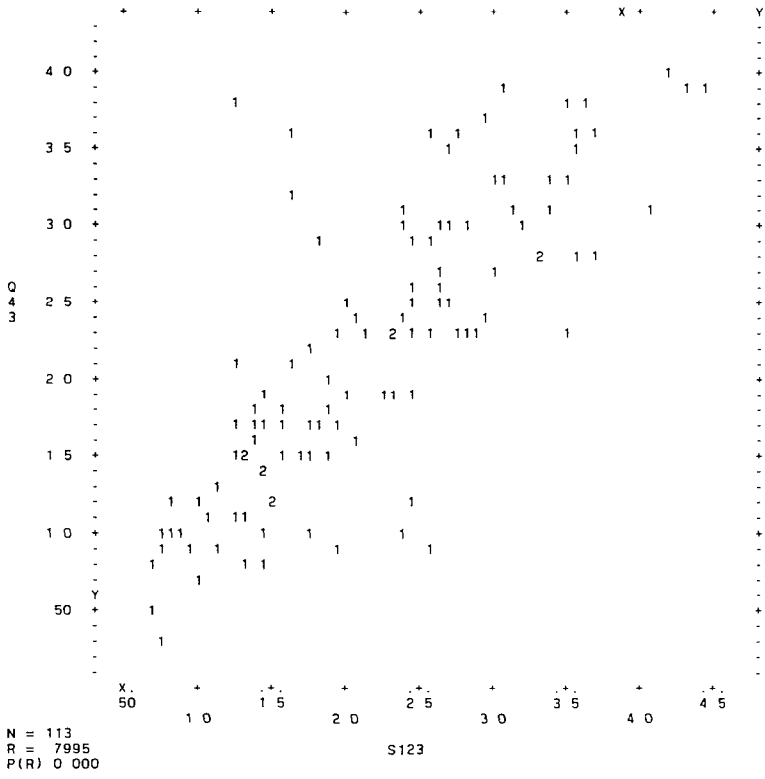

Fig 5 Log SF from RMS method (S123) on abscissa versus log SF from trend surface method (Q43) on ordinate Correlation coefficient $r = 0\ 7995$, $p<<0\ 001$

Using the calculations of Bebie *et al* [3], the SF estimate using the trend surface method is likely to be within 25% of the true SF of the visual field at the 95% confidence level. This may be compared with the SF estimate based on double determinations at all 52 points in the 24-2 pattern which is likely to be within 19% of the true SF (0.95 level), and with the SF estimate based on double determinations at only 10 points, which is likely to be within 44% of the true SF (0.95 level)

Thus, the SF estimate from trend surface analysis is likely to be more precise than the standard SF determination based on 10 preselected points It is also more robust, since aberrant findings at one or two points will not unduly affect the SF estimate

We used the 24-2 program for this study to avoid undue fatigue after three repetitions The trend surface method is theoretically applicable to any regular grid of visual field data (*e g* , programs 30-1, 30-2, or 10-2) If more peripheral points are included, SF estimates would be expected to increase regardless of the method employed[4]

We conclude that SF may be estimated using visual field data from a single threshold determination at each point, using a trend surface method of analysis In this study,we were able to validate the trend surface method of SF estimation on an independent series of patients. Since the method is simple to program and is not proprietary, it may be considered for inclusion in resident software of automated perimeters

The effect of the number of threshold determinations on short-term fluctuation

Balwantray C. Chauhan[1], Raymond P. LeBlanc[1], Stephen M. Drance[2], Kees Wijsman[2] and Arturo M. Cruz[1]

[1]*Department of Ophthalmology, Dalhousie University, Halifax, Nova Scotia;* [2]*University of British Columbia, Vancouver, British Columbia, Canada*

Abstract

The authors wanted to assess whether the number of multiple threshold determinations in automated perimetry had a significant effect on the local and global (RMS) short-term fluctuation Their sample contained 30 subjects (ten normals, ten glaucoma suspects and ten glaucoma patients) whose mean age was 56 70 years. One eye of each subject was first tested with both the standard Octopus programs G1 and 31, followed by five custom (Sargon) programs The latter were designed to test all locations twice, ten locations thrice, six locations five times, three locations ten times and two locations 15 times, respectively. There were two principal locations [(0,12 and (0,-12)] where all five sets of replications were carried out. The total number of threshold determinations in the five custom programs were equal The order of the standard and custom programs was randomized The authors' results show that local fluctuation increased sharply when calculated from two to five determinations after which it remained virtually constant. On the other hand, the number of determinations did not have a significant effect on RMS fluctuation. A comparison of the RMS obtained from the standard and custom programs indicate no significant differences ($p>0$ 05). Their results suggest that the current standard programs which do only double determinations may be underestimating local fluctuation Furthermore, local fluctuation is deemphasized by a "watering-down" effect of calculating RMS fluctuation.

Address for correspondence Dr B.C Chauhan, Nova Scotia Eye Centre, Halifax Infirmary, 1335 Queen Street, Halifax, Nova Scotia, Canada B3J 2H6

Perimetry Update 1990/91, p 209
Proceedings of the IXth International Perimetric Society Meeting,
Malmö, Sweden, June 17-20, 1990
edited by Richard P Mills and Anders Heijl

Correlation of reliability indices and test-retest reproducibility in normal subjects undergoing automated perimetry on the Humphrey Visual Field Analyzer

G. Richard Bennett[1], Elliot B. Werner[2] and Louisa Seraydarian[3]

[1]*The Eye Institute of the Pennsylvania College of Optometry, Departments of* [2]*Ophthalmology and* [3]*Mental Health Sciences, Hahnemann University, Philadelphia, PA, USA*

Abstract

Thirty ocularly normal subjects ranging in age from 24 to 60 were tested using program 24-2 on the Humphrey Visual Field Analyzer. Each subject underwent three examinations within six weeks The number of fixation losses, false positive responses, and false negative responses were each correlated with the difference of the mean defect between the second and third visual fields The first visual field was used as a training field on naive subjects The large majority of subjects had very good reliability indices There was no correlation demonstrated in this sample between any of the reliability indices on the second examination and the test-retest reproducibility.

Introduction

The reliability of a patient's visual field test is critical when attempting to use that information for accurate diagnosis and management. The perimetrist traditionally has made a subjective assessment of the reliability of an individual visual field test by monitoring the patient's responses, attention, and fixation during manual visual field testing. The visual field chart must be labeled with the perimetrist's evaluation of steadiness of fixation, consistency of responses, speed of responses, and overall reliability of the visual field[1]. Of course, this assessment is quite subjective and variable with the individual perimetrist.

Automated perimeters have greatly reduced the perimetrist's role in evaluating the reliability of an individual perimetric test result by using standardized algorithms to assess several indices of reliability. The Humphrey Visual Field Analyzer (Allergan Humphrey, San Leandro, CA) uses three quantitative measures of reliability: number of fixation losses, number of false negative errors, and number of false positive errors. Fixation losses are evaluated by the Heijl-Krakau blind spot monitoring technique which assesses fixation by periodically exposing stimuli in the blind spot during the field test[2]. A positive response indicates a fixation loss A false positive error is recorded when the patient responds to the movement of the projector when no stimulus actually has been presented to the patient. Excessive false positive responses may indicate a "trigger happy" patient or a patient responding to the rhythm of the testing procedure. A false negative is recorded when a suprathreshold stimulus is presented to an area where a sensitivity has already been measured and the patient does not respond. A high false negative score may indicate that the patient is fatigued or not attending to the task The manufacturer generally advises the perimetrist that if the reliability indices suggest that the data are "unreliable" then the test results must be interpreted with caution. Retesting is advised[2].

Reliability as measured by the manufacturer's criteria has been investigated by several authors[3-6]. Enger and Sommer have reported that 40% of glaucomatous eyes and 23% of normal eyes were considered unreliable based upon exceeding the manufacturers' allowed fixation losses, false positives, or false negatives[3]. In a study by Katz and Sommer, 30% of normals and 45% of glaucomatous subjects were considered unreliable by the manufacturers' reliability criteria[4]. These high percentages of "unreliable" results cause one to question the usefulness of the reliability indices and their relationship to the data.

The purpose of this study is to investigate the relationship between subject performance on the Humphrey Visual Field Analyzer using the C-24-2 program and the reproducibility of the visual threshold measurements on repeat testing as measured by the difference in mean devia-

Perimetry Update 1990/91, pp. 211-215
Proceedings of the IXth International Perimetric Society Meeting,
Malmö, Sweden, June 17-20, 1990
edited by Richard P. Mills and Anders Heijl

TABLE 1

RELIABILITY NORMALS

RELIABILITY/REPRODUCIBILITY STUDY NORMALS PROSPECTIVE

CASE		FIRST									DELTA
NUMBER	AGE	EYE	FLOSS N	FLOSS D	FPOS N	FPOS D	FENG N	RNEG D	MD1	MD2	MD
1	24	OD	1	21	0	13	0	10	0.32	0.42	0.10
2	25	OD	0	19	0	10	0	9	-0.52	-0.47	0 05
3	27	OD	0	21	0	15	0	9	0.92	0.79	0.13
4	24	OD	0	19	0	4	0	9	0 33	0.44	0.11
5	24	OS	0	19	0	10	1	9	-0.77	-1.04	0.27
6	24	OD	2	18	0	7	0	9	0.23	0.27	0.04
7	32	OS	1	18	0	14	0	8	1 19	0.35	0.84
8	25	OS	0	19	0	7	1	15	-1.84	-1 64	0.20
9	26	OD	1	20	0	12	1	10	-2.70	-3.01	0.31
10	26	OS	0	19	0	7	0	12	-0.17	-0.63	0.46
11	47	OD	2	23	1	16	0	13	-1.97	0.35	2.32
12	60	OS	2	19	1	11	0	9	1.61	1.65	0 04
13	24	OD	0	18	0	14	0	10	-0.57	-0.19	0.38
14	25	OD	1	20	0	10	0	11	-0.27	0.17	0.44
15	25	OD	1	19	2	7	0	10	-0 55	-0.87	0.32
16	26	OS	0	18	0	8	0	8	1.18	-0 64	1.82
17	27	OD	2	20	0	13	0	11	-0.69	-0.49	0.20
18	26	OD	1	18	0	8	0	9	0.80	0.95	0.15
19	28	OD	3	19	0	7	0	10	1.83	-1.24	3.07
20	25	OD	1	19	0	6	0	7	0 23	-0.93	1.16
21	60	OS	3	21	2	13	2	16	-2 09	0.96	3 05
22	25	OS	1	19	0	19	1	10	-0 39	0 22	0.61
23	25	OD	0	18	0	6	0	8	-0 61	-0.55	0 06
24	24	OD	1	19	0	13	0	7	0 98	0 54	0.44
25	25	OS	0	18	0	14	0	7	-0.36	-0 28	0.08
26	25	OD	0	20	0	13	0	10	-1.59	-0.92	0 67
27	25	OD	0	20	0	8	0	9	-0 36	-0.15	0 21
28	25	OD	1	18	0	9	0	8	1 24	0.86	0.38
29	27	OD	1	20	0	13	1	12	-1.91	-1.39	0.52
30	29	OD	0	19	0	9	0	5	0.01	0.12	0.11

TABLE 2

RELIABILITY NORMALS

M	N	O	P	Q	R	S	T	U	V	W
SECOND									DELTA	CASE
EYE	FLOSS N	FLOSS D	FPOS N	FPOS D	FNEG N	FNEG D	MD1	MD2	MD	NUMBER
OS	1	19	0	4	1	7	-0.05	-0 71	0 66	1
OS	4	19	0	7	0	9	-1 23	-1 50	0.27	2
OS	1	18	0	9	0	9	0 44	0 20	0 24	3
OS	1	20	2	16	0	11	0.93	-0.43	1 36	4
OD	0	18	0	6	0	8	-0.69	-0.50	0 19	5
OS	2	19	0	12	0	9	-0 16	0.39	0 55	6
OD	0	20	0	9	0	8	0 36	0 14	0 22	7
OD	0	18	0	7	0	4	-2 43	-2.14	0.29	8
OS	0	19	0	8	0	10	-2 10	-1 96	0.14	9
OD	0	18	0	8	0	12	-0 20	-0 34	0 14	10
OS	0	19	0	18	0	9	0 59	0.53	0 06	11
OD	2	19	0	9	0	10	1.42	1 30	0.12	12
OS	0	18	0	14	0	4	-0.29	0 23	0.52	13
OS	0	18	0	13	1	4	-0 33	0 47	0 80	14
OS	0	18	0	10	0	9	-1.34	-2 06	0.72	15
OD	0	20	1	17	0	10	-0 48	0 98	1 46	16
OS	5	20	1	15	0	8	-0 20	0.83	1 03	17
OS	1	19	0	11	0	9	0.69	0.14	0.55	18
OS	1	18	0	7	0	8	-0.85	-1 33	0 48	19
OS	0	19	0	10	0	9	-0 24	-1.97	1.73	20
OD	0	20	0	10	1	13	0 34	-0.12	0.46	21
OD	0	16	0	5	0	3	-0 80	0 00	0.80	22
OS	1	18	0	10	0	9	-0 41	-1.48	1.07	23
OS	0	19	1	13	0	9	-0.12	0 24	0.36	24
OD	1	19	0	8	0	10	-0.17	0 37	0 54	25
OS	0	21	0	14	1	11	-1.92	-1 17	0.75	26
OS	0	19	0	12	0	10	-0 65	-1.67	1.02	27
OS	1	20	0	12	0	9	0 08	0 98	0 90	28
OS	0	20	0	14	1	13	-1 90	-1 23	0.67	29
OS	0	18	0	7	0	11	-0 45	-0.78	0 33	30

tion (MD). Patient performance was measured by the Humphrey reliability indices of fixation losses, false positives, and false negatives.

Subjects and methods

Thirty normal volunteers ranging in age from 24 to 60 years old were tested using the C-24-2 program on the Humphrey Visual Field Analyzer. The first eye tested (right or left) was chosen randomly and then consistently tested first on each of three subsequent automated visual fields. Visual field testing was performed on both eyes on three separate days. The interval between tests was one to two weeks. All subjects were considered to be healthy normals, having visual acuities of 20/25 in each eye and no evidence of ocular disease. In addition subjects were excluded who exhibited any significant field defects as defined by a total deviation or pattern deviation equal to or less than the 5% level of significance using the Humphrey Statpac Analysis. All subjects had a subjective refractive error of not more than -5.00 diopters or +5.00 diopters, intraocular pressures of 20 mm Hg or lower as measured by Goldmann applanation tonometry, and no previous experience with automated perimetry.

Prior to threshold automated visual field testing the patient was instructed and the training program was used to familiarize the patient with the operations of the perimeter. The training sequence and instructions were repeated as necessary. One perimetrist was present during the entire visual field to encourage the subject to maintain position and fixation and to monitor eye position through the telescope during the testing procedure. Although three separate visual fields were performed, only the last two fields were used for analysis in order to eliminate any learning effects.

Three different reliability measurements were collected for the first and second eyes of each of the 30 subjects: fixation losses, false positives and false negatives. In addition to reliability measurements, the mean deviation for the second and third visual field was recorded and the absolute difference between values for each eye was calculated (delta MD). The delta MD was used as an index of the reproducibility of the visual field measurements. The patient performance indicators of fixation losses, false positives, and false negatives were tabulated for each eye The first eye tested and second eye tested were analyzed separately. Each group of eyes was further divided into two response groups for analysis; eyes having zero errors and eyes having one or more errors.

Results

Tables 1 and 2 show the raw data for each eye of the thirty subjects FLOSS N refers to the number of fixation losses and FLOSS D refers to the number of catch trials, FPOS N refers to the number of false positives and FPOS D refers to the number of catch trials for false positives, and FNEG N refers to the number of false negatives and FNEG D refers to the number of catch trials for false negatives. MD1 is the mean deviation for the second visual field and MD2 is the mean deviation for the third visual field. Delta MD is the absolute difference between MD1 and MD2. Each subject is referenced by case number. Table 3 shows the mean delta MD for the first and second eye tested for the zero error group and the one or more error group.

The two tailed unpaired t value was t=-1.57, p=0.129 for the first eye tested and t=-0.346, p=0.732 for the second eye tested. Based on this analysis, no significant difference in mean delta MD was found between groups for either first eye tested or second eye tested. Because there were so few false positives and false negatives for each patient tested, the t-test could not be used to evaluate difference between groups

Table 3

	Zero fixation losses	*One or more fixation loss*	*p**
First eye tested	Number = 13 Mean delta MD = 0 35±0 48 dB	Number = 17 Mean delta MD = 0 82±1 00 dB	0 129
Second eye tested	Number = 18 Mean delta MD = 0 59±0.46 dB	Number = 12 Mean delta MD = 0 65±0 37 dB	0.732

*two tailed unpaired "t" test

Table 4

	Zero false positives	*One or more false positives*	*p**
First eye tested	Number = 26 Mean rank = 15.02	Number = 4 Mean rank = 18.63	0.46
Second eye tested	Number = 26 Mean rank = 14 27	Number = 4 Mean rank = 23.50	0.52

*Mean-Whitney U-Wilcoxon Rank Sum W test

Table 5

	Zero false negatives	*One or more false negatives*	*p**
First eye tested	Number = 24 Mean rank = 14 60	Number = 6 Mean rank = 19.08	0 27
Second eye tested	Number = 25 Mean rank = 14.90	Number = 5 Mean rank = 18 50	0 42

*Mann-Whitney U-Wilcoxon Rank Sum W test

The Mann-Whitney U-Wilcoxon Rank Sum W test was used to analyze data for false negative and false positive responses. Table 4 shows these results for first and second eye tested with respect to false positives and Table 5 shows these results with respect to false negatives.

For false positives, the exact two-tailed p value for the first eye tested was found to be 0.4607 (not significant) and 0.0523 for the second eye tested (not significant). For false negatives, the exact two-tailed p value for the first eye tested was found to be 0.2728 (not significant) and 0.4156 for the second eye tested (not significant).

Comment

Within the sample of healthy normal subjects we found no significant relationship between test-retest reproducibility as measured by absolute difference in mean deviation and patient performance using the reliability indices of fixation losses, false positive responses, and false negative responses. The subjects tested in this study were very reliable with virtually all subjects scoring well by the manufacturers' reliability criteria. The small sample size available in this pilot study of normal individuals was skewed towards young, healthy volunteers. A large sample size with more older subjects would probably provide a more representative group of normal subjects for study. Another variable in this study was the use of only one, very experienced perimetrist who monitored each testing experience carefully after patient education. Other studies with worse reliability reported for normal subjects used the first automated threshold field performed and did not use a training threshold field for naive subjects[4]. Reliability may be improved with experience with automated threshold perimetry

Further research needs to be done to investigate the relationship between the performance of individual subjects using the reliability indices and test-retest reproducibility of other normals and subjects with ocular disease.

References

1. Anderson DR: Testing the Field of Vision St Louis: CV Mosby Co 1982
2 Haley MJ (ed): The Field Analyzer Primer, 2nd edn San Leandro: Allergan Humphrey 1987
3 Enger C, Sommer A: Recognizing glaucomatous field loss with the Humphrey Statpac Arch Ophthalmol 105:1355-1357, 1987
4. Katz J, Sommer A: Reliability indexes of automated perimetric tests Arch Ophthalmol 106:1252-1254, 1988
5. Nelson-Quigg J, Twelker JD, Johnson CA: Response properties of normal observers and patients during automated perimetry Arch Ophthalmol 107:1612-1615, 1989
6. Bickler-Bluth M, Trick GL, Kolker AE, Cooper DG: Assessing the utility of reliability indices for automated visual fields: testing ocular hypertensives. Ophthalmology 96:616-619, 1989

Is the variability in glaucomatous field loss due to poor fixation control?

David B. Henson and Heather Bryson

Department of Optometry, University of Wales College of Cardiff, PO Box 905, Cardiff CF1 3YJ, UK

Introduction

There is a well-documented increase in the variability of visual field results from patients with and suspected of having glaucoma[1-7]. This increase hinders both the detection and monitoring of visual field loss. It often requires several visual field records before a significant trend can be detected[8].

The causes of this variability are at present unknown although various researchers have suggested that it is the result of disturbed homeostasis[5], reduction in the number of nerve fibers, increased susceptibility to fatigue and poor fixation control[2,9].

The isolated scotomas found in glaucoma often have steep sensitivity profiles[10], and even small inaccuracies of fixation can result in a stimulus falling into or climbing out of one of these defects. Even small inaccuracies of fixation can, therefore, in the presence of steep sensitivity gradients, result in apparent changes in sensitivity and increases in variability from one session to another.

The amount of variability caused by fixation inaccuracy will depend upon the number of steep sensitivity gradients. A patient who has a large number of isolated scotomas will have more steep sensitivity gradients than one who has a single large scotoma of equivalent area. Fixation inaccuracy should, therefore, produce a degree of variability proportional to the number of steep sensitivity gradients within the measured field.

The physiological blind spot is bounded by a steep sensitivity gradient. Fixation inaccuracy will, therefore, have a similar effect upon the physiological blind spot as it will on glaucomatous scotomas.

This paper investigates the relationship between variability and the number of steep edged sensitivity gradients in both normal and glaucomatous patients. It concludes that these two factors are highly correlated and that the results from blind spot evaluations in patients with normal visual fields form a continuum with those from glaucomatous defects, evidence which supports the hypothesis that a significant proportion of the variability seen in patients with glaucoma is the result of fixation inaccuracy.

Material and methods

Results were collected over a period of two years from patients attending a glaucoma clinic at Bristol Eye Hospital.

Visual fields were collected with a Henson CFS2000[11] using a threshold-related, multiple stimulus, suprathreshold strategy which tested 132 locations within the central 25 degrees of the visual field. The instrument initially tests at 5 dB above the estimated threshold, any stimulus missed twice at this intensity is further tested at 8 and 12 dB above the threshold estimate.

Two groups of patients were included in this study. One group consisted of those who, on no occasion, missed any stimulus other than the ones that fall within the blind spot region. These patients were classified as having normal visual fields. The second group had visual field scores which placed them within the defect category of the CSF2000's quantification system[11]. These patients were classified as having glaucomatous visual field loss.

A total of 121 eyes from 90 patients met either of these conditions. Fifty-two eyes were classed as having glaucomatous loss while 69 were classed as having normal visual fields. Each

Perimetry Update 1990/91, pp 217-220
Proceedings of the IXth International Perimetric Society Meeting,
Malmö, Sweden, June 17-20, 1990
edited by Richard P. Mills and Anders Heijl

eye was examined between two and five times. Analysis was based on pairs of consecutive visual field records, and totalled 138 glaucomatous and 85 normal pairs.

A measure of variability was derived by counting the number of stimulus locations whose recorded sensitivity either improved or deteriorated from one visit to the next. The size of the defect/blind spot was established by counting the total number of missed stimuli within each visual field record. The number of steep edged gradients within each visual field was established by searching around each missed stimulus and counting the number of immediate neighbors which were missed or seen at different intensity levels.

Results and discussion

The basic results from both groups of patients are given in Table 1, while Fig. 1 is a plot of variability versus the number of steep edged sensitivity gradients. Each point in this figure comes from the results of two consecutive visits. The number of steep edged sensitivity gradients is averaged over the two visits. It can be seen from these figure that these two measures are highly correlated and that results from the analysis of the blind spot misses in normal patients form a continuum with those from the glaucoma patients.

Table 1. Results from glaucomatous and normal samples

	Average interval between consecutive records (months)	*Average No missed stimuli*	*Average No edges*	*Average variability between consecutive records*	*Average variability per missed stimuli*	*Average variability per edge*
Normals (n=85)	5.42 (2 73)	1 87 (0 83)	7 48 (3 57)	1 87 (1.26)	1.09 (0.66)	0 27 (0 16)
Glaucomatous patients (n=138)	5.64 (3 08)	29 82 (27 74)	80 00 (53 82)	23 69 (14 97)	1 15 (0 50)	0.31 (0 08)

Fig. 2 is a plot of variability versus the number of missed stimuli. Again, each point in this figure comes from the results of two consecutive visits. The number of misses is the average

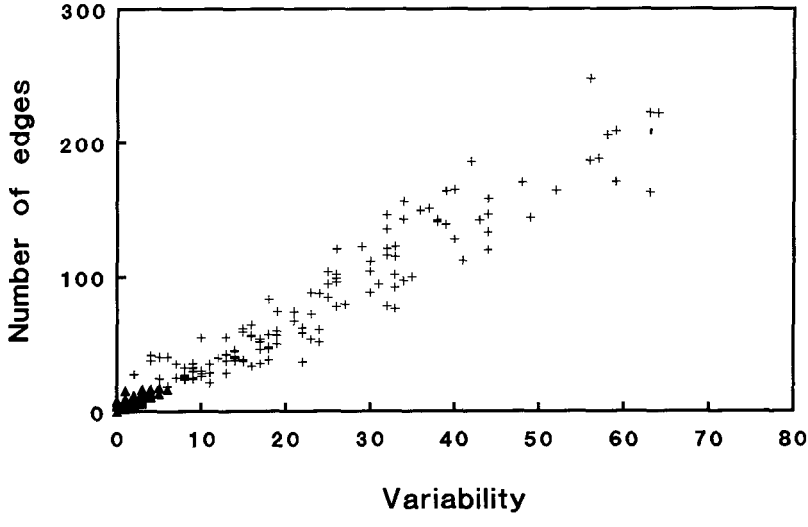

Fig 1 Visual field variability measured from consecutive visits versus the number of edges in the visual field (average of two visits) in both glaucomatous patients and normals.

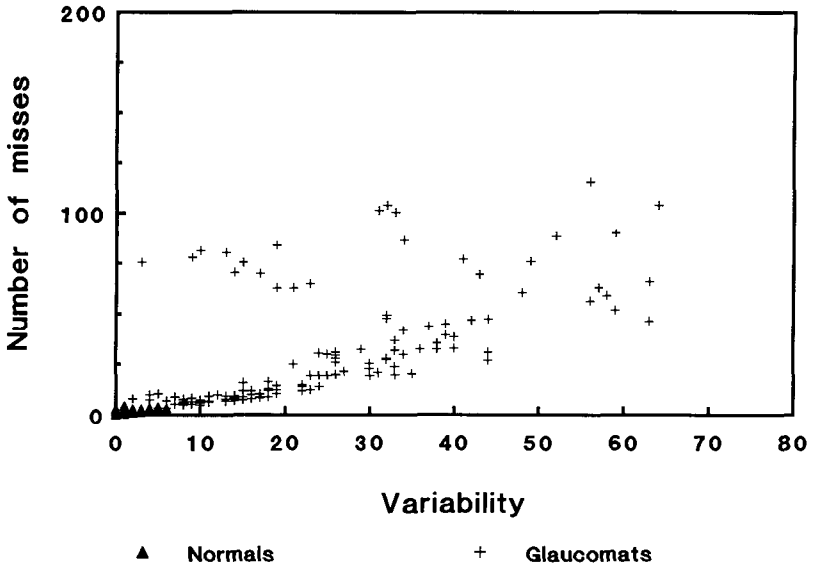

Fig 2 Visual field variability measured from consecutive visits versus number of missed stimuli (average of two visits, maximum 132).

of the two visits. While the two measures are highly correlated for small numbers of missed stimuli, as the numbers of missed stimuli increase, the correlation breaks down. Some patients with large numbers of missed stimuli have very little variability while others have a lot. Those patients with large numbers of missed stimuli and little variability have fewer edges in their visual field defects than do those with a similar number of missed stimuli and a large degree of variability.

The results from the patients with glaucomatous loss could be explained by a number of different hypotheses. One of these is that the variability in glaucomatous defects primarily occurs at the edges of the scotoma where the nerve fibers are compromised but still functioning. Such a hypothesis cannot explain the results from the blind spot analysis of normal patients where no damage has taken place.

It could also be hypothesized that the results from the glaucoma patients are an artifact of the experimental technique. Defects were only measured to a depth of 12 dB Once defects became deeper than this, as may occur in the center of a scotoma, any variability may have been obscured by not quantifying the defect depth beyond 12 dB. Again, this hypothesis cannot explain the results from the normal patients.

The results from the normal patients can, however, be explained by fixation errors which could also account for a large degree of the variability found in the glaucoma patients.

While Fig. 1 shows that the results from the normals form a continuum with the data from the glaucoma patients, an analysis of the average variability per edge (the value for the number of edges being the average from the two consecutive visits), see Table 1, indicates that glaucoma patients have a significantly higher value (p=0.006). While drawing a large number of inferences from this difference may be premature, it could be concluded that while a significant amount of the increased variability seen in glaucoma can be accounted for on the basis of errors in fixation, there is still a residual amount which is as yet unexplained.

The large amount of variability seen in the visual field results from glaucoma patients severely limits the value of visual field analysis in the monitoring of glaucoma and in predicting trends. A change in the visual field needs to be greater than the variability/fluctuation before it can be recognized as genuine. This research concludes that a significant proportion of the variability in glaucoma patients may be the result of errors in fixation. By controlling these errors or by developing protocols and quantification systems which are less sensitive to them, it may be possible to improve the ability of visual field measures to monitor glaucomatous loss.

References

1. Werner EB, Drance SM: Early visual field disturbances in glaucoma Arch Ophthalmol 95:1173-1175, 1977
2. Donovan HC, Weale RA, Wheeler C: The perimeter as a monitor of glaucomatous damage. Br J Ophthalmol 62:705-708, 1978
3. Holmin C, Krakau CET: Variability of glaucomatous visual field defects in computerised perimetry. Graefe's Arch Ophthalmol 210:235-250, 1979
4. Werner EB, Saheb N, Thomas D: Variability of static threshold responses in patients with elevated IOPs. Arch Ophthalmol 100:1627-1631, 1982
5 Flammer J, Drance SM, Zulauf M: Differential light threshold short and long-term fluctuation in patients with glaucoma, normal controls and patients with suspected glaucoma. Arch Ophthalmol 102:704-706, 1984
6 Langhorst CT, Van den Berg TJTP, Van Spronsen R, Greve EL: Results of a fluctuation analysis and defect volume program for automated static threshold perimetry with the scoperimeter. Doc Ophthalmol Proc Ser 42:1-6, 1984
7 Werner EB, Bishop KI, Davis P, Krupin T, Petrig B, Sherman C: Visual field variability in stable glaucoma patients Doc Ophthalmol Proc Ser 49:77-84, 1986
8 Holmin C, Krakau CET: Regression analysis of the central visual field in chronic glaucoma cases Acta Ophthalmol 60:267-274, 1982
9. Vingrys AJ, Verbaken JH: Perimetric fluctuation in normal and diseased eyes. ARVO Abstract No 1296, 1990
10. Drance SM: The glaucoma visual field defect and its progression. In: Drance SM, Anderson DR (eds) Automatic Perimetry in Glaucoma: A Practical Guide Orlando: Grune & Stratton 1984
11. Henson DB, Bryson H: Clinical results with the Henson-Hamblin CFS2000 Doc Ophthalmol Proc Ser 49:233-238, 1986

An investigation into the black-hole effect in autoperimetry

N.A. Jacobs and M.L. Harris

London, UK

Introduction

Light emitting diodes have become a popular method of presenting the stimulus in automated perimeters. The brightness of individual diodes can be easily modulated, which is ideal for static threshold field testing. However, to incorporate these into the device, the perimeter bowls are drilled and present multiple "black holes" to the subject. Various authors[1-3] have raised the possibility that these interruptions of the otherwise uniform background illumination may cause inaccuracies in threshold determinations due to local retinal dark adaptation.

In this study we compare the threshold values obtained from the Topcon SBP1000 and the Dicon AP2000. In the former, all the LEDs are kept at background intensity between stimulus presentations to eliminate any potential "black-hole" effect. The latter presents black holes between stimuli.

Method

Twenty normal subjects (age range 18-38 years) were assessed. Static thresholds were determined along the 135 degree meridian at 5-degree intervals to 30 degrees eccentricity using each of the automated perimeters. The Goldmann projection perimeter using stimulus sizes II and III was used as a standard. Refractive errors were fully corrected and a presbyopic correction included where appropriate.

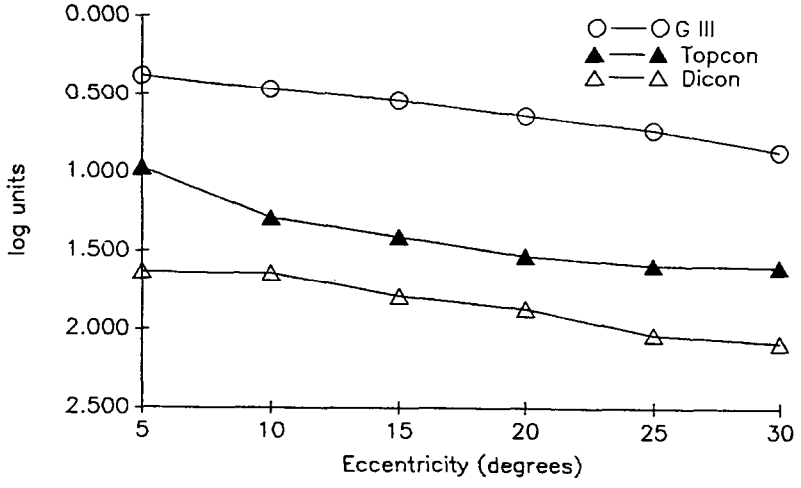

Fig 1 Threshold against eccentricity uncorrected data

Perimetry Update 1990/91, pp 221-223
Proceedings of the IXth International Perimetric Society Meeting,
Malmö, Sweden, June 17-20, 1990
edited by Richard P Mills and Anders Heijl

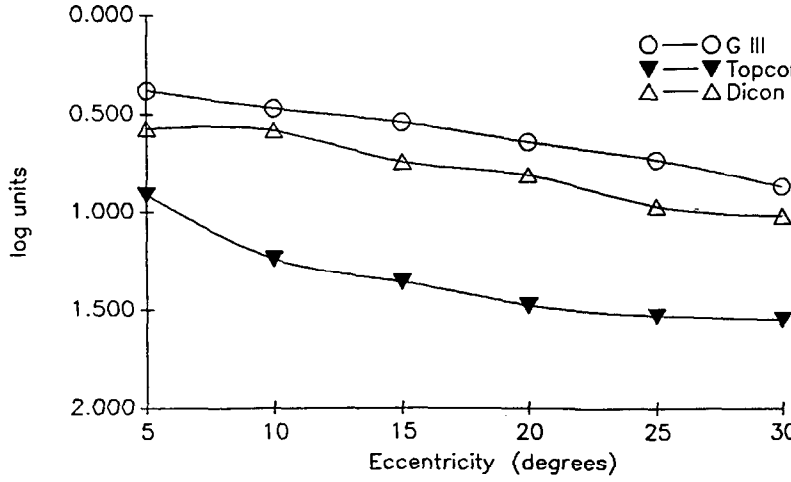

Fig 2 Threshold against eccentricity corrected data.

Results

Fig. 1 shows the threshold data in apostilbs as recorded from each perimeter.

Using the Goldmann II and III mean values to determine the relationship of stimulus intensity to size for this group of subjects, we have corrected the brightness values to take account of the stimulus sizes found on the autoperimeters. Differences in the calibration method of the autoperimeters were also allowed for. The Dicon values are derived by comparison with Goldmann I stimulus, whereas the Topcon values are a true representation of the LED brightness. Fig. 2 presents the adjusted results which are directly comparable.

In Fig. 2 beyond the 10-degree point the gradients are similar, but the levels for the autoperimeters are brighter than those for the Goldmann, the mean differences being 0.2 LU for the Dicon and 0.7 LU for the Topcon.

Discussion

In recent years there has been a proliferation of automated perimeters. Variations in their background illumination, method of stimulus presentation and testing strategy have brought difficulties with the interpretation of fields recorded on different devices. Johnson *et al* have devised an empirical approach to overcome this problem[5]. This investigation was designed to assess the influence of a specific factor, the "black-hole" effect. The perimeters selected have identical background illumination and use similar thresholding strategies. The significant difference is whether or not the LEDs are maintained at background illumination between stimuli.

When we compared the adjusted threshold values the mean difference between the autoperimeters was 0.5 LU. Contrary to our expectations it was the perimeter with black holes (Dicon) which related closer to the Goldmann standard. The reason for this is not immediately apparent. In the Topcon perimeter used in this experiment the LEDs were lit at the same luminance as the background bowl but there is a difference between the spectral output of the LEDs and the reflected white light from the bowl. The LED output peaks sharply at 585 nm, and therefore its intensity at this wavelength is much greater than that of the same wavelength within the reflected white light. The assumption has been made that the differing spectral output of the test stimuli would not affect the results of threshold sensitivity testing. Our results suggest that this is not true.

References

1. Hart WM, Gordon MO: Calibration of the Dicon autoperimeter 2000 compared with that of the Goldmann perimeter. Am J Ophthalmol 96:744-750, 1983
2 Mills RP: Quantitative perimetry: Dicon. In: Drance SM, Anderson D (eds) Automatic Perimetry in Glaucoma, Ch 9, pp 99-112. Orlando: Grunc and Stratton 1985
3 Jacobs HA: Modern Perimetry. Sem Ophthalmol 1:14-34, 1986
4. Britt JM, Mills RP: The black hole effect in perimetry Invest Ophthalmol Vis Sci 29:795-801, 1988
5. Johnson CA, Keltner JL, Lewis RA: JAWS (joint automated weighting statistic): a method of converting results between autoperimeters. Doc Ophthalmol Proc Ser 49:563-568, 1987

Accurate estimation of local defects in glaucoma

Christine T. Langerhorst, George Lambrou, Francois Temporelli and Thomas J.T.P. van den Berg

Departments of Ophthalmology and Medical Physics and Informatics, Academic Medical Center, Meibergdreef 9, 1105 AZ Amsterdam, The Netherlands

Abstract

During the past years the authors have extensively studied fluctuation behavior in automated perimetry in glaucoma. Most research was done with an experimental apparatus with a relatively low background luminance (0 1 cd/m^2), which may in itself enhance fluctuation. They showed that estimating an individual general reference level by means of double threshold measurements considerably increases the accuracy of the estimation of local defects. In this study they tested the original population of normals, glaucoma suspects and glaucoma patients with the commercially available Octopus 500 EZ, with a background level of 1.0 cd/m^2, using the G1 program, but applying their own analysis algorithm. The authors found the short-term fluctuation per point to be lower in all subjects. This was especially true for the pathological areas. The general level of the field did not differ between the two perimeters. They claim that by using a perimeter with a higher background luminance, local defects can be estimated more accurately, due to less fluctuation in pathological points. It will still be necessary, however, to use double threshold measurements to exclude the fluctuating influence of the general level of the field

Introduction

It is well known that fluctuation of perimetric measurements occurs in normals as well as glaucoma patients. We previously studied fluctuation in automated perimetry in glaucoma (short-term as well as long-term), the factors influencing it and the consequences of such fluctuation for the judgment of glaucomatous visual fields[1]. The important finding was that fluctuations can be considerable, not only locally but also more globally, such as for the long-term fluctuation of the general sensitivity level of the whole visual field. By separating, using a special computer analysis, the individual thresholds into the general level component and a strictly local defect component, the estimation of the local defect volume could be made much more accurate. Essential for this analysis was that each threshold was determined twice. For this fluctuation study we used a research perimeter[2] with a relatively low background luminance of 0.1 cd/m^2. It could be argued that usage of this instrument with such a low background may in itself enhance fluctuation[3], necessitating a complicated analysis to minimize its influence in defect estimation. We therefore undertook to study the original research population again with a more established instrument (Octopus 500 EZ) at a higher background luminance (1.0 cd/m^2). Our aim was to find out whether the short-term fluctuation would indeed be lower, and whether this would influence the accuracy of estimation of local defects.

Subjects and methods

A detailed description of the subject groups can be found in the original study[1]. In summary, we studied over an extended period of time altogether 51 subjects, divided into five more or less equally large groups: normals, ocular hypertensives, and primary open angle glaucoma patients with low, medium or high intraocular pressures. For the present study we invited as many of the original subjects as were available and willing to participate, to have an additional test with a different instrument. Thus we were able to test 32 subjects. As perimeter we used the Octopus 500 EZ automated perimeter, with a background luminance of 1.0 cd/m^2. The program used was the G1 program: phase one and then immediately again phase one in exactly the same manner (total testing time 12 minutes). Each subject was tested once in this manner.

Perimetry Update 1990/91, pp. 225-227
Proceedings of the IXth International Perimetric Society Meeting,
Malmö, Sweden, June 17-20, 1990
edited by Richard P. Mills and Anders Heijl

The double threshold values thus obtained for every measured location were analyzed with the computer algorithm developed previously[1] for accurate local defect estimation. In summary, this algorithm first makes a selection of normal points based on one of the two series of thresholds and then determines an individual general sensitivity (IGS) level based on the second series. Next the points estimated to be normal are determined using the short-term fluctuation. From these points a final most accurate IGS is estimated. Subtraction of this IGS from the average threshold in each point renders the estimation for the local defect. The mean gives the mean local defect (MLD) for each field.

Results

The most important reduced variables obtained after computer analysis are presented in Table 1. It can be seen that for all groups the short-term fluctuation in healthy points (SFh) is indeed lower with the use of the Octopus. The same holds true for the short-term fluctuation in pathological areas (SFpa), but to a greater extent. The values for the level of the individual general sensitivity (IGS) do not seem to differ much between the two perimeters used. This applies to the average values as well as to the standard deviations, with the exception of the standard deviation value of the low tension glaucoma group.

Table 1 Comparison of results of original and present study

	NOR		*OHT*		*MTG*	
	original study	*present study*	*original study*	*present study*	*original study*	*present study*
Number of patients	*10*	*3*	*10*	*9*	*12*	*5*
age (years)	67 8 ± 10 1	69.0 ± 0.9	55 7 ± 13 8	56 7 ± 11 0	65.6 ± 6.6	64 8 ± 8 5
IGS (dB)	29 4 ± 2.0	30.7 ± 1.7	30 5 ± 1 4	31 3 ± 1.7	27.6 ± 1.4	29 1 ± 2.0
MLD (-dB)	0 6 ± 0.2	0.8 ± 0.7	0 4 ± 0 2	0 6 ± 0 5	3.2 ± 1.6	5 2 ± 2.7
SFh (dB)	2 4 ± 0.8	1.5 ± 0 3	2 0 ± 0 5	1 8 ± 1 3	2.4 ± 0.5	1.8 ± 0 5
SFpa (dB)					4.4 ± 0.7	2 4 ± 0 9
LF-MLD (dB)	0 3 ± 0.1		0 2 ± 0 1		1.1 ± 0 7	
LF-IGS (dB)	1 2 ± 0.5		1 3 ± 0 7		1.7 ± 1 0	

	HTG		*LTG*	
	original study	*present study*	*original study*	*present study*
Number of patients	*10*	*9*	*9*	*5*
age (years)	50.6 ± 10 9	54 1 ± 12.4	72 4 ± 8.8	70.3 ± 6 6
IGS (dB)	27 8 ± 1 5	29 7 ± 1.2	25 7 ± 3.0	25.6 ± 6 1
MLD (-dB)	2 6 ± 2 5	3 0 ± 2.9	5 6 ± 2 1	7.5 ± 1 5
SFh (dB)	2 3 ± 0 4	1.6 ± 0 4	2 8 ± 0 8	1 8 ± 0 7
SFpa (dB)	4.6 ± 1.1	2.4 ± 0 8	4 9 ± 0 8	2 6 ± 0 9
LF-MLD (dB)	0.6 ± 0.3		1 1 ± 0 6	
LF-IGS (dB)	1.3 ± 0 4		1.8 ± 0 5	

NOR: normals; OHT: ocular hypertensives; MTG, HTG and LTG: medium, high and low tension glaucoma patients; IGS: individual general sensitivity; MLD: mean local defect; SFh: short-term fluctuation in healthy points; SFpa: short-term fluctuation in pathological points: LF: long-term fluctuation.

Discussion

In this study it was found, in accordance with the literature, that the short-term fluctuation of threshold measurements of a group of subjects was influenced by the perimetric technique used: with a perimeter with a low background luminance there was more fluctuation. It was especially interesting to note that the SF in pathological points was increased even more than in normal points under the low background conditions.

This could be important in two ways. If one believes that increased scatter is perhaps an early sign of glaucomatous field damage[4], then testing at a low background luminance might be a "provocation" test to bring out the early defective points. Arguing the other way around, how-

ever, we think that it is more important to test at higher background luminance, thereby reducing SFpa and thus also reducing the deleterious influence of a large SFpa on the estimation of the defect volume of a visual field. The testing of our original subjects with a higher background luminance perimeter did not seem to have a specific effect on other reduced data of the visual field, such as the general level (IGS) as it is estimated by our algorithm. The group values estimated for each instrument used seem to be well comparable. The differences in mean local defect (MLD) for the glaucoma patient groups in Table 1 can be accounted for by the different composition of the original and present groups.

In the original study[1], we tested the subjects repeatedly over time, and were thus able to estimate the long-term fluctuation (LF) of the reduced variables IGS and MLD. For the sake of clarity these values are also indicated in Table 1. The MLD proved to have a much smaller LF than the IGS. This means that the general level component of a visual field will hamper through its fluctuation an accurate estimate of visual field behavior in the follow-up of a patient or subject. In our algorithm this IGS fluctuation is more or less eliminated by determining the IGS level for each individual field, and subtracting it from the individual threshold. The resulting MLD was indeed shown to fluctuate much less over time and would therefore be a better, more accurate estimate of local glaucomatous field damage. In the present study we did not repeat the double threshold test with the Octopus, so we have no actual data concerning LF with this apparatus. However, in view of the similar results for the IGS and MLD itself with both instruments, it seems reasonable to assume that the LF of the variables would also not differ much between instruments This would mean that background luminance has no direct influence on the (relatively large) fluctuation of IGS over time, and it would therefore still be advisable to eliminate the general level from the local defect estimation as is done in our algorithm. We have shown earlier that the IGS can be estimated relatively accurately with double threshold measurements[5].

Testing at a higher background luminance would however still be useful, because it minimizes SFpa and thus will render the estimation of the MLD even more accurate. This will ultimately help the clinician in deciding on progression of the visual field

Conclusions

- Testing at a higher background luminance decreases short-term fluctuation in normal and pathological points.
- Especially the lower SF in pathological points may render the estimation of local defects more accurate.
- The hampering effect of IGS fluctuation does not seem to be improved by a higher background luminance.
- Therefore it still seems advisable to estimate local defects without the influence of the general level of the field. This can only be done in an unbiased way by using double threshold measurements.

References

1. Langerhorst CT: Automated Perimetry in Glaucoma: Fluctuation Behavior and Local and General Reduction of Sensitivity Amsterdam/ Berkeley/Milano: Kugler & Ghedini Publ 1988
2 de Boer RE, van den Berg TJTP, Greve EL, de Waal BJ: Concepts for automatic perimetry, as applied to the Scoperimeter, an experimental automatic perimeter Int Ophthalmol 5:181-191, 1982
3 Klewin CM, Radius RL: Background illumination and automated perimetry Arch Ophthalmol 104:395-397, 1986
4. Flammer J, Drance SM, Zulauf M: Differential light threshold: short- and long-term fluctuation in patients with glaucoma, normal controls, and patients with suspected glaucoma Arch Ophthalmol 102:704-706, 1984
5. Langerhorst CT, van den Berg TJTP, van Spronsen R, Greve EL: Results of a fluctuation analysis and defect volume program for automated static threshold perimetry with the Scoperimeter Doc Ophthalmol Proc Ser 42:1-6, 1985

Computer-assisted analysis

Statpac 2 compared to clinical evaluation of visual fields

Anja Tuulonen and P. Juhani Airaksinen

Department of Ophthalmology, University of Oulu, Oulu, SF-90220 Finland

Abstract

The purpose of this study was to evaluate how the Statpac 2 Change Probability Analysis correlates to routine clinical interpretation of visual fields and to the assessment of progression of glaucomatous optic disc cupping. The authors included in the study 20 consecutive patients (38 eyes) with glaucoma or ocular hypertension who had had five Humphrey 30-2 visual fields taken during two to four years. Using Statpac 1 the authors subjectively evaluated independently the progression of the visual fields of the 38 eyes without any knowledge of the patients' clinical data The agreement between Statpac 2 and one observer was 87% and the other 76%, respectively. The agreement between the two observers was 79% One or both observers deemed seven eyes (18%) stable, but Statpac 2 indicated deterioration. Four of these seven eyes showed progression of disc abnormalities The results of this study indicate that Statpac 2 Change Probability Analysis correlates well with routine clinical evaluation of progression of visual field changes

Introduction

The inter-test variation of the threshold values of computerized perimetry is quite large[1-3], especially in abnormal visual fields[4-6]. Therefore, it may be sometimes difficult to differentiate between true progression and random variation. Visual field indices have been developed to facilitate interpretation between normal and abnormal automated threshold visual fields[7]. However, when assessing the deterioration of visual field damage over time the visual field indices did not correlate well with clinical interpretation of progression[8].

Statpac 2 statistical analysis package has been developed to facilitate the follow-up of visual field changes in patients with glaucoma[9]. It is based on empirical data obtained from repeated visual field testing with Humphrey 30-2 program on stable glaucomatous eyes in different stages of the disease. The pointwise variability has been reported to depend on the depth of the defect, the location of the test point, and general level of depression[6]. In the change probability printout of Statpac 2 the points showing deterioration at the 5% level are indicated by black triangles and the points showing improvement with white triangles. The points not changing are indicated by a single solid dot. A small cross indicates that the program is not able to judge whether the change is significant or not.

The purpose of this study was to evaluate how Statpac 2 change probability analysis correlates with routine clinical interpretation of progression of visual field and optic disc damage.

Material and methods

Twenty consecutive patients (38 eyes) with five Humphrey 30-2 visual fields were selected for the study. We evaluated the deterioration of the visual field damage independently, using the overview printout and change analysis printout of Statpac 1 without any knowledge of the patients' clinical data.

Statpac 2 change probability analysis, based on two baseline visual fields and three follow-up visual fields, was performed on all eyes. From the three follow-up visual fields we counted the total number of black triangles, that is points showing deterioration significant at the 5% level, and the total number of white triangles, that is points showing improvement significant at the 5% level. It was decided that when the difference between the number of points deteriorating and improving was larger than four, the three follow-up visual fields showed a clinically significant change for better or worse. For example, if the number of black triangles was 17 and

Perimetry Update 1990/91, pp 231-233
Proceedings of the IXth International Perimetric Society Meeting,
Malmö, Sweden, June 17-20, 1990
edited by Richard P. Mills and Anders Heijl

the number of white triangles nine, the difference of eight was determined to indicate visual field deterioration. The numbers of points with questionable significance (small crosses) were ignored.

The changes of the optic disc cupping were analyzed by comparing the optic disc stereophotographs taken at the beginning and at the end of follow-up period without any knowledge of the patients' clinical data or the results of visual field analysis. The clinical evaluation, results of Statpac 2 analysis and optic disc assessment were then compared with each other.

Results

The mean age (±SD) of the 15 females and five males was 64±14 (range 35 to 84) years. The follow-up ranged from 2.0 to 4.2 (mean 3.2±0.6) years. There were six patients with simple glaucoma, six with capsular glaucoma, four with low tension glaucoma, one with secondary glaucoma due to uveitis, one with juvenile glaucoma and two patients with ocular hypertension.

The mean MD and PSD indices at the beginning and at the end of the follow-up period are presented in Table 1. The mean MD slope was -0.59 dB/year (range from +2.91 to -3.67 dB/year). The MD slope showed deterioration significant at the 5% level in two eyes and at the 1% level in three eyes.

Table 1 The mean (±SD) MD and PSD indices at the beginning and at the end of follow-up of the 20 patients (38 eyes) with glaucoma or ocular hypertension included in the study

Follow-up	*Mean MD index (dB)*	*Mean PSD index (dB)*
Beginning	−4.36 ± 5.49	5.30 ± 3.44
range	+2.53 to −20.26	1.62 to 12.52
End	−5.65 ± 6.20	4.83 ± 3.24
range	+1.44 to −25.70	1 43 to 12 17

Table 2 The results of clinical evaluation of visual fields, Statpac 2 statistical analysis package and assessment of glaucomatous progression from optic disc stereo photographs

	Glaucomatous VF and optic disc damage					
	Deteriorated		*Improved*		*Stable*	
	Number of eyes (%)					
Observer 1	14	(37%)	3	(8%)	21	(55%)
Observer 2	15	(39%)	3	(8%)	20	(53%)
Statpac 2	21	(55%)	9	(24%)	8	(21%)
MD change of at least 2 VF $p<5\%$*	14	(37%)	1	(3%)	23	(61%)
MD change of last VF $p<5\%$**	21	(55%)	–		17	(45%)
MD slope $p<5\%$***	5	(13%)	1	(3%)	32	(84%)
Optic disc cupping	12	(32%)	–		26	(68%)

* the change of mean deviation (MD) index significant at the 5% level of at least two out of three follow-up visual fields when compared to baseline visual fields

** the change of MD index significant at the 5% level of the last follow-up visual field when compared to baseline visual fields

*** MD slope significant at the 5% level

The results of clinical evaluation of visual fields, Statpac 2 statistical analysis package and assessment of glaucomatous progression from optic disc stereo photographs are presented in Table 2. When the visual field changes were classified as (1) stable or improved, or (2) deteriorated, the agreement between Statpac 2 and Observer 1 was 87%, and Observer 2 76%, respectively. The agreement between the two observers was 79%.

Among the 12 eyes which were assessed to show progression of the glaucomatous optic disc abnormality (Table 2) Statpac 2 indicated no deterioration of visual fields in five eyes (42%);

Observer 1 in four eyes (33%), and Observer 2 in seven eyes (58%), respectively.

Visual fields of seven of 38 eyes (18%) were deemed stable by Observer 1 and/or 2 but Statpac 2 indicated deterioration. Four of the seven eyes showed progression of glaucomatous optic disc cupping.

Discussion

The results of this study show that Statpac 2 Change Probability Analysis correlates well with our clinical interpretation of visual field changes. In some eyes with progressive optic disc changes it located subtle changes of visual field damage which were missed by one or both observers. On the other hand, there were eyes with progressive optic disc damage whose visual fields were deemed stable both by Statpac 2 and Observer 1 and 2.

The study design is, of course, unnatural because in clinical situations the decision making is always based both on optic disc and visual field evaluation It remains for the practitioner to decide whether the changes indicated by the statistical analysis package are clinically significant, and due to glaucoma or some other disease

References

1. Parrish RK, Schiffman J, Anderson DR: Static and kinetic visual field testing: reproducibility in normal volunteers. Arch Ophthalmol 102:1497-1502, 1984
2. Lewis RA, Johnson CA, Keltner JL, Labermeier PK: Variability of quantitative automated perimetry in normal observers. Ophthalmology 93:878-881, 1986
3. Heijl A, Lindgren G, Olsson J: Normal variability of static perimetric threshold values across the central visual field. Arch Ophthalmol 105:1544-1549, 1987
4. Holmin C, Krakau CET: Variability of glaucomatous visual field defects in computerized perimetry Graefe's Arch Clin Exp Ophthalmol 210:235-250, 1979
5. Werner EB, Bishop KI, Davis P, Krupin T, Sherman C, Petrig B: Visual field variability in stable glaucoma patients Doc Ophthalmol Proc Ser 77-84, 1987
6. Heijl A, Lindgren A, Lindgren G :Test-retest threshold variability in glaucomatous visual fields Am J Ophthalmol 108:130-135, 1989
7. Flammer J: The concept of visual field indices Graefe's Arch Clin Exp Ophthalmol 224:389-392, 1986
8. Chauhan BC, Drance SM, Douglas GR: The use of visual field indices in detecting changes in the visual field in glaucoma Invest Ophthalmol Vis Sci 31:512-520, 1990
9. Statpac User's Guide: Introducing Statpac 2. San Leandro, CA: Allergan Humphrey 1989

Classification of glaucomatous visual field defects using the Humphrey Field Analyzer box plots

Yeong Se Shin, Hirotaka Suzumura, Fumio Furuno, Kayoko Harasawa, Niriyoshi Endo and Harutake Matsuo

Department of Ophthalmology, Tokyo Medical College Hospital, 6-7-1, Nishishinjuku, Shinjuku, Tokyo 160, Japan

Abstract

The authors have reported several methods for evaluation of glaucomatous visual field defects and have developed a system for classification of glaucomatous visual field defects by numerical values. Approximately 1300 eyes with glaucoma were examined with the Humphrey Field Analyzer (HFA) and these were divided into 16 groups These visual fields were represented by box plots and were classified by the minimum, the lower limit of the box and the median Using this system, it was possible to classify the glaucomatous visual field defects into five major stages and five minor subgroups. This methods permits an objective, analogous representation of the extent of visual field defects that can be rapidly and accurately grasped

Introduction

Although there have been many classifications of glaucomatous visual fields, most of them are based on results obtained by quantitative kinetic perimetry. In this study, we attempted to classify the glaucomatous visual fields numerically using the Humphrey Field Analyzer (HFA) box plot of the type proposed by Heijl *et al* [1].

Methods and subjects

The central 30 degrees of the visual field was measured by HFA program 30-2 (stimulus size III) and the whole field was measured by the Goldmann perimeter (GP)

Glaucomatous visual fields were classified into 16 groups based on the static and kinetic results (Table 1, Fig. 1). Box plots were printed out according to these 16 groups, and a mean box plot of each group was then calculated. Based on the resulting mean box plots, classification of glaucomatous visual fields was performed.

Table 1 Glaucomatous visual fields are classified into 16 groups based on kinetic and static perimetry

	GP	*HFA*	*No of cases*
1	Normal	Normal	40
2	Slight depression	Normal	14
3	Normal	Slight depression	44
4	Small isolated scotoma	Single relative arcuate depression	6
5	Slight depression	Single relative arcuate depression	19
6	Nasal step without scotoma	Single nasal defect	15
7	Single relative arcuate disturbance with absolute nucleus	Single arcuate and nasal defect	25
8	Nasal step with or without scotoma	Double arcuate depressions	19
9	Single arcuate defect	Double arcuate depressions	8
10	Single absolute arcuate defect and nasal step	Single arcuate defect and nasal step	13
11	Single absolute arcuate defect and nasal step	Double arcuate defects	11
12	Double arcuate defects without breakthrough of 1/4	Double arcuate defects	13
13	Single complete breakthrough	Complete breakthrough	4
14	Double arcuate defects with breakthrough of 1/4	Complete breakthrough	14
15	Complete breakthrough and arcuate scotoma	Double arcuate defects	8
16	Central and/or temporal rest	Central (and/or temporal) test	27

Perimetry Update 1990/91, pp. 235-243
Proceedings of the IXth International Perimetric Society Meeting,
Malmö, Sweden, June 17-20, 1990
edited by Richard P. Mills and Anders Heijl

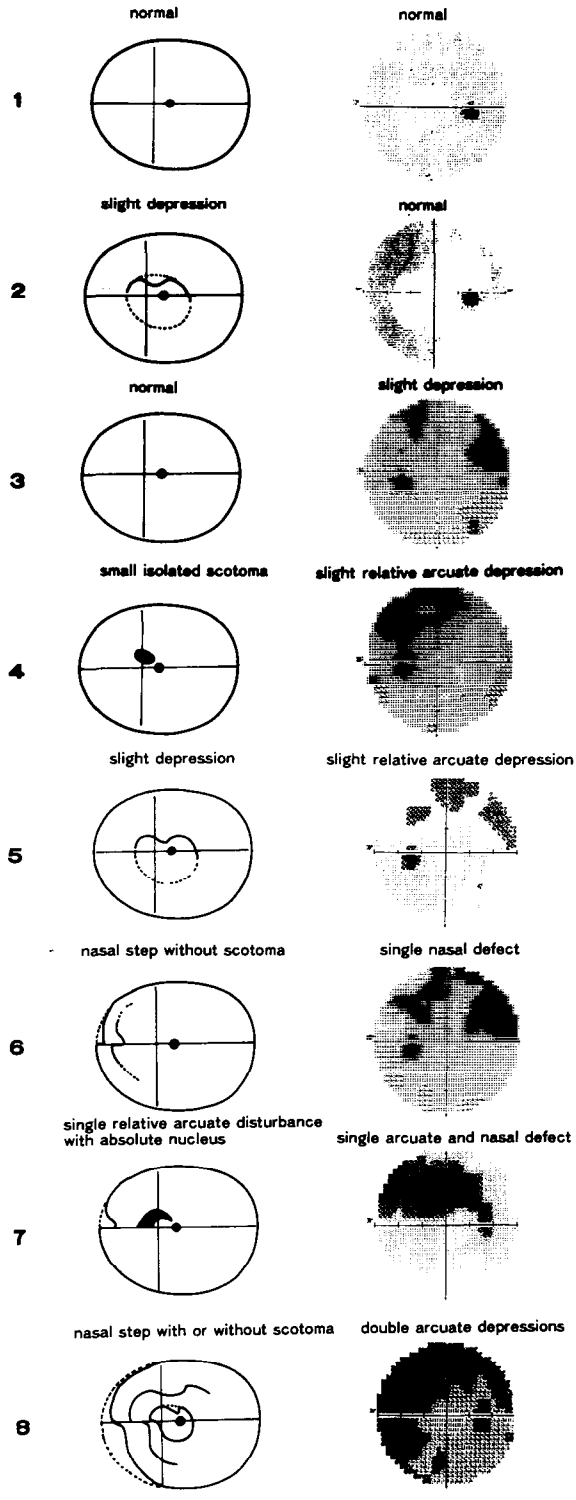

Fig 1 Visual fields of 16 groups Groups 1–8.

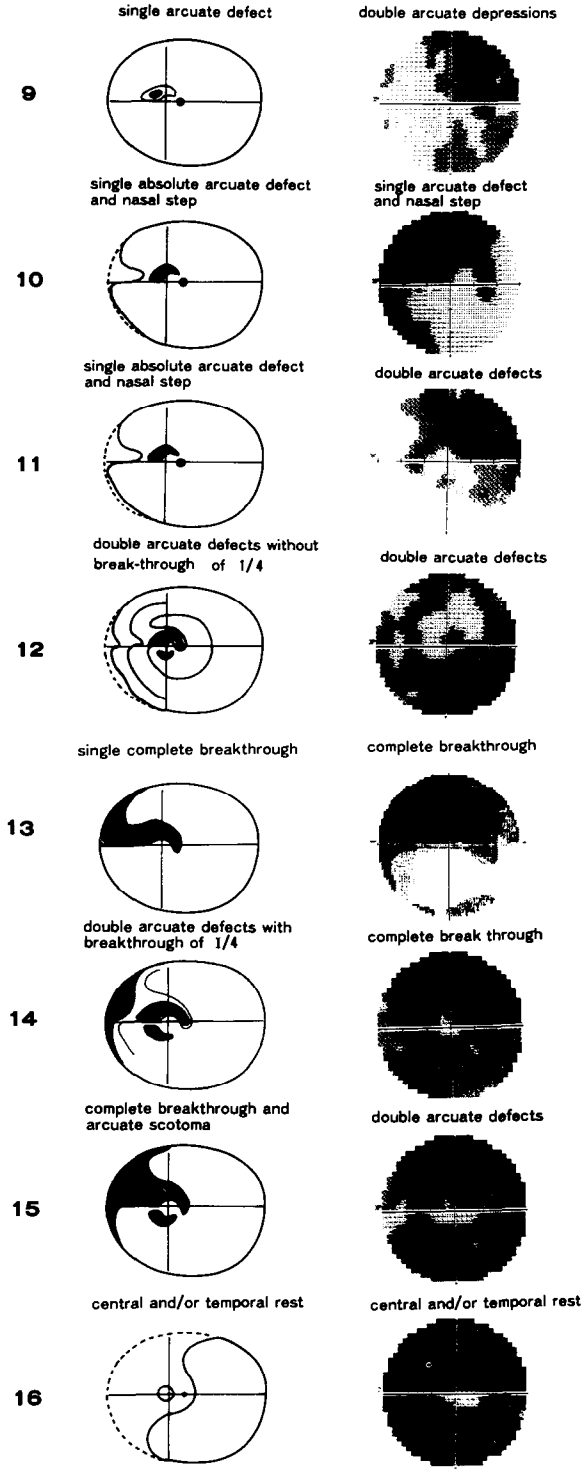

Fig 1 Visual fields of 16 groups. Groups 9–16

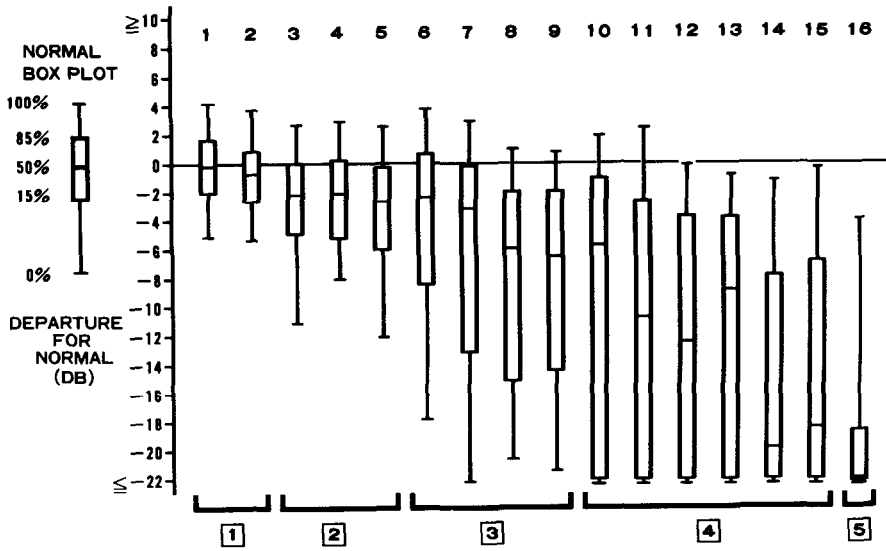

a.

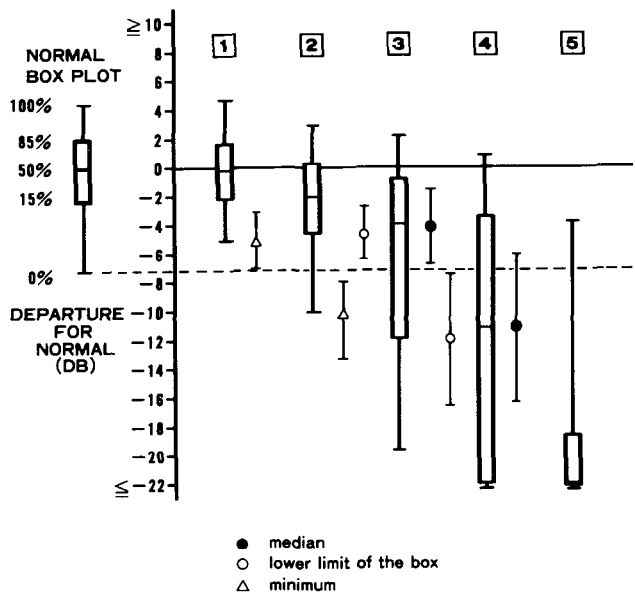

b.

Fig 2 a. Box plots of 16 groups; b. averaged box plots of five major stages.

Among about 1300 eyes with glaucoma examined by HFA from January 1987 to January 1990, we found 280 eyes with a visual acuity of 0.7 or more, a pupillary diameter of 3 mm or more, and without other diseases. These were selected for the present study. The average age of the patients was 56.0±15.7 years, ranging from eight to 87 years.

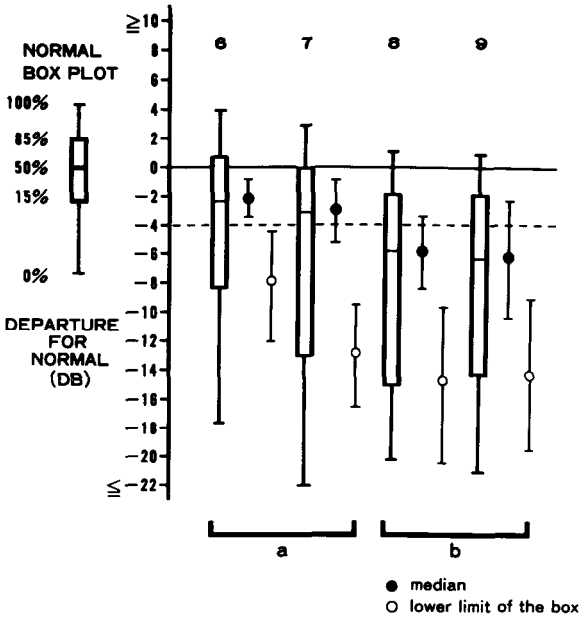

Fig 3a. Two minor subgroups of Stage 3

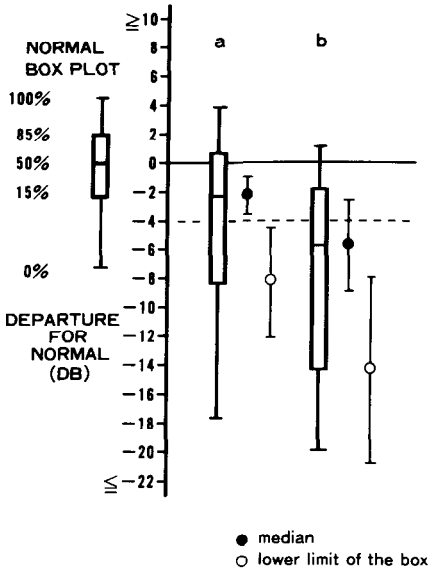

Fig 3b Averages of two minor subgroups "a" and "b".

Results

The means of box plots for each 16 groups using both GP and HFA are indicated in Fig. 2a Classification was made into five stages, based on the minimum, the lower limit of the box and the median. As shown in Fig. 2b, it was considered that the minimum of Stage 1 was better than the minimum of the normal box plot, and Stage 1 was defined as the box plots with a minimum of -7 dB or better. In Stage 2, the length of the negative tail increased and the lower limit of the box was better than the minimum of normal box plot. Thus, Stage 2 was defined

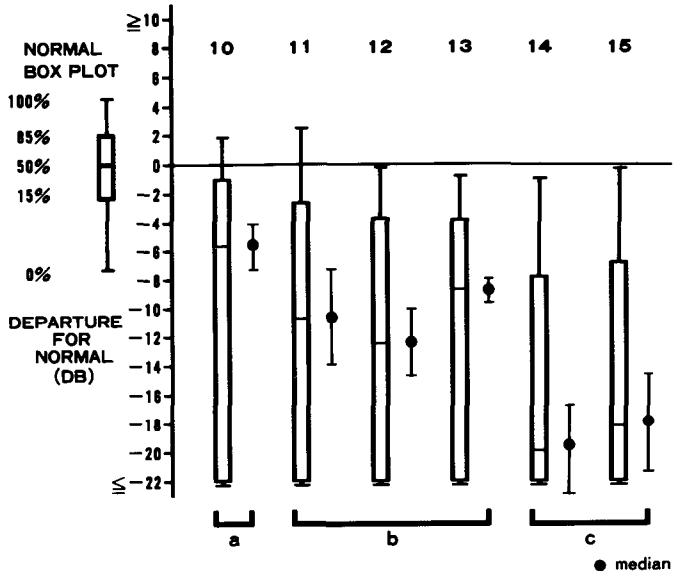

Fig 3c Three minor subgroups of Stage 4

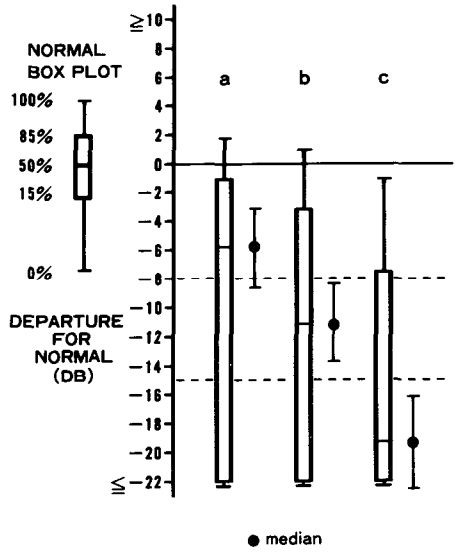

Fig 3d Averages of three minor subgroups "a", "b" and "c"

as fields with box plots in which the minimum was -8 dB or worse and the lower limit of the box was -7 dB or better. Stage 3 was defined as cases of box plots in which the lower limit of the box was -8 dB or worse. Stage 4 consisted of cases of box plots in which the lower limit of the box was -22 dB or worse. In Stage 5, the median of the box plot was -33 dB or worse (Table 2a)

In this classification, the spectra of Stages 3 and 4 were extremely wide, so they were broken down further. Stage 3 was divided into two minor subgroups (Fig. 3a and b). Subgroup "a" consisted of cases with a single arcuate defect on HFA and subgroup "b" of cases with double arcuate defects on HFA. From these findings, the median played an important role in the classification but at the lower limit of the box. It was considered best that the median was defined as -4 dB or better for subgroup "a" and as -5 dB or worse for subgroup "b". Stage 4 was divided

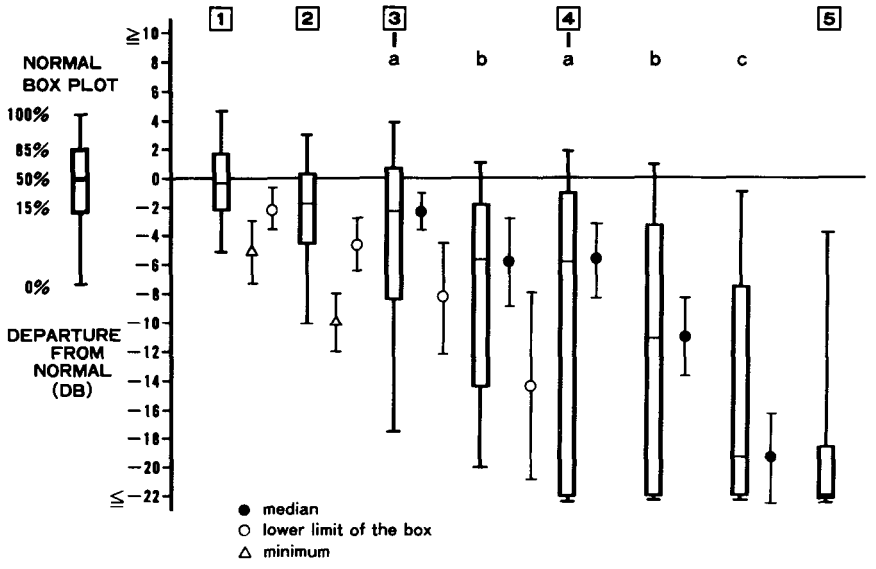

Fig 4 Five major stages and five minor subgroups

into three minor subgroups based on the median (Fig. 3c and d). Subgroup "a" consisted of fields with a single arcuate defect on HFA and its median was -8 dB or better. Subgroup "b" consisted of fields with double arcuate defects; its median was -9 to -15 dB. Subgroup "c" also had double arcuate defects but with a median of -16 to -21 dB. We propose a classification consisting of five major stages and five minor subgroups, as shown in Fig. 4 and Table 2.

Table 2a

Stage 1	Minimum -7 dB or better
Stage 2	Minimum -8 dB or worse Lower limit of box -7 dB or better
Stage 3	Lower limit of box depressed from -8 to -21 dB
Stage 4	Lower limit of box depressed to -22 dB or worse
Stage 5	Median reaches -22 dB or worse

Table 2b

Stage 3	
Subgroup "a"	Median -4 dB or better
Subgroup "b"	Median -5 dB or worse
Stage 4	
Subgroup "a"	Median -8 dB or better
Subgroup "b"	Median from -9 to -15 dB
Subgroup "c"	Median -16 dB or worse

Discussion

Classification and progressive states of glaucomatous visual fields measured by quantitative kinetic perimetry have been reported by various authors[2-7]. However, the results differ from examiner to examiner, due to subjective bias. Although there are objective evaluation criteria such as areas, measurement of three-dimensional visual fields[8,9] and the grid method of Esterman[10], these methods all require complicated calculations.

We used box plots because they give the objective information needed for the determination of a visual field defect and the depth of the depression. As a result, changes in glaucomatous

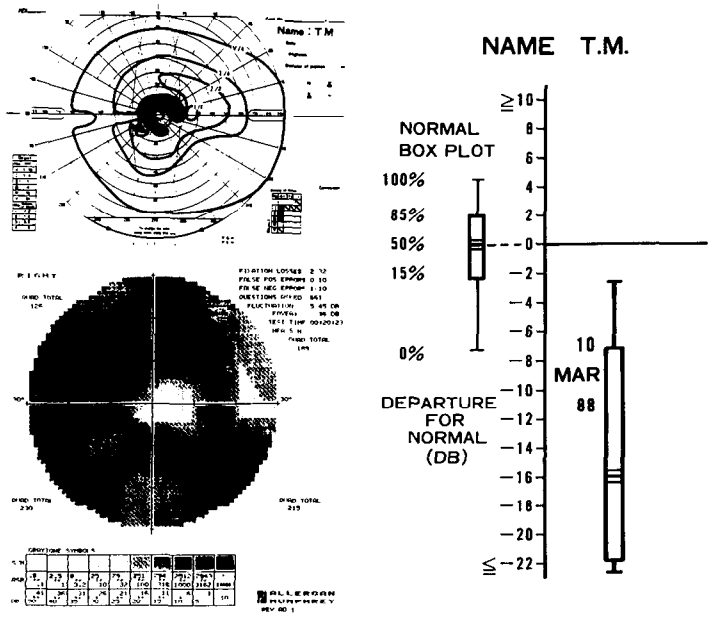

a.

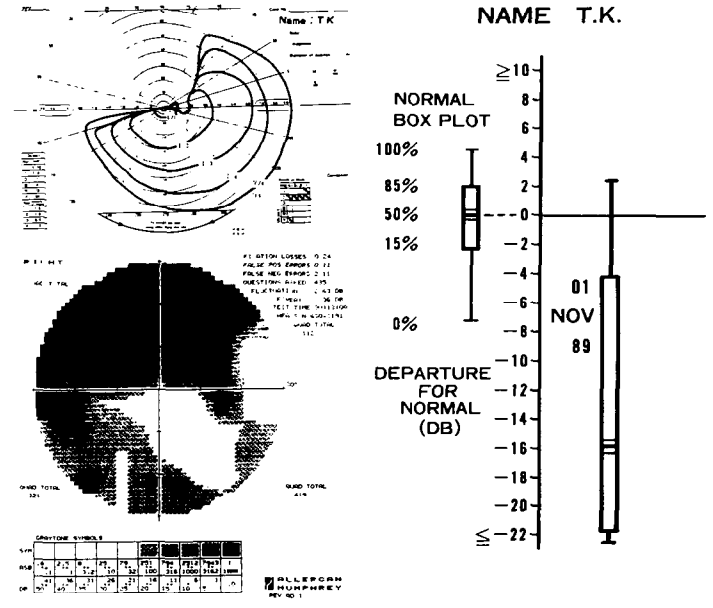

b.

Fig 5 a Double arcuate defects; b breakthrough

visual fields could be divided into five major stages, and further subdivided into five minor subgroups. In these five major stages, visual fields with GP were as follows:

- Stage 1: normal visual field or slight depression;
- Stage 2: normal visual field, slight depression or small isolated scotoma;
- Stage 3: nasal step with/without scotoma or single arcuate depression/defect;

- Stage 4: single arcuate defect with nasal step or double arcuate depression/defect;
- Stage 5: central and/or temporal rest.

As shown above, we found that even visual fields with the same box plot had different changes. For example, we found one case with double arcuate scotomas, as shown in Fig. 5a, and one field with breakthrough, as shown in Fig. 5b. The latter seemed to be a more advanced visual field change than the former. But it showed a similar depression when determined by HFA box plot. This discrepancy resulted from the fact that the HFA measured the field within the central 30 degrees, and that the HFA could detect depressions which kinetic perimetry failed to detect. The box plots were influenced not only by the depth of the defect but also by its extension.

We proposed that classification by box plots can offer a better and more objective method of evaluating glaucomatous visual field disturbance than conventional methods.

References

1. Heijl A, Lindgren G, Olsson J: A package for the statistical analysis of the visual fields Doc Ophthalmol Proc Ser 49:153-168, 1986
2 Richardson KT: Functional status of the glaucoma patient Invest Ophthalmol 11:102-107, 1972
3. Harrington DO: The Visual Fields, 3rd ed CV Mosby 1971
4 Traquair HM: Clinical detection of early changes in the visual field Arch Ophthalmol 22:947, 1939
5. Aulhorn E, Harms H: Early visual field defects in glaucoma Glaucoma Tutzing Symposium, pp 151-186 Basel: Karger 1966
6 Aulhorn E, Karmeyer H: Frequency distribution in early glaucomatous visual field defects Doc Ophthalmol Proc Ser 14:75-83, 1977
7 Drance SM: The early field defects in glaucoma Invest Ophthalmol 8:84-91, 1967
8. Hamada H, Juruno F, Matsuo H: Morphometric study of the quantitative kinetic perimetry Jpn J Ophthalmol 85:1644-1654, 1981
9 Suzumura H, Furuno F, Matsuo H: Volume of 3-dimensional visual field and its objective evaluation by shape coefficient: normal values by ages and abnormal visual field Fol Ophthalmol Jpn 34:2448-2457, 1983
10. Esterman B: Functional scoring of the binocular visual field Doc Ophthalmol Proc Ser 35:187-192, 1982

Improved threshold estimates using full staircase data

Jonny Olsson[1], Peter Åsman[1], Holger Rootzén[1] and Anders Heijl[2]

Departments of Mathematical Statistics[1] and Ophthalmology[2], Malmö General Hospital, University of Lund, Sweden

Abstract

In 1988 the authors described a method for estimation of reliability parameters based on maximum likelihood analysis. They have now developed a new algorithm for threshold estimation (Bayesian posterior mean threshold estimation, BPM) based on the same concepts. The method uses all patient responses and also to some extent spatial dependence of thresholds. The performance of the BPM method was studied in 20 eyes of ten normal subjects and 24 eyes of 15 patients with glaucomatous field loss All subjects underwent at least four 30-2 threshold tests on the Humphrey perimeter with approximately one week intervals. Pointwise inter-test threshold variances were calculated and averaged for each eye The use of BPM decreased these variances significantly in both groups ($p<0.001$); to 73% in the normal fields (range: 57%-93%) and to 93% in the glaucoma group (range: 61%-104%) Improvement of threshold estimates in glaucoma patients were seen mainly in fields with mild field loss Thus the reproducibility of threshold estimates may be significantly improved without any increase in test time, if all patient responses are utilized

Introduction

Decreasing the time required to administer perimetric tests, without loss in the quality of the data obtained, is an important task. It is, of course, trivial to decrease test time; one can for example devise a program which measures the threshold at each point less carefully. Such strategies are not attractive, however, because of the associated losses in reproducibility and accuracy. Similarly it is easy to increase reproducibility and accuracy; one needs only to measure each threshold several times. Patient fatigue will surely provide diminishing returns in such an endeavor, and there will be significant costs in increased clinical time.

Perimetric thresholds are usually estimated by staircase testing. Visual field results might then be viewed as an aggregate of staircases of stimulus intensities and responses, one staircase for each tested point. We and others have pointed out that there is information in these staircases which is as yet ignored and lost[1,2], because clinical threshold estimates now are based only on the points of reversals of the staircases.

At the IPS meeting in Vancouver, we described a method for using the otherwise ignored data in the staircases in order to estimate frequencies of false positive and false negative responses[2]. That method which is based on maximum likelihood analysis, can often reliably estimate these parameters from the staircases without the need to perform any catch trials at all

We have now carried this project further by developing an extension to that method, intended to improve estimation of thresholds, Bayesian posterior mean threshold estimation (BPM). The procedure estimates the threshold by the posterior mean[3], using all patient responses in the staircases. It can provide either higher quality data from the same thresholding procedures which are currently in use, or shorter tests with the same quality as is now available.

Estimation of perimetric thresholds

To use the BPM procedure two things are required: the probability of a staircase as a function of the threshold value and a prior distribution of the threshold value.

Address for correspondence Jonny Olsson, Department of Mathematical Statistics, Box 118, S-221 01 Lund, Sweden

Perimetry Update 1990/91, pp 245-249
Proceedings of the IXth International Perimetric Society Meeting,
Malmö, Sweden, June 17-20, 1990
edited by Richard P. Mills and Anders Heijl

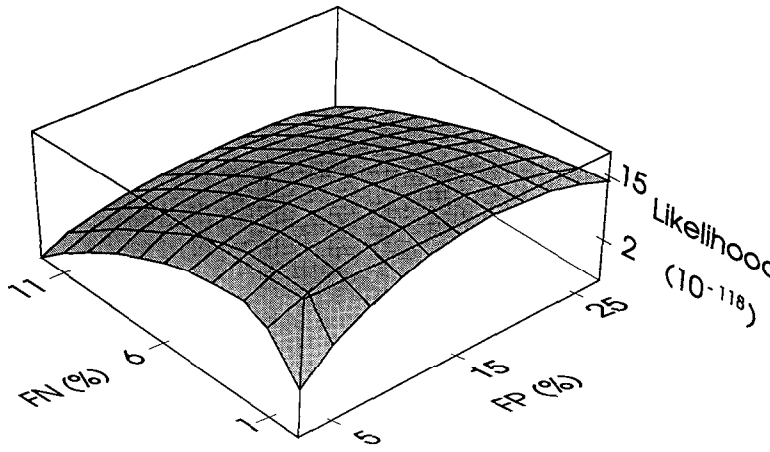

Fig 1 Likelihood function of aggregate of staircases in the 30-2 threshold test of one glaucoma subject Likelihood plotted versus FP and FN. Maximum likelihood estimates of FP (14 1%) and FN (1 3%) obtained at the maximum of surface Furthermore, likelihood depends on slope of frequency-of-seeing curve Results for σ = 3 dB, which gave the highest likelihood, are shown

To calculate the probability of a staircase the shape of the patient's frequency-of-seeing curve was needed. We assumed that the shape depended on the false positive ratio (FP), false negative ratio (FN), and a parameter describing the steepness of the frequency-of-seeing curve in the tested field (σ) as shown in Equation 2 below. These parameters were estimated using the aggregate of all staircases in the test, one staircase from each tested point. The estimation was performed by the maximum likelihood method[2]. An example of how the likelihood function of an aggregate of staircases depends on the FP and FN ratios is shown in Fig. 1

It would have been possible to estimate the threshold values by the maximum likelihood method. However, for reasons to be explained, the Bayesian procedure was chosen instead. A prior distribution of the deviation of initial stimulus intensity from the true threshold was specified. At a given test location, the intensity of the initial stimulus presentation in the Humphrey 30-2 test is based on thresholds in neighboring points and aims at being 3 dB below the true threshold This level will, of course, be influenced by chance. It is also likely that the prior distribution varies between subjects and between tests. We assumed the prior distribution to be Gaussian, and its mean, m_p and standard deviation, σ_p, were estimated for each field test.

Finally, we estimated the threshold values at each point using the probability of the staircase and the prior distribution. Thus, in the ith point the posterior mean threshold estimate was calculated and used as the threshold estimate, *i e* , by the formula

$$\text{estimated threshold}_i = \frac{\int_{-\infty}^{\infty} z \Pr(\text{staircase}_i) \frac{1}{\sigma_p} \phi \left(\frac{(z - (\text{initial stimulus level})_i) - m_p}{\sigma_p} \right) dz}{\int_{-\infty}^{\infty} \Pr(\text{staircase}_i) \frac{1}{\sigma_p} \phi \left(\frac{(z - (\text{initial stimulus level})_i) - m_p}{\sigma_p} \right) dz} \quad (1)$$

in which, for each point

$$\Pr(\text{staircase}) = \prod_{\textit{stimuli with responses}} \left(FP + (1 - FP - FN)\ \Phi \left(\frac{z - (\text{stimulus intensity})_j}{\sigma} \right)\right)$$

$$\times \prod_{\textit{stimuli without responses}} \left(1 - FP - (1 - FP - FN)\ \Phi \left(\frac{z - (\text{stimulus intensity})_j}{\sigma} \right)\right) \quad (2)$$

Here z represents the possible threshold values in dB and $(\text{stimulus intensity})_j$ is the jth stimulus intensity of the staircase in dB. The normal density function used for the prior distribution is denoted by ϕ, the normal distribution function used for the frequency-of-seeing curve by Φ, products by Π and probability by Pr.

The posterior mean threshold estimation offers two advantages as compared to a maximum likelihood estimation. First, it provides an explicit expression for the calculation of the threshold estimate. Second, by using the prior distribution, it gives the very estimate which minimizes the expected value of the square of the measurement error[3].

Testing of method

We wanted to compare the results of the BPM procedure with the traditional threshold estimates currently obtained in most perimeters. Humphrey 30-2 full threshold fields were measured prospectively in 20 eyes of ten normal subjects and 24 eyes of 15 patients with glaucoma using a special software enabling the storage of all stimulus presentations and responses. All eyes were tested a minimum of four times at one week intervals For each field pointwise threshold values were estimated with the BPM procedure as well as with the traditional method. Because of inevitable limitations in the dynamic range of perimeters, staircases in points with absolute defects will, of course, be truncated It is possible to use also these staircases but in the current version of the estimation program we did not use truncated staircases. Instead for the present study we modified the BPM procedure to set thresholds equal to the traditional estimates in points with truncated staircases and furthermore in all points of fields containing more than five such truncated staircases. In 12 of the 24 glaucoma eyes all fields had more than five such truncated staircases.

Comparison of threshold estimates

Ideally, threshold estimates should be both as close as possible to the true values (*i e* , have high accuracy) and as reproducible as possible (*i.e* , have a high degree of precision). The accuracy, or rather the comparability of the two methods was evaluated by calculating the average difference between the BPM and the traditional threshold estimates for each eye The reproducibility for the two methods was assessed by calculating test-retest variability for each eye. Thus, for each eye, the average of the pointwise inter-test threshold variances was calculated for each method Finally the ratio of the averages was calculated for each eye

Results

The BPM procedure gave slightly higher threshold estimates than the traditional method (Table 1), but the difference averaged only 0 1 dB The traditional estimates were actually the values (or the averages of the two values in case of double threshold determinations) appearing on the standard printout. Since these values represented the last seen level we added 1 dB to those values converting them to the average of the last two levels making them more comparable to the BPM estimates

Test-retest variability of the BPM procedure was significantly lower than that of the traditional method in both groups of eyes (Table 2). In normal fields the BPM procedure diminished the variance by 27% and in glaucomatous fields by 7%. The 7% reduction includes glaucomatous fields in which the BPM procedure was modified, as well as those in which it was not; in those glaucoma fields where the unmodified BPM procedure *was* used, variance was reduced by 13%. In the glaucoma group decreased variability was seen mainly in fields with mild field loss.

The standard deviations of the prior distributions, σ_p were found to be comparably small in the normal eyes but considerably higher in glaucomatous eyes (Table 3)

Table 1 Average differences between threshold estimates of new and traditional methods

Group	*n*	*Mean (dB)*	*SEM (dB)*	*Significance*
Normal	20	0.1	0.04	$p<0.001$
Glaucoma	24	0.1	0.03	$p<0.001$

Table 2 Ratio of test-retest variability of threshold estimates New versus traditional method

Group	*n*	*Mean ratio (%)*	*Range (%)*	*Significance*
Normal	20	73	57- 93	$p<0.001$
Glaucoma	24	93	61-104	$p<0.001$

Table 3. Estimated standard deviation, σ_p, of differences between initial stimulus level of thresholding algorithm and the true threshold estimates

Group	*n*	*Mean (dB)*
Normal	20	2.4
Glaucoma	24	6.2

Discussion

Our results demonstrate that the precision of perimetric threshold estimates may be significantly improved by using currently ignored information. Improvements were most pronounced in normal fields. A probable explanation is that the error of the predicted level of the true threshold has considerably smaller standard deviations in normal fields. Consequently, the prior distribution provided more spatial information regarding the true threshold values in normal fields.

We did not apply the Bayesian method to any truncated staircase for two reasons. The most important reason was to reduce computation time in the estimation of frequency-of-seeing curve parameters. That method was iterative, and to increase the speed, tables of numerical values of staircase probabilities were computed. The tables were handled much quicker if only non-truncated staircases were used. For the Posterior Mean threshold estimates (*c.f.*, Equation 1) computation time was short. The second reason was that points with a "true sensitivity" much below the 0 dB limit of the perimeter might cause violations of the assumptions on which the method is based. More precisely it is possible that the prior distribution is considerably different in such points. Excluding staircases, of course, influences the estimation of FP, FN and σ. Since the latter parameters are used by the BPM, this may then in turn affect the Bayesian threshold estimates in points with non-truncated staircases. This is also why the BPM procedure was modified to retain traditional threshold estimates in fields with more than five truncated staircases.

Traditionally, increased test quality is bought at the expense of increased test time and increased patient fatigue. In our opinion the described approach of improving test quality and/or reducing test time by analysis of available data using basic statistical principles, is so attractive that it must be used clinically Our particular method may be applied beneficially almost regardless of the actual test algorithm used. These types of methods are certainly quite computer-intensive, and they would have been very difficult to implement up to now. With increasing availability of computational power, however, these types of methods can and should be incorporated into clinical instruments.

The incorporation of prior knowledge of normal and abnormal fields can give even further improvements of the threshold estimation and test procedures[4]. Allowing both the prior distribution and the frequency-of-seeing curve to vary with eccentricity and defect depth as well as making use of truncated staircases might provide such improvements.

References

1. Lynn JR, Batson EP, Fellman RL: Internal inconsistencies vs root mean square as measures of threshold variability. Doc Ophthalmol Proc Ser 42:7-15, 1985
2. Olsson J, Rootzén H, Heijl A: Maximum likelihood estimation of the frequency of false positive and false negative answers from the up-and-down staircases of computerized threshold perimetry In: Heijl A (ed) Perimetry Update 1988/89, pp 245-251. Amsterdam/Berkeley/Milano: Kugler & Ghedini Publ 1989
3. Lindgren BW: In: Statistical Theory, 3rd edn, p 412. New York: Macmillan Publ Co 1976
4. Olsson J, Rootzén H, Heijl A: Improving perimetric threshold estimation without changing test procedures. Invest Ophthalmol Vis Sci (Suppl) 31/4:17, 1990

A rapid heuristic test procedure for automated perimetry

Chris A. Johnson[1] and Lionel R. Shapiro[1,2]

[1]*Optics and Visual Assessment Laboratory, Department of Ophthalmology, University of California, Davis;* [2]*Department of Cognitive Sciences, University of California, Irvine, CA, USA*

Abstract

RIOTS is a two phase heuristic test strategy for automated perimetry The first phase is a low resolution partitioning of the visual field, which uses a modified MOBS procedure[6,9] at critical primary visual field locations This establishes expectations for the second high resolution phase of RIOTS In the second phase, expected "seen" and "not seen" target locations are alternated in a checkerboard pattern Responses are evaluated by comparison with neighboring points, *a priori* population information, individual response reliability and a variety of decision rules to interactively determine subsequent presentations and hypotheses. Threshold estimates are obtained by reaching or exceeding predetermined decision criteria. By using their Kraken perimetry simulation program[8], the authors have demonstrated a significant improvement in performance of RIOTS as compared to the staircase procedures typically used for automated perimetry (*e g* , Humphrey full threshold test) Although RIOTS shows a slightly better test-retest reliability, its main advantage is a dramatic reduction in test time For both patients and normals, RIOTS requires 230 to 275 presentations for a central 30° visual field exam (Humphrey 30-2 test pattern), whereas the full threshold procedure includes between 325 and 500 presentations for normals and between 400 and 900 presentations for patients Test time for RIOTS is therefore six to eight minutes for all individuals, as compared to 12 to 27 minutes for the full threshold procedure Preliminary clinical comparison studies support the simulation results, except that the performance characteristics of RIOTS are slightly better than predicted. The authors have also found it possible to make simple classification judgments for patient reliability based solely upon information available within the RIOTS procedure This precludes the need for redundant threshold measurements to compute reliability measures

Introduction

Quantitative automated static perimeters currently use rapid staircase procedures to measure visual field sensitivity Previous studies (both computer simulations and clinical evaluations of patients) indicate that the accuracy and efficiency of these staircase procedures are at nearly optimal expected levels of performance Further refinements of staircase parameters are therefore unlikely to produce substantial improvements in either the accuracy or efficiency of automated perimetric test strategies, suggesting that a new methodology is needed[1-5]

In this view, we have developed a new heuristic test procedure for automated perimetry referred to as RIOTS (real-time interactive optimized test sequence). RIOTS (patent pending) was developed with the assistance of Kraken, a computer simulation program for perimetry RIOTS is a multi-pass strategy that utilizes *a priori* population characteristics, real-time comparison and correlation of neighboring test locations and a series of decision rules to establish threshold estimates for each visual field location in a highly efficient manner

RIOTS takes advantage of the fact that both normal and abnormal visual fields exhibit distinct and contiguous spatial patterns of sensitivity The sensitivity at each visual field location is not independent of other locations in the visual field, especially in immediate neighboring regions. RIOTS generates a pattern of expected response characteristics and analyzes the agreement between expected and obtained responses, as well as agreement between individual lo-

Supported in part by National Eye Institute Research Grant #EY03424 (to CAJ) and an Unrestricted Research Grant from Research to Prevent Blindness, Inc

Address for correspondence Chris A Johnson, Ph D , Optics & Visual Assessment Laboratory, Department of Ophthalmology, University of California, Davis, CA 95616, USA

Perimetry Update 1990/91, pp 251-256
Proceedings of the IXth International Perimetric Society Meeting,
Malmö, Sweden, June 17-20, 1990
edited by Richard P Mills and Anders Heijl

cations and their neighbors. Between passes of RIOTS, heuristic decision rules are applied to detect response errors, refine threshold estimates and define areas of high, intermediate and low agreement. RIOTS uses an average of 3.0 to 3.4 stimulus presentations per location to obtain threshold measurements. Fankhauser and his associates have previously reported a multi-pass strategy for visual field evaluation that utilized spatial information[6]. However, their spatial analysis was primarily directed towards detection of scotomas and discrimination of real *versus* pseudoscotomas; subsequent evaluation of visual field loss was then determined by staircase procedures. RIOTS differs from this previous approach by using a much smaller number of stimulus presentations, a different method of deriving initial threshold estimates, and utilizing a series of neighbor comparisons and decision rules to obtain final threshold values.

Methods and procedure

In this paper, we describe the RIOTS test strategy as it has been applied to the Humphrey Field Analyzer 30-2 target presentation pattern. However, RIOTS can be implemented for any target presentation pattern that contains a regular geometric relationship of target locations in Cartesian or polar coordinate space.

A schematic representation of the sequence of testing for RIOTS is shown in Fig. 1. The initial stage of RIOTS (Pass 0) consists of threshold determinations at 12 "seed" and two blind spot locations. Seed locations are strategically placed so that all other visual field locations are neighbors. Thresholds are determined by a MOBS (modified binary search[7]) procedure that has been optimized for clinical automated perimetry applications The enhanced MOBS procedure provides significantly greater accuracy and reproducibility over standard staircase procedures used in automated perimetry. Approximately one-third of the total test time is devoted to ensuring that there are accurate determinations of the seed points.

Thresholds for seed locations are used to calculate expected thresholds for other locations. All visual field locations are then arranged in a checkerboard pattern of "expected seen" (pre-

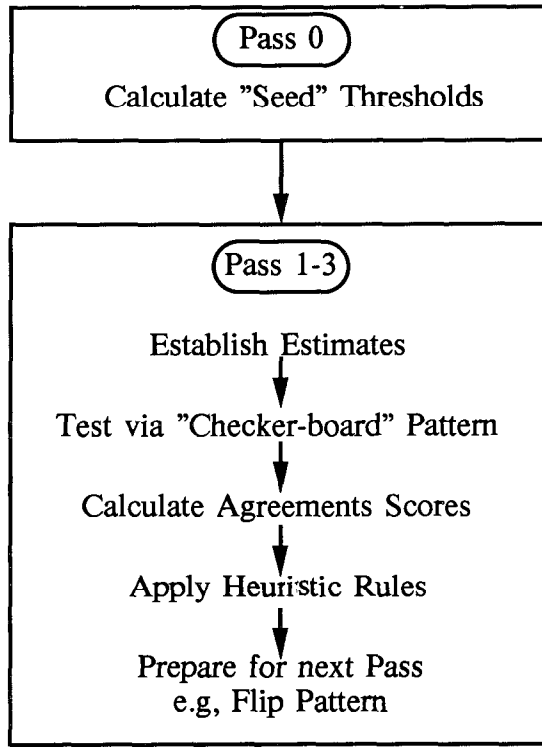

Fig 1 Outline of procedural flow for RIOTS.

sumed super-threshold) and "expected not seen" (presumed sub-threshold) targets for Pass 1. The interval between presumed super- and sub-threshold stimuli is individually adjusted for each location, based on optimal results from simulation studies. A single stimulus presentation is made for each location (except for seed locations).

Following Pass 1, the degree and spatial pattern of agreement is evaluated for each location and its neighbors. Locations for which the agreement pattern suggests a spurious response (false positive or false negative) are immediately rechecked. The checkerboard is then reversed ("expected seen" locations become "expected not seen" and *vice versa*) after heuristic decision rules have adjusted the expected threshold value and the interval between presumed super and sub-threshold stimuli at each individual location.

Pass 2 is then conducted by performing a single stimulus presentation at each location (except for seed locations). Following Pass 2, the degree and spatial pattern of agreement is again evaluated for each location and its neighbors, and spurious responses are promptly retested. Pass 3 is only performed for those locations that have not yet achieved the criteria for good agreement. For Pass 3, the checkerboard is again reversed and other parameters are adjusted according to optimal heuristic decision rules identified from our simulation studies.

Results

Extensive computer simulation comparisons of RIOTS and standard staircase procedures (Humphrey Field Analyzer 30-2 strategy) have been conducted for normal and abnormal visual fields for a variety of response characteristics (response fluctuations, false positive and false negative errors) using the Kraken simulation program[8]. These studies indicate that RIOTS is slightly more accurate, but is considerably more efficient than standard staircase procedures, especially for abnormal visual fields Typically, RIOTS is 1.5 to 2.0 times faster than the 30-2 test strategy for normal observers, and is two to three times faster for observers with abnormal visual fields. Unlike standard procedures, RIOTS exhibits little or no difference in testing time for normal and abnormal visual fields. RIOTS is also more resistant to response variability and response errors (false positives and false negatives) than standard staircase procedures. An example of our simulation comparisons is presented in Table 1. The average accuracy (difference between actual and obtained thresholds in dB) and efficiency (total number of presentations) of RIOTS and the 30-2 test strategy are presented for 350 normal visual fields with 0 to 5 dB of response variability (fluctuation). Note that the differences between RIOTS and the 30-2 strategy become greater as response variability increases. A similar pattern of results occurs for various false positive rates, false negative rates and various combinations of fluctuation and response errors. All of these characteristics are augmented for abnormal visual fields with localized visual field loss.

Table 1 Mean performance characteristics for differing levels of response variability*

	Variation (dB)					
	0	*1*	*2*	*3*	*4*	*5*
*Accuracy***						
30-2	0.49	1.29	1 53	1 78	2.03	2 33
RIOTS	0.18	0 72	0 81	0 98	1 16	1 36
*Efficiency****						
30-2	322 7	356.6	376 4	396.1	412 5	424.4
RIOTS	226 7	241.2	257.9	268.1	272.6	278.5

*based on 350 tests per mean; **difference of actual-test (dB); ***mean number of presentations

Preliminary clinical comparison studies of RIOTS *versus* standard automated perimetry test strategies are in agreement with the predictions of simulation studies. To date, our clinical studies confirm the greater efficiency of RIOTS. In addition, RIOTS appears to have slightly better test-retest reliability. RIOTS often reports slightly higher sensitivity than standard procedures, especially for the superior visual field. This may be due to a diminishing of fatigue effects as a result of the dramatic reduction in testing time.

Existing test procedures in automated perimetry frequently obtain information about the

patient's response reliability during testing by evaluating the response to double threshold determinations (short-term fluctuation), false positive trials, false negative trials and targets presented to the blind spot region (fixation losses). The added stimulus trials needed to obtain this information can add a significant amount of test time.

Since the main advantage of RIOTS over existing automated perimetry test procedures is the large reduction in test time, it would be desirable to obtain information about the patient's reliability during the test without the necessity of performing additional stimulus presentations. Schulzer and his colleagues have recently shown that it is possible to accurately determine the short-term fluctuation of a visual field, without the need for double determinations, through the use of a statistical model applied to the threshold data[9]. In this view, we have derived an analysis procedure that allows the patient's response reliability to be assigned to good, fair or poor categories. Rather than using a statistical model, we apply a Boolean logic model to derive a set of optimal decision rules for classifying response reliability.

A key element of the RIOTS test procedure is its ability to rapidly recognize response errors and inconsistencies during the test procedure through comparisons of expected *versus* actual responses and comparisons of responses at one location with those of neighboring locations. We analyzed this information to determine whether it could be used to categorize a patient's response reliability. One of the many functions performed by RIOTS is the immediate retesting of locations that reflect spurious or inconsistent responses (as determined by the heuristics present in the RIOTS strategy). Since this retesting is often a direct consequence of response errors and variability, we examined the total number of retests, and the pattern of retested points for EXPECTED SEEN and EXPECTED NOT SEEN locations on passes 1, 2 and 3 of the RIOTS procedure This evaluation was then used to determine optimal methods of sorting the visual field results into good, fair and poor response reliability.

The previous visual field data represented in Table 1 (350 normal visual fields with 0 to 5 dB of response variability) was reanalyzed. We determined the optimal method of sorting the results into good (0 and 1 dB), fair (2 and 3 dB) and poor (4 and 5 dB) reliability categories on the basis of the pattern of retested points. We were able to find decision rules which were highly successful in isolating the three response reliability categories.

Table 2 Classification performance by rules (values are proportional accounted for by appropriate application of rules)

	Variation (dB)					
	0	*1*	*2*	*3*	*4*	*5*
Good reliability						
rule	0 994	0 891	0 337	0 160	0.183	0.182
rule + unique cases	0 994	0 891	0 051	0 006	0.000	0 000
Poor reliability						
rule	0.009	0.151	0.717	0 822	0 817	0.897
rule + unique cases	0 003	0 034	0 551	0 486	0 809	0.903

The results of applying the optimal "good reliability" decision rule (less than seven total retests *and* less than two retests for "expected not seen" locations on pass 1) are presented in Table 2. The proportion of cases satisfying the "good reliability" decision rule is shown in the "rule" row for each of the variability levels. Removing unique cases (response patterns that never occur with low variability) yielded even better separation of the 0 and 1 dB tests from the 2-5 dB variation. Table 2 also presents the results of applying the optimal "poor reliability" decision rule (greater than eight total retests OR 1 or more retests for "expected not seen" locations on pass 3). Again removing unique cases (response patterns that never occur with high variability) improved the isolation of "poor reliability" cases.

The results of applying both rules,with their respective unique cases, to the group of simulated visual field tests (350 normal eyes, 0 to 5 dB of response variability) is shown in Table 3. These findings demonstrate that it is possible to accurately categorize a patient's response reliability (good, fair, poor) during automated perimetry using the RIOTS test strategy without the need for performing additional stimulus presentations.

New methods of analysis of serial visual fields

Marshall Cyrlin[1,4], Joseph Rosenshein[2,3], Steven Cunningham, Charles Tressler[4], Christine Czedik[4] and Roselyn Fazio[4]

[1]*Michigan State University, Lansing;* [2]*Sinai Hospital, Detroit;* [3]*Oakland University, Rochester;* [4]*Franklin Eye Consultants, Southfield; Michigan, USA*

Abstract

The authors have developed new methods for displaying and analyzing serial automated visual field data Using a computer graphic display, field losses at all 76 points of the Octopus 32 field can be seen for up to 16 different exams on a single map of the field This view allows trends in local and diffuse field loss to be rapidly identified as well as sequelae of treatment. They then consider the threshold sensitivity of each point in the field to represent a vector lying along one dimension in n-dimensional space where n equals the total number of points tested They calculate the total field vector (TFV) which is representative of the overall state of the field. Diffuse loss (or gain) in sensitivity is seen as the difference in magnitude between the TFV and a calculated normal field vector (NFV). The distribution of the threshold sensitivities is represented by the vector angle (VA) between the TFV and the NFV An increasing VA would thus correspond to a focal change in sensitivity. A change in the TFV length without a change in the VA would correspond to a diffuse change Analysis of a series of fields using this method yields a "trajectory" of the visual field in vector space which can be used to characterize the localization and magnitude of field changes The authors will present the strengths and weaknesses of this approach as compared with standard Global Indices and the Delta program to evaluate a series of Octopus #32 visual fields in patients with unstable glaucoma.

Introduction

The evaluation of change in a series of automated visual fields is difficult without the calculation of global indices and graphical displays of the visual field data The Octopus Delta software program[1], the Octopus G1 field indices[2] and the Humphrey StatPac[3] are examples of methods for evaluating serial visual field data.

We have developed the multi-dimensional vector field analysis (MDVFA) indices of MDVFA loss and MDVFA angle as alternatives to the calculation of mean defect and corrected loss variance respectively. We felt that identifying the state of the overall field by using a multi-dimensional vector approach would enable the clinician or researcher to better characterize the current state and trends in the patient's field than with the standard indices of visual fields[2,4]. The multi-dimensional vector representation has been used in many different applications requiring comparisons of complex data such as in database searches[5]. The application of this representation gives similar results to the mean defect in terms of overall loss, but this representation seems to be more robust and informative about the degree of inhomogeneity of the visual field than is the corrected loss variance (CLV) which is typically associated with the degree of localization of defects.

In addition, it is useful to be able to visualize point by point changes in sensitivity and determine trends with regression and time series analysis techniques[6-8]. We have developed a new way, the Serial Graphic Display© (SGD), for displaying on a single plot all of the points in a series of up to 16 visual fields with a trend analysis to illustrate the significance and direction of the linear trend at each point in the field. This method facilitates the easy identification of local changes and can be used in conjunction with the MDVFA indices for making decisions regarding serial changes in fields.

Address for correspondence Marshall N Cyrlin, M D , Franklin Eye Consultants, 29275 Northwestern Highway, Suite 100, Southfield, MI 48034, USA

Perimetry Update 1990/91, pp. 257-271
Proceedings of the IXth International Perimetric Society Meeting,
Malmö, Sweden, June 17-20, 1990
edited by Richard P. Mills and Anders Heijl

Methods

Data from an Octopus 201 perimeter were transmitted via an RS232 port to an IBM PC-compatible computer using the Octopus BATRAN software and a custom reception program. The transmitted field data was stored in ASCII format and then converted to the database format of KnowledgeMan (KMAN), a database management program commercially available from MDBS, Inc.

The custom serial visual field analysis software we have developed using KMAN performs and graphs a multi-dimensional vector field analysis (MDVFA) and plots a Serial Graphic Display© (SGD) of all the points in every field of a series of tests. In addition, the custom software calculates and plots the standard global indices for comparison with the results of the MDVFA. The custom software provides a screen display of the serial visual field data and a printout of the screen display. The descriptive data from each Octopus test, the calculated values of the MDVFA and the global indices are also available in ASCII format for export to other applications for further analysis and display.

Calculating the total field vector (TFV)

An Octopus Program 32 visual field consists of the measurement of the sensitivity at 76 points. We use the 74 points outside the blindspot to calculate a 74 dimensional TFV. We illustrate the calculation of the TFV using a simplified visual field which consists of only three points resulting in a three dimensional vector space.

Imagine a simple visual field consisting of only three points whose sensitivities are P_1, P_2 and P_3. We construct a three-dimensional vector space by assigning a vector, P, to each point. The length of each vector is proportional to the sensitivity of the point, and the direction of the vector is perpendicular (orthogonal) to all the others. The vectors are added together, using conventional vector addition, to obtain the TFV as shown in Fig 1.

Note: the MDVFA assumption of independence of each point in the visual field to allow for the assignment of each point to an orthogonal dimension is not completely correct. There is some correlation between the value of each point measured in the visual field and the values of its neighbors. It will require further work to determine the minimal number of vectors required to represent the field which are orthogonal and independent. However, as long as the vector assignments are made consistently (as they are in our method), the results will be useful and consistently related to each other.

The length of the TFV is determined as follows: Since P_1 and P_2 are orthogonal, we can calculate an intermediate vector $P_{1,2}$ using the Pythagorean Theorem.

The length of $P_{1,2}$ is:

$$|P_{1,2}| = (P_1^2 + P_2^2)^{-1/2}$$

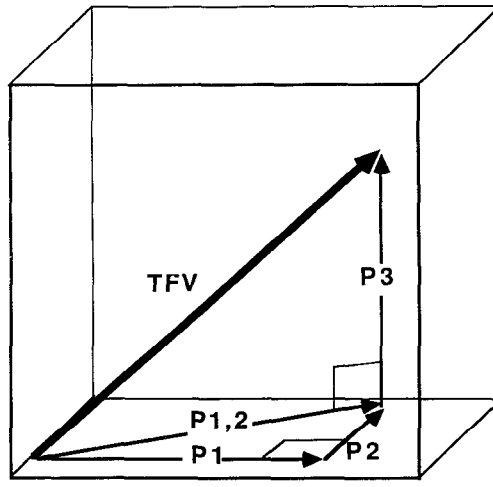

Fig 1 Vector addition for the calculation of the total field vector (TFV)

Table 3 Overall performance of classification by applying both rules (values are proportional accounted for by appropriate application of rules)

	Variation (dB)					
	0	*1*	*2*	*3*	*4*	*5*
Good[a]	0 994	0.891	0 051	0 006	0 00	0.000
Fair[b]	0.003	0.075	0.438	0 508	0.191	0 097
Poor[c]	0.003	0 034	0 511	0.486	0.809	0 903

[a](A*(¬B)); [b](A*B)+((¬A)*(¬B)); [c](B*(¬A)); where A is defined as the application of the "good reliability" + unique cases rule, and B is defined as the application of the "poor reliability" + unique cases rule
Note: * is logical *and*; + is logical *or*; ¬ is logical *not*

Our current analysis is based solely on the number and pattern of retests for "expected seen" and "expected not seen" locations on passes 1, 2 and 3 of the RIOTS test procedure. However, it is also possible to extend this analysis procedure by examining additional parameters (*e.g.*, the level and pattern of neighbor agreement for each location on each pass of the RIOTS strategy). In this manner, it may be possible to generate a quantitative estimate of reliability and the contribution of different sources of variability (response fluctuation, false positives, false negatives, etc.) to the patient's overall response reliability during testing.

The current process of categorizing the patient's response reliability as good, fair or poor is satisfactory for most practical clinical purposes. Good reliability indicates that a high degree of confidence can be placed in the test results, whereas poor reliability suggests that the patient's response inconsistency may have significantly affected the test results. Fair reliability suggests that one should be cautious of the influence of response variability on the test results

In the present study, we set a criterion of greater than 3 dB as an indicator of poor reliability, less than 2 dB as an indicator of good reliability, and 2 to 3 dB as an indicator of fair reliability. Ideally, good, fair and poor categories should be determined by population studies of normal individuals at all ages The results of large population studies will require slight alterations of our optimal decision rules, but the procedure can still be used as an effective means of analyzing the patient's response reliability during automated perimetric evaluations using the RIOTS test strategy.

Discussion

RIOTS has several advantages over conventional automated perimetry test strategies based on staircase procedures: (1) RIOTS is significantly more efficient; it requires considerably fewer presentations to complete testing. (2) RIOTS has a more consistent test time; normals and patients with visual field loss are all tested in 230 to 275 presentations, regardless of response variability. (3) RIOTS has slightly better accuracy. (4) RIOTS has slightly better test-retest reliability. (5) RIOTS performs immediate detection and correction of response errors. (6) RIOTS is less susceptible to the influences of fatigue and boredom (7) By examining the neighborhood agreement matrices for RIOTS, it is possible to accurately classify response reliability as good, fair or poor without the need for additional "catch" trials.

References

1 Fankhauser F, Bebie H: Threshold fluctuations, interpolations and spatial resolution in perimetry Doc Ophthalmol Proc Ser 19:295-309, 1979
2. Heijl A Computer test logics for automated perimetry Acta Ophthalmol 55:837, 1977
3. Johnson CA: The test logic of automated perimetry. In: Henkind (ed) Acta: XXIV International Congress of Ophthalmology. Philadelphia: JB Lippincott 1983
4. Johnson CA: Properties of staircases in automated perimetry. Invest Ophthalmol Vis Sci (Suppl) 26:217, 1985
5 Johnson CA, Shapiro LR: A comparison of MOBS (modified binary search) and staircase test procedures in automated perimetry: noninvasive assessment of the visual system 1989 Technical Digest Series 7:84-87, 1989

6. Fankhauser F, Koch P, Roulier A: On automation of perimetry. Graefe's Arch Klin Exp Ophthalmol 184:126-150, 1972
7 Tyrrell RA, Owens DA: A rapid technique to assess the resting states of the eyes and other threshold phenomena: the modified binary search (MOBS). Behav Res Methods Instruments & Computers 20:137-141, 1988
8. Shapiro LR, Johnson CA, Kennedy RL: Kraken: a computer simulation procedure for static, kinetic, suprathreshold static and heuristic perimetry. In: Heijl A (ed) Perimetry Update 1988/89: Proceedings of the VIIIth International Perimetry Society Meeting. Amsterdam/Berkeley/Milano: Kugler & Ghedini 1989
9. Schulzer M, Mills RP, Hopp RH, Lau, W, Drance, SM: Estimation of the short-term fluctuation from a single determination of the visual field Invest Ophthalmol Vis Sci 31/4:730-735, 1990

Notice that $P_{1,2}$ is orthogonal to P_3 since $P_{1,2}$ lies in the plane of P_1 and P_2 both of which are orthogonal to P_3. So we can use the Pythagorean Theorem again to calculate |TFV|:

$$|TFV| = (P_1^2 + P_2^2 + P_3^2)^{-1/2}$$

This calculation can then be extended to any n dimensions:

$$|TFV| = (P_1^2 + P_2^2 + P_3^2 + \ldots P_n^2)^{-1/2} \quad (1)$$

For the case of the Octopus Program 32 field with 74 points, $n = 74$.

Calculating the vector angle (VA)

The TFV has length and a direction. The direction of the TFV is referenced to the age normal visual field vector (NFV). The vector angle (VA) between the TFV and the NFV can be calculated from the vector dot (inner) product between the TFV and the NFV The vector dot product is defined as the product of the length of the NFV with the length of the perpendicular projection of the TFV onto the NFV. This can be seen in Fig. 2.

In this calculation, the lengths of the vectors TFV and NFV will be represented by |TFV| and |NFV| to distinguish them from the actual vector quantities. Both |TFV| and |NFV| can be calculated from Equation (1).

The vector dot product is defined as:

$$TFV \quad NFV = \Sigma T_i \quad N_i = |TFV| \quad |NFV| \quad \text{Cos (VA)} \quad (2)$$

Where $\Sigma T_i \quad N_i = T_1 \quad N_1 + T_2 \cdot N_2 + \ldots T_n \quad N_n$ and $n = 74$ in this case.

The T_i's and N_i's are the i^{th} components of the TFV and the NFV, respectively.

The angle between TFV and NFV can be found by solving Equation (2) for VA:

$$VA = \text{arcCos} \; (\Sigma \; T_i \cdot N_i) \div (|TFV| \quad |NFV|) \quad (3)$$

The MDVFA requires linearization of the sensitivity values of the field to calculate the VA while the actual sensitivities in dB (log units) are used to calculate |TFV| and |NFV| otherwise. This inelegant necessity results from the difference in mapping length and angle quantities in the vector space when the field values are nonlinear units (dB). In order to maintain angles under uniform scaling, it is necessary to linearize the values of the sensitivities of points used to calculate VA, *i e.*, T_i, N_i, |TFV| and |NFV|, in Equation (3) by the following conversion:

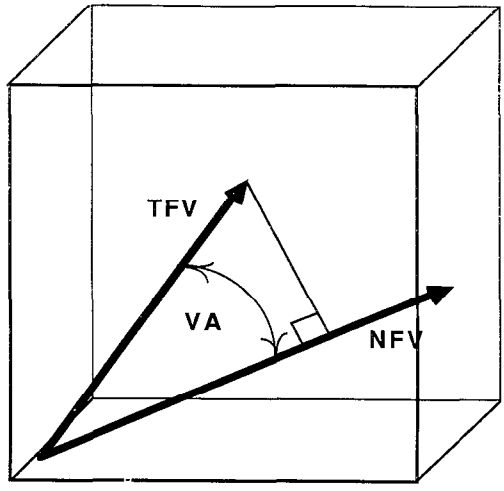

Fig 2 Relationship of total field vector (TFV) and normal field vector (NFV) in the calculation of the inner product to find the vector angle (VA)

Linear value of $P_i = 10^{Pi/10}$

Where P_i = sensitivity (in dB) of the point i.

Diffuse loss

The effect of a uniform reduction of sensitivity in the visual field due to a cataract or diffuse glaucomatous loss leads to a reduction in |TFV| but does not result in a significant change in the VA.

For example: Suppose there is a 6 dB loss of sensitivity in each of the three points of the simple visual field TFV of our previous example shown in Fig. 1. Let the initial values of P_1, P_2 and P_3 be 30 dB each. The loss results in final values of 24 dB for each of the points. We assume correspondingly simple age normal field values of 30 dB for each of the three points of the normal field.

Using Equation (1) to calculate |TFV| and |NFV|, we find:

Original $|TFV| = (3 \cdot 30^2)^{-1/2} = 52$ dB = |NFV|
Final $|TFV| = (3 \quad 24^2)^{-1/2} = 41.6$ dB
|NFV| - |TFV| = -10.4 dB

Linearizing the sensitivities for the VA calculation results in the initial values of P_1, P_2 and P_3 becoming:

Initial $P = 10^{30/10} = 10^3 = 1000$

and the final values become:

Final $P = 10^{24/10} = 10^{2\,4} = 251.2$
Original linear $|TFV| = (3 \cdot 1000^2)^{-1/2} = 1732$
Final linear $|TFV| = (3 \cdot 251.2^2)^{-1/2} = 435$

The original VA = 0 since the TFV and the NFV are identical. The final VA is:

$$VA = \arccos \{3 \quad (251.2 \cdot 1000) \div (1732 \cdot 435)\} = \arccos \{1\} = 0$$

Since the original VA = final VA = 0, there is no change in angle, only a decrease in the length of the TFV as shown in Fig. 3

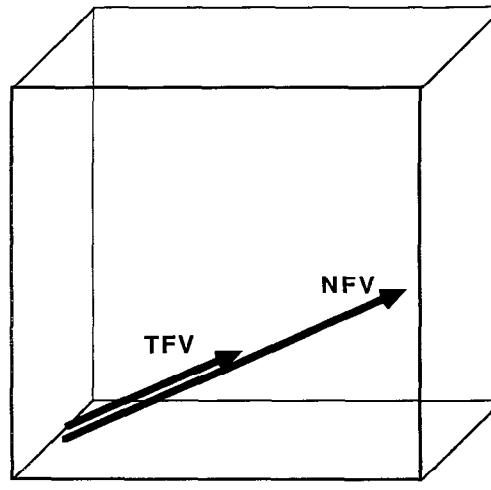

Fig 3 Illustration of diffuse loss The TFV is reduced with respect to the NFV, but remains oriented in the same direction

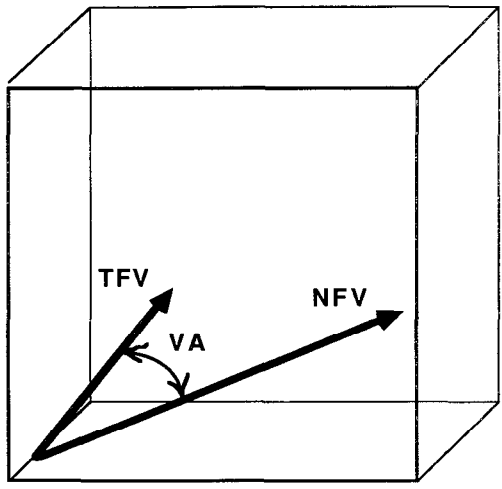

Fig 4 Illustration of local loss The vector angle (VA) increases as the length of the TFV decreases somewhat

Localized loss

In the case where there is a localized defect in the visual field, there will be a nonuniform reduction of the sensitivities of the points in the visual field. An example of such a localized defect might be a glaucomatous scotoma. The effect of a non-uniform reduction of the field values leads to both a reduction of the length of the TFV with respect to the NFV and a change in the VA with respect to the NFV. This can be seen in Fig. 4.

The value of the VA is correlated with the non-uniformity of the change in the field while the difference between the |TFV| and the |NFV| corresponds to the magnitude of the defect in the entire field. Calculating values of the VA and the change in |TFV| for the hemispheres or quadrants gives an even more precise evaluation of the nature and location of the change in the field.

In cases where there is a localized improvement of a defect, there will be a corresponding increase in |TFV| and a decrease in VA as the values of the field points approach their normal values. As a defect enlarges in extent, the VA would first increase as the field becomes more inhomogeneous, and then decrease as the spreading of the defect produced a more uniform, but depressed field.

Application of MDVFA to patient data

We use the calculated values of |NFV|, |TFV|, and VA to calculate a new set of global indices: the MDVFA loss and MDVFA angle. The MDVFA calculation was carried out for up to 16 serial visual fields for individual patients. The |TFV|, |NFV| and VA were calculated for each field along with the global indices for the whole field, the upper and lower hemifields, and the temporal, nasal, upper and lower quadrants. The MDVFA data are presented as MDVFA loss and MDVFA angle. These values are calculated as follows:

$$\text{MDVFA loss} = 100 \quad (|\text{NFV}| - |\text{TFV}|) \div |\text{NFV}|$$
$$\text{MDVFA angle} = 100 \quad \text{VA} \div (\pi/2)$$

For the purposes of comparison, the global indices of mean defect and corrected loss variance (CLV) are calculated as follows:

$$\%\text{mean defect} = 100 \quad \text{mean defect} \div \text{age normal mean sensitivity}$$
$$\text{LOG10 CLV} = \log_{10} \text{CLV}$$

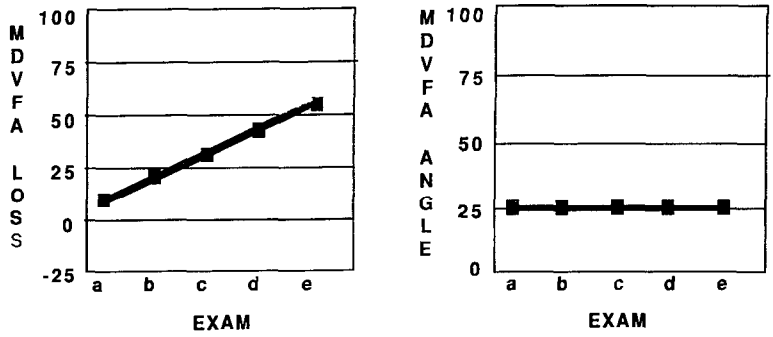

Fig 5 Illustration of MDVFA loss and MDVFA angle graphs for simulated progressive diffuse field loss.

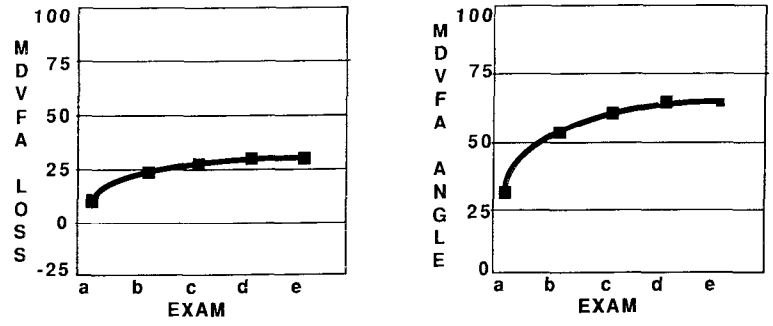

Fig 6 Illustration of MDVFA loss and MDVFA angle graphs for simulated, progressive localized (non-uniform) field loss.

Normalization of the changes as percentages of normal or reference values provides a more consistent and meaningful presentation of the data for comparison purposes than does absolute change in values.

Note: in the illustrations and patient examples which follow, the data are presented for serial exams and are *not* displayed as a function of time.

MDVFA illustrations of diffuse and local loss

Pure progressive diffuse loss. In this illustration, the field starts out with a 3 dB uniform depression of sensitivity and then uniformly decreases 3 dB with each subsequent exam. The MDVFA loss increases uniformly with each exam but the MDVFA angle remains unchanged as shown in Fig. 5

Pure progressive local loss · In this case, an initial, limited scotoma deepens without spreading in each successive test. The MDVFA loss increases until reaching a limit, while the MDVFA angle rises rapidly initially and also saturates as the scotoma becomes absolute as shown in Fig. 6.

Serial Graphic Display© (SGD) of visual fields

On single display, for a series of up to 16 of visual fields, SGD shows relative change of sensitivity (ΔS) at every point tested: up to 1216 values of ΔS simultaneously. The relative

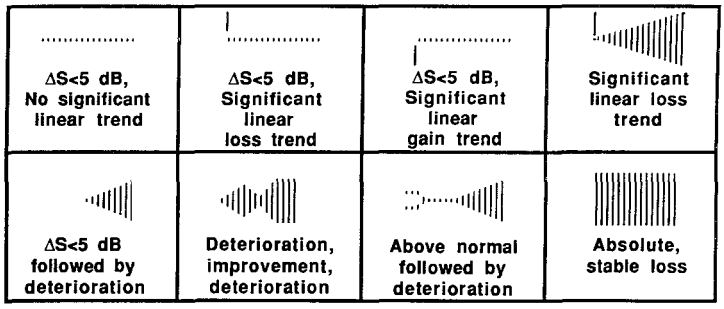

Fig 7 Illustration of typical patterns in display of sensitivity change at a single point of the field in the Serial Graphic Display© (SGD)

change in sensitivity, ΔS, is the actual value minus the reference value. The reference can be age-adjusted normal values or the values of a patient's baseline test

In the SGD, the ΔS for a test is displayed as a vertical line of variable length symmetrically placed about the zero axis at each point in the field The ratio,

$$R = \Delta S \div \text{display line length},$$

is a vertical scaling factor. Usually, R is set at 4 dB per symmetric pixel pair to show the full range of possible change The use of a symmetric display of a vertical line representing ΔS in the SGD enhances the pattern of change at each point and makes the pattern more easily discerned.

The relative change in sensitivity is represented as:

Solid line = Loss ($\Delta S \leq 0$)
Vertical space bounded by dots = Gain ($\Delta S \leq 0$).

A linear regression was performed for ΔS versus time at each point measured in the field. The chi-squared test was used to find the "goodness of fit" of the regression line. Significance bars (up indicates deteriorating trend, down indicates improving trend) are plotted preceding the series of ΔS lines at some points. The length of the bar indicates the significance of the fit. The minimum slope of the linear regression line to be considered significant (and thus displayed) could be set at any value. In the cases shown in this paper, the minimum slope to be indicated was set at 0.2 dB per year although it could have been set at 2 dB per year or even more. The value of 0.2 dB per year was chosen since it is twice the normal aging loss of 0.1 dB per year which is seen in the age normal values for the Octopus program 32.

Some typical patterns of change in sensitivities at a single point are illustrated in Fig. 7.

Results

Example 1 · progressive loss

Progressive loss is shown in Figs. 8a, b and c. The MDVFA loss graph shows the sporadic changes in the examinations A through G. The field improves and eventually stabilizes in the examinations H through L in this series of 12 tests in the right eye of this patient with progressive glaucoma. The MDVFA angle graph illustrates that the rapid increase in localization in the upper hemisphere is greater than in the lower hemisphere. This asymmetry is not as clearly depicted by the LOG10 CLV graph. The SGD clearly shows the areas in which the changes in sensitivity for each examination are localized. The significance bars, indicating significant deterioration trends, are circled for emphasis.

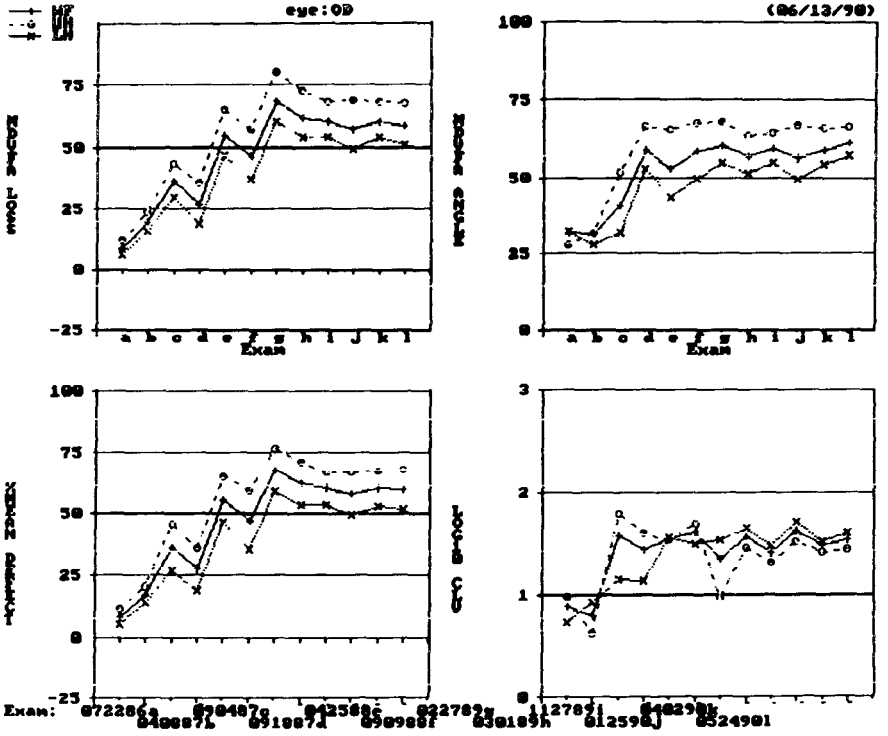

Fig 8a Example 1: progressive loss is shown in these graphs of the MDVFA and global indices.

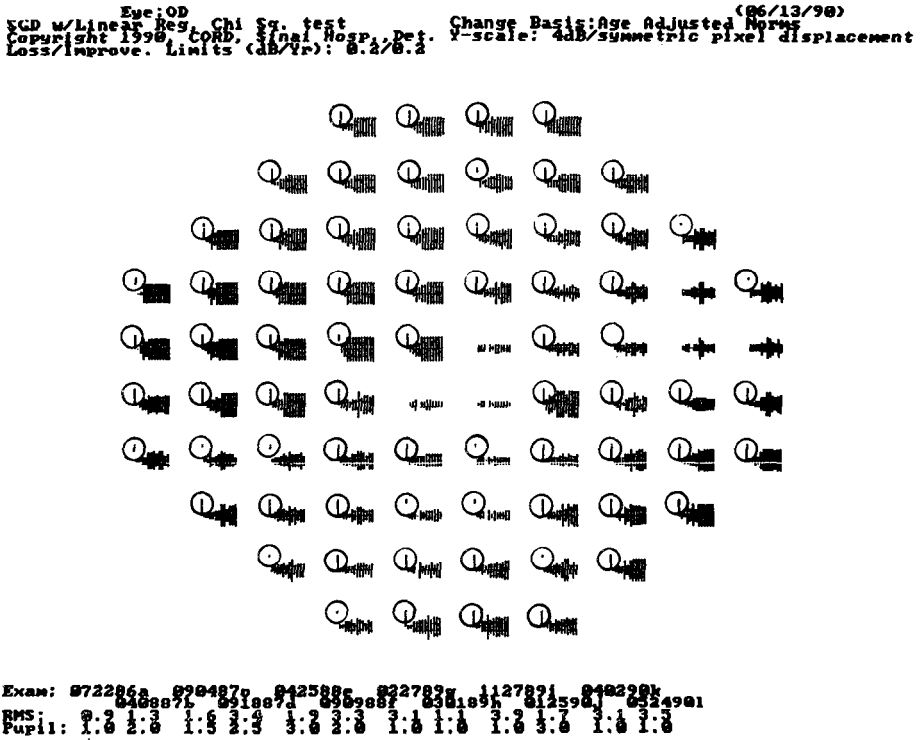

Fig 8b Example 1: progressive loss is shown by the SGD

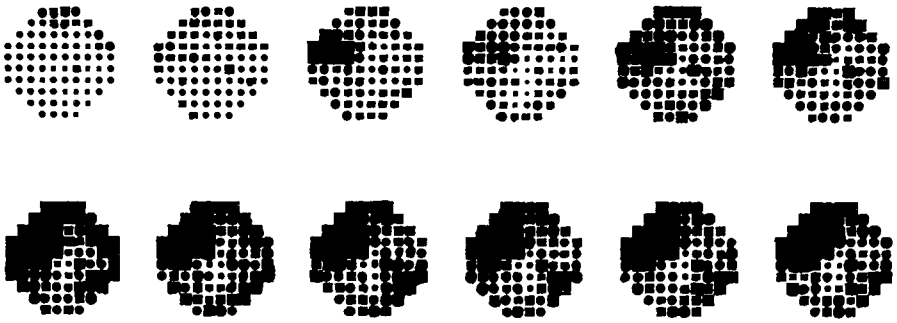

Fig. 8c. Example 1: progressive loss in the Delta series printouts (shown for comparison)

Example 2. gradual improvement/gradual loss

Gradual improvement followed by loss is shown in Figs. 9a, b and c. The MDVFA loss graph shows the gradual improvement in examinations A through E (following laser and filtration surgery) followed by a small loss in the upper quadrants and in the lower temporal quadrant between examinations E and F. There was a great improvement from examination F to G which remained stable from examination G to H with a subsequent loss of sensitivity in the upper quadrants from examination H to L. The sensitivities remained stable in the lower quadrants for the rest of the examinations. The MDVFA angle graph illustrates that the loss localized in the upper nasal quadrant remains relatively constant. The greatest decrease in non-homogeneity (smoothing of the field) occurs in the lower nasal quadrant in examinations F through L. The LOG10 CLV graph, for comparison, is much less sensitive to changes in localization. The SGD

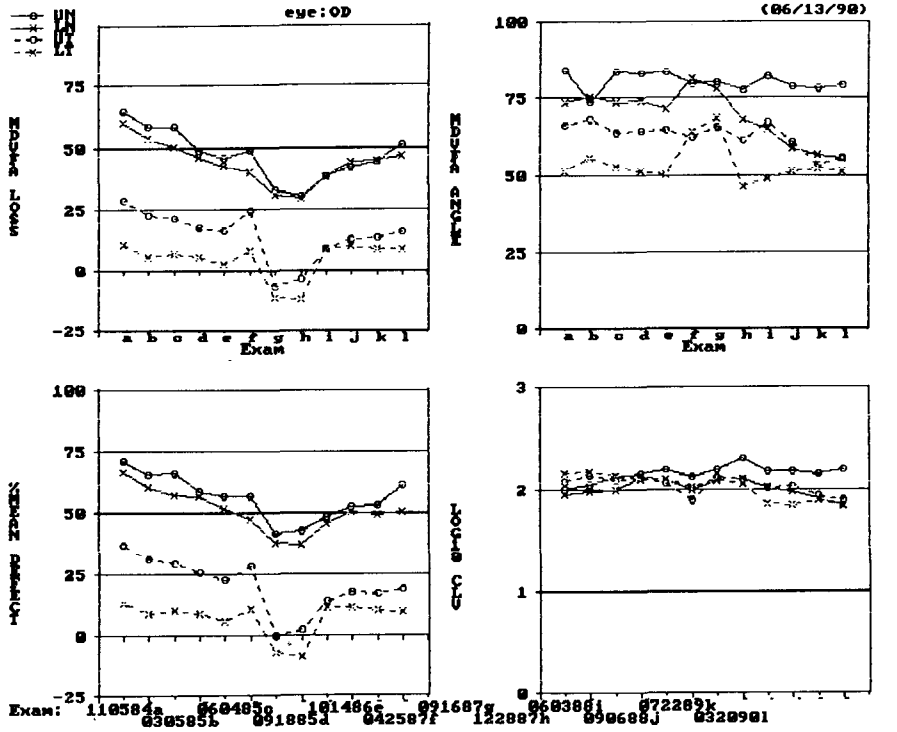

Fig 9a Example 2: gradual improvement/gradual loss is shown in these graphs of the MDVFA and global indices.

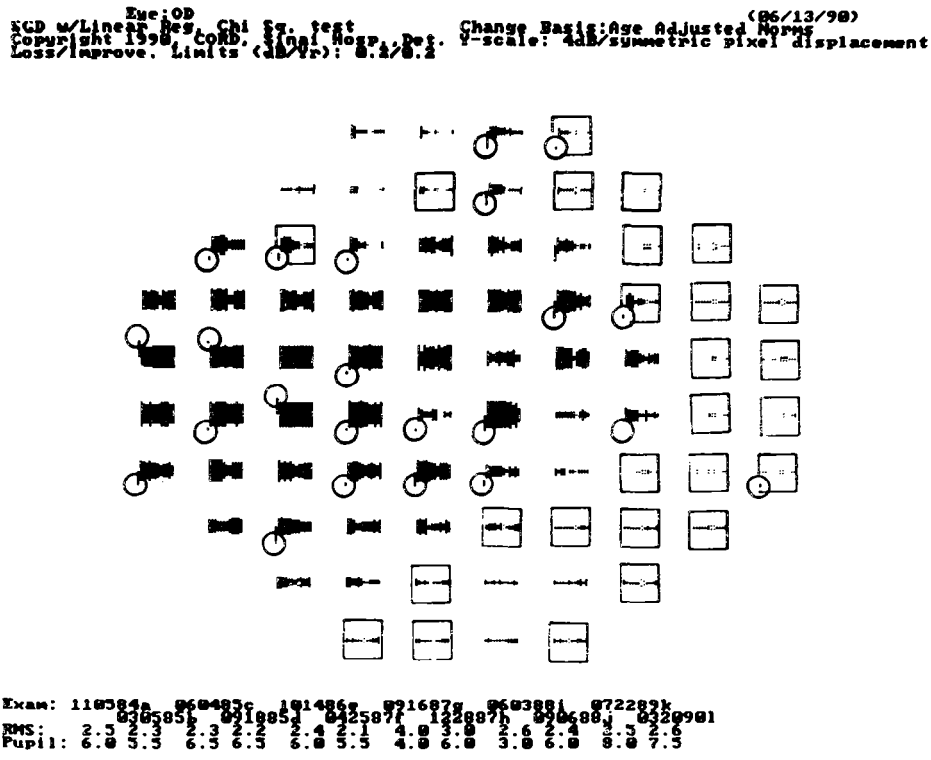

Fig 9b Example 2: gradual improvement/gradual loss is shown in this SGD Particularly note the improvement above normal primarily in the right hemisphere

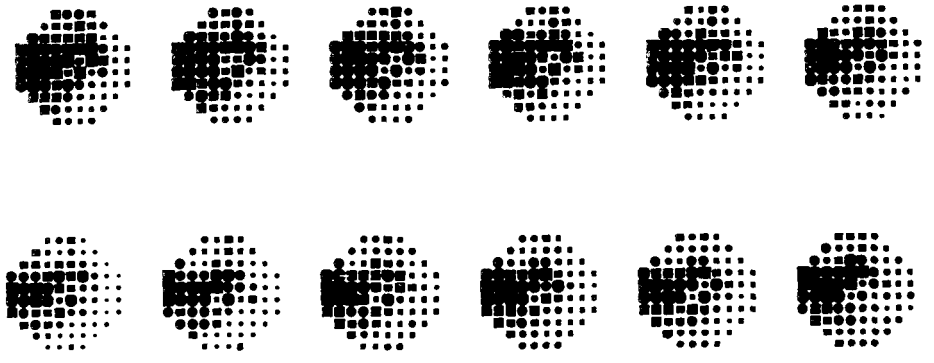

Fig 9c Example 2: gradual improvement/gradual loss in the Delta series printouts (shown for comparison)

plot depicts a local improvement to above normal sensitivity (points highlighted by boxes) in examinations G and H in many of the temporal points which return to normal sensitivity on subsequent examinations. Significance bars (circled for emphasis) show many points with linear trends.

Example 3 subtle diffuse progression

Subtle diffuse progression is shown in Figs. 10a, b and c The MDVFA loss graph shows a small, but gradual loss in sensitivity in the right eye in examinations A to L. The MDVFA angle graph shows the loss to be primarily in the upper quadrants. In the upper temporal quadrant

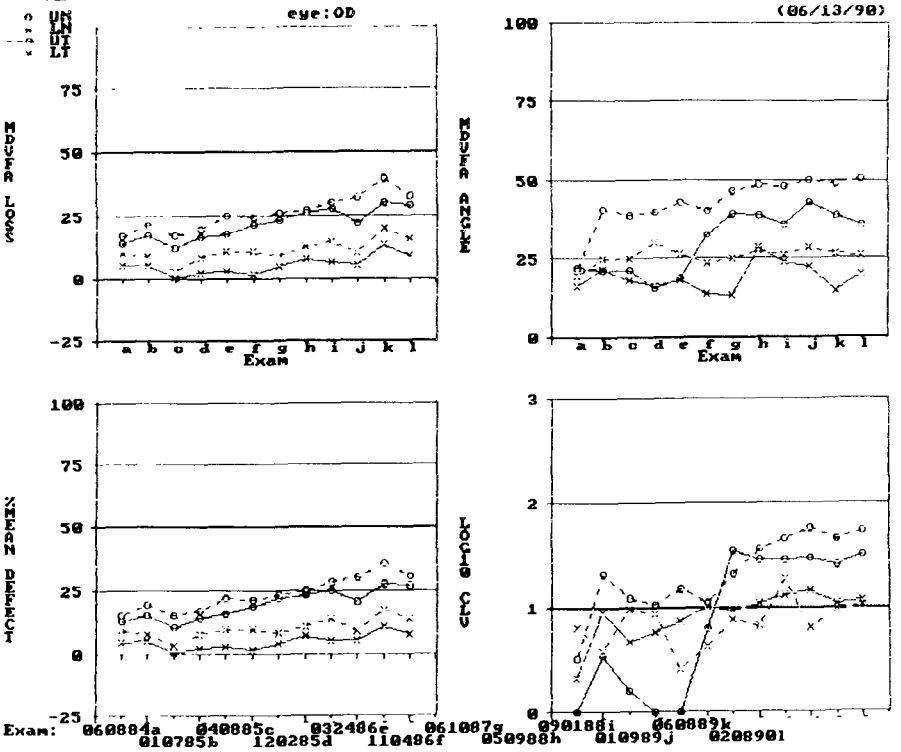

Fig 10a Example 3: subtle diffuse progression is shown in these graphs of the MDVFA and global indices.

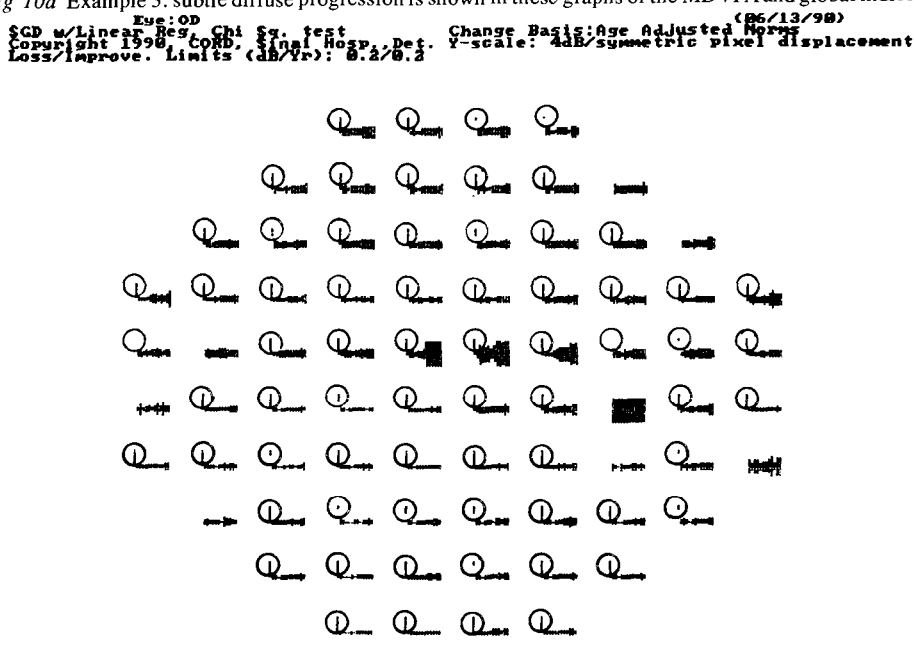

Fig 10b Example 3: subtle diffuse progression is shown in this SGD

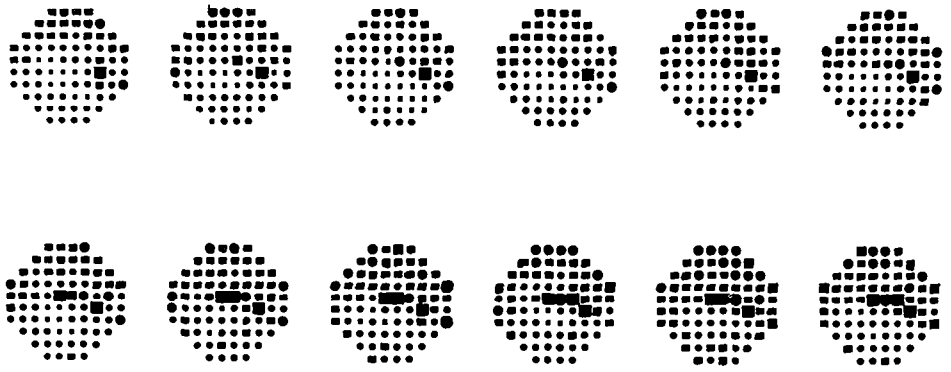

Fig 10c Example 3: subtle diffuse progression in the Delta series printouts (shown for comparison).

the localization increased rapidly from examination A to B with subsequent gradual increase. In the upper nasal quadrant the localization does not increase until examination F. The changes in the LOG10 CLV graph are more erratic and are not as easily interpreted. The SGD plot clearly demonstrates the rapid increase in loss in the arcuate area above fixation. On casual inspection the remainder of the points appear to be relatively stable or have minimal progression. The significance bars (circled for emphasis), however, demonstrate broadly distributed, significant, progressive loss.

Trajectories in vector space

The TFV traces out a path in n-dimensional space as the visual field, which it represents, changes with time. Mathematically, it is possible to describe the path, but it is difficult to visualize. The two quantities, |TFV| and VA describe the general state of the visual field. The MDVFA loss and MDVFA angle correspond to changes in the |TFV| and VA respectively. By examining the path or "trajectory" corresponding to the changes of the field in the two-dimensional space which is formed by the MDVFA loss and MDVFA angle, it is possible to understand some details of the nature of the changes in the visual field without recourse to the entire data.

In Fig. 11a, the diagram, MDVFA angle *versus* MDVFA loss, indicates the nature of changes in the field when plotted in these two dimensions. Change toward the upper half of the diagram indicates increasing non-uniformity in the distribution of field sensitivities. Change toward the lower half indicates a smoothing or leveling of the distribution of sensitivities. A change toward

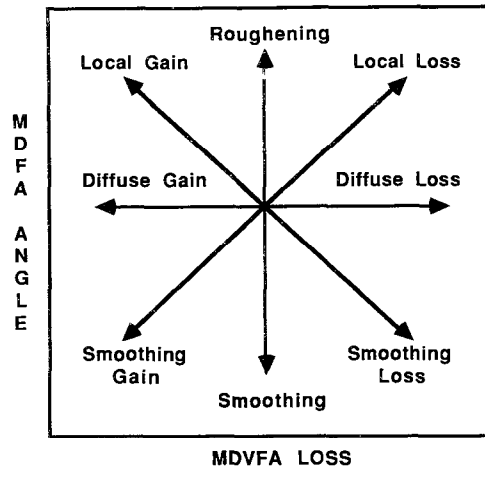

Fig 11a The plot of MDVFA angle *versus* MDVFA loss shows the eight basic types of change encountered in plotting "trajectories" in this space.

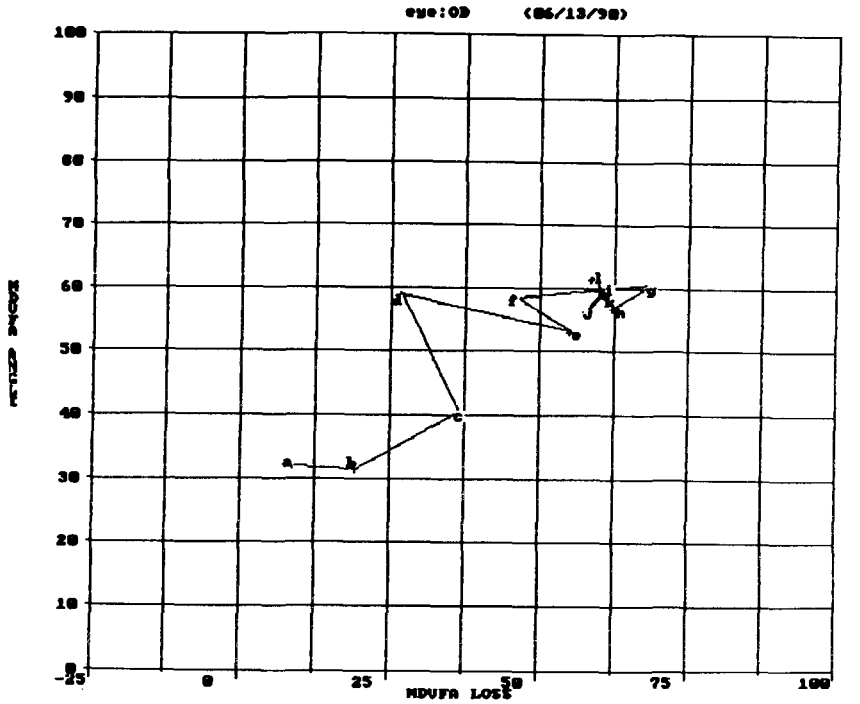

Fig. 11b. Example 1: progressive loss trajectory.

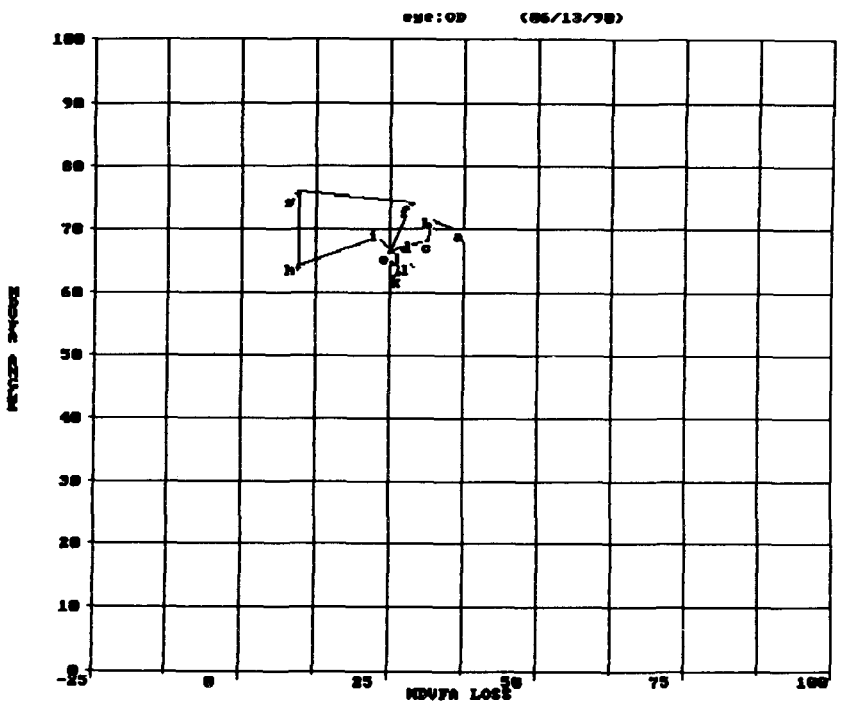

Fig 11c. Example 2: gradual improvement/gradual loss trajectory.

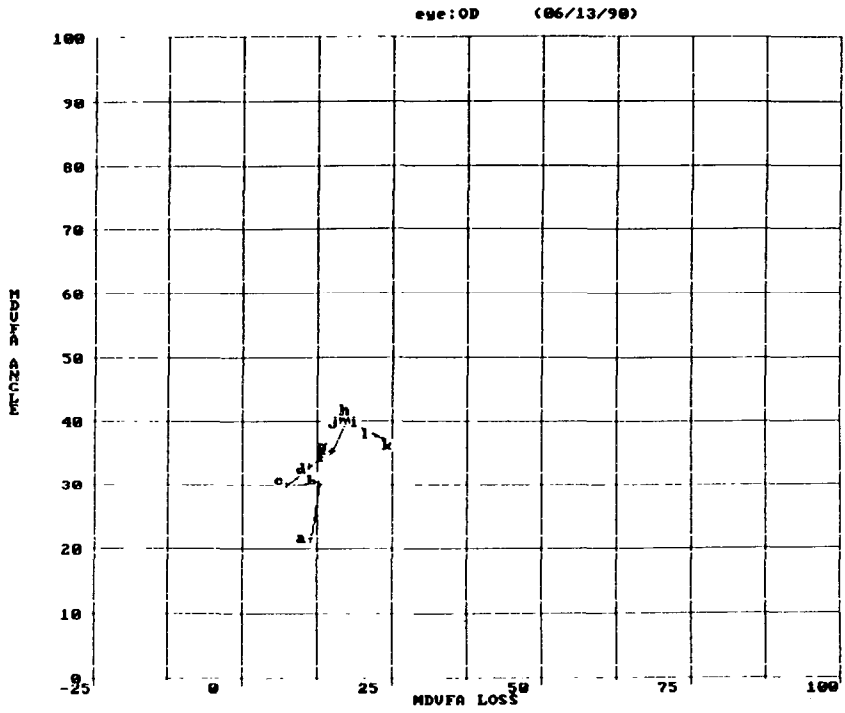

Fig 11d Example 3: subtle diffuse progression trajectory

the right corresponds to increasing diffuse loss while a change to the left indicates a diffuse improvement in sensitivity. The eight arrows indicate the various combinations of change which might be encountered. The scaling of the axes will affect the actual angles displayed. In Figs 11b, c and d, the "trajectories" for each of the actual clinical examples previously discussed are shown:

In Figure 11b, example 1: progressive loss, the trajectory shows strong growth of local defects. In Fig. 11c, example 2: gradual improvement/gradual loss, the trajectory shows little net local gain after a large diffuse gain and loss. In Fig. 11d, example 3: subtle diffuse loss, the trajectory shows growth of field inhomogeneities accompanied by only a small loss.

Conclusions

The MDVFA indices and graphs used with the SGD represent new methods for the analysis of serial visual fields The MDVFA indices allow the reduction of the visual field data to two independent values which characterize the state of the field and can be used for plotting "trajectories" of the field in the two-dimensional space defined by them. The MDVFA loss behaves very similarly to the %mean defect, but the MDVFA angle, unlike the CLV, is relatively unaffected by changes in the RMS, or the value of the short-term fluctuation[9], and is more consistent in representing non-homogeneous change of the visual field.

The SGD allows the clinician or researcher to compare changes point by point in a series of up to 16 exams and performs regression analysis at each point measured in the field to identify significant trends. The SGD makes it possible, in a series of fields, to identify subtle patterns of local changes not apparent from field indices alone. The SGD displays more examinations and provides more information than the Octopus Delta Series and Change Program.

The MDVFA and SGD methods are not specific to a single test program or to the Octopus perimeter. The MDVFA graphs and SGD present a possible uniform graphic output for the

results of serial examinations on a wide range of instruments. We are currently investigating the application of these techniques to other Octopus programs and to the data output of the Humphrey Perimeter.

References

1. Bebie H, Fankhauser F: Handbook for Operation and Application of Octopus Delta Program. Schlieren, Switzerland: Interzeag AG 1981
2. Flammer J: The concept of visual field indices Graefe's Arch Clin Exp Ophthalmol 224:389-392, 1986
3 Haley MJ (ed): The Field Analyzer Primer. San Leandro, CA: Allergan Humphrey 1986/87
4. Hirsch J: Statistical analysis in computerized perimetry. In: Whalen WR, Spaeth G (eds) Computerized Visual Fields, pp 307-344, 1986
5. Salton G, Buckley C: Parallel text search methods Comm ACM 31:202-215, 1988
6. Wu DC, Schwartz B, Nagin T: Trend analysis of automated visual fields. Doc Ophthalmol Proc Ser 49:175-189, 1987
7. Wild JM, Dengler-Harles M, Husse MK, Crews SJ, Cole MD, Searle AFT, O'Neill FC: Regression techniques in the analysis of visual field loss In: Heijl A (ed) VIII International Perimetry Society, pp 202-216. Amsterdam/Berkeley/Milano: Kugler & Ghedini Publ 1989
8. Fitzke F, Pointswami S: Private communication 1990
9. Cyrlin M, Rosenshein J, Cunningham S, Tressler C, Czedik C, Fazio R: Multi-dimensional vector analysis of visual fields. Invest Ophthalmol Vis Sci 3:15, 1990

Automated visual field management in glaucoma with the PERIDATA program

Paolo Brusini[1], Stefano Nicosia[1] and Jörg Weber[2]

[1]Department of Ophthalmology, General Hospital, I-33100 Udine, Italy, [2]University Eye Clinic, Cologne, Germany

Abstract

PERIDATA* is a program created for the transmission, storage and processing of visual field data from the Humphrey Field Analyzer and the Octopus automated perimeters Its graphic and statistical capabilities make it useful in the management of glaucomatous visual fields, both for diagnosis and for follow-up. In the authors' experience, this powerful and flexible package has been found to perform well for clinical, scientific, and didactic purposes.

PERIDATA is a program which reads visual field data either from a Humphrey Field Analyzer (HFA) or Octopus automated perimeters (all versions), stores them in a personal computer (PC), and can process them in different ways[1,2]. The present version 4.5 (13.12.89) has interesting features, which may be useful in the management of glaucomatous patients.

The test data can be acquired either from the original HFA discs or with an RS-232 connection between the HFA and the PC. With Octopus perimeters, the data are read from Octopus Octosoft files and from Octopus ASCII files.

It is possible to display the results of a single test, to merge up to five threshold tests, to compare either two or four threshold tests of a patient either in chronological or free sequence order, to compare the threshold tests of two eyes of the same patient, and to compare either the right and the left or the upper and the lower halves of one single field. Using the HFA, it is possible to insert notes and the diagnosis for every test.

The results of a test can be displayed using a combination of seven factors, with more than 1000 different display modes. These factors are:

1. value (measured threshold value, deviation from age-corrected normal threshold, corrected deviation, number of stimulus presentations at each point, age-corrected normal values);
2. unit (decibel, standard decibel, physiological perimetric units, a new scale at present on trial);
3. calculation mode (mean value, single values, difference of two values);
4. picture mode (numerical values, interpolated, non-interpolated, and non-extrapolated grayscale, statistics 1 and 2, which we will discuss later, and three-dimension);
5. scale (10°, 60°, 90° or free choice between 1° and 90°);
6. inversion coordinates (either X, Y or both axes);
7. projection (standard, retinal nerve fiber related projection either rectangular or polar[3], chiasma lesion related projection).

Moreover, it is possible to delete either the blind spot area or other parts of the field, according to the decision of the perimetrist.

The tests can be printed in different print modes: large, small and high resolution print, and three standard display modes on one page, as with the HFA

A new version of PERIDATA (4.8), at present on trial, offers a "Peridata standard printout", which has a combination of topographical and numerical representations: numerical values of deviations, grayscale of deviations, Bebie-curve, and visual field indices (MD, LV, CLV, PSD, CPSD, SF, CSF).

*The PERIDATA program is available on request from BIT CONNECTION, Ralf Geiger, Auf der Loeh 20, D-5204 Lohmar 1, Germany

Perimetry Update 1990/91, pp. 273-277
Proceedings of the IXth International Perimetric Society Meeting,
Malmö, Sweden, June 17-20, 1990
edited by Richard P. Mills and Anders Heijl

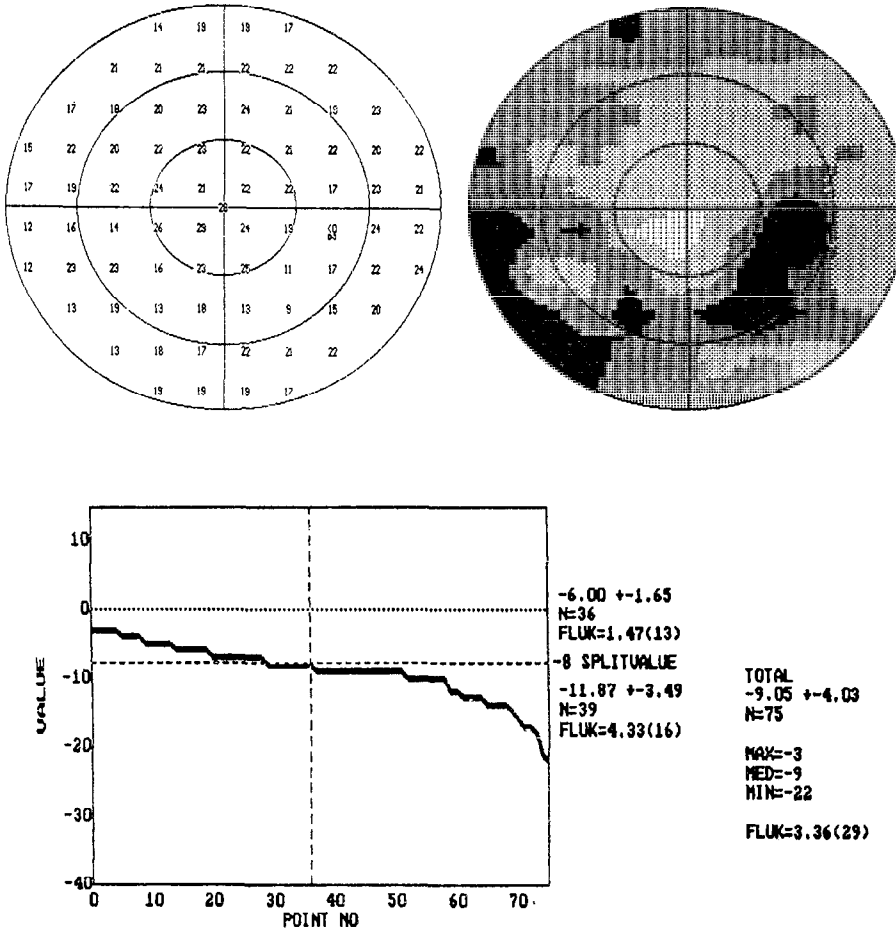

Fig 1 HFA 30-2 program in a 78-year-old glaucomatous patient In the cumulative curve of deviations (bottom), the split value, selected at 8 dB, divides the test points into two groups (each with their own indices), according to their deviation from age-corrected normal values (the blind spot was deleted)

In the management of visual fields with glaucomatous defects, some PERIDATA capabilities are particularly interesting

We report here our experience with this program, used in connection with an HFA. In most cases the threshold 30-2 program was used.

Using a grid custom test to improve the definition of a suspect defect, the "merge" function allows us to superimpose these data over a standard test on a single page, supplying a precise and clear printout, both in numerical values and in grayscale.

If the STATPAC program is not available, it may be useful to use the deviation from age-corrected normal threshold or the corrected deviation display modes; in the latter case the general influence on the field is estimated and subtracted from each point's value to make the local deviation visible.

PERIDATA also has two statistical displays. In Statistics 1, the frequency of values (or the frequency of deviation values) is displayed; some visual field indices, similar to those of the HFA and Octopus (mean sensitivity, mean defect, root of loss variance, and short term fluctuation), are also calculated. In Statistics 2, the cumulative frequency of values is shown. It is also possible to obtain a cumulative curve of deviations, as in the "Bebic curve"[4]. When two tests of a patient are compared, a single-point statistics of a trend is supplied[5].

With both statistical displays, the test points can be split into two groups, selecting a "split

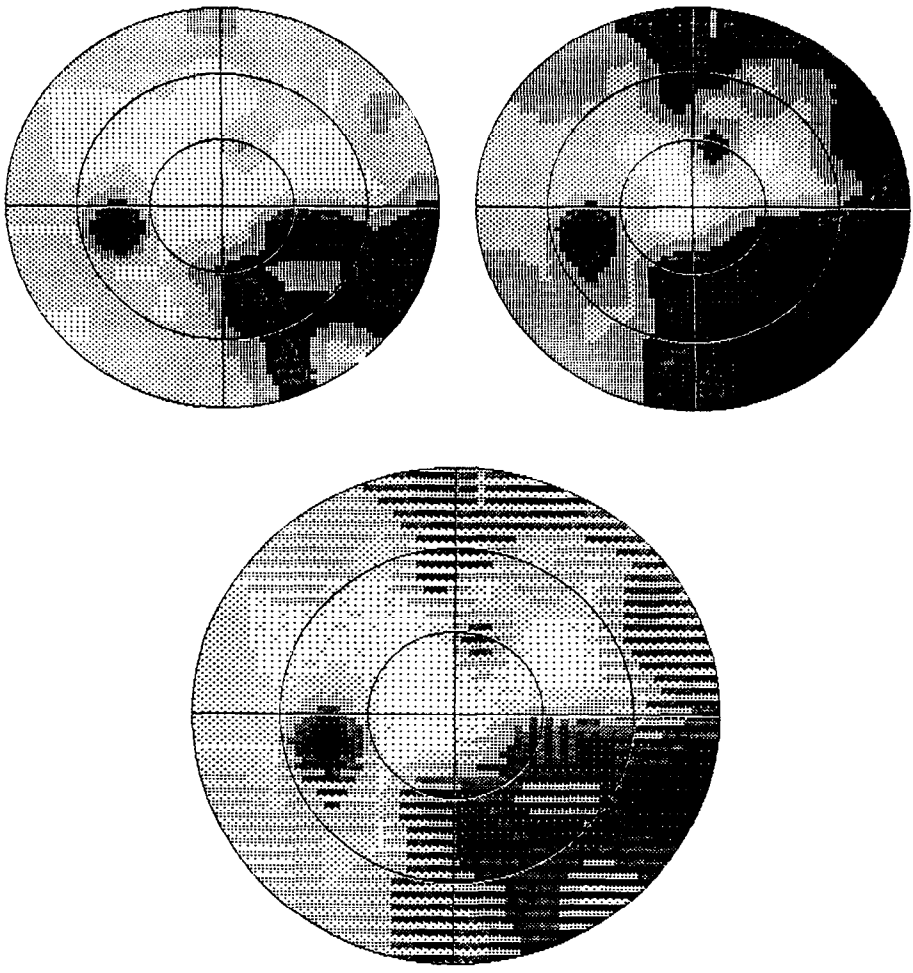

Fig 2 Progression of a glaucomatous visual field defect over time (top), as shown by Graphical Analysis of Topographical Trends (bottom)

value". In this case the visual field indices are calculated independently for both groups (Fig 1).

The comparison of two threshold tests, one from the right and one from the left eye of the same patient, can be useful in early glaucoma to show subtle differences between the eyes, particularly if no local defect is evident. In some cases, a more precise analysis of results of a visual field with suspect defects can be obtained by comparing the matching points of the upper and the lower, and the right and the left halves of the field.

The differences between two or four tests can also be shown with the Graphical Analysis of Topographical Trends (GATT), using the grayscale print mode[6,7]. With this special printout the differences are represented in alternating stripes, whose contrast is in relation to the amount of change, either vertical, if the second value is better, or horizontal, if it is worse (Fig. 2) The same procedure can be used to show: (1) the differences between first and second threshold values in a single test (Graphical Analysis of Fluctuation – GAF); (2) the difference between left and right eye threshold tests (Graphical Analysis of Bilaterality – GAB); and (3) the differences between the two halves of a single visual field (Graphical Analysis of Symmetry – GAS).

The delete area option allows the operator to remove the blind spot area (useful in statistics and in symmetry analysis), the most peripheral points in 30° programs (artifact due to lens rim), half of the field (glaucoma associated with hemianopia) or, if necessary, the field either

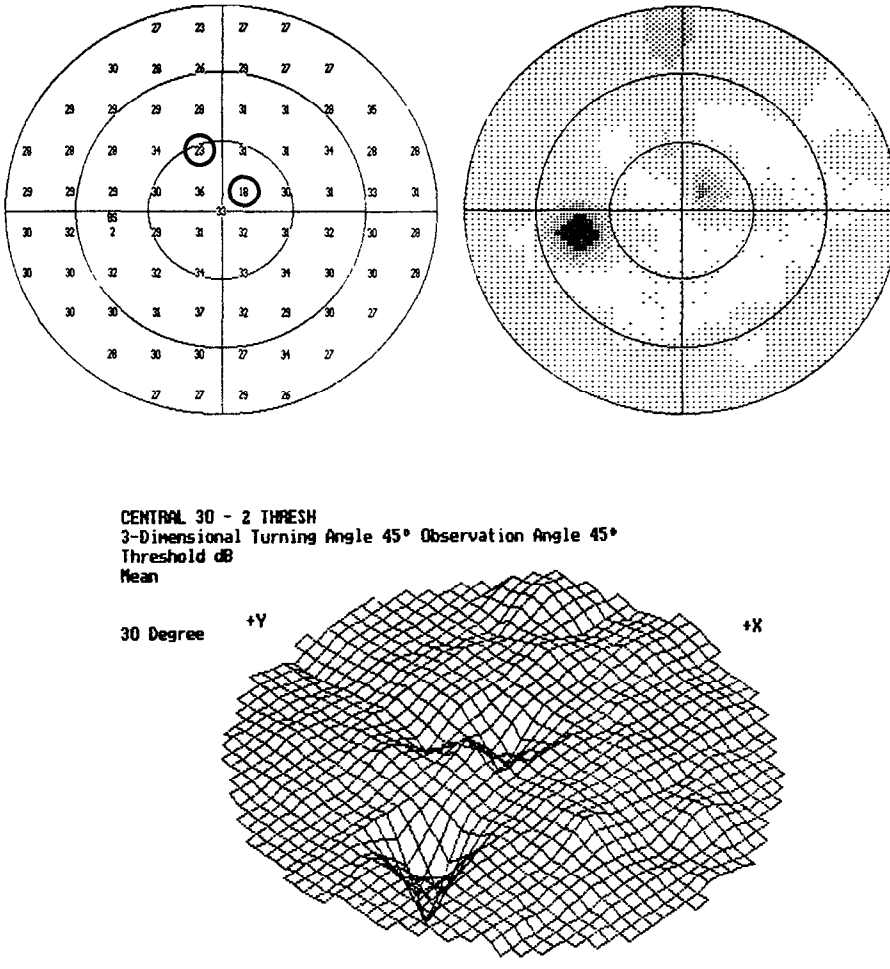

Fig 3 Shallow paracentral scotomas (encircled), clearly shown by the three-dimensional display.

outside or inside a given eccentricity, etc. This option can be employed to compare particular visual field areas over time, especially using Statistics 1 and 2.

With the three-dimensional display, the visual field can be turned around and the observation angle can be raised as much as one likes. Although it does not provide any further information when compared to more traditional displays, it could be useful in some selected cases, *e.g.*, to show small sensitivity depression, which are not clearly visible on the grayscale display (Fig. 3), and for didactic purposes (the color display is particularly impressive). Using the 3-D display either with deviation or corrected deviation mode or even with compare mode, homonym, heteronym, symmetry, analysis, etc., the color can be used to convey further information, adding a fourth dimension to the representation[8].

In conclusion, the PERIDATA program, particularly for glaucomatous patients, seems to us to be useful for clinical purposes (storage of data), for research (statistics, different display modes and options), and also for teaching (3-D color display).

The disadvantages, in our opinion, are the difficulty to easy manage the program, a bit complicated for beginners, and the lack of an exhaustive operator's handbook with clear examples of various available options and capabilities. The following version (4.8) has been improved into that direction by presenting – by choice – a simplified menu, with only six standard displays and one standard print-out.

A manual supplement, explaining the use and interpretation of the results, is in preparation.

References

1. PERIDATA manual 1989: Lohmar, Germany: Bit Connection 1989
2. Weber J: Experiences with the perimetric data program Peridata Third European Octopus Users' Meeting, Luzern, August 30-September 2, 1989
3. Weber J, Georgopoulos G, Ulrich H: The nerve fiber projection chart: a new way to represent perimetric data Glaucoma Meeting, Budapest, April 13-15, 1989
4. Bebie H, Flammer J, Bebie Th: The cumulative defect curve: separation of local and diffuse components of visual field damage. Graefe's Arch Clin Exp Ophthalmol 227:9-12, 1989
5. Weber J, Krieglstein GK: New methods for the perimetric follow-up of glaucoma Int Symp Glaucoma Soc, Singapore, March 16-17, 1990
6. Weber J, Krieglstein GK: Graphical analysis of topographical trends (GATT) in automated perimetry Int Ophthalmol 13:351-356, 1989
7. Weber J, Krieglstein GK, Papoulis G: Use of Graphic Analysis of Topographical Trends (GATT) for perimetric follow-up of glaucoma. Klin Mbl Augenheilk 195:319-322, 1989
8. Lambrou GN, Schalk Ph, Rechenmann RV, Bronner A: Computer-assisted visual field assessment: quantification, three- and four-dimensional representations Doc Ophthalmol Proc Ser 49:207-215, 1987

Octosmart: a computerized aid for interpreting visual field examination results

Arthur T. Funkhouser, Hans-Peter Hirsbrunner, Franz Fankhauser and Josef Flammer

University Eye Clinics, Bern and Basel, Switzerland

Introduction

Octosmart is a new computer program running on an IBM PC or compatible which is able to take examination results obtained with the Octopus G1 program and evaluate them[1]. Examination conditions for obtaining visual fields were standardized by Goldmann. With automation, artifacts due to subjective judgement of the perimetrist were largely eliminated. As a further step in this evolution, Octosmart seeks to make visual field evaluation clearer, easier and more standardized in that it offers commentary about the examination results based on statistical considerations and the accumulated experience of several visual field experts.

Utilizing Octosmart's menu-oriented structure, the user is first able to locate the examination to be studied and then has several evaluation tools available. These include:

- facts about the examination conditions (administrative data);
- sector analysis (including rudimentary cluster analysis),
- numerical tables of the loss values (both phases separately);
- numerical tables of the combined loss values along with the visual field indices of program G1 and a graphic indicator of the degree of pathology as determined by the program;
- a summary evaluation of the examination results in which many factors, such as the short-term fluctuation, the catch trial error rates and repetitions are taken into account and commented upon The comments are in easily understandable language;
- a cumulative defect curve along with a display of the visual field and two indices (MD and CLV).

While the final evaluation, especially in borderline situations, must still be made by the ophthalmologist, Octosmart is able to process a large amount of information and reduce it to manageable proportions. It highlights aspects which might otherwise escape routine screening and can thus serve as a real help in the evaluation of a visual field examination. It may also be utilized in the training of new visual field interpreters

A comparison of human and automated visual field interpretation

In order to check its performance, some results produced by the Octosmart diagnostic software have been compared with those of three interpreters analyzing 27 visual fields obtained with program G1.

The study[2,3] revealed highly consistent judgments between interpreters and, hence, between interpreters and Octosmart only in cases of obvious pathology. In cases considered as "normal" or "borderline" by some interpreters, the "personal styles" of human interpreters implicitly guide the decision process. Since uncertainty in human interpreters results in unpredictable inter-individual differences, visual field interpretation, assisted by an automated visual field evaluation, such as the program Octosmart, based on standardized and explicit evaluation criteria, is considered to be superior to unaided human visual field interpretation.

While fluctuations in the decision processes between interpreters may be a strong argument and justification for an automated visual field evaluation, the hidden mechanisms that produce contradictory results in human interpreters must be taken into account and carefully studied in any attempts to evaluate automated visual field interpretation. The complexity of the perimetric

Address for correspondence Dr A.T Funkhouser, University Eye Clinic, Insel Hospital, 3010 Bern, Switzerland

Perimetry Update 1990/91, pp 279-280
Proceedings of the IXth International Perimetric Society Meeting,
Malmö, Sweden, June 17-20, 1990
edited by Richard P Mills and Anders Heijl

task, on the other hand, requires suitable tools foı adequate description of the underlying processes. In the study, it was shown that the standardized performance of the Octosmart - diagnostic software can best be described in terms of the "personal styles" of human interpreters.

References

1 Bebie H: Computer-assisted evaluation of visual fields Graefe's Arch Clin Exp Ophthalmol 228:242-245, 1990
2. Hirsbrunner HP, Fankhauser F, Funkhouser AT, Jenni A: Evaluating human and automated interpretations of visual field data in perimetry *Jpn J Ophthalmol* 34:72-80, 1990
3. Hirsbrunner HP, Fankhauser F, Jenni A, Funkhouser AT: Evaluating a perimetric expert system: experience with Octosmart. Graefe's Arch Clin Exp Ophthalmol 228:237-241, 1990

Evaluation of the diagnosis of visual fields

Lionel R. Shapiro[1,2] and Chris A. Johnson[1]

[1]*Optics and Visual Assessment Laboratory, Department of Ophthalmology, University of California, Davis, CA 95616,* [2]*Department of Cognitive Sciences, University of California, Irvine, CA; USA*

Abstract

Expert systems and artificial intelligence techniques have been useful in the study of diagnostic decision making and judgments in radiology, cardiology, and internal medicine Clinical diagnosis of visual fields may be seen as a similar problem of obtaining agreement among experts. The present study uses established techniques in Cognitive Science (*i.e* , protocol analysis) to specify the diagnostic knowledge for a group of experts and novices using a given set of normal and pathologic visual fields. However, this approach goes beyond traditional techniques by exploiting non-verbal classifications extracted from the data and visual field set. Verbal reports of visual field experts are analyzed using the following variables: classification features, subsequent diagnosis, as well as time into the report for features and diagnosis The results from preliminary experiments as well as examples of their application are presented. These data may be used to study diagnostic decision making as well as establish a basis for an expert system in clinical perimetric diagnosis and evaluation of visual fields

Introduction

Harrington[1] has stated that the sum total of diagnostic information must be meaningful and reliable in order to allow for intelligent diagnosis. To be meaningful, the assumptions of the procedure, as well as any limitations, must coincide with those understood by the diagnostician. To be reliable, the diagnostic information resulting from any procedure used by a diagnostician or expert system must be robust across time, patients and clinics, in that patients with similar normal or pathological characteristics should elicit similar results. These important criteria must be addressed in any attempt to create new tests or diagnostic procedures. This paper will use techniques developed in cognitive science to investigate the first issue: how one may begin to characterize what is meaningful diagnostic information Specifically, we will outline our preliminary efforts at obtaining the relevant information in the domain of diagnosis of visual fields.

Past research attempting to characterize the components of medical expertise is extensive (*e.g.*, refs[2-5]). Each study has made critical assumptions of how experts in medicine derive diagnostic conclusions and plans for treatment. Most artificial intelligence in medicine (AIM) systems make use of a scoring of certainty or confidence. However, it has been difficult to characterize these measures for anything but the crudest of information without getting into problems associated with exact Bayesian analysis. The AIM systems also rely greatly upon the biases of individual researchers which may or may not reflect actual cognitive "weightings" (if such processes do take place). Furthermore, little empirical backing has been given for these systems of quantified observations.

These medical diagnosis systems typically incorporate strictly verbal-predicate knowledge representations (*i.e* , [FieldContains [What Depression] [Where Nasal]] or similar representations utilizing descriptive terms and values for given functions). Non-verbal information is converted to verbal-predicate form (usually by the system designers) before being incorporated into the knowledge base. This simple assumption in representation has broad ramifications. In light of research in human problem solving[6], it is unrealistic and limiting to assume that human cognition operates strictly upon verbal-predicate representations. To develop an

Supported in part by National Eye Institute Research Grant No EY-03424 (to CAJ), and an Unrestricted Research Grant from Research to Prevent Blindness, Inc

Perimetry Update 1990/91, pp 281-285
Proceedings of the IXth International Perimetric Society Meeting,
Malmö, Sweden, June 17-20, 1990
edited by Richard P. Mills and Anders Heijl

display, experts were instructed to give detailed verbal descriptions of the display (short of giving a diagnostic impression) for 30 sec. These descriptions were digitally recorded by the Macintosh II using a Farallon MacRecorder. Following this, the visual field was removed. At this point experts were given 10 sec to list up to three impressions for diagnosis of the visual field in order of likelihood. Short breaks of approximately 30 sec were given after every ten of these trials.

Results

Verbal protocol files were generated from transcriptions of the recordings of the visual field descriptions and the diagnoses. Two preliminary analyses are reported here. Analysis of correspondence of the diagnostic categorizations across subjects was done to provide a measure of clinical "agreement" amongst the experts. Comparisons within subjects of diagnostic categorizations for the two presentations of the same visual field (one flipped horizontally) provide an estimate of the reliability of the expert diagnostic process. Preliminary findings, calculated based upon the percentage correspondence for (a) number of exact matches for first diagnosis, and (b) number of at least one diagnosis match, are given in Table 1.

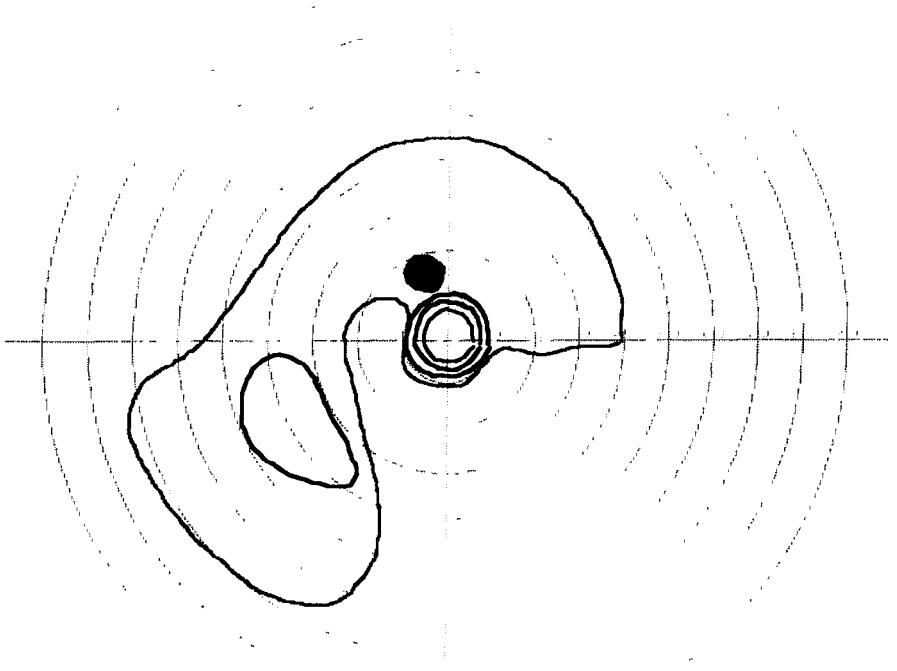

Fig 1 Visual field display eliciting the following similar diagnostic judgments and respective protocols Expert #1: Dx: glaucoma, ischemic optic neuropathy Protocol: "Visual field shows severe inferior; visual field loss and a superior focus of sensitivity loss; in the arcuate nerve fiber bundle region. A very distinct nasal step; along the horizontal meridian Compression of the isopters throughout; overall depression of the entire field. It looks like an arcuate, slightly greater sensitivity loss Overall depression " Expert #2: Dx: glaucoma; ischemic optic neuropathy Protocol: "This field is generally very severely constricted; and depressed with preservation of the central visual island. There is a dense inferior absolute arcuate field defect with a superior scotoma coming off the blind spot There is overall marked depression of the field above and an absolute arcuate; with an altitudinal-type defect inferiorly."

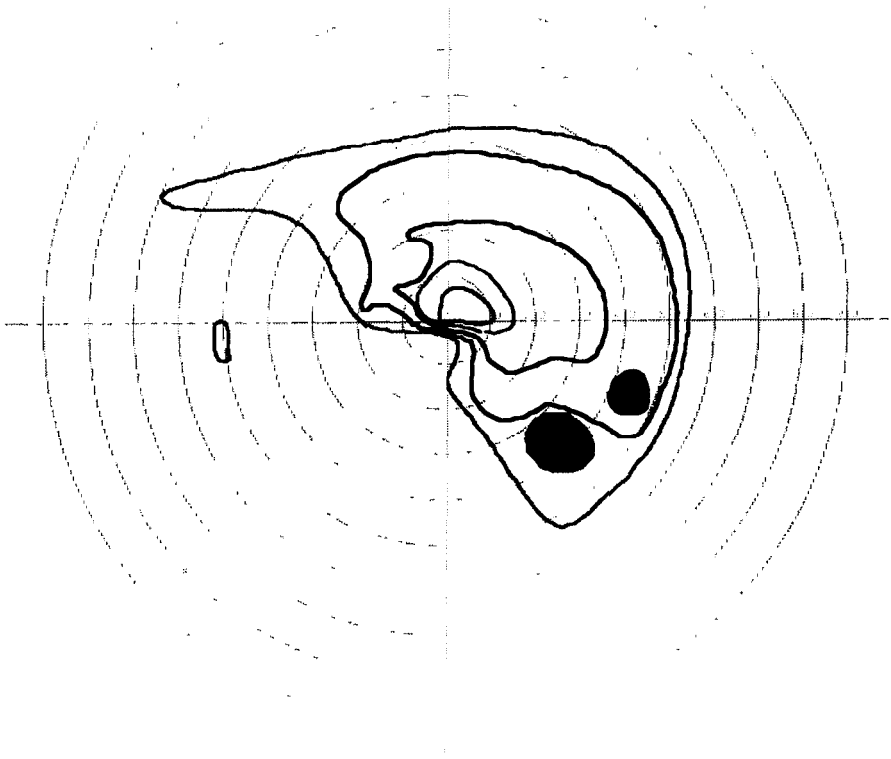

Fig 2 Visual field display eliciting the following differing diagnostic judgments and respective protocols Expert #1: Dx: optic neuropathy; optic neuritis Protocol: "Visual field appears to have significant sensitivity loss in the inferior and temporal region and sloping edges to the defect. There is an inferior temporal quadrant defect extending to fixation. The possibility of some respecting of the vertical for that inferior isopter, significant sensitivity loss, sloping edges to.." Expert #2: Dx: glaucoma; drusen of the optic nerve. Protocol: "I assume this is a right eye of a patient who has inferonasally a field defect and a superior nasal field defect of the inferior temporal scotomas; most likely the diagnosis would be double arcuate scotomas from glaucoma; another consideration would be drusen of the optic nerve head Without seeing the other eye "

Table 1 Correspondence for diagnosis matches

	Exact match on Dx #1	*At least one common Dx*
Within expert		
1	75.0%	92.5%
2	70 0%	97 5%
Between experts (by visual field)	42 5%	82 5%

Figs. 1 and 2 show examples of visual fields with elicited diagnostic judgments and descriptive protocols. Fig. 1 shows an example where the experts were in good agreement, whilst Fig. 2 shows an example where the between expert agreement was poor.

Verbal protocols files were generated from transcriptions made from the verbal description recordings overlaid with timing reference tones at five second intervals (defining the resolution *epoch* length). Analyses based upon a detailed review of the protocols and their relationship to diagnostic judgments are beyond the scope of this report. Preliminary results, however, suggest strong individual differences in the use of both localizing and feature-descriptive terms.

Discussion

The description and diagnosis of kinetic visual field plots in isolation of contextual information is a non-trivial task. Preliminary findings suggest that the study participants were able to overcome the handicap imposed by this restriction of information.

As mentioned above, more detailed analyses are currently being examined. These include the relationships between diagnosis, localizing terms, feature-descriptive terms, as well as actual visual field spatial/feature characteristics. These data provide the parameters by which planned studies of the perceptual nature of information used in diagnostic tasks will be examined.

These and forthcoming findings will aid in the development of models for expert clinical diagnosis of visual fields. This is done by providing an empirically derived base from which analytic tools (*e g.*, traditional expert systems modeling, neural network modeling, etc.) may be applied. Without this base set of knowledge representations and an understanding of their underlying structure, inappropriate assumptions may cause modeled performance to approach that of a reasonably good novice as opposed to a true expert.

The applications of an expert visual field diagnostic model include: (a) aiding diagnosis in a clinical environment, (b) quality control for clinical trials incorporating visual fields, (c) ophthalmologic education and testing, (d) aid in the development of new perimetric testing techniques, and (e) assistance in the structuring of ophthalmologic knowledge and discovery of new structures. Visual field expert systems may never replace clinicians, but they greatly assist in advancing the quality of patient care. They also provide a formal model for the diagnosis of visual fields.

References

1. Harrington DO: The Visual Fields. St Louis: CV Mosby 1976
2. Schaffner KF: Logic of Discovery and Diagnosis in Medicine. Berkeley: University of California Press 1985
3 Schwartz WB, Patil RS, Szolovits P: Artificial intelligence in medicine: where do we stand? New Engl J Med 316:685-688, 1987
4. Szolovits P, Patil RS, Schwartz WB: Artificial intelligence in medical diagnosis Ann Int Med 108:80-87, 1988
5. Szolovits P (ed): Artificial Intelligence in Medicine AAAS Selected Symposium 51 Boulder Co: Westview Press 1982
6. Posner MI: Cognition. Glenview IL: Scott, Foresman and Co 1973
7. De Groot AD: Thought and Choice in Chess The Hague: Mouton & Co 1965
8 Cranberg LD, Albert ML: The chess mind In: Obler K, Fein D (eds) The Exceptional Brain: Neuropsychology of Talent and Special Abilities New York: Guilford 1988
9. Segalowitz SJ: Two Sides of the Brain: Brain Lateralization Explored Englewood Cliffs, NJ: Prentice-Hall 1983
10 Chase WG, Simon HA: Perception in chess Cognit Psychol 4:55-81, 1973
11. Lesgold AM: Acquiring expertise In: Anderson JR, Kosslyn SM (eds) Tutorials in Learning and Memory San Francisco: Freeman 1984
12 Rosch E: Principles of categorization In: Rosch E, Lloyd BB (eds) Cognition and Categorization Hillsdale NJ: LEA 1978
13. Husaim JS, Cohen LB: Infant learning of ill-defined categories Merrill-Palmer Quarterly 27:443-456, 1981
14 Newell A, Simon HA: Human Problem Solving Englewood Cliffs, NJ: Prentice-Hall 1972
15. Miller JR, Polson PG, Kintsch W: Problems of methodology in cognitive science In: Kintsch W, Polson PG (eds) Method and Tactics in Cognitive Science Hillsdale, NJ: LEA 1984
16. Shapiro LR, Johnson CA, Kennedy RL: KRAKEN: a computer simulation procedure for static, kinetic, suprathreshold static and heuristic perimetry In: Heijl A (ed) Perimetry Update 1988/89 Proceedings of the VIIIth International Perimetry Society Meeting Amsterdam/Berkeley/Milano: Kugler & Ghedini Publ 1989

A neural network can differentiate glaucoma and optic neuropathy visual fields through pattern recognition

Shalom E. Kelman, Howard F. Perell, Lynne D'Autrechy and Robert J Scott

The University of Maryland, School of Medicine, 22 S Greene Street, Baltimore, MD 21201, USA

Introduction

Neural networks are an information processing technology that have recently gained in popularity[1,2]. Neural network technology, also known as parallel distributed processing, has been inspired by studies of the brain and nervous system. A feature of neural networks that distinguishes them from conventional computer programs is their ability to learn[3]. Pattern recognition is one area where neural networks have been successfully put to practical use. Several investigators have recently applied neural networks to visual field interpretation[4-6].

At present the experienced clinician uses his cumulative experience of interpreting visual fields to recognize pattern differences in visual fields of patients with glaucoma and other types of optic neuropathy. We attempted to have a neural network emulate the thought process of the experienced clinician by performing pattern recognition in distinguishing visual field loss in glaucoma from other types of optic neuropathy.

Overview of a neural network model

We will borrow some terms from linear algebra to describe the workings of our neural network[7]. For the purposes of this paper we will consider a visual field as a vector. A vector is an array of numbers that measures a particular function In the case of a Humphrey 30-2 visual field, the 76 decibel levels could be viewed as a 76 dimensional vector. It could then be used as an input vector or a pattern in a neural network. We wish to classify our vectors or patterns into two groups, the glaucoma group and the optic neuropathy group. In the parlance of linear algebra, we are performing a mapping of the input vector space (the various vectors representing the assorted visual fields) into the output space (the two diagnostic groups). A neural network can be viewed as a computerized algorithm that efficiently and accurately carries out this mapping. Once this mapping is completed, one can submit unknown data (visual fields that have not been classified) and ask the network to classify them. In doing so the network evaluates numerous hidden relations in the input data that go beyond measurable characteristics such as mean deviation and global indices but are detected by the network's reading of the data presented.

Network architecture

In a neural network the unit analogous to the biological neuron is referred to as a processing element. A processing element has many input paths and combines by simple summation the values on these input paths. The combined input is then modified by a transfer function. This transfer function can be a threshold function that passes information only if the combined input reaches a certain level, or it can be a continuous function of the combined input such as a sigmoid function. The transfer function is used as a means of "squashing" the values of the input into a limited range, often between 0 and 1. The value derived by the transfer function is generally passed directly to the output path of the processing element. The output path of the processing element is connected to input paths of other processing elements through con-

Perimetry Update 1990/91, pp. 287-290
Proceedings of the IXth International Perimetric Society Meeting,
Malmö, Sweden, June 17-20, 1990
edited by Richard P. Mills and Anders Heijl

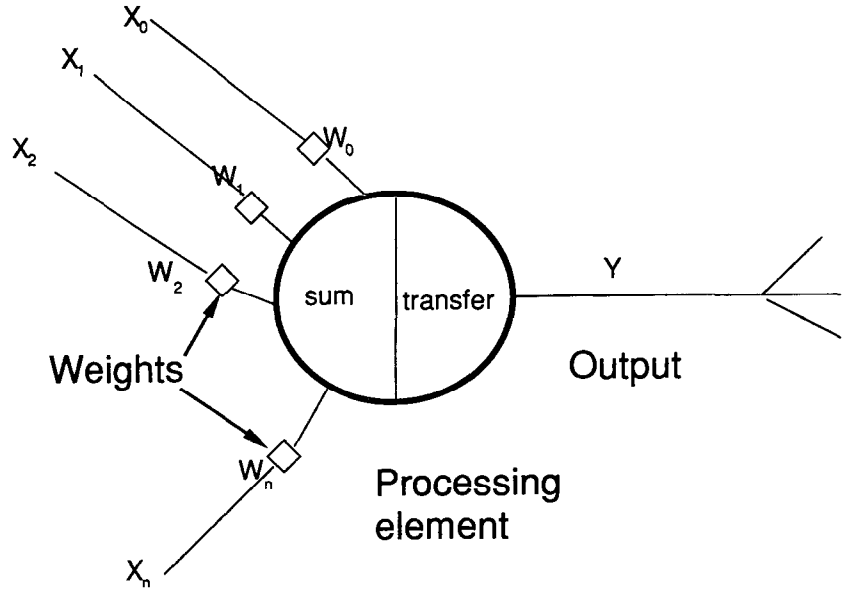

Fig 1 Neural network processing element

nection weights that correspond to the synaptic strength of neural connections. Fig. 1 illustrates the above description. Because each connection has a corresponding weight, the signals on the input lines to the processing element are modified by these weights prior to being summed. Thus the summation function can be thought of as being a weighted summation.

A neural network consists of many processing elements joined together in the above manner. Elements are usually organized into a sequence of layers with full or random connections between successive layers. Fig. 2 shows a simple three-layer neural network architecture. The input layer is where data is presented to the network, and the output layer stores the response of the network for a given input. The intermediate layer is known as the hidden layer, and it is here that encoding of the data presented to the network takes place.

Unlike traditional expert systems, where knowledge is made explicit in the form of rules, neural networks generate their own rules by learning from example. Learning in a network is the process of adjusting the connection weights of the processing element in the response to stimuli presented at the input and output layers.

One type of learning that is employed in neural networks is back propagation learning. In back propagation the network is trained on data consisting of an input associated with a desired

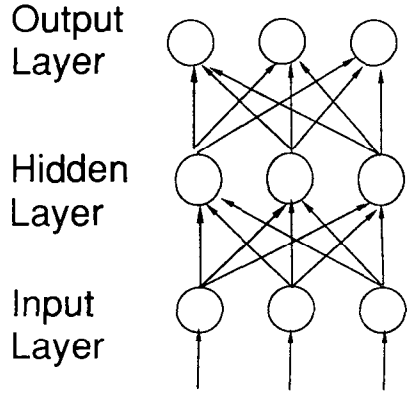

Fig 2 Three-layer neural network

output. The connection weights are adjusted on each presentation of the training data set until the network is able to produce the appropriate output for each input. The network is then tested with inputs it has not seen during training. During this phase the connection weights are fixed and are no longer allowed to change. The degree to which the network can correctly classify the test data is the measure of its ability to generalize. The ability to generalize is an attribute of neural networks that resembles biologic systems[3].

In the present model the input layer consisted of 76 processing elements each processing element representing a point in the Humphrey 30-2 visual field. Because the system requires the input points to have values less than 1 the decibel value was divided by 50. The hidden layer consisted of 14 units. The initial value of the weights between the input and hidden unit layer were initialized to small random values uniformly distributed between -0.3 and 0.3. The input layer was fully connected to the hidden unit layer meaning that each processing element in the input layer was connected to each and every processing element in the hidden unit layer. Similarly the hidden unit layer was fully connected to the output layer which consisted of a single processing element.

During training of the neural network the output processing element was assigned a value of 1 if the visual field presented to the network was classified as glaucoma and assigned the value of 0 if the visual field was classified as an optic neuropathy. During testing of the neural network a visual field was considered successfully classified if the value of the output layer was 0.7 or greater for a glaucoma visual field and 0.3 or less for an optic neuropathy visual field. The back propagation learning algorithm was used with a learning rate of 0.9. The network was run on commercially available software produced by Neural Ware Inc., and implemented on an IBM AT computer.

The training set consisted of 50 glaucoma visual fields and 37 optic neuropathy visual fields The testing set consisted of 23 glaucoma visual fields and ten optic neuropathy visual fields.

Clinical material

Humphrey 30-2 visual fields were obtained on patients with primary open angle glaucoma and optic neuropathies secondary to either ischemic optic neuropathy, optic neuritis or compressive optic neuropathy. Visual fields where fixation losses were greater than 20% or false positive/false negatives were greater than 33% were excluded. A total of 73 glaucoma visual fields and 47 optic neuropathy visual fields were collected. Fifty of the glaucoma and 37 of the optic neuropathy visual fields were chosen for the training set with the remaining fields used for the testing of the trained network.

Results

After being repeatedly presented to the network 64,000 times, the visual fields in the training set were successfully classified into the appropriate categories with an accuracy of 100%. By this we mean that the network was able to adjust the weights of the network to the point where each of the visual fields in the training set when presented to the network at the input layer was correctly classified in the output layer. The weights of the neural network were then fixed and a test data set was presented to the network. Eighty-two percent (19/23) of the glaucoma test set and 80% (8/10) of the optic neuropathy test set were correctly classified by the trained network.

Discussion

A neural network successfully achieved high accuracy in learning to separate visual fields into two categories – glaucoma and optic neuropathy. It was able to achieve this by the use of back propagation learning. The network was able to generalize what it had learned from the training data to successfully classify visual fields it had not previously seen.

The network had learned to distinguish the fields on the basis of the pattern differences it had learned from the training set. The ability to learn from experience and the facility to gener-

alize what it had learned from the training set are features the network shares with the experienced clinician. What exactly the network learned, however, is encoded in the diverse strengths of the connection weights between the processing units and more specifically in the hidden unit layer. At this point in time hidden unit layer analysis is in its infancy[8,9]. What particular blend of patterns the network has assimilated as a result of learning remains hidden in the "hidden layer".

It is of interest to compare other statistical methodologies that could similarly analyze the data. One branch of classification analyses which deals with this kind of problem is linear discriminant analyses. It is similar to neural networks in that a "classifier" is used to analyze inputs and appropriately classify them into separate categories. The development of the linear discriminant classifier depends on assumptions of multivariate normality. Due to the robustness of the technique, the classifier often succeeds where multivariate normality does not exist. This is to be contrasted with the back propagation algorithm which does not depend on any underlying assumptions of multivariate normality. It classifies more in a geometric sense and, again in the parlance of linear algebra, develops a hyperplane to separate the various vectors in the input space[10]. Attempts have recently been made to apply discriminant analyses to visual fields[11]. Which approach will yield the more useful classifier is yet to be seen.

Conclusions

A neural network utilizing back propagation learning can differentiate glaucoma and optic neuropathy Humphrey 30-2 visual fields. In addition, the network was able to generalize from the training set and correctly classify 80% of visual fields not encountered during training.

References

1 Kelman SE: Introduction to neural networks with applications to ophthalmology In: Masters BR (ed) Noninvasive Diagnostic Techniques in Ophthalmology, Ch 31. New York: Springer-Verlag, 1990
2 McClelland JL, Rumelhart DE, Hinton GE: The appeal of parallel distributed processing. In: Rumelhart DE, McClelland JL (eds) Parallel Distributed Processing, pp 3-44 Cambridge, MA: MIT Press 1986
3. Rumelhart DE, Hinton GE, Williams RJ: Learning internal representations by error propagation In: Rumelhart DE, McClelland JL (eds) Parallel Distributed Processing, pp 318-362 Cambridge, MA: MIT Press 1986
4 Banks GE, Coffey D, Small SL: A connectionist visual field analyzer. Presented at the Thirteenth Annual Symposium on Computer Applications in Medical Care, Washington, DC 1989
5 Goldbaum MH, Sample PA, White H, Weinreb RN: Discrimination of normal and glaucomatous visual fields by neural network Invest Ophthalmol Vis Sci (Suppl) 31:503, 1990
6 Shields SM, Trick GL: Applying neural networks in glaucoma: prediction of the risk of visual field loss Invest Ophthalmol Vis Sci (Suppl) 31:503, 1990
7 Jordon MI: An introduction to linear algebra in parallel distributed processing In: Rumelhart DE, McClelland JL (eds) Parallel Distributed Processing, pp 365-411. Cambridge, MA: MIT Press 1986
8 Gorman RP, Sejnowski TJ: Analysis of hidden units in a layered network trained to classify sonar targets. Neural Networks 1:75-89, 1988
9. Lang KJ, Witbrock MJ: Learning to tell two spirals apart In: Touretzky DS, Hinton GE, Sejnowski TJ (eds) Processing of the 1988 Connectionist Models Summer School. San Mateo, CA: Morgan Kaufmann Publishers 1988
10 James M Classification Algorithms. New York: Wiley 1985
11 Caprioli T, Miller E: Combined use of structural and functional measurements improves discrimination between normal and glaucomatous eyes Invest Ophthalmol Vis Sci (Suppl) 31:503, 1990

A computer-assisted visual field diagnosis system using a neural network

Satoru Nagata[1], Kazutaka Kani[1] and Akihiro Sugiyama[2]

[1]*Department of Ophthalmology, Shiga University of Medical Science, Seta Tsukinowa, Shiga 525,* [2]*Topcon Japan, Hasunuma 75-1, Itabashi, Tokyo 174, Japan*

Abstract

A system was developed enabling the Topcon SBP-1000 perimeter to assist in the diagnosis of ophthalmologic disorders The system utilizes the computer's neural network, which is taught through repetition to recognize various pathologic conditions through analysis of visual field disturbances The network, composed of three layers of cells, was educated using the back propagation method In three days of learning with a 32 bit computer, the system memorized 40 types of visual field patterns, enabling it to classify 13 types of illness The computer-generated classifications showed an 85% rate of concurrence with the diagnosis arrived at by the attending physicians.

Introduction

Perimetry is gaining increasing acceptance as a diagnostic technique by ophthalmologists, brain surgeons, and other specialists. While providing indispensable information on neural diseases, however, the data it provides requires considerable experience for accurate interpretation. Static perimetry, in particular, tends to be harder to utilize than kinetic perimetry for physicians without specialized training In an attempt to resolve some of these difficulties, we produced a computerized system for the assistance of visual field diagnosis.

There are various possible approaches to the development of such a system, one involving the training of a neural network and the other the programming of an expert system. We chose the former course. Expert systems, using the "if...then" rule, can serve as useful diagnostic aids, but are exceedingly difficult to program in such a way as to recognize visual field data and other graphic patterns. Neural networks are harder to control than expert systems, but they have the capacity to work with graphic data, and are hence suitable for the development of assisting systems for visual field diagnosis

Several types of neural networks were produced and then trained to recognize visual field data. The present report describes one of the systems which was successfully trained and proved useful as a diagnostic aid.

Methods

The neural network we developed is composed of three cell layers, 291 cells and 5168 connections. The input layer is made up of 257 cells, with the input value of each cell determined by the corresponding visual field value obtained with the SBP-1000[1]. The ability of the neural network to recognize graphic patterns is affected by the number of cells in the network's hidden layer; trial and error indicated that for the analysis of visual field data with our system the optimal number of hidden layer cells is 19 The outer layer is composed of 15 cells, with each individual cell corresponding to one of the 15 visual field diagnoses the system is capable of reaching. The 15 diagnoses include normalcy, glaucoma (Bjerrum-upper, Bjerrum-lower, arcuate-upper, arcuate-lower, server), hemianopsia (temporal, nasal, upper, lower), scotoma (ring, central, others), concentric contraction, and others.

The neural network was implemented on a 32-bit work station (Toshiba AS3260C) using a C language program. Training was done with a series of 40 representative visual field patterns using the back propagation method[2,3] The system was trained in such a way as to minimize

Perimetry Update 1990/91, pp 291-295
Proceedings of the IXth International Perimetric Society Meeting,
Malmö, Sweden, June 17-20, 1990
edited by Richard P. Mills and Anders Heijl

the value of the error function, represented by the following formula:

$$\text{error function} = \sum_{j=0}^{\text{output layer's cells}} (\text{out}(j)-\text{teacher}(j))^2$$

"Out(j)" in this formula represents the output value (*i e.*, diagnosis) determined by the output layer's cells. "Teacher(j)" indicates the diagnosis reached by the attending physicians on the basis of all available data. Hence the value of the error function decreases as the system's diagnoses approach those of the attending physicians. Learning iterations were halted after approximately 50,000 in three days, as the error function had decreased to less than 0.0001. Following the learning process the network was able to reach an accurate diagnosis on all of the 40 training patterns used.

One important feature of this neural network is that it is not limited to single diagnosis. When new or complex visual field patterns are shown to the system, reactions occur in several of the output layer cells, indicating the range of likely diagnoses (Figs. 1-4).

Results

The functioning of the system was checked using data from 305 visual fields obtained with the SBP-1000 perimeter. Eighty-five percent of the system's conclusions were in agreement with the diagnosis reached by the attending physicians. When the second and third diagnoses of the neural network are taken into account, the rate of agreement rises to 89% and 93%, respectively.

The following are data from several representative cases:

Case 1. a 72-year-old female with primary open angle glaucoma. The patient's left eye ratio was 0.7. The network indicated arcuate glaucomatous visual field loss as its first choice, and severe glaucomatous visual field loss as its second choice (Fig. 1).

Case 2. a 36-year-old male with pituitary adenoma. The system indicated temporal hemianopsia as its first choice, with glaucoma as a weak but possible second choice (Fig. 2).

Case 3 a 63-year-old female also with pituitary adenoma. This patient's visual field pattern was interpreted as glaucomatous by many inexperienced physicians, but was correctly read as temporal hemianopsia by the network (Fig. 3).

Case 4 a 52-year-old female with pigmentary retinal degeneration accompanied by pituitary adenoma. The network indicated uncertainty regarding the diagnosis through the use of the "Others" classification as its first choice, but suggests the strong possibility of temporal hemianopsia in its second choice (Fig.4).

Discussion

The system was designed to assist the visual field screening process for physicians lacking extensive experience in perimetry. It proved able to accurately classify typical visual field defects, and to suggest likely possibilities when confronted with complex or unusual patterns.

Glaucoma and hemianopsia are often difficult to recognize on the basis of a single visual field pattern; in such cases the system is capable of bringing the physician's attention to the possible existence of these conditions.

We are in the process of developing new neural networks capable of a greater range of diagnoses. One of these systems combines right and left visual field data for higher recognition rate of hemianopsia and other intracranial diseases.

The training of these networks must be performed on a 32-bit work station, but once the system is complete it can be transferred to fixed modules for use with 16-bit computers. This makes it possible for most hospitals to use visual field diagnosis networks similar to those described above.

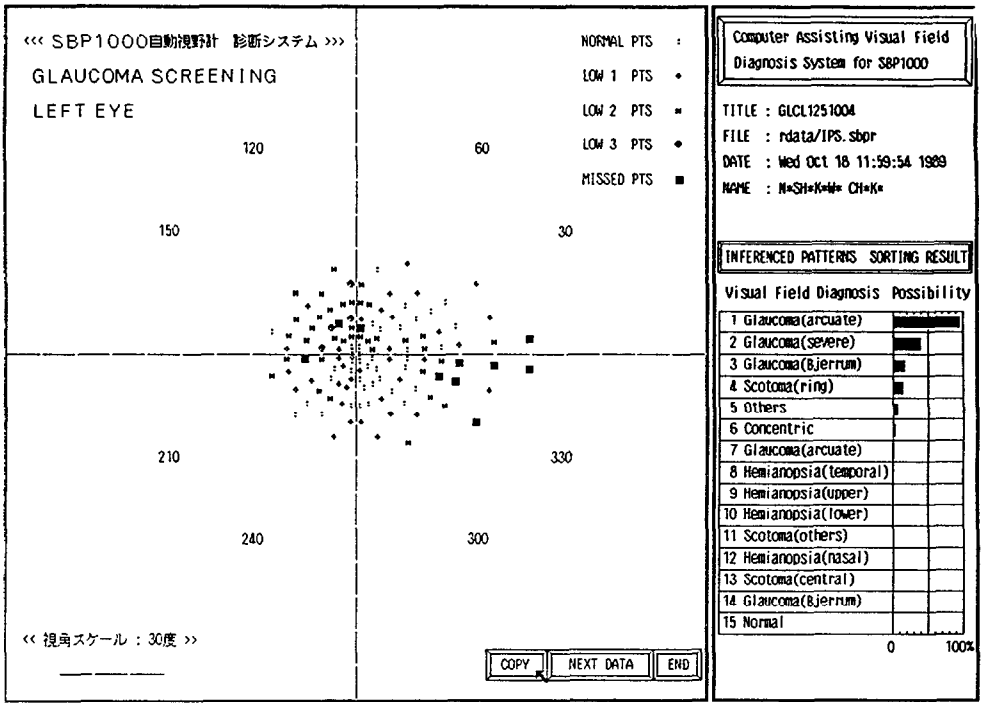
«« SBP1000自動視野計 診断システム »»
GLAUCOMA SCREENING
LEFT EYE
NORMAL PTS :
LOW 1 PTS •
LOW 2 PTS ×
LOW 3 PTS ●
MISSED PTS ■
120
60
150
30
210
330
240
300
« 視角スケール : 30度 »
COPY
NEXT DATA
END
Computer Assisting Visual Field Diagnosis System for SBP1000
TITLE : GLCL1251004
FILE : rdata/IPS.sbpr
DATE : Wed Oct 18 11:59:54 1989
NAME : M×SH×K×W× CH×K×
INFERENCED PATTERNS SORTING RESULT
Visual Field Diagnosis Possibility
1 Glaucoma(arcuate)
2 Glaucoma(severe)
3 Glaucoma(Bjerrum)
4 Scotoma(ring)
5 Others
6 Concentric
7 Glaucoma(arcuate)
8 Hemianopsia(temporal)
9 Hemianopsia(upper)
10 Hemianopsia(lower)
11 Scotoma(others)
12 Hemianopsia(nasal)
13 Scotoma(central)
14 Glaucoma(Bjerrum)
15 Normal
0
100%

Fig 1

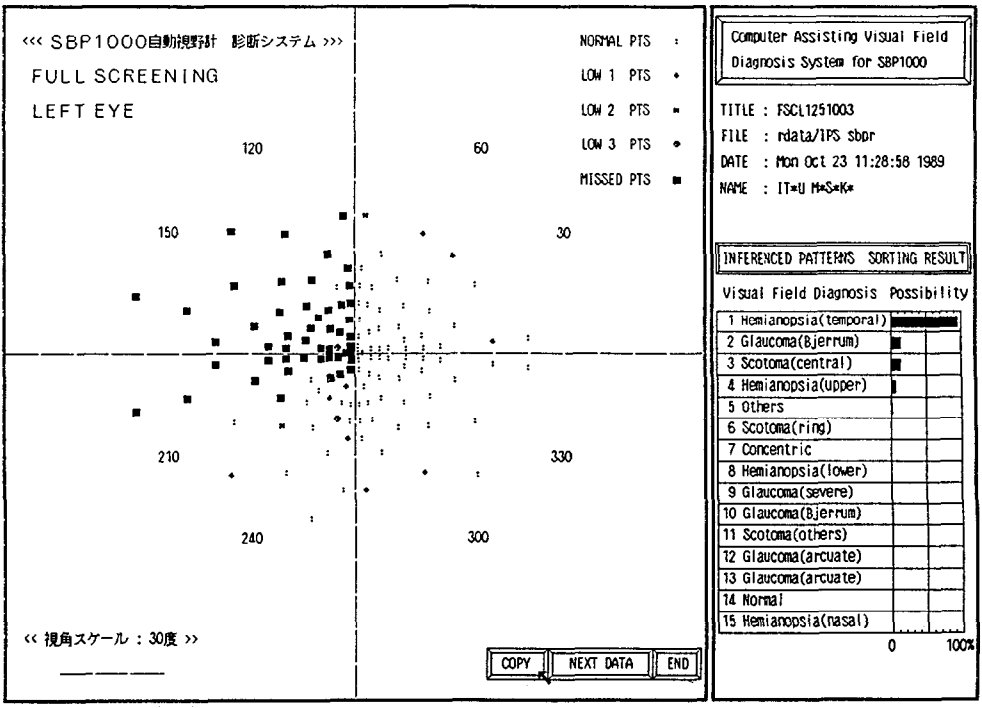
«« SBP1000自動視野計 診断システム »»
FULL SCREENING
LEFT EYE
NORMAL PTS :
LOW 1 PTS •
LOW 2 PTS ×
LOW 3 PTS ●
MISSED PTS ■
120
60
150
30
210
330
240
300
« 視角スケール : 30度 »
COPY
NEXT DATA
END
Computer Assisting Visual Field Diagnosis System for SBP1000
TITLE : FSCL1251003
FILE : rdata/IPS.sbpr
DATE : Mon Oct 23 11:28:58 1989
NAME : IT×U M×S×K×
INFERENCED PATTERNS SORTING RESULT
Visual Field Diagnosis Possibility
1 Hemianopsia(temporal)
2 Glaucoma(Bjerrum)
3 Scotoma(central)
4 Hemianopsia(upper)
5 Others
6 Scotoma(ring)
7 Concentric
8 Hemianopsia(lower)
9 Glaucoma(severe)
10 Glaucoma(Bjerrum)
11 Scotoma(others)
12 Glaucoma(arcuate)
13 Glaucoma(arcuate)
14 Normal
15 Hemianopsia(nasal)
0
100%

Fig 2

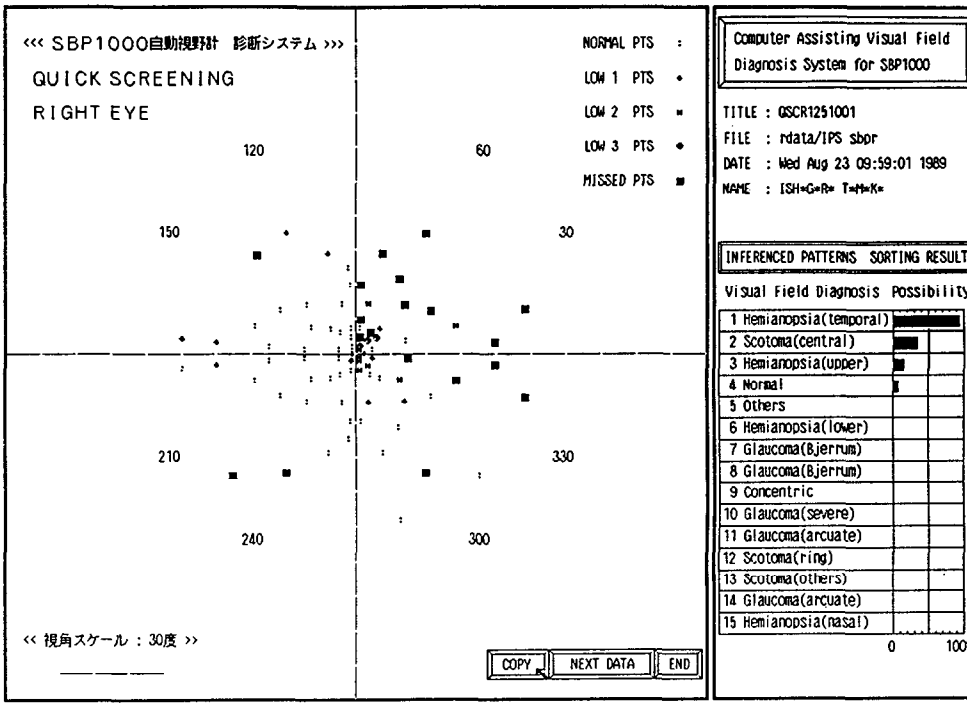
«« SBP1000自動視野計 診断システム »»
QUICK SCREENING
RIGHT EYE
NORMAL PTS :
LOW 1 PTS
LOW 2 PTS
LOW 3 PTS
MISSED PTS
120
60
150
30
210
330
240
300
« 視角スケール : 30度 »
COPY
NEXT DATA
END
Computer Assisting Visual Field Diagnosis System for SBP1000
TITLE : QSCR1251001
FILE : rdata/IPS sbpr
DATE : Wed Aug 23 09:59:01 1989
NAME : ISH=G=R= T=M=K=
INFERENCED PATTERNS SORTING RESULT
Visual Field Diagnosis Possibility
1 Hemianopsia(temporal)
2 Scotoma(central)
3 Hemianopsia(upper)
4 Normal
5 Others
6 Hemianopsia(lower)
7 Glaucoma(Bjerrum)
8 Glaucoma(Bjerrum)
9 Concentric
10 Glaucoma(severe)
11 Glaucoma(arcuate)
12 Scotoma(ring)
13 Scotoma(others)
14 Glaucoma(arcuate)
15 Hemianopsia(nasal)
0
100%

Fig 3

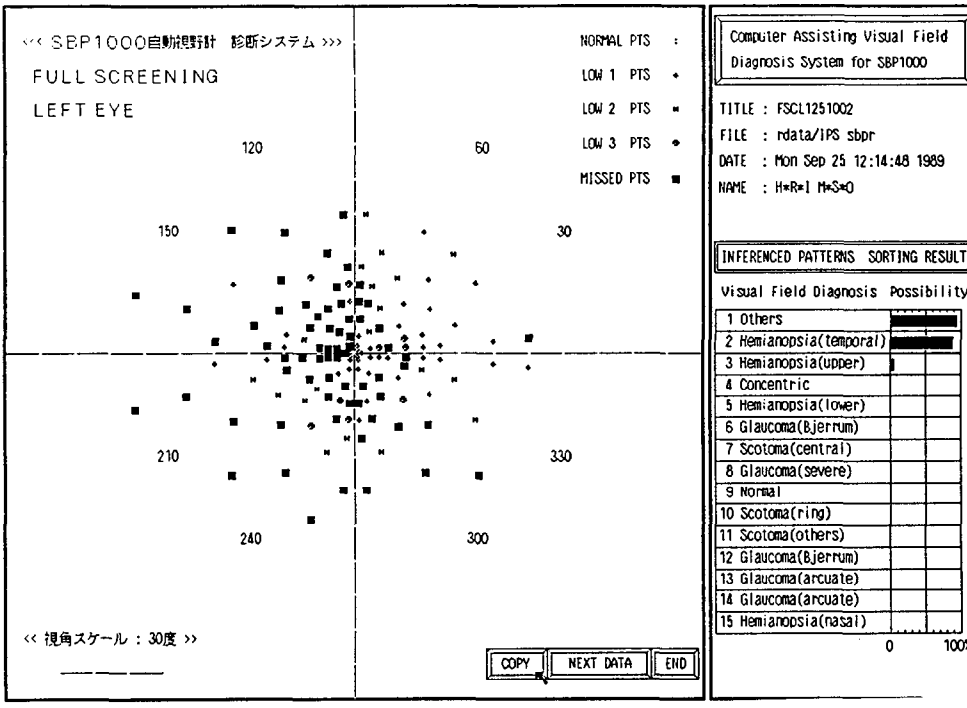
«« SBP1000自動視野計 診断システム »»
FULL SCREENING
LEFT EYE
NORMAL PTS :
LOW 1 PTS
LOW 2 PTS
LOW 3 PTS
MISSED PTS
120
60
150
30
210
330
240
300
« 視角スケール : 30度 »
COPY
NEXT DATA
END
Computer Assisting Visual Field Diagnosis System for SBP1000
TITLE : FSCL1251002
FILE : rdata/IPS sbpr
DATE : Mon Sep 25 12:14:48 1989
NAME : H=R=I M=S=O
INFERENCED PATTERNS SORTING RESULT
Visual Field Diagnosis Possibility
1 Others
2 Hemianopsia(temporal)
3 Hemianopsia(upper)
4 Concentric
5 Hemianopsia(lower)
6 Glaucoma(Bjerrum)
7 Scotoma(central)
8 Glaucoma(severe)
9 Normal
10 Scotoma(ring)
11 Scotoma(others)
12 Glaucoma(Bjerrum)
13 Glaucoma(arcuate)
14 Glaucoma(arcuate)
15 Hemianopsia(nasal)
0
100%

Fig 4

References

1 Kani K, Tago N, Kobayashi K, Shioiri T: A new automatic perimeter Doc Ophthalmol Proc Ser 42:69-73, 1985
2. Rumelhart DE, Hinton GE, Williams RJ: Learning representations by back propagating errors Nature 323:533-536, 1986
3. Rumelhart DE, McClelland JL, PDP Research Group: Parallel Distributed Processing, Vol 1 & 2. Cambridge, MA: MIT Press 1986

Computer-assisted evaluation of the results from high-pass resolution perimetry: a knowledge-based system

Lene M. Martin-Boglind and Peter Wanger

Department of Ophthalmology, Sabbatsberg Hospital, P O. Box 6401, S-113 82 Stockholm, Sweden

Abstract

High-pass resolution perimetry (HRP) is a computer-based method for measuring resolution thresholds in the central 30 degree visual field. As with any other computerized perimetric technique, HRP generates a large number of data to be considered when the examination results are evaluated The aim of the present study was to develop a computer program for at least a preliminary evaluation of visual fields, obtained using the high-pass resolution perimetric system The performance of a program prototype was compared with that of clinical observers with various degrees of experience of the HRP system Sixty visual fields from 30 patients, selected to be non-trivial for evaluation, were used in this test The number of correct diagnoses made by the program was higher compared to clinical observers when evaluating individual visual fields and equal to the best observer when evaluating visual field pairs Computerized evaluation of the results of high-pass resolution perimetry can be expected to give considerable support to the final diagnostic decision.

Introduction

The recently developed high-pass resolution perimetry (HRP) relies on acuity measurements in the 30 degree central field. A direct linear correlation has been demonstrated between retinal ganglion cell density and the resolution threshold[1]. This finding has been corroborated by means of comparisons with retinal nerve fiber layer photography[2,3] and measurements in the photocoagulated retinas of diabetic patients[4]. HRP has been shown to be a sensitive test for optic nerve damage in glaucoma[5] and minor optic neuropathies after resolved optic neuritis[6] The variability of the test has been found to be low[5,7-9].

Computerized perimeters generate vast amounts of data that can be manipulated in many different ways. HRP produces more than 35 values and indices to be evaluated when performing an exact interpretation of the fields. Although interpretation support is given by graphic presentation of the results and numerical comparison with reference data, the evaluation still requires expertise.

In computer science the development of knowledge-based systems (KBS), also called expert systems, is a rapidly growing area. The knowledge in a KBS has to be formally represented, often as rules based on if-then statements, for example:

- "IF the temporal hemifield of the right eye shows decreased sensitivity
- AND the nasal hemifield of the left eye shows decreased sensitivity
- THEN a right homonymous hemifield defect is present."

Since the late 1970s it has been recognized that an "intelligent" program has to be provided with high-quality and specific knowledge about the "domain", *i.e.*, the problem area the program is intended to analyze[10]. A useful KBS should perform equally well or better than an expert and be able to explain its reasoning leading to the presented conclusion[11] The knowledge built into the system has to be well-defined and the domain not too wide In visual field (VF) analysis the basic knowledge is well recognized[12] and the domain is narrow. Thus, the evaluation of HRP results seems to be an appropriate task for a KBS application. Krakau[13] has presented a preliminary model for the use of expert system techniques in visual field evaluation.

The aim of the present study was to provide the set of rules needed for a KBS application and to develop and test a program prototype for evaluation of HRP results.

Perimetry Update 1990/91, pp. 297-301
Proceedings of the IXth International Perimetric Society Meeting,
Malmö, Sweden, June 17-20, 1990
edited by Richard P. Mills and Anders Heijl

Material and methods

Visual fields

The VF from 122 eyes in 68 normal subjects, 43 eyes in 34 glaucoma patients, 74 eyes in 37 patients with known disorders affecting the optic chiasm or the retrochiasmatic pathways, and 24 eyes from 24 patients with minor optic neuropathy after resolved optic neuritis, were used to define the values needed by the program for making the VF diagnosis. Since the aim was to define the limits between normal and pathologic findings, patient VFs with small abnormal changes were over-represented in the material.

Normative data

In order to define normal age-corrected limits, the mean scores, differences between quadrant mean scores, thresholds of central test locations, form indices, and quadrant standard deviations, were obtained from two groups of normal subjects. The first group consisted of 22 subjects aged 24±3 years and the second of 30 subjects aged 66±3 years.

The resolution thresholds were compared in each of the 50 test locations from 11 normals, (age-matched to glaucoma patients), nine subjects with ocular hypertension and 15 glaucoma patients, all with a mean score in the upper normal range (5-5.7 dB). The aim was to find out if there were any differences between the groups in thresholds from single or clustered test locations. In addition, the difference in thresholds between test locations above and below the horizontal meridian were calculated.

The normal limits for differences between the mean scores of the four quadrants in the same eye were estimated by visual inspection of frequency histograms based on data from the normal groups.

The resolution thresholds from the eight central test locations from the 24 patients with minor optic neuropathies were compared to corresponding values from age-matched normal subjects. These points were also compared to the 12 adjacent points in the same eyes.

Program development

A program prototype was produced, using the expert system programming language CLIPS (C Language Production System, Cosmic Inc)

The following factors were taken into account:

A Quality of examination.
1 examination time
2 number of presentations
3 number of responses to blanks
4 reaction time
5 number of premature responses
6 number of missed catch targets
7. number of deleted responses
8 retest value
9. retest standard deviation

B Test results
1. age corrected mean score
2. difference between quadrant mean scores
3. standard deviations of quadrant mean scores
4. form index

Program testing

In order to compare the performance of the program prototype with that of clinical observers 30 VF pairs, non-trivial for evaluation, were selected from the 263 VFs. The criterion for selection was that the number of correct diagnoses made by the program should be about 50%. Thus, the clinical observers could be expected to have approximately equal chances of performing either better or worse compared with the program. Eleven of these 30 VF pairs came

from normal subjects, six from glaucoma patients, six from patients with chiasm and seven from patients with retrochiasmatic lesions. Eight ophthalmologists and six perimetrists with experience of the HRP system, ranging from three months to more than two years (mean 17 8 months), participated in the test Each observer was asked to decide whether the VF were normal or pathologic and to define the type of defect

Results

Visual fields

The program prototype correctly identified 98 out of 122 (80%) normal fields, 27 out of 43 (63%) glaucomatous fields (increase in mean score) and 47 out 74 (64%) ncurologic fields (hemifield/quadrant defects) The program considered 13 out of the 24 (54%) VFs from patients with minor optic neuropathy as pathologic (increased mean score in four fields, abnormal form index in five and both indices pathologic in four fields) The given percentages should not be regarded as sensitivity measures since the material was selected and was not representative of the respective patient population. The VF diagnosis was regarded as correct when the indicated type of defect corresponded to the patient's known disorder or when VFs from normal subjects were labelled normal.

Normative data

Means and standard deviations of mean scores from the two normal groups, aged 24±3 and 66±3 years, respectively, were 3 67±0 75 and 4 45±0.78 dB. Linear interpolation gave a rate of threshold increase of 0.018 dB per year Form index was 0 69±0.09 with no difference between the two groups of normal subjects (younger 0 69±0 09, elderly 0 69±0 10)

The normal quadrant mean scores were 3.8±1.1 (lower temporal quadrant), 4.1±1.0 (upper nasal) and 4.2±1.1 (upper temporal and lower nasal quadrants). The limits for normal difference between quadrant mean scores in the same eye ranged from 1 3 to 1 6 dB Regarding standard deviations of the quadrant mean scores, the upper normal limit was 2 dB

Analysis of thresholds from the central eight or 20 test locations did not reveal any significant difference between the patients with minor optic neuropathy and the normal groups. Mean form index from these patients was 0.60±0 20

Regarding thresholds from single or clustered test locations, no difference was observed

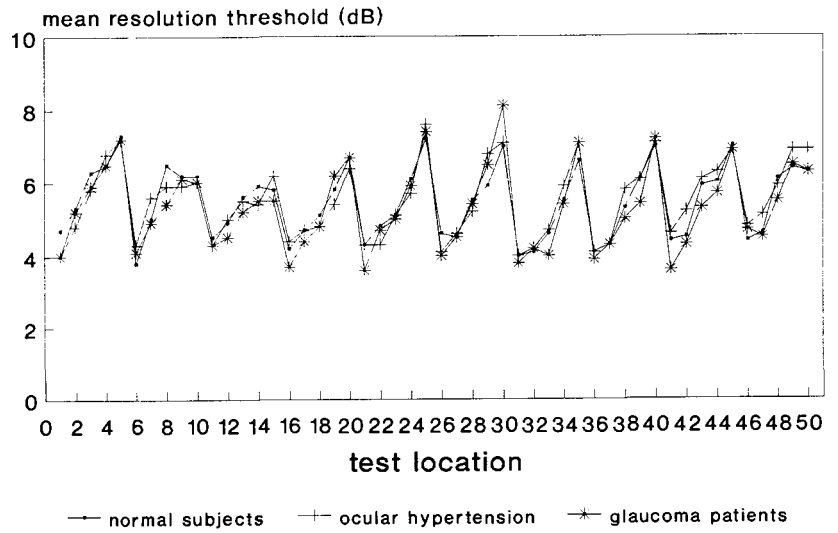

Fig 1 Mean resolution threshold in each test location from 11 normal subjects, age-matched with the 15 glaucoma patients and eight patients with ocular hypertension, all with mean scores in the upper normal range (5-5.7 dB) Note the similarity between the groups in the thresholds at every test location

when fields from normal subjects, glaucoma patients or patients with ocular hypertension were compared (Fig. 1.). Analysis of the test locations above and below the horizontal meridian[14] showed no difference between normal subjects and glaucoma patients.

Program development

Program prototyping, using the CLIPS expert programming language, was found to be straight-forward. CLIPS is a flexible tool, which allows addition or removal of rules from the knowledge base without extensive reprogramming. The tested program consisted of approximately 120 rules and evaluated 19 of the more than 35 parameters from each eye, calculated by the HRP system. The remaining parameters were not judged necessary for the development of the program prototype.

Program testing

In the 60 fields, selected for the comparison with clinical observers, the program prototype performed better than the average observer and equally well when compared with the best observer. The program prototype presented a correct diagnosis in 39 of the 60 individual fields and 16 of the 30 field pairs. It should be recalled that these fields were chosen to be non-trivial for evaluation. The average clinical observer correctly identified the diagnosis in 29 of the 60 individual fields and 14 of the 30 field pairs. The best observers made correct evaluations of 33 individual fields and 16 pairs.

Discussion

In the present study, a commercially available expert system programming language was used to produce a program prototype for evaluation of the results of high-pass resolution perimetry (HRP). Normative data were established in order to provide the program with the necessary knowledge. The tested prototype consisted of some 120 rules. In comparison with clinical observers the program performed better than the average observer and equally well as the best observers. Similar findings have been reported regarding the performance of expert systems in other fields of medicine[15,16]

The rules in the program were derived from the standard knowledge of perimetry[12] regarding hemifield and quadrant defects. This knowledge is based on the anatomy of the visual pathways. In glaucoma increased mean score has been reported to be the cardinal HRP sign[5]. This view is supported by the findings in the present study. The visual field changes in early glaucoma[17-19] observed using differential light threshold technique, *i.e* , paracentral scotoma and nasal step, do not seem to add any diagnostic information in the HRP system. Form index has been reported to be a sensitive sign of minor optic neuropathy[6]. In the present study the mean form index from normal subjects was lower than previously reported[6] but still significantly different from the mean form index from the patients with minor optic neuropathies. The normative data in the present study agrees well with previously reported findings regarding mean score and the influence of age[20,21].

The expertise required by the program was rather limited, most of the relevant evaluations could be performed using less than 200 rules Explanation of the proposed visual field diagnosis can simply consist of a list of the observed abnormalities. As in most physiologic tests, the borders between normal and pathologic HRP values are blurred rather than crisp. A structured analysis of borderline findings can be performed using the available KBS techniques for "reasoning under uncertainty"[11]. Adding rules to the program for this purpose will be trivial, once the relevant data have been gathered.

In conclusion, computerized evaluation of the results from high-pass resolution perimetry was found to be at least as competent as evaluations made by clinical observers and can be expected to give a considerable support to the final diagnostic decision.

Acknowledgements

The authors are grateful to Klas Orsvärn, civil engineer, Swedish Institute of Computer Science, for his friendly support during the program development. The study was supported by grants from the Karolinska Institute and from Alcon Laboratories Inc.

References

1. Frisén L: A computer-graphics visual field screener using high-pass spatial frequency resolution targets and multiple feed-back devices. Doc Ophthalmol Proc Ser 49:441-446, 1987
2. Lindblom B: High-pass resolution perimetry: a new method for the early detection of visual field defects. Chibret Int J Ophthalmol 7:33-41, 1990
3. Airaksinen PJ, Tuulonen A, Välimäki J, Alanko HI: Retinal nerve fiber layer abnormalities and high-pass resolution perimetry. Acta Ophthalmologica 68:687-689, 1990
4 Lindblom B: Effects of laser-induced retinal lesions on perimetric results (submitted)
5. Wanger P, Persson HE: Pattern-reversal electroretinograms and high-pass resolution perimetry in suspected or early glaucoma. Ophthalmology 94:1098-1103, 1987
6. Frisén L: A shape statistic for visual field evaluation: utility in minor optic neuropathy Neuro-ophthalmology (Amsterdam) 9:347-354, 1989
7. Douglas GR, Drance SM, Mickelberg FS, Schulzer M, Wijsman K: Variability of the Frisén ring perimeter In: Heijl A (ed) Perimetry Update 1988/89 Amsterdam/Berkeley/Milano: Kugler & Ghedini Publ 1989
8. Drance SM, Douglas GR, Schulzer M, Wijsman CS: The learning effect of the Frisén ring perimeter In: Heijl A (ed) Perimetry Update 1988/89 Amsterdam/Berkeley/Milano: Kugler & Ghedini Publ 1989
9 Martin-Boglind LM, Wanger P: The influence of feed-back devices, learning and cheating on the results of high-pass resolution perimetry. In: Heijl A (ed) Perimetry Update 1988/89 Amsterdam/Berkeley/Milano: Kugler & Ghedini Publ 1989
10 Waterman DA: A Guide to Expert Systems Reading: Addison-Wesley 1985
11 Giarratano J, Riley G: Expert Systems: Principles and Programming Boston: PWS-KENT Publ Co 1989
12 Harrington DO: The Visual Fields: A Textbook and Atlas of Clinical Perimetry. St Louis: CV Mosby Co 1981
13. Krakau CET: Artificial intelligence in computerized perimetry Doc Ophthalmol Proc Ser 49:441-446, 1987
14. Sommer A, Enger C, Witt K: Screening for glaucomatous visual field loss with automated threshold perimetry. Am J Ophthalmol 103:681-684, 1987
15 Chard T: Human versus machine: a comparison of a computer expert system with human experts in the diagnosis of vaginal discharge Int J Bio-Med Computing 20:71-78, 1987
16. Miller PL: The evaluation of artificial intelligence systems in medicine. Comp Meth Prog Biomed 22:5-11, 1986
17 Aulhorn E, Harms H: Early visual field defects in glaucoma. In: Leydhecker W (ed) Tutzing Symposium 1966, pp 171-186. Basel: Karger 1967
18 Hart WM, Becker B: The onset and evolution of glaucomatous visual field defects Ophthalmology 89:268-279, 1982
19 Heijl A, Lundqvist L: The location of earliest glaucomatous visual field defects documented by automatic perimetry Doc Ophthalmol Proc Ser 35:153-158, 1983
20. Frisén L: Perimetric variability: importance of criterion level. Doc Ophthalmol Proc Ser 70:323-330, 1989
21. House PH, Schulzer M, Drance SM, Douglas GR: Do lens opacities affect the resolution visual field in normal subjects? (submitted)

Extended empirical statistical package for evaluation of single and multiple fields in glaucoma: Statpac 2

Anders Heijl[1], Georg Lindgren[2], Anna Lindgren[2], Jonny Olsson[2], Peter Åsman[1], Steven Myers[3] and Michael Patella[3]

[1]*Department of Ophthalmology, Malmö General Hospital, Sweden;* [2]*Department of Mathematical Statistics, University of Lund, Sweden,* [3]*Allergan Humphrey, San Leandro, CA, USA*

Abstract

A statistical package, based on empirically determined normative physiologic data, has been available for the Humphrey perimeter since 1986. The authors have now developed an extension of that package, providing improved analyses for change in glaucomatous visual fields, and a new routine for recognition of glaucomatous field loss in single fields Data from repeated threshold testing of glaucoma patients over a one-month period were used to establish empirical significance limits for change in glaucomatous fields These limits depend on test point location, initial defect depth, number of tests available, and global sensitivity as measured by mean deviation (MD). They are used to calculate change probability maps showing the significance of deteriorations or improvements at each test point Significance limits for change in MD are also incorporated into the package. The linear regression analysis of changes in MD over many tests has been improved; in cases where significant learning can be identified by the program, the analysis is done ignoring the first test. The extended package also provides a plain text analysis of single fields, the glaucoma hemifield test (GHT). The GHT is primarily based on significance of deviations from normal threshold values as expressed in pattern deviation probability maps Results in five sectors in the superior field are compared with those in five corresponding mirror-image sectors in the inferior field. The text indicates if these up-down differences exceed or fall within the limits of normality, or if the result is borderline. Generalized shifts in sensitivity are also recognized and flagged

Introduction

Inter-test threshold variability is high in glaucomatous visual fields[1-8], making differentiating between random fluctuations and true change a common and important problem in glaucoma management. None of the generally available analysis aids for detecting visual field change have made use of knowledge of pathophysiological test-retest variability in glaucomatous visual fields.

We have previously described random test point variability in glaucoma using data from 51 glaucoma patients, who were tested four times each during a one month period; we found that point-by-point inter-test threshold variability increased with increasing eccentricity and depended upon baseline defect depth[9]. Further and more recent analyses of these fields have shown that point-by-point variability increased not only with increasing eccentricity but also with increasing baseline defect depth, and depended on general field status as expressed by MD[10]. We set out to devise a statistical method which makes use of these findings in judging change.

Determination of normality or abnormality of single visual field results has become simpler with the availability of normative values, deviation maps, visual field indices and particularly probability maps. Interpretation may still be problematic in many cases, however, and a need to standardize and codify visual field interpretation also exists. Cross-meridional comparisons have often been used in visual field interpretation, and one numerical method has been devised with the intent of better judging the normality of field results[11]. Our earlier work has suggested that it is possible to improve such up-down comparison methods by basing them on the signif-

Address for correspondence Anders Heijl, Department of Ophthalmology, Malmö General Hospital, S-21401 Malmö, Sweden

Perimetry Update 1990/91, pp 303-315
Proceedings of the IXth International Perimetric Society Meeting,
Malmö, Sweden, June 17-20, 1990
edited by Richard P. Mills and Anders Heijl

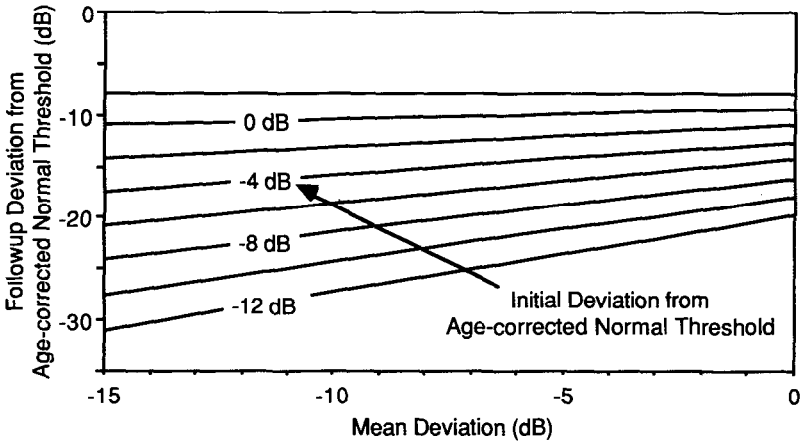

Fig. 1. Derived confidence limits ($p<0.05$) for deterioration for the most peripheral zone of the central visual field. Plots are for the case of a single baseline and a single follow-up test. Note that variability is larger for higher baseline defect depths than for lower values, and that variability depends on MD. Variability is also larger peripherally than centrally

icance of departures from normal values at each point instead of using simple threshold values[12,13]. The package described here uses such comparisons of test point significance as the basis for an automated method of assessing fields in patients having or suspected of having glaucoma

Methods

Analysis for change

We measured and analyzed random inter-test variability in glaucomatous visual fields (details about the material in ref[9]). Distributions of point-by-point threshold changes (in decibels) were plotted for different point locations, types of points (normal to severely depressed), and types of visual fields (abnormal to severely depressed) (Fig. 1)[9,10]. Point-by-point significance limits were produced for inner, central, and outer zones of the 30-2 pattern. We produced separate tables for the cases of one and two baseline fields.

We also wished to identify and indicate those clinical cases where the MD change exceeds

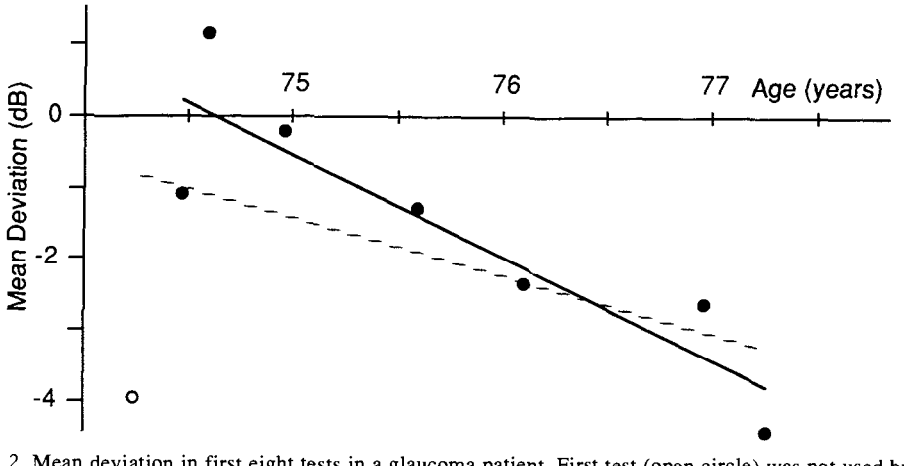

Fig 2 Mean deviation in first eight tests in a glaucoma patient First test (open circle) was not used by linear regression analysis since hypothesis of unchanged perimetric experience was rejected at a $p<5\%$ level. Slope -1 4 dB/year, significant at a $p<0.7\%$ level (solid line) Ignoring the difference in perimetric experience by including the first test gives a much less significant ($p<20\%$) slope (dotted line).

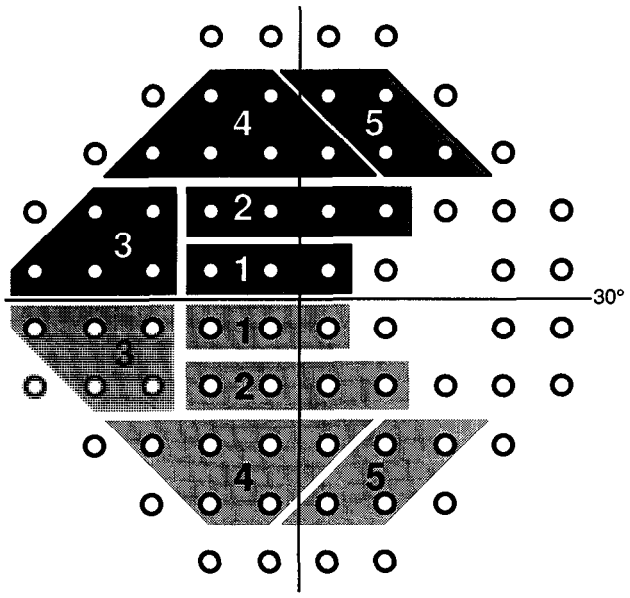

Fig. 3. Zones used in the glaucoma hemifield test (GHT) for determination of normality. The sum of probability scores is calculated for each sector. Significant up-down differences, as well as significant defects occurring simultaneously in mirror-image sectors, are reported

the random variability typically seen in glaucoma patients. Up to now, detection of significant changes in MD has required a minimum of five tests since only linear regression techniques have been available. The same empirical data employed for the change probability maps were used to produce significance limits for changes in mean deviation[14] at 10%, 5%, and 2.5% levels, which can then be used as early as at the second test session.

Finally, we wished to correct for learning effects in cases where such increased experience was likely to adversely affect judgments of change over time[15]. Thus, we have modified the previously available linear regression on MD[14] to ignore the first test result in the series if its MD is significantly out of line with and worse than the trend shown in later tests at the 5% level (Fig. 2)[16]. This is accomplished by performing a separate regression analysis on the MD values for all but the first test, and then determining if this gives a significantly better linear model. If it does, the first test is not considered. The analysis for learning effects is automatically performed whenever five tests are available. In cases where a test is eliminated from the linear regression, it is also not used as one of the baseline tests in forming the change probability maps and in calculating changes in MD.

Analysis for normality

We intended to provide a sensitive automated method for detecting localized loss, as well as overall shifts in sensitivity.

The central field was divided into five sectors in the superior field and five mirror-image sectors in the inferior field (Fig. 3). Photographs of nerve fiber layer patterns in normal subjects were used when these sectors were defined. Measurement results in these sectors are graded according to a score assigned to the point-by-point significance in the Statpac 1 pattern deviation probability map. Visual field normality is primarily judged in terms of score differences between pairs of mirror-image sectors, superior *versus* inferior; in some cases it is also based upon absolute scores in each of the ten sectors. Overall depression or super-normality is determined based on results at a subset of the most sensitive points in the field, independent of sector groupings.

Scoring for each sector is done as follows: non-significant test points are given a score of 0; points which are significant at the 5% level, a score of 2; points which are significant at the

2% level, a score of 5. Points reaching significance of 1% and greater are given a calculated score of 10 or more; if the pattern deviation happens to coincide with the 1% limit, a score of 10 is assigned; if the deviation is larger, the score is ten times the pattern deviation divided by the 1% significance limit. The program then calculates the sum of such scores for each sector, and calculates the up-down score differences between each of the five pairs of sectors.

Empirical distributions were determined for these sector score differences from the normal database used for the creation of the Statpac 1 program package (details about the Statpac 1 data base are given in ref[14]) From these distributions we determined limits of normality. For example, only 1% of measurements from our normal population lies outside the 1% limit of normality. Both positive and negative differences can be signs of disease and consequently the limits were calculated for a two-sided test.

We wanted the GHT to be sensitive to nasal steps and similar defects. The presence of trial lens artifacts in the normal material would, however, seriously widen the limits for nasal up-down differences Therefore the normal database for the GHT includes no tests having two or more absolute defects in the most peripheral points; such points obviously are test artifacts if occurring in normal eyes. Obviously such a strategy causes the GHT to be more likely to classify fields as abnormal due to simple trial lens artifacts, but we believe this to be a reasonable trade-off We also excluded fields having significantly super-normal threshold results based on the general height as described below. However, in determining the empirical frequency distributions no tests were eliminated from consideration based upon reliability indices alone. Thus included were 540 tests from 265 subjects.

Fields with one or more pairs of mirror image sectors showing up-down differences reaching the upper or lower 0.5% limit of normality are classified as abnormal. If no sector pair difference reaches the upper or lower 1.5% limit of normality the field is classified as normal Otherwise the field is classified as borderline.

Fields with symmetric defects in the superior and inferior field, for example a double arcuate scotoma, could sometimes be missed in a scheme sensitive only to differences across the horizontal meridian We therefore also used the normal data base to determine one-sided significance limits for the scores in each of the ten individual sectors alone, without reference to the corresponding sector in the other hemifield. Using these limits Statpac 2 also classifies fields as abnormal if two mirror-image sectors both individually reach the 0 5% significance limit.

We also wanted to detect generally depressed and overtly supernormal fields. The degree of general reduction or increase of sensitivity, called general height (GH), is determined by analyzing the measured threshold value at the most sensitive points in the field. The deviations from normal for all points in the 24-2 pattern are ranked from most positive (often supernormal) to most negative, and the 85th percentile point's deviation from age normal is set equal to the general height. Thus, in computing GH for a 30-2 test, only a subset of the points, those comprising the 24-2 pattern, are considered. We have calculated the distribution of GH in the material of normal fields In this analysis no fields were excluded. GH is the same value which is used to shift from total deviation to pattern deviation maps of the original Statpac program The messages "GENERAL REDUCTION OF SENSITIVITY" or "ABNORMALLY HIGH SENSITIVITY" are printed when the 0 5% high and low limits respectively for GH are exceeded.

Results

General findings

Determination of change

Finite instrument dynamic range, high variability, and the necessarily limited number of patients tested in the data base only allowed calculation with acceptable certainty of confidence intervals for deteriorations from initial deviations from normal in the range -12 dB to +2 dB; for improvements from initial deviations between -28 dB and 0 dB, and also only for MDs better than -15 dB.

General observations, however, allow us to make statements in many cases falling outside these limits. The observation that variability increased with increasing defect depth allows the ruling out of significant change for deteriorations from initial deviations more negative than -12 dB in cases where the change is less than that required for significance at -12 dB. Similarly,

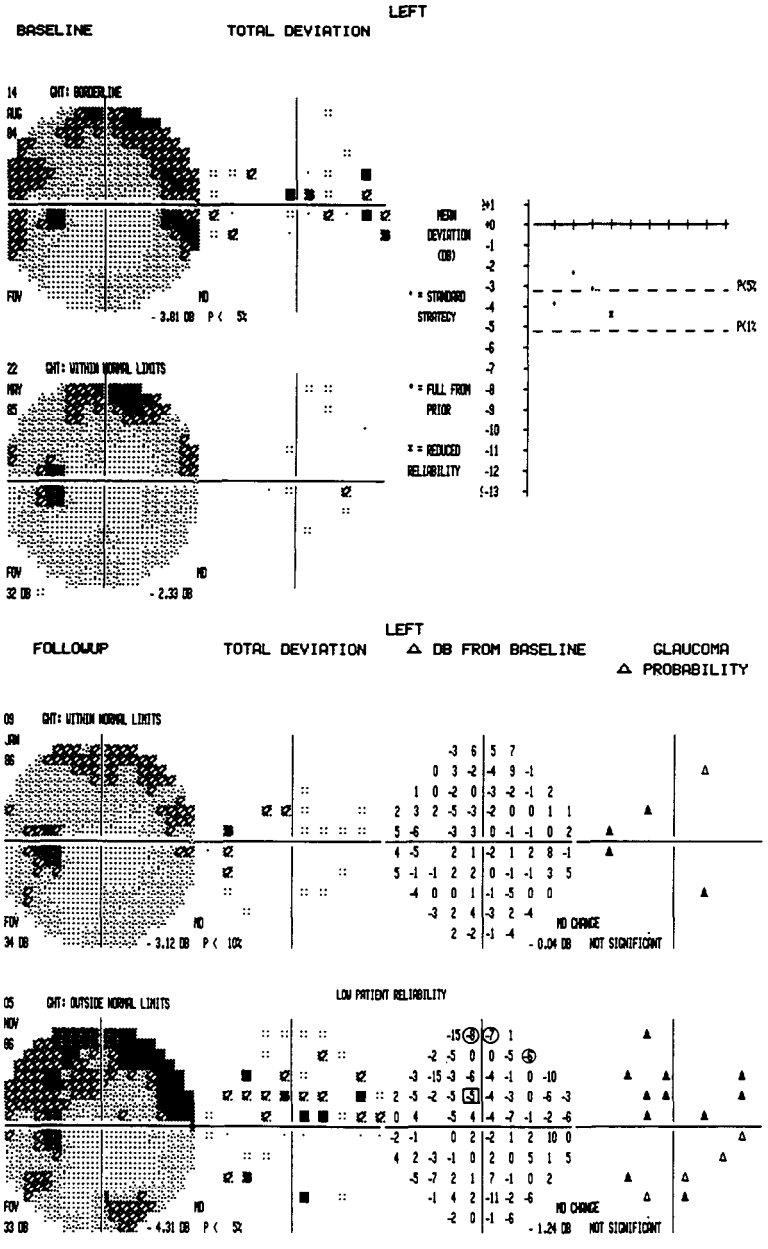

Fig 4 Change probability maps for a glaucoma patient having moderate visual field loss. In the follow-up test dated 05.11.86 a change of -5 dB in the most central area (boxed value) was computed to be significant, while changes of -5, -7, and -9 dB in more peripheral locations (circled values) were not significant, illustrating that significance is affected by both initial defect depth and by eccentricity Significance levels also vary with MD and with the number of initial baseline tests

improvements from initial deviations more negative than -28 dB are significant if they reach a sensitivity which would have been significant if starting from -28 dB. Deteriorations from initial levels more positive than +2 dB are significant if the same follow-up sensitivity would have been significant based on a starting level of +2 dB better than the age-corrected normal

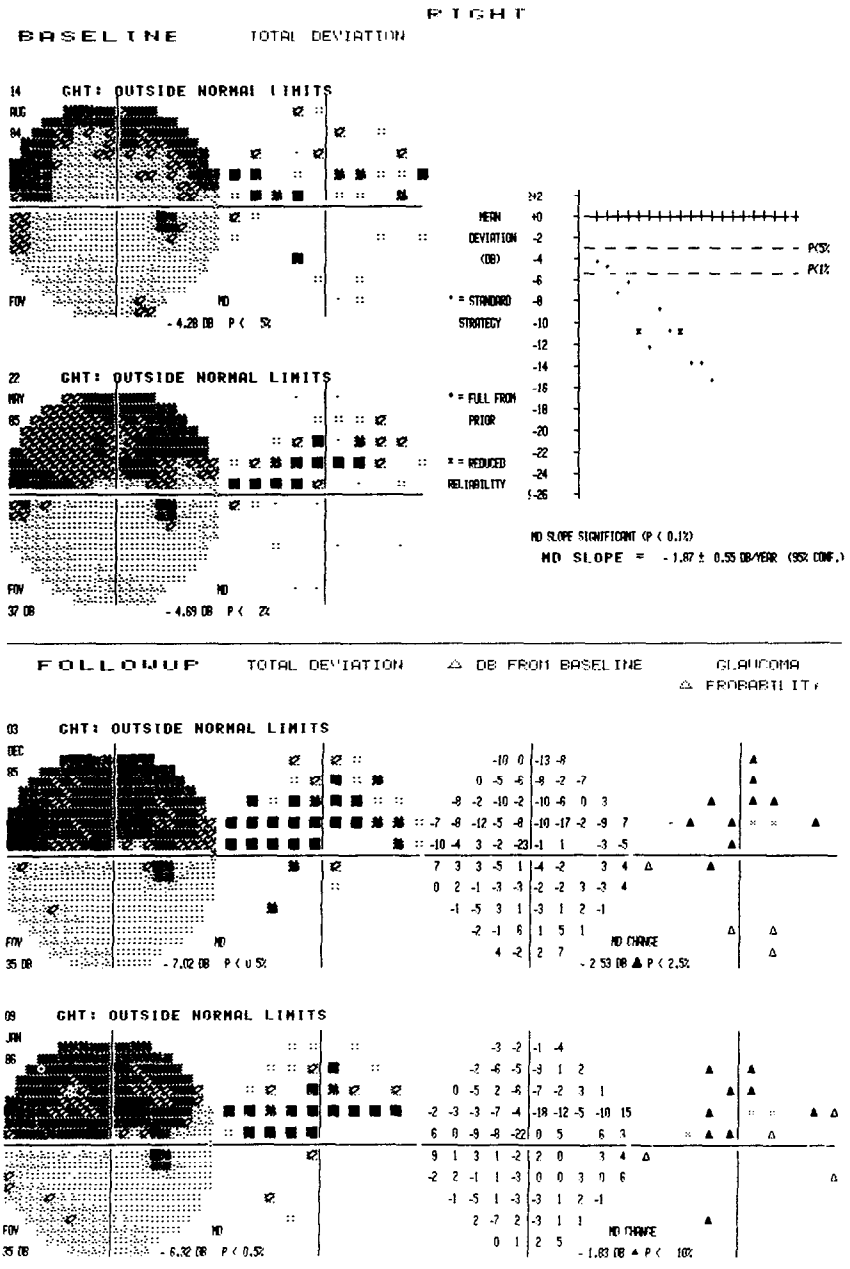

Fig 5 Change probability maps in a glaucomatous field Progressive field loss is seen in the superior hemifield. Only four tests are shown here but later change probability maps showed the same results. Points not addressed by the database are indicated by x.

threshold level.

Limited statements may also be made about change probability maps made from fields with mean MDs more negative than -15 dB. We found in glaucomatous fields that the point-by-point deteriorations required in order to reach significance became larger with increasingly negative MDs, while point-by-point improvements required became smaller. Thus, it is possible to say that patients having MDs more negative than -15 dB, whose fields do not appear to be deteri-

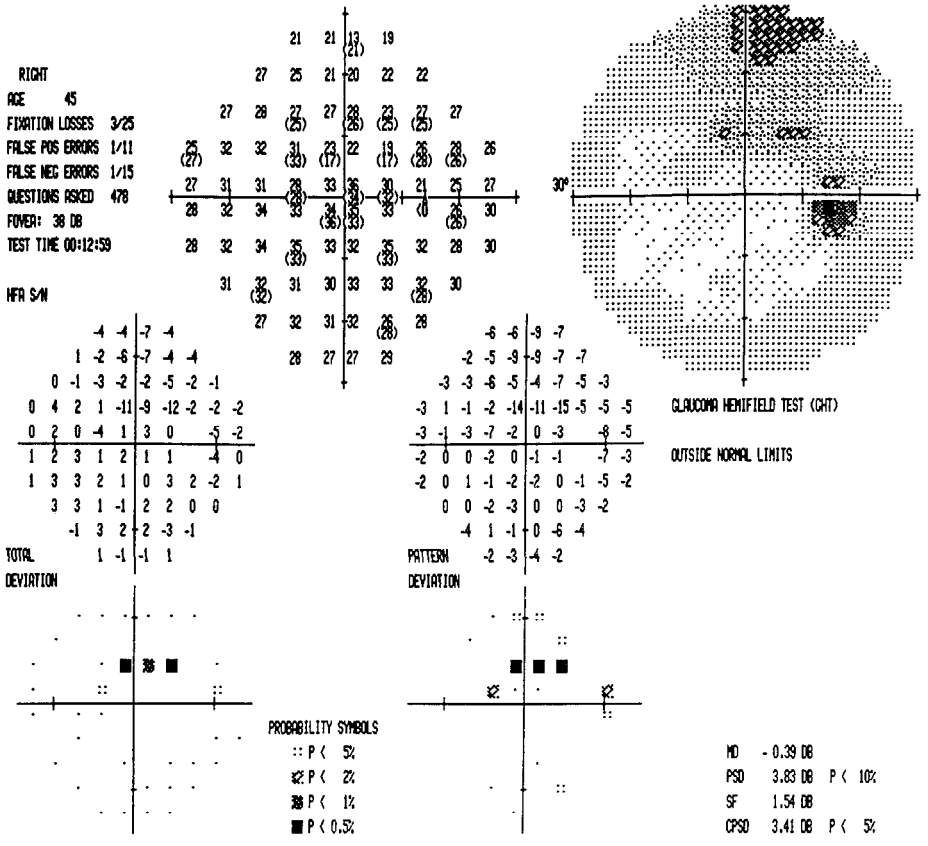

Fig 6 Glaucomatous visual field. GHT has judged this field to be abnormal based on vertical asymmetry in area 2 (cf Fig 3). All fields with one or more pairs of mirror-image sectors showing up-down score differences seen in fewer than 1% of normals are classified as abnormal

orating when judged relative to the limits appropriate for an MD of -15 dB, most likely are not deteriorating.

It may be noticed that since all perimeters have a limited dynamic range, it will, in points with an initial absolute defect, be impossible to know if a change is small enough to be non-significant. Explicitly flagging such points on printouts would be more confusing than helpful. Instead we decided to indicate only if the change to or from a sensitivity below 0 dB was at least large enough to be significant.

Significance limits for change in MD were found to be dependent on MD itself similarly to what was seen for individual deviations.

Judgment of normality

In calculating the distributions for upper minus lower sector scores, we found them to be asymmetric and therefore determined separate upper and lower significance limits for differences. Thus, in the central and nasal sectors larger differences were generally required when the lower hemifield was most disturbed, while for the temporal areas the upper and lower limits were more similar to each other.

Explanation of printouts

In general, change probability maps are produced using the combined results of the two earliest tests as baseline. In cases where only a single baseline test is chosen by the operator,

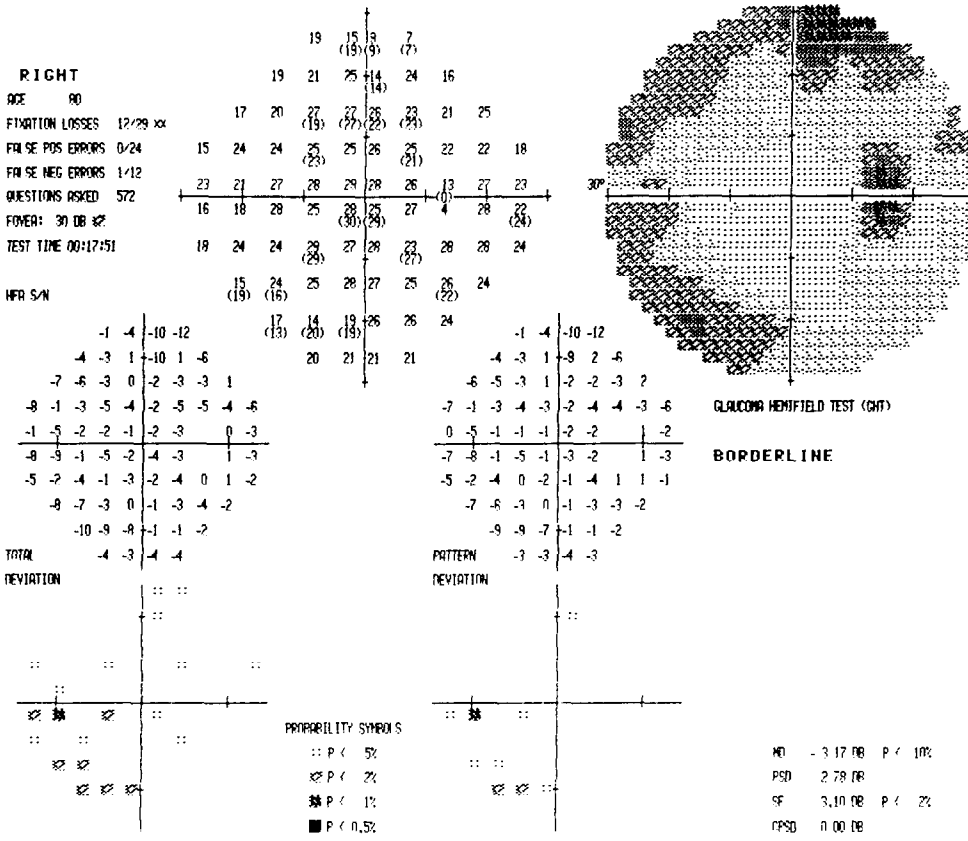

Fig 7 Visual field in a subject with increased intraocular pressure. Field evaluation is borderline since the difference for sector pair 3 reaches the 3% limit for normals, but no pair reaches the 1% limit.

a warning is printed suggesting that any apparent changes found be confirmed prior to institution of a modification to the patient's therapy Each follow-up test is compared on a point-by-point basis with that baseline, and a change map is produced showing points deteriorating or improving by more than the significance limits for random variability in glaucomatous visual fields (Figs. 4 and 5). Changes falling outside the 5% and 95% limits are indicated by triangles, dark for deterioration and open for improvement. Points changing by amounts which are not significant are indicated by a dot Those changing by amounts for which no information about significance is available within the data base are indicated with an X.

The mean MD of the baseline tests is subtracted from that of each follow-up test, and the difference is printed below the associated change probability plot (Figs. 4 and 5). Changes in MD exceeding the significance limits for normal variability in glaucomatous visual fields are indicated numerically and symbolically, with open triangles indicating improvement and dark triangles indicating loss. The level of significance is also indicated.

Individual gray scales, total deviation probability maps[14], the decibel change from baseline at each point, MD, foveal threshold, and the results of the glaucoma hemifield test are also shown for each follow-up. Tests scoring outside the reliability limits of the original Statpac program have a low reliability message appended (see Discussion); such a status does not exclude them from analysis by Statpac 2, however, since its data bases include low reliability results.

Fig. 6 illustrates a simple case where a field was judged to be abnormal due to loss in the superior field in sector No. 2, and Fig. 7 shows a borderline case. Fig. 8 illustrates loss which is largely symmetrical around the horizontal meridian.

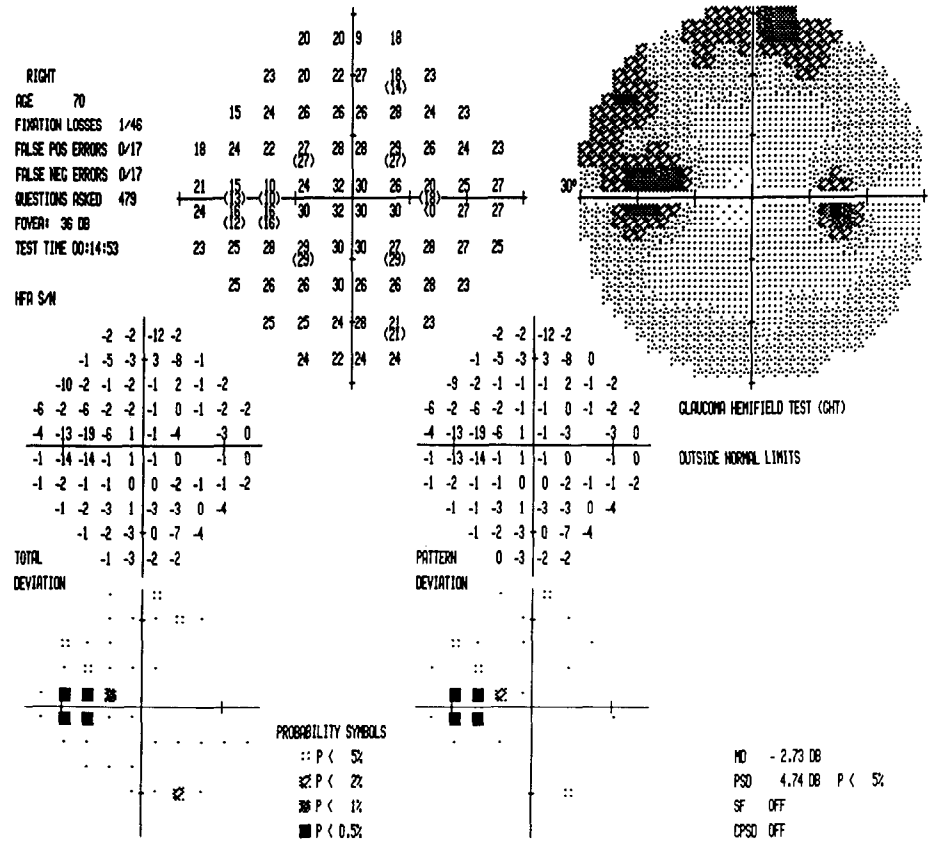

Fig 8 Abnormal field with symmetrical defects in superior and inferior fields The sum of the probability scores in the upper and lower nasal sectors both reach the 0 5% significance limit

Fields showing abnormally high sensitivities are not further classified as normal, borderline or abnormal (Fig. 9) since threshold measurements in such fields often are highly unreliable. Fields are classified as having a general reduction of sensitivity only if they have not been found to be abnormal under any other test in the GHT (Fig. 10). The reason for this is to stress the presence or absence of localized field defects as are typically seen in glaucoma.

Statpac 2 analyses may be applied to any available 30-2 or 24-2 threshold tests, including those produced prior to its availability.

Discussion

One of the most difficult tasks in the management of glaucoma is judging between medically important change and random variability in visual field results. The analyses we present here are the first to make these judgments with the help of prospectively acquired empirical limits for inter-test variability in glaucomatous visual fields. We are of the opinion that such a cautious empirical approach is of critical importance in designing diagnostic methods. We have shown in previous communications[17,18] that, in the absence of empirical information to the contrary, the assumptions of eccentricity independence and Gaussian distributions would have produced misleading information in the probability maps of the Statpac 1 statistical package. We think that an empirical method is similarly essential when addressing the complex issue of change over time in glaucomatous fields, and that this approach makes our change probability maps very different from previously produced maps of this sort[19].

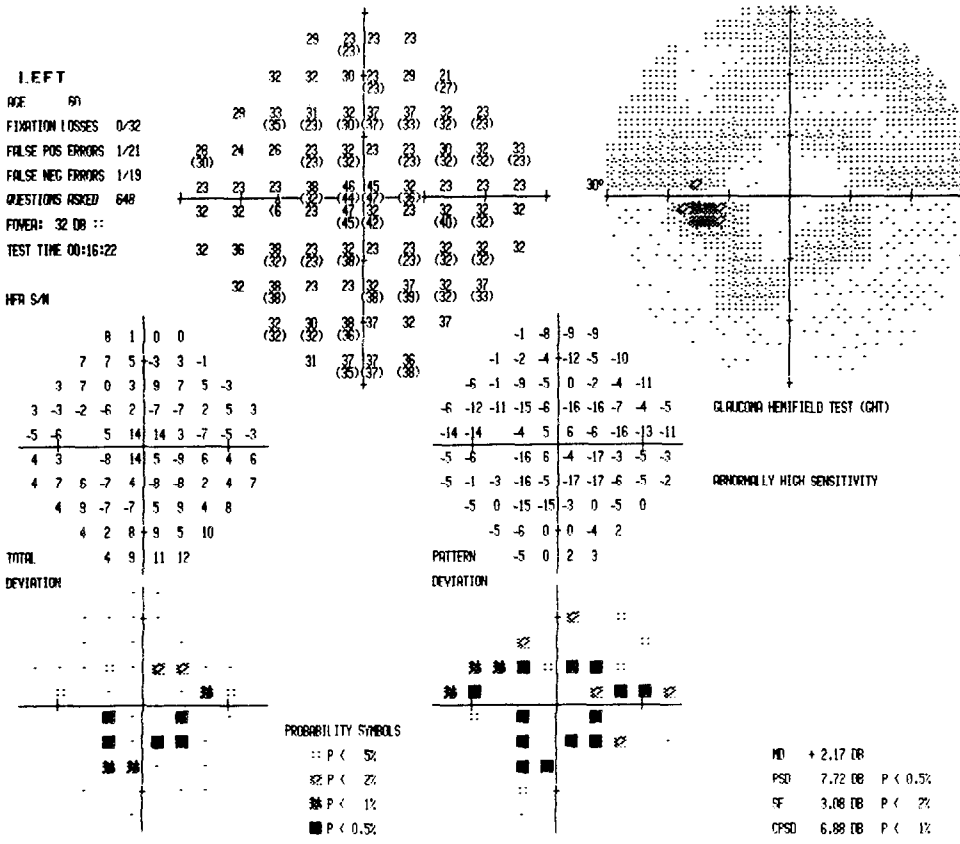

Fig 9 Visual field in a patient with ocular hypertension Several abnormally high sensitivities are seen in the central area General height exceeds the upper 0 5% limit while false positive answers are within normal limits. Such super-normal results are almost exclusively produced by "trigger-happy" patients, *i e* , patients who also tend to press the response button when no stimulus is seen.

It is also clear from our results that any efforts at classifying changes in individual points or visual field sectors on the basis of raw numerical dB changes alone, without consideration of eccentricity, field status, or initial degree of normality/abnormality[6,7] are, at best, non-optimal.

In our opinion change probability maps are considerably easier to interpret than threshold data. However, since the maps use the 5 and 95% limits, random variability should be expected to give a few significant points even in stable eyes. Repeated occurrences suggest true and persistent change. It would be desirable to provide also higher limits for the change maps than the 5 and 95% significance levels presented here, and we have reason to expect that a reanalysis of our basic data using yet more sophisticated techniques may provide these to some extent. We believe, however, that major improvements will only be achieved through the execution of considerably larger prospective studies of variability in glaucoma patients.

We are aware of the limitations of using MD and other global indices to detect change[14,20] and do not advocate sole reliance on MD as an indicator of change. One clear and important benefit of our method of analyzing for change in MD, however, will be to point out cases where a change from baseline to one later test session is not as significant as one might have expected based on clinical judgement only. In our opinion, random variability in glaucoma is often underestimated and therapeutic decisions often made based upon measured changes which are well within these random changes.

The GHT is a first attempt to reduce information in Statpac 1 probability maps into a single plain text expression of field status. Up-down comparisons have been suggested before in field

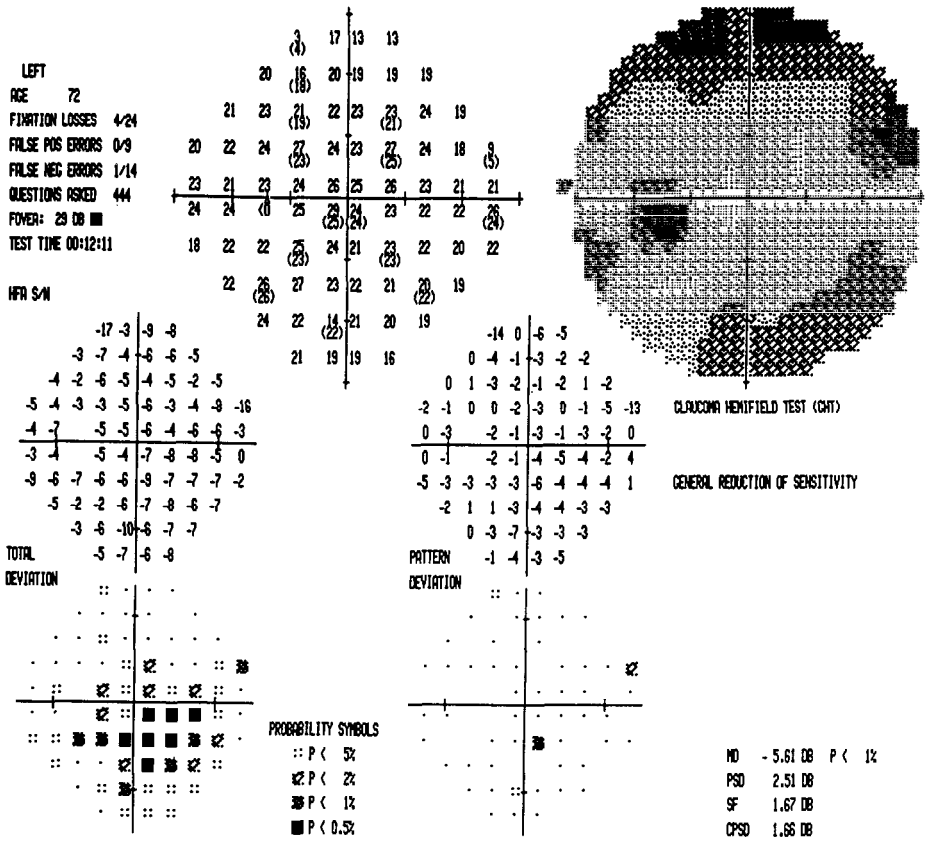

Fig 10 Visual field in a patient with cataract GHT has found a significant general reduction in sensitivity Overall sensitivity shifts are detected by ranking deviations from normal for all points in the 24-2 pattern from most positive (often super-normal) to most negative. The 85th percentile point's deviation from age-corrected normal is compared with significance limits derived from our normal population The 0 5% and 99 5% levels are considered the limits of normality.

evaluation. The use of test-point significance is a considerable improvement. In addition, the GHT has the ability to detect defects which are symmetric around the horizontal meridian. Such defects are not common but will often escape detection if only up-down differences are used. By using the 0.5% limits for both corresponding sectors in this check, we aimed at making the GHT highly specific regarding symmetric defects, since identifying up-down differences is the main purpose of the program. The limits still ensure that clear symmetric field loss will not pass undetected. In order to produce a low number of false positive results in normals (approximately 5%), we chose the upper and lower 0.5% limits of normality for up-down differences. Another 10% of normals would be expected to be classified as "borderline" at the same time as, from our clinical experience, most glaucomatous field defects would be identified as at least "borderline". Basing sector definition on RNFL anatomy allows identification of shallow glaucomatous defects following this arcuate pattern while disregarding non-specific trial lens induced artifacts[21].

It is important to be able to identify fields with general reduction of sensitivity as a single finding since it will draw the attention to the possibility of, for example, media opacities or miotic therapy being the actual explanation for a dark field[22]. The GHT effectively recognizes this type of field. It is also important to recognize abnormally high sensitivities since the interpretation of such fields often is hazardous and they are not always detected by the catch trials for false positive answers (Fig. 9). We have found the GHT to identify such cases on a

regular basis. Such fields are most often obvious to the trained observer but are surprisingly often missed by perimetrically less experienced clinicians.

We wanted to present the single field evaluation in a comprehensive way and decided upon a plain text display. More detailed analyses of this type may well be used more frequently in the future, but require careful design based on thorough knowledge of normal and abnormal visual fields and field variability. Analyses based only on the current field without knowledge of the frequency with which the findings are encountered in normals, on the other hand, have little value.

The Statpac 2 package has primarily been designed for use in glaucoma. None of the methods of the package require the user to disregard test results which show low reliability as indicated by the reliability tests (FN, FP, fixation losses). This does not mean, however, that good judgement should be suspended in analyzing tests. Tests in which the patient was obviously inattentive, where there are obvious trial lens induced artifacts, or where the perimetrist noted continually poor fixation must be judged in light of those observations.

Acknowledgements

Data for the normal retinal nerve fiber layer anatomy were provided by Drs PJ. Airaksinen and A. Tuulonen, University of Oulu, Finland This project was sponsored by Allergan Humphrey. MP and SM are employed by the company AH was a consultant None of the authors has any proprietary interest in the program or the perimeter.

References

1. Heijl A, Lindgren A, Lindgren G: Inter-test variability of computer-measured individual differential light threshold values in glaucomatous visual fields. In: Heijl A (ed) Perimetry Update 1988/89, pp 165-172 Amsterdam/Berkeley/Milano: Kugler & Ghedini Publ 1989
2. Heijl A: Computer test logics for automatic perimetry Acta Ophthalmol 55:837-853, 1977
3. Holmin C, Krakau, CET: Variability of glaucomatous visual field defects in computerized perimetry. Graefe's Arch Clin Exp Ophthalmol 210:235-250, 1979
4. Flammer J, Drance SM, Zulauf M: Differential light threshold: short-and long-term fluctuation in patients with glaucoma, normal controls, and patients with suspected glaucoma Arch Ophthalmol 102:704-706, 1984
5. Wilensky JT, Joondeph BC: Variation in visual field measurements with an automated perimeter Am J Ophthalmol 97:328-331, 1984
6. Hoskins HD, Magee SD, Drake MV, Kidd MN: A system for the analysis of automated visual fields using the Humphrey Visual Field Analyzer. Doc Ophthalmol Proc Ser 49:145-151, 1987
7. Werner EB, Bishop KI, Davis P, Krupin T, Petrig B, Sherman C: Visual field variability in stable glaucoma patients Doc Ophthalmol Proc Ser 49:77-84, 1987
8. Starita RJ, Piltz J, Lynn JR, Fellman RL: Total variance of serial Octopus visual fields in glaucomatous eyes. Doc Ophthalmol Proc Ser 49:85-90, 1987
9. Heijl A, Lindgren A, Lindgren G: Test-retest variability in glaucomatous visual fields Am J Ophthalmol 108:130-135, 1989
10. Heijl A, Lindgren A, Lindgren G, Patella M: Inter-test threshold variability in glaucoma: importance of censored observations and general field status (this volume, pp 189-192)
11. Sommer A, Enger C, Witt K: Screening for glaucomatous visual field loss with automated threshold perimetry Am J Ophthalmol 103:681-684, 1987
12. Åsman P, Heijl A: Improved recognition of glaucomatous field loss using test point significance instead of threshold value. Invest Ophthalmol Vis Sci (Suppl) 30/3:176, 1989
13. Åsman P, Heijl A: Hemifield test for detection of glaucomatous field loss. Invest Ophthalmol Vis Sci (Suppl) 31/4:15, 1990
14. Heijl A, Lindgren G, Olsson J: A package for the statistical analysis of visual fields. Doc Ophthalmol Proc Ser 49:153-168, 1987
15. Heijl A Lindgren G. Olsson J: The effect of perimetric experience in normal subjects Arch Ophthalmol 107:81-86, 1989
16. Besley DA, Huh E, Welsch RE: Regression Diagnostics: Identifying Influential Data and Sources of Collinearity, p 20 New York: John Wiley & Sons 1980
17. Heijl A, Lindgren G, Olsson J, Åsman P: Visual field interpretation with empiric probability maps. Arch Ophthalmol 107:204-8, 1989
18. Heijl A, Åsman P: A clinical study of perimetric probability maps. Arch Ophthalmol 107:199-203, 1989

19. Schwartz B, Nagin P: Probability maps for evaluating automated visual fields Doc Ophthalmol Proc Ser 42:39-48, 1985
20. Chauhan BC, Drance SM, Douglas DR: The use of visual field indices in detecting changes in the visual field in glaucoma. Invest Ophthalmol Vis Sci 31:512-520, 1990
21. Åsman P, Heijl A: Spatial considerations in cluster analysis for detection of glaucomatous field loss. (this volume, pp. 317-318)
22. Heijl A: Lack of diffuse loss of differential light sensitivity in early glaucoma Acta Ophthalmol 67:353-360, 1989

Spatial considerations in cluster analysis for detection of glaucomatous field loss

Peter Åsman and Anders Heijl

University of Lund, Department of Ophthalmology, Malmö General Hospital, S-214 01 Malmö, Sweden

Clusters of test points with depressed sensitivity are not uncommon in visual fields of normal subjects and may sometimes cause diagnostic problems. Based on previous knowledge of normal visual field variability it seems likely that location may influence frequency, size and depth of clusters of depressed points in fields from normal subjects. Furthermore, defects in glaucoma often have arcuate shape due to the anatomy of the retinal nerve fiber layer.

These factors made it reasonable to assume that it should be possible to improve separation of clusters caused by glaucomatous damage from those due to random variability or artifacts, if shape and position of individual clusters were accounted for. We therefore devised a method where RNFL anatomy and cluster location and depth were taken into account. The performance of such a method of quantifying clusters in normal and glaucomatous eyes was compared to the results obtained after depriving the method of information regarding cluster location, depth and RNFL anatomy.

We studied Humphrey 30-2 threshold fields from 177 eyes of 177 normal subjects none of whom were included in the Statpac normal database, and 58 eyes of 46 patients with glaucoma. Glaucoma diagnoses were based on optic disc photographs. Fields with defects larger than Aulhorn's grade II were excluded. All subjects had some previous experience of automated perimetry.

A cluster was defined as a group of tested points, where each reached the $p<5\%$ level in the Pattern Deviation Probability Map of the Statpac program. In *traditional* clusters all points were contiguous, and in *arcuate* clusters (AC) they also had to be located along the directions of the normal retinal nerve fiber layer. To define the *position* of a cluster, the average test point eccentricity (in degrees from point of fixation) and meridian (in degrees from 0° to 360° relative to temporal horizontal meridian) were used. An aggregate defect score, *cluster volume*, was calculated for each cluster. This was defined as the sum of probability scores (Table 1), which were based upon significances in the Pattern Deviation Probability Map Traditional clusters were also evaluated according to the number of points within the cluster, *cluster size*.

Table 1 Calculation of probability scores

Significance reached in Pattern Deviation Probability Map	*Probability score*
Non-significant	0
$p<5\%$	2
$p<2\%$	5
$p<1\%$	$\frac{10 \times \text{Pattern Deviation (dB)}}{\text{1\% significance limit}}$

Empiric limits of normality for clusters were calculated using all visual field tests incorporated in the Statpac normal database. Separate cluster volume limits were determined for each of eight geographical areas in the central 30° and for both types of clusters. Limits were also determined for traditional cluster size for the same areas. All fields were classified as normal or abnormal according to these limits. Thus a field was classified as abnormal if any arcuate cluster volume reached the 0.5% limit, or if any traditional cluster volume reached the 0.5% limit, or if any traditional cluster size reached the 0.5% limit for traditional cluster size. The ability of these three methods to separate the normal and the glaucoma group was studied separately.

Perimetry Update 1990/91, pp. 317-318
Proceedings of the IXth International Perimetric Society Meeting,
Malmö, Sweden, June 17-20, 1990
edited by Richard P. Mills and Anders Heijl

Analysis of traditional cluster size identified 62% of the glaucomatous eyes and 89% of the normal eyes. For the analysis of traditional cluster volume the results were 74% and 89% respectively and finally arcuate cluster volume analysis identified 78% of the glaucomatous eyes and 90% of the normal eyes. Thus, cluster volume analysis was superior to analysis of cluster size and best performance was achieved when arcuate cluster analysis was applied. In the normal group common test artifacts often resulted in falsely positive verdicts with the traditional cluster volume analysis while arcuate cluster analysis gave normal results. At the same time arcuate cluster analysis was able to detect paracentral defects in no less than five glaucomatous fields which were missed with analysis of traditional cluster volume. When only the *size* of the clusters was considered many clear glaucomatous defects were missed. Sensitivity would of course have been higher if larger defects were included but still, arcuate cluster analysis would have shown best performance. The distribution of significant arcuate clusters was slightly different in the two groups. Thus, in the glaucoma group these clusters were most common in the nasal and central areas; in the normal group they were slightly more frequent in the temporal and lower mid-periphery.

We conclude that empirical knowledge about the normal frequencies of cluster volumes in different areas of the visual field provides important help in the interpretation of automated visual fields. The usefulness of cluster analysis in glaucoma was markedly improved by accounting for location and volume of clusters. Our findings also clearly support the idea that it is easier to identify glaucomatous field defects if analysis takes retinal nerve fiber layer anatomy into account. Further improvements in the evaluation of cluster shape may provide even better diagnostic aids in glaucoma.

Color

Blue stimuli versus white stimuli in glaucoma

Allan I. Friedmann

32 Wimpole Street, London, W1M 7AE, UK

In the last 15 years or so, there have been an increasing number of papers showing that short-wave stimuli (blue) can detect very early field defects in glaucoma and ocular hypertension that could not be detected by achromatic (white) stimuli. In fact during this period I can find only one significant paper which proposes exactly the opposite, namely that white stimuli are more sensitive than blue[1]. I will return later to explain this apparent anomaly.

Another important matter to be explained is the reason why earlier very eminent workers were led to the conclusion that chromatic or colored perimetry did not add much to the visual field examination done by achromatic (white) stimuli[2,3].

In order to find some answers to these and other questions, we need to look at the retinal organization for color vision, namely the color coding of the retina. An invited paper given at the 5th Color Deficiencies Symposium 1979 from the Jules Stein Institute and UCLA School of Medicine so clearly describes the blue cone function and its differences from the Red and Green cones that I can do no more than to quote directly from it[4]:

"The blue cones furthermore are unique in their distribution and connectivity. In fish as in man they are the most non-randomly distributed cones. Blue cones and rods fail to converge on the same bipolar cells in fish at least, and ganglion cells which carry rod signals are in general R or R+G dominated in fish and monkeys. In other words the Blue Cone system appears to be largely independent of neutral and/or luminosity systems which rely primarily on the far more numerous R and G cones (about 90% in primates). The B cone dependent ganglion cells furthermore appear to be mainly if not exclusively on center in fish and monkeys. That is short wavelengths are best appreciated by simultaneous color contrast of relatively small blue objects against a large non-blue field. Finally B cone systems appear not to play a significant role in best visual acuity. This is assured by their wide spacing and agrees well with the expected correlation of high acuity associated with the higher density of the red and green cones and their bipolars associated with photopic function."

This may well account for the fact that in early glaucoma damage to foveal function may be found to be depressed by other measures than visual acuity.

This very succinct description of the B cone system makes clear that this system is in many ways very different from the M (medium) and L (long) wave systems.

Virtually all the papers showing blue more sensitive than white used either a color opponent background or mesopic adaption, and occasionally scotopic adaptation. These techniques are used so that the background illumination will not cause loss of sensitivity in the cone system being tested, and thus be able to detect the smallest drop in blue cone sensitivity. The fact that white on white or color on white is so relatively insensitive is one of the main reasons for the earlier criticisms of color stimuli in perimetry[2,3].

A paper from the Division of Applied Science of Harvard University in 1989 is to my mind one of the most significant in explaining many of the unanswered questions in clinical perimetry[5]. The authors measured the contribution of short wave (S) cones to luminance and movement by moving patterns that selectively stimulated short wave cones, and the long wave cones, and calculated that the S cones contributed as little as 1/35 or 1/50 to the detection of movement, the rest was contributed by the M and L cones. The implications of this are very important for clinical perimetry, because they highlight the difference between static and kinetic perimetry, especially with blue stimuli, and also explain the apparent anomaly in the paper by Hart mentioned previously[1] in which the author showed the superior sensitivity of white over blue. But

Perimetry Update 1990/91, pp. 321-324
Proceedings of the IXth International Perimetric Society Meeting,
Malmö, Sweden, June 17-20, 1990
edited by Richard P. Mills and Anders Heijl

as all Hart's testing used kinetic (moving) targets, he could not detect the early losses in blue sensitivity. It is impossible to say at this state how much white light perimetry causes fluctuations because of blue cone involvement, but Harrington's observations in 1964[6] are interesting:

"Using an ultra-violet background with luminescent targets with a wavelength of 450-470 nm, nerve fiber defects of glaucoma which appear to come and go with standard light and very small test objects are often clearly and consistently detected with the same size or smaller luminescent targets."

Whether the difference in movement detection between the S cone system and the M and L cone systems contributes to stato-kinetic dissociation is not clear.

All the evidence now points to the early involvement of the S cone system connecting to large ganglion cells with large axons, and it is the loss of these large ganglion cells and large nerve fibers (axons) that is the hallmark of the condition. A recent paper shows these changes in postmortem examinations of retinae of patients who had had glaucoma before they died[7].

It is logical to assume that in long-term raised intraocular pressure of primary open angle glaucoma after early damage to the B cone system and its ganglion cells, similar damage would occur to the L and M cone systems thereby damaging all the cone responses which would then be equally sensitive to white light as to blue light. This could explain the findings that in low tension glaucoma spectral increment thresholds showed greater loss to short wave stimuli than to white stimuli, whilst in high tension glaucoma the fields by the two methods were similar[8].

In a classical paper, the author[9] compared the Analyzer white and blue and the Tubinger perimeter white and blue, but using mesopic adaptation in the Tubinger perimeter similar to the background illumination of the analyzer. In cases of glaucoma with retinal nerve fiber layer abnormality, blue stimuli were found to be more sensitive in both instruments, confirming the earlier findings on the analyzer[10].

Another paper[11] I think is significant is that in which the authors used a modified Humphrey Field Analyzer and compared white on white, and blue on a yellow background in cases of early glaucoma and ocular hypertension, and found that more abnormalities were detected with the shortwave stimuli. Interestingly, they found that yellow on a yellow background was no more sensitive than white on white. The importance of these papers is that the authors have shown that standard commercially available perimeters, perhaps with some modifications, can be used for the detection of early glaucoma field defects using shortwave stimuli.

Although this paper deals essentially with the blue cone system, it would be woefully inadequate if no mention were made of the medium wave (green) and long wave (red) systems, because all three cone systems are interrelated to some extent. This is highlighted in a paper[12] which describes a patient who had a nerve fiber bundle defect due to a micro-infarct. A red stimulus showed the largest and densest defect, yellow was the next most sensitive, blue the next, and white the least sensitive The authors describe the fact that red was considerably more sensitive than white as "a better signal to noise ratio".

There are not documented a variety of conditions in which the blue cone system is either initially or preferentially vulnerable. Whether this vulnerability is part of the glaucoma group of conditions cannot be assumed, especially as the optic disc changes are so often part of this group of conditions.

Case 1 is a 52-year-old housewife who was found to have a slightly elevated intraocular pressure eight years ago. Since then she has been regularly monitored with intraocular pressure measurements and visual field examinations with either white or blue stimuli. Her intraocular pressure varied between 23 and 30. However on 25 May 1990 her right visual field was found to be no longer normal. Her optic discs were normal.

Fig. 1 shows a composite chart with the findings of the charts of the blue stimuli and white stimuli tests placed on it. All stimuli showing a loss of sensitivity to white stimuli are marked with one to four vertical lines below the stimulus, each line represents a loss of function of 0.2 log units. The losses of function to the blue stimuli were similarly marked, but above each stimulus. This allows an immediate comparison between the losses to blue and white stimuli. The chart also shows the working thresholds for the blue and white stimuli.

It is interesting to note that almost all the stimuli showing a reduction of function were detected by the white and the blue stimuli, but in almost all cases the loss of sensitivity was

greater with the blue stimuli. The tests with the blue and white stimuli take the same time.

In virtually all the comparisons published between blue and white stimuli in early glaucomatous field defects done with static perimetry, the blue stimuli are shown to be either more sensitive or at least as sensitive as white stimuli. This strongly suggests that blue stimuli should be either the first line of perimetric examination to detect these early field defects, or if white stimuli result in a normal or doubtful response this should be followed by blue stimuli examination, although this latter procedure means two examinations.

Diminished foveal function has been reported in a number of cases of early glaucoma. This is not detectable by Snellen testing because it is due to low spatial frequency loss, but is detectable by contrast sensitivity tests or macular threshold tests.

Case 2 is a case of central serous retinopathy showing the difference between visual acuity findings and macular threshold findings (Table 1). The author whose paper was quoted earlier in discussing color-specific pathways in the retina says that such studies are in their infancy, and suggests an order of complexity that will be difficult to manage philosophically or experi-

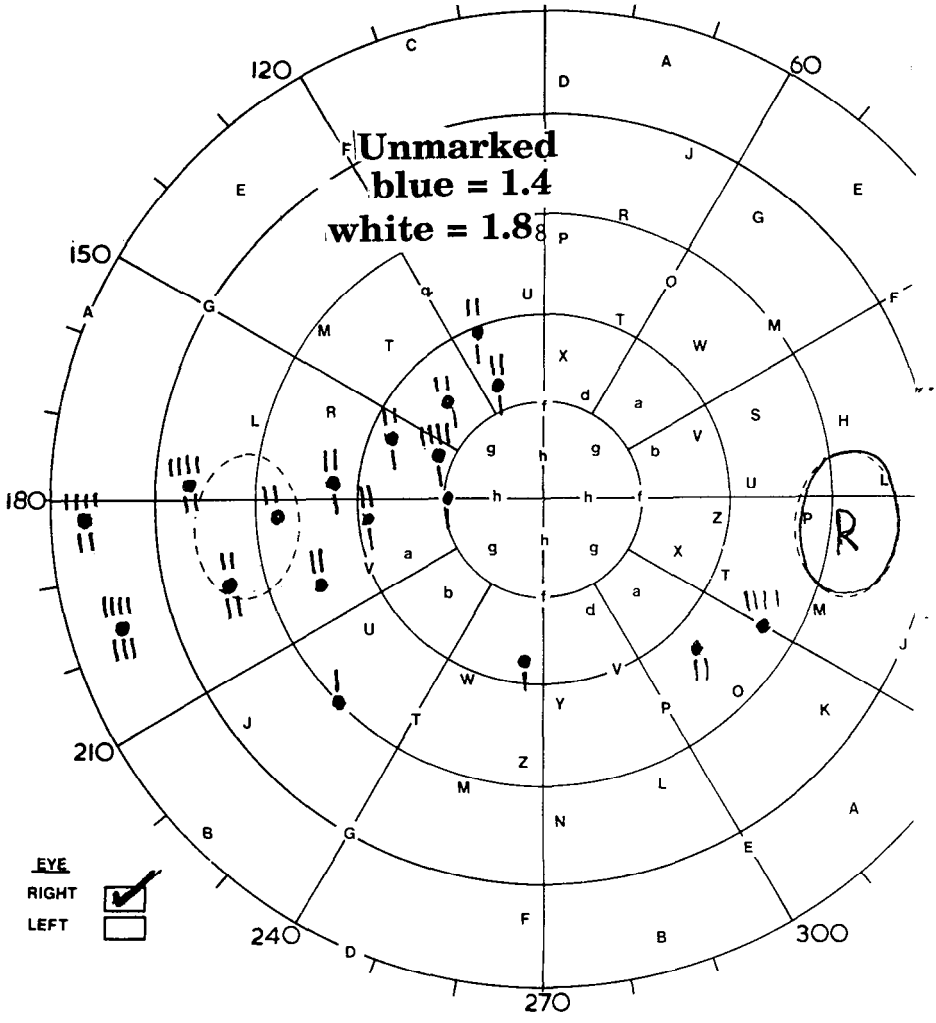

Fig 1 Composite chart in a case of early glaucoma. Marked stimuli are abnormal. Each line drawn above the stimulus represents a loss of 0.2 log units of function to blue stimuli, Each line below a stimulus represents 0.2 loss of function to white stimuli. Working thresholds to blue and white respectively are marked on the chart.

mentally. I feel that color perimetry is at much the same stage, but does open exciting new possibilities.

Table 1 Visual acuities and macular thresholds in a case of central serous retinopathy affecting one eye

		Affected eye	*Normal eye*
Three days after onset	Visual acuity	6/4	6/4
	Macular thresholds	1.6	2.6
Four weeks later	Visual acuity	6/4	6/4
	Macular thresholds	1.6	2.6

References

1. Hart WM: Blue-yellow contrast perimetry compared to conventional kinetic perimetry in patients with established glaucomatous visual field defects. In: Heijl A (ed) Perimetry Update 1988/1989, pp 23-30. Amsterdam/Berkeley/Milano: Kugler & Ghedini 1989
2. Dubois-Poulsen A: In: Le Champ Visuel, pp 490-496. Paris: Masson 1952
3. Aulhorn E, Harms H: Visual perimetry. In: Jameson D, Hurvich LM (eds) Handbook of Sensory Physiology, Vol V11/4, p 125. Berlin: Springer Verlag 1972
4. Stell WK: Photo-receptor specific synaptic pathways in goldfish retina: a world of colour, a wealth of connection. In: Verriest G (ed) Fifth Colour Deficiencies Symposium, pp 1-14 Bristol: Adam Hilger 1980
5 Lee J, Stromeyer CF: Contribution of human short-wave cones to luminance and motion detection J Physiol 413:563-593, 1989
6 Harrington DO In: The Visual Fields, pp 64-67. St Louis: CV Mosby Co 1964
7. Quigley HA, Dunkelberger GR, Green WR: Retinal ganglion cell atrophy correlated with automated perimetry in human eyes with glaucoma. Am J Ophthalmol 108/4:453-464, 1989
8. Yamazaki Y, Lalowski R, Drance SM: A comparison of the blue cone mechanism in high and low tension glaucoma. Can J Ophthalmol 96/1:12-15, 1989
9. Yamazaki Y: A comparison between white stimulus profiles and blue stimulus profiles in the mesopic condition in early glaucoma. Nihon Univ J Med 26:113-126, 1984
10. Genio C, Friedmann AI: A comparison between the white light and blue light in 70 eyes in patients with early glaucoma using the mark II Visual Field Analyzer. Doc Ophthalmol Proc Ser 26: 1981
11. Johnson CA, Adams AJ, Lewis RA: Automated perimetry of short-wavelength mechanisms in glaucoma and ocular hypertension. In: Heijl A (ed) Perimetry Update 1988/1989, pp 31-37 Amsterdam/Berkeley/Milano: Kugler & Ghedini 1989
12 King-Smith PE, Vingrys AJ, Benes SC, Havener WH: Differences between perimetric thresholds for white and equiluminous red, blue and yellow in a nerve-fiber bundle defect. In: Drum D, Verriest G (eds) Proceedings IX Color Deficiencies Symposium Dordrecht: Kluwer Acad Publ 1989

Equiluminant blue/yellow color contrast perimetry (CCP) in high risk ocular hypertension (OHT) and glaucoma (POAG)

William M. Hart Jr., Mae O. Gordon, Scott E. Silverman and Michael A. Kass

Department of Ophthalmology and Visual Sciences, Washington University School of Medicine, St. Louis, MO, USA

Abstract

The authors designed a cross-sectional study to determine if threshold static CCP of the central 30° of the visual field improved detection of glaucomatous damage. Masked readers independently graded age-corrected gray-scale plots for CCP and Statpac plots for the 30-2 program of the Humphrey perimeter (HP). Visual fields were graded for the presence or absence of defects, and the extent and topography of defects. Comparable visual fields were collected for 55 age-matched normal eyes, 54 OHT eyes and 19 POAG eyes. For the central 30° of the visual field, both CCP and conventional perimetry successfully differentiated POAG from normal There was very good agreement between the readings of CCP and conventional fields for the presence of defects (Fisher's exact test $p<0.0001$), but there was no evidence of significantly improved sensitivity or specificity when comparing the two forms of perimetry for the detection of defects.

Introduction

As there is a well known acquired form of tritanopia in patients with OHT and POAG[1-4], it has been suspected for some time that CCP in the blue/yellow dimension might increase perimetric sensitivity for detection of visual field defects in patients with incipient glaucomatous damage to the optic nerve[5-7]. A few reports have appeared in which it seemed that this might be the case[8]. However, most of this work has not used methods that adequately control for the variables of both luminance and color contrast in perimetric testing. We report here data collected by a form of blue/yellow color contrast perimetry in which the variable of photopic spectral luminance was strictly controlled, so that test-object (variably blue) and adapting background (constantly yellow) lights were empirically matched in luminance for each subject examined.

Methods

One eye of each subject was selected for study, including 55 normals, 54 with OHT and 19 with POAG. Normal eyes were those of both volunteers as well as patients seeking routine ophthalmic care who had normal ophthalmic examinations and negative personal and family histories for ophthalmic disease. Those with OHT were from a previously described group, and were intentionally selected for having high individual estimates for the risk of future glaucomatous visual field damage (for each OHT subject the eye with the greater risk estimate was chosen). OHT eyes were known to have IOPs in excess of 21 mm Hg on three or more occasions, and normal visual fields, as previously measured by program 30-2 of the Humphrey automated perimeter. (Method of visual field interpretation given below.) Eyes with POAG were known to have IOPs greater than 21 mm Hg on three or more occasions, pathologic cupping of the optic disc, and visual field defects in one of the nerve fiber bundle patterns characteristic of the disease.

This work was supported by Grant No EY-06582 from the National Eye Institute and by an unrestricted grant from Research to Prevent Blindness

Perimetry Update 1990/91, pp. 325-329
Proceedings of the IXth International Perimetric Society Meeting,
Malmö, Sweden, June 17-20, 1990
edited by Richard P. Mills and Anders Heijl

Each eye in this study was examined by both conventional and CCP methods. Conventional perimetry was done with program 30-2 of the Humphrey automated instrument within one month of the day of CCP examination. CCP was done with a modification of a previously described instrument, using an automated, binary, bracketed threshold static algorithm. The same 76 locations examined by program 30-2 of the Humphrey instrument were examined by the CCP method. Test objects were variably blue, against a yellow background, and were equated for photopic luminance with the background by means of heterochromatic flicker photometry. Stimulus values were expressed on a logarithmic scale with the maximum stimulus value being 100% of blue saturation (threshold sensitivity of zero); a 10% blue saturation stimulus value corresponded to 1 log unit of sensitivity (10 dB); a 1% blue saturation stimulus value indicated 2 log units of sensitivity (20 dB), etc.

The conventional visual fields were printed as gray scale representations along with Statpac analyses. CCP data from a group of 64 normal eyes were used to construct a data base of age-corrected mean values for each of the 76 locations in the 30° field, for each half decade of age from 40 years to 80 years of age. All CCP data were then expressed as defect depths (in dB units), as compared to expected half-decade age-matched normal mean values for each of the 76 locations studied. CCP fields were plotted as pseudo gray-scale representations with overlying isopters (of defect depth) at 0, 5, 10 and 15 dB.

Both conventional and CCP fields were graded by two experienced observers (WMH and MAX). Grading was done with patient identities and diagnoses being masked. Each field was scored according to a pre-determined algorithm as: (1) normal; (2) probably normal; (3) suspicious; (4) probably abnormal; and (5) definitely abnormal. For those fields adjudged probably or definitely abnormal, field defects were further sub-classified as being superior or inferior nasal steps; superior and/or inferior arcuate scotomas; superior and/or inferior paracentral scotomas; and mild, moderate, or severe generalized depression. CCP fields were graded as normal or probably normal if no areas exceeding 5 dB of defect were found, while those with 10 dB or more of defect in any location were graded as probably or definitely abnormal. Those with areas of defect depth between 5 and 10 dB were judged either suspicious or probably abnormal depending on the spatial distribution of color contrast defect. Infrequent, non-contiguous areas of 5-10 dB defect were given less weight than contiguous areas matching expected patterns for nerve fiber bundle defects.

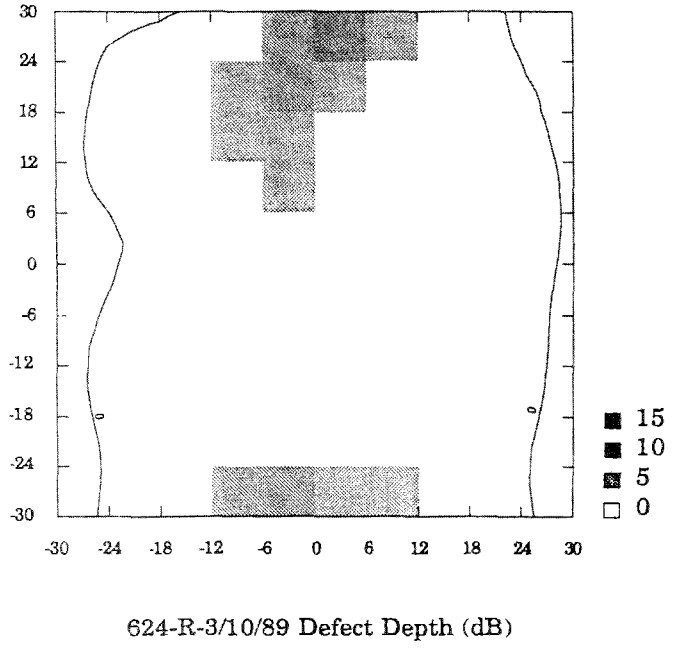

Fig 1 CCP field of a normal eye. Results plotted as defect depth relative to age-corrected normals at each location. Typically, a few scattered locations of defect appear with depths of less than 5 dB.

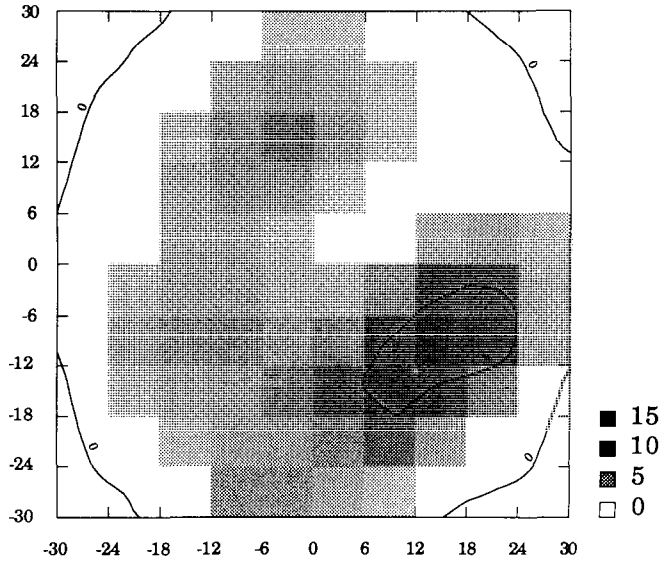

Fig 2 CCP field of an OHT eye, showing a focal depression exceeding 5 dB in the inferior Bjerrum region. This defect was also found by conventional perimetry (Note that this eye was previously categorized as an OHT eye prior to this discovery)

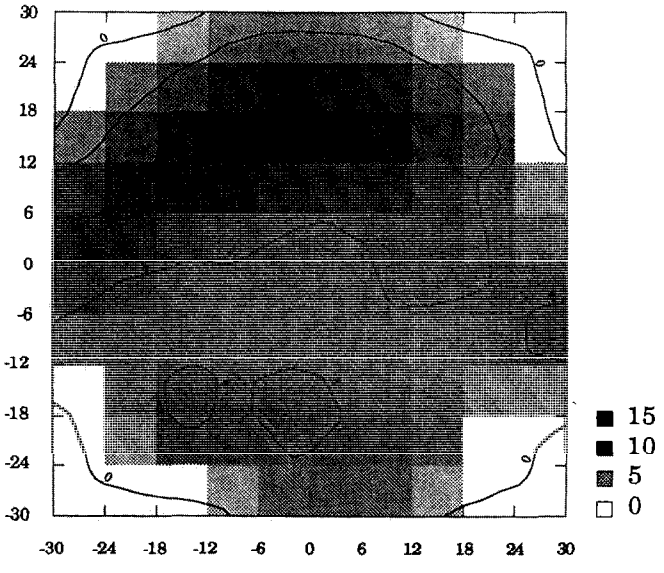

Fig 3 CCP field of a frankly glaucomatous eye, showing an arcuate scotoma in the superior Bjerrum region and focal scotomas in the inferior Bjerrum region.

Results

Three examples of CCP fields are shown in Figs. 1, 2 and 3. These are representative of the patterns of blue/yellow color contrast perimetric defects found in normal, OHT, and POAG subjects. A summary of the comparison for all eyes between conventional and CCP field readings is given in Table 1. There was generally very good agreement between the two methods; and while CCP identified 17 eyes as abnormal that were either normal or only suspicious by conventional perimetry, it should be noted that conventional perimetry identified 14 eyes as abnormal that were either normal or only suspicious by CCP. (Of the 128 eyes in the study, two had conventional fields that were more than one month separated from the CCP fields and were eliminated from this comparison.

Table 1. Comparison of masked readings of CCP and conventional perimetry for 126 eyes

		CCP perimetry reading			
		Abnormal	*Suspicious*	*Normal*	*Totals*
Conventional perimetry reading	Abnormal	18 (56%)	7 (22%)	7 (22%)	32 (100%)
	Suspicious	4 (67%)	1 (17%)	1 (17%)	6 (100%)
	Normal	13 (15%)	9 (10%)	66 (75%)	88 (100%)
	Totals	35	17	74	126

Table 2 Masked interpretations of CCP for 128 eyes by prior diagnosis

		CCP reading			
		Abnormal	*Suspicious*	*Normal*	*Totals*
Prior diagnosis	POAG	13 (68%)	4 (21%)	2 (11%)	19 (100%)
	OHT	13 (24%)	8 (15%)	33 (61%)	54 (100%)
	Normal	9 (16%)	5 (17%)	41 (75%)	55 (100%)
	Totals	35	17	76	128

Table 3 Masked interpretations of conventional visual fields for 126 eyes by prior diagnosis

		CCP reading			
		Abnormals	*Suspicious*	*Normal*	*Totals*
Prior diagnosis	POAG	14 (74%)	0	5 (26%)	19 (100%)
	OHT	12 (22%)	4 (8%)	38 (70%)	54 (100%)
	Normal	6 (11%)	2 (4%)	45 (85%)	53 (100%)
	Totals	32	6	88	126

Tables 2 and 3 summarize, respectively, the results of reading CCP and conventional visual fields of eyes classified by prior diagnosis (normal, OHT, and POAG). The two tests performed very similarly. Using both abnormal and suspicious readings as positive for detection, CCP had a sensitivity for POAG detection of 89%, while conventional perimetry had a sensitivity of 74% ($p = 1.00$, sign test, two-tailed). False positives among normal eyes for CCP were 25% and for conventional perimetry were 18% ($p = 0.18$, sign test, two-tailed). False positives among OHT eyes for CCP were 39% and for conventional perimetry were 30% ($p = 0.26$, sign test, two-tailed).

Discussion

By studying OHT patients with the greatest likelihood of having incipient glaucomatous visual field defects, we attempted to maximize the chance of detecting extrafoveal defects for color contrast perception in areas of the visual field that seem normal by conventional measures. If CCP is in fact more sensitive than conventional perimetry for the detection of early disease, we should have been able to demonstrate a significant number of "false positive"

results when examining these patients. In those with manifest disease, we might also expect to find areas abnormal by CCP that are either unaffected or less badly damaged, as measured by conventional perimetry. Although "false positive" CCP readings were greater among OHT than normal eyes, the same was true for conventional perimetry, and the differences between the two tests were not statistically different. Also, even though defects in POAG eyes were demonstrable by CCP in areas apparently unaffected as measured by conventional perimetry, the same was also true for the opposite comparison. There were some defects found by conventional perimetry that appeared in areas of the visual field that were normal or unaffected, as measured by CCP.

One of the disadvantages of a cross sectional study such as this one is that the prognostic significance of a test's false positive results cannot be known. Thus, the presence of such defects by CCP in an eye with incipient disease may in fact be a more sensitive means of detecting early glaucomatous damage. If so, this will require continued prospective follow-up for definitive proof.

References

1. Drance S, Lakowski R, Schulzer M et al: Acquired color vision changes in glaucoma: use of 100-hue test and Pickford anomaloscope as predictors of glaucomatous field change. Arch Ophthalmol 99:829-831, 1981
2. Fişhman G, Krill A, Fishman M: Acquired color defects in patients with open-angle glaucoma and ocular hypertension. Mod Probl Ophthalmol 13:335-338, 1974
3. Grützner P, Schleicher S: Acquired color vision defects in glaucoma patients. Mod Probl Ophthalmol 11:136-140, 1972
4. Lakowski R, Drance S: Acquired dyschromatopsias: the earliest functional losses in glaucoma. Doc Ophthalmol Proc Ser 19:159-165, 1979
5. Hart WM Jr, Gordon MO: Color perimetry of glaucomatous visual field defects. Ophthalmology 91:338-346, 1984
6. Hart WM Jr: Blue/yellow color contrast perimetry compared to conventional perimetry in patients with established glaucomatous visual field defects. In: Heijl A (ed) Perimetry Update 1988/1989, pp 23-30. Amsterdam/Berkeley/Milano: Kugler & Ghedini 1989
7 Hart W Jr., Silverman S, Trick G et al: Glaucomatous visual damage: luminance and color contrast sensitivities Inv Ophthalmol Vis Sci 31:359-367, 1990

Perimetric isolation of the SWS cones in OHT and early POAG

John G. Flanagan[1], Graham E. Trope[2], Warren Popick[1] and Arvinder Grover[2]

[1]*University of Waterloo, Waterloo,* [2]*University of Toronto, Toronto, Ontario, Canada*

Abstract

Recent psychophysical and histopathological evidence has demonstrated that the larger diameter optic nerve axons are selectively damaged in early glaucoma. Thus, psychophysical isolation of mechanisms most related to the large axon nerve fiber damage should enable early diagnosis of glaucoma. The aim of this study was to perimetrically isolate the short wavelength sensitive (SWS) cone system served by the largest of the parvocellular projecting ganglion cells Various studies have measured the foveal SWS function but only two groups have investigated the entire central visual field. The results were conflicting with one group finding both diffuse and localized reduction in SWS function and selective loss in some OHT and early POAG patients The other group found the technique less useful than standard perimetry on a small group of established glaucoma patients, but subsequently agreed that it may be more sensitive in the detection of early glaucoma. The authors investigated 45 normals, 18 OHTs and 26 early POAG subjects. All were between the ages of 45 and 60 years with clear optical media to reduce the effect of differential ocular media absorption Pupils were larger than 2 mm and acuity greater than 6/15. A routine 24-2 or 30-2 program was conducted for each subject on a HFA 630 using a white, 0.431° target The same target locations were also examined using a blue (OCLI, 500 nm cutoff filter), 0.431°, target against a yellow background (Schott OG530, 530 nm cutoff filter) of 300 cdm^{-2} Results were analyzed on a point-by-point basis by establishing normal 95% confidence limits for every target location for each test condition. Ten out of 26 early POAG subjects and three out of 18 OHT subjects demonstrated a selective loss to the blue on yellow target. The early POAG subjects gave a cumulative abnormal score double that of standard testing when SWS function was determined. The results confirm that testing SWS function is of potential clinical value in patients with early POAG and OHT.

Introduction

Perimetric investigation is still considered by many the most reliable means of diagnosing glaucoma[1] in spite of evidence to suggest extensive optic nerve fiber loss before focal visual field abnormality can be found[2,3]. Perimetry has failed to demonstrate any associated reduction in overall retinal sensitivity due to such a diffuse axonal loss[4-6]. There is however growing psychophysical evidence to indicate that early damage occurs before field defects become apparent. Many color vision studies have shown a decreased hue discrimination along the blue-yellow axis[6-9]. Both chromatic and achromatic sensitivity loss has been found, with the largest changes at the blue end of the spectrum[10]. Many ocular hypertensives show similar results[11-14]. Airaksinen *et al* [15] linked foveal color vision loss to diffuse retinal nerve fiber loss.

Other techniques which have found changes that seem to precede focal visual field loss include both spatial and temporal contrast sensitivity[7,16]; fluctuations of the visual field area[17]; electrodiagnostic techniques[18-20] and photostress recovery time[21].

A recent report by Quigley *et al* [22] has demonstrated that the larger diameter optic nerve axons are the first to be damaged in chronic human glaucoma. Therefore it may be hypothesized that the early psychophysical losses which may be apparent prior to the development of perimetric visual field loss are related to damage of the more susceptible larger axon ganglion cells

At photopic levels of adaptation the cone system provides both chromatic and achromatic information. The chromatic signals appear to be divided into two separate channels; one which compares the response from long wavelength sensitive (LWS) cones with the mid-wavelength sensitive (MWS) cones; and a second which responds to short wavelength sensitive (SWS)

Address for correspondence Dr. J G. Flanagan, School of Optometry, University of Waterloo, Waterloo, Ontario N2L 3G1, Canada

Perimetry Update 1990/91, pp 331-337
Proceedings of the IXth International Perimetric Society Meeting,
Malmö, Sweden, June 17-20, 1990
edited by Richard P. Mills and Anders Heijl

cones mediated by LWS and MWS cones[23]. The achromatic channel also summates signals from the LWS and MWS cones[24]. The SWS cones are very different however, only sending signals to the chromatic pathway[25]. Like rods, they are absent at the center of the fovea[26] and are diffusely spread throughout the perimacula[27]. Of particular interest is that the SWS cones send information via larger axons than the LWS or MWS cones.

All cone types respond to blue stimuli, but only the LWS and MWS cones are significantly stimulated by a yellow adapting field. Increased luminance effectively decreases contrast for the LWS and MWS cones but has a minimal effect on the SWS cones (Stiles pi- 1, 2 and 3)[28]. Although various studies have shown loss of sensitivity to short wavelength stimuli, most have restricted their investigation to the foveal response[8,9,13,15,29,30] and have proposed that measures of blue or blue-yellow sensitivity may be predictive of the eventual development of glaucoma.

Heron *et al.*[8], using a blue on yellow stimulus, measured peripheral sensitivity at several points along the 40° meridian and reported the presence of both diffuse and localized reductions in sensitivity in some OHT, and POAG patients. Only two groups have attempted to isolate the SWS cones over the entire central visual field (30°) using a static threshold technique. Johnson *et al.*[31] found evidence of both diffuse and localized reduction in SWS cone sensitivity and selective loss in approximately 7% of the OHTs and 15% of the early glaucoma patients. They concluded that these results represent early glaucomatous damage which might be a precursor to conventional visual field loss. Hart *et al.*[32] found blue on yellow perimetry to be less useful than standard perimetry on a small group of established glaucoma patients. However, a subsequent study[33] agreed that the technique may be more sensitive in the detection of early glaucoma but maintained that there is little benefit in established glaucoma patients.

The aim of this study was to psychophysically isolate the short wavelength sensitive (SWS) cone system served by the largest of the parvocellular projecting ganglion cells, over the central 30 degrees using blue on yellow perimetry; to establish the sensitivity of reduced SWS function in the detection of early glaucomatous damage; and to initiate a prospective study to establish the specificity of reduced SWS function in identifying those OHTs at risk of developing glaucoma.

Methods

Subjects included 45 normal volunteers, 18 ocular hypertensives (OHT) and 26 subjects with early primary open angle glaucoma (POAG). The normal group consisted of 24 males and 21 females with a mean age of 51.6 (SD 4.91) years. Exclusion criterion for all subjects included subjects younger than 45 and older than 60 years; obvious media opacity; pupil sizes of less than 2 mm; visual acuity of less than 6/15; aphakia and pseudophakia; diabetes; macula disease; optic nerve head drusen; history of ocular surgery; history of previous ocular disease; myopia greater than 6D; and astigmatism greater than 3D. All subjects were under the age of 60 with clear optical media as individual media absorption was not assessed in this preliminary study[31,34]. The OHTs were defined as "normal" but with an IOP of greater than 21 mm Hg. The group consisted of 6 males and 12 females with a mean age of 47.12 (SD 10.20) years. The POAG group had 12 males and 14 females with a mean age of 50.16 (SD 6.90) years.

The right eye of each normal subject was examined using the 30-2 program on a Humphrey 630 Field Analyzer (HFA) with a white 0.431° target. The same target locations were also examined using a blue (OCLI, 500 nm cutoff filter), 0.431° target against a yellow background (Schott 0G530, 530 nm cutoff filter) of 300 cdm^{-2} generated by an auxiliary projected light source. The testing sequence was randomized to reduce the effect of learning. Both eyes of the OHT and POAG subjects were examined when time and patient fatigue permitted, but all testing was completed on one eye before the other.

The mean sensitivity and 95% confidence limit for each target location was established for the normal population to enable a point by point analysis. The four points immediately surrounding the blind spot were excluded. The results from each of the OHT and POAG subjects were then compared to the normal 95% confidence limits. If two or more points were below the specified sensitivity the field was considered abnormal. The number of abnormal points within each field and test condition were noted and tabulated by visual field quadrant and hemifield. The analysis for this preliminary study using 95% confidence limits to define abnormality was insensitive to subtle differences between test conditions.

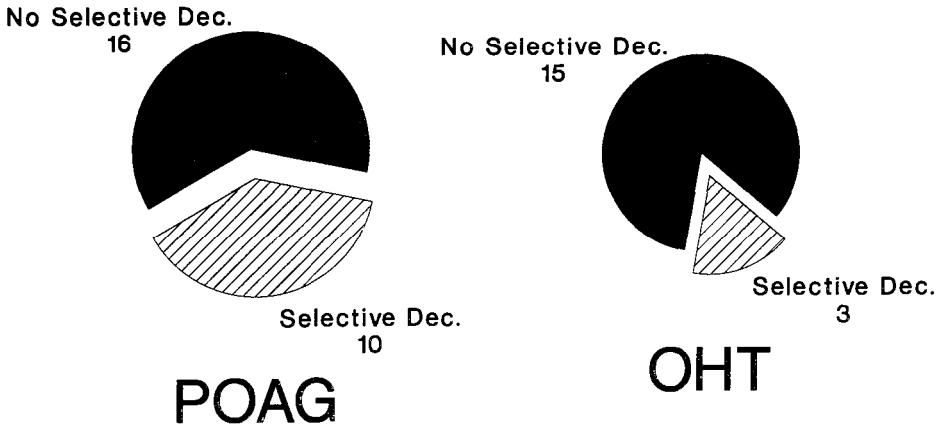

Fig 1 Pie charts illustrating the proportion of POAG and OHT subjects who demonstrated a selective decrease (Dec) in blue/yellow sensitivity.

Results

Fig. 1 illustrates the number of subjects that demonstrated a selective decrease in blue on yellow sensitivity when compared to white on white sensitivity Three out of 18 OHTs and 10 out of 26 POAG subjects had two or more abnormal points for the blue or yellow stimulus when compared to the standard white on white All the OHTs gave white on white results that were within normal limits. Fig. 2 gives the percentage of subjects considered to be abnormal for each test condition and visual field quadrant. Fig. 3 shows the proportion of abnormal points in each quadrant (A) and hemifield (B). It is apparent that the blue on yellow perimetry gave almost double the total number of abnormal points and that the inferior and temporal fields are the most sensitive to decreased SWS cone function.

Discussion

Three out of 18 OHTs and ten out of 26 early POAG subjects demonstrated a selective loss to blue on yellow perimetry when compared to standard white on white perimetry. The total number of abnormal points in the POAG group was almost double for the blue on yellow perimetry, with the inferior and temporal visual fields appearing to be particularly sensitive to decreased SWS cone functions. These results support the previous findings of both diffuse and localized SWS deficits in selected subjects with OHT and early POAG[31,33]

However, only a larger prospective study will determine the specificity within the OHT group, *i e* , will the subjects who demonstrated a selective deficit eventually develop glaucoma and how many of the "normal" OHT subjects will go onto develop glaucoma. The results of this preliminary study are encouraging and suggest that testing SWS function throughout the central visual field is of potential clinical value in patients with early POAG or OHT. To expand the technique to include subjects over the age of 60 years it would be necessary to quantify and correct for individual media absorption characteristics[31,34].

Acknowledgements

We thank E. Coyle, I. Finklestein and G Cinel for their assistance in collecting data, and gratefully acknowledge the technical support provided by T Griesbach, M Reich, R Jones and computer technologist J. Cassidy. We thank A Zorian for secretarial support and J Simpson and A La for graphics services This work was supported in part by the Medical Research Council of Canada

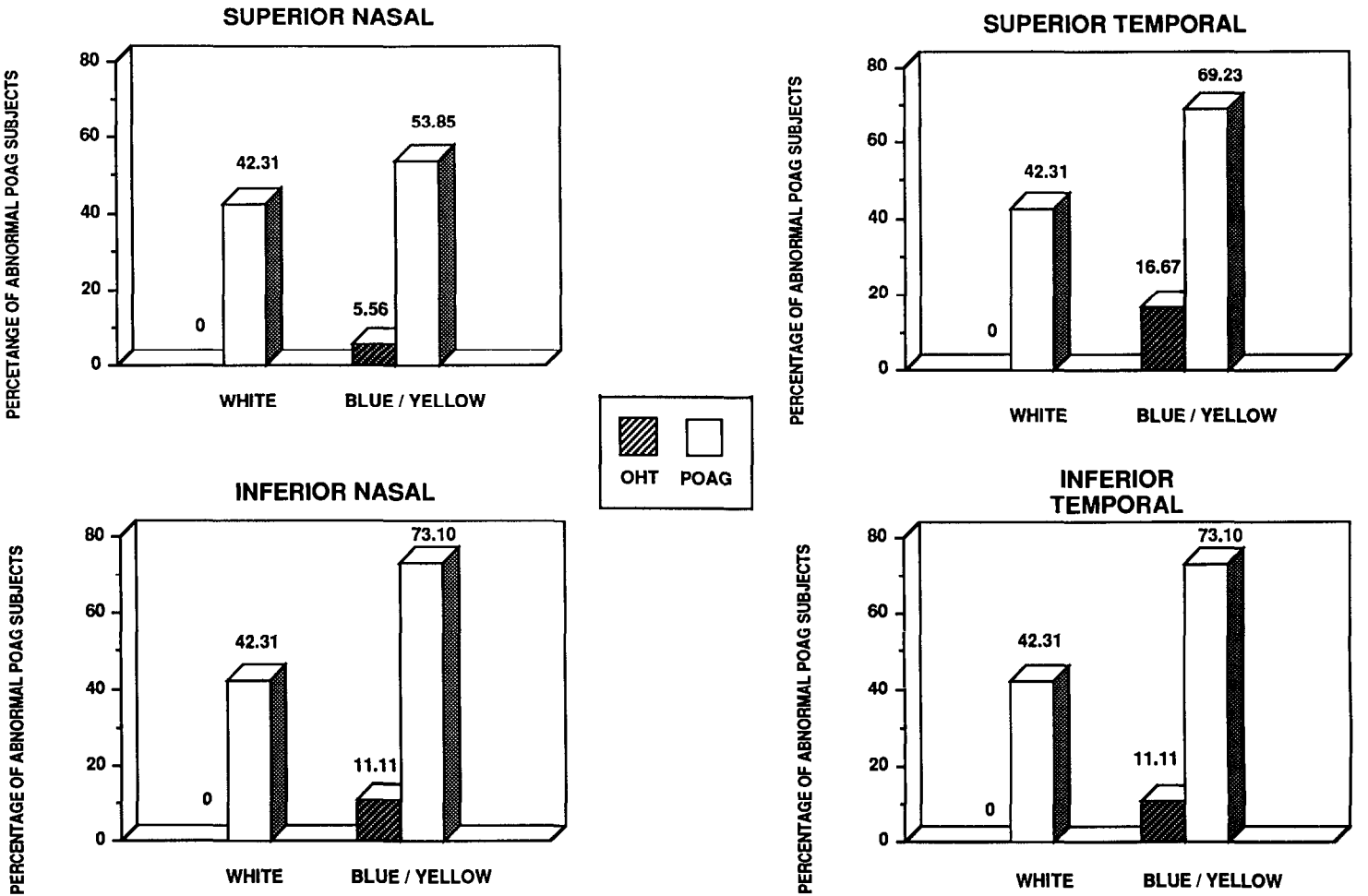

Fig. 2. Histograms illustrating the percentage of subjects outside the 95% confidence limits for each test condition and visual field quadrant.

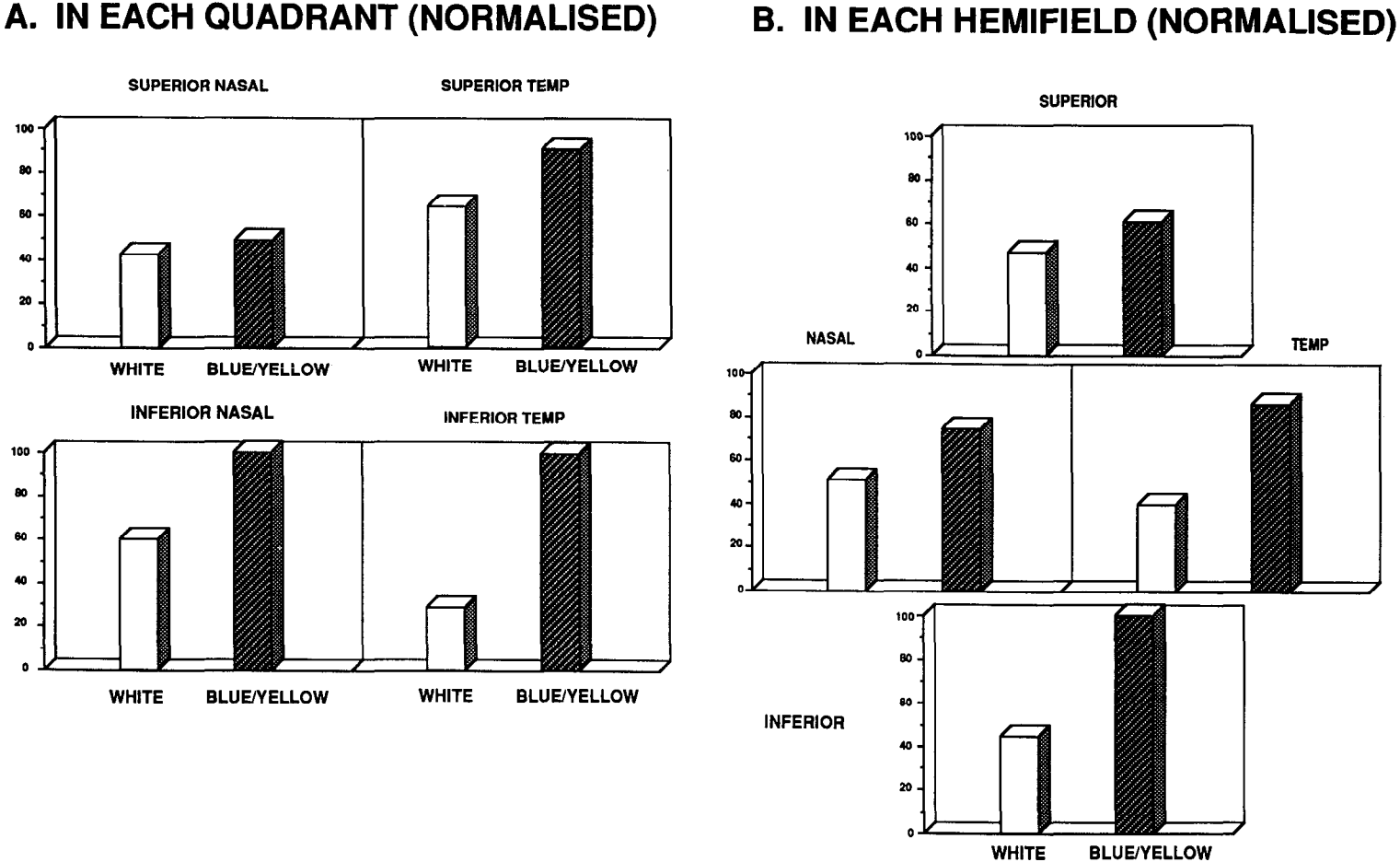

Fig. 3 A. Histograms illustrating the number of points considered abnormal in each quadrant (normalized). B. Histograms illustrating the number of points considered abnormal in each hemifield (normalized).

References

1. Heijl A: Visual field changes in early glaucoma and how to recognize them. Surv Ophthalmol (Suppl) 33:403-404, 1989
2. Quigley HA, Addicks EM, Green WR: Optic nerve damage in human glaucoma III: quantitative correlation of nerve fiber loss and visual field defect in glaucoma, ischemic neuropathy, papilledema, and toxic neuropathy. Arch Ophthalmol 100:135-146, 1982
3. Hart WM, Becker BB: The onset and evolution of glaucomatous visual field defects. Ophthalmology 89:268, 1982
4. Anderson DR: What happens to the optic disc and retina in glaucoma? Ophthalmology 90:766, 1983
5 Anctil JL, Anderson DR: Early foveal involvement and generalized depression of the visual field in glaucoma Arch Ophthalmol 102:363 1984
6 Drance SM: Physiological changes in early glaucoma (summary). Surv Ophthalmol (Suppl) 33:407-408, 1989
7. Stamper RL: Psychophysical changes in glaucoma. Surv Ophthalmol (Suppl) 33:309-318, 1989
8. Heron G, Adams AJ, Husted R: Central visual fields for short wavelength sensitive pathways in glaucoma and ocular hypertension Invest Ophthalmol Vis Sci 29:64-72, 1988
9 Sample PA, Weinreb RN, Boynton RM: Acquired dyschromatopsia in glaucoma. Surv Ophthalmol 31:54-64, 1986
10. Adams AJ, Heron G, Husted R: Clinical measures of central vision function in glaucoma and ocular hypertension. Arch Ophthalmol 105:782, 1987
11. Poinoosawmy D, Nagasubrmanian S, Gloster J: Color vision in patients with chronic simple glaucoma and ocular hypertension Br J Ophthalmol 64:852, 1980
12 Flammer J, Drance SM: Correlation between color vision scores and quantitative perimetry in suspected glaucoma Arch Ophthalmol 102:38-39, 1984
13. Adams AJ, Rodic R, Husted R, Stamper R: Spectral sensitivity and color discrimination changes in glaucoma and glaucoma-suspect patients. Invest Ophthalmol Vis Sci 23:516-524, 1982
14. Ham TR, Post RB, Johnson CA, Keltner JL: Correlation of color vision deficits and observable changes in the optic disc in a population of ocular hypertensives Arch Ophthalmol 102:1637-1639, 1984
15 Airaksinen PJ, Romuald L, Drance SM, Price M: Color vision and retinal nerve fiber layer in early glaucoma Am J Ophthalmol 101:298-213, 1986
16 Bron AJ: Contrast sensitivity changes in ocular hypertension and early glaucoma (summary) Surv Ophthalmol (Suppl) 33:405-406, 1989
17. Drance SM, Airaksinen PJ: Signs of early change in open angle glaucoma. In: Weinstein GW (ed) Contemporary Issues in Ophthalmology, pp 17-31. New York: Churchill Livingstone 1986
18. Trick GL, Nesher R, Cooper DG, Kolker AE, Brickler-Bluth M: Dissociation of visual deficits in ocular hypertension. Invest Ophthalmol Vis Sci 29:1486-1491, 1988
19 Weinstein GW, Arden GB, Hitchings RA, Ryan S, Calthorpe CM, Odom JV: The pattern electroretinogram (PERG) in ocular hypertension and glaucoma Arch Ophthalmol 106:923-928, 1988
20 Price MJ, Drance SM, Prince M, Schulzer M, Douglas GR, Tansley B: The pattern electroretinogram and visual-evoked potential in glaucoma Graefe's Arch Clin Ophthalmol 226:542-547, 1988
21 Sherman MD, Hendkind P: Photostress recovery in chronic open angle glaucoma. Br J Ophthalmol 72:641-645, 1988
22 Quigley H, Dunkelberger GR, Green WR: Chronic human glaucoma causing selectively greater loss of large optic nerve fibers Ophthalmology 95:357-363, 1988
23. DeValois RL, Abramov I, Jacobs GH: Analysis of response patterns of LGN cells J Opt Soc Am 56:966-977, 1966
24 Ingling C, Martinez E: The spatiochromatic signal of the r-g channel In: Mollen JD, Sharpe LT (eds) Color Vision, pp 433-444 London: Academic Press 1980
25 Gouras P: Antidromic responses of orthodromically identified ganglion cells in monkey retina. J Physiol 204:407, 1969
26. Bron AJ: Contrast sensitivity changes in ocular hypertension and early glaucoma (summary). Surv Ophthalmol (Suppl) 33:405-406, 1989
27 Drance SM, Airaksinen PJ: Signs of early change in open angle glaucoma In: Weinstein GW (ed) Contemporary Issues in Ophthalmology, pp 17-31 New York: Churchill Livingstone 1986
28. Kallonaitis M, Harwerth RS: Differential adaptation of cone mechanisms explains the preferential loss of short wavelength sensitivity in retinal disease. In: Drum B, Verriest G (eds) Color Vision Deficiencies IX, pp 353-364 Kluwer 1989
29. Adams AJ, Heron G, Husted R: Clinical measures of central vision function in glaucoma and ocular hypertension. Arch Ophthalmol 105:782-787, 1987
30 Drance SM, Lakowski R, Schulzer M, Douglas GR: Acquired color vision changes in glaucoma: Use of 100-Hue test and Pickford anomaloscope as predictors of glaucomatous field change. Arch Ophthalmol 99:1019-1022, 1981

31. Johnson CA, Adams AJ, Lewis RA: Automated perimetry of short-wavelength mechanisms in glaucoma and ocular hypertension. In: Heijl A (ed) Perimetry Update 1988/89, pp 31-38. Amsterdam/Berkeley/Milano: Kugler & Ghedini 1989
32. Hart WM Jr, Trick G, Nesher R, Gordon M: The effect of glaucomatous damage on static perimetric thresholds determined with luminance increment and blue/yellow color increment thresholds. ARVO abstracts. Invest Ophthalmol Vis Sci (Suppl) 29:422, 1988
33. Hart WM Jr, Silverman SE, Trick GL, Nesher R, Gordon MO: Glaucomatous visual field damage: luminance and color-contrast sensitivities. Invest Ophthalmol Vis Sci 31:359-367, 1990
34. Pokorny J, Smith VC, Lutze M: Aging of the human lens. Appl Optics 26:1437-1440, 1987

Central differential sensitivity to blue stimuli in glaucoma and ocular hypertension

Anita Garavaglia, Paolo Bettin, Maurizio Buscemi, Cristina Nassivera, Carlo Capoferri and Rosario Brancato

Department of Ophthalmology, San Raffaele Hospital, University of Milan, Milan, Italy

Abstract

The aim of this study was to verify whether testing differential sensitivity in the macular area with the Humphrey automated perimeter could detect early damage from glaucoma The authors selected 39 eyes with primary open angle glaucoma, free from defects within the central 5° of the field, 49 eyes with ocular hypertension, and 48 eyes of normal age-matched controls They underwent the macula threshold test on a Humphrey perimeter, using white and blue targets. Statistical analysis showed that: (1) differential sensitivities to blue were significantly depressed in the eyes with glaucoma and ocular hypertension; (2) glaucomatous eyes were distributed in a distinct domain compared to normal eyes; (3) sensitivities to blue were related to the severity of glaucoma and poorly influenced by other variables; (4) among controls, sensitivities to blue were instead related to subjects' ages Differential sensitivities to white stimuli were not significantly different in glaucomatous and normal eyes. These results suggest the possibility of detecting early glaucomatous alterations of central visual function using an automated perimeter and its built-in color filters.

Introduction

A significant loss of optic nerve axons takes place in ocular hypertensive eyes with no evident signs of disease using current methods of investigation[1]. Since clinical studies have demonstrated that lowering intraocular pressure (IOP) can often stop the progression of the disease, and possibly reverse some early damage[2], it is of great importance to identify the earliest changes of glaucoma.

Disturbances of central visual function are particularly being investigated, since a large number of optic nerve fibers are devoted to the central retina. Thus, color discrimination and differential sensitivity to colored test targets can be affected in early glaucoma and ocular hypertension[3-8].

In previous studies, using the Humphrey Field Analyzer, we measured central retinal differential sensitivities to white and blue stimuli in primary open angle glaucoma and in a strictly selected group of glaucoma suspects at high risk for developing visual field loss[9,10]. We found a significant decrease of sensitivity to blue targets, compared to age-matched controls.

In the present work, we studied differential sensitivities of white and blue targets in a group of ocular hypertensives, and compared them to both glaucomatous and control subjects.

Methods

Subjects

We recruited 39 glaucoma patients, 40 ocular hypertensives and 48 normal controls from our perimetry service. One eye per patient was studied.

Criteria for section were: (1) best corrected visual acuity equal to or better than 0.8; (2) subjective refraction ranging between -2 and +3 diopters; (3) no significant lens changes at slit

Address for correspondence Carlo Capoferri, M.D , Clinica Oculistica, Ospedale San Raffaele, Via Olgettina 60, 20132 Milan, Italy

Perimetry Update 1990/91, pp. 339-342
Proceedings of the IXth International Perimetric Society Meeting,
Malmö, Sweden, June 17-20, 1990
edited by Richard P. Mills and Anders Heijl

lamp biomicroscopy, and no other possible sources of reduced differential sensitivity or poor hue discrimination; (4) at least two IOP measurements and one visual field examination with the Central 30-2 Threshold test of the Humphrey perimeter, performed in the preceding three months. Pupillary diameters were measured and recorded in 0.5 mm steps. Horizontal cup/disc (C/D) ratios were measured on fundus photographs.

Glaucoma subjects were affected by primary open angle glaucoma. They had various field defects on the Central 30-2 test, but no deficits within the central 5° of the field. Their mean age was 58.8 years (1 SD 7.3), refraction was 0.44 diopters (1 SD 1.48), mean pupillary diameter was 4.31 mm (1 SD 0.83). Low-tension glaucoma was excluded. C/D ratios ranged between 0.5 and 0.9 (mean 0.64; 1 SD 0.12). Intraocular pressure (IOP) measured immediately after the study tests was <22 mm Hg on non-miotic therapy.

Ocular hypertensives had an IOP of ≥22 mm Hg on at least two occasions. they had normal visual fields, normal C/D ratios and no changes of the optic nerve head. Their mean age was 56.8 years (1 SD 7.7), their refraction 0.52 diopters (1 SD 1.20), and pupillary diameter 4.25 mm (1 SD 0.89).

Normal subjects had normal appearance of the optic disc and normal C/D ratios, and IOPs below 20 mm Hg. Their mean age was 57.8 years (1 SD 6.8), mean refraction was 0.23 diopters (1 SD 1.28), and pupillary diameter 4.08 mm (1 SD 0.77).

Test procedures

All subjects underwent the macula threshold test of the Humphrey Field Analyzer. In this test, 16 points, arranged in a square pattern at 2° intervals, are thresholded three times each; the fovea is tested separately. The test was run both with white and blue targets, using the built-in blue filter (OCLI Dichroic). All other settings of the instrument were left on the default mode (stimulus size: Goldmann III, *i.e.*, 0.43°; background illumination: 31.5 asb), except for the test speed which was set to "slow" when advisable. During the examinations, the subjects used an appropriate near correction.

We used the Student's *t*-test to compare the sensitivities of pairs of study groups and linear regression to assess the influence of age, refraction, pupil size, and C/D ratios on thresholds.

Results

Differential sensitivity to white targets, averaged over the 17 test locations, was 32.42 dB (1 SD 1.19) in the glaucoma group, 32.57 dB (1 SD 1.69) in ocular hypertensives, and 33.02 dB (1 SD 1.19) in the control group; none of these differences were statistically significant. Mean sensitivity to blue targets was 18.51 dB (1 SD 1.69) in glaucoma subjects, 20.11 dB (1 SD 1.95) in ocular hypertensives, and 22.21 dB (1 SD 1.22) in normals; these differences were all significant ($p<0.001$). The subjects in the glaucoma and controls groups were distributed in two relatively separate domains with respect to the sensitivity to blue targets, whereas ocular hypertensives were more scattered (Fig. 1).

Sensitivity values to white were significantly higher centrally, *i.e.*, at the fovea and the four most central locations, than peripherally in the three groups. With blue targets, central and peripheral sensitivities were comparable in the control group (22.20 *versus* 22.21 dB; n.s.), whereas in the other study groups they were higher at the most peripheral locations (18.27 *versus* 18.62 dB in glaucoma, $p<0.01$; 19.97 *versus* 20.17 dB in the ocular hypertensives, $p<0.05$).

Blue thresholds showed a significant relation to age in the control group ($r=0.62$, $p<0.001$) but not in the ocular hypertensive and glaucoma groups. In the latter, blue sensitivities were related to horizontal C/D ratios ($r=0.62$; $p<0.001$).

Pupil size and refraction showed no significant influence on either white or blue thresholds.

Discussion

We could detect clinically relevant differences among the three study groups with the blue targets only. This result is consistent with the results obtained by other authors using different

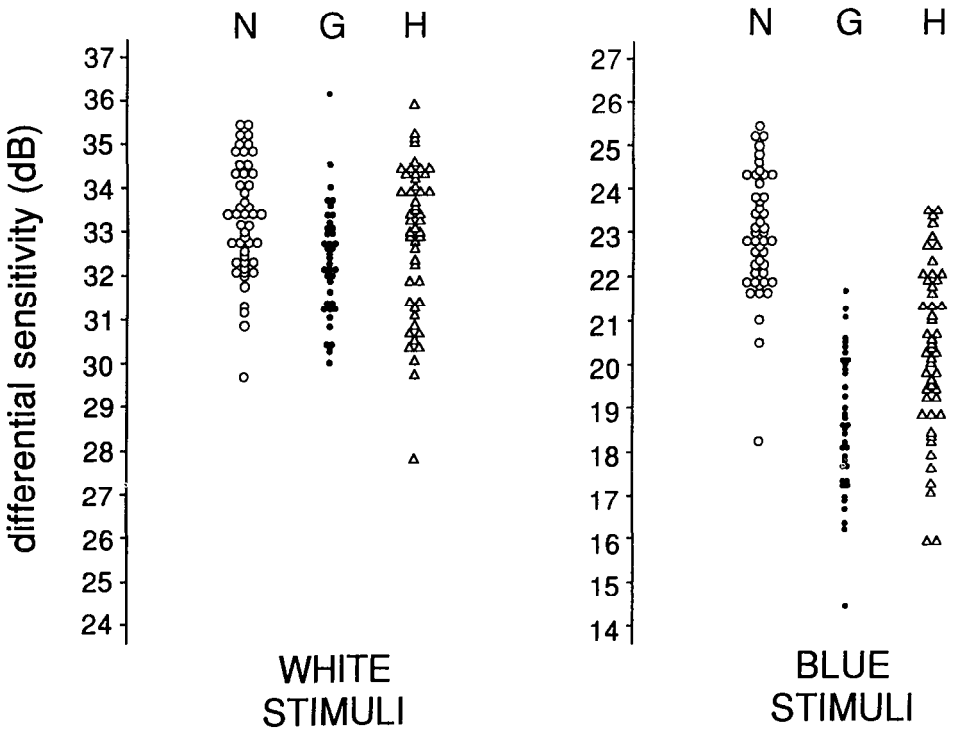

Fig 1 Distribution of mean differential sensitivities to white and blue stimuli in glaucomatous (G), ocular hypertensives (H) and normals (N).

techniques[4,5,7,8,11-13]. As Fig. 1 shows, in our series blue thresholds of the glaucoma and control groups lie in two relatively distinct ranges: this suggests that the macula test could be sensitive enough for screening for early glaucomatous central damage

In ocular hypertensives, differential sensitivities to blue distributed over a wider domain, with some values in the glaucoma range and others in the normal range. This could mean that this group includes different subjects: normal with transient ocular hypertension, normal with IOP permanently over 21 mm Hg, and glaucoma with no damage or very early alterations.

Age significantly influenced sensitivities to blue in normals only: no such relationship could be found in the glaucoma or hypertension groups. Blue thresholds were strongly related to horizontal cup/disc ratios in the glaucoma group: this suggests that glaucoma and its stage of evolution are major determinants of sensitivity to blue targets.

Averaging over a central subset of test locations does not seem to alter the sensitivity of the test: this suggests the possibility of reducing the number of points tested, thus saving time.

Since we selected our study populations in order to exclude any source of sensitivity loss other than glaucoma, no data are available on the specificity of this technique. We would expect a reduction of sensitivity to blue stimuli in various conditions, particularly nuclear sclerosis of the lens. Quantification of lens opacities by means of lens meters[14], or the combined use of different color targets[15,16] could possibly be of help in discriminating between losses due to glaucoma.

The fact that central threshold testing with a commonly available automated perimeter could identify early damage from glaucoma is interesting. A prospective study is needed to demonstrate that eyes less sensitive to blue targets will actually develop clinical glaucoma in the long run.

References

1. Quigley HA, Hohman RM, Addicks EM et al: Morphological changes in the lamina cribrosa correlated with neural loss in open-angle glaucoma. Am J Ophthalmol 95:673-691, 1983
2. Schwartz B, Takamoto T, Nagin P: Measurement of reversibility of optic disc cupping and pallor in ocular hypertension and glaucoma. Ophthalmology 92:1396-1407, 1985
3. Drance SM, Lakowski R, Schulzer M et al: Acquired color vision changes in glaucoma: use of 100-Hue test and Pickford anomaloscope as predictors of glaucomatous field change. Arch Ophthalmol 99:829-831, 1981
4. Genio C, Friedmann AI: A comparison between white light and blue light on about 70 eyes of patients with early glaucoma using the Mark II Visual Field Analyzer. Doc Ophthalmol Proc Ser 26:207-214, 1981
5. Abe H, Sakai R, Yamazaki Y: The selective impairment of the three color mechanisms (red-, green-, and blue-sensitive mechanisms) isolated by the new color campimeter in pathological eyes with fundus disease. II. Studies of static threshold campimetry in early glaucoma Acta Soc Ophthalmol Jpn 87:950-957, 1983
6. Adams AJ, Heron G, Husted R: Clinical measures of central visual function in glaucoma and ocular hypertension. Arch Ophthalmol 105:782-787, 1987
7. Steinschneider T, Ticho U: Thresholds for blue and white stimuli in glaucoma: preliminary results. Doc Ophthalmol Proc Ser 52:281-287, 1987
8. Patel B, Deutsch TA, Deutsch WE: Detection of glaucomatous visual fields by blue stimulus automated perimetry Invest Ophthalmol Vis Sci (Suppl) 29:240, 1988
9 Capoferri C, Garavaglia A, Buscemi M et al: Clinical detection of early glaucomatous foveal involvement In Ophthalmol 13:259-264, 1989
10 Capoferri C, Garavaglia A, Nassivera C et al: Clinical measures of central differential sensitivity in glaucoma Can J Ophthalmol 25:193-196, 1990
11 Friedmann AI: A preliminary report on the use of colour filters in the Mark II visual field analyzer. In: Verriest G (ed) Color Vision Deficiencies V, p 221 Bristol: Adam Hilger Ltd 1980
12 Hart WM, Gordon M: Color perimetry of glaucomatous visual field defects Ophthalmology 91:338-346, 1984
13 Heron G, Adams AJ, Husted R: Central visual fields for short wavelength sensitive pathways in glaucoma and ocular hypertension Invest Ophthalmol Vis Sci 29:64-72, 1988
14 Flammer J, Bebie H: Lens opacity meter: a new instrument to quantify lens opacity. Ophthalmologica 195:69-72, 1987
15 Van Norren D, Vos JJ: Spectral transmission of the human ocular media Vis Res 14:1237-1244, 1974
16 Capoferri C, Garavaglia A. Buscemi M et al: Threshold automated perimetry of the foveal area and early glaucomatous damage: preliminary results Ann Ottal 114:151-156, 1988

The vulnerability of the blue cone system in glaucoma

Ryutaro Tamaki, Kenji Kitahara, Atsushi Kandatsu and Yoshiteru Nishio

Department of Ophthalmology, The Jikei University School of Medicine, Tokyo, Japan

Abstract

Applying spectral sensitivity measurements on an intense white background, the authors investigated the characteristics of opponent channel damage in patients with glaucoma with normal visual acuity, by measuring the spectral sensitivity at the fovea and the extrafovea. They found that although there was a loss of sensitivity for both the blue cone system and the red and green cone system at both the fovea and the extrafovea, there was still a more prominent peak at both locations in the short wavelength region

Introduction

Previously, we reported that spectral sensitivity measurements on an intense white background might be useful not only to investigate the characteristics of opponent channel damage but also to detect minor visual disturbances in optic nerve diseases[1].

Using the same method, we investigated the characteristics of opponent channel damage in patients with glaucoma with normal visual acuity by measuring the spectral sensitivity at the fovea and the extrafovea.

Method

A two-channel Maxwellian view optical system with a 150 watt xenon arc as a light source was used. A 1° diameter circular test light was superimposed in the center of an 8° circular xenon white background field of 1000 photopic trolands. Interference filters with dominant wavelengths of between 400 and 700 nm with 6 to 10 nm half-band widths were used for the test light which was exposed for 200 ms every two seconds.

Measurements were made at the fovea and 4° temporal retina on ten patients with glaucoma with normal visual acuity. Their pupils were dilated with 1% tropicamide Prior to the measurements, the patients were adapted to the background for three minutes and the detection threshold for the test flash was measured at least three times for each test wavelength.

Results

Although the spectral sensitivities on a white background for some of the patients show that there was a loss of sensitivity for both the blue cone system and the red and green cone system, there was still a prominent peak in the short wavelength region at both the fovea and the extrafovea (4° temporal retina)

Fig. 1 shows the results of a representative case, MS, whose results show that there was a loss of sensitivity for both the blue cone system and the red and green cone system. The Goldmann visual field is shown in the lower panel. The upper left and upper right panels show the spectral sensitivity curves at the fovea and the extrafovea, respectively. The results of the test sensitivities (photons^{-1} sec. deg.^{2}) were plotted as a function of the wave number (cm^{-1}). In both panels, the solid lines represent the normal pattern and the open circles represent the mean

Address for correspondence: Ryutaro Tamaki, Department of Ophthalmology, The Jikei University School of Medicine, 19-18 Nishi-Shinbashi 3-chome, Minatu-ku, Tokyo, Japan

Perimetry Update 1990/91, pp. 343-345
Proceedings of the IXth International Perimetric Society Meeting,
Malmö, Sweden, June 17-20, 1990
edited by Richard P Mills and Anders Heijl

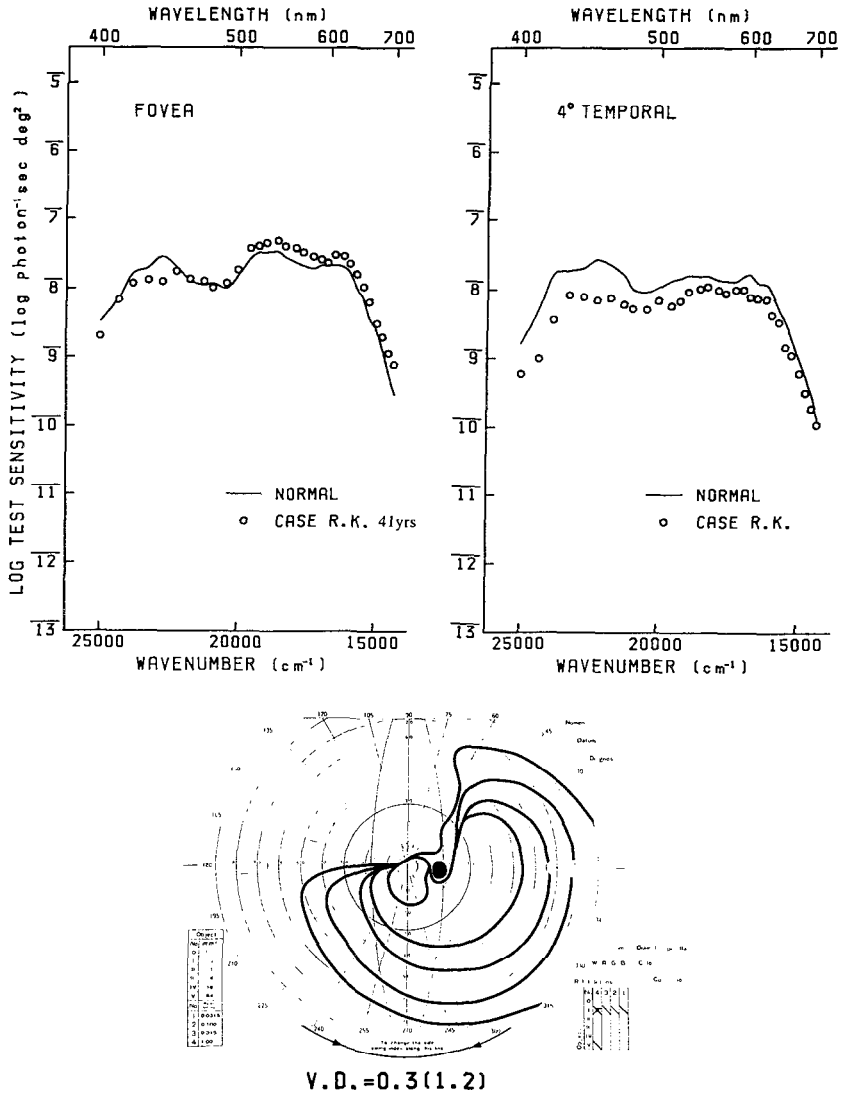

Fig 1 Case MS: the two upper panels represent the spectral sensitivity curves at the fovea and the 4° temporal retina The lower panel shows the Goldmann visual field

values of the three measurements for patient MS. Although there was a loss of sensitivity for both the blue cone system and the red and green cone system at both the fovea and the extrafovea, there was still a more prominent peak in the short wavelength region.

The results of the other representative case, RK, are similar to the normal patterns (Fig. 2)

Discussion

Previously, we reported that there was a definite lack of a peak in the short wavelength region in most optic nerve diseases when testing spectral sensitivity on an intense white background.

The purpose of this experiment was to determine whether or not there was a definite lack of a peak in the short wavelength region in glaucoma patients. In performing this experiment, the spectral sensitivities for a 1°, 200-ms test flash on a 1000 photopic troland white background

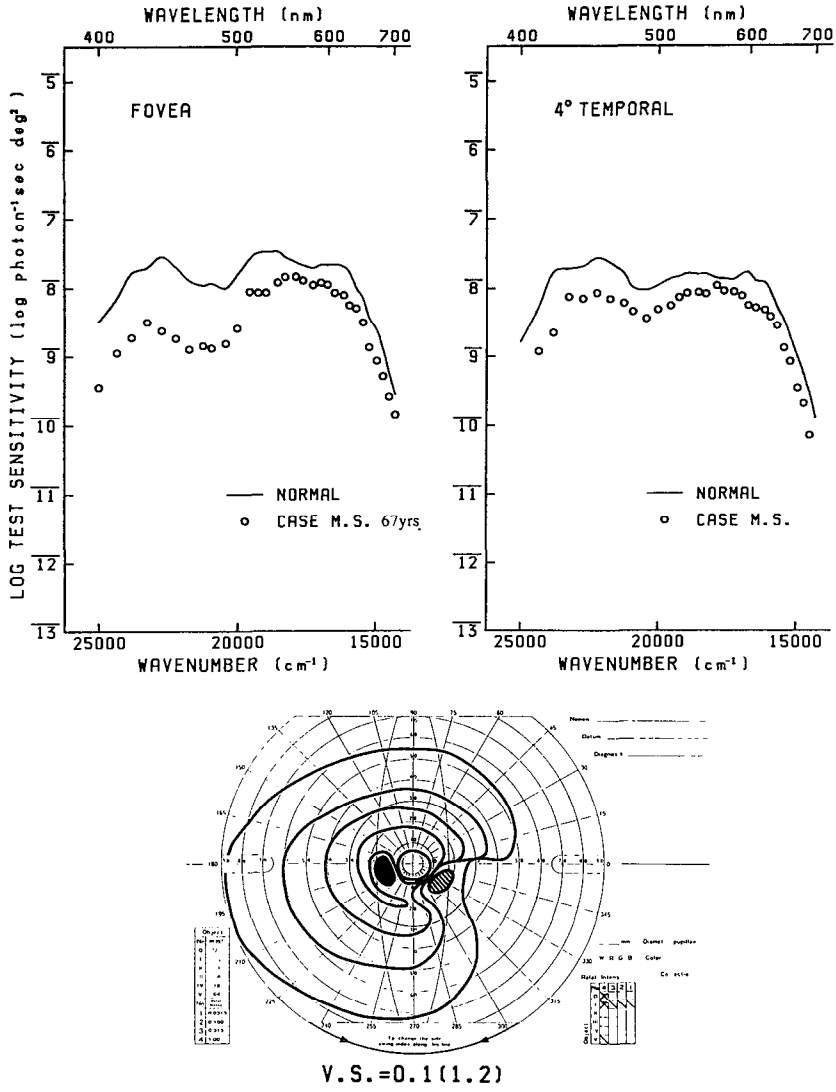

Fig 2 Case RK: upper panels: spectral sensitivities; lower panel: Goldmann visual field

were measured only at the fovea and 4° temporal retina on glaucoma patients with normal visual acuity. There was a loss of sensitivity for both the blue cone system and the red and green cone system, but there was still a prominent peak in the short wavelength region at both the fovea and 4° temporal retina. Because of these results, we feel it is still necessary to carry out more tests in the extrafoveal region.

References

1. Kitahara K et al: The usefulness of sensitivity measurements on a white background for detecting minor changes in visual disturbances in optic nerve diseases In: Heijl A (ed) Perimetry Update 1988/89, pp 39-44. Amsterdam/Berkeley/Milan: Kugler & Ghedini Publ 1989

Newer techniques and instruments

A child's play version of high-pass resolution perimetry

Lars Frisén

Department of Ophthalmology, University of Göteborg, S-413 45 Göteborg, Sweden

The computer graphics environment of high-pass resolution perimetry offers many possibilities of securing good cooperation, even in subjects with fixation difficulties[1,2]. The test strategy introduced here involves flashing one out of several distinctive symbols (drawn at random) in the test display's center and, simultaneously, a regular ring target in some other location. Presentation time is 165 ms, which frustrates refixation attempts. Each presentation is triggered by the subject who has to (1) identify the central symbol and (2) point to the location of any seen ring target. The examiner records the subject's responses on the computer's keyboard or by means of a mouse or a trackball.

There are three sets of central fixation targets. A pictorial set is meant for non-reading subjects. Another set uses the HOTV letters, and the third the full alphabet. If the latter set is selected, the subject has to name the letter displayed. For the other two, the subject can point to a panel of symbols on the test display. Both visual and auditory feedback is provided.

Except for the manual triggering and recording routines, the test is closely similar to the regular Ophthimus Ring Visual Field Test. There are only 16 test locations, to comply with the limited endurance of most subjects with fixation difficulties. There are no blindspot tests. The same pattern is used for right and left eyes. The test can be aborted at any stage, without loss of partial results. Preliminary experience is encouraging.

Acknowledgement

The author has a proprietary interest in the Ophthimus system but not in the design principles

References

1. Frisén L: High-pass resolution perimetry: recent developments In: Heijl A (ed) Perimetry Update 1988/89, pp 369-375. Amsterdam/Berkeley/Milano: Kugler & Ghedini Publ 1989
2. Frisén L: Automatic perimetry: possibilities for feedback and adaptation Doc Ophthalmol 69:3-9, 1988

Perimetry Update 1990/91, p 349
Proceedings of the IXth International Perimetric Society Meeting,
Malmö, Sweden, June 17-20, 1990
edited by Richard P Mills and Anders Heijl

Light-sense, flicker and resolution perimetry in glaucoma: a comparative study

Bernhard J. Lachenmayr*, Stephen M. Drance, Gordon R. Douglas and Frederick S. Mikelberg

Department of Ophthalmology, University of British Columbia, Vancouver, BC, Canada

Abstract

One hundred and six eyes of 106 patients with different types of glaucoma were examined by automated light-sense, flicker and resolution perimetry (Humphrey Field Analyzer, program 30-2; flicker perimeter as described by Lachenmayr[12,13]; resolution perimeter devised by Frisén[6-11]). The fields were classified in masked fashion as being normal or having purely diffuse loss, purely localized loss or diffuse as well as localized loss. Resolution perimetry showed a markedly lower sensitivity in the detection of glaucomatous damage compared with both light-sense and flicker perimetry (77% and 75%), but a high specificity (93% and 85%) When flicker perimetry was compared to light-sense perimetry and *vice versa* the sensitivity was high (95% and 94%), but the specificity low (57% and 62%). The prevalence of detection of diffuse loss for both light-sense and resolution perimetry was related to visual acuity whereas flicker perimetry did not show such a relationship

Introduction

Currently light-sense perimetry measuring the distribution of light-difference sensitivity in the visual field is the most important diagnostic tool for assessing functional glaucomatous damage. Localized field defects in the form of circumscribed scotomas, and diffuse loss producing a generalized depression of light sensitivity may occur in this disease[1-5]. Recently automated perimetric techniques were developed using more complex psychophysical threshold criteria such as resolution perimetry described by Frisén[6-11], or flicker perimetry developed by Lachenmayr[12,13]. The aim of the present study was to compare flicker and resolution perimetry to traditional clinically established light-sense perimetry in detecting glaucomatous damage.

Material and methods

One hundred and six eyes of 106 patients with glaucoma were included in the present study. The diagnosis of glaucoma was established if there was either visual field loss measured with light-sense perimetry and/or if there were glaucomatous disc changes Eighty-six eyes (81%) had both disc and field changes, six eyes (6%) had visual field damage without recognizable disc changes, 14 eyes (13%) had disc changes without a field defect. Twenty-seven eyes had normal tension glaucoma, 68 eyes had primary open-angle glaucoma and 11 eyes had other types of glaucoma with current or previous very high pressures (five eyes with pigmentary glaucoma, three eyes with chronic angle closure glaucoma, two eyes with secondary glaucoma due to heterochromic cyclitis, one eye with mesodermal dysgenesis of the chamber angle). The patients were not selected but had to confirm to the inclusion criteria and volunteer for the tests. All eyes had to have a best corrected visual acuity $\geq$ 20/30 (0.7), a pupil diameter $\leq$ 2.0 mm, a refractive error $\geq$ 6.5 dpt. sph., $\geq$ 3 dpt. cyl., clear optical media and no relevant ocular

This study was supported by research grant La517/2-1 (BJL) from the German Research Foundation (Deutsche Forschungsgemeinschaft, DFG, Bonn, Germany) and by the Medical Research Council of Canada Grant 1578

**Present address and address for correspondence* Bernhard J Lachenmayr, M D , Ph D , University Eye Hospital, Mathildenstrasse 8, D-8000 Munich 2, Germany

Perimetry Update 1990/91, pp. 351-356
Proceedings of the IXth International Perimetric Society Meeting,
Malmö, Sweden, June 17-20, 1990
edited by Richard P. Mills and Anders Heijl

pathology. Their age distribution ranged from 31 to 80 years (median 65.0 years, mean 62.3 ± 11.2 years).

Static light-sense perimetry was performed with the Humphrey Field Analyzer (HFA)[14] using program 30-2. Computerized flicker perimetry using critical flicker fusion frequency as threshold criterion was conducted with the automated flicker perimeter developed by Lachenmayr[12,13] which tests 77 points in the central 40°, 69 of the points being within the central 30°. For resolution perimetry the system of Frisén was used[6-11] which tests 50 points in the central visual field. For the assessment of diffuse field loss cumulative defect curves according to Bebie[15,16] were calculated. Confidence intervals for the Bebie curves were derived from normal populations for all three testing modalities. Details concerning the inclusion criteria and parameters of the normal populations are described elsewhere[17]. All fields were classified in masked fashion by two of the authors (SMD and BJL) as being normal or having purely diffuse loss, purely localized loss or diffuse as well as localized loss using the following quantitative criteria: Diffuse loss was identified when the Bebie-curve of the individual field fell below the 84th percentile in at least 80% of the values of the entire curve. A localized defect for the study was the presence of at least two adjacent points depressed by more than 2.0 standard deviations or three adjacent points or more depressed by 1.6 standard deviations from corresponding mean values for the age groups and there had to be a difference between the defect and its surround of at least 1.6 standard deviations.

Results

In our glaucomatous population 27 (25.5%) of field defects were entirely localized, eight (7.5%) were entirely diffuse and 57 (53.8%) had a combination of localized and diffuse field loss. There were 14 eyes (13.2%) with normal visual fields but abnormal discs.

In order to clarify the abilities of the various techniques to identify the types of field defects the data were classified into "normal fields" and "abnormal fields" (Table 1) and into "localized defects" and "no localized defects" (Table 2), as well as into "diffuse loss" and "no diffuse loss" (Table 3).

The classification into "normal fields" and "abnormal fields" (Table 1) is identical in 95 cases (89.6%) for the comparison of light-sense and flicker perimetry as opposed to only 84 cases (79.3%) for the comparison of light-sense and resolution perimetry and 81 cases (76.4%) for the comparison of flicker and resolution perimetry. There are 21 (19.8%) and 23 (21.7%) cases with a normal field in resolution perimetry which were abnormal in light-sense and flicker perimetry. The classification into "localized defects" and "no localized defects" (Table 2)

Table 1

Flicker perimetry / *Light-sense perimetry*	*Normal*	*Abnormal*	*Total*
Normal	8	6	14
Abnormal	5	87	92
Total	13	93	106
Resolution perimetry / *Light-sense perimetry*	*Normal*	*Abnormal*	*Total*
Normal	13	1	14
Abnormal	21	71	92
Total	34	72	106
Resolution perimetry / *Flicker perimetry*	*Normal*	*Abnormal*	*Total*
Normal	11	2	13
Abnormal	23	70	93
Total	34	72	106

Table 2

Flicker perimetry / *Light-sense perimetry*	*Not localized*	*Localized*	*Total*
Not localized	13	9	22
Localized	8	76	84
Total	21	85	106

Resolution perimetry / *Light-sense perimetry*	*Not localized*	*Localized*	*Total*
Not localized	19	3	22
Localized	20	64	84
Total	39	67	106

Resolution perimetry / *Flicker perimetry*	*Not localized*	*Localized*	*Total*
Not localized	15	6	21
Localized	24	61	85
Total	39	67	106

Table 3.

Flicker perimetry / *Light-sense perimetry*	*Not diffuse*	*Diffuse*	*Total*
Not diffuse	32	9	41
Diffuse	22	43	65
Total	54	52	106

Resolution perimetry / *Light-sense perimetry*	*Not diffuse*	*Diffuse*	*Total*
Not diffuse	35	6	41
Diffuse	23	42	65
Total	58	48	106

Resolution perimetry / *Flicker perimetry*	*Not diffuse*	*Diffuse*	*Total*
Not diffuse	38	16	54
Diffuse	20	32	52
Total	58	48	106

shows a similar trend. The situation is different for the classification into "diffuse loss" and "no diffuse loss" (Table 3) with an identical result in only 75 (70.8%), 77 (72.6%) and 70 (66.0%) cases. There are 22 (20.8%) and 23 (21.7%) cases with a diffuse loss in light-sense perimetry which was not present in flicker and resolution perimetry. Twenty cases (18.9%) had a diffuse loss in flicker perimetry which was not present in resolution perimetry and 16 cases (15.1%) had a diffuse loss in resolution perimetry which was not found in flicker perimetry.

In order to analyze the influence of visual acuity on the classification into "diffuse loss" and "no diffuse loss", the study population was divided into those with a visual acuity of 20/20 or better or less than 20/20. Fifty-nine subjects had a visual acuity of 20/20 or better and 47 subjects had a visual acuity of less than 20/20 (Table 4). The prevalence of diffuse loss for light-sense and resolution perimetry is higher in those eyes with a visual acuity less than 20/20 compared to eyes with a visual acuity equal or better than 20/20 while for flicker perimetry the diffuse loss is similar in both groups.

Table 4

	Visual acuity	
	<20/20 (1 0)	*≥20/20 (1 0)*
Light-sense perimetry		
Normal field + purely localized loss	15/47	26/59
Diffuse and localized loss + diffuse loss	32/47	33/59
Flicker perimetry		
Normal field + purely localized loss	25/47	29/59
Diffuse and localized loss + diffuse loss	22/47	30/59
Resolution perimetry		
Normal field + purely localized loss	22/47	36/59
Diffuse and localized loss + diffuse loss	25/47	23/59

Discussion

Resolution perimetry showed a normal test result in approximately 20% of cases when both light-sense and flicker perimetry indicated visual field defects (Table 1). In less than 2% of cases resolution perimetry indicated field damage when both light-sense and flicker perimetry were normal. This corresponds to a sensitivity of resolution *versus* light-sense and flicker perimetry of 77% and 75% and a specificity of 93% and 85%. In this study Frisén's resolution perimetry[6-11] is therefore markedly less sensitive in detecting glaucomatous field damage than light-sense perimetry with the Humphrey Field Analyzer, program 30-2, or flicker perimetry with the system described by Lachenmayr[12,13], but the specificity is high. The ability of resolution perimetry to identify localized defects is similarly poor. Only 76% and 72% of cases with localized defects in light-sense and flicker perimetry were identified with resolution perimetry, 86% and 71% of cases with no localized defects in light-sense and flicker perimetry were also classified in resolution perimetry as having no localized defects (Table 2). The low sensitivity of resolution perimetry is probably due to the fact that the visual field area which is tested and the number of test locations is smaller[17]. The high specificity of resolution perimetry and the very few cases in which resolution perimetry finds an abnormal field when light-sense and flicker perimetry are still normal shows that resolution perimetry does not provide additional information.

The situation is quite different for the comparison of flicker and light-sense perimetry: the sensitivity of flicker perimetry to identify abnormal fields is 95%, but the specificity is only 57%. The proportion of cases identified as normal with light-sense perimetry which are called abnormal with flicker perimetry and *vice versa* is 4.5% and 5.7% (Table 1). Similarly, 91% of cases with localized defects in light-sense perimetry were also identified with flicker perimetry and only 59% of cases with no localized defects in light-sense perimetry were classified identically in flicker perimetry (Table 2). Our results show that flicker perimetry as used in the present study[12,13] is comparable to light-sense perimetry (HFA, program 30-2) in identifying glaucomatous field changes in general and localized defects in particular. The low specificity of flicker perimetry implies that there are cases where light-sense perimetry does not show a visual field defect and flicker perimetry already indicates damage and *vice versa*. As light-sense and flicker perimetry use different threshold criteria the discrepancy suggests that both techniques may provide different information about glaucomatous damage.

A comparison of the ability to identify a diffuse field loss shows an interesting trend (Table 3). In some 20% of cases flicker perimetry and resolution perimetry do not show a diffuse damage when light-sense perimetry finds it. Diffuse damage is however shown by flicker perimetry in 8.5% of cases and resolution perimetry in 5.7% of cases in which light-sense perimetry does not indicate it. Light-sense perimetry obviously finds a diffuse loss more often than the other two perimetric techniques. The fact that the prevalence of diffuse field loss in both light-sense (Table 4, top) and resolution perimetry (Table 4, bottom) is related to visual acuity as opposed to flicker perimetry (Table 4, middle) suggests a possible influence of retinal image quality. From a theoretical point of view, such an influence has to be expected for threshold criteria using spatial information, such as light-difference sensitivity or spatial resolution, but not for threshold criteria using temporal information, such as flicker fusion frequency. Experi-

mental studies have shown that blurring of the retinal image by a small defocus may cause a measurable effect on light-difference sensitivity[18], whereas flicker perimetry is less affected by the quality of the retinal image[19,20].

The following practical conclusions may be drawn:

1. Resolution perimetry according to Frisén[6-11] is less sensitive for the detection of glaucomatous field damage than light-sense perimetry (HFA, program 30-2) and flicker perimetry according to Lachenmayr[12,13]. There are almost no fields which have a normal result in light-sense and flicker perimetry which show an abnormality in resolution perimetry.
2. Light-sense perimetry and flicker perimetry are comparable in their sensitivity to identify abnormal fields and also in their ability to identify localized defects. There are fields which have damage in flicker perimetry which is not found in light-sense perimetry and *vice versa*. Both techniques may provide different information about glaucomatous damage.
3. The assessment of diffuse field loss by light-sense and resolution perimetry is influenced by visual acuity even with slight reductions of visual acuity to 20/30 or better, which is not the case with flicker perimetry.

Acknowledgements

The authors are grateful to B C Chauhan, Ph D , and P.H House, M.D., for calculating the Bebie-curves for the data of the Humphrey Field Analyzer and the Frisén perimeter. Chris A Johnson, Ph.D , Department of Ophthalmology, University of California, Davis, made his normal data on the Humphrey Field Analyzer available to us, which we used for calculating the confidence intervals for the Bebie-curves We are especially grateful to K. Wijsman and S Lalani, O D , for their technical help

References

1. Aulhorn E, Karmeyer H: Frequency distribution in early glaucomatous visual field defects Doc Ophthalmol Proc Series 14:75-83, 1977
2. Caprioli J, Sears M, Miller JM: Patterns of early visual field loss in open-angle glaucoma Am J Ophthalmol 103:512-517, 1987
3 Drance SM: The glaucoma visual field defect and its progression In: Drance SM, Anderson D (eds) Automatic Perimetry in Glaucoma: A Practical Guide, pp 35-42. Orlando: Grune and Stratton 1985
4. Flammer J: Psychophysics in glaucoma: a modified concept of the disease. In: Greve EL, Leydhecker W, Raitta C (eds) The Second European Glaucoma Symposium, pp 11-17 The Hague: Junk Publ 1985
5. Glowazki A, Flammer J: Is there a difference between glaucoma patients with rather localized visual field damage and patients with more diffuse visual field damage? Doc Ophthalmol Proc Series 49:317-320, 1987
6. Douglas GR, Drance SM, Mikelberg FS, Schulzer M, Wijsman K: Variability of the Frisén ring perimeter. In: Heijl A (ed) Perimetry Update 1988/1989, pp 197-198 Amsterdam/Berkeley/Milano: Kugler & Ghedini Publ 1989
7. Drance SM, Douglas GR, Schulzer M, Wijsman K: The learning effect of the Frisén high pass resolution perimeter. In: Heijl A (ed) Perimetry Update 1988/1989, pp 199-201 Amsterdam/Berkeley/Milano: Kugler & Ghedini Publ 1989
8. Frisén L: A computer-graphics visual field screener using high-pass spatial frequency resolution targets and multiple feedback devices. Doc Ophthalmol Proc Series 49:441-461, 1987
9. Frisén L: High pass resolution targets in peripheral vision Ophthalmology 94:1104-1108, 1987
10 Frisén L: Acuity perimetry: estimation of neural channels Int Ophthalmol 12:169-174, 1988
11. Frisén L: High pass resolution perimetry In: Heijl A (ed) Perimetry Update 1988/1989, pp 369-375 Amsterdam/Berkeley/Milano: Kugler & Ghedini Publ 1989
12. Lachenmayr B: Analyse der zeitlich-räumlichen Übertragungseigenschaften des visuellen Systems: Ein neuer Weg zur Frühdiagnose von Netzhaut- und Sehnerverkrankungen? Thesis (Habilitationsschrift), University of Munich 1988
13. Lachenmayr B, Rothbächer H, Gleissner M: Automated flicker perimetry versus quantitative static perimetry in early glaucoma In: Heijl A (ed) Perimetry Update 1988/1989, pp 359-368. Amsterdam/Berkeley/Milano: Kugler & Ghedini Publ 1989
14 Heijl A: The Humphrey Field Analyzer, construction and concepts Doc Ophthalmol Proc Series 42:77-84, 1985
15 Bebie H, Flammer J, Bebie Th: The cumulative defect curve: separation of local and diffuse components of visual field damage. Graefe's Arch Clin Exp Ophthalmol 127:9-12, 1989
16. Kaufmann H, Flammer J: Clinical experience with the Bebie-curve In: Heijl A (ed) Perimetry Update 1988/1989, pp 235-238. Amsterdam/Berkeley/Milano: Kugler & Ghedini Publ 1989

17. Lachenmayr B, Drance SM, Chauhan BC, House PH, Lalani S: Diffuse and localized glaucomatous field loss in light-sense, flicker and resolution perimetry. Graefe's Arch Clin Exp Ophthalmol 1991 (accepted for publication)
18. Weinreb RN, Perlman JP: The effect of refractive correction on automated perimetric thresholds. Am J Ophthalmol 101:706-709, 1986
19. Kleberger E: Untersuchungen über die Verschmelzungsfrequenz intermittierenden Lichts an gesunden und kranken Augen. I. Mitteilung. Graefe's Arch Ophthalmol 155:314-323, 1954
20. Gleissner M, Lachenmayr B: Influence of defocus, artificial media opacities and pupil size on thresholds in light-sense and flicker perimetry. Proc Int Conf on Optics in Life Sciences, Garmisch-Partenkirchen 1990 (in press)

Perimetry and retinal lesions: a pathophysiological study

Bertil Lindblom

Department of Ophthalmology, University of Göteborg, S-413 45 Göteborg, Sweden

Differential light sensitivity (DLS) and high-pass resolution (HRP) thresholds were studied before and after panretinal photocoagulation in eight eyes with proliferative diabetic retinopathy. A defined area temporal to the macula was chosen for measurements. A 4° perimetric test grid composed of 50 test positions was used. The relative photocoagulated area was measured and the relative change in space-average functioning ganglion cell separation was calculated. These calculations were based on the assumption that photoreceptor destruction was functionally equivalent to disconnection of retinal ganglion cells.

After treatment, the difference in DLS thresholds, expressed in decibels, was linearly related to the calculated change in ganglion cell separation. A 5-dB average sensibility loss corresponded to a change in ganglion cell separation by 13%, equivalent to treatment to 21% of the retinal area. While this log/lin relation may be practically useful, the theoretical rationale remains to be defined.

For HRP, the change in threshold expressed in min arc was linearly related to the change in ganglion cell separation, without the need for logarithmic transformation. This is in agreement with resolution theory, stating that resolution is proportional to the distance between working retino-cortical connections. Thus the HRP result seems directly to reflect the anatomical state of the visual system.

The complete article will be published elsewhere

Perimetry Update 1990/91, p. 357
Proceedings of the IXth International Perimetric Society Meeting,
Malmö, Sweden, June 17-20, 1990
edited by Richard P Mills and Anders Heijl

Graphic visual field difference plots

Lars Frisén

Department of Ophthalmology, University of Göteborg, S-413 45 Göteborg, Sweden

Abstract

Visual field maps depicting differences between observed and reference results merit evaluation. In this study, regular ring perimetry plots and difference plots were examined in masked fashion by four examiners. Observer sensitivity was estimated from 24 subjects who had made a good recovery after demyelinating optic neuropathy. On average, 91% ± 7 (SD) were judged abnormal in the regular format but full agreement occurred in only 18 cases. With the difference plot, there was full agreement in all cases, 79% being classified as abnormal. Statistical indices identified 75% abnormal results When categorizing the field defects, observer agreement was better with the difference plots. Observer specificity averaged approximately 80% in normal subjects, irrespective of map type, but full agreement was more common in the difference map (79% *versus* 67). Indices identified 23 normal results, for a specificity of 96%

Introduction

Every teacher of graphic visual field evaluation knows how difficult it is to impart understanding of threshold surfaces. This is true for both normal and abnormal fields. A possible solution is to change the format of representation so that only *deviations* from normal are shown. This is fairly straightforward in Ophthimus ring perimetry, which represents thresholds directly, without interpolation or lumping together of several threshold levels[1]. The only problem concerns the selection of reference values. The solution proposed here involves a heightwise shift of the individual threshold surface so that the most sensitive part of the observed field is made to coincide with the normal average.

The utility of this "difference plot" was illuminated by four examiners, who evaluated masked sets of plots from normal controls and from subjects with resolved demyelinating optic neuropathy. It is well known that the latter disorder generally leaves only subtle field defects in its wake[2-4]

Subjects and methods

Subjects

Visual field records were retrieved from 24 subjects who had made a good recovery after one or more attacks of classical retrobulbar demyelinating optic neuropathy. Age distribution was 36± 6 (SD) years. Four had a letter visual acuity of 0.8 (20/25); all the others were better. The same number of records was retrieved from age-matched normal controls. Each subject contributed one record only.

Perimetry

Perimetry was performed with the Ophthimus high-pass resolution perimeter (HRP) (High-Tech Vision, Malmö, Sweden), version 1.4, which determines resolution thresholds in 50 locations in the 30° central visual field. HRP uses ring-shaped targets of constant contrast There are 13 targets with a size interval of 0.1 $\log_{10}$ unit (1 decibel (dB)): No. 0 has a stroke width of 10'. Normally, results are described by ring plots, with the ring size representing the threshold printed in each test location (Figs. 1A and C). Extensive numerical analyses and reference values are contained in the software[1].

Perimetry Update 1990/91, pp 359-363
Proceedings of the IXth International Perimetric Society Meeting,
Malmö, Sweden, June 17-20, 1990
edited by Richard P Mills and Anders Heijl

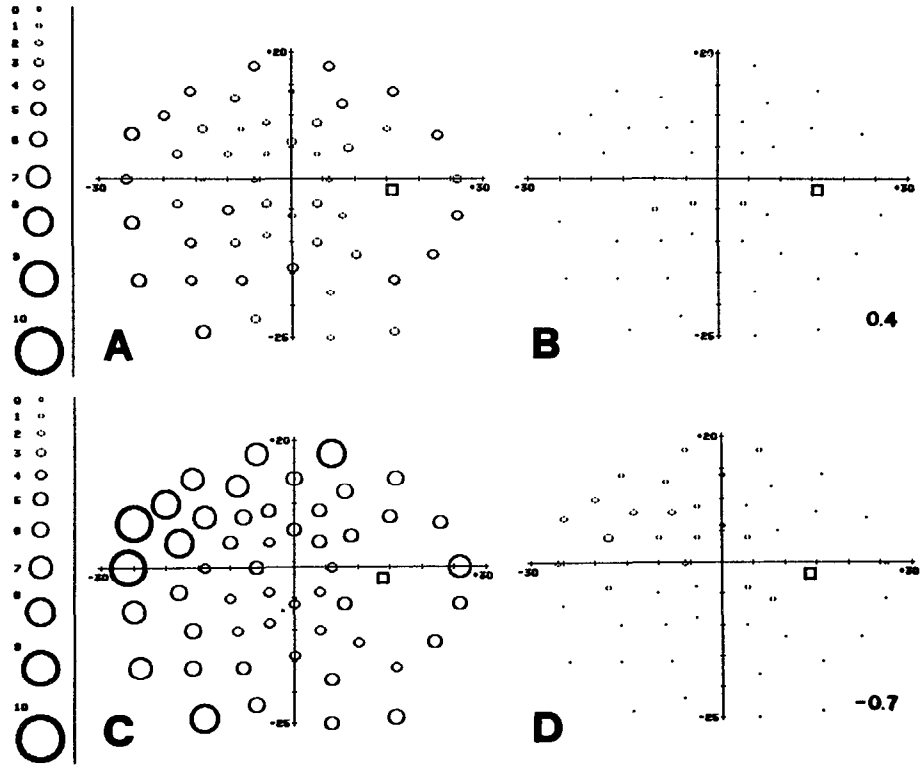

Fig 1 Examples of regular (left) and difference plots (right) from a control subject (top) and a patient (below) Part of target series is shown to the left Inset: adjustment factor α. Examiners' judgments: A: normal (two examiners) or abnormal (2); B: normal (4); C: abnormal, with uniform (2) or upper nasal depression (2); D: abnormal with upper nasal depression (4) Patient record was outside normal limits for global deviation statistic only

Difference plots

Difference plots were based on the normal reference values contained in the Ophthimus database. For each subject and each test location, the age-adjusted normal average was subtracted from the observed threshold to obtain a δ value. Because of normal variation most normal subjects will obtain multiple non-zero δ values. Therefore, plots of plain δ values will produce a cluttered display that may interfere with recognition of minor abnormalities. A simple remedy is to calculate an adjustment α from a subset of test locations, namely those that show the lowest δ values. These locations are likely to be normal, or near normal, also in abnormal eyes (see further below). Here, the 15 lowest δs were identified. The three lowest among these were discarded to prevent influence from fortuitously good results. The remaining 12 were averaged to obtain α, which was then subtracted from each δ value. The results were truncated to integers. Finally, the ring size corresponding to each positive (int) (δ - α) was plotted in the corresponding location (Figs. 1B and D).

Presentation formats

Two masked and randomly ordered sets of 48 graphs were prepared. The one shown first was in the regular format while the second comprised difference plots. The examiners were provided with a written instruction, asking for purely subjective evaluations, without discussion with the others. Neither patients (or their diagnoses) nor controls were known to the examiners. The patient/control ratio was not disclosed.

The following normal criteria were suggested for the regular plot. Threshold levels should all be within the normal range and there should be a monotonous increment in threshold level with increasing eccentricity. Up to three locations with higher thresholds should be accepted as normal provided that all neighboring locations showed normal levels and deviation was ≤ 2 dB. For the difference plot, the suggested normal criteria were 0 dB in all locations, or up to three isolated locations with difference levels ≤ 2 dB.

Examiners

Two examiners had had several years of experience with different forms of automated perimetry, including HRP, one had had about one year's experience with HRP, and one, a medical student, had had only one hour of training in HRP evaluation. The author did not participate in the evaluations.

Statistical analyses

Sensitivity was calculated as the percentage of records from the patient group that were identified as abnormal while specificity was calculated as the percentage of records from the control group that were identified as normal. Two-tailed student's t was used to evaluate differences between means, $p < 0.05$ being considered significant.

Results

With the regular result plot, subjective recognition of minor visual field abnormality, as exemplified in Fig. 1C, proved to be fairly variable. Observer sensitivities ranged between 83 and 100% and averaged 91% ± 7 (SD) (Table 1). Full agreement was reached in only 75% of cases while three out of four examiners agreed in 92%. Objective evaluation identified 18 abnormal results, for a sensitivity of 75% (Table 1).

There was more divergence of opinion in the classification of normal subjects, with 3/4 agreement in only 71%. Average specificity was 79% ± 3. Statistical indices identified a single abnormal result, for a specificity of 96% (Table 1).

All examiners felt that the difference plots (Figs. 1B and D) were easier to evaluate. This was confirmed by less divergence of opinion in the patient group (Table 1). There was complete agreement in *all* cases, 79% being unanimously judged abnormal (for a sensitivity of 79% ± 0) and 21% normal. The normal group presented more problems, with full agreement in only 71% and 3/4 agreement in 79%. Mean specificity was 81% ± 4.

Observer experience did not appear to influence sensitivity or specificity with either type of chart, the novice performing essentially on par with the most experienced examiner (Table 1).

Table 1 Summary of subjective and objective evaluations

Examiner No *	*Ordinary plot*		*Difference plot*		*Statistic*	*Limit*	*Sensitivity*	*Specificity*
	sensitivity	*specificity*	*sensitivity*	*specificity*				
1	100	79	79	83	Raw score	5 30 dB	17	100
2	88	75	79	83	Global dev	1 34 dB	46	96
3	92	83	79	83	Local dev	0 79 dB	38	100
4	83	79	79	75	Form index	0 66	50	100
Average	91±7	79±3	79±0	81±4	Neural cap	73%	38	100
Majority (3/4 vote)	92	71	79	79	Combined indices	–	75	96

*listed in order of increasing experience

The examiners were also asked to classify the spatial distribution of any field defects. The given alternatives comprised predominantly central, upper or lower temporal, upper or lower nasal, and uniform depressions. Again, the difference plots resulted in better uniformity of description, with a 3/4 majority agreement obtained in 75% of cases. The corresponding number for the regular plots was 50%. The most common classification was a shallow central scotoma, followed by shallow upper nasal or upper temporal depressions.

Discussion

The introduction of automated perimeters has caused a radical change in visual field evaluation, shifting emphasis from subjective "eye-balling" to objective "number-crunching". The change has been so pervasive that most automated perimeters offer only meager aids for subjective evaluation. The most common format of graphic representation, the grey-scale, lumps several different threshold levels to one and the same shade of grey. This effectively prevents visual identification of defects that are shallow enough to fit within one and the same grey-scale level. Unfortunately, it is precisely these abnormalities that also are the most difficult to identify by objective means. Therefore, exploration of new formats of graphic representation is desirable.

Difference plots are not new. As a matter of fact, some automated perimeters present numerical difference plots and a few can produce graphic plots, although several threshold levels are lumped to one and the same graphic symbol. These plots all seem to depict plain differences from normal averages. Formal evaluations of their properties seem to be lacking. The technique described here takes the procedure two steps further, by adjusting the differences to minimum (which minimizes clutter) and abstaining from lumping (which exposes deviations with maximum clarity).

The adjustment procedure is effectively an individualized and uniform height-wise shift of the threshold surface, where the best thresholds are brought to coincide with the average normal threshold surface. This works well in visual fields with minimal abnormality, as shown above. However, in fields with more extensive and more severe abnormalities, this procedure will tend to underrate the deficit. This can be prevented by setting α to zero if it exceeds a limiting value, *e g* , the average normal standard deviation. This is a valid procedure in ring perimetry, where standard deviations are essentially constant across the normal threshold surface[1], in contrast to ordinary perimetry[5].

Major problems in studies of sensitivity and specificity involve the selection of a model disorder, the certification of abnormality in the examined cases, and the assessment of the severity of abnormality. Resolved optic neuritis can be held to be one of the best model disorders because of its ubiquity, the ease of diagnosis in the acute phase, and the high prevalence of various low-degree abnormalities after recovery. An additional advantage is the relatively young age of onset, which ensures that the frequency of complicating disorders like cataract and macular degeneration is low. The sole disadvantage seems to be the lack of an independent indicator of field abnormality. This prevents estimation of true sensitivity. Comparing indicated sensitivities for different analytical approaches in one and the same case material is valid, however[4]. Other case materials selected on the same grounds can be expected to show similar results because of the fairly stereotype course of the disease.

Mean observer sensitivity was clearly higher with the regular plot (91% *versus* 79, $p < 0.001$) but this statistic obscures the considerable disagreement between the observers. If sensitivity instead is calculated from those cases where all observers agreed in their evaluations, it amounts to 75%, or very nearly the same as in the difference plot. For comparison, the pooled results of the objective analyses was 75%. Interestingly, no single objective index came near the detection rate of the least sensitive observer (Table 1), attesting to the need of multi-facetted analyses.

Specificity was closely similar for the two types of maps (79% *versus* 81, $p = 0.16$) although agreement was slightly better in the difference plot (Table 1). The objective indices gave a specificity of 96%, implying that all observers over-diagnosed abnormality, in both types of plots. The suggested guidelines may have appeared too severe to the present examiners.

The problem of defining the severity of abnormality has a unique solution in the Ophthimus perimeter, which estimates the "functional fraction" of retino-cortical neural channels[6]. This averaged 47% ± 16 for the neuropathy subjects and 109% ± 35 for the controls ($p < 0.001$). The large normal standard deviation depends in part on a square transform used in estimating the number of functional retinal ganglion cells per square degree. A new software version 2 omits this step and estimates cell density per *linear* degree. This statistic, termed "neural capacity", averaged 74%± 13 in the patient group and 109% ± 18 for the normals ($p < 0.001$).

Because of the better agreement between different examiners, the graphic difference plot proposed here appears to be a useful complement to existing techniques for visual field evaluation. It should also prove useful when teaching visual field diagnosis to newcomers to the field. Yet another application is determination of loci of maximum impact on the visual field with different disorders, as exemplified in Table 2, for maximum efficiency in allocation of test points.

Table 2.

Lesion	*No of cases*	*Locus*	*% of cases*
Midchiasmal, compression	23	near fixation	65
		remote	13
		uniform	22
Retrochiasmal, compression	17	near fixation	70
		remote	24
		uniform	6
Retrochiasmal, ischemic	15	near fixation	27
		remote	53
		uniform	20

Acknowledgements

The efforts of the four examiners is gratefully acknowledged. The author has a proprietary interest in the Ophthimus system but not in the design principles

References

1 Frisén L: High-pass resolution perimetry: recent developments In: Heijl A (ed) Perimetry Update 1988/89, pp 369-375 Amsterdam/Berkeley/Milano: Kugler & Ghedini Publ 1989
2 Burde RM, Gallin PF: Visual parameters associated with recovered retrobulbar optic neuritis. Am J Ophthalmol 79:1034-1037, 1975
3. Fleishman JA, Beck RW, Linares OA, Klein JW: Deficits in visual function after resolution of optic neuritis. Ophthalmology 4:1029-1035, 1987
4 Frisén L: A shape statistic for visual field evaluation Utility in minor optic neuropathy Neuro-Ophthalmology (Amsterdam) 9:347-354, 1989
5. Heijl A, Lindgren G, Olsson J: Normal variability of static perimetric threshold values across the central visual field. Arch Ophthalmol 105:1544-1549, 1987
6 Frisén L: Acuity perimetry: estimation of neural channels Int Ophthalmol 12:169-174, 1988

Octopus program G1X

Ch. Messmer[1], J. Flammer[2] and H. Bebie[3]

[1]*Augenklinik Kantonsspital, CH-6016 Luzern,* [2]*Universitäts Augenklinik, CH-4056, Basel,* [3]*Institut für theoretische Physik, CH-3000 Bern, Switzerland*

Abstract

The glaucoma program G1 is widely employed by Octopus users. Besides a specific distribution of the test locations, its main advantage is the quick comparison of results with normal values as well as an easy follow-up. However, the program is relatively time-consuming and thus tiring for some patients For this reason, the program was modified to "G1X" This program can be interrupted at any time and provides information, including statistical analyses, based on the available data. The test sequence is rearranged in accordance with the importance of the information. The available information, including the confidence limits, is continuously calculated and presented on the display screen of the Octopus 1-2-3 during the test procedure. This provides the possibility of adapting the measurement to the patients and their diseases The principal features as well as clinical applications were described

Perimetry Update 1990/91, p. 365
Proceedings of the IXth International Perimetric Society Meeting,
Malmö, Sweden, June 17-20, 1990
edited by Richard P Mills and Anders Heijl

Threshold-related suprathreshold field testing: which is the best technique of establishing the threshold?

David B. Henson and Roger Anderson

Department of Optometry, University of Wales, P.O. Box 905, Cardiff CF1 3YJ, UK

Abstract

The reliability of several abbreviated multiple stimulus threshold estimation techniques was assessed by comparing them with a longer, more elaborate "accurate" technique, to try to derive an optimum strategy for visual field screening purposes. A one-reversal technique stepping down from seeing to an intensity at which all the stimuli were missed was found to combine reasonable accuracy with short testing while also being robust to the presence of visual field defects.

Introduction

There are many different strategies for examining the visual field: some are more appropriate for the detection of defects while others are more appropriate for the quantification of established visual field loss.

A static suprathreshold strategy has repeatedly been advocated as the most appropriate for screening the visual field[1-4]. With this strategy stimuli are presented at an intensity calculated to be above the patient's threshold. If the patient reports that they can see this stimulus, then it is assumed that no significant defect exists and that no further testing of that point is necessary.

Some of the early suprathreshold strategies were one-level: they presented stimuli at a single intensity across the whole visual field, no account being taken of the retinal gradient of sensitivity. These tests have largely been superseded by the gradient adapted suprathreshold strategy, where the retinal gradient of sensitivity is compensated for by using larger (Friedmann VFA), or brighter (Henson CFS2000) stimuli towards the periphery. In any suprathreshold test, some estimate of threshold must be made, from which the intensity can be incremented to its "suprathreshold" level. The sensitivity and specificity of suprathreshold testing will depend on the accuracy of this initial threshold estimate. If the initial threshold estimate is incorrect and as a result the suprathreshold stimuli set either brighter or dimmer than the assumed optimal level, then this will have an adverse effect on the test's sensitivity and specificity. Various techniques of threshold estimation have been put forward. One of the simplest of these is to set the threshold according to the age of the observer, called age-related suprathreshold testing[5]. Others involve an actual measurement of the threshold made at the beginning of the examination, a technique referred to as threshold-related suprathreshold testing.

The way in which the threshold is measured at the beginning of a threshold-related suprathreshold strategy also varies from one instrument/report to another. The Humphrey has a threshold-related suprathreshold strategy in which it establishes the threshold at four separate locations of 10 degrees eccentricity, using steps of 4 dB, reducing to 2 dB after the first reversal and then extrapolating backwards by 1 dB at the second reversal to obtain the final value. It then takes the second most sensitive value to establish the height of the "hill of vision" and increments by 6 dB to the suprathreshold testing level. No explanation is given as to why the Humphrey chooses the second most sensitive value.

Gutteridge[6], using the Friedmann VFA, suggested using paracentral stimuli at suprathreshold levels' decreasing the intensity until half or more escaped detection, and then incrementing by 4 dB to obtain a suitable suprathreshold level. Bakto *et al* [7] also with the Friedmann VFA, used locations near fixation and determined "the weakest stimulus that could be seen at least one half of the time". The Henson CFS2000[8] recommends a reversal technique from seeing to non-seeing and back to 50% seeing. Henson *et al.*[9], again with the Friedmann VFA, used a

Perimetry Update 1990/91, pp 367-372
Proceedings of the IXth International Perimetric Society Meeting,
Malmö, Sweden, June 17-20, 1990
edited by Richard P. Mills and Anders Heijl

technique of presenting approximately 30 stimuli across the central 25 degrees of the field and taking threshold as the intensity at which 20-30% were missed.

With the above techniques, no details are given as to how the threshold is established in patients with moderate or advanced field loss who may never see more than 50% of the stimuli.

Other manuals and researchers suggest different methods again, but little has really been done to ascertain reasons for choosing a certain technique and the benefits or otherwise of using one compared to another. One of the reasons for the lack of consistency in the actual techniques of threshold estimation is the absence of any systematic study, detailing the relative merits of the various strategies. While most researchers have adopted a threshold-related rather than age-related technique, what is the cost with respect to accuracy and time? Henson and Anderson[10] compared the reliability of threshold estimates using single and multiple stimuli and found an increased reliability as well as a reduced estimation time using multiple stimuli.

For this reason this study uses multiple stimuli and presents data from an evaluation of the accuracy of various techniques including: age setting, single staircase up or down (*i.e.*, one reversal), two reversal, and one reversal double estimate. In addition to this the study will investigate the possible effects of the number of stimuli in the pattern, the position and eccentricity of the stimuli in the field, whether or not the stimuli fall on defects, attention, comprehension and age of the observer

Method

For the study a Henson CFS2000[11] was used with specially developed software to present the stimuli and store the results on magnetic disc for later analysis. Multiple stimulus patterns were used throughout. In order to determine the accuracy of the various thresholding techniques, it is first necessary to have a standard against which to compare them. For this "accurate technique" the method used was that described by Henson and Anderson[10]. This involved using multiple-stimuli and making an initial threshold estimate using a single staircase from seeing to non-seeing in 1 dB steps. Patterns of stimuli were then presented over a range of intensities from 3 dB below to 3 dB above this estimate in 1 dB steps. In normal observers this invariably gave a range from 0-100% seeing. A minimum of 20 presentations were then made at each intensity level, 140 presentations in all.

The observer reported the number seen at each presentation which was entered into the computer. All the stimuli were located at an eccentricity of 10-15 degrees.

The 50% seeing value and the standard deviation of the threshold estimate were calculated, using the summation method[12]. This technique was employed twice consecutively on 20 normal observers to give an estimate of its repeatability.

The "accurate" strategy was used, in random sequence with other techniques (see later for descriptions), on 70 normal observers taken from a private optometric practice. Ages ranged from nine to 77 years (mean 42 years), with approximately equal numbers of males and females.

The other thresholding programs run on the 70 normal observers involved:

1. a single staircase from seeing to non-seeing (in steps of 1 dB), reversing to give a staircase from non-seeing to seeing in 11 steps of 1 dB;
2. the reverse, *i e* , a single staircase from non-seeing to seeing followed by a reversal from seeing to non-seeing.

Each staircase covered, in normal patients, the range of intensities from 0-100% seeing. From this data the following information could be extracted:

Stepping up, the level at which the stimuli were

a. first seen
b. at least two seen
c. all seen

Stepping down, the level at which stimuli were

a. first missed
b. at least two missed
c. all missed

It was also possible to extract information on: (a) repeat measures of one-reversal techniques, *i.e.*, two up or down staircases; (b) two-reversal techniques starting from either seeing or non-seeing; (c) age settings.

These techniques were then repeated on a group of 18 glaucoma patients. Ages ranged from 42 to 78 years, again with equal numbers of males and females.

Results

In giving an estimate of the reliability or repeatability of a given technique we have chosen to use two statistical measures:

1. The first is the mean difference in thresholds between any given technique and the "accurate" technique. This data can be used to decide an appropriate suprathreshold increment.
2. The second is the standard deviation of the differences between any given technique and the "accurate" technique. This statistic, which gives a result in dBs, can be used to estimate the likely number of false positives and false negatives for any given suprathreshold increment.

The mean standard deviation of the threshold estimate for the 70 normals was found to be 1.17 dB with an SD of 0.26 dB. No significant relationship was found between the SD of the threshold estimate and age.

Repeat measures of the threshold with the accurate technique were found to have a mean difference of 0.016 dB and a standard deviation of 0.18 dB. This standard deviation should be taken into account when looking at the abbreviated techniques of threshold estimation.

The results of the accurate technique were plotted against patient age for the 70 normals (Fig. 1). The best fitting straight line gave a negative gradient of -0.0756 dB/yr. This line was used to give a predicted age threshold which would be compared to the actual threshold. This comparison gave a standard deviation of the differences of the threshold estimates of 1.738 dB.

The results from the one-reversal staircase techniques and the techniques that averaged the results from two one-reversal techniques are set out in Table 1.

A two-reversal technique stepping down to "all missed" and back to "at least two seen" was also extracted, and calculated using the average of the latter two values. This gave an SD of 0.717 dB which is of a similar order to a repeat staircase down to "all missed".

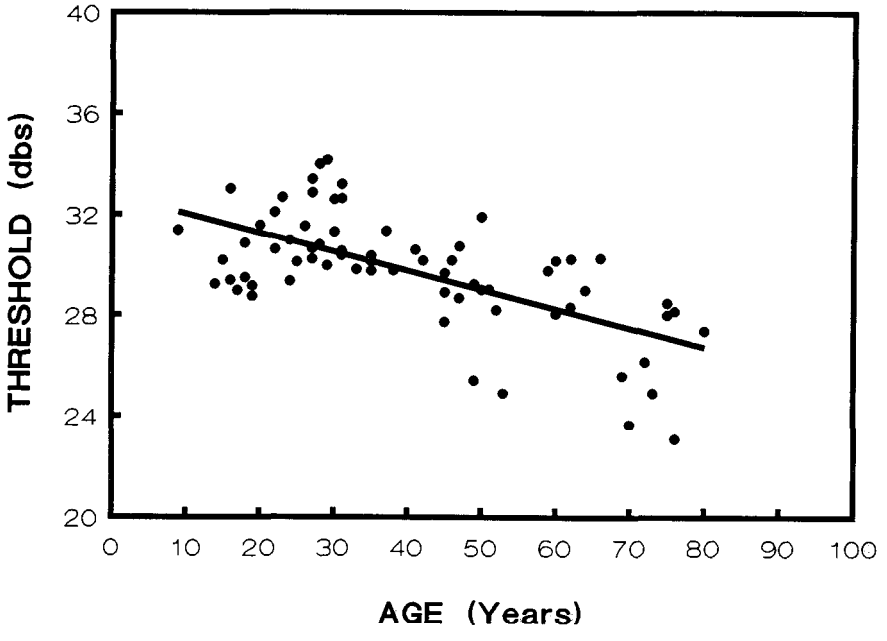

Fig 1 Threshold sensitivity as determined by the "accurate" technique *versus* patient age

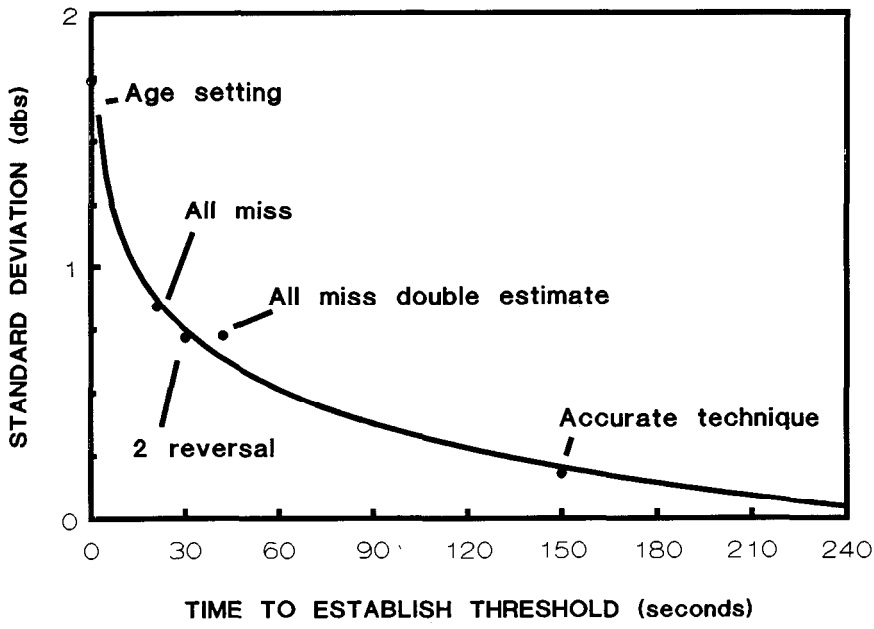

Fig 2 Accuracy of threshold estimate, represented by the standard deviation of the differences *versus* the average time taken to establish the threshold.

Table 1 Results from the one-reversal techniques

Technique	*Mean difference (SD of differences) dBs*		
	First seen/missed	*At least two seen/missed*	*All seen/missed*
Single estimate down	0 03 (1 06)	1 18 (0 85)	0 87 (0 86)
Single estimate up	–0 10 (1 17)	–0 51 (1 00)	–1 34 (0 73)
Double estimate down	0 03 (0 86)	1 18 (0 71)	1 87 (0 73)
Double estimate up	–0 10 (0 98)	–0.51 (0 81)	–1 34 (0 71)

It should be noted that, in this case, the threshold was calculated as the mean of the reversals whereas the Octopus and Humphrey instruments only use the final reversal value. Thresholds calculated with these instruments, therefore, would be of a similar accuracy to those of a one-reversal single estimate

The approximate duration of each abbreviated technique was calculated by multiplying the average number of presentations by the mean time taken for each presentation (mean = 3.4 sec, SD 0.24 sec). Each technique started off 6 dB from the appropriate age setting.

The duration of each technique ranged from zero using an age setting to 2.5 minutes using the "accurate" technique (Fig. 2).

All the methods were repeated on a group of 18 glaucoma patients. The accurate technique gave an average SD of 1.170 dB in normal subjects and an average SD of 1.766 dB in glaucoma patients. This will be discussed later.

Discussion

Any technique which establishes a threshold estimate is subject to variability. The accurate technique used in this study took an average of 2.5 minutes to perform and had an SD of the differences (obtained from repeat measures) of 0.18 dB. This technique has limited use in patients with visual field defects where it may be impossible to reach an intensity at which 100% of the stimuli will be seen. The technique also has limited use in screening programs

where the time taken to establish the threshold is long in comparison to the abbreviated techniques described in this study.

The rate of sensitivity loss with age (0.76 dB/decade), is in broad agreement with those of Jaffe *et al.*[13] (0.74 dB/decade), Heijl *et al* [14] (0.64 dB/decade), and Johnson *et al.*[15] (0,80 dB/decade). The SD of the differences between the age-related technique and the accurate technique is large (1.73 dB) in comparison to other techniques. If this technique were to be used in a screening program then to ensure high specificity the suprathreshold increment would have to be increased which would decrease the test's sensitivity to shallow defects. The advantages of an age-related technique are its simplicity and speed. There is practically no scope for operator error and no valuable time spent on establishing the threshold. The gain in time would not always be as great as that indicated in Fig. 2 because the perimetrist would have to demonstrate the test to the patient, a process which could be included in the time taken to establish the threshold with a decreasing staircase strategy.

The one-reversal techniques, either stepping down from seeing to non-seeing or up from non-seeing to seeing, give more accurate estimates of the threshold (Table 1), than does an age setting while taking less than 30 seconds to complete. Stepping down from seeing to non-seeing has certain advantages over stepping up from non-seeing to seeing. The test starts off at a suprathreshold value at which some or all of the stimuli are seen. This serves as a good demonstration/training to the patient, and he/she learns better what to look for. By informing the patient that the stimuli will get dimmer with each presentation until they can no longer be seen also assists patient understanding. The slightly improved performance of the stepping down to "all missed" versus stepping up to "all seen" may be accounted for on this basis.

Another advantage of stepping down, particularly to "all missed", relates to the way in which these strategies work in the presence of visual field defects. In cases where there is some visual field loss it may prove impossible to reach an intensity at which all stimuli will be seen whereas it will always be possible to decrease the intensity until none are seen. There is a possibility, in cases of advanced loss, that all the stimuli will fall within defective areas. The likelihood of this occurring can be reduced by ensuring that the number of stimuli within each presentation is kept to three or four and that they are located both above and below the horizontal midline, which is often respected in early glaucomatous loss. Stepping down to "first missed" and "at least two missed" will be more susceptible to this problem than that of stepping down to "all missed".

Repeating a one-reversal technique and taking the average of the two results improves the accuracy of the threshold estimate (a 0.15-0 20 dB reduction in the SD of the differences) but takes longer to perform. The increase in time would not be double that of a single estimate in that it would not be necessary to go back as far for the second estimate. The two-reversal technique has a similar accuracy to a single-staircase double-estimate but takes slightly less time to perform. Clearly, there are many ways in which a two-reversal technique can be defined with multiple-stimulus patterns. In this report we have chosen to use one which starts off above threshold, reduces to "all missed", and then reverses back to "at least two seen". This particular option was chosen because it is relatively robust to the presence of visual field defects, although not quite so robust as a repeat one-reversal technique to "all missed".

For this research, patterns incorporating points 10-15 degrees from fixation were used. This location was chosen to reduce the problems likely to be encountered when the patient's gradient of sensitivity from the central to peripheral field does not match that of the instrument[16]. If the gradient of the instrument is too shallow, or too steep, and points around fixation are used to estimate the threshold, a larger over- or under-estimation of the threshold level will result at the periphery than if the threshold was established with points lying between 10 and 15 degrees of eccentricity. A disadvantage of using this region of the field is that it is more likely to be affected by glaucomatous damage.

What then is the best technique to use? In a routine screening procedure in which the time taken to examine the visual field is an important parameter, the one-reversal stepping down to "all missed" combines reasonable accuracy with a short testing time. It is also easy to administer and easily understood by patients.

In an environment in which time is less of a constraint and accuracy more important, a repeated single staircase to "all missed", the final threshold being the average of the two measures, has a lot to commend it. The accuracy of an age-related technique is low and two-reversal techniques along with single-reversal stepping-up techniques are less robust to the existence of visual field loss.

References

1. Dyster-Aas K, Heijl A, Lundqvist L: Computerized visual field screening in the management of patients with ocular hypertension. Acta Ophthalmol 58:918-928, 1980
2. Greve EL, Verduin WM: Detection of early glaucomatous damage. Part 1: visual field examination. Doc Ophthalmol Proc Ser 14:103, 1976
3. Heijl A: Automatic perimetry in glaucoma visual field screening. Graefe's Arch Clin Exp Ophthalmol 200:21-37, 1976
4. Kosoko O, Sommer A, Auer C: Screening with automated perimetry using a threshold related three-level algorithm. Ophthalmology 93:882-886, 1986
5. Bedwell CH: The Visual Fields. London: Butterworths 1982
6. Gutteridge IF: The working threshold approach to Friedmann visual field analyzer screening. Ophthalmol Physiol Opt 3/1:41-46, 1983
7. Bakto KA, Anctil J, Anderson DR: Detecting glaucomatous damage with the Friedmann analyzer compared with the Goldmann perimeter and evaluation of stereoscopic photographs of the optic disk. Am J Ophthalmol 95:435-447, 1983
8. Henson CFS2000 Central Field Screener: Operating Instructions. Windsor UK: Keeler
9. Henson DB, Dix SM, Oborne AC: Evaluation of the Friedmann visual field analyzer Mark II. Part 1: results from a normal population. Br J Ophthalmol 68:458-462, 1984
10. Henson DB, Anderson RS: Thresholds using single and multiple stimulus presentations. In: Heijl A (ed) Perimetry Update 1988/89, pp 191-196 Amsterdam/Berkeley/Milano: Kugler & Ghedini 1989
11. Henson DB, Bryson H: Clinical results with the Henson-Hamblin CFS2000 Doc Ophthalmol Proc Ser 49:233-238, 1987
12. Guildford JP (ed): Psychometric Methods New Delhi: Tatum and McGraw Hill Publ 1954
13. Jaffe GJ, Alvarado JA, Juster RP: Age related changes in the normal visual field. Arch Ophthalmol 104:1021-1025, 1986
14. Heijl A, Lindgren G, Olsson J: Normal variability of static perimetric threshold values across the central visual field. Arch Ophthalmol 105:1544-1549, 1987
15. Johnson CA, Adams JA, Lewis RA: Evidence for a neural basis of age-related visual field loss in normal observers. Invest Ophthalmol Vis Sci 30:2056-2064, 1989
16. Van den Berg TJTP, Nooteboom PJ, Langerhorst CT, Greve EL: Fluctuation and population differences in automated perimetry and the influence on defect volume estimation. Doc Ophthalmol Proc Ser 49:103-107, 1987

Optimizing dot size and contrast in pattern discrimination perimetry

Bruce Drum and Regina Bissett

Wilmer Eye Institute, Johns Hopkins University School of Medicine, Baltimore, MD 21205, USA

Abstract

In pattern discrimination perimetry, target patches of non-random dots are embedded in a surround field of dynamic random dots. Target visibility is lowered by reducing target coherence, *i e* , by randomizing some of the target dots. A second-generation prototype pattern discrimination perimeter has been developed that provides control of the dot size and contrast of the stimulus display In initial studies with the new instrument, the authors have scaled dot size with eccentricity starting with either 1′ or 3′ foveal dots, to match the spatial resolution capabilities of either the parvocellular (P) or the magnocellular (M) pathways, respectively, and have compared coherence thresholds for spatial (static checkerboard) and temporal (scrolling random dot) stimulus patterns in normal subjects Coherence thresholds for large-dot peripheral test conditions are almost unchanged by contrast reductions down to near-threshold levels, and are nearly flat functions of eccentricity By comparison, thresholds for foveal and, to a lesser extent, small-dot peripheral conditions are more affected by contrast reductions The findings are similar for static checkerboard and scrolling random dot conditions. These results suggest that both spatial and temporal patterns are processed mainly by P pathways in the fovea and M pathways in the periphery

Introduction

For the past several years our laboratory has been developing a new type of visual field test that is based on the detection of patterns of dots within a surrounding field of dynamic random dots[1-7]. The threshold variable is usually the coherence, or degree of non-randomness, of the stimulus dots. Coherence (and visibility) is reduced by randomizing the positions of a known percentage of dots within the stimulus.

Previous studies were carried out with a prototype instrument that was limited to high-contrast stimuli with a fixed pixel size of about 15′ of arc. These studies suggested that pattern discrimination perimetry is a sensitive technique for detecting early optic nerve damage in open-angle glaucoma[4,5], and that different types of patterns might be used to assess different neural pathways[6].

A second-generation instrument has now been developed, with a more powerful computer and a high-performance CRT, making it possible to adjust the dot size and contrast of the stimulus display separately at each eccentricity These new capabilities allow a more rigorous investigation of the basic mechanisms of pattern discrimination and make it possible to more effectively optimize the sensitivity and specificity of clinical pattern discrimination tests, both for early glaucomatous damage and for vision loss arising from other disorders.

Apparatus

The new version of the pattern discrimination perimeter (PDP) consists of a high-performance monochrome CRT display controlled by an IBM-AT-compatible computer (NEC Powermate 1 Plus) and an Imagraph model AGC-1210-10 graphics controller with 1024×1280-pixel resolution, 256 grey levels and a 60 Hz non-interlaced raster (the controller is capable of handling a 24-bit/pixel RGB color display, but we are using only the green gun output). The display is an Ikegami model DM-2010A, with a P4 white phosphor and a 20-inch diagonal screen (actual display dimensions, 10.5"×12.7"). The display pixels are 0.01 inch square, which translates into visual angles (at fixation) of 4 min at a subject distance of 8.6 inches, 3 min at 11.4 inches and 1 min at 34.3 inches. Because the screen is nearly flat, pixel size decreases by

Perimetry Update 1990/91, pp 373-380
Proceedings of the IXth International Perimetric Society Meeting,
Malmö, Sweden, June 17-20, 1990
edited by Richard P. Mills and Anders Heijl

approximately a $\cos^2$ factor with increasing eccentricity.

Screen contrast and luminance were calibrated using a Spectra Spotmeter (model UBA 1/4) with a 15′ diameter detector area and a photometric filter. The photometer was placed at the normal vantage point of the subject and alternately centered in light and dark stimulus dots at either the center of the screen or at an extreme corner. The stimulus dot size was set at 4×4 screen pixels, large enough to include the entire detector area of the photometer. The maximum and minimum screen luminances were 110 and 1.3 cd/m^2 near the center of the screen and half those values for the extreme corners. Maximum contrast, computed as $(L_{max} - L_{min})/(L_{max} + L_{min})$, was thus 98% for dot sizes >15′ at all screen locations. Contrast calibrations for smaller dot sizes were obtained by bringing the photometer within 2.5 cm of the screen and inserting a 20-diopter positive lens in front of the photometer to bring the screen into focus. Contrast was 89% for 3×3-pixel dots, 77% for 2×2-pixel dots and 60% for single-pixel dots.

Stimuli

All stimulus patterns for our initial studies were 20×20-dot patches, 0.5 sec in duration. The light:dark dot ratio for both the test stimulus and the surround field was 1:1, and the space-average luminance for both was 55 cd/m^2. The coherent test stimuli were either static checkerboards (alternating light and dark dots, presented for a single surround frame) or a patch of spatially random dots that scrolled upward as a unit, one dot per surround frame within a fixed window. The static checkerboard stimulus thus contained only spatial information and the scrolling random dot stimulus contained only temporal information. We expected that "P" retinal ganglion cells, which send signals to the parvocellular layers of the lateral geniculate nucleus (LGN) would be preferentially sensitive to the purely spatial pattern and that "M" ganglion cells, which send signals to the magnocellular LGN layers, would be preferentially sensitive to the purely temporal pattern[8,9]. The surround was updated at a frequency of 2 Hz for the static checkerboard patterns and 15 Hz for the scrolling random dot patterns.

As in previous studies[1-7], coherence was defined as the percentage of predictable dots in the stimulus, either within a single stimulus frame for spatial patterns or from one frame to the next for temporal patterns. Operationally, coherence for both temporal and spatial patterns was controlled by reversing the contrast of equal numbers of light and dark stimulus dots at randomly selected positions without replacement. An independent set of dots was selected for contrast reversal in each surround frame, so that the temporal properties of the added noise were identical to those of the surround. The coherence ranged from 100%, with no dots reversed, to 0%, with 50% of the dots reversed.

If the set of stimulus dots to be reversed is selected entirely randomly, a problem with the properties of random numbers arises that can make it possible to detect a pattern whose coherence is nominally zero Because the number of stimulus dots is relatively small, there is a surprisingly high probability that one part of the pattern will have more than half of the dots reversed and another part of the pattern will be relatively spared. If the stimulus is a checkerboard pattern, the part that received too few reversals will still be visible as a noisy checkerboard and the part that received too many reversals will appear as a noisy *reversed* checkerboard. If the stimulus is a scrolling random dot pattern, similar inhomogeneities in the reversed dots can produce partial correlations between successive frames that appear as residual coherent motion. This problem was solved by dividing the stimulus pattern into four quadrants and requiring that the number of reversed dots in each quadrant had to differ by no more than one light/dark dot pair from one-fourth of the total number of reversed dot pairs.

Stimuli were centered on the fovea and on the major diagonal meridians of 45°, 135°, 225° and 315° at eccentricities of 4.2°, 12.5° and 20.3°. Respective dot sizes were 1′, 4′, 11.4′ and 21.1′ of visual angle for the small-dot (P) scale, and 3′, 11.9′, 38.1′ and 56.3′ of visual angle for the large-dot (M) scale (see Fig 1). These scales approximately followed the proportional relationship

$$S=k(1+pE), \qquad (1)$$

where S=stimulus size (min of arc), k=foveal stimulus size (min of arc), p=1/(eccentricity (deg of arc) at which S=2k) and E=eccentricity (deg of arc). For the P scale, p=1 and k=1, and for the M scale, p=1 and k=3. The dot sizes for eccentric positions were produced by a 4-bit

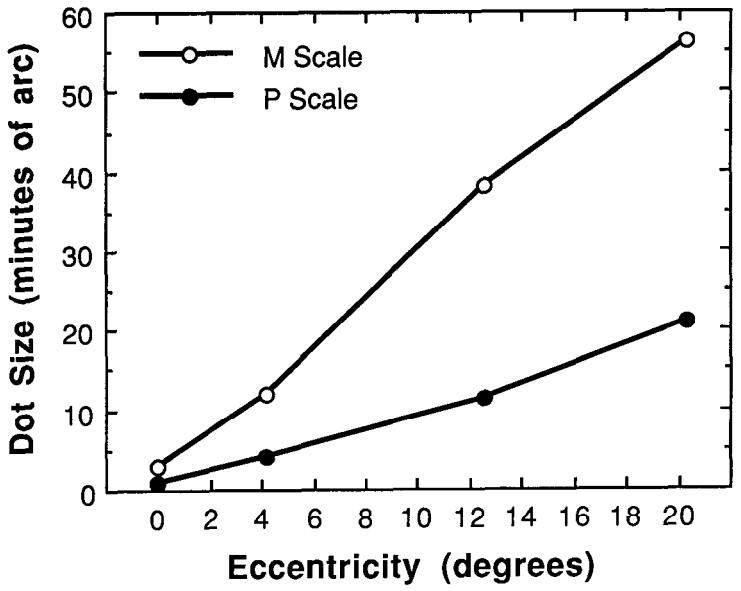

Fig 1 Dot size *versus* eccentricity for stimulus patterns matched to the estimated spatial scales of P (open circles) and M (filled circles) system receptive fields

(16-level) hardware zoom feature of the graphics controller board, and were thus limited to multiples of 4′ of visual angle except for the $\cos^2$ eccentricity corrections In order to achieve the smaller dot sizes for the foveal conditions, subjects were moved from the regular distance of 8.6" out to 11.4" for 3′ dots and to 34.3" for 1′ dots.

These scales increase more steeply with eccentricity than those proposed by Drasdo[10], Virsu and Rovamo[11] and others for resolution and detection tasks that are thought to be determined by retinal scaling factors. Much steeper scaling functions have been found for various hyperacuity tasks[12,13], but have usually been attributed to additional cortical processing of foveal stimuli. However, more recent anatomical[14,15] and psychophysical[16,17] studies suggest that previous work may have underestimated the foveal ganglion cell density, and that even very steep scaling functions may reflect primarily retinal scaling factors

All stimuli were presented both at the maximum contrast and at a low contrast that was expected, based on pilot observations, to be just sufficient for the dots to be consistently visible at all eccentricities tested. The low contrast levels selected for the four main stimulus conditions were: small-dot checkerboards, 20%; large-dot checkerboards, 10%; small-dot scrolling random dots, 10%; large-dot scrolling random dots, 5% The rationale for comparing high and low contrast conditions was that low contrasts should emphasize the M response and the high contrasts should emphasize the P response[18,19].

The fixation target for foveal stimuli consisted of horizontal and vertical crosshairs with a central gap, and for eccentric stimuli it consisted of a black central square. The fixation target for foveal stimuli was scaled with dot size. The fixation target for eccentric stimuli was kept at the same size (a 1.5° square) for small dot sizes, but was always at least 5×5 dots for dot sizes above 16′. The 5×5-dot minimum was implemented because smaller fixation targets could not be easily seen in the midst of the high-contrast random-dot surround.

Experimental procedures

Four subjects with normal vision, two males and two females ranging in age from 35 to 51 years, participated in the main experiment. Coherence thresholds were measured one eccentricity at a time, with a single staircase procedure for the single foveal target and with four simultaneous randomly interleaved staircases for the four targets at each of the three ex-

trafoveal eccentricities. Approximately 0.5 sec before each trial, a beep alerted the subject to the upcoming stimulus presentation. The subject's task was simply to press a response button when he or she detected the stimulus. Failure to press the button within the approximately 2.5 sec before the warning beep for the next trial was taken as a negative response.

The staircase started at 100% coherence, decreased by 20%/trial until the first reversal, increased 10%/trial until the second reversal, decreased 5%/trial until the third reversal and increased 2%/trial until the fourth reversal, which was taken as the threshold. Occasional blanks were interspersed with the stimulus trials to estimate the frequency of false positive responses. When threshold was reached at one of the four positions in a set of extrafoveal measurements, threshold-level stimuli were presented in subsequent trials at that position until all remaining staircases were completed. The purpose of this procedure was to prevent the development of fixation biases toward the remaining test positions

Results

Fig 2 shows coherence threshold *versus* eccentricity results for single sessions averaged over four normal observers and four meridians per observer. Each of the four stimulus conditions were tested at (nominally) 100% contrast and at a near-threshold contrast as described above. Fig. 3A shows the combined large-dot data compared to the combined small-dot data, and Fig. 3B shows a comparison of the combined static checkerboard data to the combined scrolling random dot data

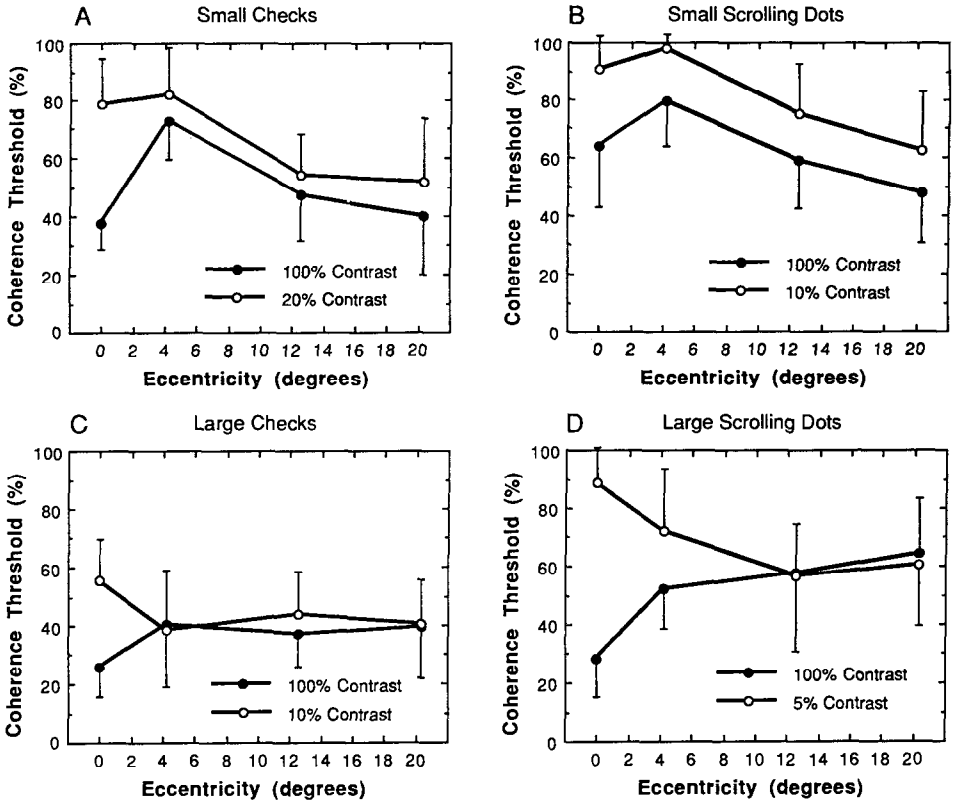

Fig 2 Coherence threshold *versus* eccentricity functions for (A) small-dot and (C) large-dot static checkerboards and for (B) small-dot and (D) large-dot scrolling random dot stimuli. Each data point is the average threshold for four normal subjects, each of which is in turn an average over four diagonal meridians. Data for high-contrast conditions are plotted with filled circles and data for low-contrast conditions are plotted with open circles. Error bars indicate standard deviations. The error bars are shown only in one direction for clarity.

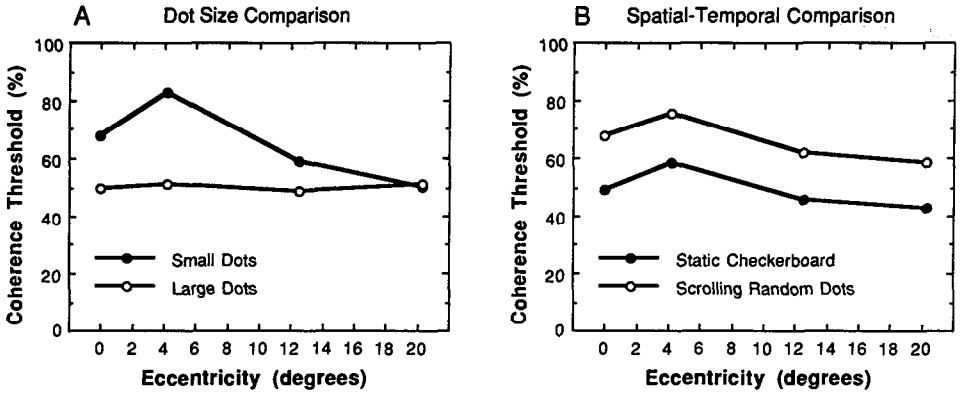

Fig. 3. Comparison of overall averages of coherence threshold *versus* eccentricity functions for the large-dot and small-dot conditions (A) and the scrolling and checkerboard conditions (B) in Fig 2

Reductions in contrast elevated foveal coherence thresholds more than peripheral thresholds for all four stimulus conditions; for the large-dot conditions, the fovea went from being the most sensitive position at high contrast to the least sensitive position at low contrast. Contrast reductions also elevated peripheral coherence thresholds somewhat for small-dot conditions (Figs. 2A and B), but left peripheral thresholds for large-dot conditions (Figs. 2C and D) virtually unchanged. In fact, all four subjects found the threshold task for large-dot peripheral conditions to be subjectively easier at low contrast than at high contrast, and three subjects actually performed better at low contrast.

Dot size strongly influenced the shape of the coherence threshold eccentricity functions, as can be seen in Fig. 3A. The overall average thresholds for the large-dot conditions were nearly constant with increasing eccentricity. Coherence thresholds for small-dot conditions, on the other hand, were consistently higher in the parafovea than in either the fovea or the periphery. Considered in terms of coherence threshold *versus* relative dot size, a threefold reduction in dot size raised the average foveal threshold nearly 20% and the parafoveal threshold over 30%, but had little or no effect on peripheral thresholds.

The average effect of spatio-temporal stimulus properties on coherence threshold is shown in Fig. 3B. Eccentricity functions for the checkerboards and scrolling patterns were the same shape, but thresholds for scrolling stimuli averaged 15-20% higher at all eccentricities. This difference cannot be explained by the use of slightly lower contrasts for the scrolling conditions than for the checkerboard low-contrast conditions, because the average threshold difference between only the high-contrast scrolling and checkerboard conditions is nearly as large as the overall difference.

Discussion

Our *a priori* hypotheses about the data in Figs. 2 and 3 were that spatial patterns with high contrast and small dots would emphasize P function, and that temporal patterns with low contrast large dots would emphasize M function. We also expected that scaling dot size with eccentricity would produce eccentricity functions that were at least approximately flat. The results bear out some of these preliminary hypotheses but not others, and, as discussed below, they suggest some revisions in the prevailing model of M and P function.

One surprising finding was the large difference in the effects of contrast changes on central and peripheral coherence thresholds, even with stimuli that were matched to the spatial scales of the underlying receptive fields. High-contrast thresholds are usually lower at the fovea than at any other position. On the other hand, low-contrast thresholds tend to be higher at the fovea than the periphery, largely because foveal thresholds are elevated by contrast reduction and peripheral thresholds are not. The fovea thus appears to be much more sensitive than the periphery to high contrast conditions and to changes of stimulus contrast. Assuming from the findings of Kaplan and Shapley[18,19] that such sensitivity to contrast change at high contrast

levels can be attributed to P function, these results suggest that the fovea is highly specialized for P system activity and the periphery is specialized for M system activity. However, the specialization does not appear to be complete, since reducing dot size to below the M resolution limit produces some threshold change with contrast at all eccentricities (Figs. 2A and B).

Several recent papers[20-22] have shown that motion sensitivity saturates at low contrast levels in the periphery, and that high contrast may even impair motion sensitivity under certain conditions. These results agree with our own finding that low contrast is as good or better than high contrast for large-dot peripheral coherence thresholds for both static checkerboards and scrolling random dots (see Figs. 2C and D), and they reinforce the idea that both types of thresholds reflect primarily M system activity.

Foveal and peripheral thresholds are differentially affected by changes in dot size as well as by changes in contrast. As Fig. 3A shows, the average large-dot eccentricity function is flat, whereas the small-dot function is non-monotonic with its maximum in the parafovea. Foveal and parafoveal thresholds are higher for small-dot conditions than for large-dot conditions, but peripheral thresholds are not. The reasons for this discrepancy are not entirely clear. The small-dot foveal thresholds are probably elevated because the effective contrast of the 1′ dots is reduced by limitations of spatial resolution in both the screen and the optics of the eye. However, a control experiment comparing coherence thresholds for 1′-dot foveal stimuli at different screen distances showed that limited screen resolution raised thresholds by only about 5%. The thresholds for 4′, single-pixel-per-dot parafoveal stimuli may also be elevated by inadequate screen resolution, but not by optical limitations in the eye. These factors therefore cannot account for the finding that the small-dot parafoveal thresholds are elevated even more than the foveal thresholds.

One possible reason for the relative elevation of small-dot parafoveal thresholds is that, because of equipment limitations, the parafoveal pixels were 23% smaller (4.0′ instead of 5.2′) than the optimal size estimated from eq 1. If eq 1 is correct, the parafoveal pixels thus might have been too small for P receptive fields to resolve. Since large- and small-dot sizes were underestimated equally, however, this explanation would imply that the M and P systems differ qualitatively in their size *vs* eccentricity scaling functions. Another possibility is that M cells can resolve the small dots in the periphery, but not in the fovea or parafovea. However, this seems inconsistent with the contrast findings showing that small-dot peripheral and parafoveal thresholds are equally affected by contrast reduction, which suggests similar levels of P cell activity at both eccentricities. A third alternative is simply that the small-dot function in Fig. 3A is characteristic of the P system, *i e* , the P system is relatively insensitive to parafoveal patterns.

While our data suggest that M and P relative sensitivities vary markedly with changes of eccentricity and dot size, the same does not appear to be true of the spatial and temporal characteristics of the stimulus. Coherence thresholds for static checkerboards and scrolling random dots are both strongly affected by foveal contrast changes and are indifferent to peripheral contrast changes, suggesting that both types of stimuli are processed mainly by the P system in the fovea and the M system in the periphery. Also the eccentricity functions of both stimulus types change in the same way with changes in dot size. When these factors are averaged (Fig. 3B), leaving an overall comparison of spatial and temporal stimulus patterns, the resulting eccentricity functions are identical except that scrolling thresholds are about 20% higher.

Our data do not necessarily imply that spatial and temporal factors are not important in distinguishing the functional roles of M and P systems, but they do suggest that, at least under our conditions, they are secondary in importance to contrast and retinal location. Once again assuming that only the P system operates best at high contrasts and the M system response saturates at low contrasts, the P system appears to be more sensitive than the M system to high-contrast foveal motion, and the M system appears to be more sensitive than the P system to peripheral static checkerboards. Previous conclusions that motion processing is handled almost entirely by the M system and the processing of spatial detail is handled predominately by the P system[23,24] may therefore need to be reevaluated.

Two features of the large-dot data have the potential for significantly improving the diagnostic capabilities of clinical pattern discrimination tests. First, the finding that reductions of contrast have little or no effect on the coherence threshold as long as the dots in the stimulus pattern remain visible suggests that a low-contrast test may be very sensitive to disorders, such as early glaucoma, that are characterized by reduced contrast sensitivity. Setting the contrast just high enough to leave the normal coherence threshold unaffected may raise the coherence

threshold substantially for a patient with only slightly reduced contrast sensitivity. Second, the flatness of the average large-dot eccentricity function in Fig. 3A suggests that it should be possible to optimize contrast in a clinical test so that the normal coherence threshold level, dynamic testing range and variability are all constant over the entire central field. This arrangement would simplify the clinical interpretation of the test by making significant deviations from the normal threshold immediately obvious and by eliminating selective ceiling effects caused by differences in the available response range.

Acknowledgements

Supported by NEI grant No EY07327. We thank Naiming Shen, Mark Powers and Matthew Severns for assistance with software development, and Robert Massof and Gislin Dagnelie for helpful comments on the manuscript. The pattern discrimination perimeter is protected by U S Patent No 4634243

References

1. Drum B, Breton M, Massof R, Quigley H, Krupin T, Leight J, Mangat-Rai I, O'Leary D: Pattern discrimination perimetry: a new concept in visual field testing. Doc Ophthalmol Proc Ser 49:433-440, 1987
2. Drum B, Breton M, Massof R, O'Leary D, Severns M: Early glaucoma detection with pattern discrimination perimetry Noninvasive Assessment of the Visual System, 1987 Technical Digest Series (Optical Society of America, Washington, DC) 4:130-133, 1987
3. Drum B, Severns M, O'Leary D, Massof R, Breton M, Quigley H, Krupin T: Pattern discrimination perimetry and conventional perimetry in early glaucoma detection. Noninvasive Assessment of the Visual System, 1988 Technical Digest Series (Optical Society of America, Washington, DC) 3:172-175, 1988
4 Drum B, Severns M, O'Leary D, Massof R, Quigley H, Breton M, Krupin T: Selective loss of pattern discrimination in early glaucoma. Appl Opt 28:1135-1144, 1989
5. Drum B, Severns M, O'Leary D, Massof R, Quigley H, Breton M, Krupin T: Pattern discrimination and light detection test different types of glaucomatous damage In: Heijl A (ed) Perimetry Update 1988/89, pp 341-347 Amsterdam/Berkeley/Milano: Kugler & Ghedini Publ 1989
6. Drum B, Quigley H, Roros J: Spatial and temporal pattern discrimination in early glaucoma. Invest Ophthalmol Vis Sci (Suppl) 30:55, 1989
7. Drum B, Quigley H, Roros J: Practice selectively improves pattern discrimination in glaucoma Noninvasive Assessment of the Visual System, 1990 Technical Digest Series (Optical Society of America, Washington, DC) 3:182-185, 1990
8 Lennie P, Trevarthen C, Wassle H, Van Essen D: Parallel processing of visual information In: Spillmann L, Werner J (eds) Visual Perception: The Neurophysiological Foundations. New York: Academic Press 1989
9 Shapley R: Visual sensitivity and parallel retinocortical channels Ann Rev Psychol 41:635- 658, 1990
10. Drasdo N: The neural representation of visual space Nature 266:554-556, 1977
11 Virsu V, Rovamo J: Visual resolution, contrast sensitivity and the cortical magnification factor Exp Brain Res 37:475-494, 1979
12. Levi DM, Klein SA, Aitsebaomo AP: Vernier acuity, crowding and cortical magnification Vision Res 25:963-977, 1985
13. Yap YL, Levi DM, Klein SA: Peripheral hyperacuity: three-dot bisection scales to a single factor from 0 to 10 degrees. J Opt Soc Am A4:1554-1561, 1987
14 Schein SJ, Klug KJ: There is one midget bipolar terminal in the b-layer of the IPL for each cone pedicle in the OPL of Macaque retina Invest Ophthalmol Vis Sci (Suppl) 31:37, 1990
15. Wässle H, Grünert U, Röhrenbeck J, Boycott B: Cortical magnification factor and the ganglion cell density of the primate retina. Invest Ophthalmol Vis Sci (Suppl) 31:396, 1990
16. Thomas JP: Effect of eccentricity on the relationship between detection and identification J Opt Soc Am A4:1599-1605, 1987
17. Farrel JE, Desmarais M: Equating character-identification performance across the visual field J Opt Soc Am A7:152-159, 1990
18 Kaplan E, Shapley R: X and Y cells in the lateral geniculate nucleus of macaque monkeys. J Physiol (Lond) 330:125-143, 1982
19. Kaplan E, Shapley R: The primate retina contains two types of ganglion cells with high and low contrast sensitivity Proc Natl Acad Sci USA 83:2755-2757, 1986
20 Van de Grind WA, Koenderink JJ, van Doorn AJ: Influence of contrast on foveal and peripheral detection of coherent motion in moving random-dot patterns J Opt Soc Am A4:1643-1652, 1987

21. Derrington AM, Goddard P: Failure of visual motion detection at high contrast: evidence for saturation. Vision Res 29:1767-1776, 1989
22. Boulton JC, Hess RF: Luminance contrast and motion detection. Vision Res 30:175-179, 1990
23. Livingstone MS, Hubel DH: Psychophysical evidence for separate channels for the perception of form, color, motion, and depth. J Neurosci 4:309-356, 1987
24 Livingstone MS, Hubel DH: Segregation of form, color, movement, and depth: anatomy, physiology, and perception. Science 240:740-749, 1988

Effect of target size, temporal frequency and luminance on temporal modulation visual fields

Jocelyn Faubert

Department of Psychology (H-663), Concordia University, 1455 de Maisonneuve O., Montreal, Quebec H3G 1M8, Canada

Abstract

The effects of five target sizes (0.125, 0.25, 0.50, 1 0, and 2 0 degrees) and four temporal rates (1, 5, 10, and 15 Hz) on temporal modulation fields (TMF) were assessed in ten observers at 3.4 cd/m^2 and five observers at 10 cd/m^2. A decrease of sensitivity was found as eccentricity increased for a 40 deg visual field. This decline in sensitivity was greater for small target sizes and higher temporal rates Increasing the luminance causes peripheral facilitation at lower temporal rates and a sensitivity improvement throughout the visual field at higher temporal rates. Small targets and high temporal rates benefit the most from a luminance increase The relevance of the data to the clinical assessment of TMFs is discussed.

Introduction

The analysis of temporal sensitivity for uniform targets throughout the central visual field in glaucoma has increased in recent years with encouraging results[1-5]. The use of temporal modulation can be particularly useful in visual diagnostics because it allows the measurement of temporal sensitivity for a potentially large number of frequencies[6]. It has been suggested that glaucoma may produce greater deficits at particular temporal frequencies[7,8]. An extension of this approach is the analysis of temporal modulation fields (TMF) which essentially evaluates the temporal modulation sensitivity throughout the visual field. The present study analyzes the effect of several parameters on the sensitivity profile of normal observers with an emphasis on target sizes similar to those used in the clinical assessment of visual fields (Goldmann sizes I to V). The parameters of interest are: (1) different eccentricities within a 40 degree visual field, (2) target size, (3) temporal frequency, and (4) luminance levels (photopic and low-photopic/mesopic levels).

Methods

Subjects

Ten eyes of ten normal observers were used for one of two luminance conditions (3.4 cd/m^2). The average age was 28.4 (SD = 4.33) with a range of 23 to 37 years. Five of these observers also participated in a second luminance condition (10 cd/m^2). All ten were experienced psychophysical observers and had undergone similar visual field testing procedures.

Apparatus

The display consisted of a 40×30 cm RGB monitor (Gigatek - 1931 cc) equipped with a medium persistence P22 phosphor. The monitor was modified to allow, under software control over the timing of the vertical sinc pulse, a 120 Hz non-interlaced full-screen refresh rate (255 lines with 560 pixels per line) and a 240 Hz half-screen refresh rate. At 5 Hz temporal frequency,

Address for correspondence Université de Montréal, École d'Optométrie, 3750 Jean Brillant C.P. 6128, Succursale A, Montréal, Québec H3C 3J7, Canada

Perimetry Update 1990/91, pp 381-390
Proceedings of the IXth International Perimetric Society Meeting,
Malmö, Sweden, June 17-20, 1990
edited by Richard P. Mills and Anders Heijl

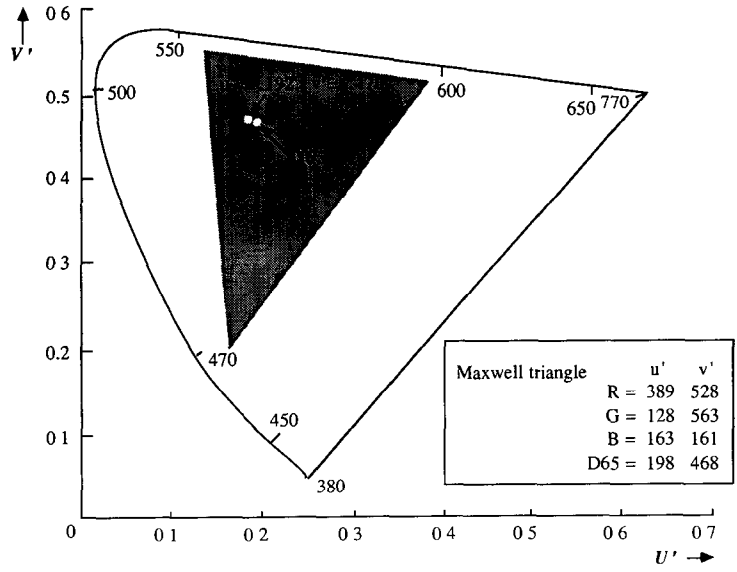

Fig 1 CIE 1976 u'v' chromaticity diagram The Maxwell triangle specifies the chromaticities available on the video monitor The dimensions of the Maxwell triangle in u'v' units are given in the highlighted box. The two white dots in the triangle represent the whites used for this study

this allows a sampling of 24 points on a sinusoidal function for the entire screen and 48 points for a half-screen.

No linearity or independence of the guns was assumed. A large range of DAC values was examined by measuring their chromaticity in CIE 1976 u',v'units (see Fig. 1) and their luminance output using a chroma meter (Minolta CL-100) The luminance was derived by comparing the illuminance output of the chroma meter and comparing it with a value obtained from a photometer reading (Spectra Spotmeter UBD-1/2). The range of DAC values was split into 10 steps (11 samples) for each gun and the 1331 combinations were evaluated. Two hundred and five combinations were eliminated because the luminance values fell into a range where the chroma meter becomes unreliable. With the measurements obtained from the remaining 1126 combinations a function for each gun was established which is used to extrapolate throughout the whole possible chromaticity range of the monitor represented by the Maxwell triangle obtained from actual measurements of the individual gun outputs. The Maxwell triangle for the monitor is shown as the grey area in Fig. 1 with the measurements listed.

Two mean luminance levels (3.4 cd/m^2 and 10 cd/m^2) were used in the following experiments. For the lower luminance level, a D65 white was used which represents the coordinates: u' = 0.198; v' = 0.468. For the second luminance level a slightly different white with the coordinates: u' = 0.192; v' = 0.470 was used. The reason is that it was impossible to obtain 100% modulation depth for 10 cd/m^2 at D65 because of the fine chromaticity sampling of the monitor (maximum luminance was 18 cd/m^2). With a slight change in u',v' values a 21 cd/m^2 maximum luminance was measured allowing us 100% modulation at 10 cd/m^2 mean luminance. Both whites relative to the CIE chromaticity diagram are shown as two adjacent white dots in Fig. 1.

The monitor was interfaced with graphics boards (Matrox - PG641) under the control of a 80386 IBM AT compatible computer. Luminance during testing sessions was measured using a Spectra Spotmeter (UBD-1/2). A chin rest was used to immobilize the head and a joy stick was used for the subject response.

Procedure

For each luminance level five target sizes (0.125, 0.25, 0.50, 1.00, 2.00 degrees of visual angle which are similar to Goldmann sizes I to V) and four temporal rates (1, 5, 10, and 15 Hz) were evaluated throughout a 40 degree visual field. The display used is shown in Fig. 2. For every target-size/temporal-rate combination eight points for each of five different eccentricities

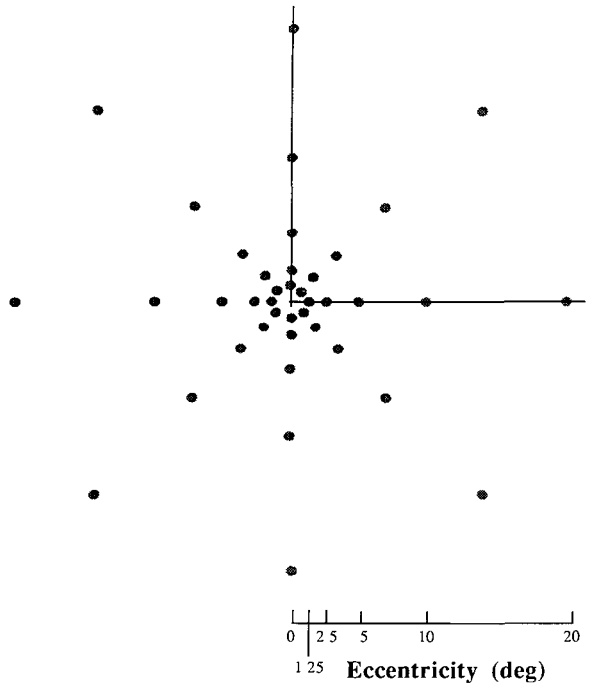

Fig 2 Display of the 40 points that were assessed. The bottom scale shows the five eccentricities used in degrees of visual angle The dark lines demonstrate that only one quadrant was presented at a time

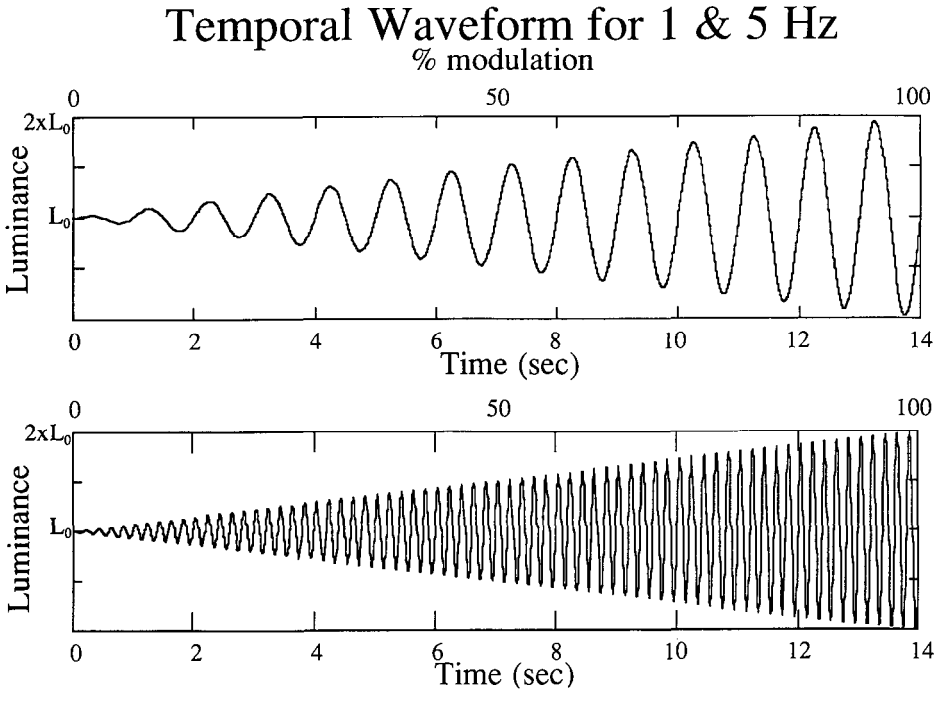

Fig. 3. Graphical representations of the luminance profile produced by the formula discussed in the text for a 1 Hz (top) and 5 Hz (bottom) temporal rate. L_o = mean luminance. The top X-axis represents modulation depth and the bottom X-axis is time in seconds.

(1.25, 2.5, 5.0, 10.0, 20.0 degrees) were assessed for a total of 40 points in the visual field. The background screen was always kept at mean luminance. This maintains the surround at adapted levels to ensure accurate sampling of the target region.

The dependent measure was depth of modulation. To produce the stimulus, a slow temporal ramp was used which can be operationally defined as:

$$L(t) = [w(t) \times s(t) + 1] \times L_o$$

where: $s(t) = sin\ (2 \times pi \times f_t \times t)$

and: $w(t) = t/14$

where L_o is the mean luminance, s(t) the sinusoidal component, w(t) the weighted function and f_t is the temporal frequency used. Graphical representations using these functions are shown in Fig. 3 for the 1 Hz and 5 Hz temporal conditions. Using such a slow onset avoids introducing abrupt temporal components in the stimulus which may interfere or interact with the temporal properties under observation. A variable onset time which randomly varied between 0.5 to 3 seconds was used. That is, prior to a given trial, an auditory signal was given and the temporal ramp would start between 0.5 to 3.0 seconds after the tone as randomly determined by the program.

In a given session, the visual field was separated into quadrants. A quadrant was randomly selected and the observer was presented with a small red fixation point in one of the four corners of the screen. Within this quadrant, any one of the potential test points was randomly chosen and a particular target-size/temporal-rate combination for that point was randomly chosen (out of a possible 20 for each point) Then the trial was initiated. Once all the test points for this particular quadrant were evaluated another quadrant was selected.

The observers were tested for two quadrants per testing session with a total of two sessions for the five observers who did only one luminance condition and four testing sessions for the other five. At the 3.4 cd/m^2 mean luminance level, the observers were adapted for 20 minutes to the mean luminance prior to the testing session. All testing was done monocularly and a 67 cm viewing distance was used.

Other features

The software developed for this particular setup is very flexible. Any target size permitted by the screen dimensions can be produced. Other psychophysical procedures such as a forced-choice staircase or other types of staircases are available. For clinical use, eye monitoring techniques where fixation is systematically assessed during testing by presenting targets in the blind spot area can be used. Special replication criteria for points which deviate from established or estimated means are available. Other features are the production of two- and three-dimensional polar maps of individual or group data. It is also possible to filter edges using gaussian functions and to use background luminances and chromaticities of choice. Different temporal waveforms are available and it is possible to produce Gabor gratings for achromatic and chromatic stimuli.

Results

Figs. 4a to 4e show the log modulation sensitivity values by retinal eccentricity for five target sizes under the 3.4 cd/m^2 luminance condition. The Y-axis represents the modulation sensitivity, so higher values mean better sensitivity. The bars shown on all the graphs are standard error bars. Each function represents a different temporal rate. For every target size a decrease of temporal sensitivity with increasing eccentricity was found which confirms previous results using single target sizes[8,9]. Increasing the size of the target reduces this peripheral drop-off and this is true for all temporal frequencies. The 5 Hz condition produces the best sensitivity levels and 15 Hz the worst sensitivity levels for all target sizes. These relationships only change in respect to the 1 and 10 Hz conditions. For the smaller targets (Figs. 4a and 4b) the 1 Hz and 10 Hz sensitivity functions are similar. With increasing target size (Figs. 4c to 4e) this relationship changes where the 1 and 10 Hz functions separate. Ultimately the 10 and 5 Hz temporal rates are alike and the 15 and 1 Hz conditions have similar sensitivity profiles (see Fig. 4e). The only deviance from this general description is the 1 Hz function which never quite drops

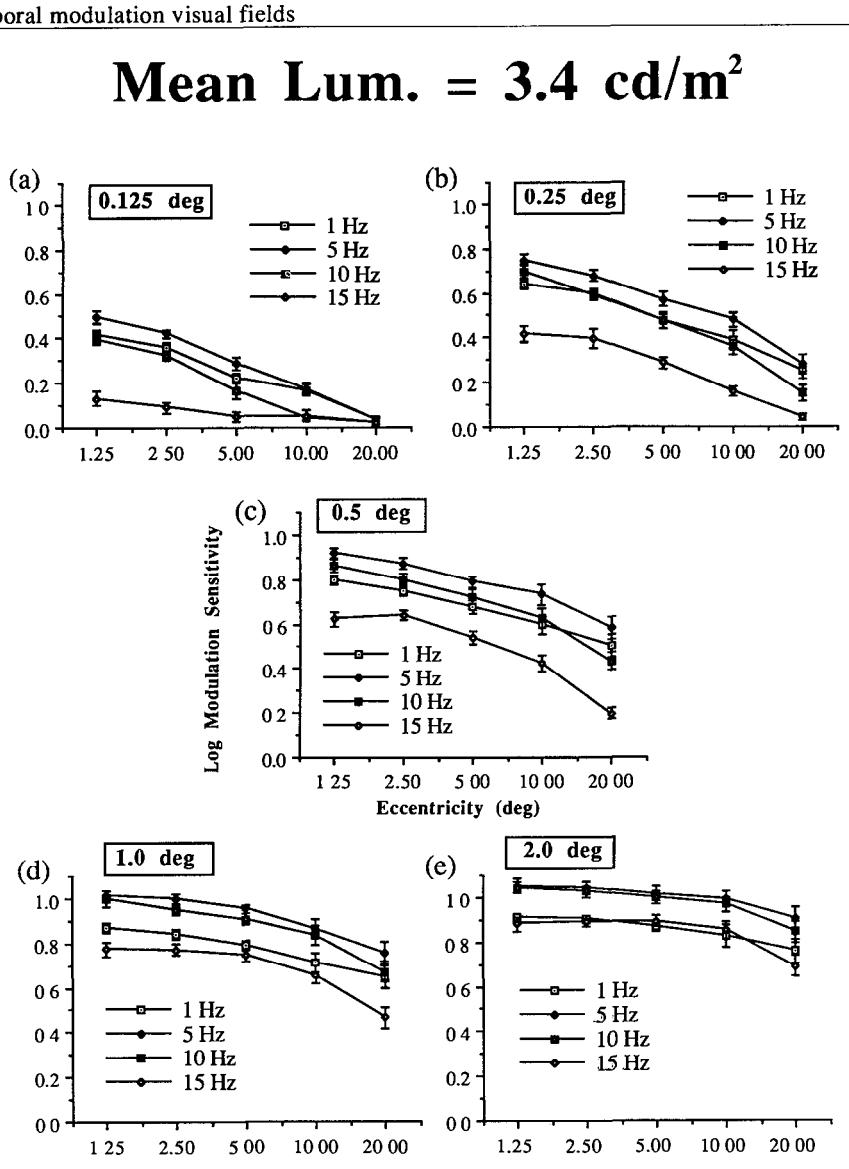

Fig 4 Graphs for the five target sizes and four temporal rates obtained for the 3.4 cd/m² condition. The Y-axis represents log modulation sensitivity and the X-axis represents retinal eccentricity

off in sensitivity from 10 to 20 degrees eccentricity as do the functions obtained for the other temporal rates. This is true for all but the smallest target size (0.125 deg). This effect is not evident for the smallest target because of a ceiling effect at 20 degrees eccentricity.

Figs. 5a to 5c show the log sensitivity values by retinal eccentricity for the different target sizes under the 10 cd/m² condition. A similar drop-off by eccentricity as for the previous luminance is observed. The 5 Hz temporal condition still produces the best sensitivity except for the largest target (Fig. 5e) where the 5 and 10 Hz conditions show identical functions. The 15 Hz condition, however, does not produce the lowest sensitivity for all target sizes as shown for the previous luminance level. For the 2.00 deg target size (Fig. 5e) the sensitivity profile is actually higher than that for 1 Hz. Again the 1 Hz function does not drop as fast as the other temporal rates especially at the two largest target sizes where the 1 Hz function is literally flat (Figs. 5d and 5e).

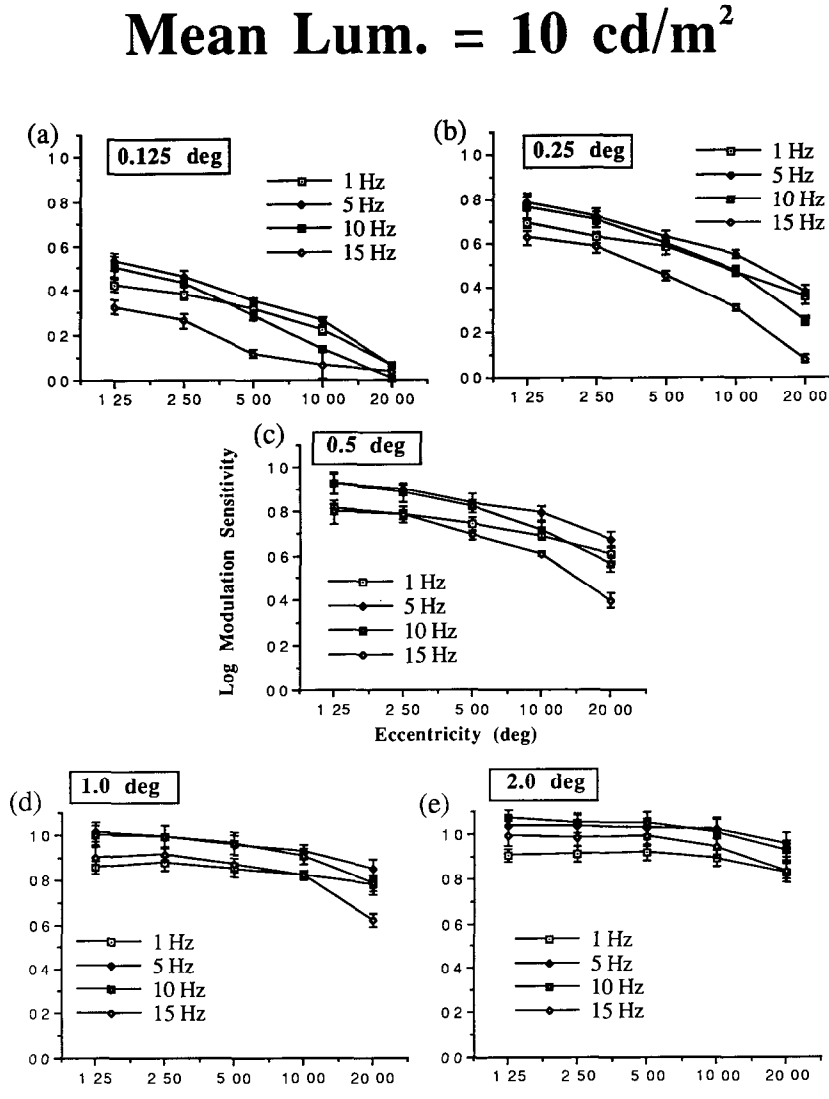

Fig 5 Graphs for the five target sizes and four temporal rates obtained for the 10 cd/m² condition. The Y-axis represents log modulation sensitivity and the X-axis represents retinal eccentricity.

Perhaps the best way to determine the beneficial or detrimental effects of luminance changes is to compare the sensitivity profiles obtained under the different luminance levels directly, which is what has been done in Figs. 6 to 10. In each of these figures, the graphs a, b, c, and d correspond to the 1, 5, 10 and 15 Hz conditions. The higher luminance level is represented by the closed symbols and the lower luminance by the open ones. In Fig. 6, which represents the data for the 0.125 degree target, a luminance increase from 3.4 cd/m² to 10 cd/m² mean luminance produces benefits at eccentricities of five degrees onward for the two slower temporal rates (not evident at 20 deg because of a ceiling effect). An increase in sensitivity is apparent for all eccentricities at the higher temporal rates (10 and 15 Hz) until a ceiling effect at 10 and 20 degrees eccentricity is reached. The same pattern is evident in Fig. 7 (size 0.25 deg) where graphs (a) and (b) show improvements from five degrees on and graphs (c) and (d) throughout the visual field except for 20 degree eccentricity at 15 Hz where a ceiling effect is again observed. A similar pattern is observed in Figs. 8, 9 and 10, except that the effect of

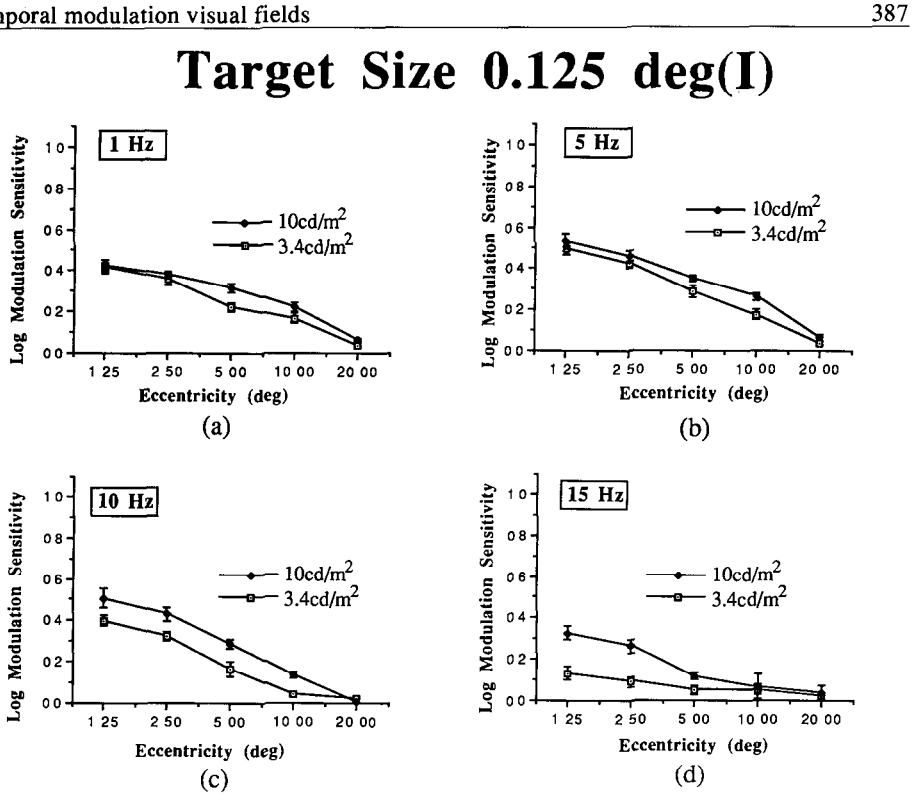
Target Size 0.125 deg(I)
1 Hz
5 Hz
10 Hz
15 Hz
10cd/m2
3.4cd/m2
Log Modulation Sensitivity
Eccentricity (deg)
1 25
2 50
5 00
10 00
20 00
(a)
(b)
(c)
(d)

Fig 6

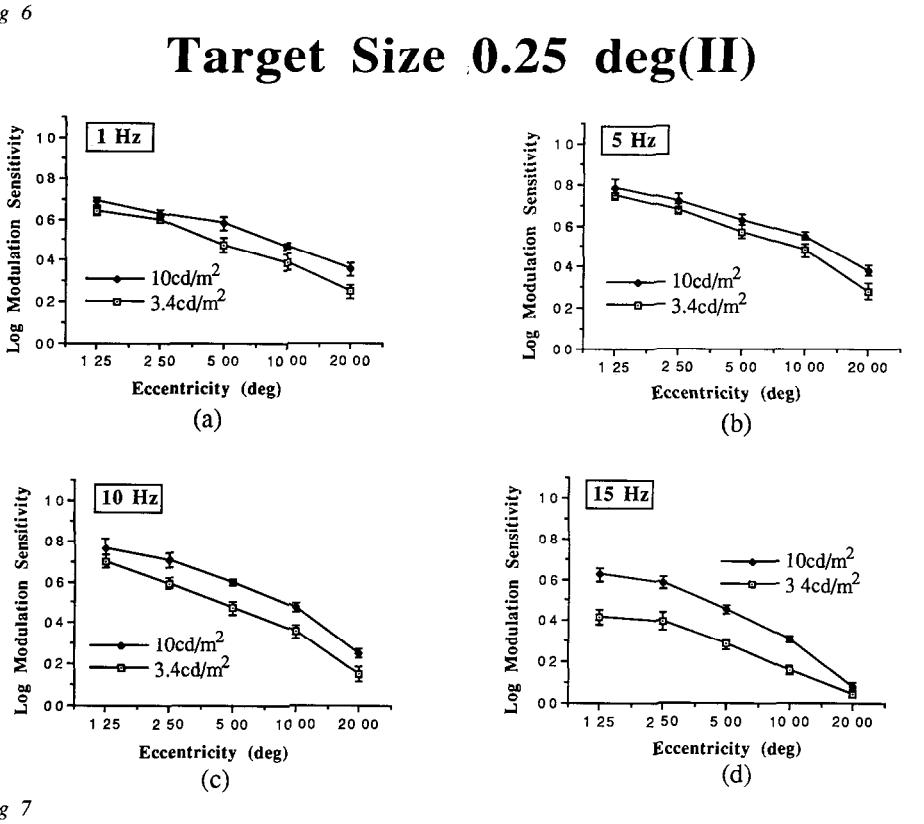
Target Size 0.25 deg(II)
1 Hz
5 Hz
10 Hz
15 Hz
10cd/m2
3.4cd/m2
3 4cd/m2
Log Modulation Sensitivity
Eccentricity (deg)
1 25
2 50
5 00
10 00
20 00
(a)
(b)
(c)
(d)

Fig 7

Target Size 0.5 deg(III)

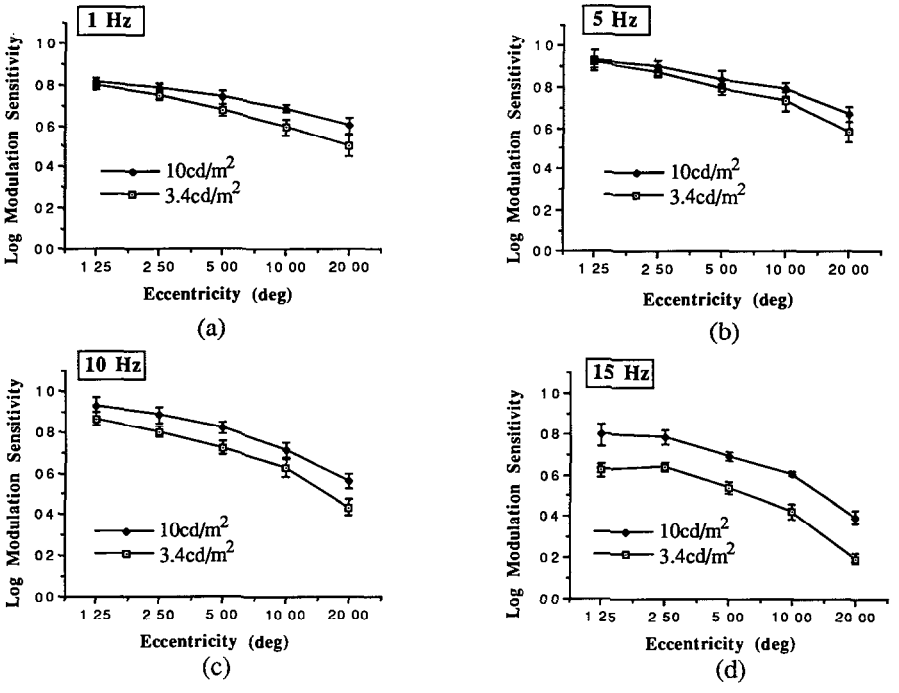

Fig 8

Target Size 1.0 deg(IV)

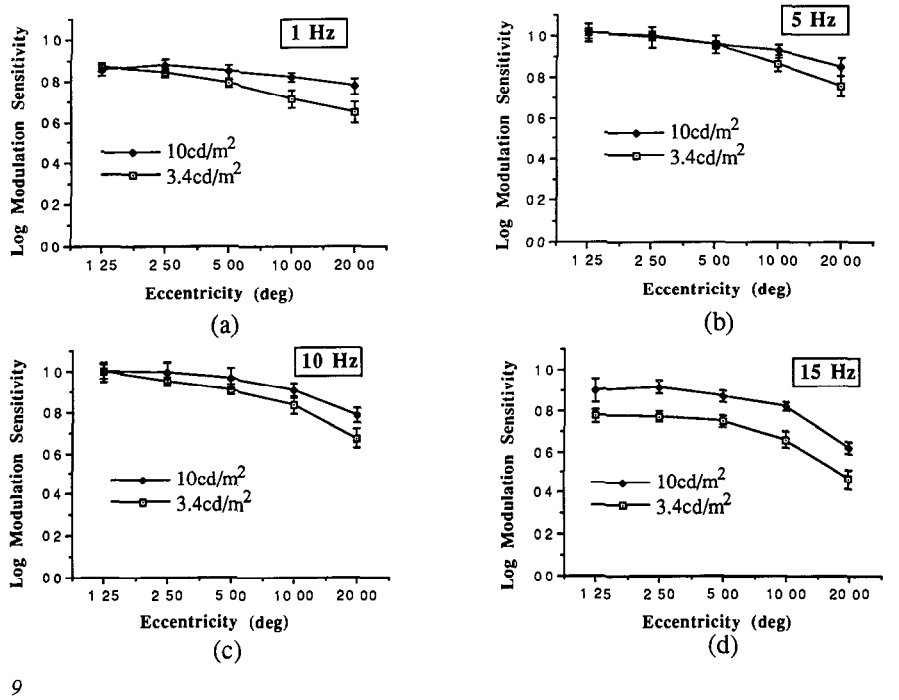

Fig 9

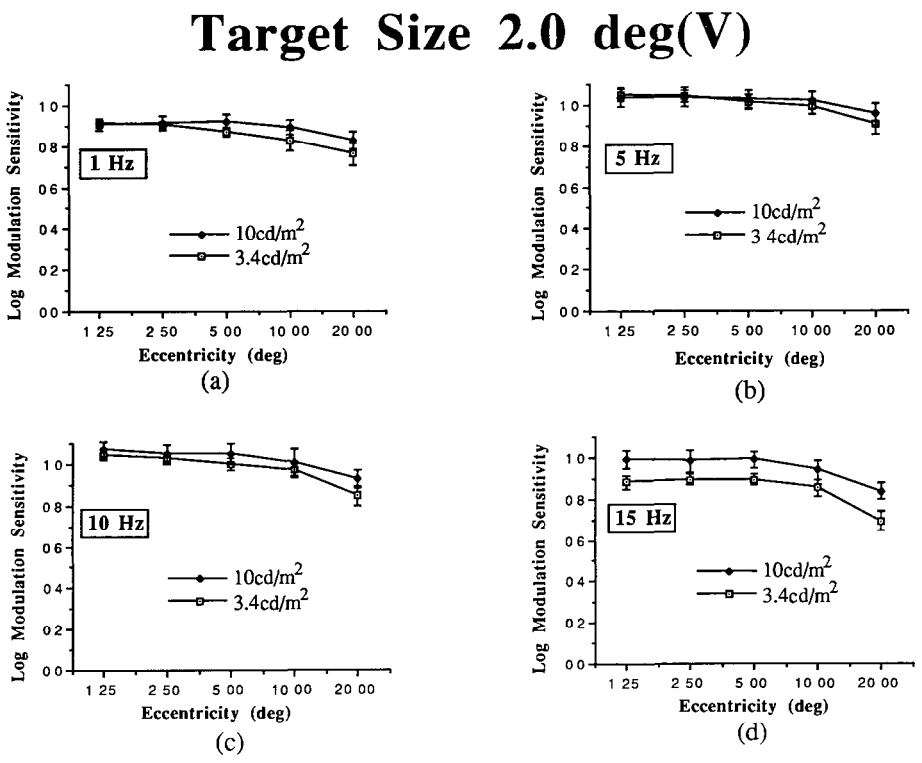

Fig 10

Figs. 6 to 10. Sensitivity profiles obtained from both luminance conditions for all parameters. Target sizes 0.125 to 2 0 deg correspond to Figs 6 to 10, respectively Please see text

higher luminance diminishes with increasing target size to the point were it is almost nonexistent at the 2.00 degree target (Fig. 10). Only the 15 Hz condition seems to have benefitted from the luminance increase at this target size.

Conclusions and discussion

A 5 Hz temporal rate generally produces the best sensitivity values and this is true for both luminance conditions. Further, there is less of a drop-off of sensitivity as the target sizes increase for all temporal-rate/luminance combinations.

Mean luminance seems to interact with target size and temporal frequency. Firstly, the larger the target the less facilitation is obtained from increased luminance. Secondly, the higher the temporal rate the more the sensitivity is raised by a luminance increase. This second facilitation tends to spread from the peripheral areas towards the central points until all eccentricities measured show some facilitation at the higher temporal frequencies. This implies that the peripheral retina is more sensitive to luminance changes at low temporal rates and the luminance increase produces a better response throughout the retina at high temporal rates. The terms low and high temporal rates used here are relative to the present conditions. Under luminances higher than in the present study all the temporal rates reported here may be considered as low to medium temporal frequencies.

The results shown here also have relevance for the clinical application of temporal modulation fields. One intent of most types of visual field measurements is to use a relatively small target size to establish localized defects. What is obvious from these results is that the choice of target size is directly dependent on the temporal rate being assessed and the luminance level

used. If a fixed target size was to be used in the assessment of TMFs, one should use a size which allows for other factors such as loss of sensitivity due to the normal aging process. It may also be desirable to leave a range of sensitivity below normal thresholds which could be useful in the monitoring of visual disorders. Under the present conditions, if one desired to assess TMFs for high temporal rates (10 Hz or 15 Hz), the use of a one or two degree target size would be necessary. Thus, there is a trade-off between temporal rate and spatial resolution.

At least two different strategies can be used when implementing TMFs. One is to use a constant target size and the other is to increase target size in proportion to some magnification factor. An assumption that often underlies the second approach is that temporal modulation sensitivity does not vary as a consequence of different temporal mechanisms as one moves towards the periphery but is a result of the neural representation at the retinal ganglion cells in combination with luminous flux[9]. Other researchers emphasize the role of photoreceptors[10]. The point is that there are no easy solutions as to what magnification function should be used. One solution is to empirically determine which scaling function should be used under particular conditions. An analysis of this issue along with the subject of visual field asymmetries has been done and will be dealt with elsewhere[11]. Generally, those results show that the scaling function cannot be made independent of luminance under low photopic/mesopic conditions.

The present results offer a reasonable building block upon which to establish what properties affect temporal modulation fields under luminance conditions where both rods and cones may be involved. A large number of implementations is possible in the assessment of TMFs in the clinical domain. Only empirical data will elucidate whether certain parameter combinations are more beneficial than others. What is certain is that TMF measurements have great potential particularly in the assessment of disorders such as glaucoma and optic neuropathies.

Acknowledgements

We would like to thank Olga Overbury for making this research possible and for her helpful comments, Gordon Balazsi for useful comments and for filling in at the conference, Peter April for excellent technical assistance, Myriam Muermans for helping with the graphs and participating in the study, and all the other observers in the study. This project is partially supported by NHRDP grant # 6605-2740-42.

References

1 Faubert J, Balazsi AG, Muermans M, Brussell EM, Kasner OP: Multi-flash campimetry and optic nerve structure in early chronic open angle glaucoma In: Heijl A (ed) Perimetry: Update 1988/89, pp 349-358 Amsterdam/Berkeley/Milano: Kugler & Ghedini 1989
2. Faubert J, Balazsi AG, Overbury O, Brussell EM: Multi-flash campimetry and other psychophysical tests in glaucoma Doc Ophthalmol Proc Ser 49:425-432, 1987
3. Faubert J, Brussell EM, Overbury O, Balazsi AG, Dixon M: Spatial vs. temporal information in suspected and confirmed chronic open angle glaucoma. In: Woo GC (ed) Low Vision: Principles and Applications, pp 79-95 New York: Springer Verlag 1987
4. Lachenmayr B, Rothbacher H, Gleissner M: Automated flicker perimetry versus quantitative static perimetry in early glaucoma In: Heijl A (ed) Perimetry: Update 1988/89, pp 359-368. Amsterdam/Berkeley/Milano: Kugler & Ghedini 1989
5 Overbury O, Faubert J, Balazsi AG, Saheb NE, Kasner OP: Temporal resolution fields and spatial contrast sensitivity in glaucoma. Invest Ophthalmol Vis Sci 31:187, 1990
6. De Lange H: Research into the dynamic nature of the human fovea-cortex systems with intermittent and modulated light I. Attenuation characteristics with white and colored light. J Opt Soc Am 48:777-784, 1958
7 Brussell EM, Muermans M, White CW, Faubert J, Balazsi AG: Chromatic flicker deficits in glaucoma patients and suspects In: Heijl A (ed) Perimetry: Update 1988/89, Amsterdam/Berkeley/Milano: Kugler & Ghedini 1989
8. Tyler CW: Specific deficits of flicker sensitivity in glaucoma and ocular hypertension. Invest Ophthalmol Vis Sci 20:204-212, 1981
9 Raninen A, Rovamo J: Retinal ganglion-cell density and receptive-field size as determinants of photopic flicker sensitivity across the human visual field. J Opt Soc Am A4:1620-1626, 1987
10. Tyler CW: Analysis of visual modulation sensitivity. II Peripheral retina and the role of photoreceptor dimensions. J Opt Soc Am A3:393-398
11 Faubert J: Temporal modulation fields: parameters and scaling. To be submitted

Scotopic and photopic CFF during manipulation of the IOP

Angela C. Kothe[1], John G. Flanagan[2] and John V. Lovasik[1]

[1]*University of Montreal, Montreal, Quebec;* [2]*University of Waterloo, Waterloo, Ontario, Canada*

Abstract

Previous studies using flash electroretinography have identified a differential susceptibility of scotopic versus photopic function to an experimentally induced, transient elevation of the IOP in man. The aim of the present study was to use the critical flicker frequency (CFF) to reproduce the results obtained electrophysiologically Two visually-trained observers were extensively investigated (20 half-hour sessions each) using a modified Rodenstock Goldmann perimeter. For each quadrant, a 5° diameter target was used at 15° eccentricity, with the addition of a central target under photopic conditions For the scotopic experiments, blue and neutral density Wratten filters were used to generate a dim target which could not be detected centrally. Three CFF determinations were recorded at one minute intervals throughout the experiment. Baseline data was derived for an initial five-minute period This was followed by a five-minute period of provocatively increased IOP Thereafter, CFF was recorded for a minimum of 20 minutes to track the recovery of flicker sensitivity Control data was established over a 30-minute period with no manipulation of the IOP and RVPP. Results indicated that CFF was immediately reduced following an increase in the IOP with a decrease in RVPP CFF was unchanged when the increase in IOP was accompanied by an increase in RVPP Results were similar for each quadrant The greater vulnerability of the dark- versus light-adapted retina to alterations of the IOP and RVPP was not confirmed.

Introduction

Experimental manipulation of the intraocular pressure (IOP), and consequently the retinal vascular perfusion pressure (RVPP) in man can be effected by body inversion[1,2] and by suction ophthalmodynamometry[3-5] Although both procedures increase the IOP, body inversion causes the RVPP to increase since arterial blood pressure is also significantly increased, whereas ophthalmodynamometry restricts blood flow in the central retinal artery and thereby decreases the RVPP.

Previous studies using such experimental manipulation of the IOP and RVPP have identified a differential susceptibility of scotopic versus photopic function to altered RVPP. For similar elevations of the IOP, rod function was more impaired when RVPP was decreased than increased, whereas cone function was not greatly altered by either an increase or decrease in the RVPP[5,6].

The aim of the present study was to establish the relationship between the retinal vascular perfusion pressure, intraocular pressure and visual function as assessed by critical flicker frequency (CFF) under both scotopic and photopic viewing conditions in an attempt to reproduce psychophysically the results reported by Lovasik and Kothe[5,6] which identified a differential susceptibility of scotopic versus photopic function to an experimentally induced, transient elevation of the IOP in man using flash electroretinography.

Method

Two clinically normal, volunteer subjects (ages 30 and 31 years) were studied. Brachial blood pressure and IOP were within normal limits. The right eye was used for all experimentation and pupils were dilated using 0.5% tropicamide. The IOP was increased in two different ways:

Address for correspondence Dr J Flanagan, School of Optometry, University of Waterloo, Waterloo, Ontario, Canada N2L 3G1

Perimetry Update 1990/91, pp 391-394
Proceedings of the IXth International Perimetric Society Meeting,
Malmö, Sweden, June 17-20, 1990
edited by Richard P. Mills and Anders Heijl

by body inversion, with an accompanying increase in RVPP; and by suction ophthalmodynamometry, with an accompanying decrease in RVPP. The derivation of RVPP has been outlined previously[5,6]. Body inversion was complete (180°) and carried out in the sitting position. Ophthalmodynamometry was performed using a Langham-type suction cup applied to the temporal sclera with a suction level of -140 mm Hg.

CFF was assessed using a modified Rodenstock Goldmann perimeter. The flickering source was produced using an episcotister mounted in the optical pathway (as previously described[7]). The stimulus was modified to give a 5° diameter. For scotopic viewing conditions the stimulus had an illuminance of 0.4×10^{-3} lux; subjects were dark adapted for 30 minutes prior to testing; and a dim red LED was used as a fixation target. For photopic viewing conditions the stimulus had an illuminance of 260 lux; the background adapting luminance was 10 cdm^{-2}; and a bright red LED was used as a fixation target.

CFF was determined at 15° eccentricity for each quadrant along the 45°/135° meridians. Fixation was also tested under photopic conditions. Baseline data was derived for an initial five-minute period. Three flicker thresholds were determined at the beginning of each minute using a method of descending limits, then averaged to give the mean CFF. IOP was provocatively increased and CFF measured for a further five minutes. Normal viewing conditions were resumed and readings continued for a further 20 minutes. Control data was established for each test condition without provocative testing, over a 30-minute period.

CFF was tested under four conditions:

1. increased IOP with decreased RVPP under scotopic viewing conditions;
2. increased IOP with decreased RVPP under photopic viewing conditions;
3. increased IOP with increased RVPP under scotopic viewing conditions;
4. increased IOP with increased RVPP under photopic viewing conditions.

Results

Table 1 shows the relative increase and decrease in IOP and RVPP for each experimental condition. Table 2 summarizes the CFF results for each condition. It can be seen that CFF was reduced for both subjects under photopic (Figs. 1 and 2) and scotopic viewing conditions when IOP was increased and RVPP decreased (suction ophthalmodynamometry). However, CFF remained unchanged when IOP and RVPP were both increased (inversion).

Table 1 The percentage increase and decrease in IOP and RVPP with suction ophthalmodynamometry and body inversion (RVPP values from Lovasik and Kothe[5,6])

	Decreased RVPP (suction)		*Increased RVPP (inversion)*	
	ACK	*JGF*	*ACK*	*JGF*
IOP	+186.7%	+187.8%	+108.8%	+135 8%
RVPP	–40%	–40%	+80%	+80%

Table 2 Summary of the results for all experimental conditions. Suction gave a significant decrease for all experiments; inversion showed no change

Subject	*Quadrant*	*Suction*		*Inversion*	
		Scotopic	*Photopic*	*Scotopic*	*Photopic*
JGF	SN	✓	✓	✗	✗
	ST	✓	✓	✗	✗
	IN	✓	✓	✗	✗
	IT	✓	✓	✗	✗
	FIX	–	✓	–	✗
ACK	SN	✓	✓	✗	✗
	ST	✓	✓	✗	✗
	IN	✓	✓	✗	✗
	IT	✓	✓	✗	✗
	FIX	–	✓	–	✗

✓: significant at 5% level; ✗: not significant; –: not measured

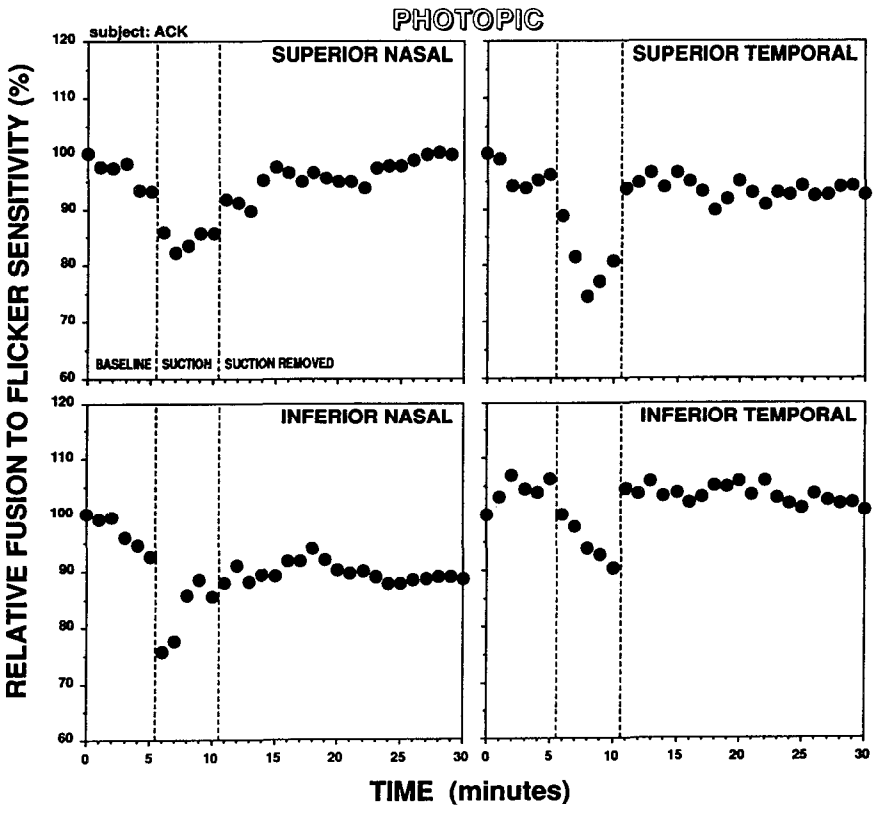

Fig 1 The influence of decreased RVPP and visual field location on flicker sensitivity with suction ophthalmo-dynamometry.

Discussion

CFF was found to be sensitive to short-term, low amplitude reductions in RVPP, under both scotopic and photopic viewing conditions. The scotopic and photopic system appeared to be similarly susceptible to these alterations in the RVPP. However, these results do not necessarily contradict those of Lovasik and Kothe[5,6]. CFF is a subjective psychophysical technique which reflects the response of the entire visual system from retina to cortex and beyond, whereas the flash ERG is an objective, electrophysiological technique which enables direct measurement of retinal function. CFF was measured foveally and at 15° eccentricity, whereas the flash ERGs reflect a mass retinal response. Autoregulation of central retinal blood flow has been well documented, but it is unclear whether there is autoregulatory activity in the peripheral retinal vessels, and the CFF was measured at relatively central locations where autoregulation is known to exist. The flash ERG is more likely to be influenced by the peripheral retina where autoregulation may not exist.

The above arguments are supported by the apparent autoregulatory response seen in both subjects when foveal function was tested with a reduced RVPP; there was an immediate drop in flicker sensitivity followed by a gradual return to baseline values over the subsequent few minutes.

Our results disagree with Berggren[8] who found no change in CFF unless IOP was increased by greater than 40 mm Hg. The changes reported above were caused by increases in IOP of between 15 and 20 mm Hg.

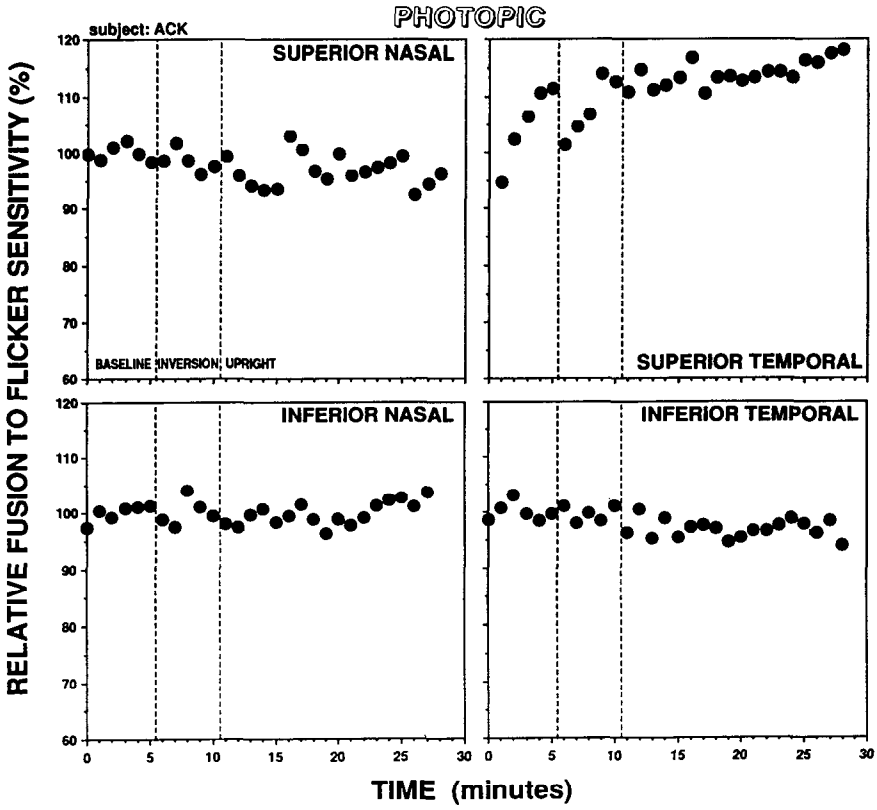

Fig 2 The influence of increased RVPP and visual field location on flicker sensitivity with body version

Acknowledgements

We thank M M Thomas, K Burns and K Pratt for their assistance in collecting data, and gratefully acknowledge the technical support provided by J Cassidy, M. Rieck, R. Jones and T Griesbach We thank Dr A P Cullen for the use of his ICOR Spectrophotometer and A Zorian for secretarial support. This research was funded in part by the MRC of Canada to Dr. Flanagan and NSERC to Dr Lovasik

References

1. Lovasik JV, Kothe AC, Spafford MM: Vascular and neural changes during body inversion: preliminary findings. Can J Optom 49:133-140, 1987
2. Friberg TR, Weinreb RN: Ocular manifestations of gravity inversion JAMA 253:1755-1757, 1985
3 Ulrich WD, Ulrich C: Oculo-oscillo-dynamography: a diagnostic procedure for recording ocular pulses and measuring retinal and ciliary arterial blood pressures. Ophthalm Res 17:308-317, 1985
4 Kergoat H, Lovasik JV: The effects of altered retinal vascular perfusion pressure on the white flash scotopic ERG and oscillatory potentials in man. Electroenceph Clin Neurophys 35:306-322, 1990
5. Lovasik JV, Kothe AC: Neural effects of transiently raised intraocular pressure: the scotopic and photopic flash electroretinogram. Clin Vis Sci 4:313-321, 1989
6 Kothe AC, Lovasik JV: A parametric evaluation of retinal vascular perfusion pressure and visual neural function in man Electroenceph Clin Neurophys 75:185-199, 1990
7 Styles T, Flanagan JG: Meridional differences in temporal response characteristics. Ophthal Physiol Opt 9:405-410, 1990
8. Berggren L: Critical flicker frequency (CFF) in man during induced ocular hypertension II. Technique, and analysis of a normal group Acta Ophthalmol 51:573-582, 1973

The concept of the new perimeter Peristat 433

Jörg Weber

Department of Ophthalmology, University of Cologne, Joseph-Stelzmann-Strasse 9, D-5000 Cologne, Germany

Abstract

Instead of several programs with fixed combinations of accuracy and spatial resolution, the new concept utilizes one flexible program that allows a free choice between three accuracy levels of the measurement strategy and between four density levels of the test point pattern. This free choice does not exist only at the beginning, but also during and at the end of the complete test. The number of possible test point patterns is much larger than four, because different density levels in different regions can be combined. Several combinations are available as "standard patterns", user-defined combinations can be added. Nevertheless, all patterns are compatible and furnish a high number of matching points because they are derived from the same basic grids. The measurement strategy uses the new and quick principle of dynamic step sizes Thus, a glaucoma test with a full threshold determination at 81 points lasts only six minutes

Introduction

Automated perimeters in current use do not always meet the needs of the majority of users. Items that are often criticized are:

1. there are too many programs;
2. once a program has started, there is almost no possibility of adapting it to an individual's specific responses; and
3. the test time for threshold tests is too long.

Therefore, a new perimeter was developed to overcome these problems. The goal was to have:

1. only one program;
2. maximum flexibility to adapt the program to the individual situation at any time during the examination; and
3. reduction of test time by at least half, while maintaining comparable accuracy

The design features three main components: the program structure, test point patterns and measurement strategies

Design of the program structure

The goal of the program design was to have maximum flexibility at any time during the examination.

Perimetric programs are combinations of a test point pattern and a measurement strategy Both determine the resolution with which the hill of vision is measured (Fig. 1). The density of the test point pattern determines the resolution in the X- and Y-dimensions. The accuracy of the measurement strategy determines the resolution in the Z-dimension.

Instead of several programs with fixed combinations of these variables of resolution, the new concept consists of one universal program that allows a free choice of resolution in any of the dimensions. This free choice does not exist only at the beginning, but also during and at the end of the complete test.

The examination is usually started at a basic resolution level that depends on the problem

Perimetry Update 1990/91, pp 395-401
Proceedings of the IXth International Perimetric Society Meeting,
Malmö, Sweden, June 17-20, 1990
edited by Richard P. Mills and Anders Heijl

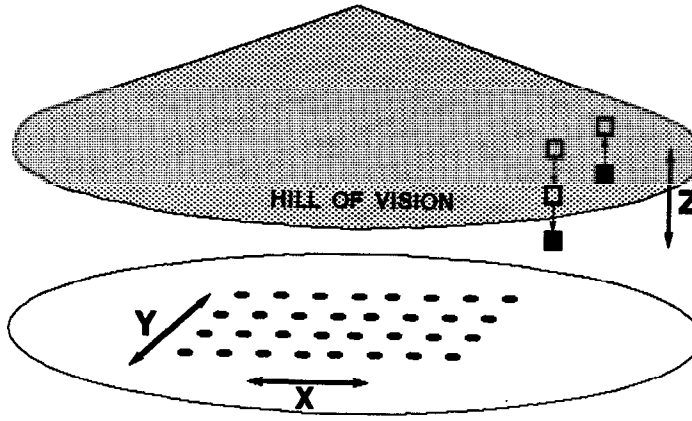

Fig 1 The "hill of vision" has three dimensions. The resolution with which it is measured depends on the test point pattern (concerning the X- and Y-dimensions) and the measurement strategy (concerning the Z-dimension).

(Fig. 2, mark 1). In most of the cases, this will be sufficient. If any uncertainties remain, the level of resolution can be increased stepwise. For example, a suspicious shallow defect can be confirmed or disclosed to be the result of normal scattering by increasing the accuracy level (Fig. 2, mark 2). The test is continued, making use of all information which has already been obtained. Thus, the test does not take any more time than a test which was started to attain that level of resolution. If a scotoma is then to be defined more exactly in spatial dimension, the density level of the test point pattern can be increased (Fig. 2, mark 3). Again, the program uses all available information to keep the test time as low as possible.

The final result is still considered to be one examination and is printed out on one sheet of paper. There is no difference in representation or test time between a stepwise and a direct choice.

Also, the internal organization of the program is stepwise concerning spatial resolution. Thus, if the examination is interrupted, *e.g.*, due to fatigue, a complete result on a lower level of resolution is likely to be obtained.

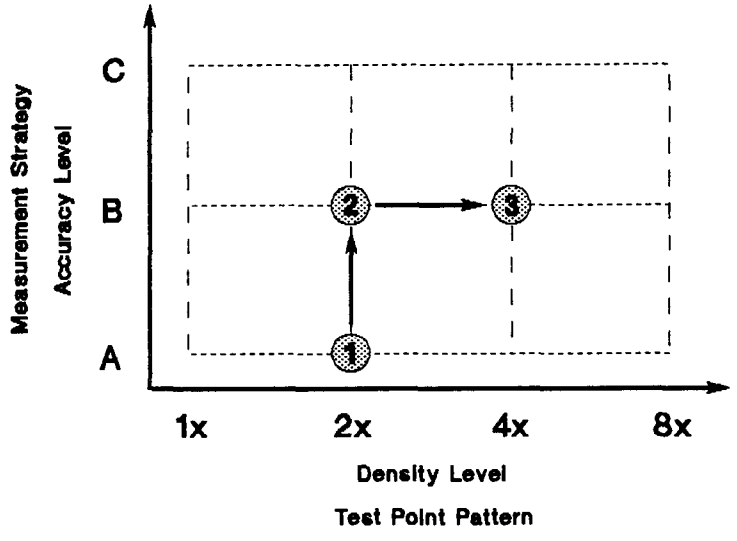

Fig 2 The program concept of the perimeter Peristat 433. Each density level of the test point pattern and each accuracy level of the measurement strategy can be combined. An enhancement of the level (such as shown with marks 1, 2 and 3) is possible at any time during the examination

Design of the test point pattern

The goal of the test point pattern design was to obtain a flexibility of density together with a maximum compatibility of different density levels.

Within 30° eccentricity, four density levels of the test point pattern are available (Fig 3): single density, double density, four-fold density and – up to 10° eccentricity – eight-fold density. The basic geometry is a 6° by 5° rectangular grid.

Rectangular grids of even interpoint distances have the advantage that the probability of detecting a circular scotoma of defined size is evenly distributed[1]. The choice of uneven distances in different directions refers to the pathophysiological phenomenon that the dimensions of field defects are unbalanced, too. In glaucoma, Johnson and Keltner[2] found a horizontal/vertical ratio greater than 1 in most of the scotomata. A similar ratio of interpoint distances (6/5 = 1.2 is close to the mean value that can be derived from Johnson and Keltner's work) increases the chance of detection compared to a ratio of 1.

The average spatial resolutions of the four density levels are 5.5°, 3.9°, 2.7° and 1.9°. The number of possible test point patterns is much larger than four because different density levels in different regions can be combined. Several combinations are available as "standard patterns", user-defined combinations can be added.

Fig. 4 shows some of the standard patterns: GL1 is a pattern with a single density which is condensed to a double density centrally of up to 10° eccentricity. Thus, it is very useful for glaucoma with its small, paracentral defects[3]. The point number is 81. GL2 has a four-fold density of up to 10°, a double density of up to 20° and a single density of up to 30°. It is recommended for the differential diagnosis and follow-up of glaucoma and has 139 points[3].

MA1 has a four-fold and MA2 an eight-fold density within 10° eccentricity and they were designed for macular processes as well as other disturbances of the most central visual field.

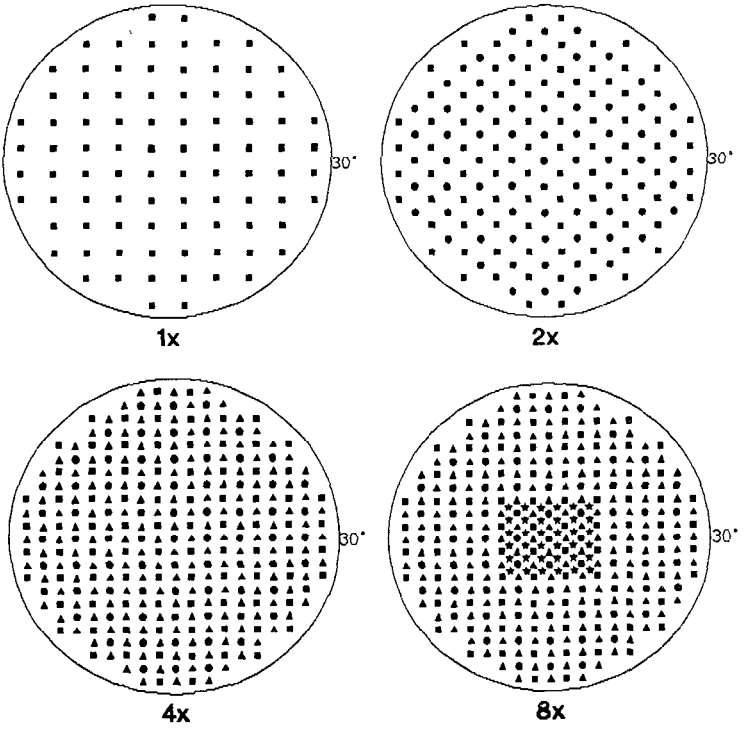

Fig 3 The four density levels of the Peristat 433 that are available within the 30° field: single, double, four-fold and eight-fold. The points added at each level are indicated by squares, circles, triangles and stars.

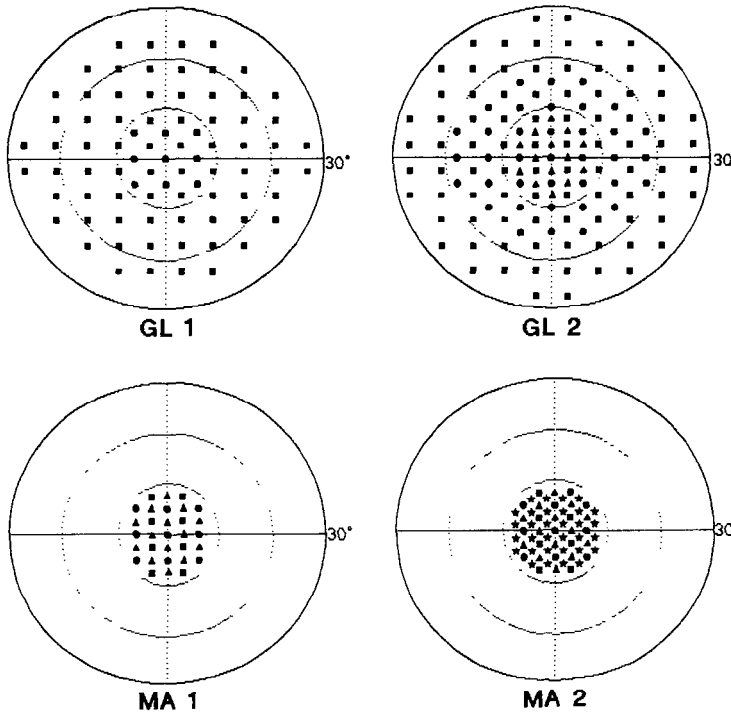

Fig 4 A selection of four "standard test point patterns": GL1 (central condensation, 81 points, "glaucoma routine"); GL2 (central condensation, 139 points, "glaucoma high resolution"); MA1 (10° field, 31 points, "maculopathy routine"); and MA2 (10° field, 63 points, "maculopathy high resolution")

The number of points is 31 or 63, respectively. The pattern NE1 (not shown) is similar to the single density pattern in Fig. 3. It is utilized for the exploration of damage to the central visual pathways. Any other combination can be defined and stored by the user

The flexible program allows infinite changes of patterns, *e g* , when a reading scotoma is suspected one may start with the MA1 pattern. If a defect is confirmed, one could continue with MA2 to outline the defect. A change from GL1 to GL2 is possible, as well as any localized pattern condensation. Nevertheless, all patterns are compatible and furnish a high number of matching points because they are derived from the same basic grids.

The peripheral pattern is a circular pattern with 52 points (not shown). The interpoint distances increase continuously with eccentricities from 10° to 15° By considering the cartographic error[4], which is reversed by the design of test point patterns[5], the radial and tangential distances of neighboring points could be kept nearly equal if measured in the bowl.

Design of the measurement strategy

The aim of the design of the measurement strategy was a maximum speed, together with the flexibility of different levels of testing

There are three levels of accuracy: levels A, B and C. Although they are all threshold strategies, they are very quick because they are based on the principle of the dynamic strategy[6].

The dynamic strategy refers to the fact that the threshold transition zone differs under varying conditions. The most important factor is the threshold level. This was proven by analysis of fluctuations[7] as well as by direct measurement of the frequency-of-seeing-curve[8]. This prior

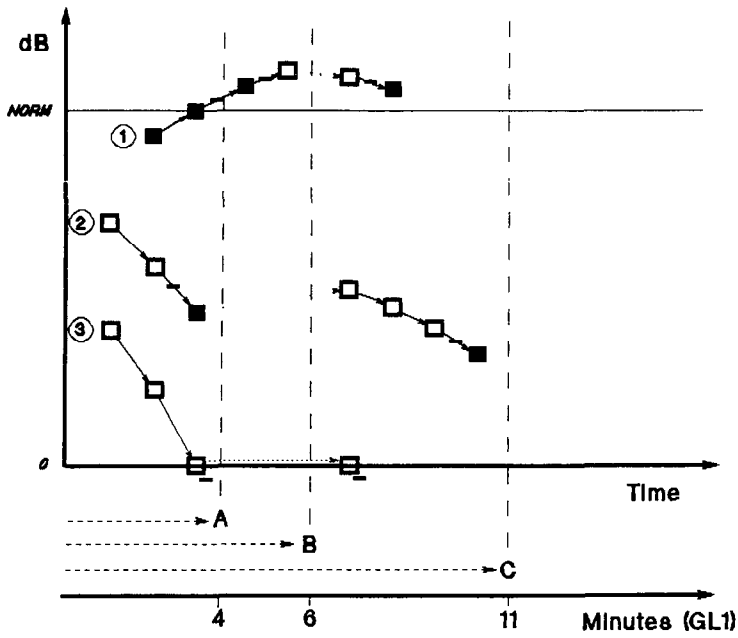

Fig 5 The three accuracy levels of the Peristat 433: level A is a single dynamic bracketing strategy with a limited measurement range (0 dB to normal threshold); level B is a single dynamic bracketing strategy without limitation; level C is a double dynamic bracketing strategy with a new determination of the staircase direction The average test time with a GL1 pattern (81 points) is indicated at the bottom.

knowledge is used to adapt the luminance steps dynamically to the average threshold coefficient of the current threshold level. Thus, the step sizes are always kept in a constant relationship with the size of the transition zone. The choice of an optimal relationship (first phase: 2 to 10 dB, see left side) increases the efficiency remarkably: *e.g* , the minimum significant distance between normal and reduced sensitivity of a single bracketing procedure (step size 2 dB above 30 dB luminance) increases by 25%[6], the test time decreases by 58% compared to the traditional 4 dB/2 dB strategy[6,9].

The difference between the three levels of accuracy of the Peristat 433 is the condition when the measurement series is finished (Fig 5). Levels A and B are nearly identical: the measurement is continued until the first reversal of the patient's response occurs. But in level A, the measurement range is not only limited by the maximum luminance (0 dB) of the perimeter (Fig. 5, case 3), but also arbitrarily by the age-related normal threshold. Thus, the test time is reduced at many normal points (Fig. 5, case 1), while the sensitivity and accuracy of pathological points is equal to level B (Fig. 5, case 2). The accuracy level C continues until the second reversal of the patient's response using step sizes down to 1 dB A new determination of the staircase direction reduces the influence of false responses (see case 2). The test time using a common test point pattern (GL1, 81 points) is four to six minutes for level A, depending on the damage. For level B, it is always six minutes. The high accuracy level C, which is seldom necessary, takes 11 minutes.

Discussion

Flexible programs are not completely new. The "SAPRO" (Spatially Adaptive PROgram)[10,11] offers an enhancement of the spatial resolution. The increase is limited to regions surrounding defect points that were detected using the basic test point grid. Only one higher level of resolution is possible. The procedure of enhancement is automatic. There is no way of changing it during the test. The test time depends on the number of defect points and is unpredictable. The

measurement strategy is a suprathreshold method with two intensity levels which are determined once at the beginning of the test.

The "Automatic Diagnostic Test" of the Humphrey Field Analyzer,[12] uses the same concept of enhancement of the spatial resolution. Also, only one higher level is possible concerning the affected regions. The standard points and the additional points are tests with two different measurement methods, both belonging to the group of suprathreshold strategies. Like the SAPRO program, there is no possibility of influencing the test during its course.

The "G1 program" of the Octopus[13] offers flexibility concerning measurement accuracy: level one, called phase one, is a traditional double bracketing procedure (4 dB/2 dB); phase two is a single bracketing procedure using 2 dB steps. The major goal of the second level is not an increase of accuracy but the exact estimation of the fluctuation. Therefore, the initial stimulus intensities of the second phase are randomized between 3 dB above and 3 dB below the assumed threshold after the first phase [14].

The "N1 program" of Safran and Mermoud[15] allows two levels of accuracy, the first of which is a suprathreshold strategy and the second a threshold strategy that makes use of the result of the first level. Additional points in the centro-macular and the blind spot region optionally increase the spatial resolution in particular areas.

Compared to these existing programs, the Peristat 433 programs offers flexibility in any dimension. Three to four levels of spatial resolution and three levels of measurement accuracy cover the whole range of clinical requirements. No additional programs seem to be necessary.

The idea of a geometric system that provides compatible test point patterns of different levels of density was proposed by Fankhauser and Bebie[1]. Their basic geometry, done with the Octopus program 31, was a square grid of 6° by 6°. Combination with program 32 provides double density and a grid constant of 4.24°. The same logic based on a 12° by 12° grid is used for the programs 41 and 42 of the Octopus. This concept has been transferred to several other automated perimeters.

The production of these programs as isolated units has turned out to be a major disadvantage. They are not able to transfer information between them. The second test starts without any prior knowledge, instead of adapting the initial stimulus intensities to results of neighboring points of the first test. Furthermore, additional effort is needed to combine the results of two compatible programs in one printout. And there are only two levels of density. A third level of four-fold density is only possible in the center of the 30-S program of Weber and Kosel[3] which is an experimental software.

The compatible patterns used by the Peritest and Perimat have a different geometry. The basic grid of 6° by 5° is condensed by additional points in the center of the 6° distance instead of in the center of a square of four points. Therefore, the denser pattern is a 3° by 5° grid. The ratio of interpoint distances changes from the optimal values of 1.2 (6/5) to the unproportionate ratio of 0.6 (3/5). On the other hand, a stepwise enhancement of density and an easy printout of the combined result is offered as well.

The compatible patterns of the Peristat 433 afford up to eight-fold density and infinite possibilities of combinations. Several predefined patterns are provided to ease the handling and provide some standardization. Because they are all derived from the same geometrical system, different standard patterns are compatible, too. For example, the center of the GL2 is identical to the MA1: both use four-fold density up to 10° eccentricity (Fig. 4). Thus, centrocecal islands of vision in glaucoma, which are assessed with the GL2 pattern at the beginning, can be followed using the MA1 test point pattern, according to the recommendations of Weber *et al.*[16].

The concept of the dynamic strategy is clear and logical. A first experimental report[9] supports the impression that the dynamic adaptation of step sizes markedly increases efficiency. The efficiency of discriminating shallow defects from normal points was measured. It is quite clear from the design, which uses increasing step sizes towards lower sensitivity, that a saving of test time is partly at the expense of less accuracy concerning deep defects. The question arises of whether the accurate depth of deep defects is an important factor for the diagnosis and evaluation of visual fields. The existence of high fluctuation in deep defects[7] may indicate that their depth is a rather unreliable figure.

References

1. Fankhauser F, Bebie H: Threshold fluctuations, interpolations and spatial resolution in perimetry. Doc Ophthalmol Proc Ser 19:295-309, 1979
2. Johnson CA, Keltner JL: Properties of scotomata in glaucoma and optic nerve disease: computer analysis. Doc Ophthalmol Proc Ser 35:281-286, 1983
3. Weber J, Kosek J: Glaukomperimetrie: die Optimierung von Prüfpunktrastern mit einem Informationsindex. Klin Mbl Augenheilk 189:110-117, 1986
4. Frisén L: The cartographic deformations of the visual field. Ophthalmologica 161:38-54, 1970
5. Papoulis C, Weber J: Der kartographische Fehler in der Perimetrie. Klin Mbl Augenheilk (in press)
6. Weber J: Eine neue Strategie für die automatische statische Perimetrie. Fortschr Ophthalmol 87:37-40, 1990
7. Flammer J, Drance SM, Fankhauser F, Augustiny L: The differential light threshold in automatic static perimetry: factors influencing the short-term fluctuation. Arch Ophthalmol 102:876-879, 1984
8. Rau S, Weber J: The frequency-of-seeing curve under perimetric conditions (this volume, p.555)
9. Weber J, Cohn H: Stratégie dynamique dans la périmétrie automatisée du glaucome 95th Congress of the Société Française d'Ophtalmologie, Paris, 7-11 May 1989
10. Häberlin H, Fankhauser F: Die Analyse parazentraler Skotome mit räumlich adaptiven Computermethoden. Klin Mbl Augenheilk 176:533-535, 1980
11. Fankhauser F, Funkhouser A, Kwasniewska S: Advantages and limitations of the spatially adaptive program SAPRO in clinical perimetry. Int Ophthalmol 9:179-189, 1986
12. Haley MJ: The Field Analyzer Primer, 2nd edn, p 26. San Leandro, CA: Allergan-Humphrey 1987
13. Flammer J, Jenni F, Bebie H, Keller B: The Octopus glaucoma G1 program. Glaucoma 9:67-72, 1987
14. Bebie H: Personal communication 1987
15. Safran AN, Mermoud CA: Neuro-ophthalmological global analysis program developed on a personal computer and the Octopus 2000R. In: Heijl A (ed) Perimetry Update 1988/89, pp 151-155. Amsterdam/Berkeley/Milano: Kugler & Ghedini Publ 1989
16. Weber J, Schultze T, Ulrich H: The visual field in advanced glaucoma. Int Ophthalmol 13:47-50, 1989

Perikon PCL 90: a new automatic perimeter

Mario Zingirian, Enrico Gandolfo, Paolo Capris and Renzo Mattioli

University Eye Clinic of Genoa, Genoa, Italy

Abstract

A new automatic perimeter (Perikon PCL 90) has recently been developed by Lectrikon-Optikon, Rome, under the supervision of the perimetry study group of the Genoa University Eye Clinic. A description of the main characteristics of this instrument is the subject of this paper. The perimeter, called "PCL 90", has the following main characteristics: projected stimuli (with optimized calibration of surface and shape); static, kinetic and mixed programs and strategies; great possibilities for adopting standard and non-standard parameters for stimuli, background and strategies (photopic and mesopic tests, color perimetry, etc); large disc memory for results storage and comparison; automated fixation control based on an optimized television system.

Introduction

In the last ten years a great number of new automatic perimeters with brilliant conceptual and technical innovations have been designed and manufactured[1-12]. In particular, new strategies and sophisticated diagnostic and statistical programs have been developed[13-19]. Our contribution to the development of a new perimeter has been stimulated by the desire to reach the following goals:

1. to incorporate in one instrument all the principal modern acquisitions in the field of electronic and mechanical engineering, in order to guarantee exact reproducibility and automatic control of every function;
2. to adopt the already well-developed and scientifically validated perimetric strategies and programs, which are considered an international standard in automatic perimetry[5,12,13,18];
3. to maintain the Goldmann stimulus and background standards, while allowing the choice of non standard parameters[20];
4. to improve the examination possibilities by making kinetic perimetry one of the standard procedures of the instrument, thus permitting a good integration of static and kinetic strategies in both diagnostic and screening programs;
5. to facilitate user operation by incorporating computer-assisted routine procedures, such as pupillary diameter measurement, visual acuity determination, headrest positioning, eye fixation monitoring and personal history registration;
6. to permit an easy dialogue between operator and computer by means of friendly software;
7. to allow software updating whenever required by the future evolution of perimetry.

The new automatic perimeter Perikon PCL 90 (Fig. 1) has been developed by Lectrikon-Optikon, Rome, under the supervision of the Perimetry Study Group of the Genoa University Eye Clinic.

A description of the main characteristics of the instrument is the subject of this paper.

Hardware

The Perikon PCL 90 is a computerized perimeter, which consists of a hemispherical screen with a stimulus projecting system, a control computer, a CRT monitor and a printer

Address for correspondence M Zingirian, Clinica Oculistica dell'Università di Genoa, Ospedale S Martino, Pad. 9, V le Benedetto XV 10, 16132 Genoa, Italy

Perimetry Update 1990/91, pp 403-407
Proceedings of the IXth International Perimetric Society Meeting,
Malmö, Sweden, June 17-20, 1990
edited by Richard P. Mills and Anders Heijl

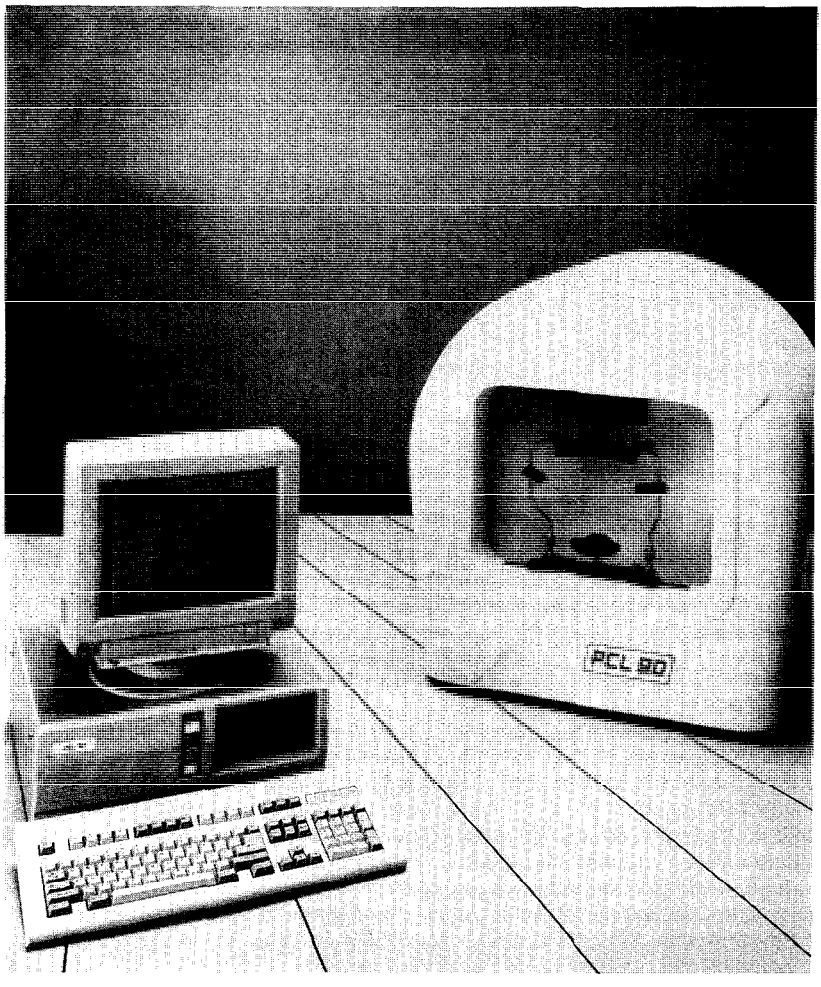

Fig 1 The Perikon PCL 90 automatic perimeter

Screen

This is represented by a 33 cm radius hemispherical cupola with a white background. The background luminance is set at 31.5 asb, but can be varied from 0.25 to 100 asb. An automatic calibration device provides for continuous assessment of the background luminance during the examination.

Stimuli

The stimulus size can be chosen from among the Goldmann conventional targets I to V (standard III). Particular care has been taken to maintain the angular value of the original Goldmann stimuli due to the different cupola radius (Goldmann 30 cm)[20]. Furthermore, a particular device has been used to correct the stimulus shape distortion due to the oblique projection and to guarantee good stimulus focusing at every eccentricity. Four stimulus colors are available. Stimulus duration can be varied from 60 ms to 5 sec (standard 200 ms). All stimulus parameters are controlled by the computer.

Both static and kinetic presentations are possible with a resolution of 0.002 to 0.004 degrees and a rate of movement of 0.5°/sec to 10°/sec for kinetic stimuli (standard 2° or 5°/sec).

Eye monitoring

This is ensured with adjustable sensitivity by a computer-controlled CCD TV camera functioning in mesopic conditions. By means of a keyboard-controlled device, the headrest can be turned in order to center the TV camera on the blind spot, thus allowing exploration of the temporal periphery up to 90°

Preliminary measurements

Pupil diameter can be measured on the visual display by a keyboard-controlled device. On-site visual acuity measurement can also be done by means of optotypes projected on the cupola.

Monitor

The monitor is monochrome, high-resolution (720 × 350 pixels) displaying both eye image and computer data.

Control computer

0.5 Megabyte RAM, 20-Megabyte hard disc and floppy disc drive

Printer

80 columns 180 cps graphic printer.

Software

Test strategies

Static and kinetic, threshold and suprathreshold strategies for both diagnostic and screening purposes are available.

Static threshold strategies

The threshold value at every test-point is measured by means of the standard double-threshold crossing method. Stimulus luminance is varied in a step-like manner (4 dB steps) until the patient's response changes. The procedure then continues in the opposite direction (2 dB steps) until a second response change is obtained. The starting level for each measurement is determined by the neighboring test-points. All the threshold values that differ by more than 4 dB from the expected value, calculated according to the neighboring-point threshold values, are thresholded again.

If a previous threshold test for the same eye is available, stored on the computer disc, these threshold values are adopted as the starting level for the examination, with a remarkable saving of time.

Static fast threshold strategies

All points of the program are tested by slightly suprathreshold stimuli and in all missed points the standard threshold strategy is performed. If no previous stored test is available, stimuli 4 dB brighter than local age-corrected normal thresholds are presented twice. If a previous test is stored on the computer disc the stimulus luminance is 2 dB brighter than previous local threshold values.

These strategies do not differ from the standard fast ones of the Octopus and Humphrey perimeters[2,5,13,14,17,18].

Static suprathreshold strategies

Four suprathreshold strategies are available for each of the screening programs.

- *Single level strategy:* at all test-points the same selected stimulus is presented.
- *Threshold-related strategy.* at all test-points 6 dB suprathreshold, threshold-related, eccen-

tricity-compensated stimuli are presented after determination of the individual sensitivity level in four points with the threshold strategy.
- *Three-zone strategy:* maximum intensity (10,000 asb) stimuli are presented at all points where 6 dB suprathreshold, threshold-related, eccentricity-compensated stimuli are missed. This permits the identification of normal, reduced sensitivity and absolute defect points.
- *Defect-quantification strategy.* threshold strategy is performed at all missed points with the 6 dB suprathreshold, threshold-related, eccentricity-compensated strategy.

Kinetic threshold strategy

Kinetic presentations are possible along every meridian with centripetal movement. Cecofugal and other non-meridional presentations are also possible. Every target size and luminance can be utilized (standard Goldmann parameters are automatically selected). Standard stimulus speed is 2°/sec inside and 5°/sec outside 30°: stimulus movement can be directly controlled on the visual display.

All non-reliable responses due to eye movement during presentation are retested. Stimulus presentation is performed in a random sequence along preselected meridians.

Printout and screen formats

All test results can be visualized on the display or printed as a numerical map (dB), symbolic map, gray-scale map (for threshold tests), comparison map (difference from normal), 3D wire-mesh presentation, interpolated meridian profiles, or isopter diagram (for kinetic tests).

During the examination many test parameters can be seen continuously on the visual display. A new index, the bracketing fluctuation, measured by the bracketing algorithm, can also be determined. It represents the root mean square of the incoherence of responses in double threshold crossing.

This information does not increase examination time. Static and kinetic short-term fluctuation can also be measured in ten double-tested points[16,19].

Programs

Nine Screening Programs and eleven diagnostic programs are available.

Diagnostic programs

Five standard-grid pattern programs with test-points aligned along orthogonal axes are available for the central area (10°, 24°, 30°) and two programs for the periphery (30°-60°). (These programs are analogous to programs 31 and 32 of the Octopus perimeter and the 30-1 and 30-2 of the Humphrey analyzer)[5,9,12,13,17,18].

A static-kinetic program explores the central visual field by means of a static-threshold standard grid test and the periphery with kinetic presentations along 20 meridians (two isopters).

Special programs can be used to explore the macula, the blind spot and the vertical meridian.

Screening programs

Three standard-grid programs explore the central visual field, the periphery or the entire field utilizing the four screening strategies. Two static-kinetic programs with two or three isopters are available. The Genoa Glaucoma Screening program, described elsewhere[21], has been partially modified to improve accuracy and time-saving. Visual disability tests for medico-legal purposes will soon be available[22].

Custom tests

Particular custom programs can be implemented by the user and stored in the computer's memory. Static grids and kinetic tests can also be combined to explore critical areas or to perform detailed tests for particular purposes

Disc routines

Each floppy disc can store more than 300 and the 20-Megabyte hard disc about 10,000 perimetric tests. The storage permits the utilization of threshold and fast strategies starting from

previous data. All stored tests can be recalled in alphabetical or chronological order, but a single patient's tests can also be recalled. In addition, all particular key-word-marked (*e g.*, hemianopsia) stored tests can be recalled and visualized.

Software for statistical evaluation of single or multiple tests will be available in the future. At the present time, only comparison with normal values and two-examination merging is possible.

"User friendly software" has been adopted to facilitate the dialogue with the computer. All choices are well indicated at every phase of the examination and all characteristics of every test and strategy can be visualized by means of help tables. The characteristics of the hardware and the software permit flexibility and thus modification and updating of procedural and statistical programs.

Conclusions

The Perikon PCL 90 is a new automatic projection perimeter which can perform static and kinetic examinations. Particular care has been taken to guarantee precision in stimulus projection and maintenance of Goldmann's standards. Screening and diagnostic suprathreshold and threshold strategies are available for standard grid and particular test patterns. Preliminary measurements, such as visual acuity and pupil diameter, as well as headrest control, are fully automated. User-friendly software has been adopted for easy utilization. Statistical software is being prepared.

References

1. Bynke H, Krakau CET, Ohman R, Aittala A: A new computerized perimeter ("Competer 750") for examination of neuro-ophthalmic patients Doc Ophthalmol Proc Ser 49:249-256, 1987
2. Fankhauser F, Spahr J, Bebie H: Three years of experience with the Octopus automatic perimeter. Doc Ophthalmol Proc Ser 14:7-15, 1977
3. Heijl A, Krakau CET: An automatic static perimeter, design and pilot study Acta Ophthalmol 53:293-310, 1975
4. Heijl A, Krakau CET: An automatic perimeter for glaucoma visual field screening and control: construction and clinical cases Graefe's Arch Clin Exp Ophthalmol 197:13-23, 1975
5. Heijl A: The Humphrey field analyzer, construction and concepts Doc Ophthalmol Proc Ser 42:77-84, 1985
6. Hong C, Kitazawa Y, Shirato S: Use of Fieldmaster automated perimeter for the detection of early visual field changes in glaucoma Int Ophthalmol 4:151-156, 1981
7. Kani K, Tago H, Kobayashi K, Shioiri T: A new automatic perimeter Doc Ophthalmol Proc Ser 42:69-75, 1985
8. Miller KN, Shields MB, Ollie AR: Automated kinetic perimetry with two peripheral isopters in glaucoma. Arch Ophthalmol 107:1316-1320, 1989
9. Schmied U: Introduction to the technique and clinical application of Octopus perimetry In: First Int Meeting on Automated Perimetry System Octopus Schlieren, Switzerland: Interzeag AG 1979
10. Zingirian M, Gandolfo E, Orciuolo M: Automation of the Goldmann perimeter Doc Ophthalmol Proc Ser 35:365-369, 1983
11. Kowa Automatic Visual Field Plotter AP-340 Operation Manual
12. Drance SM, Anderson DR (eds) Automatic Perimetry in Glaucoma Orlando: Grune & Stratton 1985
13. Bebie H, Fankhauser F, Spahr J: Static perimetry: accuracy and fluctuations Acta Ophthalmol 54:339-348, 1976
14. Funkhouser AT: Octopus examination parameters Glaucoma 11:11-20, 1989
15. Heijl A, Lindgren G, Olsson J: A package for the statistical analysis of visual fields Doc Ophthalmol Proc Ser 49:153-168, 1987
16. Flammer J, Drance SM, Augustiny L, Funkhouser A: Quantification of glaucomatous visual field defects with automated perimetry Invest Ophthalmol Vis Sci 26:176-181, 1985
17. Perimeter Digest. Schlieren, Switzerland: Interzeag AG 1983
18. The Field Analyzer Primer, 2nd edn San Leandro CA: Allergan Humphrey 1989
19. Capris P, Gandolfo E, Camoriano GP, Zingirian M: Kinetic visual field indices. In: Heijl A: Perimetry Update 1988/89, pp 223-227. Amsterdam/Berkeley/Milano: Kugler & Ghedini 1989
20. Goldmann H: Ein selbstregistrierendes Projektionskugelperimeter Ophthalmologica 109:71-79, 1945
21. Gandolfo E, Zingirian M, Capris P: The automated program "Genoa Glaucoma Screening" Doc Ophthalmol Proc Ser 42:103-107, 1985
22. Gandolfo E: Functional quantification of the visual field: a new scoring method Doc Ophthalmol Proc Ser 49:537-540, 1987

Intraocular and interocular variability of blind spot surface measurements by means of automated perimetry

Avinoam B. Safran, Leonor Almeida, Christophe Mermoud, Dominique Desangles, Catherine de Weisse and Richard Lang*

*Unit of Neuro-Ophthalmology, Ophthalmology Clinic, Cantonal University Hospital of Geneva, and *Institute of Social and Preventive Medicine, University of Geneva, Geneva, Switzerland*

Abstract

Intraocular and interocular variability of blind spot measurements was assessed in 20 normal subjects (40 eyes), using a computer program developed for the Octopus 2000R measurement unit. A single-level strategy was used, and intensity of light stimuli was set at 12 dB below mean normal age-corrected values of the threshold in locations surrounding the blind spot area Tests were located in a grid pattern constant of 1° horizontally and 1 5° vertically. Blind spot measurement was also performed in a patient with mild papilledema, using the same program Fluctuation in blind spot boundaries was high: out of a mean of 17.05 tested locations which were included within the blind spot area, a mean of 6.75 locations were found to be included in the blind spot in only one of the two successive examinations of the same eye However, the reproducibility of surface measurements proved satisfactory for clinical purposes, as the mean blind spot surface difference between two successive examinations of the same eye amounted to only 14.2% of the mean blind spot surface, mean difference between average diameter measured in two successive examinations of the same eye being 0.34°. Mean interocular difference in average diameter was only 0.54°, with more than 98% of the normal average blind spot diameters ranging from 3 31° to 5 95° This did not prevent the procedure from being sensitive enough to detect visual field changes resulting from mild papilledema.

Introduction

A number of studies have been devoted to the evaluation of the normal blind spot, a few of them using automated perimetry (see, for example,[1-5]). Marked fluctuation in differential light threshold was reported to occur at the borders of the normal blind spot[6] Limited information however is available regarding the reproducibility of measurements of the blind spot surface and the interocular variability in measurements, when using automated perimetry in large series of subjects, with the exception of the fundamental study of Haeberlin *et al* [3]. In that study, the authors performed detailed analysis of the blind spot surface by referring to areas showing absolute sensitivity loss.

We assessed intraocular and interocular variability in blind spot measurements in 20 normal subjects (40 eyes) using Octopus perimetry, with relatively dim, age-corrected light stimuli. For this purpose, a computer program was developed for the Octopus 2000R measurement unit Test stimuli were projected using a regular grid pattern, with a one-level strategy. A non-adaptive strategy was considered suitable for conducting this investigation

Subjects and methods

We examined 40 eyes of 20 normal subjects. Mean age was 37 years (range 26-47). All subjects were healthy volunteers, males and females. We defined a subject as normal if he/she

Supported in part by the Swiss National Fund for Scientific Research, Grant No 32.27842 89

Address for correspondence Professor Avinoam B. Safran, Clinique d'Ophtalmologie, Hôpital cantonal universitaire de Genève, CH-1211 Geneva 4, Switzerland

Perimetry Update 1990/91, pp 409-412
Proceedings of the IXth International Perimetric Society Meeting,
Malmö, Sweden, June 17-20, 1990
edited by Richard P Mills and Anders Heijl

fulfilled all of the following criteria: (1) best corrected visual acuity equal to or better than 20/20; (2) no history of ocular diseases; and (3) no abnormality on ophthalmological examination except for refractive errors equal to or less than 3.00 D.

For testing the blind spot area, an original examination computer program has been developed using an Octopus 2000 R measurement unit and an IBM PS/2 30 microcomputer connected with the 2000 R cupola. All tests were performed with a background illumination of 4 dB. The Octopus 2000 R stimulus size III was used. Each stimulus was presented for the standard 0.1 second duration. The stimulus intensity was 12 dB below the mean age-corrected normal value of the threshold in surrounding locations[7]. We used a 150 location grid constant of 1° horizontally, and 1.5° vertically, with a regular, single level and spatially non-adaptive strategy. Light spots were randomly projected into the nasal side in one out of six tests, in order to facilitate central fixation. Nine false positive checks were randomly performed.

Although most of the subjects (17 out of 20) had some previous experience with automated perimetry, the entire test group underwent a demonstration exercise before testing.

During each evaluation session, the subjects successively underwent examination of the right eye, the left eye, and the right eye again. The following parameters were evaluated:

1. Mean blind spot surface (and standard deviation) in right eyes, in left eyes, and in all tested eyes. Considering that tested locations are horizontally 1° distant, and vertically 1.5° distant, it was assumed that the sensitivity measured in one location reflects that of a $1.5°^2$ area (1.0° × 1.5°). Therefore, computation of the blind spot area was obtained by multiplying the number of non-seeing locations by $1.5°^2$.
2. Mean average diameter (and standard deviation) of the blind spot in right eyes, left eyes and in all tested eyes. Based on the simplified assumption that the area of the blind spot is circular in shape, computation was made according to:
   $D = 2\sqrt{S/\pi}$
   where D is the average blind spot diameter, and S the measured blind spot surface.
3. Intra-ocular variability of blind spot surface measurements, estimated by computing the mean (and standard deviation) of the absolute differences between the results of two successive examinations in each right eye
4. Fluctuation of blind spot delineation, as determined by averaging the locations which were found to be non-seeing in only one of the two successive examinations performed in the same right eye
5. Interocular variability of measured blind spot surface, *i.e* mean (and standard deviation) of the absolute differences between each blind spot surface and every other tested blind spot surface as estimated by:

$$\mu = 2 \sum_{i=1}^{n-1} \sum_{j=i+1}^{n} (S_j - S_i) / n(n-1)$$

   where μ is the mean difference, n is the number of tested eyes (*i e* 40), and S is the measured surface of the blind spot.
6. Interocular variation of the average blind spot diameter D, derived according to the procedure 5 for S.

Results

All tested subjects cooperated well and no one gave more than one false-positive answer per examination Table 1 shows computed mean values of blind spot surface, average diameter, difference in surface or diameter between first and second right eye examinations (intraocular variability), as well as difference between all tested eyes (interocular variability).

It appears that the tested population was large enough to provide reliable results, since mean surfaces and standard deviations obtained from either right eyes (n=20) or left eyes (n=20) were similar to the values computed from all tested eyes (n=40)

Table 1. Blind spot computer values, from the examinations of 20 normal subjects (40 eyes) All right eyes were tested twice

	Mean (SEM)		*Standard deviation*		*Skewness*
	No of locations	*Degrees or degrees²*	*No of locations*	*Degrees or degrees²*	
Surface					
Right eyes	17.25 (0.86)	25 88 (1.29)	3.85	5.77	–0 24
Left eyes	16 85 (0.83)	25 28 (1.24)	3 71	5 56	–0.31
All tested eyes	17 05 (0.60)	25.57 (0 90)	3 78	5 67	–0 04
Intraocular variability	2.45 (0.44)	3 68 (0 66)	1.96	2.94	+1 15
Fluctuation in boundaries	6.75 (0 72)	10 125 (1.07)	3.21	4.82	+0.10
Interocular variability	3 82 (0 23)	5.72 (0 35)	3 18	4 77	+1 17
Average diameter					
Right eyes		4 66 (0 12)		0.54	–0.46
Left eyes		4.60 (0.12)		0 53	–0 44
All tested eyes		4 63 (0 08)		0 53	–0 45
Intraocular variability		0 34 (0 08)		0.27	+1.04
Interocular variability		0 54 (0.03)		0 45	+1 22

SEM: standard error of the mean

Case report

A 55-year-old woman presented with pseudotumor cerebri She complained of transient monocular visual changes. Discrete papilledema was found in both ocular fundi. Visual acuities were normal, as were visual fields except in blind spot areas. The left eye was evaluated by means of the program designed for this study. At 27 tested locations, the light spot was not perceived. This is more than the mean normal value plus 2.5 standard deviations, *i e.*, 26.3 locations.

Discussion

In order to speed up the examination procedure for blind spot delineation, a single-level strategy was chosen, indicating either normality or defect at each tested location

Determination of light spot intensity was conditioned by the necessity of using stimuli which are intense enough for avoiding artifacts induced by angioscotomas (which can result in a loss in sensitivity of as much as 8 dB[8], while being dim enough to prevent the falsifying effects of stray light which occur at high luminance levels[2] and to detect subtle clinical defects The light intensity of the testing spots was therefore set at 12 dB below mean normal age-corrected values of the threshold in locations surrounding the blind spot area[7] Interestingly, in a study by Funkhouser *et al* [5] concerning blind-spot delineation in a normal subject, test locations exhibiting differential light threshold less than 12 dB below a reference boundary value of this subject were considered as being included within the blind spot area. Reference to a boundary value of the tested normal subject was certainly appropriate for the above-mentioned study In our study, however, designed for testing a large population, we chose to refer the intensity of light spots to age-corrected mean normal values of boundary sensitivity. Stimulus size III was used, as it is the only one available with the Octopus 2000R unit. It should nevertheless be noted that this stimulus size was found acceptable for avoiding stray light effects[2].

Tests were located using a regular grid pattern. As a grid constant of 0.6° was used by several authors for blind spot measurements[8], a grid constant of 1.4° was proposed by others[9], and a grid constant of 1° was estimated sufficient in the detailed study of Haeberlin *et al* [3], and furthermore considering that, with Octopus 2000R perimetry, tests can be located every 0.5°, and mean normal blind spot is approximately 47% larger in height than in width[10], a grid constant of 1.0° horizontally and 1.5° vertically was selected for conducting the present investigation.

This combined choice of test location pattern and light spot intensity resulted in the average inclusion of 17.5 tested locations in the blind spot area. Thus sensitive analysis of blind spot measurements was allowed.

Reliability of the technique (intra-individual variation) was evaluated by comparing the results obtained from two successive examinations of the same (right) eye in all tested subjects. It was found that the standard deviation of the difference in average diameter was 0.27°, and that mean test-retest variation in average diameter was 0.34°. Based on our experience of perimetry with the Goldmann kinetic perimeter, this value was considered reasonably stable for clinical use.

Similarly, the interocular variation of normal blind spot measurements obtained with our technique was acceptable: the standard deviation of the average blind spot diameter was 0.53°, *i.e.*, more than 98% of the normal average diameters ranged between 3.31° and 5.95° (mean ± 2.5 SD).

It may be argued that the small range of intra-individual and inter-individual variation found when using our technique possibly could reflect the use of too intense stimuli, thus reducing the clinical sensitivity of the procedure. This however was found to be erroneous, because a number of patients presenting with a moderate papilledema exhibited enlarged blind spots when tested with this method, as shown in the above-reported case.

It has been demonstrated that high values of short-term fluctuation can be found when determining blind spot boundaries[6]. In our study, it was found that, out of a mean of 17.05 tested locations within the blind spot area, a mean of 6.75 locations were found to be included in the blind spot in only one of the two successive examinations of the same eye.

However, the mean surface of the blind spot did not demonstrate substantial changes when determinations were made on two different occasions : mean surface difference between the results obtained from two successive examinations of the same eye was only 14.2% of the mean surface of the normal blind spot.

Examination of one eye with this grid appeared to require around five minutes, including false positive checks and random nasal projection of light spots. The use of a spatially-adaptive strategy should be considered for clinical practice.

References

1 Gramer E, Pröll M, Krieglstein GK: Die Perimetrie des blinden Flecks: Ein Vergleich zwischen kinetischer und computergesteuerter statistischer Perimetrie. Ophthalmologica 179:201-208, 1979
2. Fankhauser F, Haeberlin H: Dynamic range stray light: an estimate of the falsifying effects of stray light in perimetry. Doc Ophthalmol 50:143-167, 1980
3. Haeberlin H, Jenni A, Fankhauser F: Researches on adaptive high resolution programming for automatic perimeter. Int Ophthalmol 1:1-9, 1980
4. Funkhouser AT, Kwasniewska S, Fankhauser F: Clinical interest and problems related to the measurement of blind spot and the pericecal region by means of programs SAPRO, SAPPAR and BSPT Ophthalm Surg 19:485-500, 1988
5 Funkhouser AT, Fankhauser F, Kwasniewska S: SPOT: a blind spot data evaluation program for SAPRO examination Ophthalm Surg 19:590-601, 1988
6. Haefliger IO, Flammer J: Increase of the short term fluctuation of the differential light threshold around a physiologic scotoma. Am J Ophthalmol 107:417-420, 1989
7 Safran AB, Mermoud C: A neuro-ophthalmological global analysis program (N1) developed with the Octopus measurement unit In: A Heijl (ed), Perimetry Update 1988/89, pp 151-155. Amsterdam/Berkeley/Milano: Kugler & Ghedini Publ 1989
8 Zulauf M: Beitrag zur Angioscotometrie: Stimulus Grösse und Programmwahl. Kln Mbl Augenheilk 192:613-618, 1988
9. Bek T, Lund-Andersen H: The influence of stimulus size on perimetric detection of small scotomata. Graefe's Arch Clin Exp Ophthalmol 227:531-534, 1989
10 Armaly MF: The size and locations of the blind spot Arch Ophthalmol 81:192-201, 1969

Multiple stimulus bowl perimetry using a four-button, quadrant-related patient response system

Kathleen L. DePaul and William E. Sponsel

University of Wisconsin, Madison, WI, USA

Introduction

Automated perimetry in the United States has been dominated by the Humphrey Field Analyzer, a full-bowl single stimulus projection perimeter. Results are often unreliable, due in part to its long testing time (12-16 minutes per eye for 30-2 program) which produces significant patient fatigue. Many patients have difficulty repressing the normal saccadic response to a single peripheral stimulus, resulting in loss of fixation. Visual field testing using multiple stimulus patterns was first introduced by Harrington and Flocks[1] using a series of cards printed in fluorescent ink. The Friedmann Visual Field Analyzer Mark II[2], introduced in 1979, is a suprathreshold multiple stimulus perimeter which presents patterns of two to four lights. Fixation is improved due to the concentric arrangement of the stimuli and a reduced testing time of four to six minutes. Since the patient must report the number of stimuli seen, the tendency for false positive and false negative responses is reduced. The Friedmann Visual Field Analyzer Mark II principles have been incorporated into the semi- automated, flat-screen Henson-Hamblin CFS2000[3] and the Henson CFA3000 (Keeler Instruments, Inc.). The main goal of designing a new multiple stimulus perimeter was to eliminate testing variability due to technician subjectivity by fully automating the test. The Marco Technologies MT-336 perimeter (Plate 1) is a full-bowl LED perimeter which has recently been modified to perform a fully automated multiple stimulus visual field examination.

Methods

The Marco Technologies MT-336 is a full-bowl LED perimeter which is currently available for single stimulus visual field testing. In order to use it for multiple stimulus testing, the bowl has been divided into four quadrants by vertical and horizontal lines. A four-button response system has been installed, two buttons on either side of the bowl oriented vertically to each other, so that the spatial arrangement of the buttons corresponds to that of the quadrants. The multiple stimulus program has been written on an Atari ST computer. Using a 31.5 Asb background, the machine flashes patterns of two to four simultaneous stimuli for 0.2 seconds. The pattern presentation is immediately preceded by an audible warning to maximize patient attentiveness. Once the pattern has been presented, the patient responds by pressing the buttons corresponding to the quadrants in which the stimuli were seen. This allows the patient a total of 16 possible responses to a pattern. The time allowed for patient response automatically adjusts depending on the patient's speed.

U.S. and foreign patents have been applied for by Marco Equipment, Inc. (Jacksonville, FL) for various aspects of the modified MT-336 instrument. This work was funded by grants from Marco Equipment, Inc. and Chibret International.

Suprathreshold perimetry involves preliminary estimation of midfield threshold. A series of patterns are presented at 15° while varying the intensity until 50% or more of the stimuli are seen for three consecutive patterns. This procedure establishes the pretest threshold. The program automatically double checks the pretest threshold by decreasing light intensity by 2 dB

Address for correspondence William E. Sponsel, Department of Ophthalmology, F4/3 CSC, 600 Highland Avenue, Madison, WI 53792, USA

Perimetry Update 1990/91, pp 413-421
Proceedings of the IXth International Perimetric Society Meeting,
Malmö, Sweden, June 17-20, 1990
edited by Richard P Mills and Anders Heijl

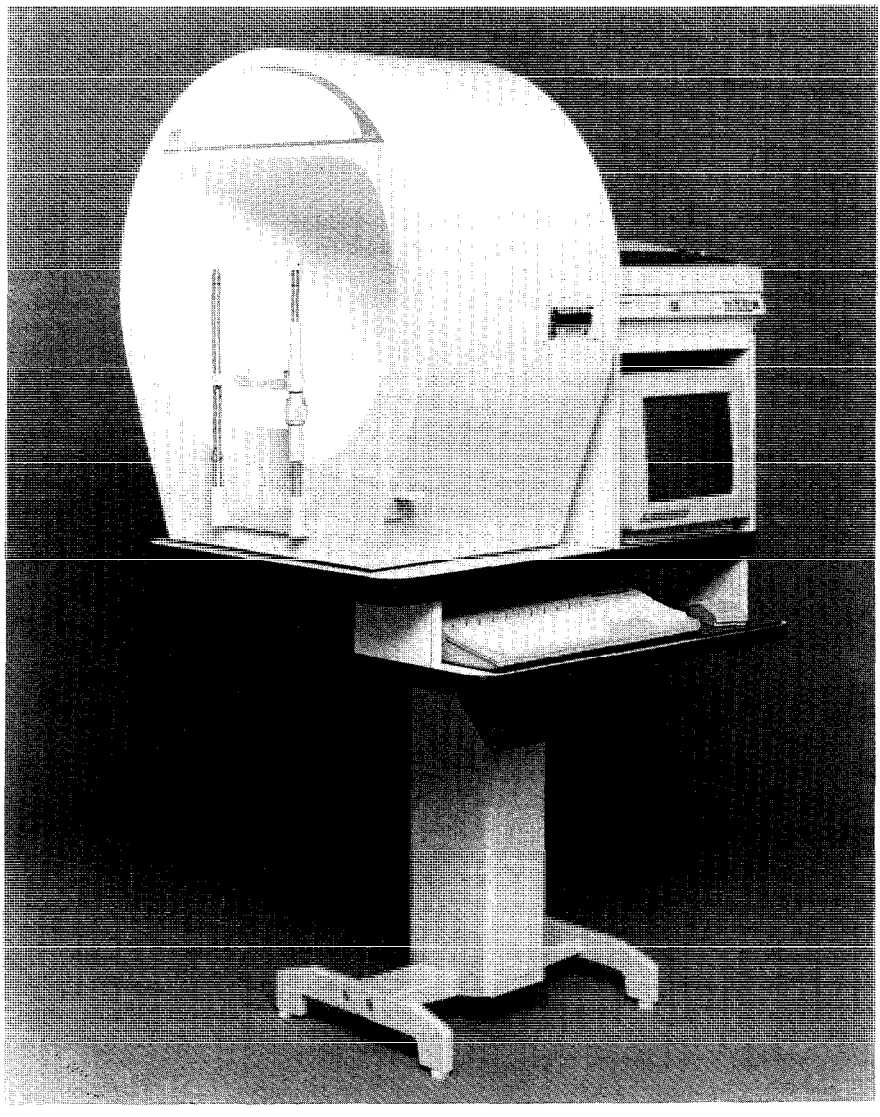

Plate 1 Marco Technologies MT-336 perimeter (unmodified)

and increasing it again in 1 dB steps until 50% or more stimuli are seen. If these two levels are not identical, a third determination is made and the median of the three is used. A slope of 2 dB per 5° is assumed for the hill of vision to provide threshold estimates for all locations in the field. Suprathreshold testing proceeds by testing all locations at 4 dB brighter than the estimated threshold. The current version of the program consists of 73 locations from 5 to 25° eccentricity

Each pattern in the suprathreshold test consists of two to four stimuli all at the same eccentricity. If any stimulus in a pattern is missed, the pattern will be retested after at least two other patterns are tested. If the same stimuli are missed the first and second time, the locations are recorded as misses at 4 dB. If not, the pattern is retested again and only those stimuli missed two times out of three will be recorded as misses at 4 dB. After all patterns have been tested at the first suprathreshold level, any patterns with one or more missed stimuli are retested at 8

dB suprathreshold one time only. Any stimuli that were missed at 4 dB and also at 8 dB will be recorded as a miss at 8 dB. These patterns will then likewise be retested once at 12 dB.

Fixation monitoring is accomplished by blind spot checking (Heijl-Krakau method)[4]. The blind spot can usually be located in one of the first six patterns of the suprathreshold test. If the blind spot is not found as part of the normal testing sequence, a blind spot routine tests a series of locations until the blind spot is found. The suprathreshold testing then proceeds with blind spot checking every sixth pattern.

Each pattern of two or three stimuli is automatically a test for a false positive response. The false positive index is expressed as the ratio of the number of false positive responses over the cumulative number of empty quadrants during the course of the test. The minimum number of empty quadrants is 23.

We report here data from the first 12 glaucoma patients or suspects tested with the modified instrument. All subjects underwent visual field testing on one eye using both the Marco Technologies MT-336 multiple stimulus program and the Humphrey Field Analyzer. Eleven were tested using the 30-2 program and one using the 24-2. The average age of these subjects was 67 years (range 34 to 84 years)

Results

Visual field examination was completed and defect areas corresponded closely on the two machines (Figs. 1 to 12). The population tested intentionally included patients who might have been expected to have difficulty with the four-button response system. Humphrey 30-2 testing was conducted by experienced perimetrists who observed the fixation monitor and interacted with each patient throughout the entire testing period. Patients were surveyed in a non-biased manner after completing both perimetric examinations. Only one patient of the twelve tested preferred the single to the multiple response method. This individual was nevertheless able to perform both examinations without difficulty.

Average false positive responses were 5% for the Marco examination and 8% for the Humphrey. Average fixation losses were 26% for the Marco examination and 31% for the Humphrey. The only patient who had significant difficulty performing the Marco examination was a 34-

Figs 1 to 11 (a) Results for patient N from Marco Technologies MT-336 multiple stimulus suprathreshold testing showing defect level from pretest threshold (top) and threshold range in dB (bottom) (b) Results for patient N from Humphrey 30-2 showing Statpac pattern deviation (top) and threshold in dB (bottom)

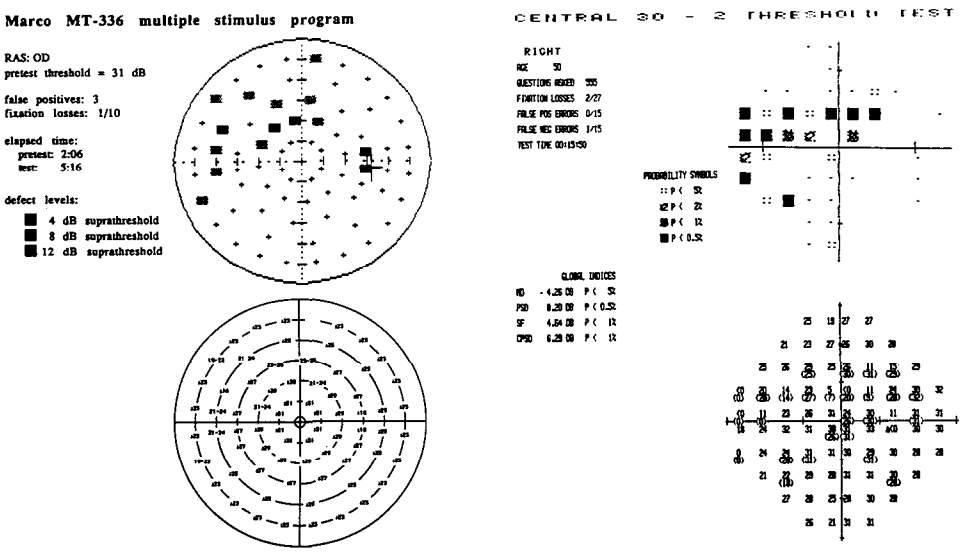

Fig 1

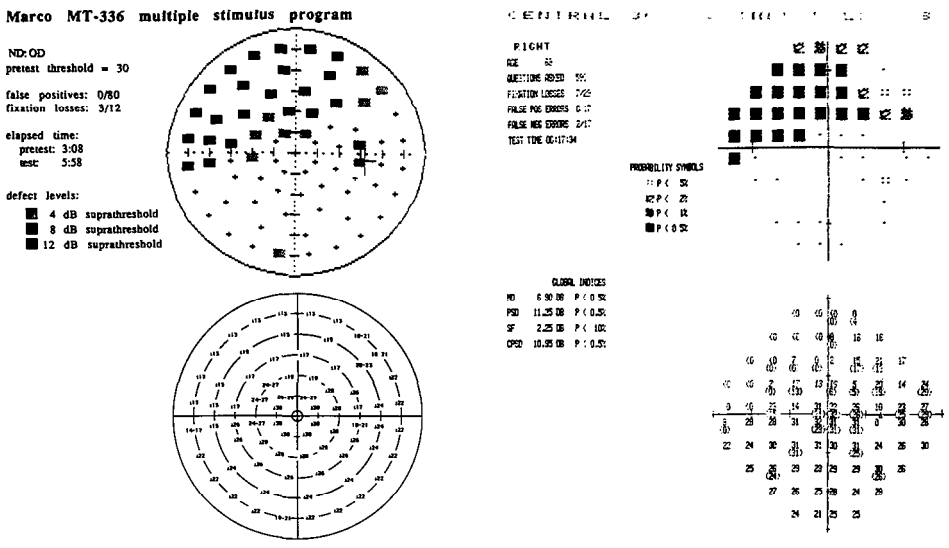

Fig 2

year-old female (Fig. 11) with intraocular pressures frequently in the 30s on maximal medical therapy. She reported recurrent phosphene-like visual disturbances during both tests, and was also the only patient to fail Statpac reliability criteria for false positive (≥30%) and false negative (≥30%) responses on the Humphrey 30-2. Eight of the twelve patients failed the reliability criteria for fixation losses (≥20%) on the Humphrey. Six patients, all of whom failed fixation criteria on the Humphrey, also exceeded the 20% fixation loss level on the Marco examination. Testing time per eye averaged 7:31 for the Marco examination (2:18 for the pretest and 5:18 for suprathreshold test) and 16:25 for the Humphrey examination.

Three of the glaucoma patients had severe field loss and obtained pre-test threshold values at or below the minimum of 19 dB. The multiple stimulus test was only able to complete one level (4 dB suprathreshold) of testing on these patients (*i.e.*, Figs. 4, 5 and 6).

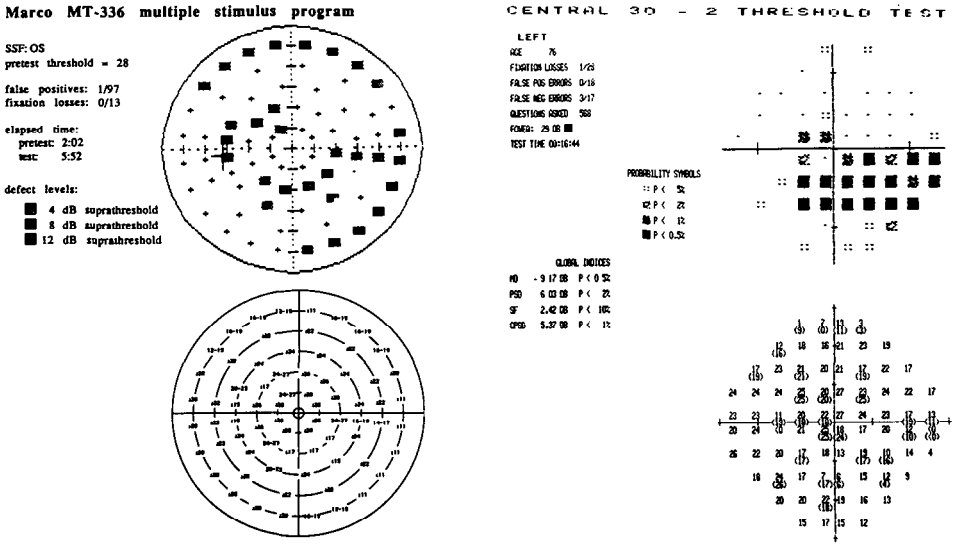

Fig 3.

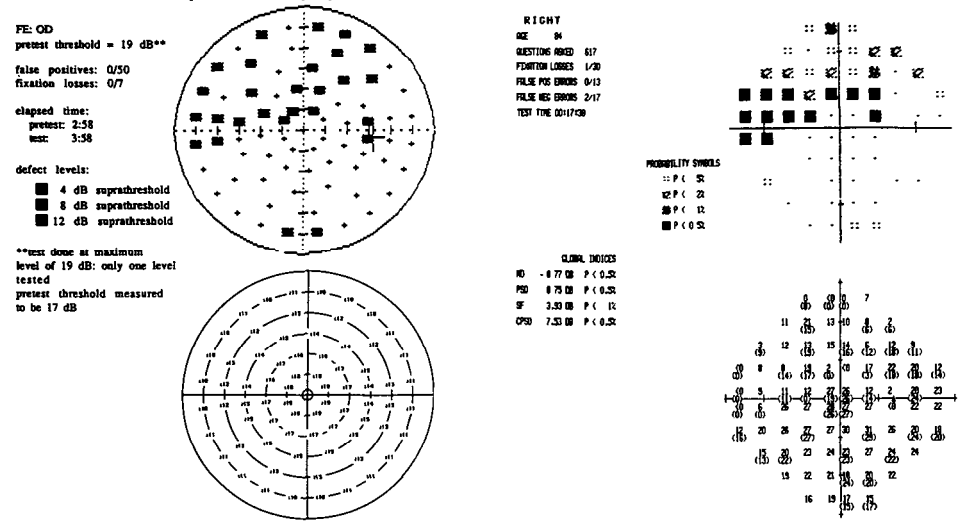
Marco MT-336 multiple stimulus program
FE: OD
pretest threshold = 19 dB**
false positives: 0/50
fixation losses: 0/7
elapsed time:
pretest: 2:58
test: 3:58
defect levels:
4 dB suprathreshold
8 dB suprathreshold
12 dB suprathreshold
**test done at maximum level of 19 dB: only one level tested
pretest threshold measured to be 17 dB
CENTRAL 30 - 2 THRESHOLD TEST
RIGHT
AGE 84
QUESTIONS ASKED 617
FIXATION LOSSES 1/30
FALSE POS ERRORS 0/13
FALSE NEG ERRORS 2/17
TEST TIME 00:17:30
PROBABILITY SYMBOLS
P(5%
P(2%
P(1%
P(0.5%
GLOBAL INDICES
MD -0.77 dB P(0.5%
PSD 0.75 dB P(0.5%
SF 3.33 dB P(1%
CPSD 7.53 dB P(0.5%

Fig 4

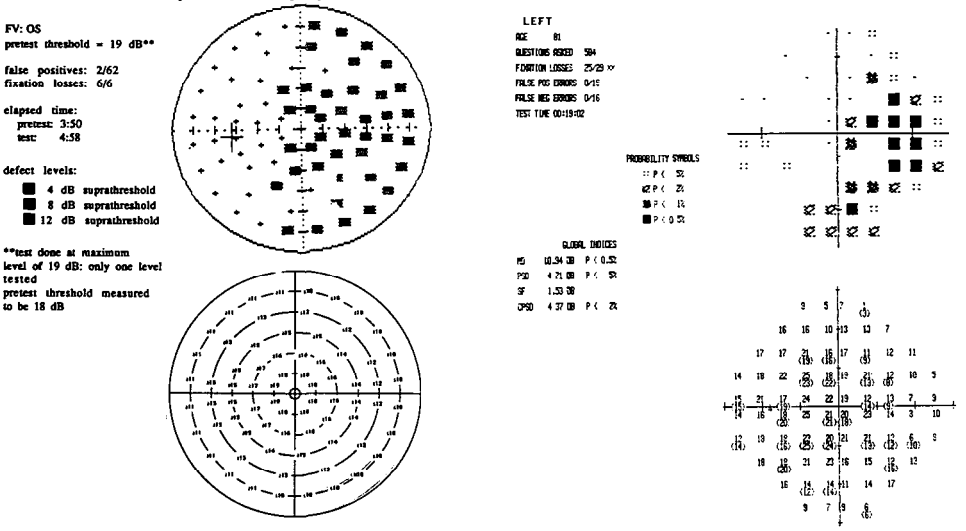
Marco MT-336 multiple stimulus program
FV: OS
pretest threshold = 19 dB**
false positives: 2/62
fixation losses: 6/6
elapsed time:
pretest: 3:50
test: 4:58
defect levels:
4 dB suprathreshold
8 dB suprathreshold
12 dB suprathreshold
**test done at maximum level of 19 dB: only one level tested
pretest threshold measured to be 18 dB
CENTRAL 30 - 2 THRESHOLD TEST
LEFT
AGE 81
QUESTIONS ASKED 584
FIXATION LOSSES 25/28 **
FALSE POS ERRORS 0/15
FALSE NEG ERRORS 0/16
TEST TIME 00:19:02
PROBABILITY SYMBOLS
P(5%
P(2%
P(1%
P(0.5%
GLOBAL INDICES
MD 10.34 dB P(0.5%
PSD 4.71 dB P(5%
SF 1.53 dB
CPSD 4.37 dB P(2%

Fig 5

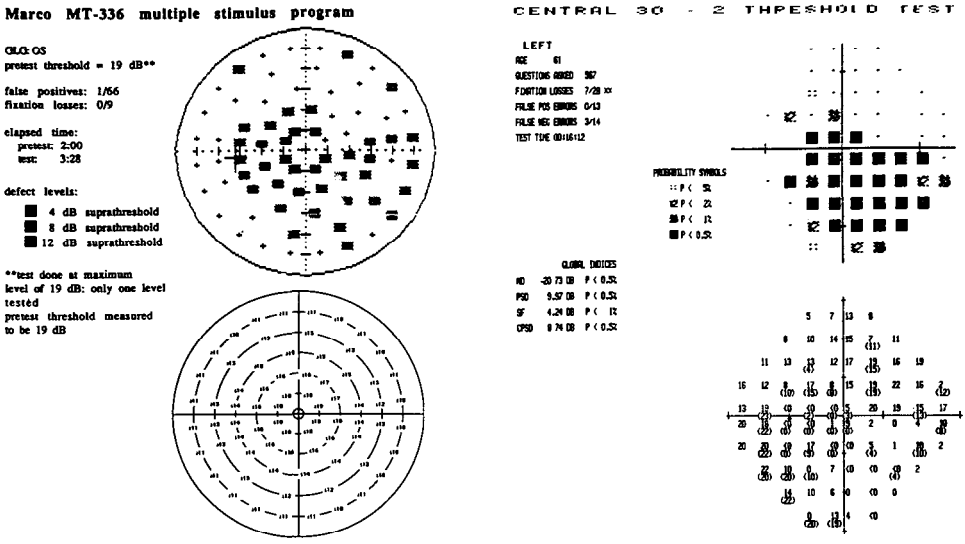
Marco MT-336 multiple stimulus program
OLG: OS
pretest threshold = 19 dB**
false positives: 1/66
fixation losses: 0/9
elapsed time:
pretest: 2:00
test: 3:28
defect levels:
4 dB suprathreshold
8 dB suprathreshold
12 dB suprathreshold
**test done at maximum
level of 19 dB: only one level
tested
pretest threshold measured
to be 19 dB
CENTRAL 30 - 2 THRESHOLD TEST
LEFT
AGE 61
QUESTIONS ASKED 567
FIXATION LOSSES 7/28
FALSE POS ERRORS 0/13
FALSE NEG ERRORS 3/14
TEST TIME 00:16:12
PROBABILITY SYMBOLS
P < 5%
P < 2%
P < 1%
P < 0.5%
GLOBAL INDICES
MD -25.73 DB P < 0.5%
PSD 9.57 DB P < 0.5%
SF 4.24 DB P < 1%
CPSD 8.74 DB P < 0.5%

Fig 6

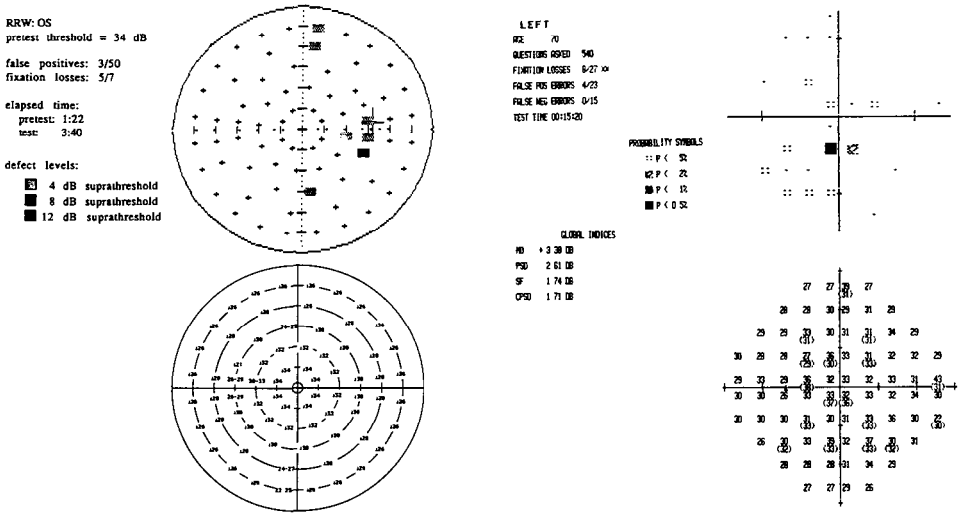
Marco MT-336 multiple stimulus program
RRW: OS
pretest threshold = 34 dB
false positives: 3/50
fixation losses: 5/7
elapsed time:
pretest: 1:22
test: 3:40
defect levels:
4 dB suprathreshold
8 dB suprathreshold
12 dB suprathreshold
LEFT
QUESTIONS ASKED 540
FIXATION LOSSES 8/27
FALSE POS ERRORS 4/23
FALSE NEG ERRORS 0/15
TEST TIME 00:15:20
PROBABILITY SYMBOLS
P < 5%
P < 2%
P < 1%
P < 0.5%
GLOBAL INDICES
MD +3.38 DB
PSD 2.61 DB
SF 1.74 DB
CPSD 1.71 DB

Fig 7

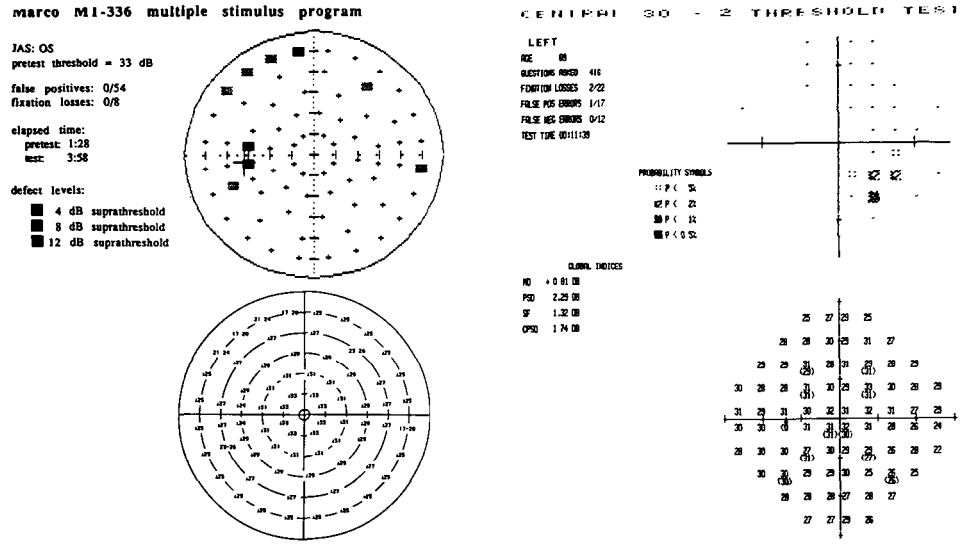
marco M1-336 multiple stimulus program
JAS: OS
pretest threshold = 33 dB
false positives: 0/54
fixation losses: 0/8
elapsed time:
pretest: 1:28
test: 3:58
defect levels:
4 dB suprathreshold
8 dB suprathreshold
12 dB suprathreshold
CENTRAL 30 - 2 THRESHOLD TEST
LEFT
PROBABILITY SYMBOLS
GLOBAL INDICES

Fig. 8.

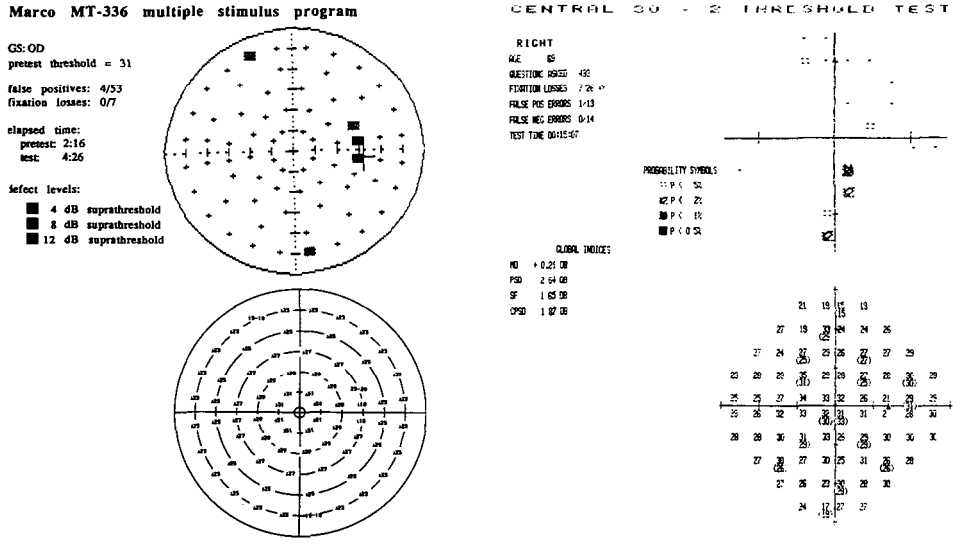
Marco MT-336 multiple stimulus program
GS: OD
pretest threshold = 31
false positives: 4/53
fixation losses: 0/7
elapsed time:
pretest: 2:16
test: 4:26
defect levels:
4 dB suprathreshold
8 dB suprathreshold
12 dB suprathreshold
CENTRAL 30 - 2 THRESHOLD TEST
RIGHT
PROBABILITY SYMBOLS
GLOBAL INDICES

Fig 9

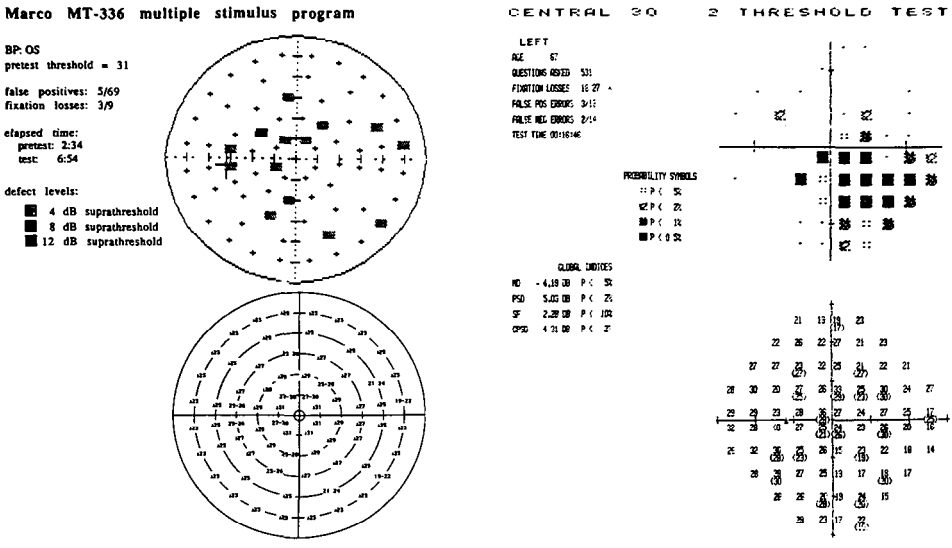
Marco MT-336 multiple stimulus program
BP: OS
pretest threshold = 31
false positives: 5/69
fixation losses: 3/9
elapsed time:
pretest: 2:34
test: 6:54
defect levels:
4 dB suprathreshold
8 dB suprathreshold
12 dB suprathreshold
CENTRAL 30 2 THRESHOLD TEST
LEFT
AGE 67
QUESTIONS ASKED 531
FIXATION LOSSES 16/27
FALSE POS ERRORS 3/13
FALSE NEG ERRORS 2/14
TEST TIME 00:16:46
PROBABILITY SYMBOLS
P < 5%
P < 2%
P < 1%
P < 0.5%
GLOBAL INDICES
MD -4.18 DB P < 5%
PSD 5.05 DB P < 2%
SF 2.29 DB P < 10%
CPSD 4.21 DB P < 2%

Fig 10

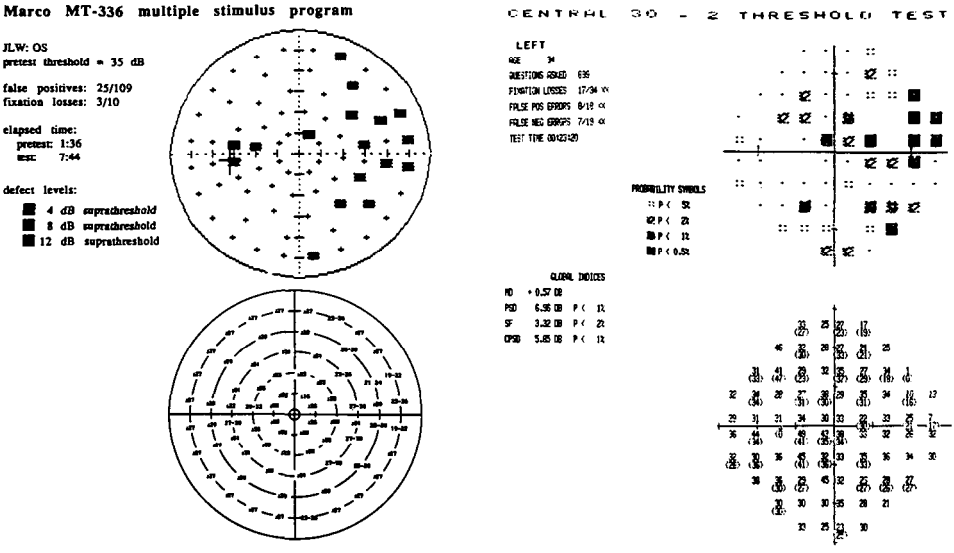
Marco MT-336 multiple stimulus program
JLW: OS
pretest threshold = 35 dB
false positives: 25/109
fixation losses: 3/10
elapsed time:
pretest: 1:36
test: 7:44
defect levels:
4 dB suprathreshold
8 dB suprathreshold
12 dB suprathreshold
CENTRAL 30 - 2 THRESHOLD TEST
LEFT
AGE 34
QUESTIONS ASKED 635
FIXATION LOSSES 17/34
FALSE POS ERRORS 8/19
FALSE NEG ERRORS 7/19
TEST TIME 00:23:20
PROBABILITY SYMBOLS
P < 5%
P < 2%
P < 1%
P < 0.5%
GLOBAL INDICES
MD +0.57 DB
PSD 6.36 DB P < 1%
SF 3.32 DB P < 2%
CPSD 5.85 DB P < 1%

Fig 11

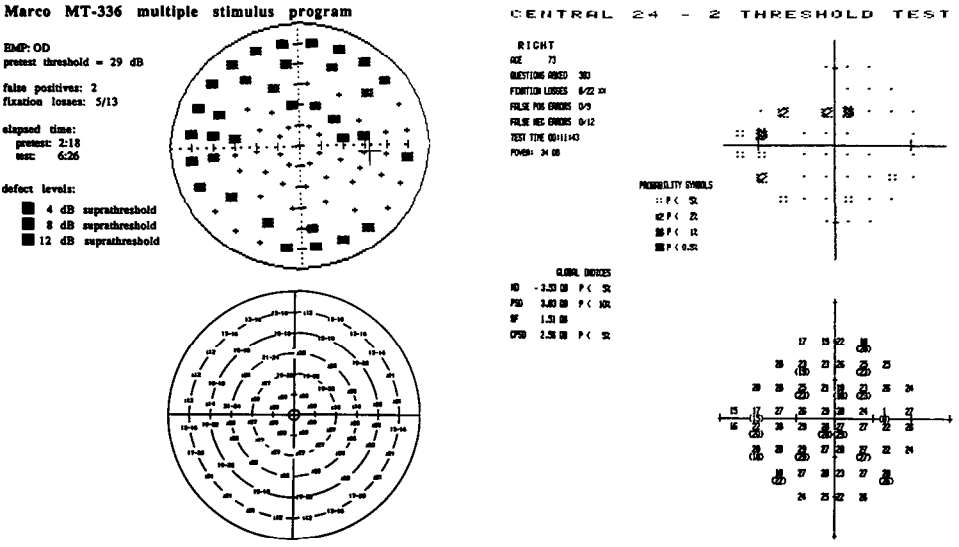

Fig 12. (a) Results for patient 12 from Marco Technologies MT-336 multiple stimulus suprathreshold testing showing defect level from pretest threshold (top) and threshold range in dB (bottom) (b) Results for patient 12 from Humphrey 24-2 showing Statpac pattern deviation (top) and threshold in dB (bottom)

Discussion

The Marco Technologies MT-336 multiple stimulus program has been designed to improve the reliability of multiple stimulus perimetric examination by fully automating the test and decreasing overall testing time. The present study intentionally included poorly compliant patients expected to have problems with perimetric testing. The novel four button quadrant-related response system appears to be a practical method for testing such patients, and should, therefore, present no difficulty for typical clinical subjects. The defect areas that are found on the Marco examination correspond closely to those found using the Humphrey in 11 of the 12 subjects tested. The only patient who showed widely differing results between the two methods (Fig. 10) was grossly non-compliant during Humphrey testing with repeated scanning eye movements and 67% fixation losses. On Marco testing, he had 33% fixation losses and claimed to have less difficulty fixating compared to the Humphrey examination.

The Marco Technologies MT-336 perimeter still requires significant modification. The LED arrangement will be converted to a grid pattern in order to distribute the stimuli more evenly across the field and avoid placing stimuli too close to the horizontal and vertical meridia. The range of light intensities will also be increased to allow better testing of patients with very low sensitivities. A telescope or video monitor will be incorporated into the system to allow for easier patient alignment and fixation monitoring, although Heijl-Krakau fixation monitoring will still be used. In addition to fixation monitoring and false positive testing, the next version of the multiple stimulus program may include indices of short-term fluctuation and false negative responses.

References

1. Harrington DO, Flocks M: Visual field examination by new tachistoscopic multiple-pattern method: preliminary report. Am J Ophthalmol 37:719-723, 1954
2 Friedmann AI: Outline of visual field analyzer Mark II. Doc Ophthalmol Proc Ser 22:65-67, 1969
3. Henson DB, Bryson H: Clinical results with the Henson-Hamblin CFS2000. Doc Ophthalmol Proc Ser 49:233-238, 1987
4. Heijl A, Krakau CET: An automatic static perimeter, design and pilot study. Acta Ophthalmol 53:293-310, 1975

Automated peripheral perimetry: kinetic *versus* suprathreshold static strategies

Howard Barnebey, Li Yi and Richard Mills

Department of Ophthalmology, University of Washington, Seattle, WA, USA

Abstract

One eye of 100 consecutive glaucoma suspect or glaucoma patients was tested with the Humphrey Field Analyzer using the suprathreshold peripheral 68 screening program (P-68), a peripheral custom kinetic program, and central 30-2 threshold program Each set of peripheral tests (P-68 and kinetic) was graded separately using previously assigned criteria for visual field defects which incorporated two levels of diagnostic confidence. Next, the paired tests were compared to one another and evaluated for concordance or discordance. Finally, the peripheral tests were compared to the central 30 degree threshold test looking for peripheral confirmation of defects found on central testing Both peripheral strategies appeared to be comparable in demonstrating peripheral defects Less time was required to perform the suprathreshold screen than to complete two kinetic isopters Isopters created with the I-2-e target were too variable to be of diagnostic usefulness in this patient population; however, a single I-4-e kinetic isopter proved to be a quick and useful screen of the peripheral field

Introduction

Computer-assisted static threshold perimetry has refocused our orientation and approach towards the examination of the visual field. The advantages of this testing method include a greater sensitivity to visual field abnormalities and the ability to collect a highly standardized data base of normal as well as stable abnormal visual fields. Major disadvantages include the length of time required to determine thresholds at each point in a finely spaced matrix and the greater threshold variability of peripheral points in the field. These disadvantages have caused clinicians to focus their attention almost exclusively on testing within the central 30 degrees.

If routine testing is limited to a central threshold field, then peripheral visual field information is ignored. Since the peripheral visual field information appears to be processed differently than that from the central field, a rapid kinetic screening of the peripheral field may be helpful, yielding valuable information In addition, there are some patients unable to perform static threshold testing who can perform kinetic testing

Recently, a kinetic peripheral screening option became available for the Humphrey Field Analyzer. This study was done to compare kinetic and suprathreshold static methods of screening the peripheral field and to relate the results to those obtained on central 30 degree threshold testing.

Material and methods

One hundred consecutive patients undergoing visual field examination for glaucoma and suspicion of glaucoma were tested on the Humphrey Field Analyzer using the following protocol. On odd calendar dates, the left eye (non-study eye) was tested first with a central 30-2 test. This decreased any influence of learning effects on the right eye (study eye) which was then tested sequentially with the peripheral 68 test, then kinetic I-2-e and I-4-e isopters, and finally, the central 30-2 threshold test.

The authors have no proprietary interest in Allergan Humphrey, Inc. or in the software described in this paper. Supported in part by an award from Research to Prevent Blindness, Inc

Address for correspondence Howard Barnebey, M D , 901 Boren Avenue #1030, Seattle, WA 98104, USA

Perimetry Update 1990/91, pp. 423-431
Proceedings of the IXth International Perimetric Society Meeting,
Malmö, Sweden, June 17-20, 1990
edited by Richard P Mills and Anders Heijl

On even calendar days, the non-study eye, in this case, right eye, was tested first with 30-2 test to minimize learning effects on left (study) eye which was tested with the kinetic I-2-e and I-4-e isopters, then the peripheral 68 test, and finally, the central 30-2 threshold test, respectively.

A custom kinetic strategy was developed which limited the number of meridians tested for each isopter. Six meridians in each nasal quadrant (5°, 10°, 15°, 30°, 60°, 80° from horizontal axis) and three meridians in each temporal quadrant (30°, 60°, 80° from the horizontal) were selected for testing. The central 30-2 threshold and peripheral-68 programs were used as currently available on the Humphrey Visual Field Analyzer.

Criteria for abnormality for the 30-2 and peripheral 68 tests were essentially the same as those used by Zamber and Mills[1] and are reproduced below in Tables 1 and 2.

Table 1 Criteria defining visual field defects using the Central 30-2 threshold strategy

Defect type	*Central 30-2*	
	Probable (Grade 2)	*Possible (Grade 1)*
Generalized depression	Mean defect and foveal sensitivity both significant	
	at the 1% level	at the 5% level
Overall peripheral depression	In the outer 2 rows (44 test points) of the pattern deviation plot 3 or more points in 3 or more quadrants significant	
	at the 1% level	at the 5% level
Focal peripheral depression	In the outer 2 rows of the pattern deviation plot in 2 *or fewer* quadrants significance reached by	
	>5 adjacent points at 1%	>3 adjacent points at 5%
Nasal depression	Considering the 10 peripheral nasal (PN) and temporal (PT) points on the pattern deviation plot significant PN minus significant PT points	
	over 2 at the 1% level	over 2 at the 5% level
Nasal step	Consider points corresponding to others on the opposite side of the horizontal meridian	
	more than 1 point at least 6 dB less sensitive	1 point at least 6 dB less sensitive, or more than 1 point >2 dB less sensitive
Hemianopic step	Consider 3 or more adjacent points corresponding to others on the opposite side of the vertical meridian	
	each at least 6 dB less sensitive	each at least 3 dB less sensitive
Remaining island of vision	Any cluster of adjacent seeing points surrounded by 0 dB points	
	More than 2 points	Not applicable

Table 2 Criteria defining visual field defects with the Peripheral 68 suprathreshold strategy

Defect type	*Peripheral 68 test*	
	Probable (Grade 2)	*Possible (Grade 1)*
Generalized depression	26 dB central reference level (default) and/or 2/3 of the test points missed	
	both criteria present	only one present
Overall peripheral depression	Of the points in each of 3 out of four quadrants	
	2/3 points missed	1/3 points missed
Focal peripheral depression	In only one or two quadrants were there	
	2/3 points missed	1/3 points missed
Nasal depression	Considering the 13 peripheral nasal (PN) and temporal (PT) points missed PN minus missed PT points is greater than	
	9 points missed	4 points missed
Nasal step	Subtract the number of missed points on one side of the horizontal meridian from those on the other side	
	2 or more points	1 point
Hemianopic step	Subtract the number of missed points on one side of the vertical meridian from those on the other side	
	2 or more points	1 point
Remaining island of vision	Any cluster of adjacent seeing points	
	more than 2 points	not applicable

Table 3. Criteria grading visual field defects using the Kinetic I-2-e test

Defect type	*Kinetic I-2-e test*	
	Probable (Grade 2)	*Possible (Grade 1)*
Generalized depression	Calculate mean eccentricity of the isopter in each of 4 quadrants. The mean of all quadrants was	
	less than 15 degrees	less than 25 degrees
Overall peripheral depression	Calculate mean eccentricity of the isopter in each of 4 quadrants. The mean of all quadrants was	
	less than 25 degrees (but I-4-e also less than 40 degrees)	more than 25 degrees (but I-4-e also less than 50 degrees)
Focal peripheral depression	Calculate mean eccentricity of the isopter in each of 4 quadrants In only 1 or 2 quadrants was mean	
	less than 15 degrees	less than 25 degrees
Nasal depression	Calculate mean eccentricity of 8 nasal points and separately of 4 temporal points Subtract mean nasal from mean temporal	
	20 degree difference	10 degree difference
Nasal step	Within 5 degrees of the horizontal meridian, there was a step defect of at least	
	10 degrees	5 degrees
Hemianopic step	Within 5 degrees of the vertical meridian, there was a step defect of at least	
	10 degrees	5 degrees
Remaining island	Any off center residual island of vision	
	anywhere	not applicable

Table 4. Criteria grading visual field defects using the Kinetic I-4-e test

Defect type	*Kinetic I-4-e test*	
	Probable (Grade 2)	*Possible (Grade 1)*
Generalized depression	Calculate mean eccentricity of the isopter in each of 4 quadrants The mean of all quadrants was	
	less than 40 degrees	less than 50 degrees
Overall peripheral depression	Calculate mean eccentricity of the isopter in each of 4 quadrants The mean of all quadrants was	
	less than 40 degrees	less than 50 degrees
Focal peripheral depression	Calculate mean eccentricity of the isopter in each of 4 quadrants In only 1 or 2 quadrants was mean	
	less than 40 degrees	less than 50 degrees
Nasal depression	Calculate mean eccentricity of 8 nasal points and separately of 4 temporal points. Subtract mean nasal from mean temporal	
	30 degree difference	20 degree difference
Nasal step	Within 5 degrees of the horizontal meridian, there was a step defect of at least	
	10 degrees	5 degrees
Hemianopic step	Within 5 degrees of the vertical meridian, there was a step defect of at least	
	10 degrees	5 degrees
Remaining island	Any off center residual island of vision	
	anywhere	not applicable

New criteria were developed for abnormalities on both I-2-e (Table 3) and I-4-e (Table 4) kinetic screening isopters. We assigned sufficiently rigorous standards for probable (Grade 2) defects so that most practitioners would agree such a defect was present. On the other hand, the standards for possible (Grade 1) defects were relaxed so that fields with questionable abnormalities would be included. Those fields which showed no defect in either category were assigned Grade 0. The criteria were designed arbitrarily on the basis of prior clinical experience and modified as necessary to avoid assignment of excessive numbers of fields into abnormal diagnostic categories.

Despite the fact that Statpac™ normative data is based on reliable subjects, we included all patients who completed the testing sequence satisfactorily. Separate analysis of reliable and total

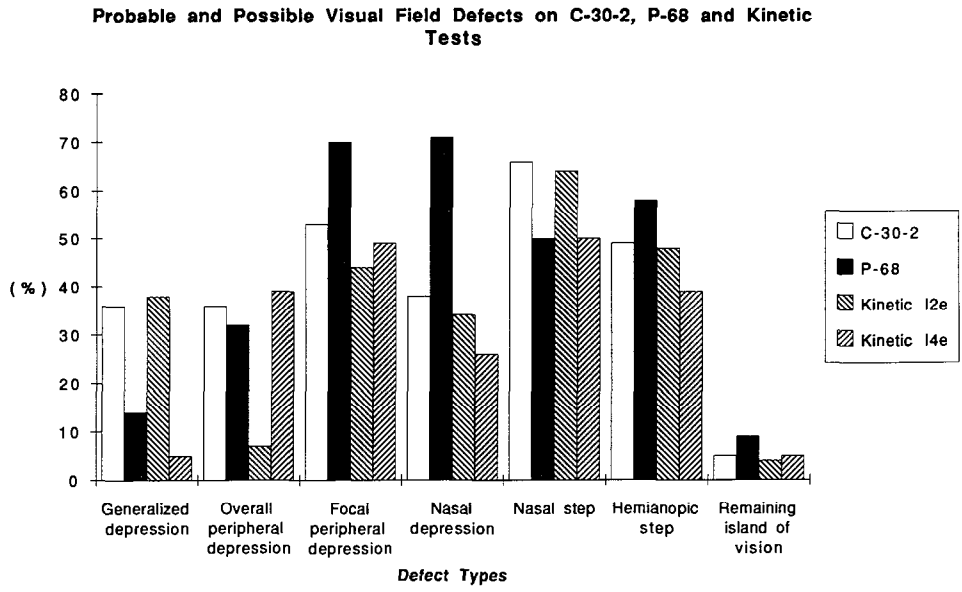

Fig 1 Frequency of field defect types with each of four test strategies Probable (Group 2) and possible (Group 1) defects are combined

patients were performed to ensure that inclusion of unreliable patients did not skew the results.

No attempt was made to determine whether the visual field was normal or abnormal by referring to a previous field or other clinical data, only whether any defects found by the 30-2 test were confirmed by the P-68 or the kinetic isopters. Similarly, when the initial test showed no defect of a given type (Grade 0), no analysis was done to determine if the second test confirmed the absence of a defect, since neither second test was as thorough as the 30-2 test.

Results

One hundred patients completed testing in one eye on the central 30-2, peripheral 68, and kinetic I-2-e and I-4-e isopters. Ninety-seven of those eyes showed at least one defect of Grade 1 or more in one of the seven defect categories. The breakdown of the frequency and types of defects identified in our population sample is summarized in Fig. 1, which combines both possible (Grade 1) and probable (Grade 2) defects together. Similar frequencies of each defect type were obtained with the four different test strategies, except that nasal depression was found more frequently using the peripheral-68 test than with other strategies, overall peripheral depression was seen less frequently with the kinetic I-2-e isopter, and generalized depression was found less frequently with the I-4-e isopter. Examples of two patients with good agreement among the test strategies are shown in Figs. 2 and 3

Figs. 4 and 5 summarize the ability of the two different peripheral test strategies to confirm defects found on central 30° threshold testing. Confirmation rates for each of the seven types of visual field defect were calculated. The rate at which probable (Grade 2) defects on the central 30-2 test were confirmed at either grade level on the peripheral-68, kinetic I-2-e and I-4-e test is displayed in Fig. 4 In Fig. 5, the rate at which both probable (Grade 2) and possible (Grade 1) central 30-2 defects were confirmed by each peripheral testing strategy (Grade 1 or 2) is displayed. Inclusion of "unreliable" patients with fixation losses greater than 33% did not appreciably change the confirmation rates.

The peripheral-68 test was somewhat superior to either kinetic isopter in confirming focal peripheral depression and nasal depression. Taken together or separately, the two kinetic isopters were better than the peripheral-68 test in confirming step defects along the nasal meridian.

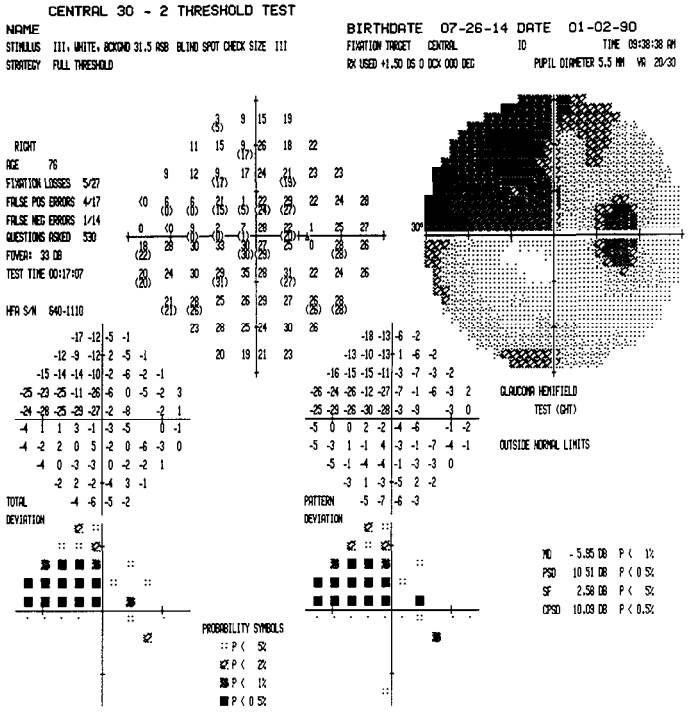
CENTRAL 30 - 2 THRESHOLD TEST
NAME
BIRTHDATE 07-26-14 DATE 01-02-90
STIMULUS III, WHITE, BCKGND 31.5 ASB BLIND SPOT CHECK SIZE III
FIXATION TARGET CENTRAL ID TIME 09:38:38 AM
STRATEGY FULL THRESHOLD
RX USED +1.50 DS 0 DCX 000 DEG PUPIL DIAMETER 5.5 MM VA 20/30
RIGHT
AGE 76
FIXATION LOSSES 5/27
FALSE POS ERRORS 4/17
FALSE NEG ERRORS 1/14
QUESTIONS ASKED 530
FOVEA: 33 DB
TEST TIME 00:17:07
HFA S/N 640-1110
30°
GLAUCOMA HEMIFIELD TEST (GHT)
OUTSIDE NORMAL LIMITS
TOTAL DEVIATION
PATTERN DEVIATION
MD -5.55 DB P< 1%
PSD 10.51 DB P< 0.5%
SF 2.58 DB P< 5%
CPSD 10.09 DB P< 0.5%
PROBABILITY SYMBOLS
:: P< 5%
P< 2%
P< 1%
P< 0.5%

Fig 2a

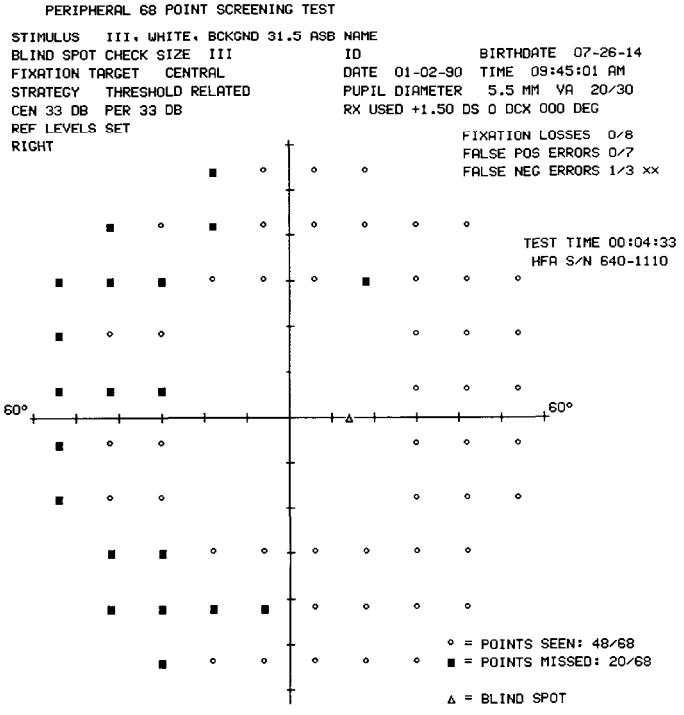
PERIPHERAL 68 POINT SCREENING TEST
STIMULUS III, WHITE, BCKGND 31.5 ASB NAME
BLIND SPOT CHECK SIZE III ID BIRTHDATE 07-26-14
FIXATION TARGET CENTRAL DATE 01-02-90 TIME 09:45:01 AM
STRATEGY THRESHOLD RELATED PUPIL DIAMETER 5.5 MM VA 20/30
CEN 33 DB PER 33 DB RX USED +1.50 DS 0 DCX 000 DEG
REF LEVELS SET
RIGHT
FIXATION LOSSES 0/8
FALSE POS ERRORS 0/7
FALSE NEG ERRORS 1/3 xx
TEST TIME 00:04:33
HFA S/N 640-1110
60°
60°
° = POINTS SEEN: 48/68
■ = POINTS MISSED: 20/68
Δ = BLIND SPOT

Fig 2b

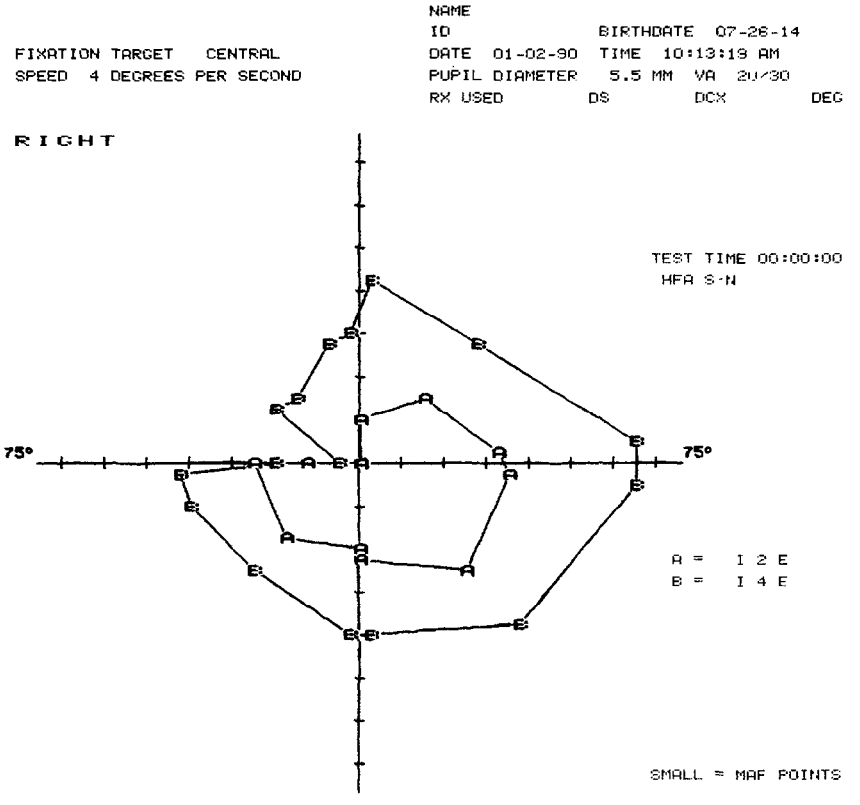

Fig 2c

Fig 2 (a) 30-2 test showing large superior nasal step defect in right eye of a 75-year-old glaucoma patient. (b) Peripheral 68 suprathreshold static test confirming probable nasal step defect. (c) Kinetic test using I-2-e isopter "A" and I-4-e isopter "B" confirming nasal step defect

Discussion

The value of testing the peripheral visual field continues to be a topic of discussion. Manual kinetic strategies have identified isolated peripheral defects without central field involvement varying between 5%[2] to 11%[3]. Threshold static peripheral field testing is not often routinely done because the time required to complete such testing is excessive in relation to the relevant information gathered New kinetic and older suprathreshold static software available on the Humphrey Field Analyzer enables two alternative ways of testing the peripheral field. This study compared the detection rates of two different peripheral testing strategies with each other and with the current central 30° threshold standard.

We found that, despite small differences in confirmation rates across all types of defect, the peripheral kinetic and suprathreshold static strategies to be roughly comparable in confirming defects discovered on the central 30-2 examination. Because of the emphasis placed on kinetic testing alongside the nasal horizontal meridian in the strategy chosen for this study, both kinetic isopters were superior in nasal step confirmation to the peripheral 68 suprathreshold static test.

With the kinetic software version we used, several problems were encountered. Isopters created with the I-2-e stimulus were often difficult to interpret subjectively because of gross irregularities in the isopter shape. In many instances, the stimulus actually crossed the fixation point before the patient responded. Such irregularities in isopter shape occurred because there was no retesting of aberrant points, as is performed routinely by technicians in manual kinetic perimetry.

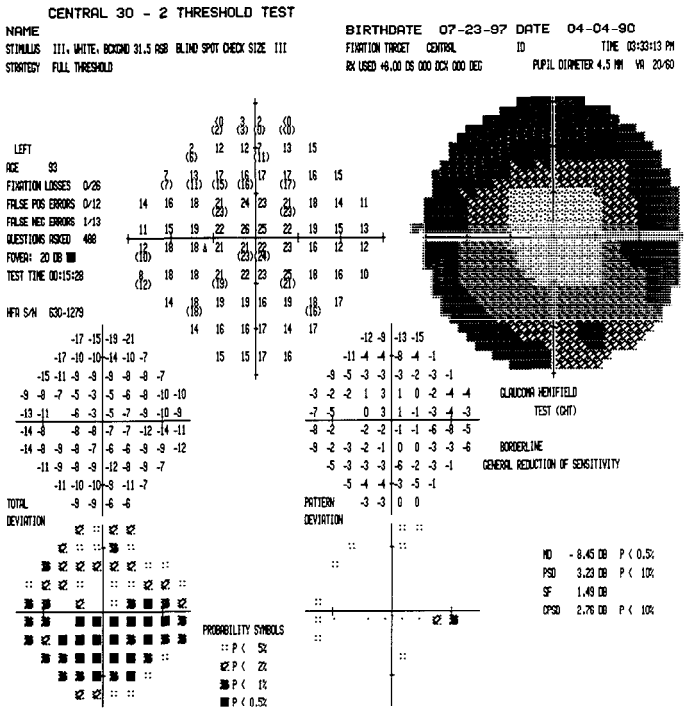
CENTRAL 30 - 2 THRESHOLD TEST
NAME
STIMULUS III, WHITE, BCKGND 31.5 ASB BLIND SPOT CHECK SIZE III
STRATEGY FULL THRESHOLD
BIRTHDATE 07-23-97 DATE 04-04-90
FIXATION TARGET CENTRAL ID TIME 03:33:13 PM
RX USED +6.00 DS 000 DCX 000 DEG PUPIL DIAMETER 4.5 MM VA 20/60
LEFT
AGE 93
FIXATION LOSSES 0/26
FALSE POS ERRORS 0/12
FALSE NEG ERRORS 1/13
QUESTIONS ASKED 488
FOVEA: 20 DB
TEST TIME 00:15:28
HFA S/N 630-1279
TOTAL DEVIATION
PATTERN DEVIATION
GLAUCOMA HEMIFIELD TEST (CHT)
BORDERLINE
GENERAL REDUCTION OF SENSITIVITY
MD -8.45 DB P(0.5%
PSD 3.23 DB P(10%
SF 1.49 DB
CPSD 2.76 DB P(10%
PROBABILITY SYMBOLS
P(5%
P(2%
P(1%
P(0.5%

Fig 3a.

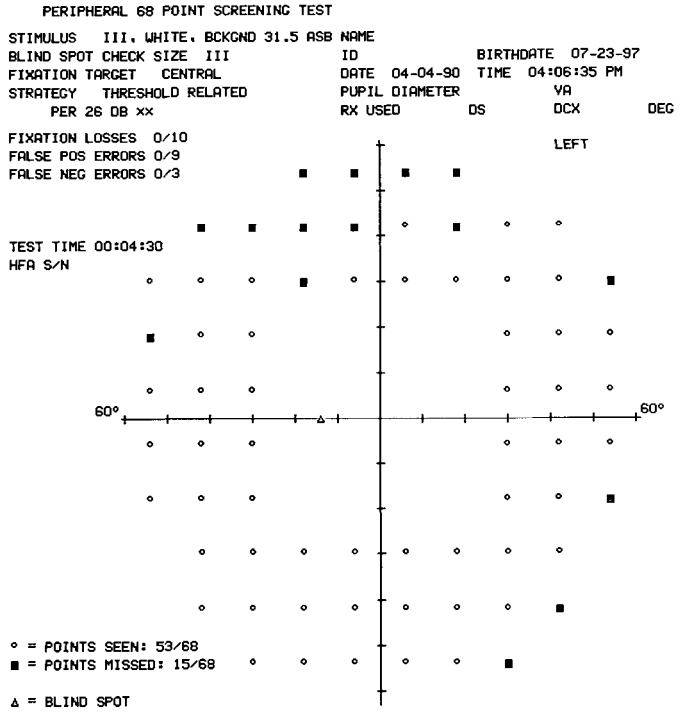
PERIPHERAL 68 POINT SCREENING TEST
STIMULUS III, WHITE, BCKGND 31.5 ASB NAME
BLIND SPOT CHECK SIZE III ID BIRTHDATE 07-23-97
FIXATION TARGET CENTRAL DATE 04-04-90 TIME 04:06:35 PM
STRATEGY THRESHOLD RELATED PUPIL DIAMETER VA
PER 26 DB xx RX USED DS DCX DEG
FIXATION LOSSES 0/10
FALSE POS ERRORS 0/9
FALSE NEG ERRORS 0/3
LEFT
TEST TIME 00:04:30
HFA S/N
60°
60°
° = POINTS SEEN: 53/68
■ = POINTS MISSED: 15/68
△ = BLIND SPOT

Fig 3b

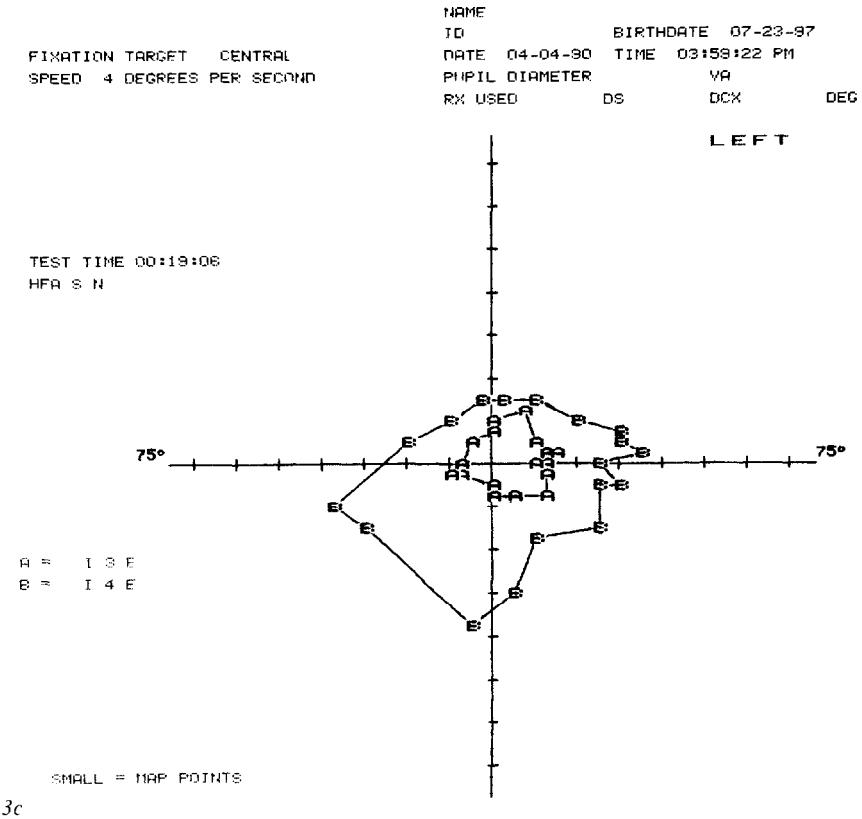

Fig 3c

Fig 3 (a) 30-2 test showing generalized depression (b) Peripheral 68 test showing only depressed central reference level (c) Kinetic I-2-e isopter "A" and I-4-e isopter "B" showing generalized constriction.

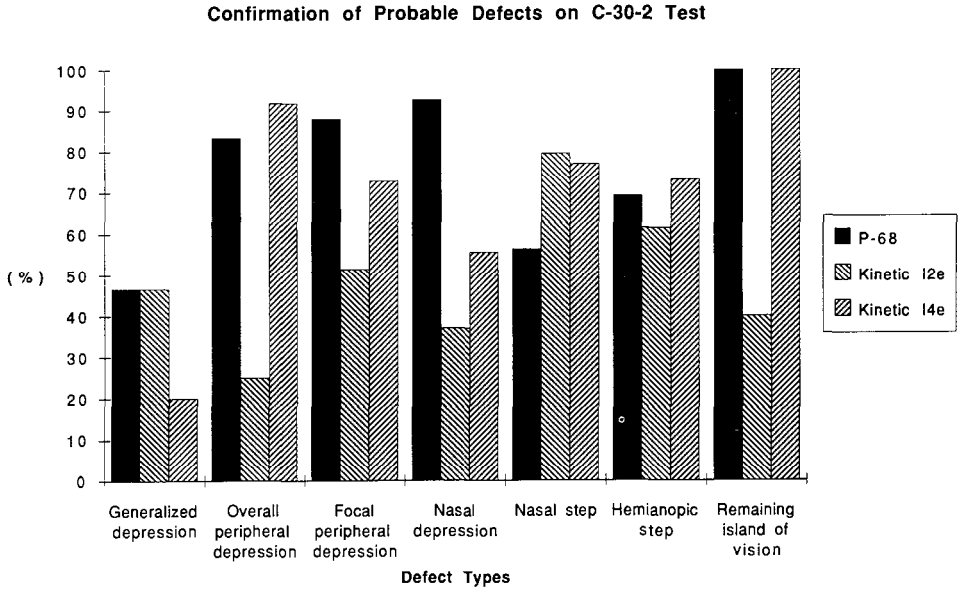

Fig 4 Confirmation rate of probable defects on 30-2 test by either possible or probable defects on the three screening tests

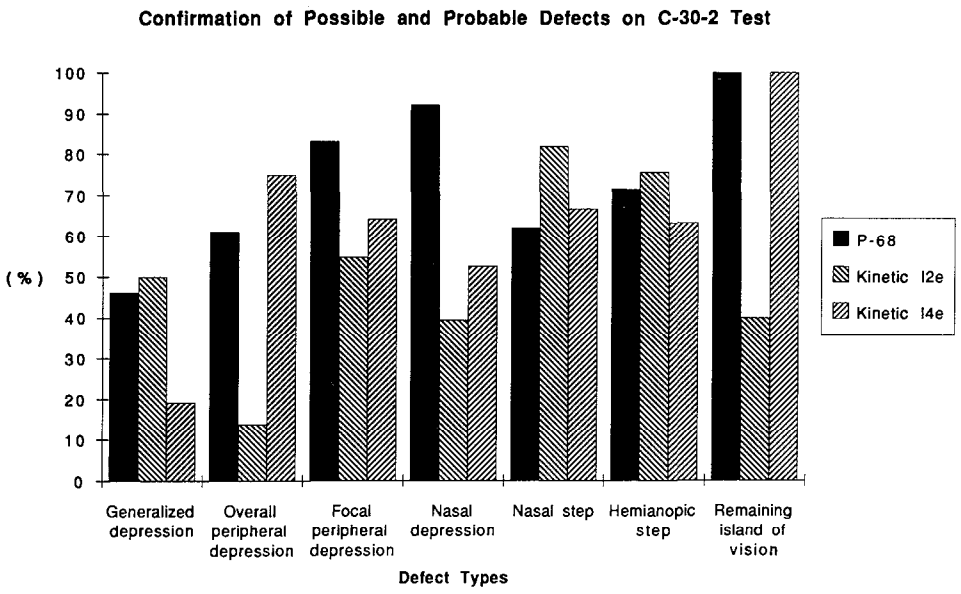

Fig 5 Confirmation rate of possible or probable defects on 30-2 test by either possible or probable defects on the three screening tests

Using the criteria outlined, an unusually high frequency of hemianopic defects was encountered and confirmed using all testing strategies in this population of glaucoma patients and suspects. Defect alignment along the vertical meridian was not observed in the fellow eye, so unsuspected neurologic disease is unlikely. Most of these "hemianopias", were probably artifactual, related to asymmetric superior depression.

The small number of patients with normal central threshold tests and abnormal peripheral tests prevented any meaningful analysis of the frequency of isolated peripheral defects in our population. Those peripheral defects which were missed on central testing included focal peripheral depression (4% of cases), nasal depression (3%), hemianopic step (3%), nasal step (2%), and overall peripheral depression (2%) Also, since no absolute standard was used with which to determine if these peripheral findings were real or artifactual, no conclusions may be drawn except that the incidence of such disagreement was low.

In summary, we found the kinetic and static peripheral screening strategies were comparable in their ability to confirm defects found on central 30-2 testing The I-2-e isopter in automated kinetic testing added insufficient additional information to compensate for the difficulty in interpretation of the often irregular isopter boundary The I-4-e kinetic isopter and the peripheral 68 suprathreshold static test proved both rapid and useful in confirming defects found on central 30-2 threshold testing.

References

1. Zamber R, Mills RP: Peripheral vs. central confirmatory testing In: Heijl A (ed) Perimetry Update 1988/89, pp 409-416 Amsterdam/Berkeley/Milan: Kugler & Ghedini Publ 1989
2 Werner EB, Beraskow J: Peripheral nasal field defects in glaucoma Trans Am Acad Ophthalmol 86:1875-1878, 1979
3 Le Blanc RP, Becker B: Peripheral nasal field defects Am J Ophthalmol 72:415-419, 1971

Evaluation of automated kinetic perimetry (AKP) with the Humphrey Field Analyzer

John R. Lynn[1], William H. Swanson[2] and Ronald L. Fellman[1]

[1]*Glaucoma Associates of Texas and* [2]*Retina Foundation of the Southwest, Dallas, Texas, USA*

Abstract

The Allergan-Humphrey Visual Field Analyzer has recently been equipped to perform technician-assisted automated kinetic perimetry (AKP). The authors compared AKP fields with manual fields obtained on a Goldmann perimeter by a highly experienced kinetic perimetrist They found that AKP was capable of providing useful additions to data from automated static perimetry (ASP), but its utility was severely compromised by a range of problems with the current implementation The most commonly encountered problems were spurious spikes on the isopters and spurious isopter lines. In addition, the available options were severely limited and a number of problems were encountered during the tests The authors suggest solutions to the problems and basic strategic considerations which should allow any manufacturer to improve if not perfect a system for automated kinetic perimetry.

Introduction

The Allergan-Humphrey Visual Field Analyzer (AHVFA) has established an excellent record for performing and analyzing automated static perimetry (ASP). The manufacturer recently provided an upgrade for the software and hardware of the AHVFA, allowing it to perform technician-assisted automated kinetic perimetry (AKP). To evaluate this new system, we com-

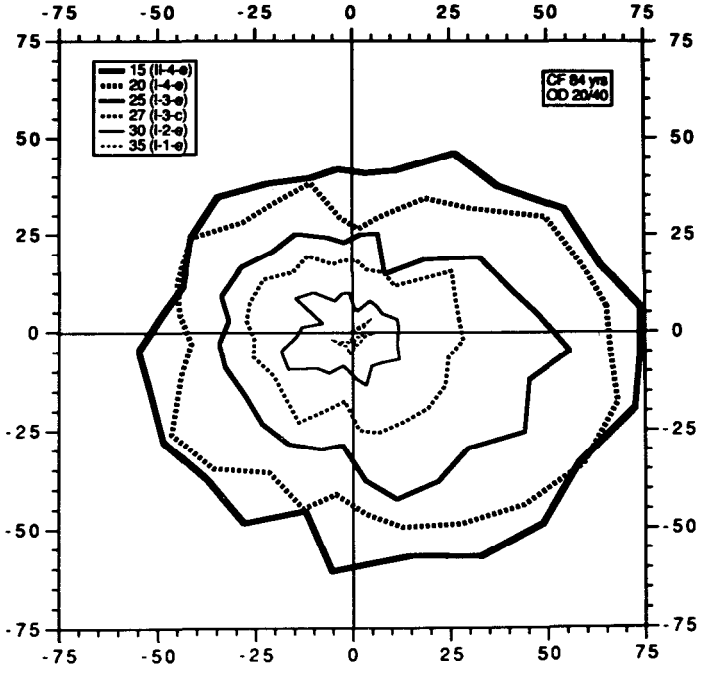

Fig 1 AKP data This normal visual field has been replotted by hand

Perimetry Update 1990/91, pp 433-452
Proceedings of the IXth International Perimetric Society Meeting,
Malmö, Sweden, June 17-20, 1990
edited by Richard P. Mills and Anders Heijl

Table 1 Equivalences of test objects on the Goldmann perimeter and the Allergan-Humphrey Visual Field Analyzer

STATIC STIMULI (ALL SPOT SIZE III)		EQUIVALENT KINETIC STIMULI		
INTENSITY (apostilbs)	STATIC VALUE (db)	KINETIC VALUE	SIZE (mm^2)	INTENSITY(apostilbs)
10,000	0	V-4-E	64	1,000
7,943	1	V-4-D	64	794
6,310	2	V-4-C	64	631
5,012	3	V-4-B	64	501
3,981	4	V-4-A	64	398
3,162	5	IV-4-E	16	1,000
2,512	6	IV-4-D	16	794
1,995	7	IV-4-C	16	631
1,585	8	IV-4-B	16	501
1,259	9	IV-4-A	16	398
1,000	10	III-4-E	4	1,000
794	11	III-4-D	4	794
631	12	III-4-C	4	631
501	13	III-4-B	4	501
398	14	III-4-A	4	398
316	15	II-4-E	1	1,000
251	16	II-4-D	1	794
200	17	II-4-C	1	631
159	18	II-4-B	1	501
126	19	II-4-A	1	398
100	20	I-4-E	0 25	1,000
79	21	I-4-D	0 25	794
63	22	I-4-C	0 25	631
50	23	I-4-B	0 25	501
40	24	I-4-A	0 25	398
32	25	I-3-E	0 25	316
25	26	I-3-D	0 25	251
20	27	I-3-C	0 25	200
16	28	I-3-B	0 25	159
13	29	I-3-A	0 25	126
10 0	30	I-2-E	0 25	100
7 9	31	I-2-D	0 25	79
6 3	32	I-2-C	0 25	63
5 0	33	I-2-B	0 25	50
4 0	34	I-2-A	0 25	40
3 2	35	I-1-E	0 25	32
2 5	36	I-1-D	0 25	25
2 0	37	I-1-C	0 25	20
1 6	38	I-1-B	0 25	16
1 3	39	I-1-A	0 25	13

Assumes that the static maximum is 10,000 apostilbs, the kinetic maximum is 1,000 apostilbs and that doubling spot diameter is equivalent to a 0 5 log unit increase in intensity

pared AKP fields gathered by inexperienced kinetic technicians with results obtained by a highly experienced kinetic perimetrist using a Goldmann perimeter Optimization methods were used in an attempt to improve the performance of the AKP system.

Why kinetic fields?

An example of AKP data obtained on the AHVFA is shown in Fig. 1. Each isopter was gathered with a stimulus value which can be translated into decibels (dB) by referring to the table of equivalences (Table 1). The results in Fig. 1 show the system is capable of obtaining reasonable kinetic thresholds, even in the hands of an inexperienced perimetrist. The lines have been replotted to avoid problems with the software's data output routines which are discussed below.

When a patient has a small defect at the edge of an ASP field, selected kinetic isopters can be helpful in differentiating between visual system damage and a lens rim artifact as shown in

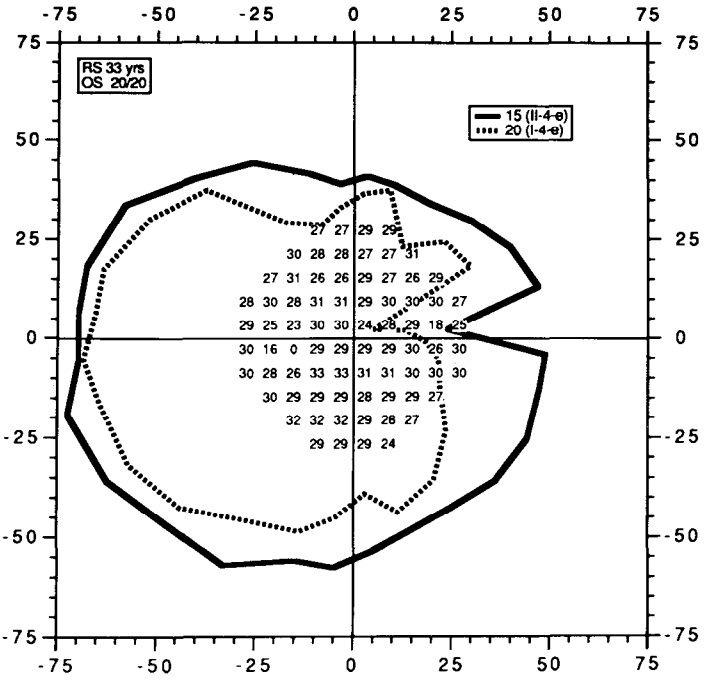

Fig 2 AKP data superimposed on ASP thresholds AKP confirms the superonasal step only suspected on ASP.

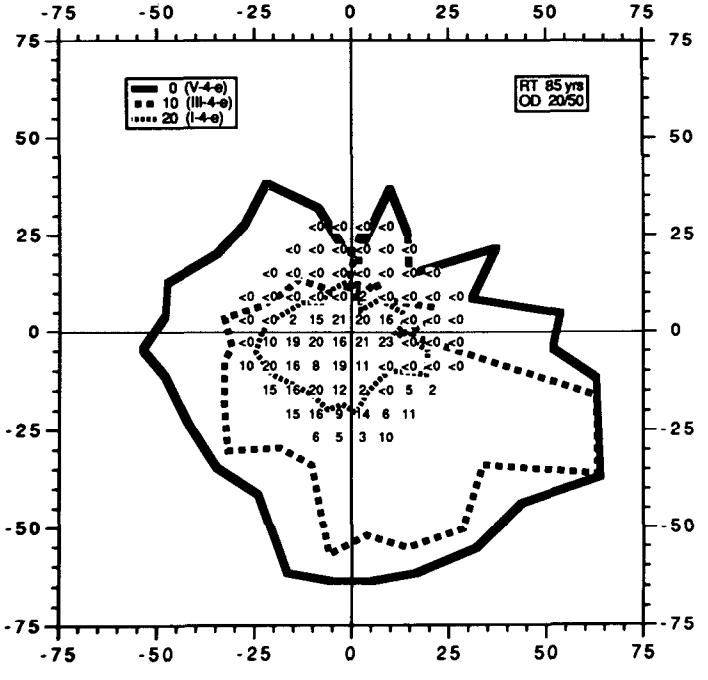

Fig 3 AKP data superimposed on ASP with severe visual field loss superiorly AKP is seen over a larger area than ASP, showing potential for better follow-up in advanced glaucoma.

Fig. 2. The numerical ASP data (shown in Fig. 2 as dB) suggested reduced sensitivity just above the horizontal raphe near the lens rim nasally. The I-4-e and II-4-e AKP isopters show a definite and consistent nasal step, confirming the significance of the mild defect suspected on ASP.

With a severely damaged visual field, many areas may appear blind during ASP. Kinetic isopters often show a larger region of useful vision, as illustrated in Fig. 3. The enlarged test field forms the basis for follow-up which might not be feasible in any other way.

Two theoretical advantages of kinetic perimetry over static were not demonstrated by this work with AKP. A shorter test time was not feasible because of the manual aspects of the protocol. Better definition of isopters than the transition between different shades on the gray scale of ASP was not realized because of problems with this configuration of the AKP strategy.

Material and methods

Twenty-two subjects were recruited from the appointment schedule of our experienced kinetic perimetrist by a technician who did not know the patients or their performance characteristics. The only requirements were a prior examination on the Goldmann perimeter within 30 days and a willingness to serve as a research subject. The patients tested either had glaucoma or were suspected of having it. Some had extensive experience as kinetic field examinees and some did not. Three patients were tested in both eyes, yielding 25 data sets. Patients ranged in age from 38 to 89 years, with a mean of 75.5 ± 11.8 years. There were nine males and 13 females. Three of the patients were of African ancestry and 19 were of European ancestry. One of the patients had hand motion vision at 12 feet, and the remaining 24 eyes had acuities ranging from 20/20 to 20/400, with a mean of 0.51 ± 0.48 log minimum angle of resolution (logMAR). Of the 18 eyes which also underwent ASP, the short-term fluctuation (SF) ranged from 0.85 to 6.08, with a mean of 2.14 ± 1.29 dB.

Automated kinetic visual fields were obtained by technicians who routinely used the AHVFA for ASP but had no experience with kinetic testing. The technicians followed a protocol designed to produce relevant standard isopters; this protocol was changed repeatedly during the study in attempts to optimize the system (Fig. 4A). Each isopter was outlined with the "auto test" option, testing 28 meridia in a pseudo-random order. Data points which were at least 5° inside or outside the expected isopter were retested using "custom test" mode (Fig. 4B). Automated scotoma tests were conducted, using rules for selecting stimulus value and visual field location based on either an ASP printout or on the AKP isopters (Fig. 4C). The rules for use of the static data required a translation of the x-y coordinates from ASP to meridian and offset coordinates (Fig. 4D), and Table 1 for equivalents of dB and Goldmann stimuli.

Comparison of isopters

An isopter is the limit of visibility where a given test object passes from unseen to seen. Isopters gathered on the AHVFA were compared with those obtained on a Haag-Streit Goldmann perimeter in order to determine biologically equivalent stimulus values for the two machines. A number of problems complicated analysis of data gathered within 30°, so statistical analysis was only performed on data outside 30°. The types of problems found are well covered below. Outside 30° we sought full 28 meridian isopters which neither crossed inside 30° nor proved detectable before movement. Of these, we sought AKP data which lay between two manual isopters whose stimulus values differed by no more than 5 dB. One isopter from each of five patients fit these criteria (three were 1-4-e and two were 1-3-e). Linearly interpolating between the manual isopters, we found that on average the stimulus on the Goldmann perimeter was 4.6 ± 0 9 dB less intense than the nominally equivalent stimulus on the AHVFA. Photometric calibration of the background on both machines revealed that the AHVFA was 1 dB dimmer than the Goldmann perimeter, which only partially explains the difference. With the current AHVFA we are unable to calibrate either size or intensity of the test objects.

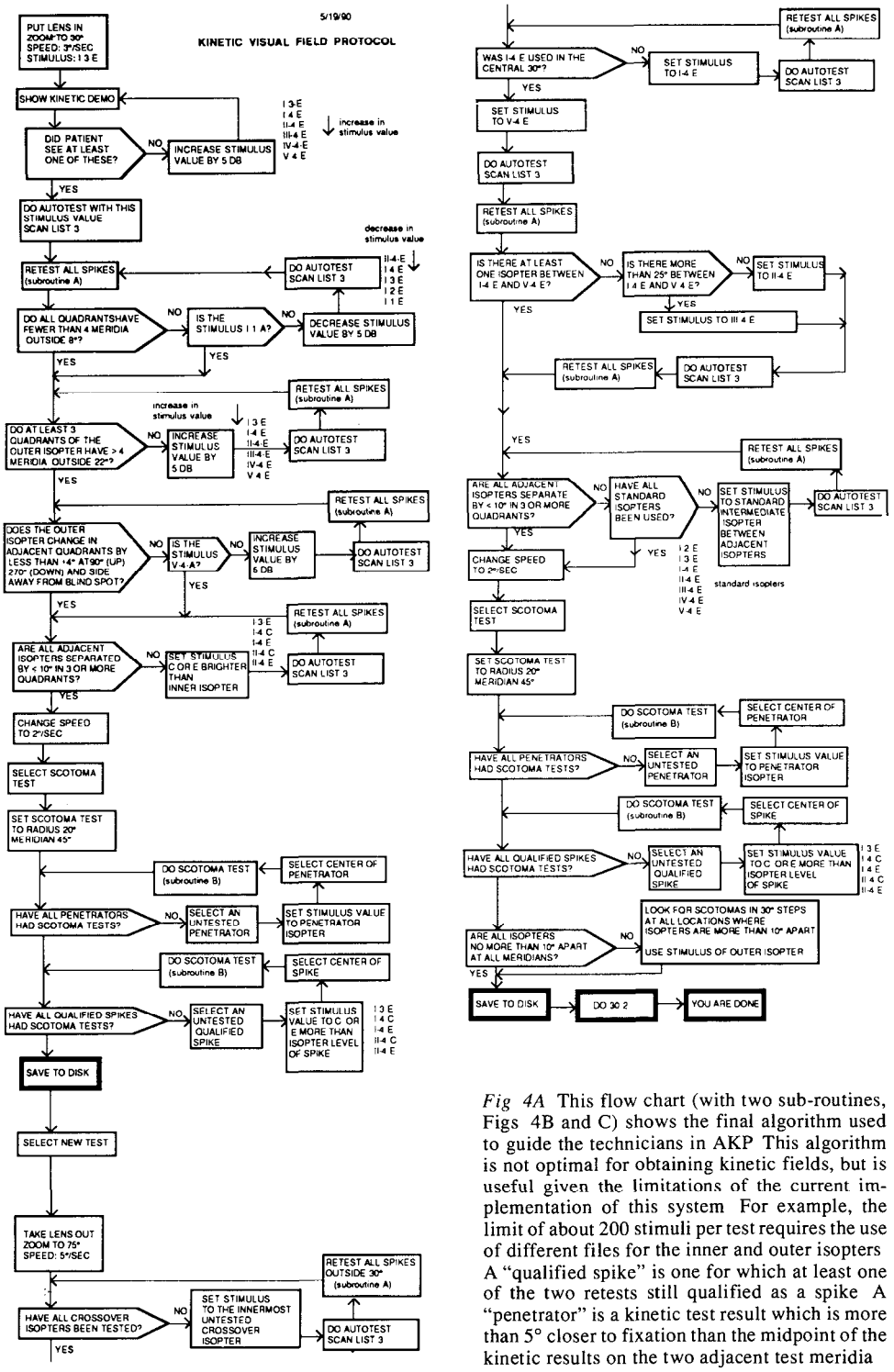

Fig 4A This flow chart (with two sub-routines, Figs 4B and C) shows the final algorithm used to guide the technicians in AKP This algorithm is not optimal for obtaining kinetic fields, but is useful given the limitations of the current implementation of this system For example, the limit of about 200 stimuli per test requires the use of different files for the inner and outer isopters A "qualified spike" is one for which at least one of the two retests still qualified as a spike A "penetrator" is a kinetic test result which is more than 5° closer to fixation than the midpoint of the kinetic results on the two adjacent test meridia

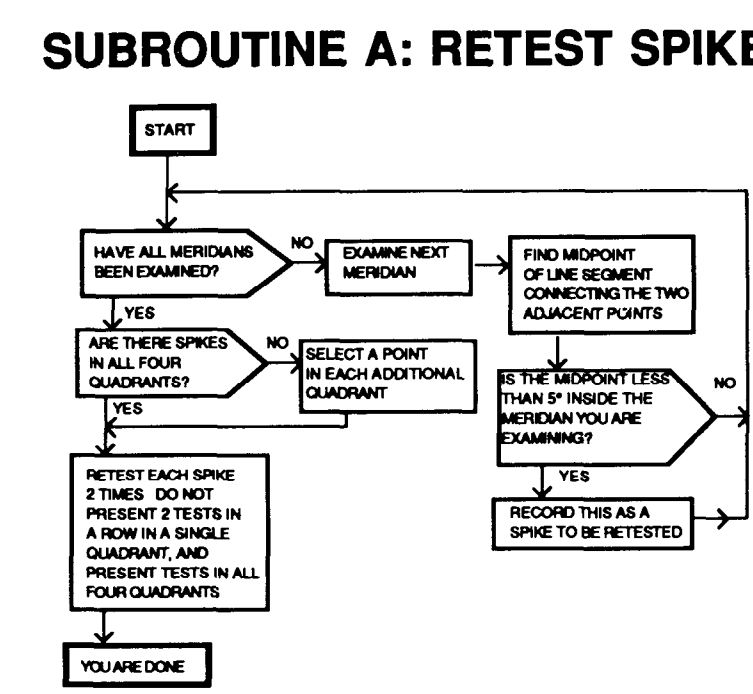

Fig 4B Flow chart for retesting AKP spikes. This sub-routine is a resource algorithm for Fig. 4A.

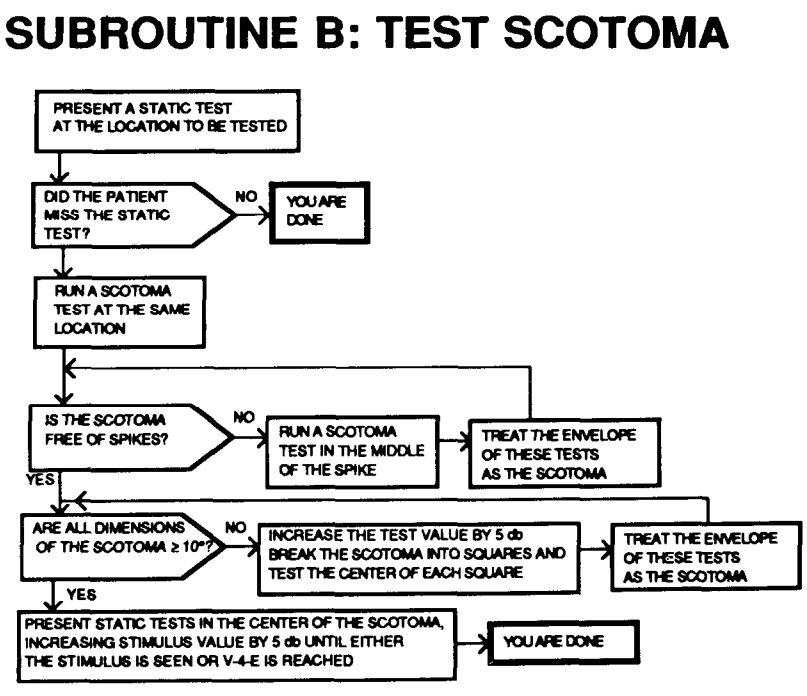

Fig 4C Flow chart for testing a scotoma on the AHVFA This sub-routine is referenced by the primary protocol, Fig 4A.

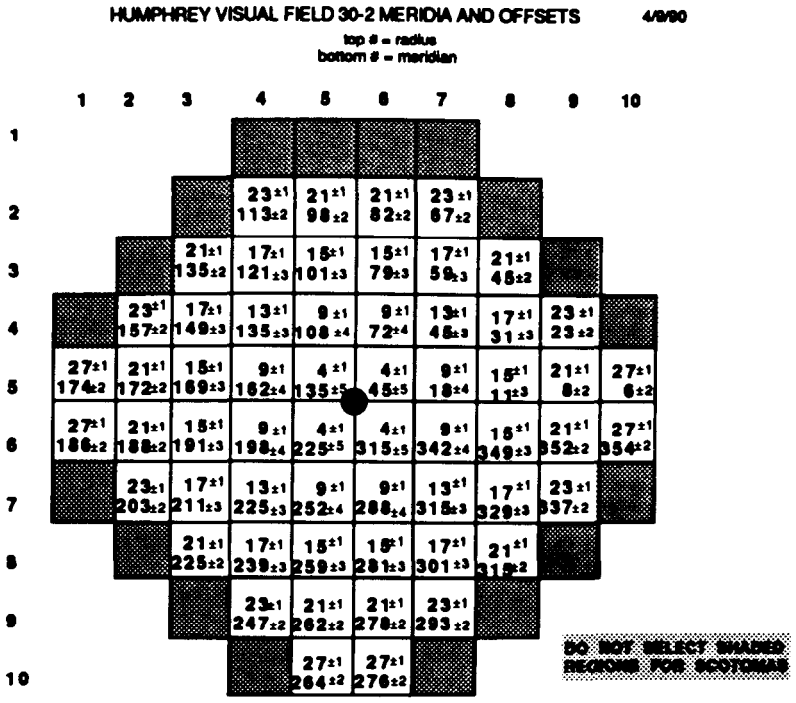

Fig 4D Locations in meridian-offset of the test pattern points in AHVFA's test of the central 30° (30-2) The acceptable variance of one radial degree in any direction is shown with each point on the 6° grid

Problems with current implementation of isopter measurement

The system can be used to measure visual fields in some normal people, but a range of problems with the current implementation make it difficult to test the kinds of isopter which occur in eyes with significant pathology. Visual fields from such diseased eyes are biologically irregular in shape. Also, due to problems with the printout, analysis of the data often requires lengthy reference to the numeric values printout which indicates starting and stopping locations, stimulus values, and visibility (Table 2). Thus, interpretation is usually difficult.

The problems which occurred most frequently are described below, with illustrative examples from four patients. For each patient, side-by-side comparisons are shown of the AKP, manual visual fields from the Goldmann perimeter, the ASP, and some recommended solutions to the AKP problem.

As we prepare to discuss problems and their solutions, we need to define a few terms. A "spike" is a kinetic test result which is more than 5° farther from fixation than the midpoint of the kinetic results on the two adjacent test meridia. A "crossover isopter" is an isopter which lies partially outside 30° and partially within the 30° limit imposed for insertion of a refractive correction. A "distractor" is a stimulus presented solely for the purpose of keeping attention global. For example, if a scotoma is being tested in one quadrant, distractors are often used in other quadrants during manual perimetry to discourage the patient from shifting their direction of gaze.

Spurious spikes

On a normal Goldmann plot, a spike is an indicator of a rare peripheral island of vision. We considered a spike to be spurious when it was not present on repeated retests of the meridian. Spurious spikes were present on 20 out of 25 fields, of which one is shown in Fig. 5A. None are shown in the corresponding Figs. 5B and 5C. Despite retests which proved the spikes were spurious, the printout showed them as part of the isopter, making interpretation difficult. By

Table 2 Numeric values printout. The loci of starting and stopping each stimulus is shown in polar and x-y coordinates as well as stimulus value and visibility in this companion to AKP

MERIDIAN START	DEGREES START	MERIDIAN STOP	DEGREES STOP	X START	Y START	X STOP	Y STOP	STIMULUS VALUE	STIMULUS RESPONSE	TEST TYPE
300	66	300	64	33	-57	32	-55	V 4 E	SEEN	STANDARD
75	55	75	38	14	53	10	37	V 4 E	SEEN	STANDARD
150	67	150	40	-58	34	-35	20	V 4 E	SEEN	STANDARD
30	66	30	43	57	33	37	21	V 4 E	SEEN	STANDARD
315	69	315	62	49	-49	44	-44	V 4 E	SEEN	STANDARD
355	74	355	52	74	-6	52	-5	V 4 E	SEEN	STANDARD
195	75	195	44	-72	-19	-42	-11	V 4 E	SEEN	STANDARD
285	64	285	64	17	-62	17	-62	V 4 E	SEEN	STANDARD
225	69	225	49	-49	-49	-35	-35	V 4 E	SEEN	STANDARD
240	66	240	48	-33	-57	-24	-42	V 4 E	SEEN	STANDARD
265	64	265	64	-6	-64	-6	-64	V 4 E	SEEN	STANDARD
95	54	95	21	-5	54	-2	21	V 4 E	SEEN	STANDARD
105	55	105	33	-14	53	-9	32	V 4 E	SEEN	STANDARD
345	75	345	56	72	-19	54	-14	V 4 E	SEEN	STANDARD
120	57	120	44	-28	49	-22	38	V 4 E	SEEN	STANDARD
330	74	330	74	64	-37	64	-37	V 4 E	SEEN	STANDARD
85	54	85	38	5	54	3	38	V 4 E	SEEN	STANDARD
165	70	165	49	-68	18	-47	13	V 4 E	SEEN	STANDARD
5	74	5	54	74	6	54	5	V 4 E	SEEN	STANDARD
175	74	175	48	-74	6	-48	4	V 4 E	SEEN	STANDARD
275	64	275	64	6	-64	6	-64	V 4 E	SEEN	STANDARD
185	75	185	54	-75	-7	-54	-5	V 4 E	SEEN	STANDARD
45	61	45	21	43	43	15	15	V 4 E	SEEN	STANDARD
210	72	210	48	-62	-36	-42	-24	V 4 E	SEEN	STANDARD
135	62	135	39	-44	44	-28	28	V 4 E	SEEN	STANDARD
255	64	255	64	-17	-62	-17	-62	V 4 E	SEEN	STANDARD
60	57	60	29	29	49	15	25	V 4 E	SEEN	STANDARD
15	70	15	20	68	18	19	5	V 4 E	SEEN	STANDARD
19	72	21	33	68	23	31	12	V 4 E	SEEN	CUSTOM
194	66	193	49	-64	-16	-48	-11	V 4 E	SEEN	CUSTOM
96	51	92	19	-5	51	-1	19	V 4 E	SEEN	CUSTOM
333	74	333	74	66	-34	66	-34	V 4 E	SEEN	CUSTOM
21	70	23	36	65	25	33	14	V 4 E	SEEN	CUSTOM
349	71	349	64	70	-14	63	-12	V 4 E	SEEN	CUSTOM

protocol, the technicians rechecked all spikes twice with intervening distractors, and then drew the isopter by hand through the median of the three values. This greatly reduced the number of spikes and disclosed a few peripheral islands of residual vision. However, the technicians found it difficult to spot all of the spikes because isopter lines are not shown on the screen. In any event, there was no provision for storing the hand-drawn isopter on disc.

Solutions

To eliminate spurious spikes, the software should evaluate each isopter directly after each automated isopter test. Whenever the value for a given meridian is more than 5° peripheral to the midpoint of a line connecting test results on the two adjacent meridia, that meridian should be selected for retest. Each selected meridian should receive two additional presentations in random order, interspersed with other relevant tests of isopter, scotomas, and distractors if needed. The printout should then connect the isopter to the median of the three tests.

Spurious isopters

Isopters represent lines of equal retinal sensitivity. Any time kinetic data points are invalid thresholds or they are joined by lines which obviously cross territory that is significantly more or less sensitive than the threshold line being sought; we have termed the resultant line a "spurious isopter".

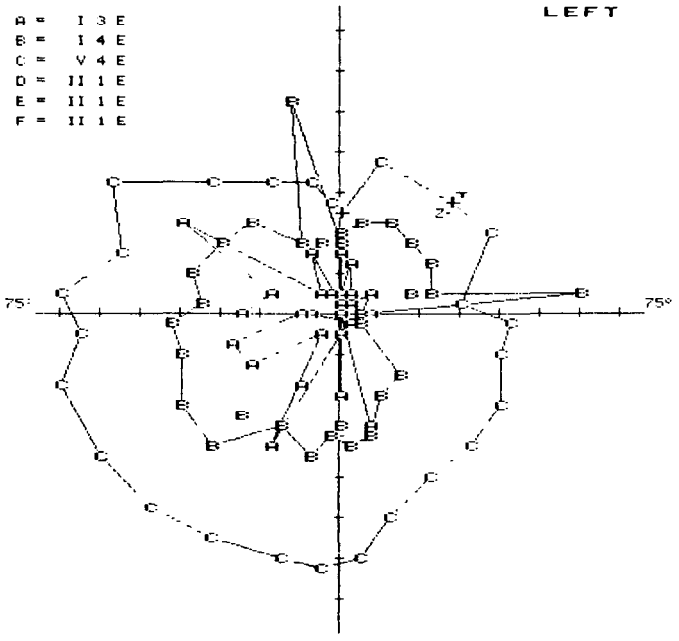

Fig. 5A. Spurious spikes. A spike is a kinetic test result which is more than 5° farther from fixation than the midpoint of the neighboring AKP thresholds. When spikes are retested twice and not confirmed, they are then called spurious.

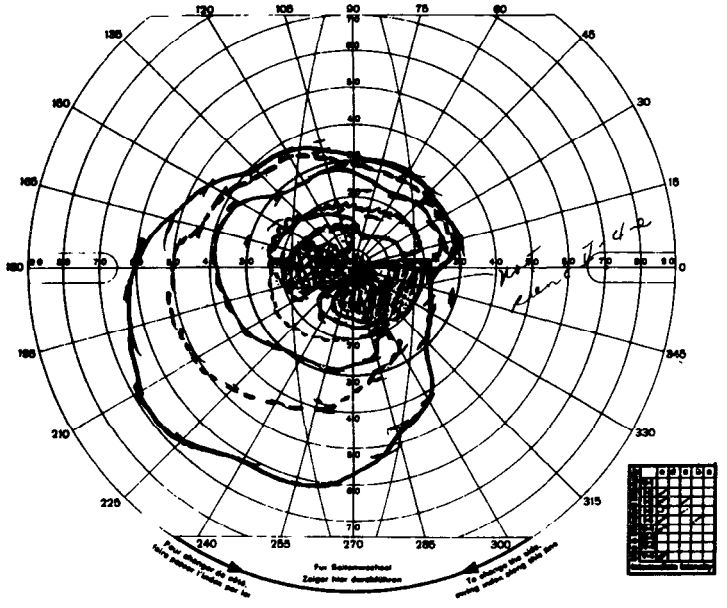

Fig 5B The manual kinetic plot of the eye in Fig. 5A. No spikes are seen in this eye with a significant pericentral defect

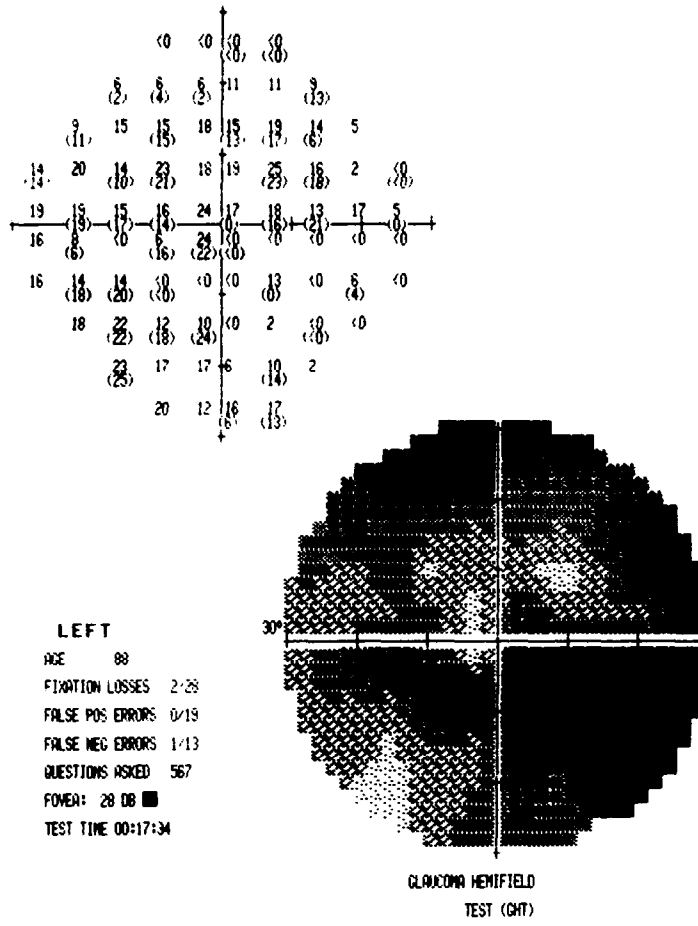

Fig 5C The ASP gray scale and thresholds of the eye in Figs 5A and 5B No spikes are seen but thresholds are high

Spurious isopters #1 crossover isopters

In 20 of 25 visual fields, isolated threshold points within 30° of fixation were connected, ignoring data outside 30° In the numeric output which forms the basis for Fig. 6A, the I-3-e isopter extends outside 30° in many areas as in Figs. 6B and 6C, yet this 30° printout from AKP (Fig 6A) shows the 1-3-e isopter entirely inside 30°

Solutions For the 30° plot, line segments should extend from threshold points toward adjacent threshold locations which are more peripheral than 30°. Fig. 6D is a replot of this patient's I-3-e and I-4-e AKP data

Spurious isopters #2 loci of static suprathreshold stimuli are connected to threshold isopters

In 19 of 25 fields, spurious isopters also arose as lines connecting loci of seen static presentations with nearby kinetic thresholds In Fig. 7A, all the V-4-e data are connected like an isopter, yet 19 of the 28 points were seen before the test moved, so these are loci of seen suprathreshold static stimuli The resultant "isopters" are closer to fixation than expected by Figs. 7B and 7C. In addition, nine static tests were performed in "custom test" mode; these were all seen, yet their loci were connected to what one might presume to be an isopter.

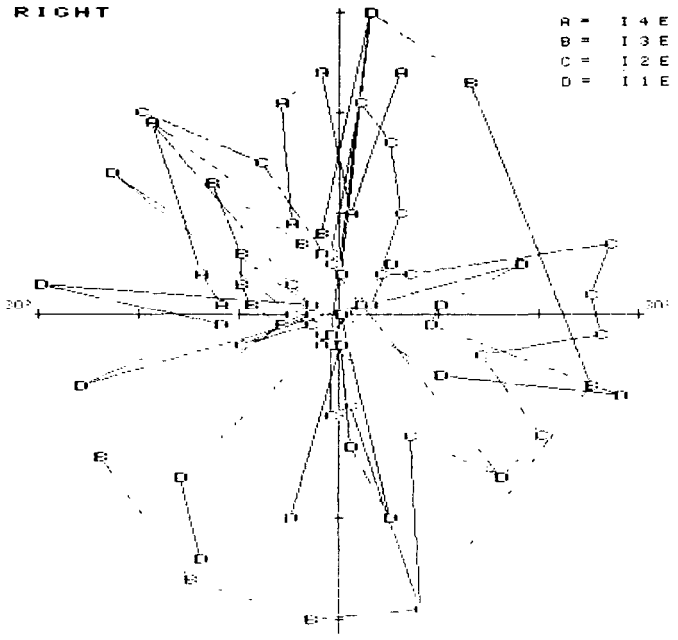

Fig 6A Spurious crossover isopter This AKP plot of the central 30° should extend inside and outside 30° but is shown entirely inside 30° with no indication of the AKP data collected outside the lens limit

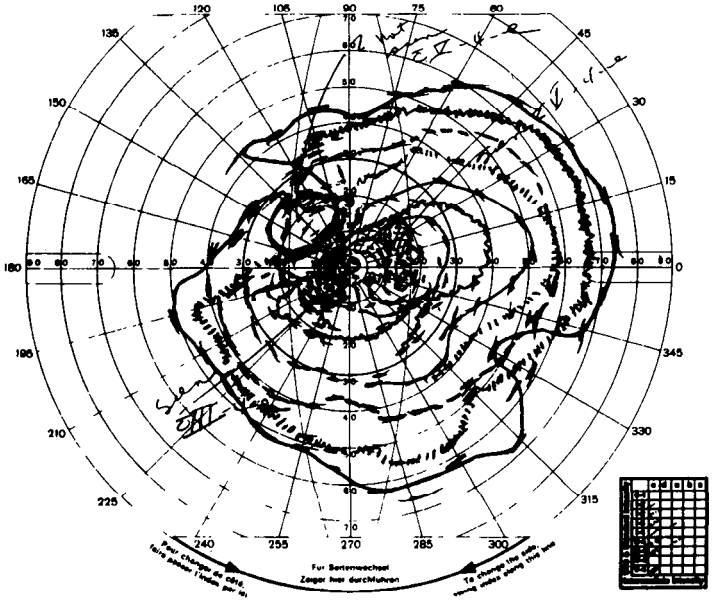

Fig 6B Manual test of the eye in Fig 6A The nominally equivalent isopter is shown well outside 30°, especially temporally and inferiorly

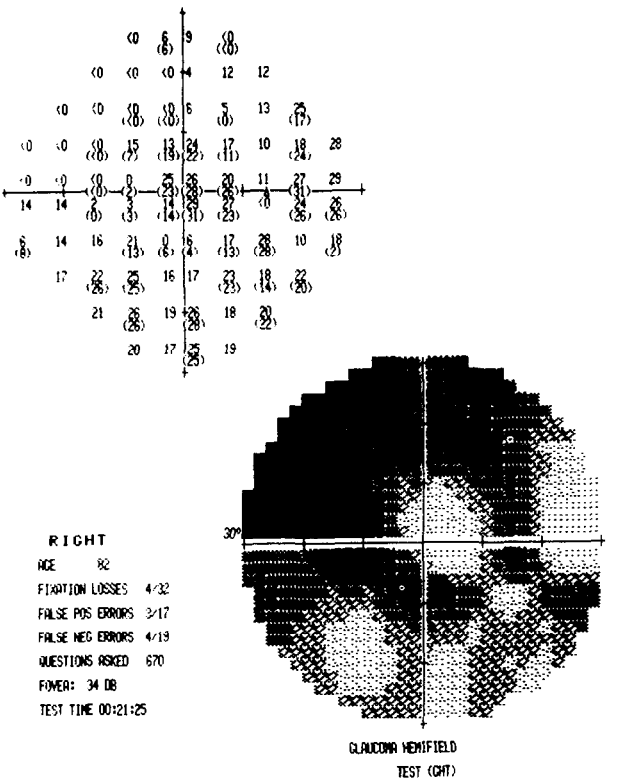

Fig 6C ASP of the eye in Figs 6A and 6B Spotty residual vision does not prove vision extends outside 30° although the temporal island touches the margin solidly.

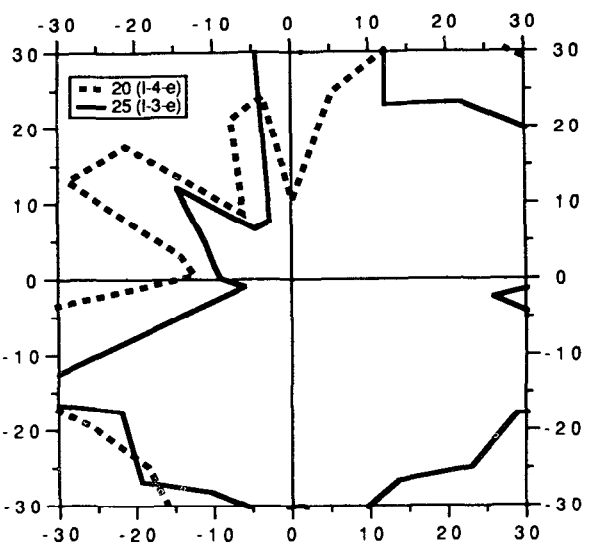

Fig 6D Data from AKP manually replotted from numeric values printout. The inferior and temporal extensions of I-3-e and I-4-e isopters cross over the 30° limit.

Solutions. During AKP, "seen" static tests should be so designated but not connected to threshold points. Unseen static points should automatically be retested and, if confirmed, undergo scotoma testing. Unseen points which are not confirmed need a threshold designation different from "seen" points, but they still should not be connected to the isopter because better vision may surround them. A replot of this patient's AKP data is shown in Fig. 7D.

Spurious isopters #3 · stimuli which pass through the center result in chaotic plots

In 14 of 25 fields, the test object crossed the point of fixation before being seen. Unfortunately, there is no indication of the direction from which the test object was moving except by tedious reference to the numeric values printout. The lines for the isopter plot are drawn from one meridian to the next, resulting in a chaotic arrangement of lines which do not in any way reflect transitions from not seen to seen. In Fig. 8A, many of the test objects passed through fixation before being seen. The speed of test object movement could have influenced this fixation crossing which is relatively rare in manual perimetry, and is certainly not expected in 14 of 25 fields. The Goldmann field (Fig. 8B) and ASP data (Fig. 8C) give a clear picture of this patient's obviously defective visual field, while the AKP printout obscures much of this information.

Solutions. When a stimulus crosses the point of fixation, it should not be connected to points which did not cross the point of fixation. In addition, the printout should indicate the direction from which the unconnected test was moved, either with an additional symbol or by rotating the letter or number. Finally, the speed of test object movement should bear a direct relationship to the distance from fixation. A replot of this patient's AKP data is shown in Fig. 8D.

Additional problems

Scotoma testing

The Allergan-Humphrey kinetic system includes a scotoma test which requires the technician to indicate the stimulus value, the speed of movement, the number of evenly spaced radii to use plus their lengths if never seen, and the location of the potential scotoma. In the hope of evaluating the scotoma test under optimal conditions the technicians used information from an ASP field to guide their selection of stimulus value and test location. Using Fig. 4D, locations were selected for scotoma testing by referring to the ASP To be chosen for scotoma testing, a defect had to be surrounded on at least three sides vertically and horizontally by sensitivities which were at least 5 dB more sensitive than the defect. Table 1 was used to select stimulus values equivalent to 13 dB higher sensitivity than the static threshold, so the stimuli would be well below threshold. When this failed to produce meaningful data, the use of prior ASP data was discontinued and the flow chart (Figs. 4A, B and C) was developed. The scotomas mapped in both ways were generally smaller than those mapped with ASP or Goldmann perimetry in the same locations This may be due to the fact that eight stimuli were automatically presented in sequence, starting from the same location without any possible distractors, a pattern which encourages small changes in fixation to make the stimuli more visible. The scotoma test yielded very little useful information, and was abandoned after 15 fields

Limited number of options

A number of additional options appear quite desirable at this stage. Implementation of many options carries a risk to replicability of test results if all parameters are not stored for use on future tests and the required comparisons. The current implementation deals with isopter irregularities by allowing the technician to delete data points during the test. Since useful information is often embedded in excessive data, none should be discarded. A useful option would be to save all patient responses but only print selected data.

The number of tests/quadrant in the auto test menu is either three or seven per quadrant. Two useful options would be four/quadrant (10°, 30°, 60°, and 80°) and five/quadrant (5°, 25°, 45°, 65°, and 85°).

The maximal number of tests is 202. This means that the auto tests which must start at 30°

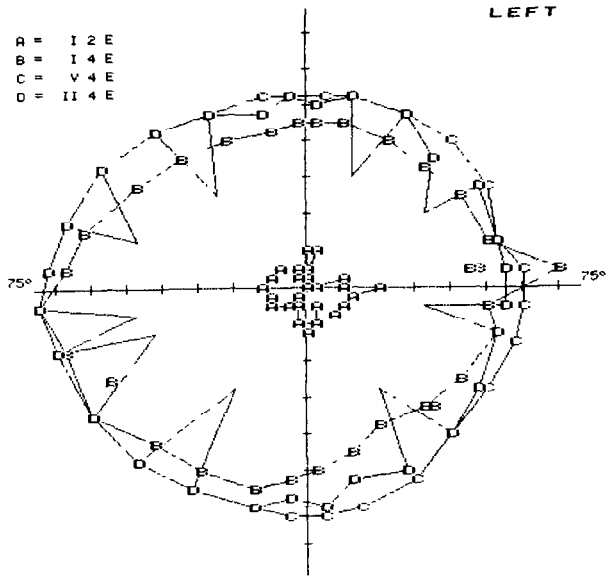

Fig 7A Spurious isopter linking suprathreshold static data to AKP thresholds Two sources of suprathreshold static data contribute to the confusion in this 75° AKP plot of a glaucoma suspect's field. The peripheral tests were usually seen before they moved and static spot testing within the field was always seen.

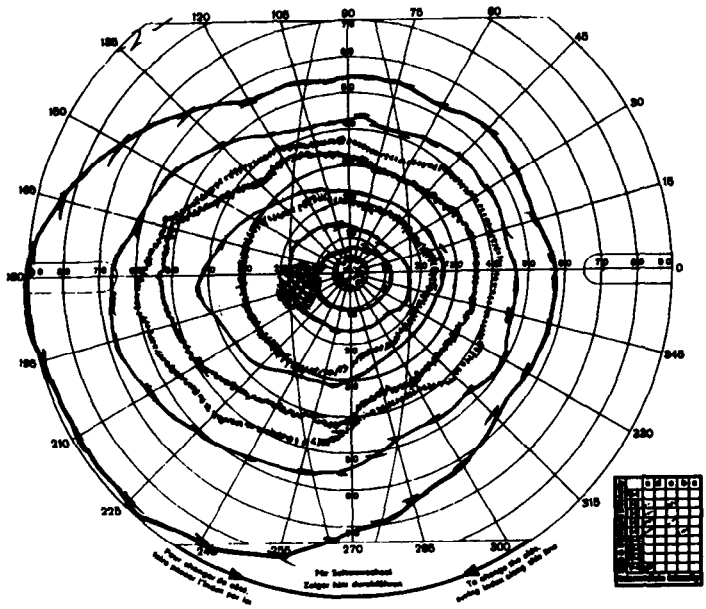

Fig 7B Plot of the field in Fig. 7A on a Goldmann perimeter. The field appears normal.

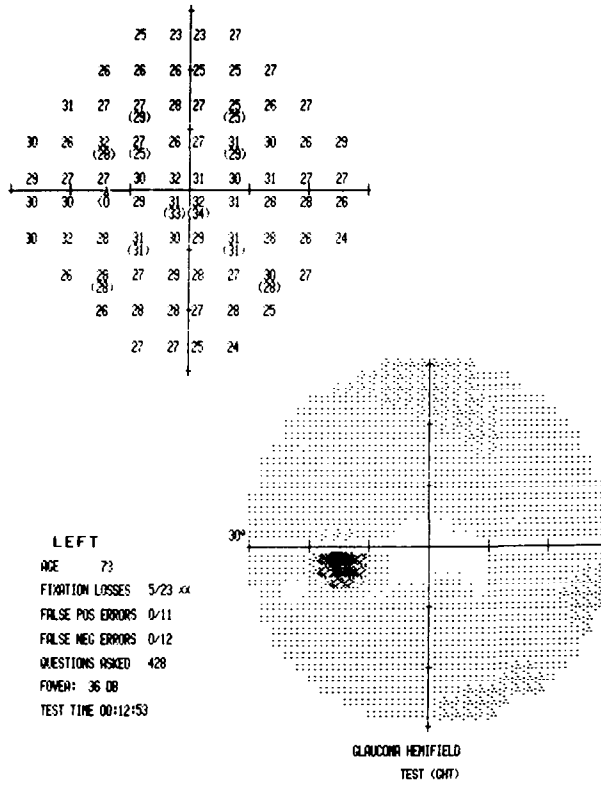

Fig 7C ASP plot of the field in Figs 7A and 7B The field appears normal

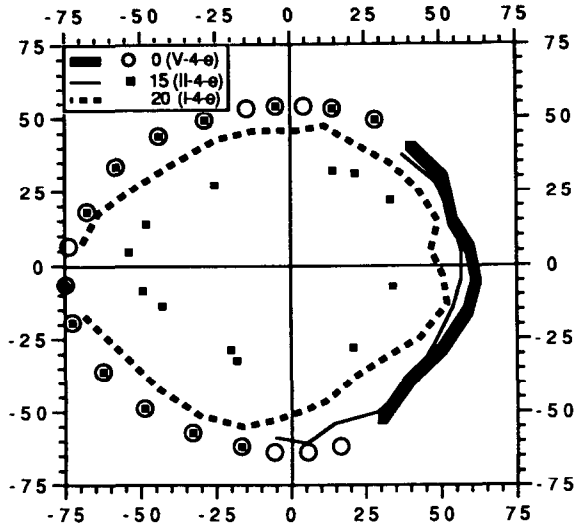

Fig 7D Replot of AKP data from Fig 7A using numeric values printout Static suprathreshold data are not connected to the kinetic threshold data which only occurred nasally to the V-4-e and II-4-e.

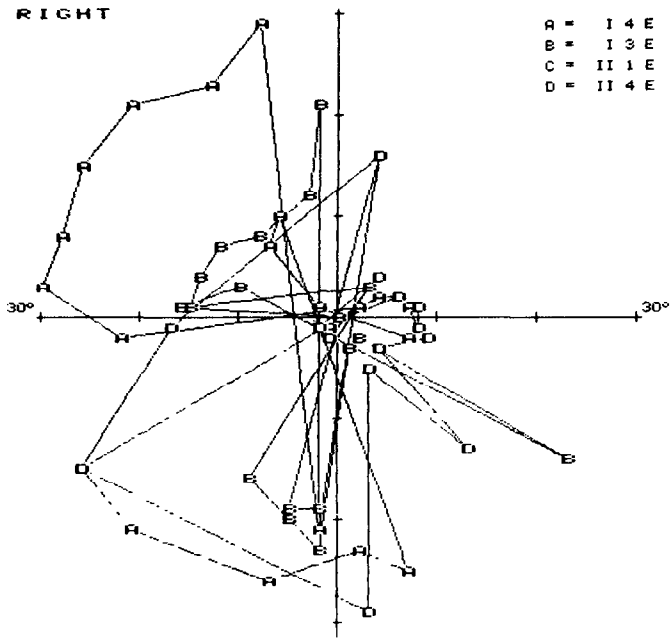

Fig 8A Spurious transcentral isopters This AKP plot of a severely damaged field is chaotic, partly because test objects passed through the center of the field, but mostly because the plotted results do not indicate this fact

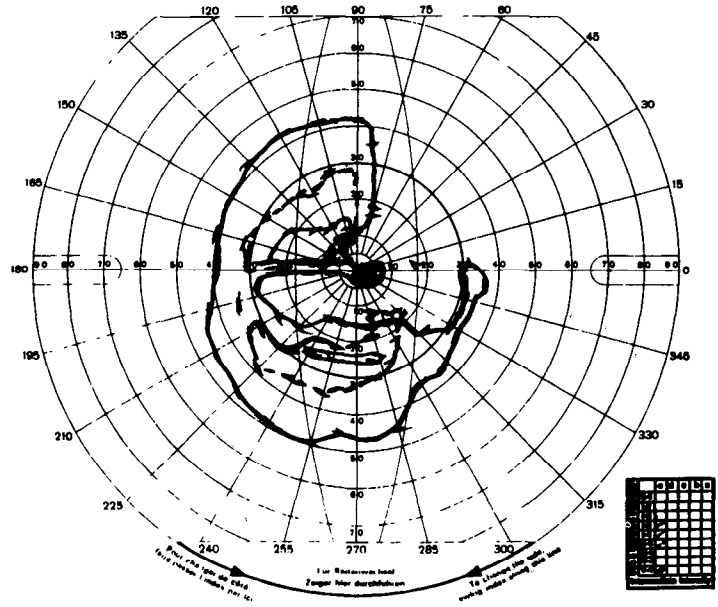

Fig 8B Inferior paracentral arcuate and superior temporal defect as plotted on the Goldmann perimeter This residual rim pattern requires an algorithm other than the simple radial testing currently available on AKP

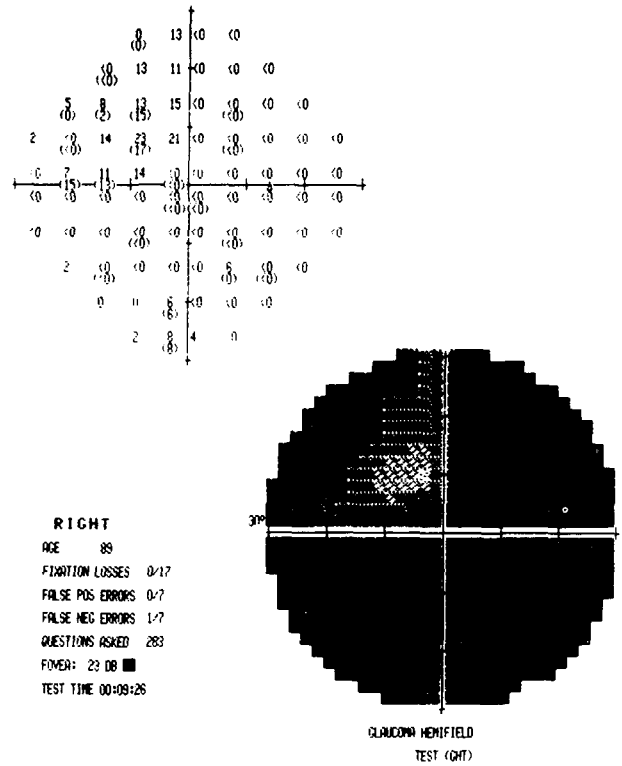

Fig 8C ASP plot of the same field shown in Figs 8A and 8B Severe loss shown in the central field does not hint that the peripheral rim persists

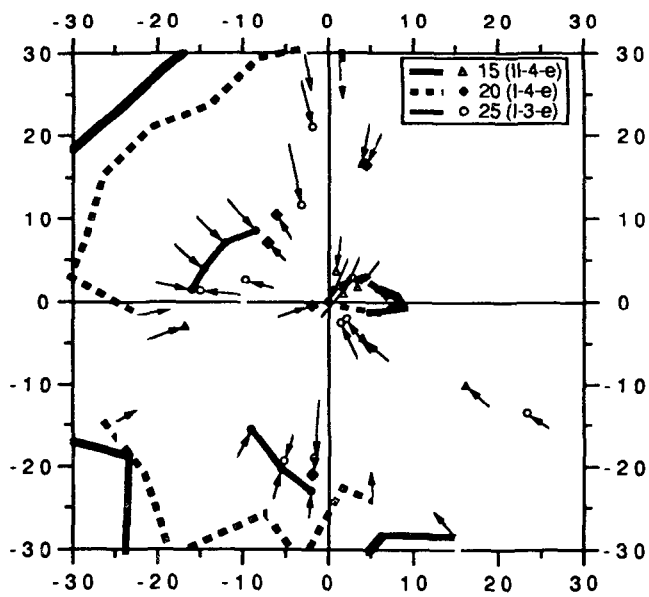

Fig 8D Replotted AKP data from Fig 8A. Inadequate data were gathered for a full exposition of the details but the field of numeric values printout does show similarities to Fig 8B

and those which must start near 75° cannot be measured and stored in a single file. Moreover, crossover isopters which are often of great interest in glaucoma cannot be fully explored without both 30° and 75° plots. The maximal number of tests should be increased. It would also be useful to have the option of merging data sets.

Although the auto test on the AHVFA may be presented in a regular order, we always elected the pseudo-random option. In this mode, stimuli are always presented in the same meridional order, so patients sometimes learn the location of the next expected test. At a minimum, the order should be randomly varied.

There is no capability for manually calibrating spot size and brightness. A menu option for manual calibration would simply turn the test object on or off.

The static test requires too rapid a response for some patients, who say they see the stimulus but their answer is not recorded. A menu-selectable delay between stimulus offset and the end of the time period for the patient's response should be provided for patients with slow reaction times. The labels for the isopters (A,B,C, etc.) are arbitrary, and may be different for each field. This makes printouts hard to decipher. A solution is to have a standard set of labels, such as identifying the isopters by the dB equivalent.

Problems during testing

When static testing reveals a defect, it is difficult to start the scotoma test at that exact location. There should be a method for beginning the scotoma test at selected locations where static tests were not seen.

The lines which connect points on the printout are not shown on the CRT display. This makes it difficult to retest spikes and to compare isopters. The isopter lines for one or two selected stimulus values could be called to the CRT at operator discretion, constantly updated and modified by plotting the median of repeated tests.

Since the kinetic hardware and software were installed, two different formerly reliable AHVFAs purchased at different times and with different options, plus a new third AHVFA have developed an intermittent problem with ASP During the middle of a test, the background light will suddenly turn off for a second and then return The patients often abandon fixation when this happens, thinking the test is over.

If the "return" button is hit instead of "continue testing", all data are lost since the last save. Given the complexity of operating the menus, several data sets were lost this way. Before discarding data the program should provide a warning that the last data set has not been saved, and offer additional options such as saving the data or canceling the termination and continuing the test

The eye monitor is turned off for 20 seconds while preparing an autotest, so fixation may change. After the test is ready there should be a pause while eye monitoring is resumed, and a menu option should begin the test once the eye is centered.

It is not possible to pause during an autotest if the patient needs a short break. For instance, one patient needed to scratch her nose. In addition to "cancel" there should be a "pause" option.

Some patients cannot respond to stimuli greater than V-4-e in the most defective part of their field Subsequent changes in that zone would thus go undetected. Since the AHVFA routinely produces 10 dB greater luminance during ASP, that should be made available as V-5-abcde and V-6- abcde for AKP testing.

Strategic considerations

Keeping attention global

For defects inside the central 30°, test stimuli must be near threshold in the region of the defect, while distractors of the same intensity and size would be well above threshold at other meridia inside the lens rim In manual perimetry this has caused patients to ignore the near-threshold stimuli being used to plot the isopters. The solution is to vary the size, intensity and location of the distractors. In order to keep all stimuli within the lens rim, the stimulus values should be allowed to differ for each quadrant.

For scotoma testing, stimuli should be intermixed from all directions to ensure that stimuli

frequently appear in each quadrant so the patient does not know where to expect the next test. This tends to keep attention global and discourage changes in fixation. To this end, the software could select scotoma candidates as soon as clues to their presence develop, then randomly test all these suspicious areas simultaneously along with the isopters, only using distractors as needed.

It would solve two problems if four, five or six autotests were available per quadrant. The user would then choose different numbers/quadrant when testing successive isopters Pseudo-random tests would appear more random to more patients and suprathreshold tests with multiple stimuli would not superimpose one another in the printout

Crossing the expected isopter perpendicularity

The most reliable data are obtained when transitions from non-seeing to seeing are abrupt. The most abrupt transitions usually occur when the stimulus is moved perpendicularly to the isopter. For many isopters in a normal visual field, radial movements may approximate perpendicular movement, but for pathological fields radial movements may be tangential to isopters near defects, producing unreliable data in regions of great interest. A solution is to use prior data to determine the direction of movement. An iterative procedure which uses the perpendicular bisector of adjacent seen loci to determine the direction of movement may provide better mapping of scotomas and other defects

Using prior information to choose starting locations

The restriction to starting all meridia in the autotest at either 30° or 75° makes it difficult to test crossover isopters and tends to increase the incidence of spurious spikes. For patients with large defects, some quadrants may require more than 30 seconds before the test object reaches the remaining field while other quadrants require a second or less. This decreases reliability and increases patient anxiety. The solution is either to start at a randomly chosen distance 5° to 15° outside the expected isopter, or to allow each quadrant to begin at a user-selectable radius.

Evaluating fixation stability

The simplest method is the Heijl-Krakau technique of testing the blind spot and allowing rejection of unreliable data sets. In order to reduce the rejection of tests with the attendant time, effort, and expense wasted, it would be better to monitor reflections from the eye electronically and have the system stop the procedure and sound a warning when fixation changes The optimal solution would be to use eye-reflection information to adjust stimulus location to compensate for fixation changes.

Using appropriate speeds

The speed should automatically change as a function of distance from the center of the field, decreasing as the stimulus approaches the center. Recommended speeds are 5°/second outside 40°, 4°/second for 30° to 40° eccentricity, 3°/second between 20° and 30°, 2°/second between 5° and 20° as well as within moderate to large scotomas, and 1° per second inside 5° eccentricity and within small scotomas.

Conclusions

- Automated kinetic isopters gathered with the Humphrey Visual Field Analyzer can be valuable additions to static field data, providing a more complete picture of the patient's visual field. Patients with previous ASP experience on the same machine have commented favorably on the new quieter performance of the AHVFA.
- The current implementation has a range of problems which make it difficult to use the printed output.
- The current implementation has a limited number of options and a range of operational

problems which make it difficult to gather complete sets of isopters.
- The current implementation is not useful for plotting scotomas, because its sequential radial presentation, starting from a single location without the possibility of distractors, attracted the patient's attention to the area and tended to generate ovoid data.
- The strategic considerations listed above should be implemented in future systems if results are to approximate those of an experienced kinetic perimetrist.
- The criticisms and suggestions point the way for any manufacturer to improve if not perfect a fully automated system for kinetic perimetry.

Glaucoma

Computerized visual fields in pediatric glaucoma

Roberto Sampaolesi and Javier Fernando Casiraghi

Department of Ophthalmology, University of Buenos Aires, Faculty of Medicine, Parana 1239-1° A, 1018 Buenos Aires, Argentina

Abstract

The authors studied the visual fields of 46 eyes divided into three groups: congenital glaucomas operated on only once, congenital glaucoma requiring reoperation, and other pediatric glaucomas including late congenital glaucoma, Rieger's syndrome and juvenile open angle glaucoma Patients' ages at the time of visual field examination ranged from six to 21 years Program G1 of the Octopus 2000 perimeter was used for testing, and the results were analyzed with Octosmart. Visual field defects were limited to diffuse loss of sensitivity. It is possible that this kind of defect was caused by the action of the intraocular pressure on the axoplasmic flow

Material and methods

Forty-six eyes of 25 patients from three pediatric glaucoma groups were studied (Table 1):
- *Group 1* · congenital glaucomas operated on only once (19 eyes);
- *Group 2*. congenital glaucomas requiring reoperation (11 eyes);
- *Group 3* other pediatric glaucomas (16 eyes).

Table 1

Group	*No of eyes*	*Males*	*Females*	*Bilateral*	*Unilateral*	*Visual fields performed at age*
1	19	12	7	14	5	6-18 years
2	11	9	2	4	7	10-21 years
3	16	4	12	16	–	8-17 years
Total	46	25	21	34	12	6-21 years (mean 11 9 years)

Groups 1 and 2 consisted of pure congenital glaucomas without any other ocular or somatic abnormalities. All surgery was performed before patients reached two years of age

Group 3 consisted of ten eyes with late congenital glaucoma, two eyes with Rieger's syndrome with glaucoma, and four eyes with open-angle glaucoma in childhood[1,2]

The visual fields were examined with the Octopus 2000 perimeter, using both phases of program G1[3,4], and analyzed with Octosmart including the Bebie curve[5]. Visual field examinations were performed between the ages of six and 21 years (X=11.9 years). In order to minimize learning effects, the number of visual fields performed was between two and five per eye[9]

The intraocular pressure was measured with the Goldmann applanation tonometer, with or without general anaesthesia, according to the patient's age[6]. Axial lengths were measured by means of the Kretz Echographer 7200 MA and the Sonokretz PR 400 FS using the immersion technique[7,8]. Visual acuity was measured using Snellen optotypes following cycloplegic refraction.

Analysis of variance including the following elements was performed with both parametric and non-parametric tests: best corrected visual acuity in decimal scale, refraction, corneal diameter, axial length, mean defect (MD) and corrected loss variance (CLV), and a reliability factor lower than 10.

The relationship between the two visual field indices (MD and CLV), axial length, visual acuity and refraction was studied statistically. The visual fields were analyzed with Bebie's

Perimetry Update 1990/91, pp 455-464
Proceedings of the IXth International Perimetric Society Meeting,
Malmö, Sweden, June 17-20, 1990
edited by Richard P Mills and Anders Heijl

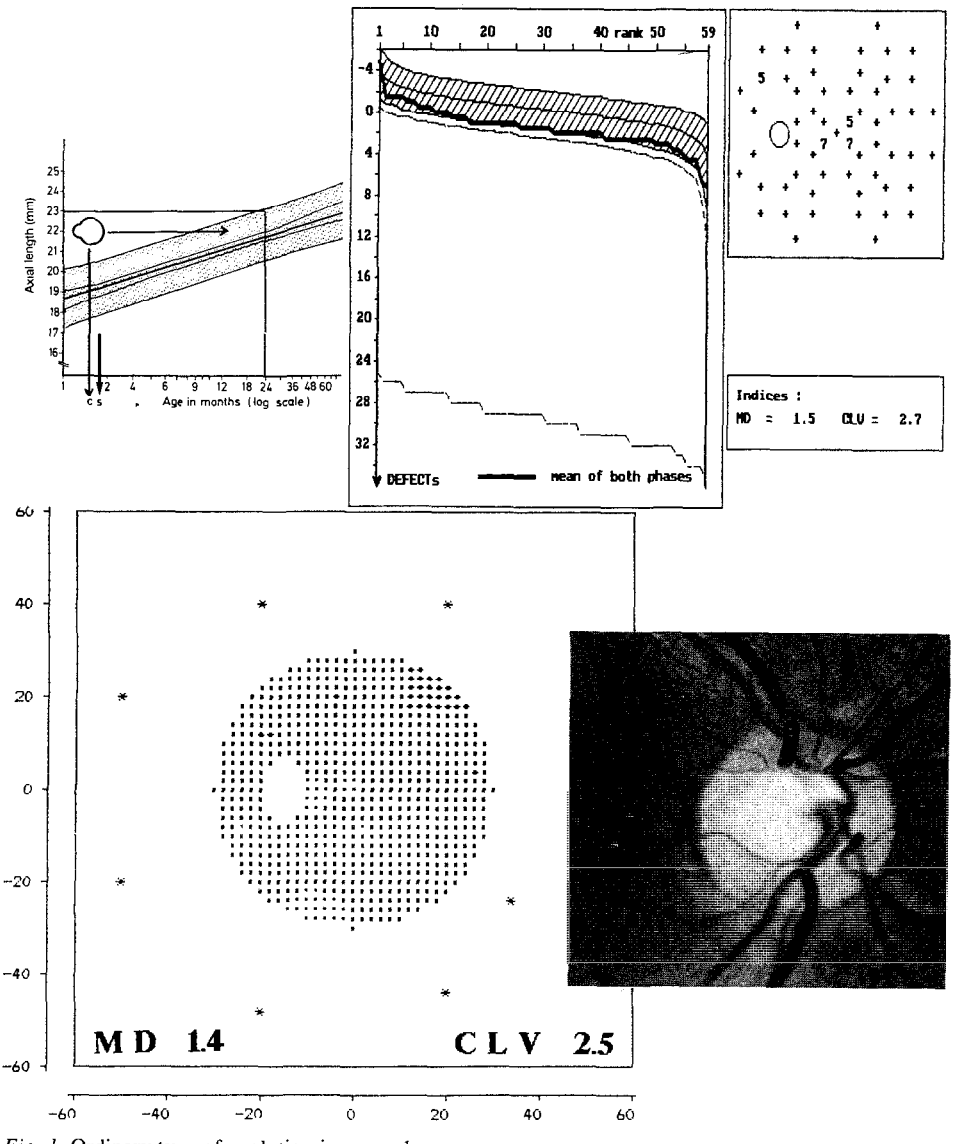

Fig 1 Ordinary type of evolution in group 1

cumulative frequency curve, and classified as diffuse, scotomatous or combined (diffuse plus scotomatous) loss[5]

In order to evaluate the normal threshold in the age group of ten to 20 years[10], we performed both phases of program G1 on ten young normal subjects with a visual acuity of 1.0, axial length between 23.50 and 24.50, normal diurnal pressure curve, who had no ocular or associated systemic pathology.

Results

Group 1

Patients with congenital glaucoma requiring only one operation generally presented within the first six months of age. They were brought to the ophthalmologist as soon as symptoms appeared,

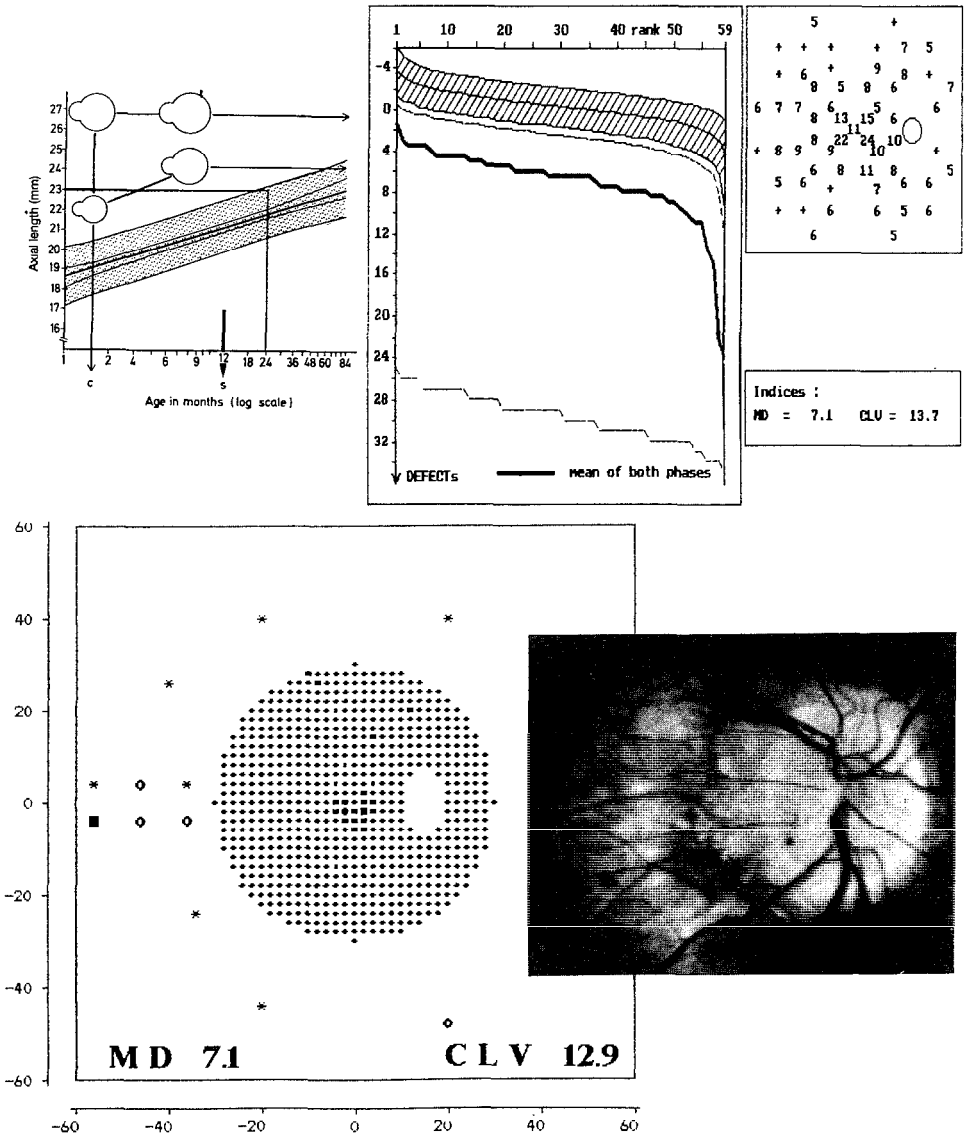

Fig 2 Special type of evolution in group 1 presenting a macular scotoma overlapped by a uniformly diffuse defect

and the time between the initial consultation and surgery was very short, only days to a week

The prognosis in these cases is very good when the surgery normalizes the intraocular pressure. The eye stops enlarging, the optic disc is normal, the visual acuity is good, and the visual field has a low degree of defect[1,2] (Fig. 1)

Other cases in group 1 were excluded from the statistical study because of probable macular abnormalities. These cases were of two clinical types. One type was congenital glaucoma presenting late to the ophthalmologist when the eye was already enlarged with an axial length of over 26 mm. The other type had a long interval between the initial consultation and the surgery during which the eye continued to enlarge. When we examined these patients later, between the ages of ten and 17 years, we found a normal disc, visual field with central scotoma and a diffuse sensitivity loss, poor visual acuity, no binocular vision, and no stereopsis (Fig. 2). The macula showed an altered or no foveal reflex, and the perifoveal reflex was abnormal and severely altered. Sometimes there was a posterior staphyloma[1,2] or a myopic crescent

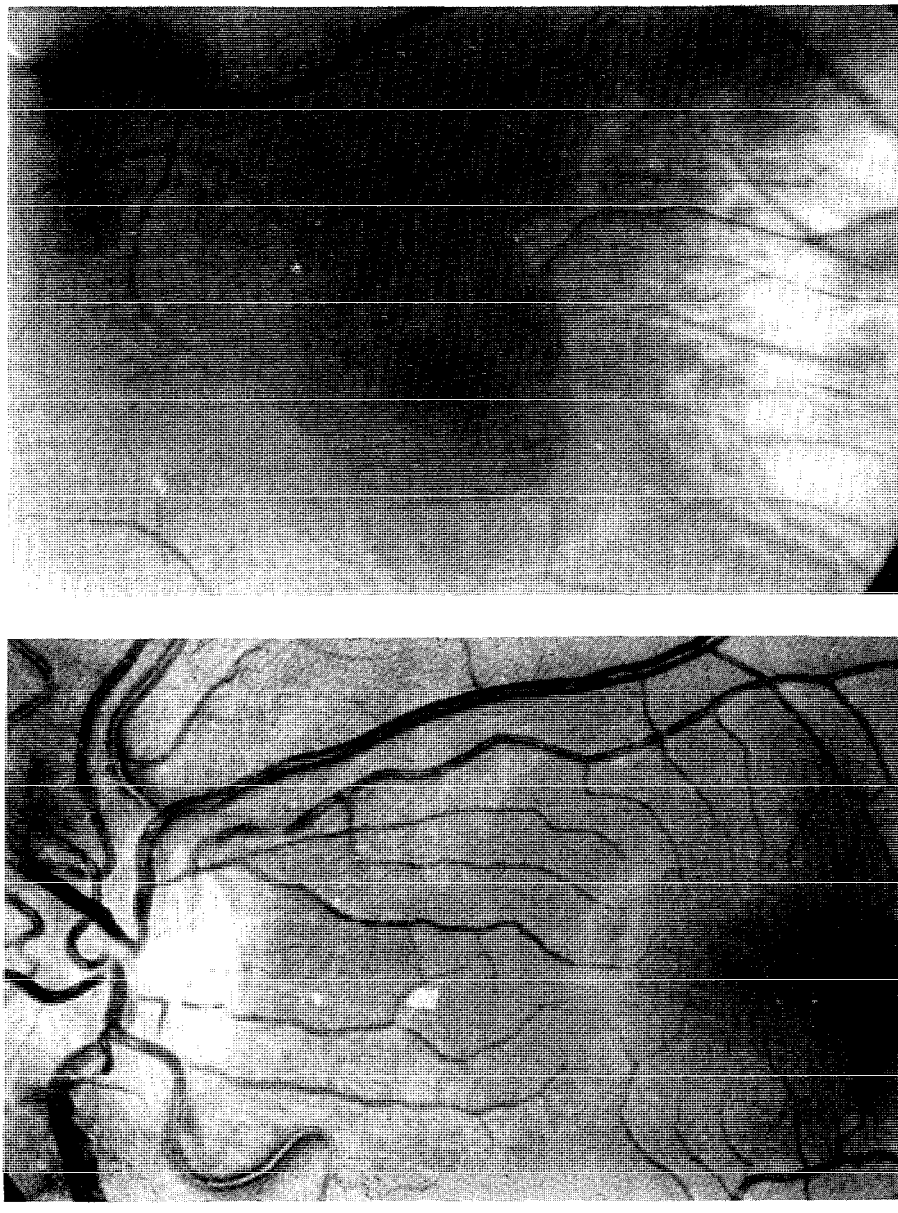

Fig 3a In the upper photograph the macular alteration corresponding to the visual field with macular scotoma can be observed In the lower photograph the normal macula of the contralateral eye can be observed

Group 2

Patients with congenital glaucoma requiring more than one operation, even though diagnosis and initial surgery were carried out very early, did not have prompt normalization of intraocular pressure. The length of the eye continued to increase, and the optic disc became cupped (Fig. 3).

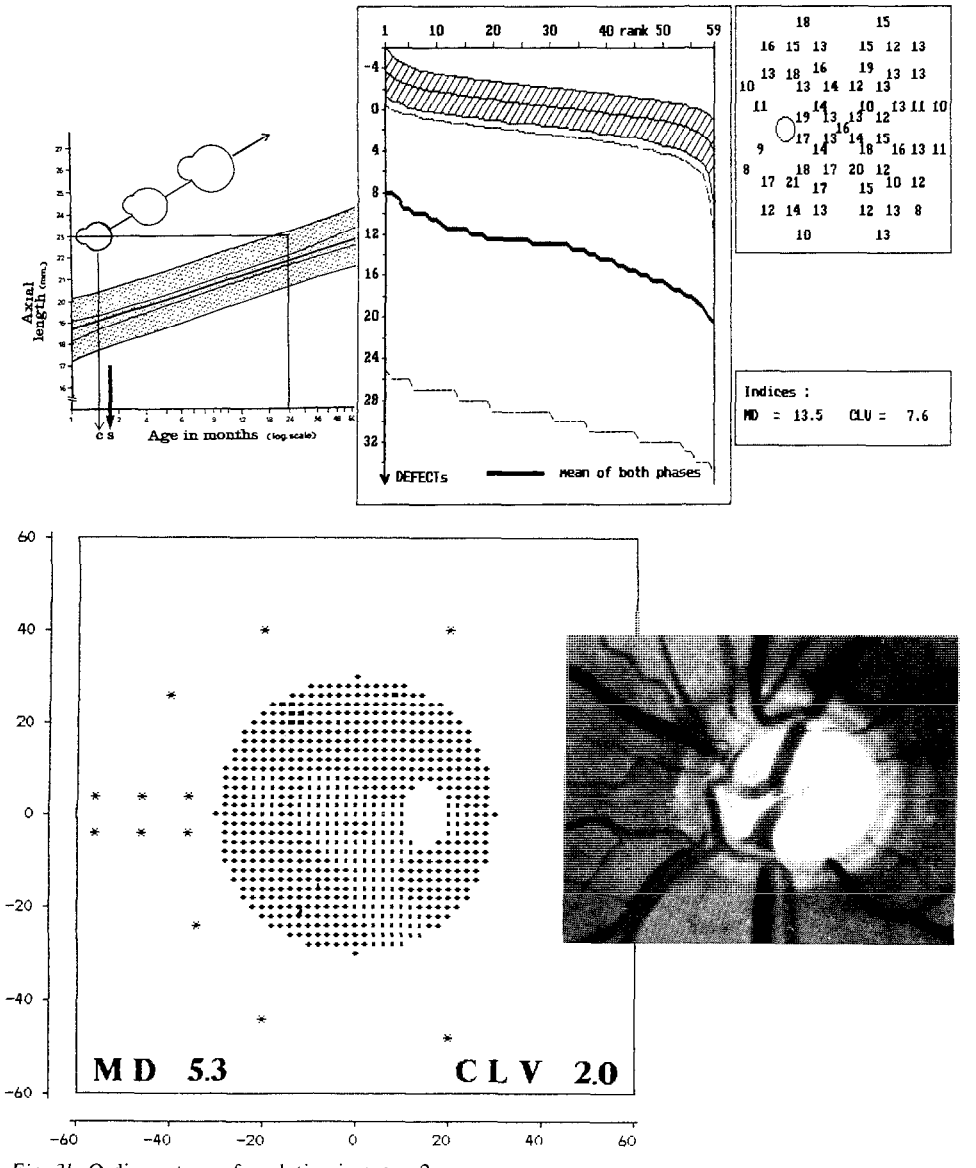

Fig 3b Ordinary type of evolution in group 2

Group 3

Children were over four and a half years of age when late congenital glaucoma, Rieger's syndrome, or open-angle glaucoma were detected. It is important to point out that four and a half years is a key age, because up to that point the eye is elastic and enlarges, while after that age this is no longer the case[7,8]. In these patients the axial length is normal, unlike the cases in groups 1 and 2.

The results of the visual fields of the 20 eyes of ten young normal subjects aged between ten and 20 years showed a mean sensitivity of 28.1 dB ±0.73.

These results are comparable to those in the Octopus normal database for the age group of 20-30 years which showed a mean sensitivity of 29.6 dB ±2.0[4,10].

The visual field results of the 46 eyes with pediatric glaucoma were as follows:

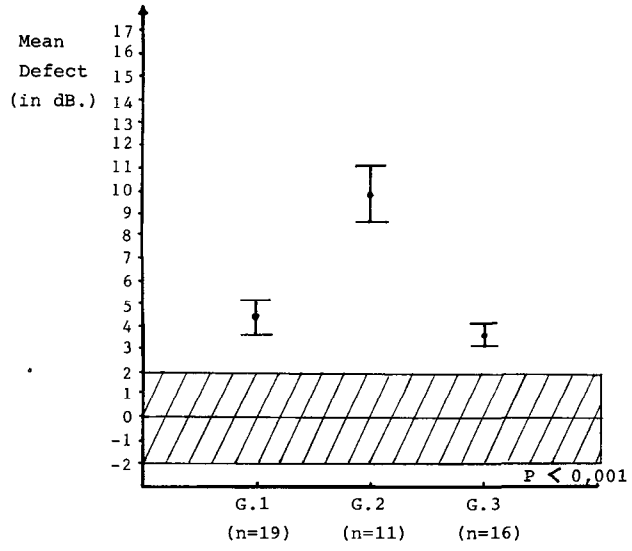

Fig 4 Mean defect.

Group 1 (19 eyes)

The average MD was 4.30 dB (standard error (SE) ±0.73) (Fig. 4); the average visual acuity (VA) was 0.71 (SE ±0.07) (Fig. 5). The average myopia was -3.03 D (SE ±0.95) (Fig. 6), and the average axial length was 25.02 mm (SE ±0.47) (Fig. 7). 36.8% (seven eyes) had tears in Descemet's membrane. The correlation between VA and MD was moderate (r = -0.63) and statistically significant (p<0.01).

The correlation between axial length and refraction is low due to the emmetropization process, which is observed in eyes with congenital glaucoma[7].

Five eyes (26.3%) out of 19 had a normal VF (MD between -2 and +2 dB)[11], a VA of 1.0, and were emmetropic with a normal axial length In a further four eyes VA was also 1.0, but VF showed an increased MD, but not CLV. The average MD for these eyes was 4.5 dB, and three of these eyes were emmetropic

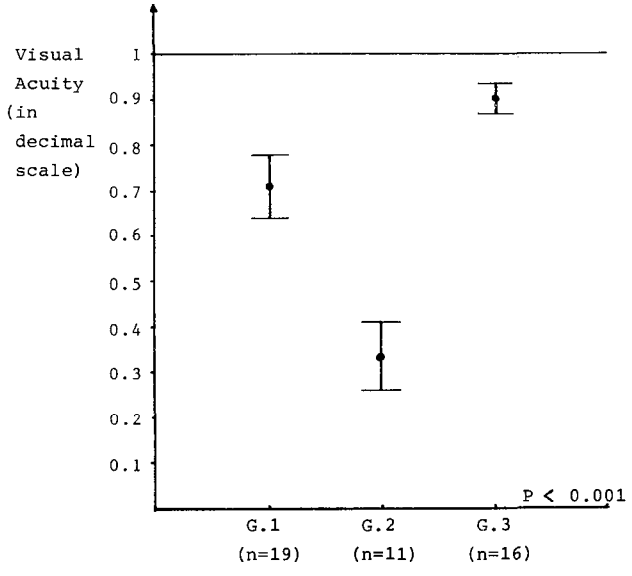

Fig 5 Visual acuity.

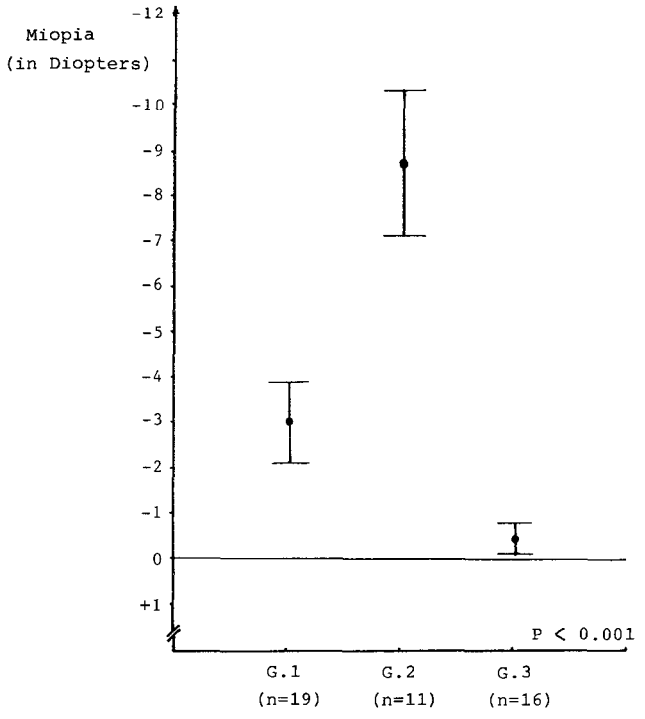

Fig 6 Refraction

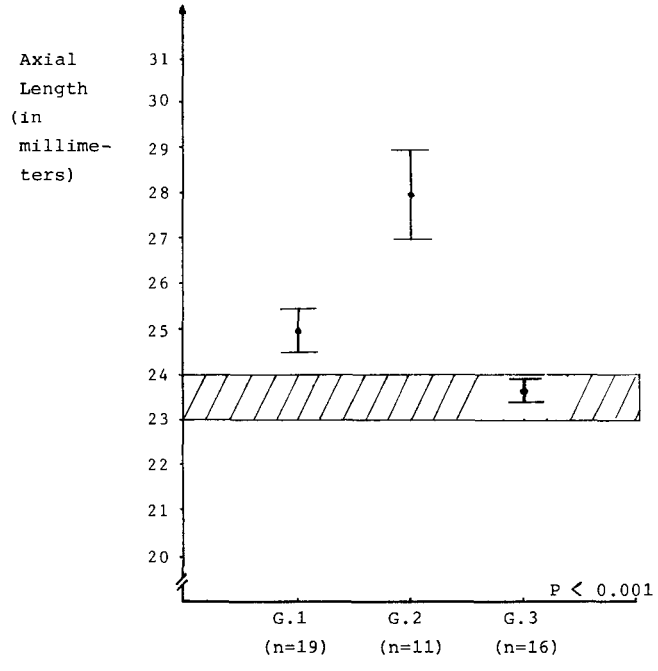

Fig 7 Axial length.

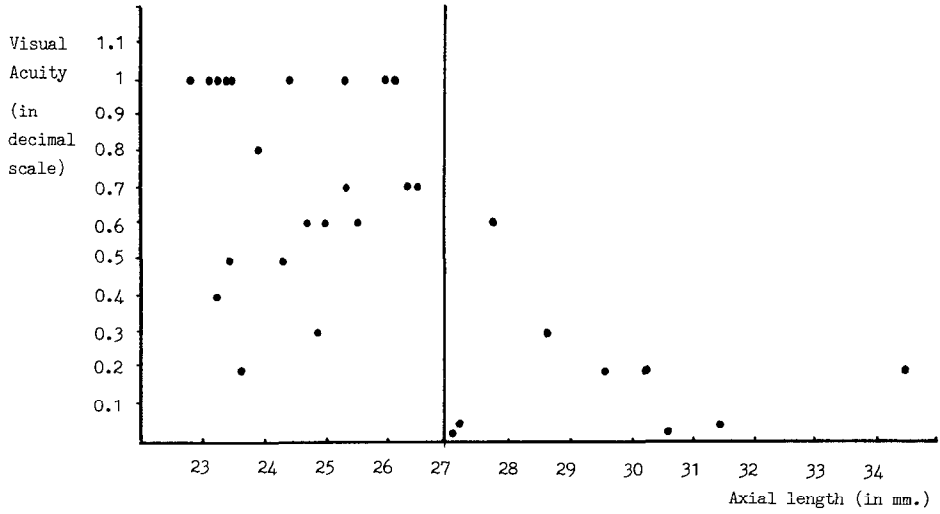

Fig 8 Relation: visual acuity - axial length

The remaining ten eyes presented a VA ranging between 0.7 and 0.2 ($\bar{X}$: 0.45), myopia between 0 and -13 D ($\bar{X}$: -5.42 D), and an axial length between 23.23 and 30.23 mm ($\bar{X}$: 25.74 mm).

Fourteen eyes out of 19 (73.7%) presented a diffuse sensitivity loss. In two out of 14 eyes, uniform diffuse depression was overlapped by a localized defect. These two cases presented with endothelium and central Descemet tears. We presumed this to be the cause of the defect and of the low VA (0.4 and 0 2)

Group 2

This group comprised 11 eyes which needed reoperation because, despite the initial surgery, the axial length continued to grow and the IOP failed to remain regulated.

The mean MD was 9.95 dB (SE ±2 29) (Fig. 4). The average VA was 0.33 (SE: ±0 08) (Fig. 5). The average myopia was -8.72 D (SE: ±1 63) (Fig 6), and the average axial length was 28.03 mm (SE: ±0.94) (Fig 7).

Seven eyes out of 11 had endothelium and Descemet tears (63.6%). All 11 eyes showed an increased MD: between 2 8 and 19 dB ($\bar{X}$: 9.95 dB), while the CLV was not increased Only in one eye with an axial length of 31 45 mm, myopia of -15 D, and macular alteration with poor vision (0.05), was a localized defect found in addition to diffuse loss of sensitivity. The VA varied between 0.7 and 0.025 D ($\bar{X}$: 0 33 D)

In this group of 11 eyes, the negative correlation between MD and VA was high (r = -0.80) and statistically significant (p<0.01).

Unlike group 1, in group 2 the correlation between axial length and refraction was high (r = -0.85), due to the fact that in this group the emmetropization had failed to compensate for the increased axial length ($\bar{X}$: 28.03 mm)[7].

As reported by Vidic and Lerchner[12], all eyes in this group with an axial length of over 27 mm, presented with a VA below 0.2 (Fig. 8).

Group 3 (16 eyes)

In these eyes congenital glaucoma appeared after four to five years of age, when the eye is no longer distensible[7,8]; therefore, the axial lengths were generally normal: $\bar{X}$ AL: 23.67 mm (SE ±0.21) (Fig. 7); the average VA was 0 90 (SE +0.03) (Table 5), and the average refraction was -0.31 D (SE ±0.22) (Fig. 6). None of the 16 eyes had Descemet tears

In three of the 16 eyes, VF was normal (MD: between +2 and -2 dB), VA was 1.0, and the refraction was emmetropic.

However, 13 of the 16 eyes (81.2%) presented with a diffuse defect of the VF (MD between 2 3 and 7 2 dB, $\bar{X}$: 4.44) (Fig 4).

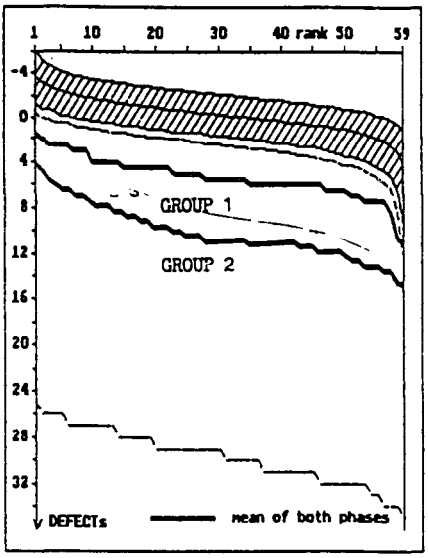

Fig 9 Cumulative curve type for groups 1 and 2: diffuse sensitivity loss

Discussion

It should be noted that, in eyes which were poorly or highly damaged by congenital glaucoma, we found no localized defects (scotomas) All the defects which were found were diffuse (Fig. 9).

It can be speculated that the increased IOP in a child's eye, whose vascular system is elastic and healthy, would only have an effect on the axoplasmic flow and would cause a diffuse defect in the differential light sensitivity.

Acknowledgement

We would like to thank Dr. V Castiglia, pediatrician and biostatistician, who carried out the statistical analysis

References

1 Sampaolesi R: Congenital glaucoma: long-term results of surgery In: Glaucoma Update III, pp 154-161 Berlin/Heidelberg/New York: Springer 1987
2 Sampaolesi R: Congenital glaucoma: long-term results after surgery Fortschr Augenheilk 85:626-631, 1988
3. Flammer J: The Octopus glaucoma G1 program Glaucoma 9:67-72, 1987
4 Flammer J: The concept of visual field indices Graefes Arch Ophthalmol 224:389-392, 1986
5 Bebie H, Flammer J, Bebie T: The cumulative defect curve: separation of local and diffuse components of visual field damage Graefes Arch Ophthalmol 226:9-12, 1989
6 Sampaolesi R, Reca R, Armando E: Normaler intraocular Druck bei Kinder bis zu 5 Jahren mit und ohne Allgemeinnarkose: Seine Wichtigkeit für die Frühdiagnose des angeborenen Glaukoms Glaucoma Symposium Würzburg, Stuttgart: Ferdinand Enke Verlag, p 278, 1986
7 Sampaolesi R: Ocular echometry in the diagnosis of congenital glaucoma Doc Ophthalmol Proc Ser 29:177-189, 1980
8 Sampaolesi R: Ocular echometry and the diagnosis of congenital glaucoma and its evaluation In: Glaucoma Update II, pp 175-184 Berlin/Heidelberg/New York: Springer 1983
9. Wild JM, Dengler-Harles M, Searle AET, O'Neill EC, Crews SJ: The influence of the learning effect on automated perimetry in patients with suspected glaucoma Acta Ophthalmol 537-545, 1989

10. Haas A, Flammer J, Schneider U: Influence of age on visual fields of normal subjects Am J Ophthalmol 101:199-203, 1986
11 Heijl A: Lack of diffuse loss of differential light sensitivity in early glaucoma. Acta Ophthalmol 64:353-360, 1989
12 Vidic B, Lerchner J: Biometrische Langzeitergebnisse bei Glaukom in Kindersalter Fortschr Augenheilk 87:25-27, 1990

The relationship of peripheral vasospasm, diffuse and localized visual field defects, and intraocular pressure in glaucomatous eyes

Jody R. Piltz, Stephen M. Drance, Gordon R. Douglas and Frederick S. Mikelberg

Department of Ophthalmology, The University of British Columbia, Vancouver, British Columbia, Canada

Introduction

Increasing evidence has identified vasospasm as one of the risk factors in the development of glaucomatous optic nerve damage. In 1985, Corbett and Phelps noted a high frequency of migraine in patients with low tension glaucoma (LTG) compared with controls[1,2]. Drance and coworkers measured fingertip bloodflow using a laser Doppler flow meter in LTG patients with and without a history of migraine, and noted vasospastic tendencies in LTG patients even in the absence of a migrainous history. Vasospasm in the fingertip was present in approximately 65% of LTG patients without migraine, and in 26% of non-glaucomatous, non-migrainous individuals[3].

Reversible and irreversible visual field abnormalities have been described in vasospastic patients. Gasser and Flammer have documented visual field abnormalities in patients with a vasospastic syndrome who exhibited one or more of the following findings: cold hands, Raynaud's phenomena, migraine and/or variant angina[4]. These patients exhibited abnormal capillaroscopic responses to cold in the nailfold of the finger. The visual field abnormalities were often associated with pale optic nerve heads in younger patients, while older individuals had pale and excavated optic nerve heads reminiscent of LTG. The visual field abnormalities worsened with cooling of the hand prior to perimetry, and improved with the calcium channel blocker, nifedipine[5].

The site(s) of vasospasm resulting in the ocular findings is not yet known. Lewis and coworkers found a 35% prevalence of visual field defects in patients with a history of migraine who were not having an attack; the majority of these defects were monocular and were therefore attributed to ischemia anterior to the chiasm[6]. Choroidal vasospasm has been documented by Prunte and Flammer using indocyanine green video-fluorescence angiography. The choroidal vasospasm was associated with visual field defects which improved after nifedipine administration[5].

Varied patterns of visual field defects in glaucoma have been identified and the study of the relationship of these different patterns to possible pathophysiologic mechanisms has been initiated. The ability to detect different mechanisms of glaucomatous damage in a clinical setting would be advantageous in designing appropriate treatment strategies. If a vasospastic mechanism could be identified clinically by evaluating visual field or optic disc characteristics, appropriate treatment could be instituted without extensive ancillary testing.

There is now a good deal of evidence to suggest that visual field loss may occur both diffusely as well as locally[7-13]. We investigated the occurrence of diffuse and local visual field damage in vasospastic and non-vasospastic glaucoma patients in order to study possible pathophysiologic mechanisms. The interrelationship of vasospasm and intraocular pressure to the type of visual field loss was also examined.

This research was funded by the Medical Research Council of Canada MT 1578

Address for correspondence J R Piltz, M D , Department of Ophthalmology, University of Pennsylvania, Scheie Eye Institute, 51 North 39th St., Philadelphia, PA 19104, U.S.A

Perimetry Update 1990/91, pp 465-472
Proceedings of the IXth International Perimetric Society Meeting,
Malmö, Sweden, June 17-20, 1990
edited by Richard P Mills and Anders Heijl

Material and methods

Automated perimetry and fingertip blood flow measurements were performed on 91 patients with primary open angle glaucoma. Patients were recruited from the glaucoma service of the University of British Columbia, which is both a consultation and continuing care service. High and low tension glaucoma patients were studied, and patients were not selected by the extent of glaucomatous damage. The sample therefore included individuals with most levels of glaucomatous involvement Patients with a visual acuity of less than 6/7.5 were excluded, which removed many patients with end-stage disease. All patients had refractive errors of <8 diopters of myopia or hyperopia and <3 diopters of astigmatism. One eye of each patient was studied. When both eyes were eligible, the eye with the better visual acuity was chosen; when the acuity was equal, a coin toss was used to choose the study eye.

The diagnosis of glaucoma was based on clinical evaluation of the optic discs, retinal nerve fiber layer and visual fields for each patient. Optic disc changes included localized notching, saucerization, generalized rim loss, or an abnormal neuroretinal rim area measured with manual planimetry. Retinal nerve fiber layer defects were either generalized or focal. Visual field defects included focal paracentral or arcuate scotomas, nasal steps or generalized depression on automated perimetry. LTG eyes had intraocular pressures of <21 mmHg without therapy on diurnal testing, while high tension glaucoma (HTG) eyes had intraocular pressures of ≥22 mmHg. No other relevant ocular pathology was present in study eyes.

Fingertip blood flow was measured with a laser Doppler flow meter in a method previously described[3]. Blood flow was measured at baseline, after immersing the hand in warm water (40°C) for two minutes, and after cooling the hand in ice water (4°C) for ten seconds. Patients were arbitrarily divided into vasospastic and non-vasospastic groups by the ratio of maximum flow after immersion in warm water to minimum flow after cooling. Patients were labelled vasospastic if the ratio was ≥7, patients were labelled non-vasospastic if the ratio was <6

Automated visual fields were performed using either Humphrey program 30-2 or Octopus program G1 The pupil diameter was ≥3 mm for all field tests Pharmacologic mydriasis was used if pupils were less than 3 mm.

Localized field loss on the Humphrey perimeter was defined as a minimum of three adjacent defective points in one hemifield on the pattern deviation plot with one point having a probability of abnormality of $p<1\%$ and two adjacent points with a probability of abnormality of at least $p<2\%$ Three points of the cluster, including the $p<1\%$ nucleus, were not located on the peripheral ring of test locations. The localized loss was considered mild if fewer than ten adjacent points within one hemifield were depressed $p<2\%$

Localized field loss on the Octopus perimeter was defined as a cluster of at least three adjacent abnormal points in one hemifield with one point depressed at least 10 dB and two adjacent points depressed by ≥5 dB from age matched controls. The cluster of points was surrounded by points with sensitivities at least 10 dB higher than the nucleus, except for the side of the defect extending to the outer edge of the tested area Three points of the cluster, including the 10 dB depressed nucleus, were not located on the peripheral ring of test locations. The localized loss was considered mild if fewer than nine adjacent points within one hemifield were depressed ≥5 dB from surrounding points.

Diffuse visual field loss was identified using cumulative defect curves (Bebie curves)[14]. If 90% of the points of a Bebie curve for an individual visual field examination fell below the 95th percentile, then the field was considered to exhibit diffuse loss Visual fields were categorized into those exhibiting purely localized loss (L), those exhibiting diffuse and localized loss (diffuse loss with moderate to severe localized loss) (DL), those exhibiting predominantly diffuse loss (diffuse loss alone or diffuse loss with mild localized loss) (PD), and those considered normal by the above criteria (N)

All intraocular pressure readings recorded on the patient's chart were tabulated. The highest intraocular pressure reading and the average of all pressure readings were incorporated into the analysis If the patient was on ocular hypotensive therapy during their evaluation on the glaucoma service, then an attempt was made to contact the referring doctor to supply the maximum intraocular pressure recorded off medications.

Each patient was also assigned to an intraocular pressure group based on the frequency of elevated intraocular pressure readings over the last decade (Table 1). Patients in group 1 had fewer than 25% of pressure readings over 16 mmHg, group 2 had ≥25% of IOPs over 16 mmHg

but <25% over 20 mmHg, group 3 had ≥25% of IOPs over 20 mmHg but <25% over 25 mmHg, and group 4 had ≥25% of IOPs over 25 mmHg.

The prevalence of the various visual field groupings in the vasospastic and non-vasospastic patients were compared with chi square analysis. Analysis of variance was performed on raw and transformed data to evaluate the relationship of intraocular pressure to the type of visual field damage in vasospastic and non-vasospastic patients.

Results

Forty-seven patients were called vasospastic and 44 non-vasospastic. The mean age in the vasospastic and non-vasospastic groups were 61.3 and 61.4, respectively. Half the patients in each of the LTG and HTG groups were vasospastic and half were non-vasospastic Approximately 25% of patients in each of the vasospastic and non-vasospastic groups had LTG and 75% had HTG (Table 1).

Table 1 Demographic characteristics of patients

	Vasospastic	*Non-vasospastic*	
Number	47	44	
Sex	26 M, 21 F	29 M, 15 F	
Age	61 3±10 7	61 4±11.4	NS
%HTG	74.5	70 5	NS
%LTG	25 5	29 6	NS

Diffuse loss was rarely seen in the absence of some degree of localized field loss Only two of 91 patients had pure diffuse loss; both of these patients were non-vasospastic. Overall, approximately half of the field defects were purely localized and the remaining defects were divided between the DL and PD groups. There was no statistical difference between the prevalence of localized and diffuse loss in the vasospastic and non-vasospastic groups (chi square) (Table 2).

Table 2 Prevalence of type of visual field loss in vasospastic and non-vasospastic patients

	None	*Localized*	*Diffuse and local*	*Predominantly diffuse*
Vasospastic	12 eyes	18 eyes	10 eyes	7 eyes
Non-vasospastic	6 eyes	18 eyes	16 eyes	4 eyes

Table 3 Intraocular pressure characteristics of vasospastic and non-vasospastic patients

	Localized	*Diffuse-localized*	*Predominantly diffuse*
Vasospastic			
IOP max: mean	23.2±6.8	23 3±5 4	28 1±7 5
IOP max: median	23	24	27
IOP mean	17.0±3 5	16 1±3 0	19 3±2 8
IOP group	2 1±0.75	2 4±0 97	3 0±0 82
Non-vasospastic			
OP max: mean	22 9±6.0	28 8±6 6*	29 0±7 4
IOP max: median	21 5	26 5	26
IOP mean	17 4±3.7	18.1±3 5	20 0±2 8
IOP group	2 4±0.93	2.7±0.80	3 0±82

*significantly different than localized, $p<0$ 05

Fig. 1 shows the histograms for the maximum intraocular pressure (IOP max) in each group, Fig. 2 shows the cumulative frequency plots of the maximum intraocular pressure, and Table 3 lists the mean and median of the maximum intraocular pressures, the overall mean IOP, and the mean IOP group for each category

In eyes with localized field loss (Figs. 1A and 2A), the distribution of pressures is similar in the vasospastic and non-vasospastic groups In eyes with DL field loss (Figs. 1B and 2B), the

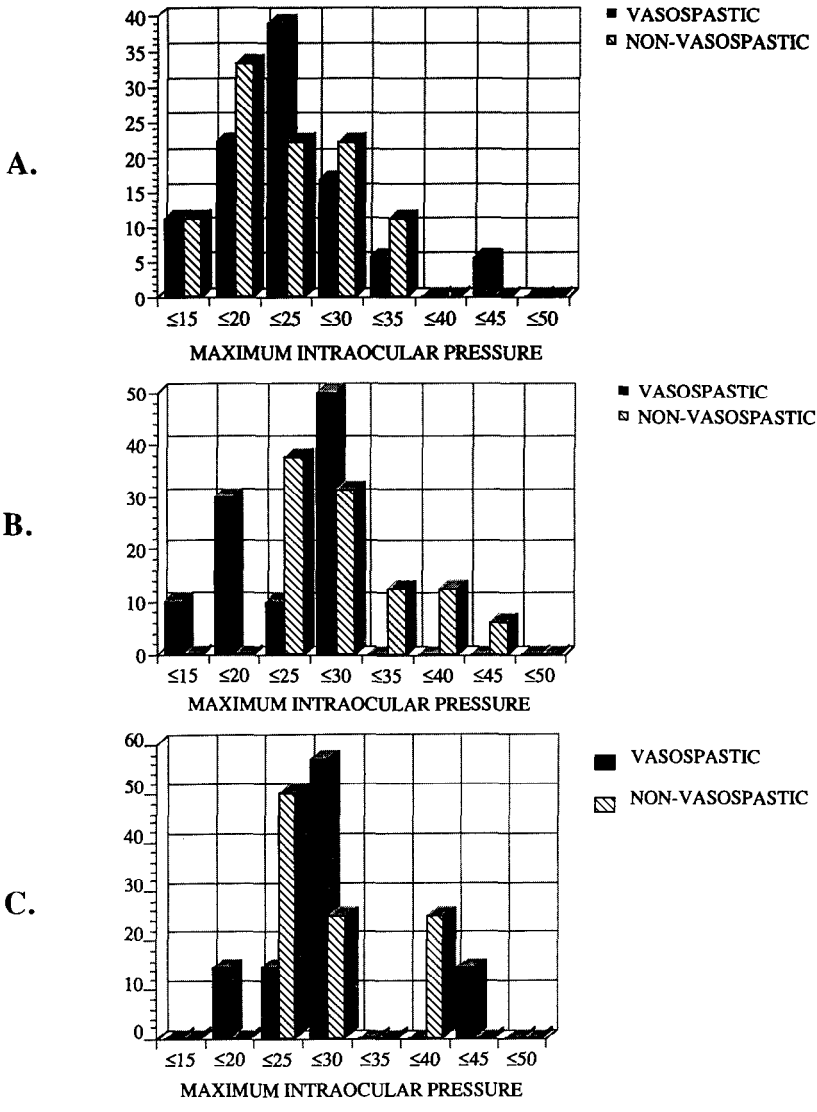

Fig 1 Histogram of maximum intraocular pressure in vasospastic and non-vasospastic patients A: patients with localized visual field loss (L); B: patients with localized and diffuse visual field loss (DL); C: patients with predominantly diffuse visual field loss (PD)

intraocular pressures are higher in non-vasospastic patients than in vasospastic patients; these differences, however, were not statistically significant (p=0 077, analysis of variance with Bonferroni procedure for multiple comparisons).

Fig. 3 shows the cumulative frequency plots of the maximum intraocular pressure in the different patterns of visual field loss. The curve is skewed toward higher pressures in eyes with diffuse loss (DL and PD) compared to eyes with purely localized loss. This relationship, however, is only present in the non-vasospastic patients. In the non-vasospastic group, the IOP was significantly greater in the DL group than in the L group (p<0.05, analysis of variance with Bonterroni procedure for multiple comparisons). In the vasospastic patients, the pressure in the L and DL groups are similar, while the PD group exhibited higher IOPs; these differences were not statistically significant. Similar trends were seen between the vasospastic and non-vasospastic groups when analyzing overall mean intraocular pressure and pressure group designations.

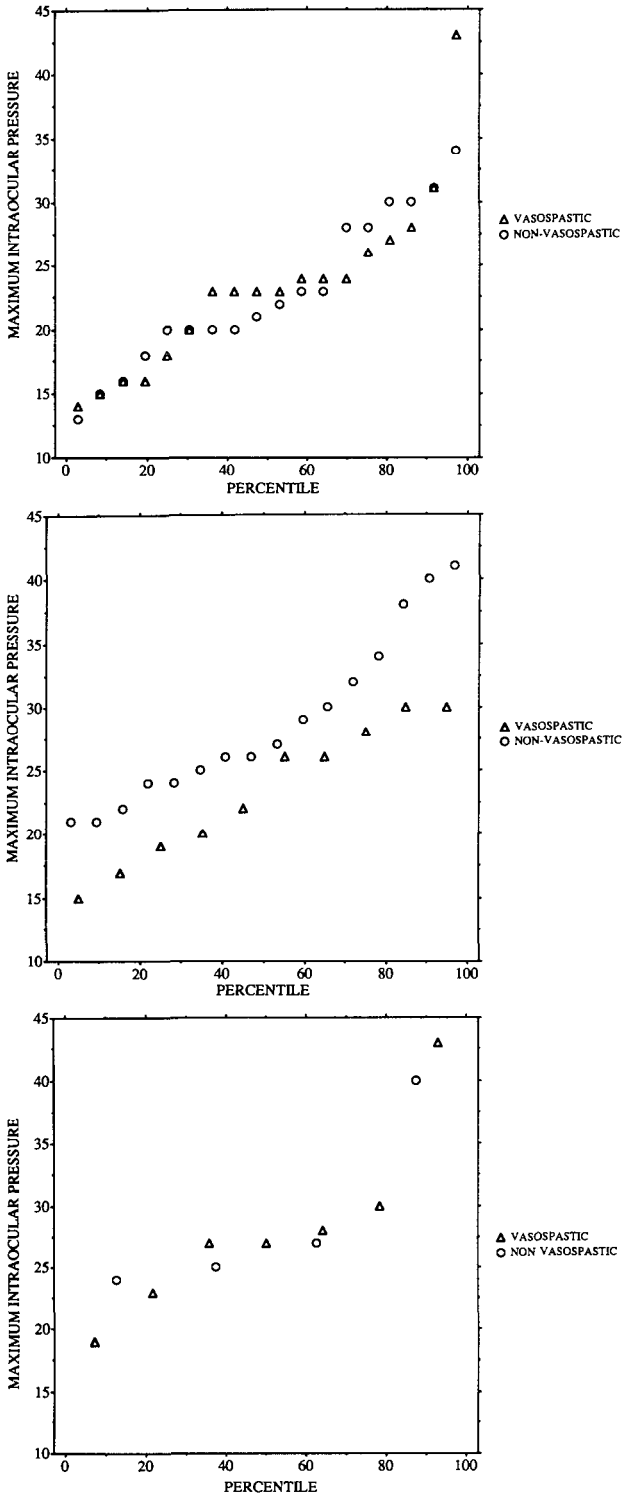

Fig 2 Cumulative frequency curves of the maximum intraocular pressure in vasospastic and non-vasospastic patients A: patients with localized visual field loss (L); B: patients with localized and diffuse visual field loss (DL); C: patients with predominantly diffuse visual field loss (PD).

A.

All patients.

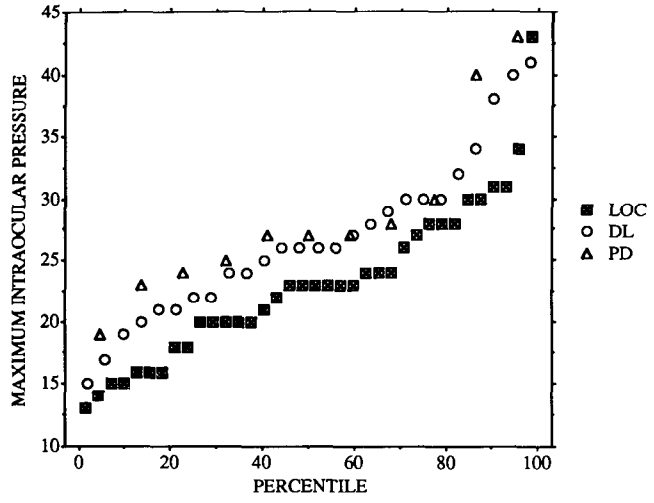

B.

Vasospastic

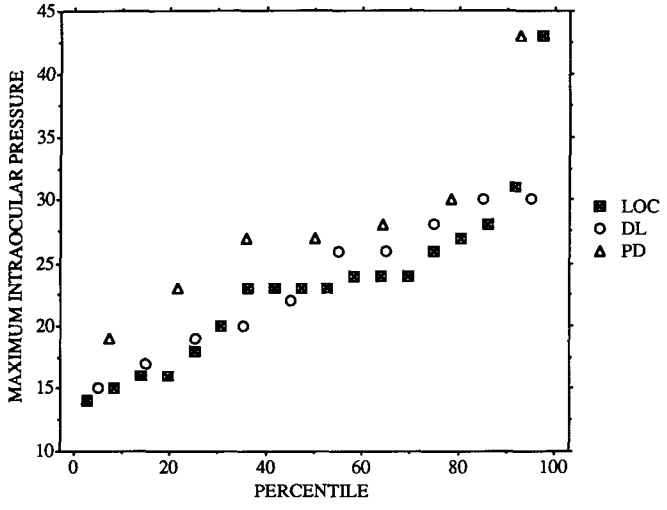

C.

Non-vasospastic

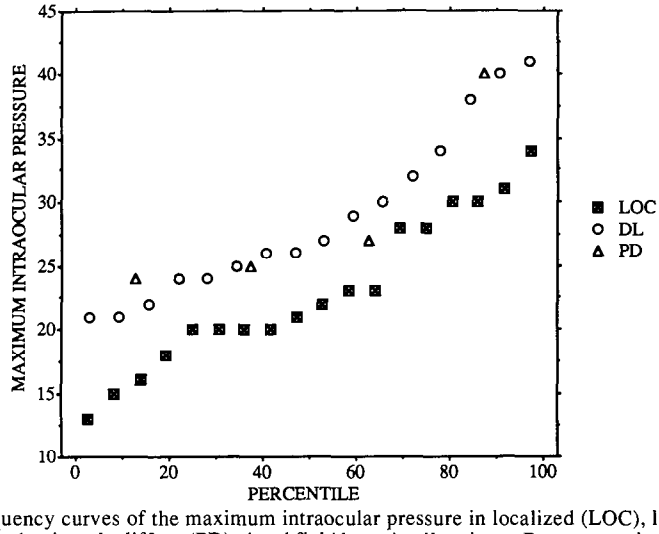

Fig 3 Cumulative frequency curves of the maximum intraocular pressure in localized (LOC), localized and diffuse (DL), and predominantly diffuse (PD) visual field loss. A: all patients; B: vasospastic patients; C: non-vasospastic patients

Discussion

While the literature has shown that vasospasm may be one of the risk factors in the development of LTG, the role vasospasm plays in the mechanism of glaucomatous damage remains unclear. Attempts by other investigators to identify mechanistic patterns of visual field loss have often been unsuccessful. Previous reports have claimed that the characteristics of the field loss in LTG and HTG are different[15,16], but other studies were unable to confirm these findings[17-22]. Studying an acute ischemic mechanism, Motolko and Drance found that visual field changes in LTG patients with a history of a hemodynamic crisis were indistinguishable from field changes of other LTG patients[17,21]. Greve was unable to identify differences in the characteristics of the visual field defects in two populations of glaucomatous eyes which likely had different mechanisms of damage[18]. These studies, however, looked at patterns of localized loss and did not address the occurrence of diffuse visual field loss

Examination of diffuse and localized patterns of visual field loss has shed some light on the mechanisms of glaucomatous damage, particularly to the role of increased IOP. For example, studies have suggested that elevated intraocular pressure may be involved in the development of diffuse changes in the visual field[7-10,12,13,23]. The main purpose of this study was to see whether a characteristic pattern of localized and diffuse visual field loss could be identified in the vasospastic patients. The introduction of Bebie curves as a clinical tool has facilitated the identification of diffuse visual field loss.

We were unable to find a particular pattern of diffuse and localized visual field loss in vasospastic patients compared to non-vasospastic patients We did, however, confirm the association of elevated intraocular pressure and diffuse visual field loss, and found this relationship to be stronger in non-vasospastic patients.

The pressure distributions of eyes with diffuse loss were skewed to higher levels compared to eyes with localized field loss. This skewing of the pressure distributions was more pronounced in the non-vasospastic patients than in the vasospastic patients. In eyes with DL field loss, non-vasospastic patients had higher pressures than vasospastic patients. While the pressure differences between these groups did not reach statistical significance, a trend was noted. This trend was seen whether we examined the maximum IOP recorded, the mean IOP or the overall IOP group designation. This finding may suggest that diffuse damage can occur at lower intraocular pressures in vasospastic patients compared with non-vasospastic patients.

This investigation was unable to characterize a "vasospastic pattern" of visual field damage in glaucoma. Since vasospasm is seen in a significant percentage of the general population, and only a minority of vasospastic individuals develop glaucoma, the clinical identification of vasospasm by visual field criteria may be masked While the literature has shown that vasospasm may be one of the risk factors in the development of LTG, the role vasospasm plays in the development of glaucomatous damage remains unclear

References

1 Phelps C, Corbett J: Migraine and low-tension glaucoma Invest Ophthalmol Vis Sci 26:1105-1108, 1985
2. Corbett J, Phelps C, Eslinger P, Montague P: The neurologic evaluation of patients with low-tension glaucoma Invest Ophthalmol Vis Sci 26:1101-1104, 1985
3. Drance S, Douglas G, Wijsman K, Schulzer M, Britton R: Response of blood flow to warm and cold in normal and low-tension glaucoma patients. Am J Ophthalmol 105:35-39,1988
4. Gasser P, Flammer J: Influence of vasospasm on visual function. Doc Ophthalmol 66:3-18, 1987
5. Prunte C, Flammer J: Choroidal angiography findings in patients with glaucoma-like field defects Doc Ophthalmol Proc Ser 325-327, 1989
6 Lewis RA, Vijayan N, Watson C, Keltner J, Johnson C: Visual field loss in migraine Ophthalmology 96:321-326, 1989
7 Drance S, Douglas G, Airaksinen P, Schulzer M, Hitchings R: Diffuse visual field loss in chronic open-angle and low-tension glaucoma Am J Ophthalmol 104:577-580, 1987
8 Lachenmayr B, Drance S, Chauhan B, House P, Lalani S: Diffuse and localized glaucomatous field loss in light-sense, flicker and resolution perimetry Invest Ophthal Vis Sci 31(Suppl):91, 1990
9 Caprioli J, Sears M, Miller J: Patterns of early visual field loss in open angle glaucoma Am J Ophthalmol 103:512-517, 1987

10 Chauhan B, Drance S, Douglas G, Johnson C: Visual field damage in normal-tension and high-tension glaucoma. Am J Ophthalmol 108:636-642, 1989
11. Drance S: Mechanisms of optic nerve damage Fortschr Ophthalmol 85:611-613, 1988
12. Flammer J: Psychophysics in glaucoma: a modified concept of the disease Doc Ophthalmol Proc Ser 43:11-17, 1985
13 Glowazaki A, Flammer J: Is there a difference between glaucoma patients with rather localized visual field damage and patients with more diffuse visual field damage? Doc Ophthalmol Proc Ser 49:317-320, 1987
14 Bebie H, Flammer J, Bebie T: The cumulative defect curve: separation of local and diffuse components of visual field damage Arch Ophthalmol 127:9-12, 1989
15 Anderton S, Hitchings R: A comparative study of visual fields of patients with low-tension glaucoma and those with chronic simple glaucoma Doc Ophthalmol Proc Ser 35:97-99, 1983
16 Caprioli J, Spaeth G: Comparison of visual field defects in the low-tension glaucomas with those in the high-tension glaucomas Am J Ophthalmol 97:730-737, 1984
17 Drance S: The visual field of low tension glaucoma and shock induced optic neuropathy Arch Ophthalmol 95:1359-1361, 1977
18 Greve E, Geijssen H: Comparison of glaucomatous visual field defects in patients with high and with low intraocular pressures Doc Ophthalmol Proc Ser 35:101-105, 1983
19 King D, Drance S, Douglas G, Wijsman K: Comparison of visual field defects in normal-tension glaucoma and high-tension glaucoma Am J Ophthalmol 101:204-207, 1986
20 Lewis R, Hayreh S, Phelps C: Optic disk and visual field correlations in primary open-angle and low-tension glaucoma Am J Ophthalmol 96:148-152, 1983
21. Motolko M, Drance S, Douglas G: The visual field defects of low tension glaucoma: comparison of defects in low-tension glaucoma and chronic open angle glaucoma Arch Ophthalmol 100:1074-1077, 1982
22. Phelps C, Hayreh S, Montague P: Visual fields in low-tension glaucoma, primary open angle glaucoma, and anterior ischemic optic neuropathy Doc Ophthalmol Proc Ser 35:113-124, 1983
23 Greve E, Geijssen H: The relation between excavation and visual field in glaucoma patients with high and with low intraocular pressures Doc Ophthalmol Proc Ser 35:35-42, 1983

Reassessing split fixation in advanced glaucoma: preliminary studies with computerized perimetry

Marc F. Lieberman[1] and Robert H. Ewing[2]

[1]*Departments of Ophthalmology, Pacific Presbyterian Medical Center, San Francisco;*
[2]*Kaiser-Permanente Medical Center, Redwood City and Department of Ophthalmology, Stanford University Medical Center, Stanford, CA, USA*

Abstract

Defining "split fixation" as involvement of one of the four innermost test points on the Humphrey Central 30-2 or 24-2 tests, 28 eyes of 22 glaucoma patients were followed for a mean of 44 months and administered Macular Threshold Tests (MTT) with foveal thresholding at each perimetric follow-up examination (mean 9.1 tests/eye) Data on intraocular pressure (IOP) control and visual acuity were collected. Only three of 28 eyes lost vision by more than two Snellen lines; none fell below 20/70. There was no obvious correlation between IOP levels and visual loss A new graphic display of the long-term data from the 16 point grid used in the Macular Threshold Test was developed Two different patterns of foveal-perifoveal dissociation were seen The MTT yielded much valuable data about the stability and large amount of fluctuation seen in glaucomatous split fixation.

Introduction

In 1977 Kolker published his seminal study on the prognosis of advanced visual field defects involving the central 5° in eyes with primary open angle glaucoma (POAG)[1]. This was an important study because it sought to clarify the conditions under which visual acuity is retained in end-stage disease, related both to the character of the central field involvement and its relationship to long-term intraocular pressure (IOP) control.

Kolker retrospectively evaluated the fate of 101 eyes treated by medications alone, by glaucoma surgery, or after intracapsular cataract extraction. Follow-up was at least 48 months, and/or six months after a surgical procedure Entrance criteria required vision better than 20/60. If to a I2e stimulus with Goldmann perimetry (or a 2/1000 target with tangent screen testing) the central 5° was affected along the horizontal meridian, fixation was said to be "split"; otherwise it was "spared".

The key observations of this study were as follows:

1. eyes which already began the study period with split fixation had a rate of central visual loss twice that of eyes in which the central field was spared;
2. all eyes that lost central fixation invariably progressed from sparing, through splitting, to "snuff out"; *i e* , splitting was a necessary perimetric stage preceding loss;
3. the higher the IOP, the greater the likelihood of visual loss: 4% lost fixation with IOPs <18 mmHg, 18 9% lost with IOPs in the 18-22 mmHg range, and 28.6% lost if IOPs were >22 mmHg;
4. post-surgical loss was immediately evident, and occurred only with antecedent split fixation (transient IOP elevation was thought to be contributory)

Alerted to these clinically relevant findings, many ophthalmologists became sensitive to the appearance of split fixation in the Goldmann fields of glaucoma eyes with advanced loss, and vigorously sought to reduce the IOP as much as possible.

Supported in part by grants from the Northern California Society for the Prevention of Blindness, Research to Prevent Blindness, and the Pacific Vision Foundation

Address for correspondence Marc F Lieberman, M D , Ophthalmology-5th Floor, Pacific Presbyterian Medical Center, 2340 Clay Street, San Francisco, CA 94115, USA

Perimetry Update 1990/91, pp 473-489
Proceedings of the IXth International Perimetric Society Meeting,
Malmö, Sweden, June 17-20, 1990
edited by Richard P Mills and Anders Heijl

However, with the advent of computerized static perimetric testing on the Octopus and Humphrey machines in the early 1980s, such split fixation seemingly appeared more common than with Goldmann testing A combination both of the standardized resolution of the test pattern for the central field and of the superior sensitivity of threshold testing (compared to kinetic suprathreshold stimuli) yielded many fields where scotomata involved one or more of the central four test points, lying within the central 5°. This specifically occurred when using the most popular threshold test patterns[2], where the 6°-spaced points straddle the test axes: *i e.,* the Octopus 32 or 34 programs, or the Humphrey 30-2 or 24-2 programs.

Uncertain of whether Kolker's observations regarding the visual prognosis of split fixation and its correlation with IOP applied to central involvement as detected by computerized threshold testing, we designed a prospective long-term study which explores the central 5° of the visual field in eligible glaucoma patients, using a high-resolution grid pattern. We present here the preliminary analysis of this ongoing project

Methods

From 1985 until the present, the following perimetric policy has been in effect at three different ophthalmology services (Kaiser-Permanente, Redwood City, CA; Stanford University, Stanford, CA; and Pacific Presbyterian Medical Center, San Francisco, CA). All pupils are routinely dilated to at least 3 mm prior to field testing, and the most current refraction, with appropriate add, is used. At the completion of either the Humphrey Field Analyzer Central 30-2 or Central 24-2 examinations of one or both eyes (using either the full threshold or full from prior testing strategy), the technician inspects the innermost four test points for evidence of scotomatous involvement of one or more points. This is defined either by a loss of greater than

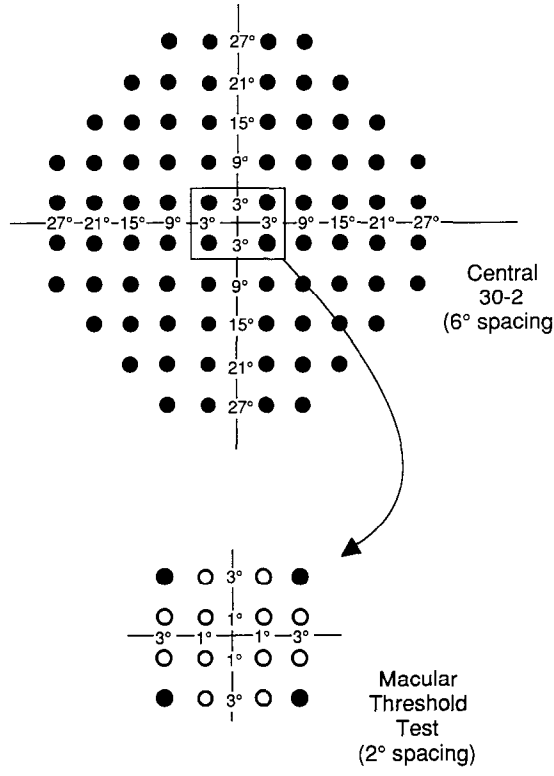

Fig 1 Centered on the fovea, which is tested separately, the MTT examines a 6° × 6° grid, each point 2-degrees apart, and thresholded three times This covers slightly less than the central 5-degrees. Note that the innermost four points of the central 30-2 and central 24-2 points are identical to the four corner points of the MTT

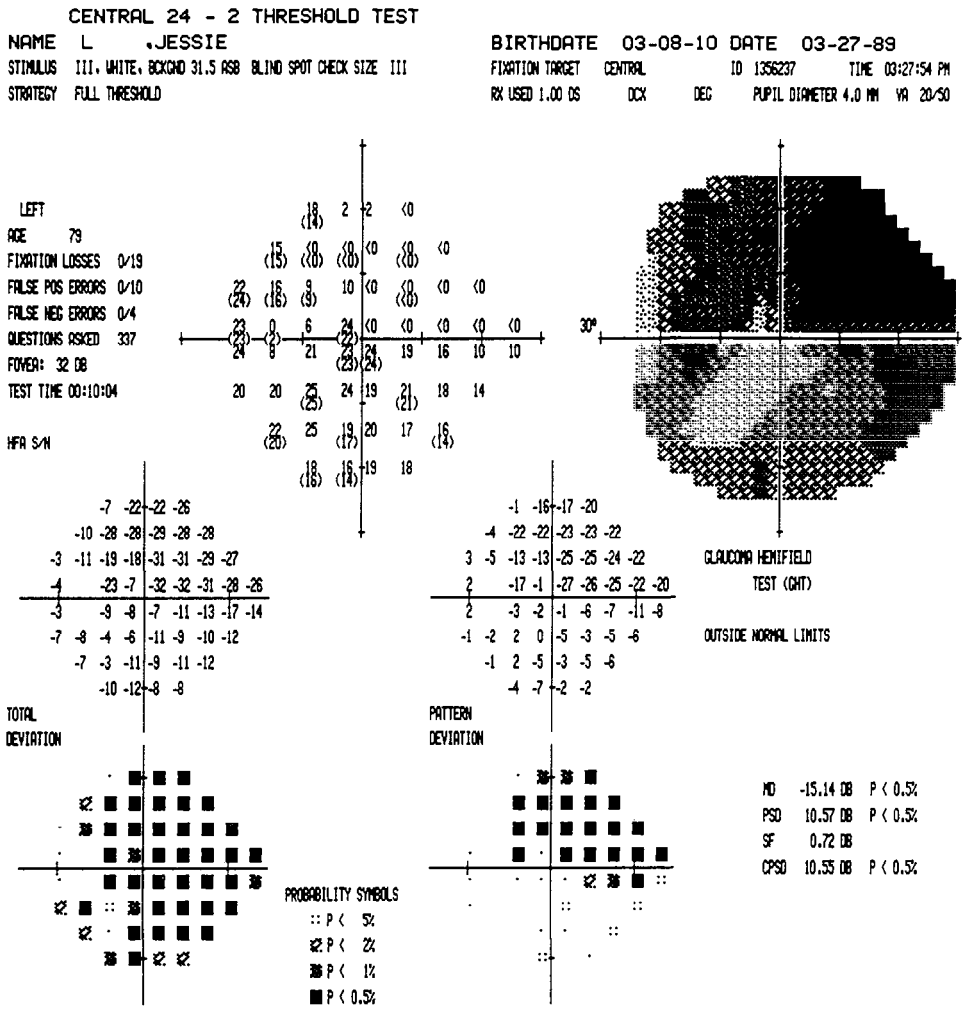

Fig 2A

Fig 2 This central 24-2 test (A) shows engulfing of fixation by a dense superior arcuate scotoma, densest nasally to fixation. This is reflected over time in the 16 point plot (B), where the upper right (superonasal) quadrant shows profound disturbance, and the upper two points in the superotemporal (upper left) quadrant reflect the threat to fixation The inferior eight perifoveal points are essentially normal

5 dB from adjacent values, or by a p-value of <0.05 as displayed on the Pattern Deviation plot with the Statpac® single view printout. After a few minutes' rest, the involved eye is tested using the Macular Threshold Test (MTT), beginning with the additional measurement of the foveal value.

The MTT uses a high-resolution square grid of the approximate central 5° area bounded by the four innermost points of the central 30-2 or 24-2 patterns. It tests at 2° intervals, thresholding each of the 16 points three times (see Fig. 1). Testing usually takes an additional seven to ten minutes per eye. For all subsequent perimetric follow-up, the MTT is obtained the same day as the central 30-2 or 24-2 examinations.

We consolidated the 4500-some computerized central and MTT fields obtained in the past five years onto a Humphrey Field Analyzer hard disc. Next, selected data was downloaded by cable through the R232 port, in ASCII code, onto a Macintosh Plus™ computer using transmission and translation software developed by Dr. Peter Åsman of Malmö, Sweden. This data

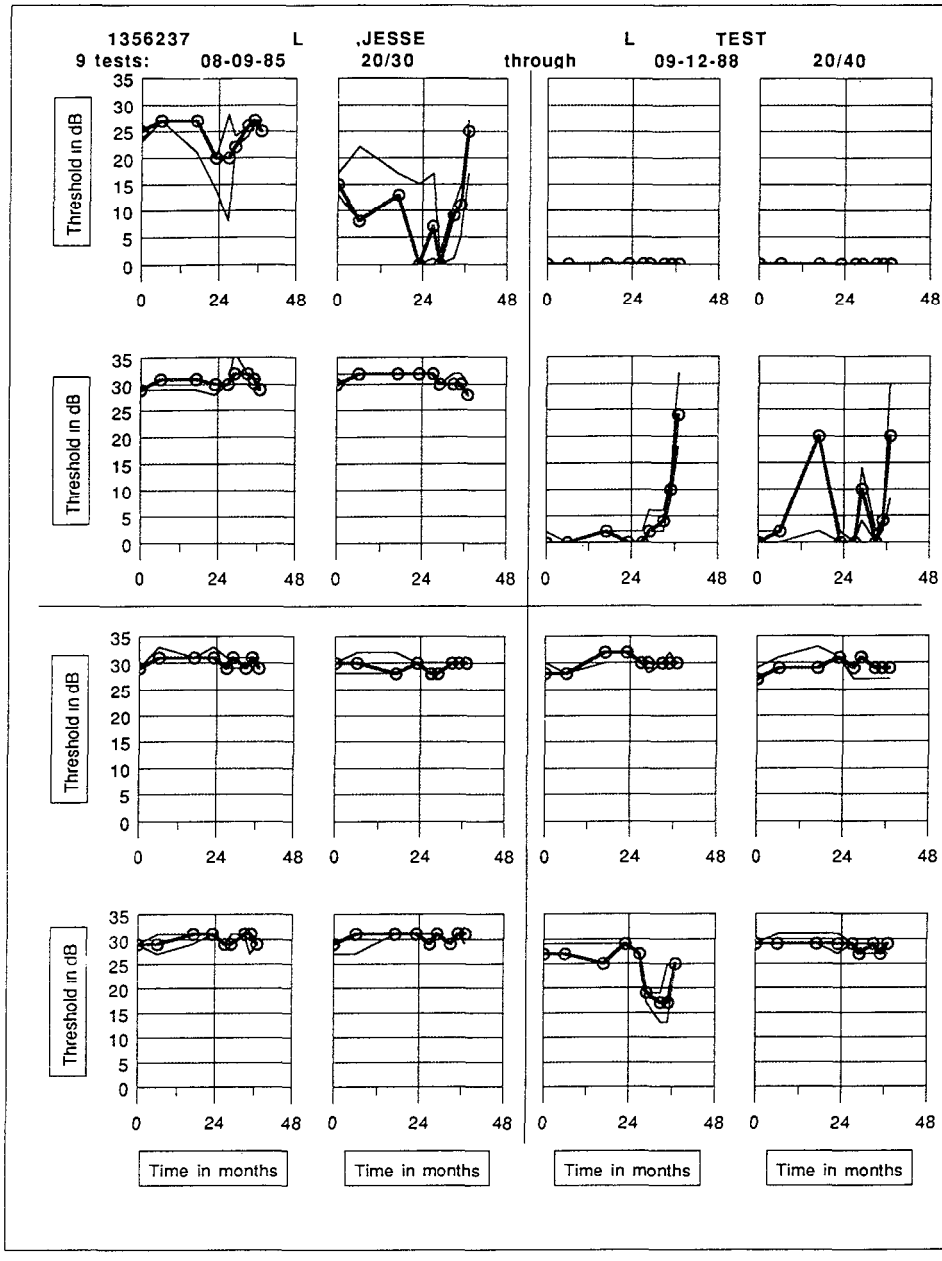

Fig 2B

was then reworked into a customized 4th Dimension® database program designed by one of us (RHE)

Our preliminary analysis of split fixation in eyes with glaucoma was confined to 28 eyes of 22 patients which met the following criteria: (a) best-corrected acuity of 20/50 or better, with annual refractions; (b) at least three Central 30-2 or 24-2 tests and three MTTs by Humphrey perimetry over at least 36 months' time; (c) applanation tonometry and other standard ophthalmic examinations at least every six months, which ruled out diseases other than glaucoma (with special attention to the macula). The average follow-up was 44 months (range 36-59 months)

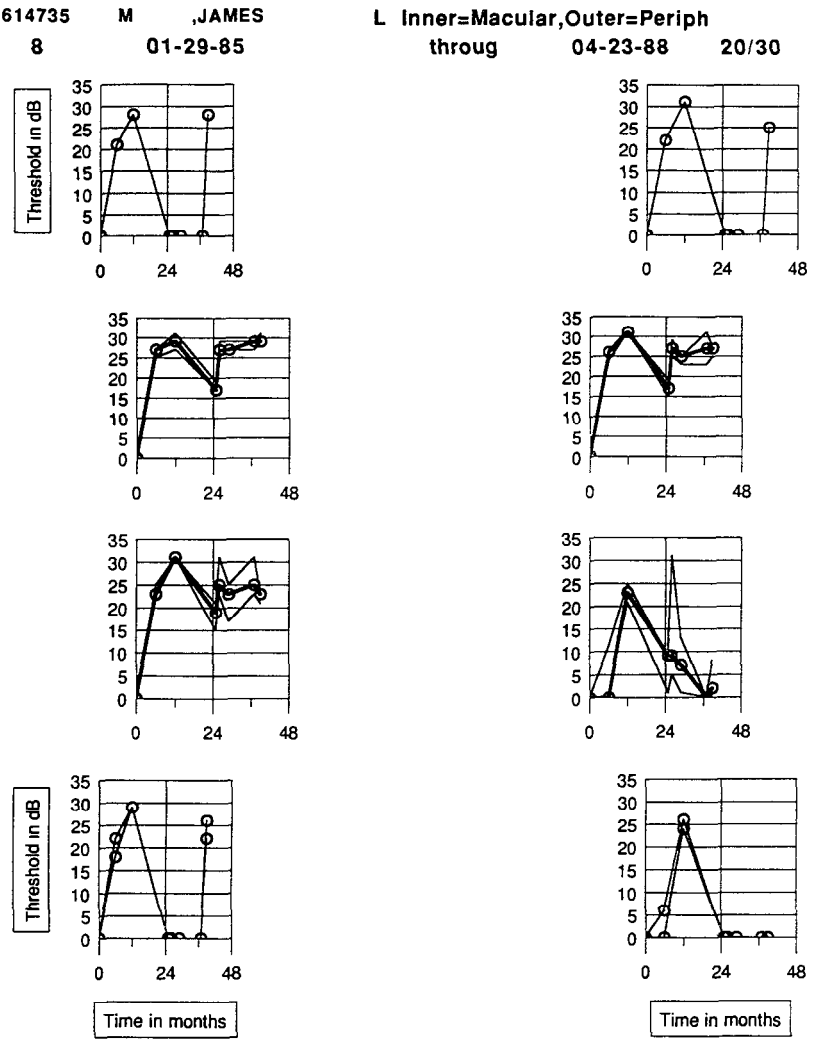

Fig 3 In this perifoveal four point plot, the four corner graphs display threshold data of the innermost four points of the central 30-2/24-2 tests The identical four points in the MTT are displayed as the central four graphs. As is frequently seen, the MTT data show less fluctuation than when the same points are sampled during the more extended threshold test Specifically this eye had greater damage and fluctuation in the lower half of the field than in the superior half: this is reflected in the greater fluctuation of the inferior two graphs of the MTT data

The average number of central tests and MTTs was 9 1 per eye (range 3-19). The average eye had 32.7 tonometry readings (range 12-59) over the course of the study; this is a greater than normal frequency because many eyes underwent laser or surgical intervention, with subsequent close surveillance.

The diagnosis for 18 patients was POAG; two patients had a secondary open angle glaucoma (pseudo-exfoliation and Sturge-Weber); one patient had mixed mechanism glaucoma, one patient had chronic narrow angle closure glaucoma. There were no attempts to control which medical glaucoma regimen each eye was receiving: nearly all eyes were on a combination of beta-blocker, miotic and/or carbonic anhydrase inhibitor. During the study period, 19 of the 28 eyes underwent pressure-lowering interventions (16 argon laser trabeculoplasties (ALTs); three trabeculectomies); one eye underwent intraocular lens implantation several years after a pre-

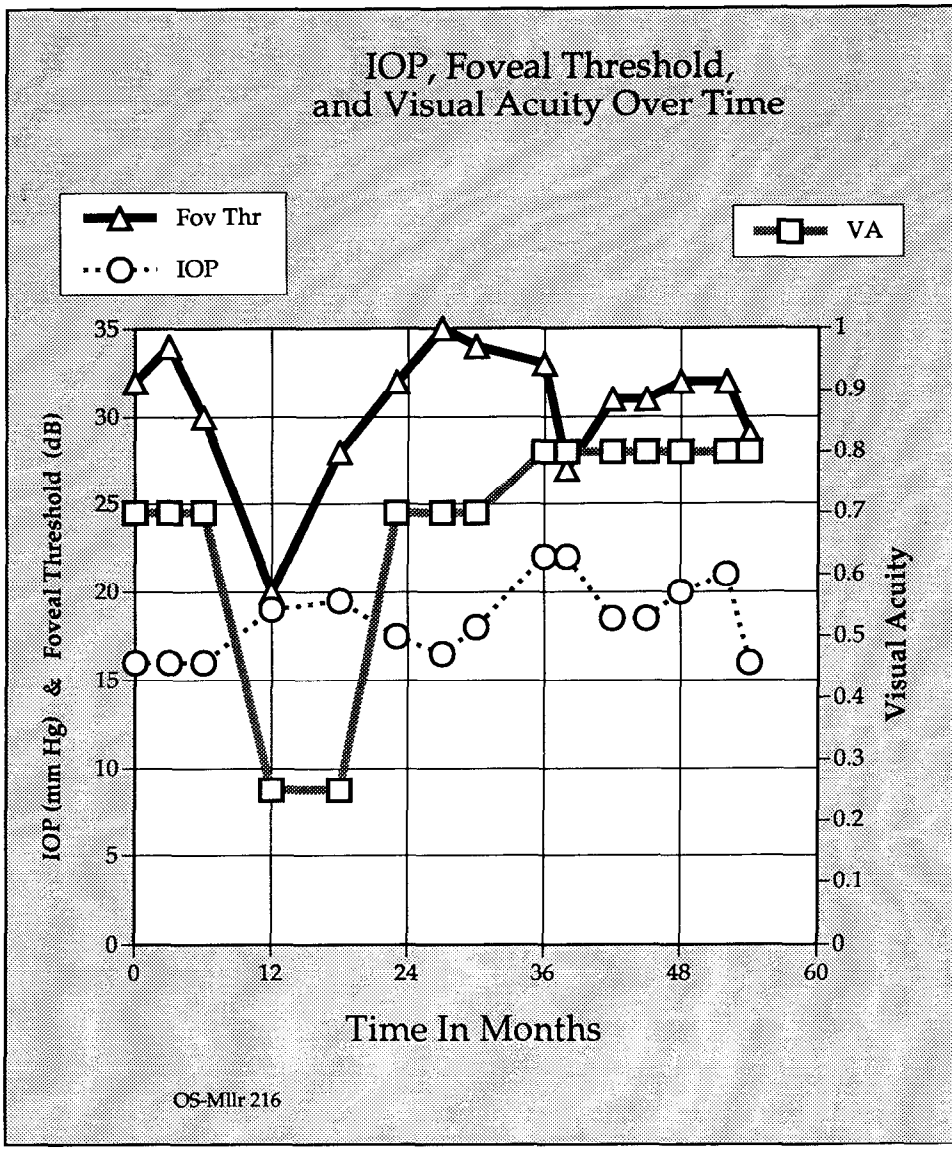

Fig 4 This display shows the course of IOP level (mmHg) and foveal values (dB), together sharing the scale of the left ordinate, and visual acuity, notated by the right ordinate. In this example, despite relative IOP stability, the foveal and acuity measures inexplicably deteriorated together on the fourth and fifth tests, then returned to normal levels

vious glaucoma filter; eight eyes were exclusively managed by medications. Visual loss was defined as a reduction of greater than two lines in Snellen acuity, unimproved by refraction and unrelated to media changes (*e g.*, cataract).

For all eyes in the study, we devised a 16-point macular threshold plot With this display, long-term MTT data was graphically plotted on a single page for ease of assessment. The MTTs for each eye had a graph prepared for each of the 16 test points, plotting the three threshold values obtained at each point *versus* time (Fig. 2).

In an attempt to meaningfully compare the vast amount of threshold data, another plot of perimetric data was devised for some eyes This displayed the threshold values obtained for

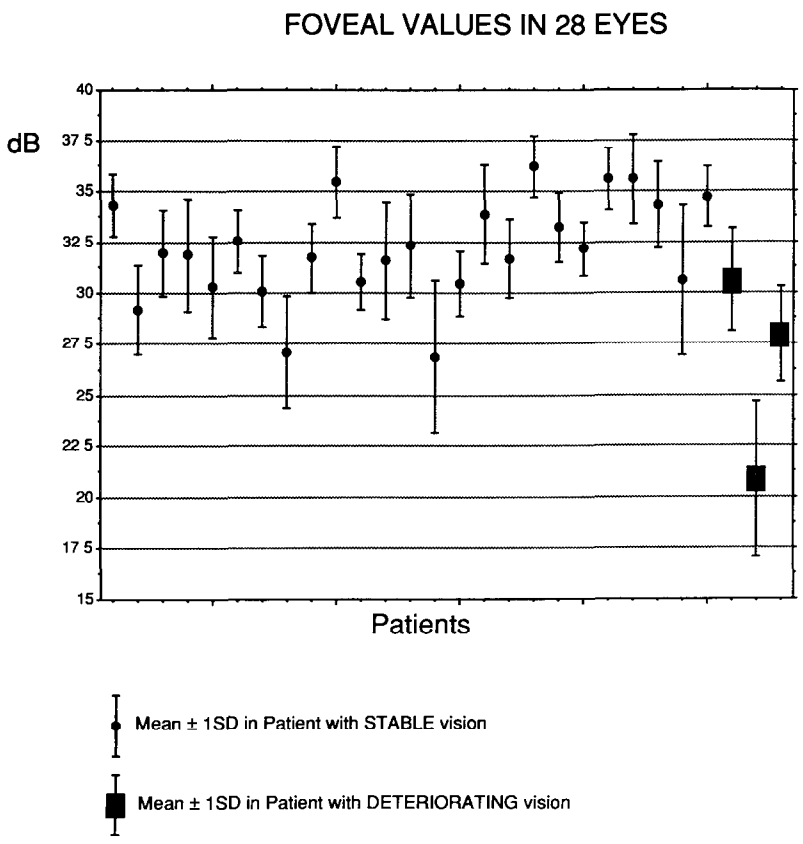

Fig 5 The mean foveal value for each of the study eyes is plotted ± 1 SD The 25 figures to the left (circle in the center) represent those eyes without loss of vision; the last three figures on the right (box in the center) are the three eyes with visual loss >2 Snellen lines

each of the innermost four central points from the central 30-2/24-2 tests *versus* time, compared to plots of the identically positioned points of the MTT (*viz* the four outermost corner points), thrice-thresholded, *versus* time (Fig. 3). This perifoveal four point plot thus displays the values and fluctuations of the same four points in the perifoveal region as tested with the central 30-2 or 24-2 tests as tested with the more focused MTT.

Clinical data reflecting the course of IOPs, foveal values, and visual acuities were also plotted against time (Fig 4)

Results

Frequency of visual loss

During the time frame of the study, only three of 28 eyes demonstrated reduction in central acuity by more than two Snellen lines. But surprisingly, the changes in foveal sensitivity comparing the earliest measures (at the time of the best acuities) and the last measures (at the time of the worst acuities) bore little relation to the measured changes in acuities. The vision of two of these eyes was reduced from 20/30 to 20/70; both these underwent laser trabeculoplasties 24 months before and 24 months after their respective vision changes. Looking at initial and final foveal values, these two eyes showed changes 23 dB to 21 dB, and 33 dB to 31 dB respectively – but had intervening measures as low as 14 dB and 28 dB, respectively. The third eye with visual deterioration went from 20/40 to 20/70, two years after a trabeculectomy; here

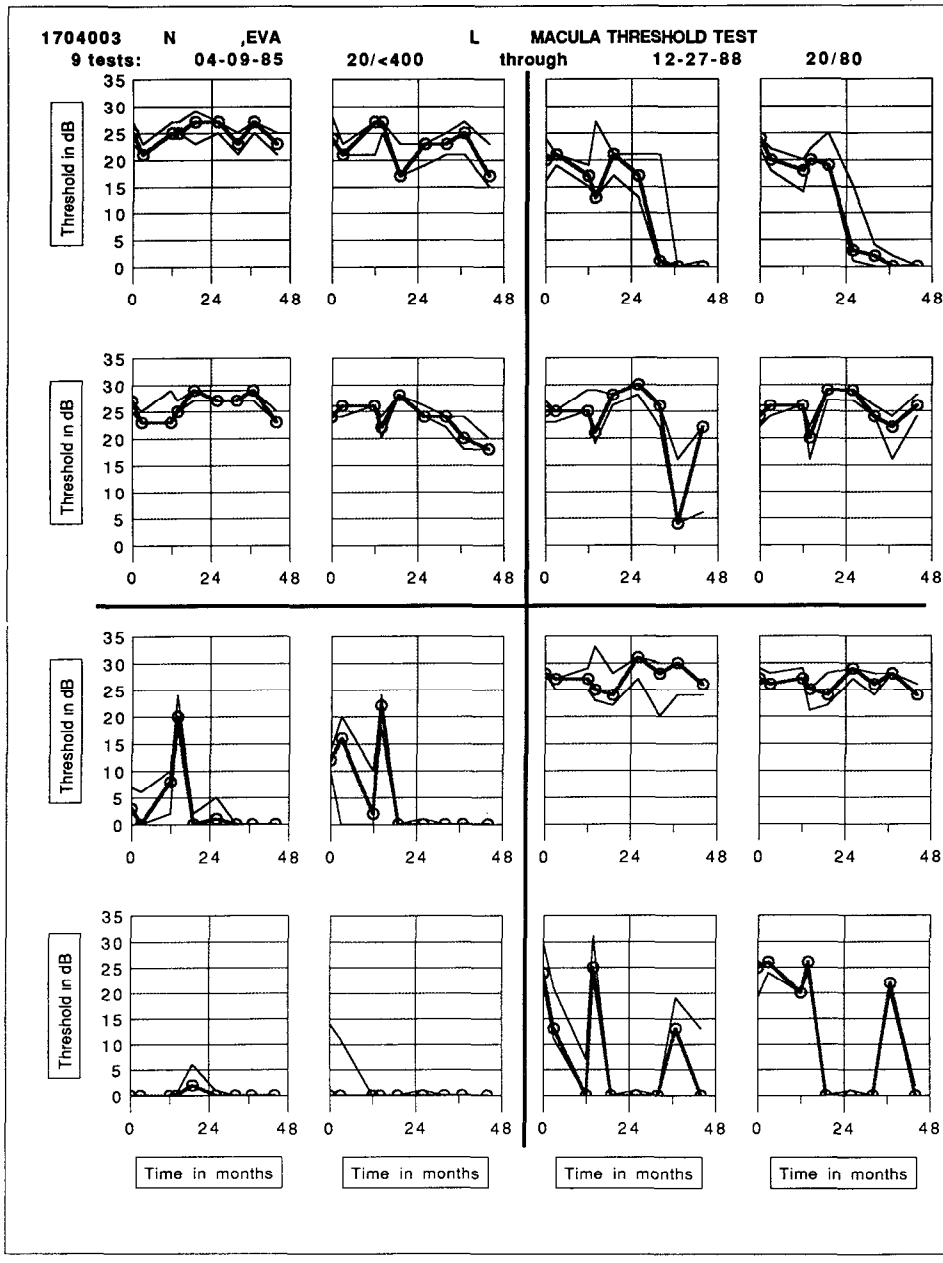

Fig 6 This 16 point macular threshold plot shows a "pincher effect", whereby the four outer nasal points (the two graphs in the upper right and the two in the lower right) showed greatest fluctuation, with relative stability of those points closest to the horizontal nasally Stability is seen in the upper left quadrant (superotemporal), but great damage below

the initial foveal value fell from 31 dB to 26 dB steadily, with little fluctuation.

The remaining 25 eyes over the course of the study fluctuated within two lines of baseline acuity: two fluctuated for the worse (*viz* 20/25 to 20/40, and 20/40 to 20/60), the rest fluctuated by one line around a median acuity of 20/30. In this larger group, foveal values showed a remarkable amount of fluctuation in the presence of long term stability of visual acuity (Fig. 5).

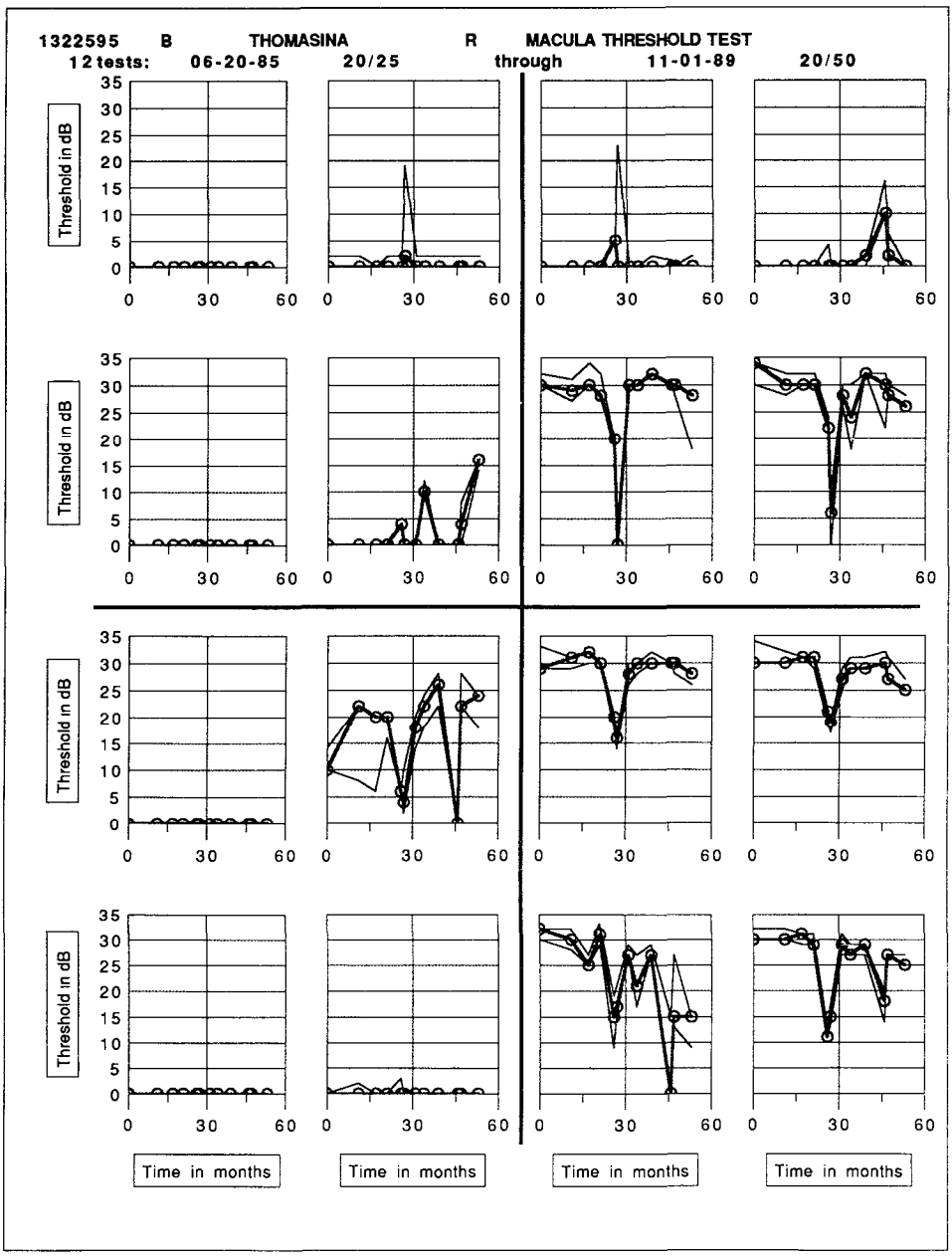

Fig 7 On the fourth and fifth macular threshold tests of this right eye, significant loss of sensitivity appeared in the seven remaining points of retained sensitivity With subsequent testing thresholds returned to earlier levels Note too the relatively later preservation of normal sensitivity in points closest to the horizontal and closest to the blind spot

IOP behavior

In only one of the three eyes with vision change was there a probable relationship to the IOP control The eye that dropped from 20/40 to 20/70 had mean IOPs of 22 prior to visual change; afterwards, with increased medications, mean tensions stabilized at 15 8 In the other two eyes,

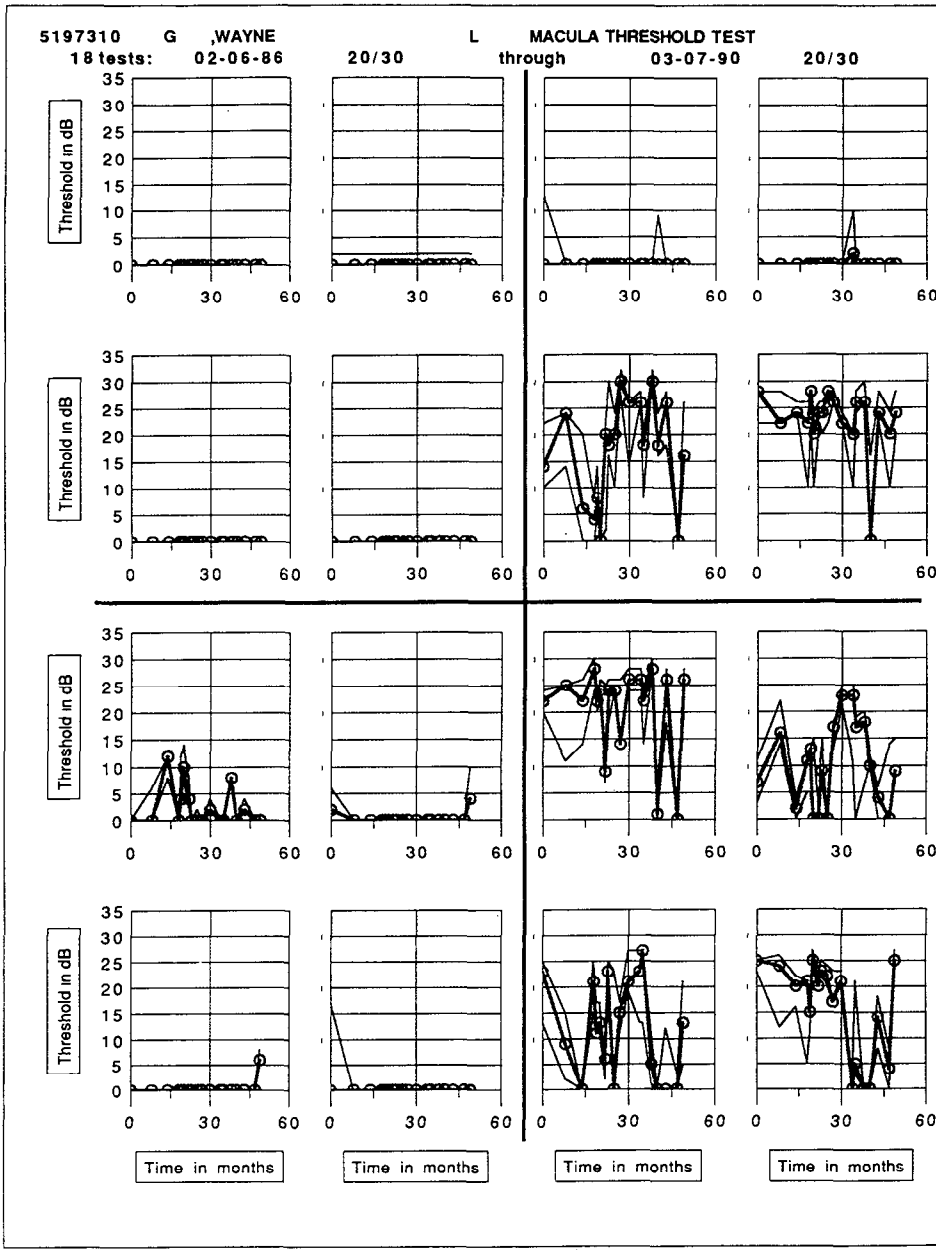

Fig 8A

Fig 8 Although only six of the 16 test points in the macular threshold test retained function in this 16 point plot (A), there was a large amount of fluctuation for better and worse over the 18 MTTs performed over four years In contrast, the clinical parameters of foveal values, acuities, and IOPs remained constant (B) The overview display from Statpac for this eye (C) shows how little useful information for perimetric follow-up from the central 24-2 test is available in such an advanced stage of field loss.

which had pre-change IOPs of 14.5 and 15.5, respectively, and IOPs of 13.7 and 15.7 afterwards, no temporal relationship was identified between tension and acuity loss.

The course of IOP control in the remaining 25 eyes is looked at by the type of intervention.

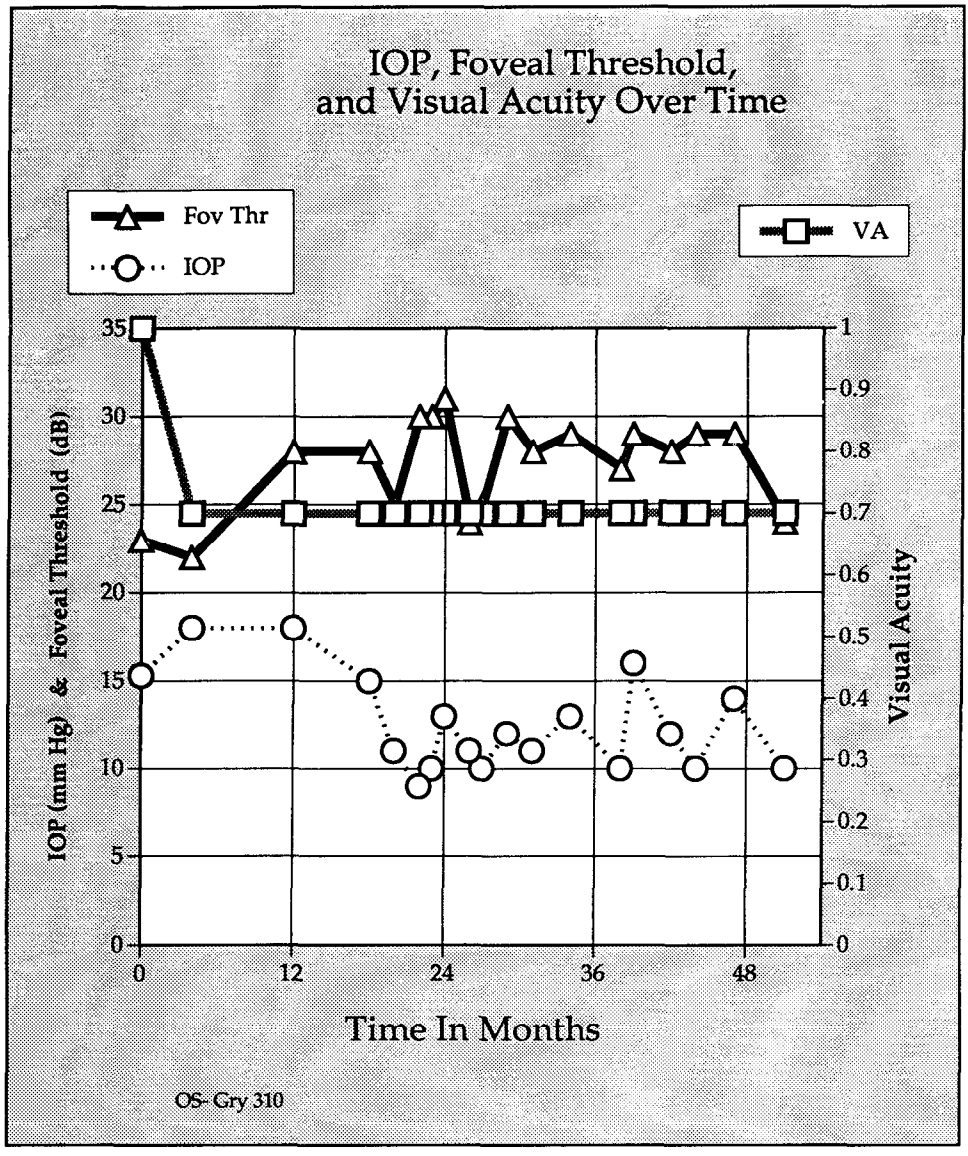

Fig 8B

For the 16 eyes that underwent ALT, the mean pre-laser IOP was 20.3; the mean post-ALT tension was 15.8. The mean pre-trabeculectomy IOP for the three operated eyes was 20.6; the mean post-operative tension was 13.6. The eye with a functioning trabeculectomy filter averaged pressures of 13.3 prior to posterior chamber lens implantation; afterwards tensions averaged 16.8. The mean pressure for the eight medically treated eyes was 16 5 No loss of central vision was seen in any of these eyes.

Assessment of 16 point macular threshold plots

By visual inspection alone, several patterns of the 16 point plots were appreciated. Frequently there was excellent agreement between the 30-2 display and the 16 point plot, yet with a higher resolution with the latter. The display often identified discrete areas of stability, contrasting

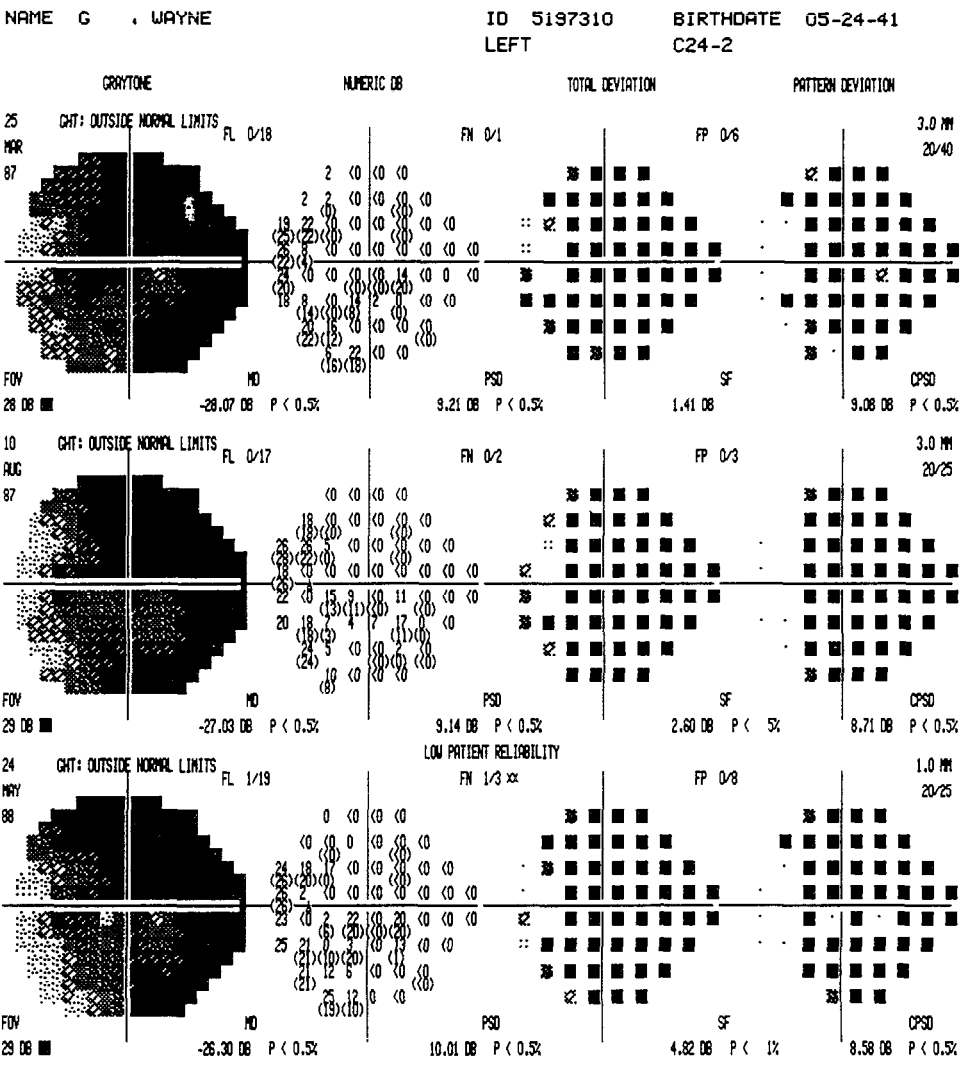

Fig 8C

with areas of fluctuation and/or deterioration (Fig. 2).

Occasionally the fluctuating points suggested patterns of progressive damage (Fig. 6.) In this example, six of the inferior eight points show profound disturbance, with normal thresholding in the two points just below the horizontal, inferonasally (lower right quadrant). Similarly, the two points immediately above the horizontal (superonasally) show obvious fluctuation, above which the two points (superonasally, in the upper right quadrant) show progressive deterioration. This sequence of damage – progressing like "pinchers" peripherally in towards the horizontal midline and temporally towards the blind spot – was a common expression of progressive arcuate deterioration Points adjacent to the horizontal midline were frequently seen to be preserved later than points 3° above or below

Another pattern reflecting fluctuation was the appearance of seeming deterioration, even apparent on repeat testing, with later recovery to the previous levels of sensitivity (Fig. 7). Though such a "bad day phenomenon" was worrisome at the time, no clinical correlation with IOP or alteration of vision was appreciated at the time of the sudden change for the worse – or for the better.

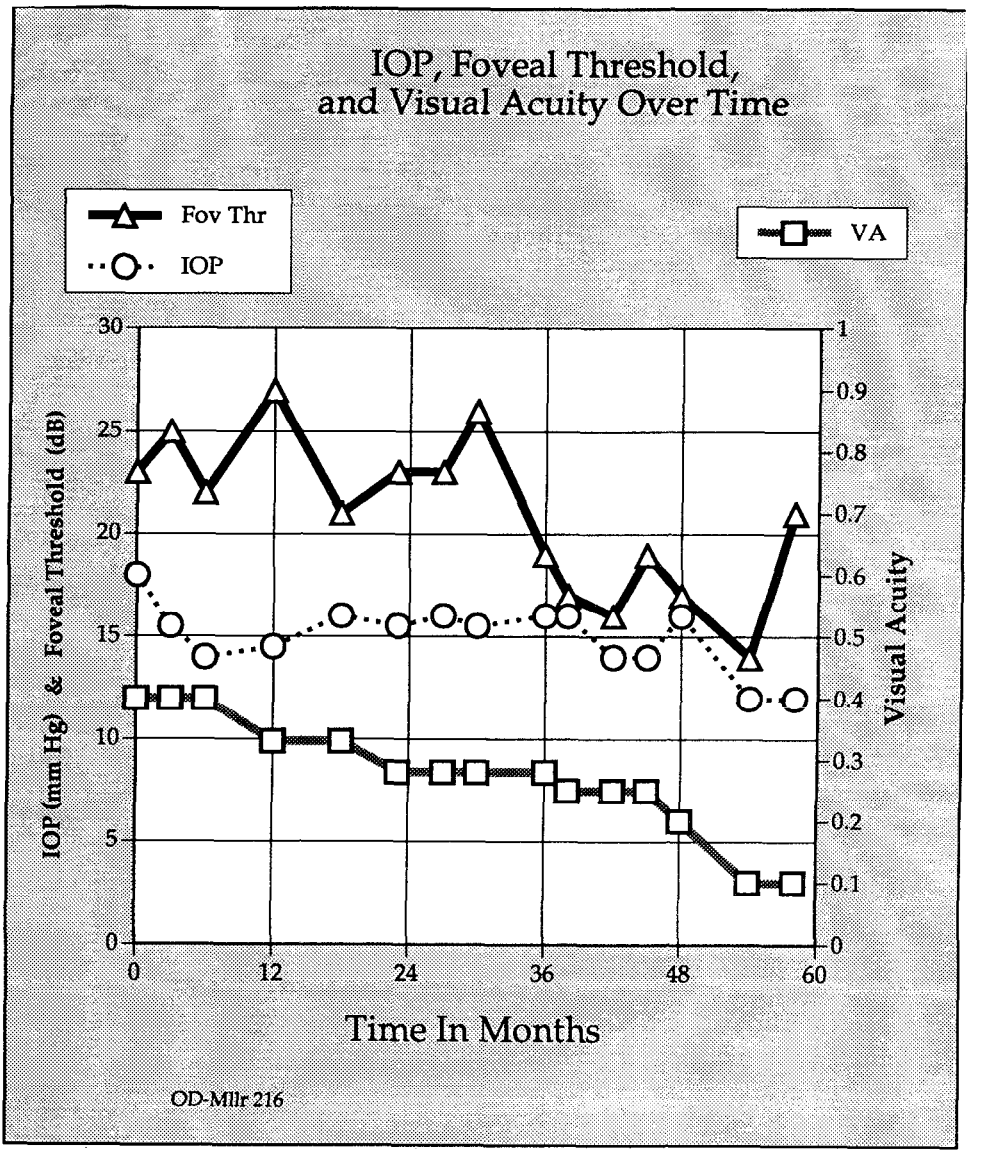

Fig 9A

Fig 9 Despite a stable level of IOP with little fluctuation over nearly five years, this plot (A) graphically illustrates the gradual decay of foveal sensitivity and visual acuity Although the trend towards deterioration is evident inferiorly in the 16 point plot (B) covering the same period, relative stability of perifoveal points appears in the superior half of the test grid This is an example of relative dissociation of perifoveal and foveal values

Less dramatic, but similarly without clinical correlation, was the pattern of profound "see-saw" fluctuation (Fig. 8). Despite consistently good IOP control (under 15 mmHg), and monotonously stable acuities of 20/30, the points of retained sensitivity showed tremendous scatter on repeat testing.

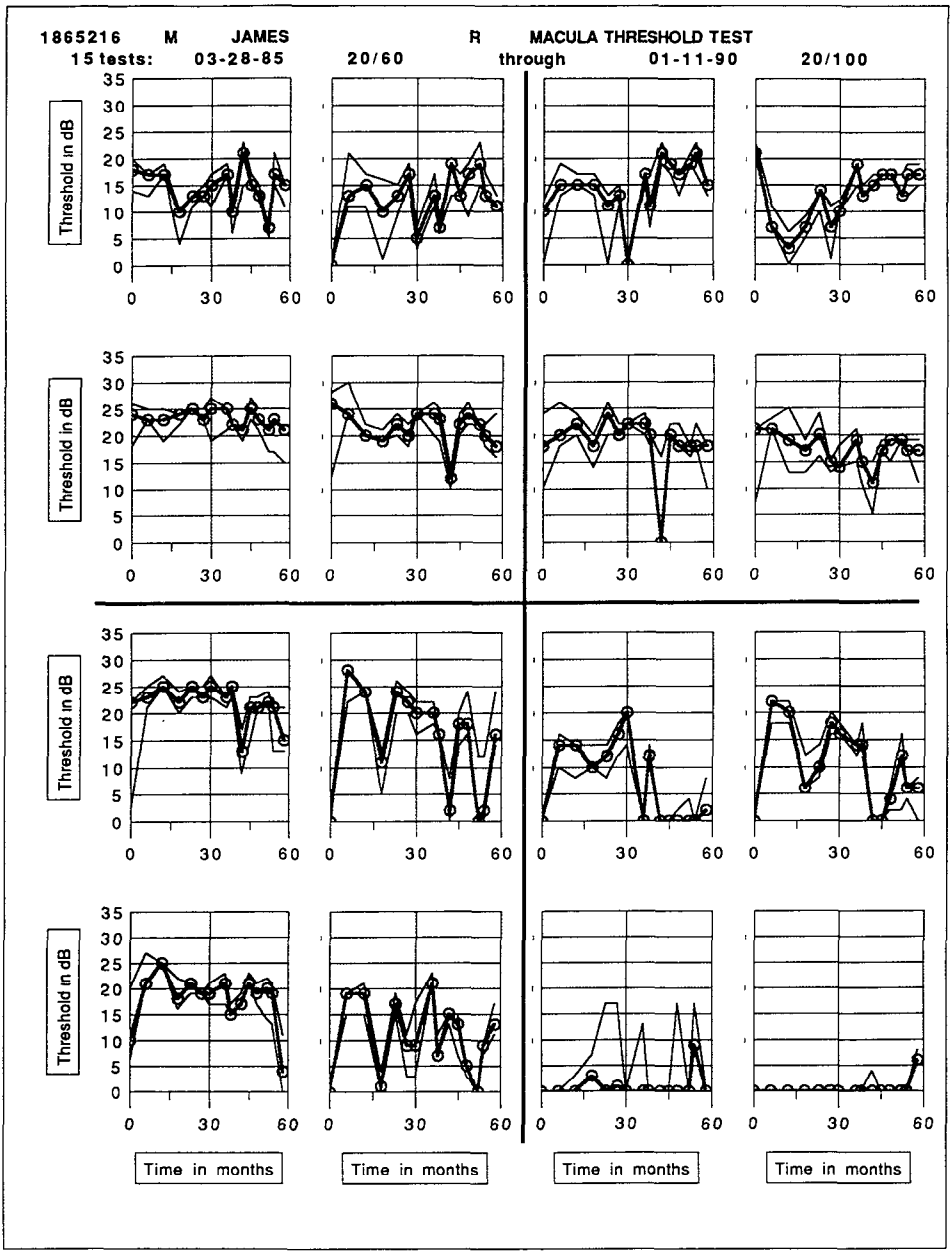

Fig 9B

Plotting of foveal values, IOPs and visual acuities

The course of one of the three patients whose vision definitely deteriorated despite IOPs consistently below 16 mmHg is visually clarified on the graph displaying tensions, visions and foveal thresholds over time (Fig. 9A). Of note was the relative preservation of the superior eight perifoveal points on MTTs over time, with only gradual loss inferiorly (Fig. 9B).

Discussion

This study was established to extend the observations of Kolker[1] based on kinetic perimetry, in a retrospective study of end-stage glaucoma eyes. Alert to the potential for central "snuff out" – defined as visual loss to <20/200 by Kolker – with increasing IOPs over 18, every attempt was made by us to keep the tension as low as possible in these eyes with demonstrated split fixation by computerized perimetry. Although our average follow-up was four months less than Kolker's four years, we suspect that the total absence of severe visual loss to the 20/200 level in our study reflected two factors: (a) the vigorous use of medical, laser and surgical therapies to keep the mean pressures for all eyes under 18 mmHg (the range in which Kolker saw only a 4% rate of severe visual loss); and (b) the presumably more sensitive and reproducible capacity of computerized perimetry to define and monitor subtle manifestations of split fixation, leading to the inclusion of eyes perhaps less damaged than in Kolker's series.

However some visual loss was appreciated Three of 28 eyes (10 7%) dropped acuity by more than two Snellen lines. Yet with a single exception, there was no association between IOP level or laser intervention (with its potential for temporary elevated pressures post-treatment) to explain the deterioration. Even with close scrutiny of the 16 perifoveal points evaluated with the MTT, one eye with visual loss showed no obvious pattern of perifoveal loss indicative of the foveal changes (Fig. 9B).

This is the reverse of the usual meaning of "foveal-perifoveal dissociation". As used by Hart[3], maculopathies can demonstrate preserved foveal function though surrounded by perifoveal depression. Optic neuropathies allegedly show concomitant depression of both foveal and perifoveal areas. In our case, however, perifoveal function was seen to persist in the presence of decreasing acuity and foveal function.

In fact, by our definition of "split fixation", all eyes in this study manifested good foveal function (acuity >20/50, with mean foveal thresholds of 31 dB ± 4 24 over three years) surrounded by at least some focus of perifoveal disruption – exactly the findings Hart described in his maculopathic eyes from vascular and degenerative processes[3] Since glaucoma is the commonest optic neuropathy, the distinction of foveal-perifoveal dissociation ascribed to macular diseases needs be reconsidered.

The expected correlation between foveal values and visual acuity – as seen by Anctil and Anderson[4] – was sometimes striking (Fig. 4). However, as in two of the cases whose acuity dropped more than two Snellen lines, the relationship could not always be demonstrated. What else might correlate with the subtle drop in acuity? Anctil and Anderson, in determining static foveal measures in select glaucoma patients, determined several patterns of field loss, including both dissociation and association with peripheral sensitivity[4]. It is possible that evidence of global visual loss might be found by monitoring the peripheral visual field beyond the central 30° for deterioration, or by careful statistical evaluation of the central 30-2 and 24-2 tests by the Statpac-2© Glaucoma Change probability plot. These strategies were not done by us, but may merit further investigation.

It is difficult to make sense of the enormous amount of numeric data present in multiple MTT displays over time. The long-term evaluation is greatly enhanced by use of the graphic 16 point macular threshold plot. Visual inspection can rapidly establish areas of stability, progressive deterioration, or fluctuation. Knowing that in the presence of clinical stability fluctuation up to 7 dB per location can manifest in threshold testing of the central field[5], caution must be used in asserting whether there is progression or not (*cf* Fig 7). It remains to be seen, however, whether statistically valid information such as linear regression analysis is clinically any more useful than visual inspection alone of the graphic display of the MTT (Fig. 10)

In looking at the displays of the perifoveal four point plots, it is remarkable that there often appears less fluctuation of values in the identically tested points of the MTT compared to the testing of the same points by the central 30-2 or 24-2, despite the fact that each eye underwent the longer tests first. It may well be that the more compact spatial focus of the test pattern, and/or shorter testing time, contribute to more consistent responsiveness. A specific statistical comparison is in progress to evaluate the short term fluctuation values of the MTT and the central 30-2/24-2 tests performed the same day

Although the value of assessing the central 10° has been asserted in the neuro-ophthalmic literature[6], the MTT specifically has received scant attention in the glaucoma literature The one exception was a report from Italy where the MTT was used with both blue and white target

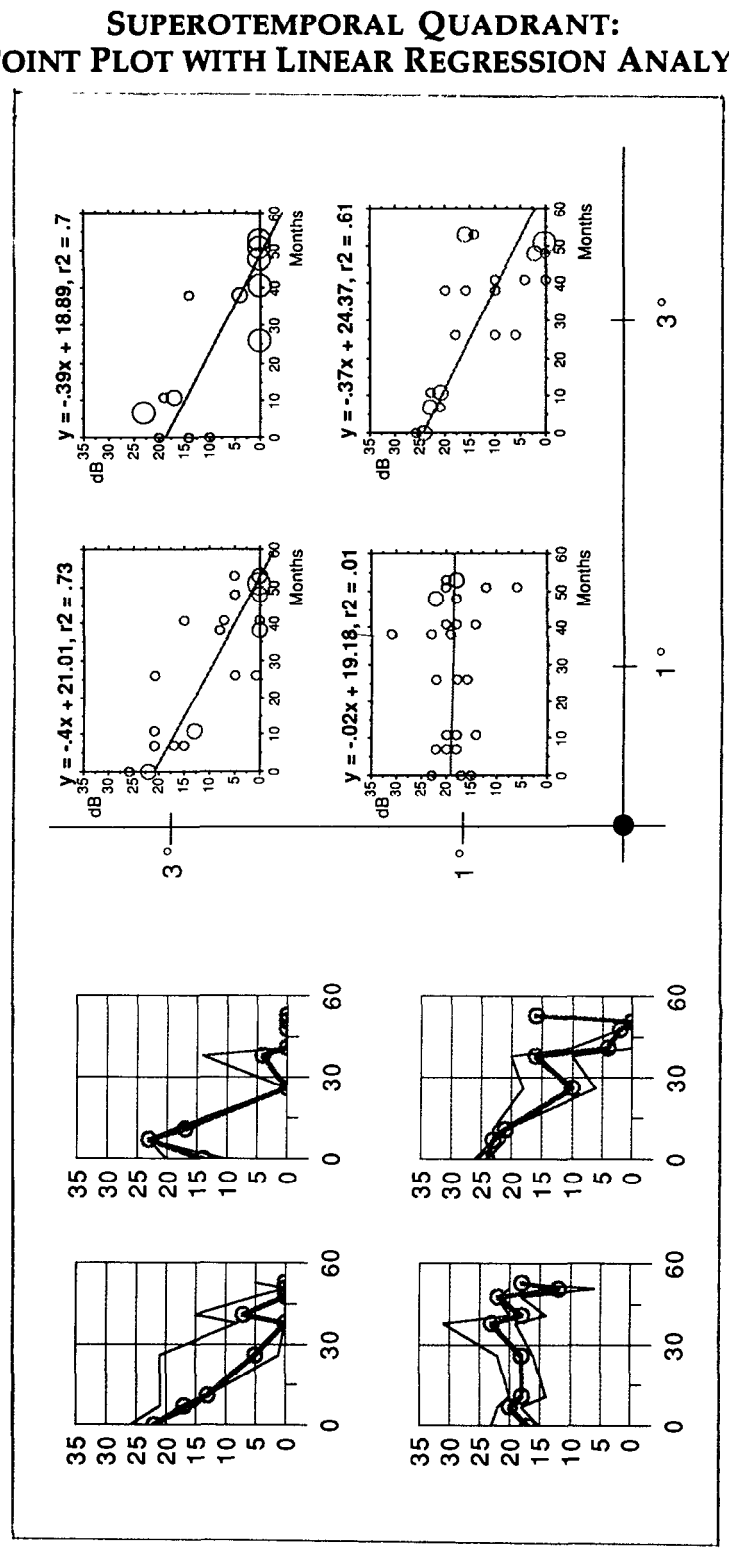

Fig. 10. Sample display of how one quadrant of the MTT (on left) is replotted, using a linear regression analysis (on right). Three points show a statistically significant deterioration, compared to the innermost (lower left) point, which remained stable.

colors to distinguish glaucoma suspects from normals[7]. In our experience, the routine clinical use of macular thresholding to refine the surveillance of glaucomatous eyes with threatened fixation has proven clinically feasible and productive. Especially in eyes with extensive field damage, careful scrutiny of the precious central field is often the only handle available in following advanced disease (*cf* Fig. 8) and monitoring preservation of function after intervention

Although there remain many unanswered questions about the properties and long-term behavior of perifoveal testing, our study is the first long-term, prospective evaluation of the MTT in a large glaucoma population Interesting data remains to be culled, especially with respect to: foveal variability with same-day testing and fluctuation over time; to the short term fluctuation in the MTT compared to 30-2 or 24-2 testing; and to the association between foveal values and measured acuities.

Clinically the MTT has already proven invaluable in carefully exploring the phenomenon of split fixation in advanced glaucoma. We have demonstrated with great precision the capacity for stability of central visual function despite encroachment by glaucomatous defects into the central 5°. As prescribed by Kolker, keeping the IOP as low as possible appears to be invaluable advice for preservation of these vulnerable fields. In cases of advanced glaucomatous damage, the MTT in conjunction with foveal threshold testing provides important information as to the function of the central field.

Acknowledgements

We wish to acknowledge the kind assistance of Dr Peter Åsman, Department of Ophthalmology, Malmö General Hospital, Malmö, Sweden, as well as the daily support by the perimetric technicians at Pacific Presbyterian Medical Center, Kaiser-Permanente, Redwood City, and Stanford University Medical Center

References

1. Kolker AE: Visual prognosis in advanced glaucoma: a comparison of medical and surgical therapy for retention of vision in 101 eyes with advanced glaucoma Trans Am Ophthalmol Soc 75:539-555, 1977
2 Lieberman MF, Drake MV: A Simplified Guide to Computerized Perimetry Thorofare, NJ: Slack Inc 1987
3. Hart WM Jr: Three-dimensional topography of the central visual field: sparing of foveal sensitivity in macular disease In: Henkind P (ed) Acta XXIV International Congress of Ophthalmology, Vol 1, pp 184-189 Philadelphia: JB Lippincott 1983
4. Anctil JL, Anderson DR: Early foveal and generalized depression of the visual field in glaucoma Arch Ophthalmol 102:363-370, 1984
5 Werner EB, Petrig B, Krupin T, Bishop KI: Variability of automated visual fields in clinically stable glaucoma In: Heijl A (ed) Perimetry Update 1988/89, pp 167-172 Amsterdam/Berkeley/Milano: Kugler & Ghedini Publ 1989
6. Wall M: Examination of the ten degrees of visual field surrounding fixation In: Wall M, Sadun A (eds) New Methods of Sensory Visual Testing, pp 94-111 New York: Springer Verlag 1989
7. Capoferri C, Garavaglia A, Buscemi M, Brancato R: Clinical detection of early glaucomatous foveal involvement Int Ophthalmol 13:259-264, 1989

Are early visual field changes topographically different between primary open-angle (high tension) and normal tension glaucoma?

Aiko Iwase, Keiko Matsubara and Yoshiaki Kitazawa

Department of Ophthalmology, Gifu University School of Medicine, Gifu, Japan

Abstract

The authors studied the early visual field defects in 13 normal tension glaucoma (NTG) eyes and 13 primary open angle glaucoma (POAG) eyes. The patterns of the early visual field defects in the two groups of patients were compared between the upper and lower hemifields In POAG eyes, the incidence of abnormal points was significantly higher in the lower nasal areas than in the upper nasal areas In contrast, in NTG eyes, it was significantly higher in the upper hemifield than in the lower hemifield

Introduction

It is not yet clear whether or not early visual field changes are different in their location between primary open-angle glaucoma (POAG) and normal tension glaucoma (NTG). In an attempt to answer this question, we studied the early glaucomatous visual field damage in the two types of glaucoma by comparing the incidence of abnormal points in the upper and lower hemifields.

Material and methods

Perimetry was performed with a Humphrey Field Analyzer using threshold program 30-2, and visual field indices were calculated with the Statpac 2 program. Total deviation (TD) and pattern deviation (PD) of each test point were judged to be either normal or abnormal according to the probability symbol of Statpac 2[1] When it was reproducible, the 5% probability level was used as the indicator of abnormality

Statpac 2 includes the program called "Glaucoma Hemifield Test" (GHT) which evaluates fields by comparing the thresholds of clusters of test points in the upper hemifields with those in the lower[1]. In the GHT program, each hemifield contains five such clusters mirrored in the opposite hemifield (Fig. 1).

The diagnostic criteria for normal tension glaucoma are listed in Table 1 We deliberately set the upper limit of normal IOP slightly low so that only patients with definitely "normal" IOP were enrolled in the NTG group

Table 1

1	Maximum IOP equal to or lower than 20 mm Hg
2	Glaucomatous cupping of the optic disc
3	The presence of glaucomatous visual field defects corresponding to the optic disc changes
4	A non-occludable normal open angle
5	Neither intracranial nor otolaryngological lesions
6.	No history of massive hemorrhage or hemodynamic crisis
7	No history of corticosteroid therapy

Address for correspondence Prof Yoshiaki Kitazawa, M D , Department of Ophthalmology, Gifu University School of Medicine, 40-Tsukawa-machi, Gifu-shi 500, Japan

Perimetry Update 1990/91, pp. 491-494
Proceedings of the IXth International Perimetric Society Meeting,
Malmö, Sweden, June 17-20, 1990
edited by Richard P Mills and Anders Heijl

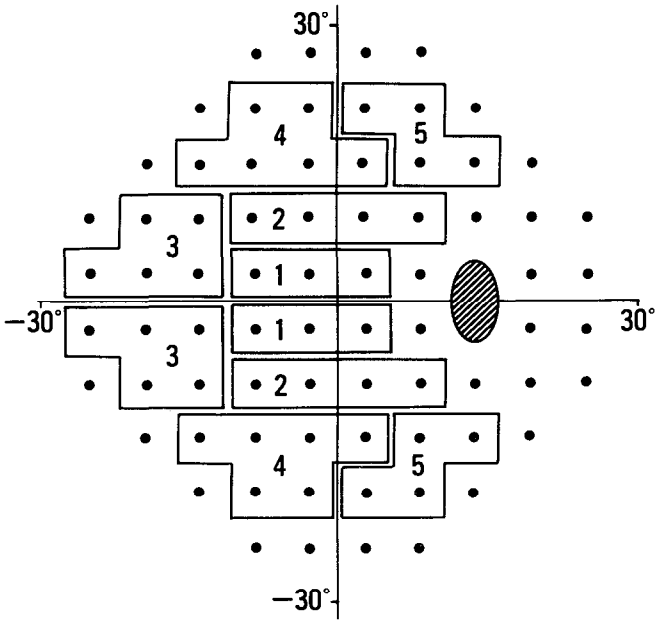

Fig 1 The five pairs of areas in the Glaucoma Hemifield Test

Thirteen normal tension glaucoma (NTG) patients and 13 primary open angle glaucoma (POAG) patients were studied. In all patients, visual acuity was equal to or better than 0.7 and the reliability of the field test was satisfactory (fixation loss, false positive, and false negative rates were less than 20%). The mean deviation (MD) was better than -4.0 dB; therefore, all the enrolled patients could be considered to have relatively mild field changes.

The clinical background of the patients is summarized in Table 2. The age of the two groups was not significantly different. The IOP of NTG patients was the mean IOP of all values obtained during the follow-up period, including a diurnal pressure profile. The IOP of POAG patients was the mean of IOPs measured throughout the observation period in the absence of glaucoma medication

Table 2 Clinical background

	NTG	*POAG*
Age (years)	56 20±10 20 (39-74)	48 02±14.80 (26-79)
Male/female	10/3	11/2
IOP (mm Hg)	13 50± 2 16	23 10± 1 45
MD (dB)	−1 94± 1 24	−2 39± 0.82

( ): range; mean ± SD

Table 3 Aulhorn classification: number of eyes

Greve's modification)	*0-I*	*I*	*II*	*Total*
NTG	1	7	5	13
POAG	3	7	3	13

The mean deviation (MD) was not significantly different between the two groups. The clinical stage of visual fields was classified according to Greve's modification of Aulhorn's classification of glaucomatous visual field damage (Table 3) and the distribution of the stages of field defects was not significantly different between the two groups.

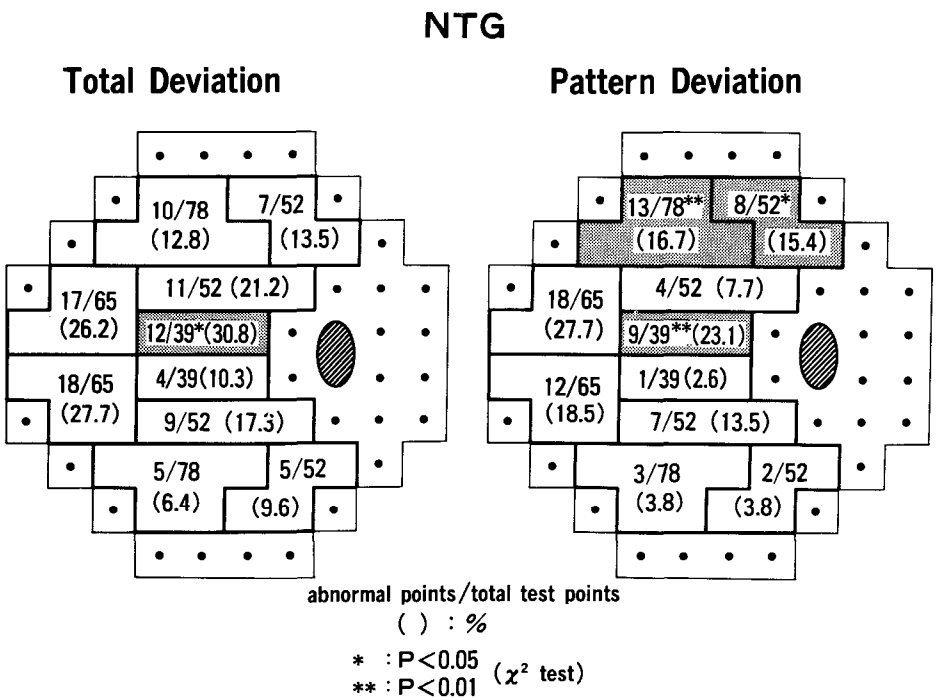

Fig 2 The incidence of abnormal points in each cell (NTG) as a ratio and (%).

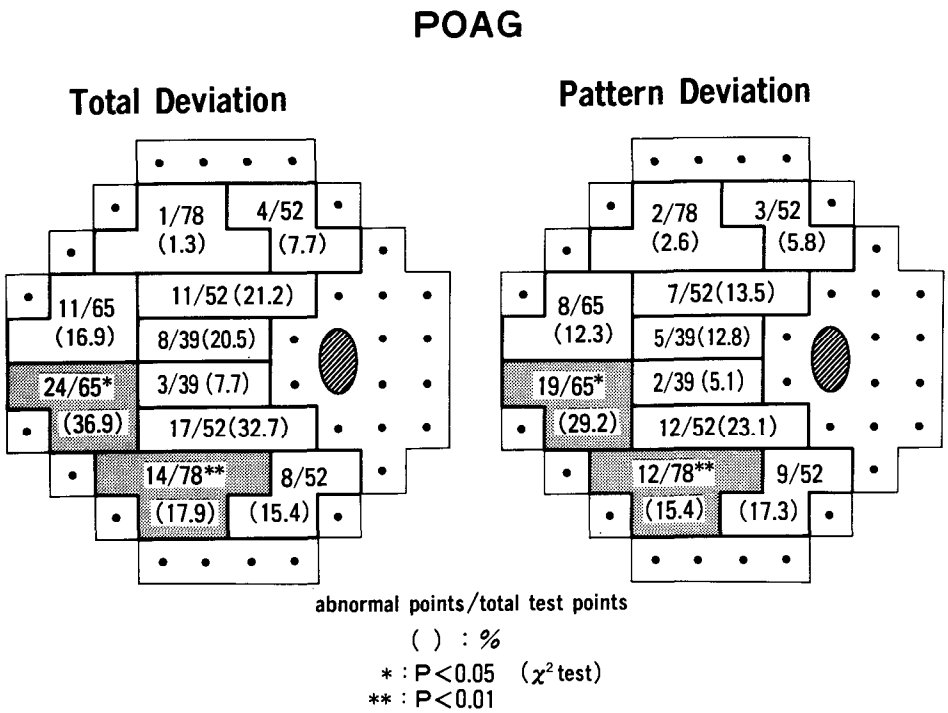

Fig 3 The incidence of abnormal points in each cell (POAG) as a ratio and (%)

Results

The results of threshold determinations in NTG patients are illustrated in Fig. 2. The ratio of abnormal points to total test points is shown in each cell. For TD, the incidence of abnormal test points was noted to be high, greater than 20%, in the upper areas 1, 2 and 3, and the lower area 3. For PD, the abnormal test points were most prevalent in upper areas 1 and 3. When the incidence of abnormal points was compared in two corresponding areas, for example, the upper area 1 to the lower area 1, the upper hemifield was found to have a higher incidence of abnormal points. That is, for TD, the upper area 1 had a significantly higher incidence of abnormal points, and for PD the upper areas 1, 4 and 5 were more frequently involved than the corresponding areas in the lower hemifield.

The results in POAG patients are similarly illustrated in Fig. 3. For TD, the incidence of abnormal test points was noted to be high, greater than 20%, in the upper areas 1 and 2, and the lower areas 2 and 3. For PD, the abnormal test points were most prevalent in lower areas 2 and 3. When the incidence of abnormal points was compared in two corresponding areas, the lower hemifield was found to have a higher incidence of abnormal points. They were the lower areas 3 and 4 for TD and PD.

The patterns of early visual field defects were compared between upper and lower hemifields in POAG and NTG, respectively. In POAG eyes, the incidence of abnormal points was significantly higher in the lower nasal areas than in the upper nasal areas. In contrast, in NTG eyes, this was significantly higher in the upper hemifield than in the lower hemifield.

Discussion

The pattern of visual field damage has been reported to be different between NTG and POAG by Levene[2], Anderton and Hitchings[3], Caprioli and Spaeth[4] and Greve and Geijssen[5]. On the other hand, many investigators, such as Motolko *et al.*[6] and Phelps *et al* [7], reported no difference in the pattern of field defects between two groups. The results of the present study, in which five pairs of corresponding point clusters in the upper and lower hemifields were compared, supports the notion that the pattern of visual field damage is different between NTG and POAG The difference in the topographic pattern of relative scotomata suggests that the mechanism responsible for the development of the optic nerve damage might be different between POAG and NTG in their early stages.

References

1 Statpac 2 User's Guide: San Leandro CA: Allergan-Humphrey 1989
2 Levene RA: Low tension glaucoma: a critical review and new material Surv Ophthalmol 24:621, 1980
3 Anderton SA, Hitchings RA: A comparative study of visual fields of patients with low-tension glaucoma and those with chronic simple glaucoma Doc Ophthalmol Proc Ser 35:97-99, 1983
4 Caprioli J, Spaeth GL: Comparison of visual field defects in the low-tension glaucomas with those in the high-tension glaucomas Am J Ophthalmol 97:730-737, 1984
5 Greve EL, Geijssen HC: Comparison of glaucomatous visual field defects in patients with high and with low intraocular pressures Doc Ophthalmol Proc Ser 35:101, 1983
6 Motolko M, Drance SM, Douglas GR: Comparison of defects in low-tension glaucoma and chronic open angle glaucoma Arch Ophthalmol 100:1074, 1982
7 Phelps CD, Hayreh SS, Montague PR: Visual field in low-tension glaucoma, primary open-angle glaucoma, and anterior ischemic optic neuropathy Doc Ophthalmol Proc Ser 35:113, 1983

The influence of intraocular pressure on visual field damage in normal-tension and high-tension glaucoma

Balwantray C. Chauhan and Stephen M. Drance

Department of Ophthalmology, University of British Columbia, Vancouver, Canada

Abstract

There have been several reports to suggest that the type of visual field damage in glaucoma is influenced by intraocular pressure (IOP) This study was undertaken to determine the extent to which patients with normal-tension glaucoma (NTG) and high-tension glaucoma (HTG) could be differentiated on the basis of some features of their visual fields The authors present results from 40 pairs of NTG and HTG patients matched very closely for the extent of visual field damage, pupil size and visual acuity Using this pooled material, the authors increased the IOP difference between the two groups in either direction, *i e* , either by progressively lowering the highest recorded IOP allowed for inclusion in the NTG group or by progressively increasing that required for inclusion in the HTG group They compared the normal areas of the visual fields by using simple visual field indices designed to quantify the undisturbed field With Receiver Operating Characteristics (ROC) analysis, the authors showed that changing the inclusion criterion in the NTG group resulted in no better separation between the groups However, when the inclusion criterion was changed in the HTG group, the two groups tended to become more separable In this case, the degree of separation appeared to be related to the difference in the highest recorded IOP between the two groups, although the separation was not complete These findings show that pressure has a greater influence on the type of visual field damage at the higher end of the IOP spectrum encountered in glaucoma and suggest that there is no common single pathophysiological mechanism in glaucoma.

Supported in part by Grant 1576 from the Medical Research Council of Canada

Address for correspondence Dr B C Chauhan, Nova Scotia Eye Centre, Halifax Infirmary, 1335 Queen Street, Halifax, Nova Scotia, Canada B3J 2H6

Perimetry Update 1990/91, p 495
Proceedings of the IXth International Perimetric Society Meeting,
Malmö, Sweden, June 17-20, 1990
edited by Richard P Mills and Anders Heijl

Contrast sensitivity measurement in the detection of primary open angle glaucoma

Joanne M. Wood and Jan E. Lovie-Kitchin

Centre for Eye Research, Queensland University of Technology, Brisbane 4001, Australia

Abstract

Contrast sensitivity is a well established psychophysical technique for identification and monitoring of visual dysfunction. Traditional methods of contrast sensitivity measurement using oscilloscope-based techniques are too time-consuming and expensive to be clinically viable A number of chart-based tests have been introduced to simplify measurement. These employ either grating or letter targets and incorporate criterion-free psychophysical strategies such as two alternate forced choice to reduce measurement error. The aim of the study was to determine the potential of such tests in the detection of primary open angle glaucoma. Twenty primary open angle glaucoma, 20 ocular hypertensive patients and 20 normal control subjects were investigated using the following chart-based contrast sensitivity tests: Cambridge Gratings, Pelli-Robson Letter Charts, High and Low Contrast Letter Charts and Melbourne Edge Test. The validity and diagnostic capability of each was evaluated with respect to oscilloscope-based contrast sensitivity and to Humphrey Field Analyzer central visual fields assessment (program 24-2), disc photographs and intraocular pressures. The validity of each of the chart-based tests relative to the oscilloscope-based standard was poor (r<0.70). ROC curves demonstrate low sensitivity and specificity (poor diagnostic capacity) at the recommended cut-off levels for all of the contrast sensitivity tests. Alternative criteria are suggested to improve diagnostic capacity.

Introduction

The three clinical tests used routinely in screening for glaucoma are optic disc evaluation, measurement of intraocular pressure (IOP) and visual field analysis. There is evidence to suggest, however, that as many as 35-50% of optic nerve fibers may be lost in glaucoma before a visual field defect measured manually can be recorded[1]. More recently, it was reported that perimetric sensitivity measured using automated static techniques decreases soon after the initial loss of ganglion cells[2], although the study examined only a small number of subjects.

Assessment of the contrast sensitivity function (CSF) has been reported to be more effective in detecting early glaucomatous changes than either measuring visual fields or IOP[3]. Traditional methods of measuring contrast sensitivity have used oscilloscope-based techniques which are both expensive and time-consuming and unsuited to clinical practice. More recently, a number of rapid and inexpensive chart-based screening tests have been introduced with the aim of making contrast sensitivity testing a clinically viable technique. These include the Arden Plates[4], Regan Low Contrast Letters[5], Vistech Contrast Sensitivity Charts[6], Bailey-Lovie High and Low Contrast Letter Charts[7,8], Melbourne Edge Test[9], Pelli-Robson Letter Charts[10] and Cambridge Gratings[11]. Although all these tests have interesting features many have been made available to the clinician without supporting evaluation of their reliability and validity, and therefore their utility in clinical practice has been questioned[12,13].

We report results of an ongoing study, the aim of which is to assess the validity and diagnostic capacity of five chart-based screening tests. The study addresses these issues with respect to the detection of primary open angle glaucoma (POAG). The tests selected for evaluation were the Cambridge Gratings, Bailey-Lovie High and Low Contrast Letter Charts, Pelli-Robson Letter Charts and the Melbourne Edge Test (MET).

The MET, Cambridge Gratings and Pelli-Robson Letter Charts are designed to measure the peak of the CSF, around 4 cycles/degree. This is based on the premise that the height of the peak of the CSF is a good predictor of visual performance[14] and is depressed in ocular and neuro-ophthalmological disease.

Perimetry Update 1990/91, pp. 497-502
Proceedings of the IXth International Perimetric Society Meeting,
Malmö, Sweden, June 17-20, 1990
edited by Richard P. Mills and Anders Heijl

The MET[9] is designed to measure edge contrast sensitivity, on the assumption that this approximates the peak of the CSF[15]. The test comprises two series of 20 circular patches with an edge on each patch, the contrast of which decreases from 0.79 to 0.001 in 0.1 log unit steps (mean luminance is constant). Subjects are required to identify the orientation of the edge (horizontal, vertical, right oblique or left oblique). Edge threshold (dB) is taken as the edge of lowest contrast which is identified correctly.

The Pelli-Robson Letter Chart[10] consists of eight rows of six uppercase Sloan letters, which are of constant size but decrease in contrast from approximately 100% in the upper left hand corner to 0.9% at the lower right. The letters are arranged in groups of three, where contrast is constant within a group, and the contrast of each group decreases by approximately 0.15 log units. Subjects are required to name the letters and continue until two or more errors are made in a group; nil responses are not allowed. Contrast threshold is determined by the last group in which at least two of three letters are correctly identified.

The Cambridge Gratings[11] consist of a series of 12 pairs of plates. Each pair comprises one plate composed of horizontal square wave gratings (4 cycles/degree) while the other plate is blank. The mean luminance of each of the plates in a pair are equal. The contrast across the series of gratings decreases from 13% to 0.14%. The plates are presented in order of decreasing contrast and for each presentation the subject is required to report on which plate the horizontal stripes appear. Subjects are not permitted to give a nil response, so the test is a true two alternate forced choice procedure. The score is given as the first plate pair on which the subject makes an error; the scores on four repeated trials are summed and converted, by means of a table, to a contrast sensitivity score

The Bailey Lovie High (85% contrast) and Low Contrast (9% contrast) Letters[7,8] are designed to measure both high and low spatial frequencies. Low contrast letters have been advocated as a good screening tool for a number of visual disorders including glaucoma[5], however more recently their usefulness as a screening device has been questioned[12,16].

Methods

The sample comprised 60 subjects: 20 POAG patients on non-miotic medication (mean age 58.2 years; SD 9.2 years); 20 glaucoma suspects (mean age 52.3 years; SD 14.3 years) and 20 age-matched normal controls (mean age 56.9 years; SD 11.6 years). The glaucoma suspects were selected on the basis of raised (≥21 mmHg) and/or asymmetrical IOP (≥5 mmHg difference). Subjects were free of ocular or neurological pathology (other than defined in the inclusion criteria) and free of systemic disease with known ophthalmic complications.

Each subject attended for one session of approximately two hours' duration. Performance measures for both eyes of each subject were obtained for oscilloscope-based contrast sensitivity, Cambridge Gratings, Bailey-Lovie High and Low Contrast Letters, Pelli-Robson Letter Charts, MET and the Humphrey Field Analyzer (HFA).

Contrast sensitivity to vertical, stationary sinewave gratings was measured using an oscilloscope screen (Millipede VR1000) driven by a microprocessor. The angular subtense of the screen was 5.34° at the working distance of 3 m. Spatial frequencies of 1, 2, 4, 8 and 16 cycles/degree were selected to evaluate the CSF. The Millipede system uses a double staircase thresholding procedure with three reversals to determine contrast threshold for each spatial frequency. Central threshold visual fields were measured with the HFA using program 24-2 for stimulus size III. Field results were analyzed using the visual field indices of the Statpac. The chart tests were employed using the procedures recommended by the manufacturer, under the specified illumination levels. Full optical correction for the appropriate working distances were employed for each test. The order of tests and eyes was balanced using a factorial design.

At the end of the session, IOP was measured using an AO non-contact tonometer to obtain three readings falling within 3 mmHg of each other. Fundus photographs were also taken and used to classify the optic discs.

Both eyes of each subject were measured to permit inter-eye comparison. Data from only one eye was included in the analysis for this paper. The selected eye was that with the greatest degree of ocular hypertension (OHT) or glaucomatous loss. For the normal subjects, the selected eye was chosen to match the number of right and left eyes analyzed for the glaucoma and glaucoma suspect groups. The results obtained using the various tests were compared. The

diagnostic capacity of each test was analyzed in terms of its sensitivity and specificity using cumulative frequency plots and receiver operator characteristic (ROC) curves.

Results and discussion

A measure of the validity of the chart tests was determined by calculating Pearson's product moment correlations (r_p) for the contrast sensitivity values obtained with the chart tests against those obtained with the oscilloscope technique for all subjects (illustrated in Table 1 for the spatial frequencies that each of the chart tests are purported to measure). None of the screening tests correlated highly with the oscilloscope-based measure. This finding is contrary to the literature advocating the chart tests, which purport that the MET[9], Pelli-Robson Letters[10] and Cambridge Gratings[11] measure the peak of the CSF, whilst the Low Contrast Letters measure the mid to low spatial frequencies[5]. The poor agreement between contrast sensitivity scores measured with the chart tests and the oscilloscope may arise from:

1. different psychophysical procedures. The chart tests employ forced choice procedures whilst the oscilloscope technique employs a double staircase with three reversals;
2. differences arising from the use of electronic as compared to chart-based techniques;
3. the presence of suprathreshold high frequency components in the chart targets masking the low spatial frequency stimuli;
4. high levels of variance associated with the measurement techniques masking any correlations between the tests. This is supported by the finding that the test-retest reliability of the chart-based techniques is poor[13].

Table 1 Correlations (r_p) between the chart tests and the oscilloscope

Test	*SF (cycles/degree^{-1})*	r_p
Cambridge Gratings	4	0 35
Pelli-Robson Letters	4	0 49*
MET	4	0 28
Bailey-Lovie HC Letters	16	0 43*
Bailey-Lovie LC Letters	4	0 37

*indicates significance >95% level

A series of one-way analyses of variance (ANOVA) was carried out for test and subject group. The ANOVA showed that there were significant differences in scores ($p<0.005$) between subject groups for all of the tests apart from the MET and the short-term fluctuation index of the HFA. A Scheffe post-hoc analysis demonstrated that these differences lay between the glaucoma and the normal groups None of the tests discriminated between the glaucoma suspect and the normal groups apart from IOP (the latter result was expected because the inclusion criterion for the glaucoma suspect group was defined by IOP) These findings are contrary to those of some other studies which have reported differences in visual performance between OHT and normal subjects with respect to contrast sensitivity (*e.g.*,[3]), color vision (*e.g.*,[17]) and fluctuations in static (*e.g.*,[18]) and kinetic (*e.g.*,[19]) perimetry. It is possible that in the present study any differences in visual performance between the OHT and normal subjects may have been masked by differing levels of experience. The OHT subjects were experienced in psychophysical testing (particularly visual fields) as their visual function had been monitored over a number of years, whereas the normal subjects had varying levels of experience. Prior experience with a psychophysical test has been reported to improve performance levels and reduce the degree of fluctuation in response (*e g.*,[20]).

The diagnostic capacity of each of the tests was determined by plotting the cumulative frequency of subjects passing or failing each test for different pass/fail criteria (illustrated for the Cambridge Gratings in Fig. 1). The percentage of abnormals failing is the sensitivity of the test for the given pass/fail criterion and the percentage of normals passing is the specificity. The point at which the number of misclassifications (*i e* , false-negatives and false-positives) is at a minimum can be chosen as a cut-off criterion for separating glaucomas and normals in the age group investigated in this study. This cut-off point is given in Table 2 for each of the chart tests, together with the associated sensitivity and specificity values. However, this point

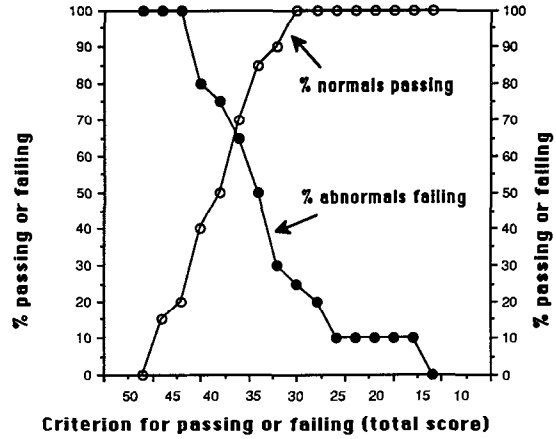

Fig 1 Cumulative frequency of subjects passing or failing the Cambridge Grating test for different pass/fail criteria.

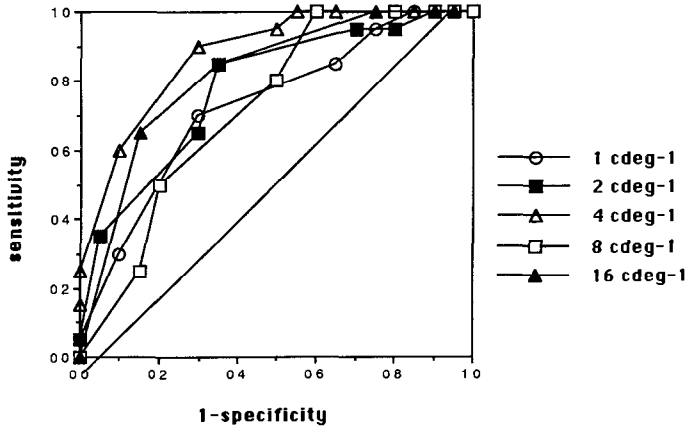

Fig 2 ROC curve for the five spatial frequencies of the oscilloscope Points along the curve represent different cut-off criteria – these were omitted from the graph to maintain the clarity of the figure.

may not always be the best cut-off criterion to use since it depends upon the relative importance attached to false-positive and false-negative errors The Bailey-Lovie Low Contrast Letters have the best sensitivity and specificity of the chart tests at a pass/fail criterion of +0.20 (log-MAR). It should be noted that this cut-off criterion should only be used for the screening of a similar population to that tested in this study and further that the relatively low sensitivities and specificities of all of the chart tests makes them unsuitable for clinical screening regardless of the cut-off criterion used.

Table 2 Optimum cut-off criteria for the chart tests and the associated sensitivity and specificity values

Test	*Pass/fail criterion*	*Sensitivity*	*Specificity*
Cambridge Gratings	35	65%	70%
Pelli-Robson Letters	1 65	40%	82%
MET	20	65%	60%
Bailey-Lovie HC Letters	–0 04	70%	60%
Bailey-Lovie LC Letters	+0 20	77%	77%

An alternative method of presenting the sensitivity and specificity data is to plot a ROC curve (illustrated for the oscilloscope technique in Fig. 2). Points along the curve represent different

cut-off criteria for the test. A point in the top left hand corner of the diagram would indicate good sensitivity and specificity; the diagonal line represents points of zero discrimination. The ROC curve may be used to give an index of the relative power of tests to differentiate between the glaucoma and normal groups if a number of tests are plotted on the same graph. The sensitivities and specificities of the oscilloscope measures are greater than those of the chart tests and are best for a spatial frequency of 4 cycles/degree (around the peak of the CSF). This finding is in agreement with previous studies[21] which have also demonstrated that spatial frequencies around the peak of the CSF have the greatest diagnostic capacity for the detection of glaucoma. The ROC curve for the chart tests indicates poor sensitivity and specificity for all of the tests, with the Bailey-Lovie Low Contrast Letters having the best discriminability of the chart-based tests (as shown in Table 2).

While oscilloscope measures of contrast sensitivity discriminated between the glaucoma and normal groups, the visual field indices obtained with the HFA yielded higher levels of sensitivity and specificity than this test. Cumulative frequency and ROC curves showed that the mean defect (MD) and pattern standard deviation (PSD) indices had the highest levels of sensitivity and specificity, at 90% (sensitivity) and 79% (specificity) for the PSD and 90% (sensitivity) and 78% (specificity) for the MD and are of a similar order to those derived by an alternative method in another study[22]. Since one of the criteria in the diagnosis of POAG is the presence of visual field defects, this result was not unexpected. Nevertheless, the findings indicate that this form of visual field testing is superior to any alternative contrast sensitivity test available.

Conclusions

Measurement of the peak of the CSF using oscilloscope-based techniques is a sensitive and specific technique for the detection of POAG. The currently available chart-based screening tests, however, correlate poorly with oscilloscope-based measures and have low diagnostic capacity for detecting known glaucoma – they are therefore unlikely to be effective in detecting glaucomas prior to field loss. It is concluded that although the screening tests are rapid and convenient, they sacrifice sensitivity and specificity and may be ineffective screening devices for early glaucoma in their current form.

References

1 Quigley HA, Addicks EM, Green WR: Optic nerve damage in human glaucoma III Quantitative correlation of nerve fiber loss and visual field defect in glaucoma, ischemic neuropathy, papilloedema, and toxic neuropathy Arch Ophthalmol 100:135-146, 1982
2. Quigley HA, Dunkelberger GR, Green WR: Retinal ganglion cell atrophy correlated with automated perimetry in human eyes with glaucoma Am J Ophthalmol 107:453-464, 1989
3. Ross JE, Bron AJ, Reeves BC, Emmerson PG: Detection of optic nerve damage in ocular hypertension Br J Ophthalmol 69:897-903, 1985
4. Arden GB, Jacobson JJ: A simple grating test for contrast sensitivity: preliminary results indicate value in screening for glaucoma. Invest Ophthalmol Vis Sci 17:23-32, 1978
5. Regan D, Neima D: Low-contrast letter charts as a test of visual function Ophthalmology 90:1192-1200, 1983
6. Ginsburg AP: A new contrast sensitivity vision test. Am J Optom Physiol Opt 61:403-407, 1984
7. Bailey IL, Lovie JE: New design principles for visual acuity letter charts Am J Optom Physiol Opt 53:740-745, 1976
8. Bailey IL: Simplifying contrast sensitivity testing. Am J Optom Physiol Opt 59: 12P, 1982
9. Verbaken JH, Johnston AW: Population norms for edge contrast sensitivity Am J Optom Physiol Opt 63:724-732, 1986
10. Pelli DG, Robson JG, Wilkins AJ: The design of a new letter chart for measuring contrast sensitivity Clin Vis Sci 2:187-199, 1988
11. Wilkins AL, Della Sala S, Somazzi L, Nimmo-Smith I: Age related norms for the Cambridge Low Contrast gratings, including details concerning their design and use Clin Vis Sci 2:201-212, 1988
12 Brown B, Lovie-Kitchin JE: High and low contrast acuity and clinical contrast sensitivity tested in a normal population Optom Vis Sci 66:467-473, 1989
13. Wood JM, Hill AR, Reeves BC: The reliability and validity of high and low contrast optotypes. Ophthalm Physiol Opt 9:106, 1989

14. Rubin GS: Reliability and sensitivity of clinical contrast sensitivity tests. Clin Vis Sci 2:169-177, 1988
15 Shapley RM, Tolhurst DJ: Edge detectors in human vision. J Physiol (London) 229:165-183, 1973
16 Lovie-Kitchin JE: High contrast and low contrast visual acuity in age related macular degeneration. Clin Exp Optom 72:79-83, 1989
17 Flammer J, Drance SM: Correlation between color vision scores and quantitative perimetry in suspected glaucoma. Arch Ophthalmol 102:38-39, 1984
18. Flammer J, Drance SM, Fankhauser F, Augustiny L: Differential light threshold in automated static perimetry: factors influencing short-term fluctuations Arch Ophthalmol 102:876-879, 1984
19 Zingirian M, Gandolfo E, Capris P, Rovida S: Kinetic threshold fluctuation and glaucoma. Glaucoma 10:21-24, 1988
20. Wood JM, Wild JM, Hussey MK, Crews SJ: Serial examination of the normal visual field using Octopus automated projection perimetry: evidence for a learning effect Acta Ophthalmol 65:326-333, 1987
21. Ross JE, Bron AJ, Clarke DD: Contrast sensitivity and visual disability in chronic simple glaucoma Br J Ophthalmol 68:821-827, 1984
22 Enger C, Sommer A: Recognising glaucomatous field loss with the Humphrey Statpac. Arch Ophthalmol 105:1355-1357, 1987

Statokinetic dissociation in glaucomatous peripheral visual field damage

N. Katsumori[1], J. Bun[2], H. Shirabe[3] and K. Mizokami[3]

[1]Akashi Municipal Hospital, [2]Kakogawa Municipal Hospital, and [3]Department of Ophthalmology, Kobe University, Japan

Abstract

In this study, the authors tested the peripheral nasal visual fields of 17 eyes of 12 patients with early glaucomatous visual field defects The Octopus program 41 was employed for static measurements and the Goldmann perimeter for kinetic measurements In the nasal peripheral Octopus test points, six pairs of two or three test points across the horizontal meridian were selected The sensitivity difference between upper and lower visual fields measured by Octopus and by Goldmann perimetry were compared. Octopus static perimetry was considered to be more sensitive than Goldmann kinetic perimetry But some cases showed statokinetic dissociation (sensitivity difference was found by Goldmann kinetic perimetry in spite of no difference being detected by Octopus static perimetry) and it tended to be found in the more peripheral field

Introduction

The nasal step is a characteristic visual field defect seen in glaucoma. In some cases, peripheral nasal defects without central field abnormalities occur as an early sign of glaucoma.

The usefulness of central 30° visual field examination with an automated static perimeter is well-known in glaucoma. But it has not yet been defined whether static perimetry is more useful than kinetic perimetry in detecting early glaucomatous peripheral visual field damage.

In this study, we tested the peripheral nasal visual fields of glaucoma patients using both static and kinetic strategies and compared the results.

Material and methods

Static and kinetic visual field testing was performed on 17 eyes of 12 patients with early glaucomatous visual field defects (six males and six females, aged 35-69 years). The Octopus program 41 was employed for static measurements and the Goldmann perimeter for kinetic ones

In the nasal peripheral Octopus test points, six pairs of two or three test points across the horizontal meridian were selected (Fig 1) for comparison of the difference in sensitivity between upper and lower fields. A difference of ±5 dB was not considered to be significant.

Octopus test points were plotted on the Goldmann visual field chart (Fig. 2) and the sensitivity of the selected points was determined as follows. The Goldmann test stimuli were expressed in decibels as referred to in the report of Anderson *et al* [1] (V-4 = -20 dB, I-4 = 0 dB, I-3 = 5 dB, I-2 = 10 dB, I-1 = 15 dB) If a test point was found between V-4 isopter and I-4 isopter, its sensitivity was determined as "a" (-20 dB ~ 0 dB). If a test point was found between I-4 isopter and I-3 isopter, sensitivity was "b" (0 dB ~ 5 dB), if it was between I-3 isopter and I-2 isopter, sensitivity was "c" (5 dB ~ 10 dB), and if it was between I-2 isopter and I-1 isopter, sensitivity was "d" (10 dB ~ 15 dB). Test points found outside the V-4 isopter were excluded from the study.

The difference in sensitivity between upper and lower fields was classified into four groups (no difference group: a→a, b→b, c→c, d→d; small difference group: c →b, d→c; middle

Address for correspondence Norio Katsumori, Department of Ophthalmology, Kobe University, Kusunoki-cho 7, Chuo-ku, Kobe, Japan

Perimetry Update 1990/91, pp 503-507
Proceedings of the IXth International Perimetric Society Meeting,
Malmö, Sweden, June 17-20, 1990
edited by Richard P. Mills and Anders Heijl

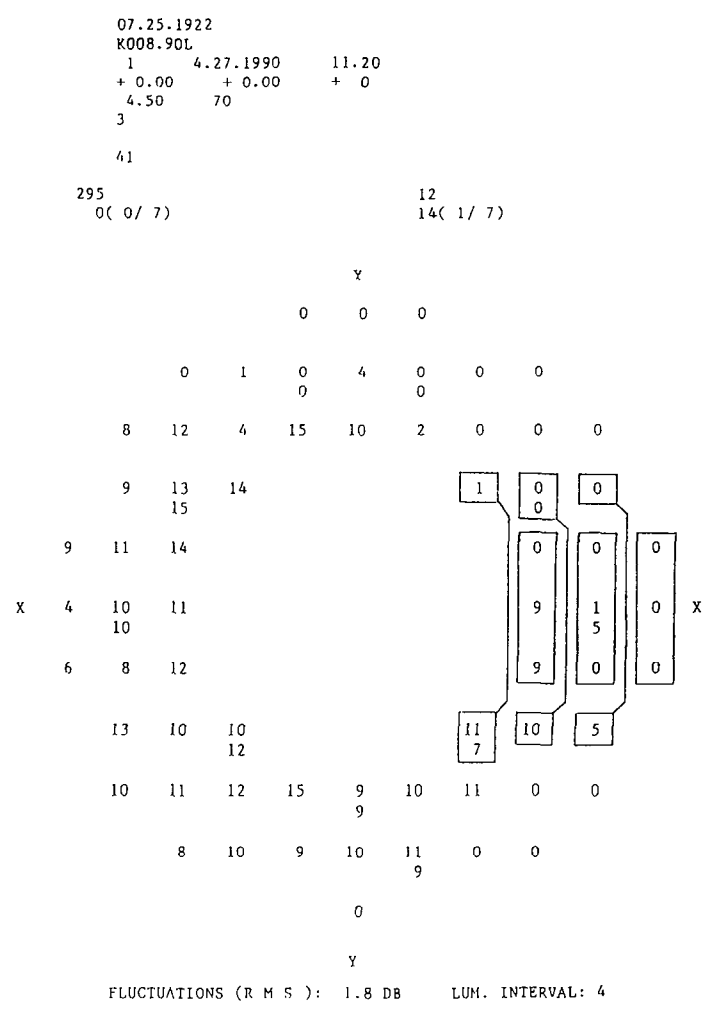

Fig 1 A selection of the test points in the peripheral nasal visual field

difference group: b→a; large difference group: c→a).

The sensitivity difference measured by Octopus and Goldmann perimetry was compared in each eye.

Results

The sensitivity differences between upper and lower visual fields measured by Octopus and Goldmann perimetry are shown in Fig. 3. The difference with Octopus measurement increased significantly in parallel with that of Goldmann measurement (Table 1, correlation ratio 0.28).

In 35 test pairs (36%), a difference of over 5 dB was detected by Octopus, although a difference could not be detected by Goldmann (Table 2). Static threshold perimetry was considered to be more sensitive and its usefulness in peripheral field examination was also demonstrated.

Eleven pairs (11.3%) which did not show a significant difference with Octopus (within 5 dB) did show a sensitivity difference with Goldmann perimetry (statokinetic dissociation). The dissociation pairs tended to be seen in the more peripheral locations (Table 3).

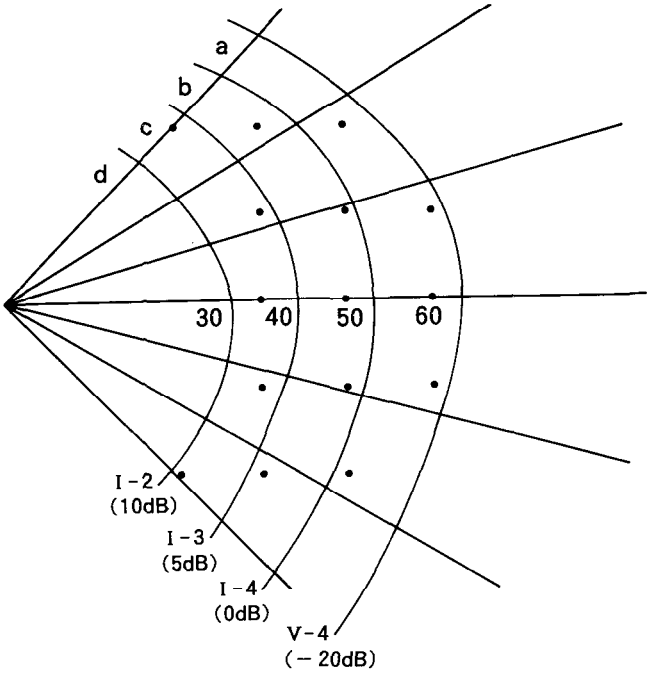

Fig 2 Test points plotted on the Goldmann visual field chart and determination of Goldmann sensitivity (a: V-4 ~ I-4; b: I-4 ~ I-3; c: I-3 ~ I-2; d: I-2 ~ I-1).

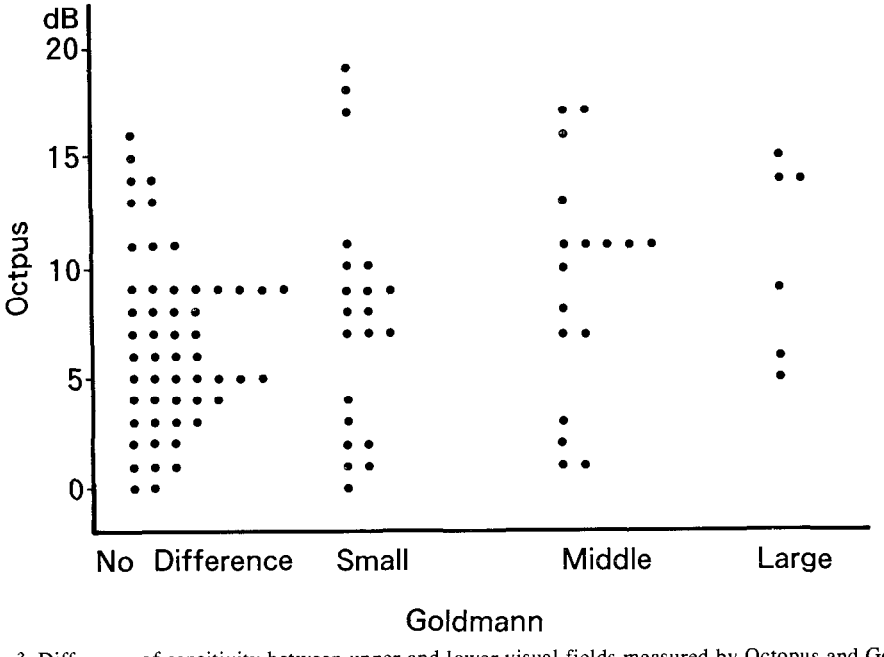

Fig 3 Difference of sensitivity between upper and lower visual fields measured by Octopus and Goldmann perimetry

Table 1 Average of the sensitivity difference

Goldmann	*Octopus*
No difference	6.6 ± 4.0 dB (*n*=53)
Small	7 7 ± 5 5 dB (*n*=21)
Middle	9 1 ± 5.1 dB (*n*=18)
Large	11 6 ± 3 9 dB (*n*=5)

correlation ratio 0.28

Table 2 Number of test pairs whose difference was over 5 dB or within 5 dB

Goldmann	*Octopus*	
	5 dB ≤	*<5 dB*
No difference	35 (36%)	17
Small	14	7 (7 2%)
Middle	14	4 (4 1%)
Large	5	0

Table 3 Location of the dissociation pairs

Eccentricity	*No of pairs*
60 degree	3 (13%)
48 degree	4 (8%)
36 degree	4 (5 3%)

Discussion

The nasal step has been recognized as one of the most characteristic visual field defects in glaucoma[2]. In addition, the presence of the peripheral nasal defect without central field abnormalities has been reported[3,4] and careful examination of the peripheral visual field is emphasized to be important. Recently, the automated static perimeter has been widely used to detect early glaucomatous damage. But the program most commonly used is mainly limited to the central field and study of the peripheral field by automated static perimetry is often ignored. Caprioli and Spaeth[5] have reported that an isolated peripheral nasal defect could be found using automated static perimetry and examination of the peripheral nasal field by sensitive threshold perimetry should be included in the careful evaluation of patients with glaucoma. In this study, we examined the peripheral nasal field using Octopus static perimetry and Goldmann kinetic perimetry and compared the results Significant correlation was found between the results of Octopus and Goldmann perimetry, and Octopus static perimetry was considered to be more sensitive than Goldmann kinetic perimetry In the peripheral field examination, the automated static perimetry could be useful in detecting glaucomatous damage.

In this study, some cases showed statokinetic dissociation (a sensitivity difference was found by Goldmann kinetic perimetry in spite of no difference being detected by Octopus static perimetry) and it tended to be found in the more peripheral field. There are some reasons why this dissociation was found. One of these is the method used to determine the sensitivity difference with Goldmann perimetry To determine the difference, we used the suggestion of Anderson *et al* [1]. They proposed conversion formulas from one instrument to another, but pointed out that the formulas they applied to Goldmann perimetry were less reliable than others.

One reason is the difference of background illumination between Octopus (4.0 asb) and Goldmann (31.5 asb). Using high background illumination, a steeper sensitivity profile can be

obtained. Therefore, Goldmann perimetry may be able to detect a large peripheral defect more readily than Octopus perimetry.

Safran and Glaser[6] reported that statokinetic dissociation was related to properties of the affected retinal ganglion cells (transient or sustained). In glaucoma, greater vulnerability of large ganglion cells has been suggested[7] and this may be a reason for the statokinetic dissociation found in our study. Further investigations is needed, however, to determine whether statokinetic dissociation is of clinical value.

References

1 Anderson DR, Feuer WJ, Alward WLM, Skuta GL: Threshold equivalence between perimeters Am J Ophthalmol 107:493-505, 1989
2. Aulhorn E, Harms H: Early visual field defects in glaucoma In: Leydhecker W (ed) Glaucoma Symposium, pp 151-186. New York: S Karger AG 1967
3. LeBlanc RP, Becker B: Peripheral nasal field defects Am J Ophthalmol 72:415-419, 1971
4. Werner EB, Beraskow J: Peripheral nasal defects in glaucoma. Trans Am Acad Ophthalmol 86:1875-1878, 1978
5. Caprioli J, Spaeth GL: Static threshold examination of the peripheral nasal visual field in glaucoma Arch Ophthalmol 103:1150-1154, 1985
6 Safran AB, Glaser JS: Statokinetic dissociation in lesions of the anterior visual pathways. Arch Ophthalmol 98:291-295, 1980
7 Asai T, Katsumori N, Mizokami K: Retinal ganglion cell damage in human glaucoma 1 Studies on the somal diameter Fol Ophthalmol Jpn 38:701-709, 1987

The mode of progression of isolated scotoma in glaucoma

Hiroyuki Miyazawa, Hiromi Yokogawa and Kuniyoshi Mizokami

Department of Ophthalmology, School of Medicine, Kobe University, 7-5-2 Kusunoki-cho, Chuo-ku, Kobe 650, Japan

Abstract

The progression mode of isolated scotomas in Bjerrum's area was studied in glaucoma patients using the Octopus 201 perimeter. Visual field abnormalities were classified into general and local types by Program Delta In patients with local depression, the direction of expansion of isolated scotomas in Bjerrum's area was studied. Isolated scotomas located in the nasal visual field showed a tendency to expand further nasally Some of those near the physiologic blind spot expanded toward the periphery of the nasal side, but other expanded toward the blind spot. This tendency differed according to the magnitude of total visual field loss.

Introduction

Recently, quantitative perimetry and statistical analysis of perimetric data have been made possible by the development of the computerized perimeter This instrument, which allows accurate analysis and assessment of the visual field from the very early stages of glaucoma, has contributed to the understanding of early visual abnormalities in glaucoma. However, there have only been a few previous reports on serial evaluation of the development and progression of the early stages of glaucoma using computerized perimeters[1,2].

Subjects and methods

Twenty-eight eyes of 25 patients (23-68 years old, mean 45 years) with early primary open angle glaucoma that showed deterioration of visual field damage measured by Program 31 of the Octopus perimeter (model 201) were studied The follow-up period was three months to two years, and the longitudinal analysis was performed by Program Delta. Since the results of the initial measurement of the visual field were considered to be subject to learning effects, the data from the second measurement were regarded as basal Only patients who showed significant deterioration (t-test) of the sensitivity in the whole field during the observation period (change mode of Program Delta) were included in the study. Glaucoma patients in whom the arcuate area showed no significant changes were regarded as having the general type of loss, and those in whom significant deterioration in the arcuate area was observed were classified as having the local type of loss

In patients with local depression, analysis was carried out on 60 points among the measurement points of Program 31, excluded those in the blind spot and those on the horizontal line passing through the fixation point. The location of isolated scotomas in which the sensitivity was reduced by 5 dB or more compared with the surrounding areas, their relationship with the total loss, and the mode of their expansion, were studied. Isolated scotomas in Bjerrum's area were classified into those on the temporal side of the vertical meridian and those on the nasal side of that line. The direction of significant expansion of the scotomas was examined according to the changes in the threshold at six measurement points immediately on the temporal and nasal sides of each scotoma (Fig. 1).

Perimetry Update 1990/91, pp 509-512
Proceedings of the IXth International Perimetric Society Meeting,
Malmö, Sweden, June 17-20, 1990
edited by Richard P. Mills and Anders Heijl

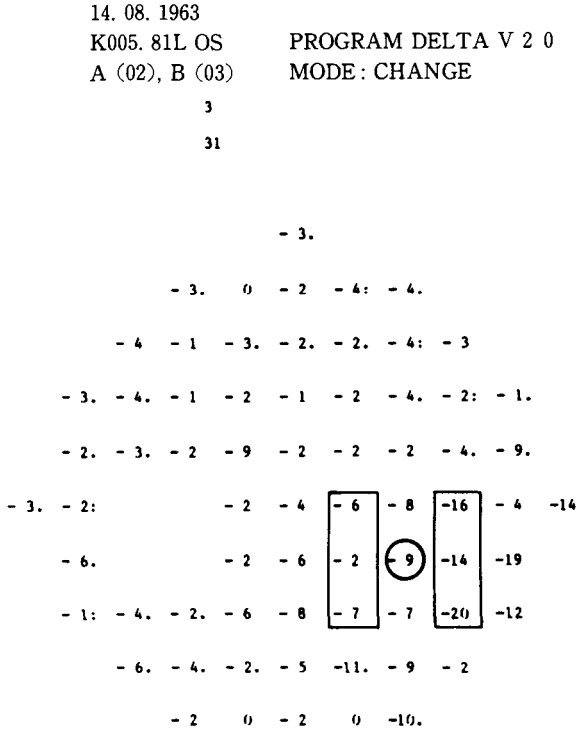

Difference Table: Mean B Minus Mean A (Negative Values Decreased Sensitivity) 0-0 all results zero <> low normal values dots indecate that some (.) or all (:) results are in normal range (fully valid)

confidence interval for mean difference/t-test
(1) pathol area (undotted) −5 5±1 7 (T-test: alteration is indicated)
(2) whole field −4.8±1.0 (T-test: alteration is indicated)

Fig 1 A case in which an isolated scotoma expanded to the nasal visual field

Results

Table 1 shows the location of the 39 isolated scotomas classified as the local type. Seventy-two percent of the scotomas were distributed in the upper visual field, and 28% in the lower visual field, but no significant difference was observed in their frequency between the temporal and nasal sides. Neither was there any difference in their location according to the value of total loss. Table 2 shows the direction of expansion of each scotoma. The scotomas in the nasal visual field tended to expand toward the periphery on the nasal side Some of those near the physiologic blind spot expanded toward the periphery of the nasal side, but others expanded toward the blind spot. This tendency showed no difference between the upper and lower visual fields Table 3 shows the correlation between the direction of expansion of scotomas and the value of total loss. Those scotomas in visual fields with a greater total loss (>100 dB) tended to expand toward the nasal periphery (Table 3b). Fig. 1 presents a case in which a local isolated scotoma expanded significantly to the nasal visual field.

Table 1 Location of solitary scotomas

	Location			
Total loss	*Upper temporal*	*Lower temporal*	*Upper nasal*	*Lower nasal*
<100	5	3	6	2
≥100	8	3	9	3

Table 2 Direction of spread of solitary scotomas

	Direction		
Location	*Blind spot*	*Peripheries of nasal visual field*	*General*
Temporal visual field	9	8	2
Nasal visual field	2	15	3

Table 3 Direction of spread of solitary scotomas according to the value of total loss

	Direction		
Location	*Blind spot*	*Peripheries of nasal visual field*	*General*
a total loss <100			
Temporal visual field	4	4	0
Nasal visual field	2	6	1
b total loss ≥100			
Temporal visual field	6	4	2
Nasal visual field	0	9	2

Discussion

Quantitative evaluation of visual field abnormalities in early glaucoma, such as isolated scotomas in Bjerrum's area, has been made easier with the advent of automatic perimeters General depression in visual sensitivity, which develops simultaneously with or in advance of isolated scotomas in Bjerrum's area, has been demonstrated in early glaucoma[3]. In this study, we examined patients who showed significant progression of visual field damage by *t*-test according to Program Delta. The visual field damage was classified into general and local types

Isolated scotomas were more frequent in the upper visual field, a finding consistent with earlier reports. In this study, we also examined the direction of their expansion. Those in the nasal visual field tended to expand toward the periphery of the nasal visual field. However, some of those in the temporal visual field expanded toward the physiologic blind spot while others expanded toward the periphery of the nasal visual field. Nerve fibers from the central retina run more superficially and enter the central portion of the optic disc[4]. In the light of this anatomical characteristic, impairment of axons located more peripherally in the optic disc would have a greater tendency to expand to involve other peripheral axons. In this study, the direction of expansion of scotomas differed according to the magnitude of total loss. Scotomas tended to expand toward the periphery of the nasal visual field if the total loss was greater, *i e* , if the disease was more advanced.

Various hypotheses have been proposed about the mechanism of visual field damage in glaucoma, and no consensus has as yet been obtained. Quigley *et al.*[5,6] classified a large series of glaucoma eyes according to the degree of visual damage and histologically examined the optic disc. They reported that mechanical compression of the lamina cribrosa is the earliest detectable change and suggested that the pattern of visual field damage is determined by the difference in the degree of the damage to nerve fibers in the pores of the lamina cribrosa. From the mode of progression of isolated scotomas in early glaucoma observed in this study, nerve fibers in the margin of the disc are considered to be first damaged in the very early stages of the disease, due to slipping of the laminar pores caused by loosening of the lamina cribrosa. Then, the

laminar pores begin to slip in a fixed direction, which may be toward the center, laterally or medially, but after a certain stage, the loss of nerve fibers is considered to progress laterally. This hypothetical mechanism of progression of visual field damage must be examined by future pathological as well as detailed anatomical studies.

References

1. Caprioli J, Sears M: Patterns of early visual field loss in open angle glaucoma. Doc Ophthalmol Proc Ser 49:307-315, 1986
2 Mikelberg FS, Drance SM: The mode of progression of visual field defects in glaucoma. Doc Ophthalmol Proc Ser 42:387-390, 1985
3 Glowazki A, Flammer J: Is there a difference between glaucoma patients with rather localized visual field damage and patients with more diffuse visual field damage? Int Perimetric Society, 7th Int Visual Field Symp, Amsterdam 1986
4. Radius R, Anderson DR: The course of axons through the retina and optic nerve head Arch Ophthalmol 97:1154-1158, 1979
5 Quigley HA, Addicks EM: Regional differences in the structure of the lamina cribrosa and their relation to glaucomatous optic nerve damage Arch Ophthalmol 99:137-142, 1981
6. Quigley HA, Hohman RM, Addicks EM et al: Morphologic changes in the lamina cribrosa correlated with neural loss in open angle glaucoma Am J Ophthalmol 95:673-691, 1983

The progression mode of visual field defects in low-tension glaucoma

Torao Sugiura, Miki Ito and Kuniyoshi Mizokami

Department of Ophthalmology, School of Medicine, Kobe University, 7-5-2, Kusunoki-Cho, Chuo-Ku, Kobe 650, Japan

Introduction

Several authors have reported statistically significant differences between the visual field defects of low-tension glaucoma (LTG) and primary open-angle glaucoma (POAG)[1,2], while other investigators have found no differences[3,4]. Progression of visual field defects in LTG over long periods of time has, however, not been well described.

We assessed the progression of visual field defects by retrospective case reviews of patients with a diagnosis of LTG. This study was designed to test the hypotheses that: (1) the pattern of visual field defects in patients with progressive LTG differs from that in patients with non-progressive LTG; and that (2) intraocular pressure (IOP) plays a role in the progression of visual field damage in LTG.

Subjects and methods

Our study included 106 eyes of 61 patients with a diagnosis of LTG. Entry criteria for all eyes included:

1. IOP <21 mmHg on every occasion on which it was measured, including a diurnal curve;
2. characteristic glaucomatous visual field defects;
3. glaucomatous optic disc changes;
4. open angles;
5. absence of any other apparent pathology to account for visual field loss and/or the appearance of the optic nerve head.

All patients were examined with program 31 on the Octopus 201 perimeter to test the central 30-degree visual field Stimulus size 3 was used in all cases. Progression of visual field defects was assessed with the Delta program. The subjects were then divided into two groups: those with and those without statistically significant progression of visual field damage.

To determine whether IOP plays a role in the progression of visual field damage, we compared maximum, mean and minimum IOPs and level of change in IOPs between the two groups To see whether there were differences in visual field damage between the two groups, the eccentricity and quadrant of scotomas were compared.

Results

Forty-one percent of the eyes showed statistically significant progression of visual field damage in 2.7±1.5 years (Table 1). Age and sex were matched between the two groups (Table 2). In the group which showed progression, level of change in IOP and maximum IOP were significantly higher ($p<0.01$) (Table 3).

Fig. 1. illustrates the prevalence of scotomas in the four quadrants. The superior-nasal quadrant was most commonly damaged in both groups, and no difference in the other quadrants was found between the two groups. A dense scotoma of up to ten degrees from fixation was more common ($p<0.05$) in the progressive group (Fig. 2). Additionally, in the earlier stage of the disease (total loss <100 dB), scotomas of up to ten degrees were more prominent in the progressive group (Figs. 3 and 4).

Perimetry Update 1990/91, pp. 513-516
Proceedings of the IXth International Perimetric Society Meeting,
Malmö, Sweden, June 17-20, 1990
edited by Richard P Mills and Anders Heijl

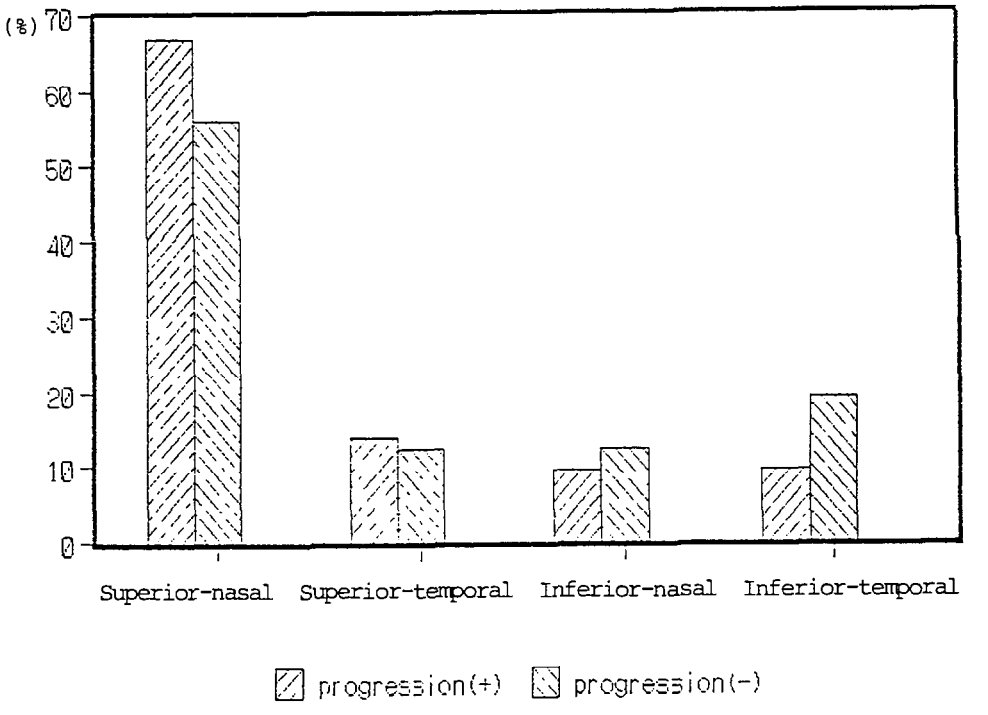

Fig 1 Prevalence of scotomas in the four quadrants

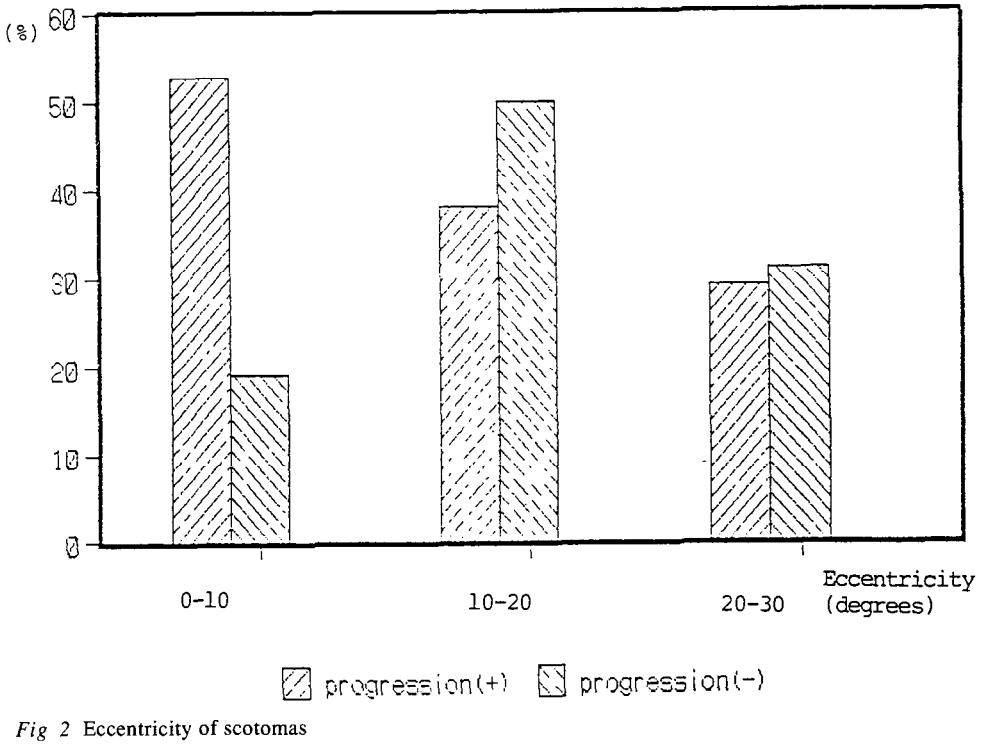

Fig 2 Eccentricity of scotomas

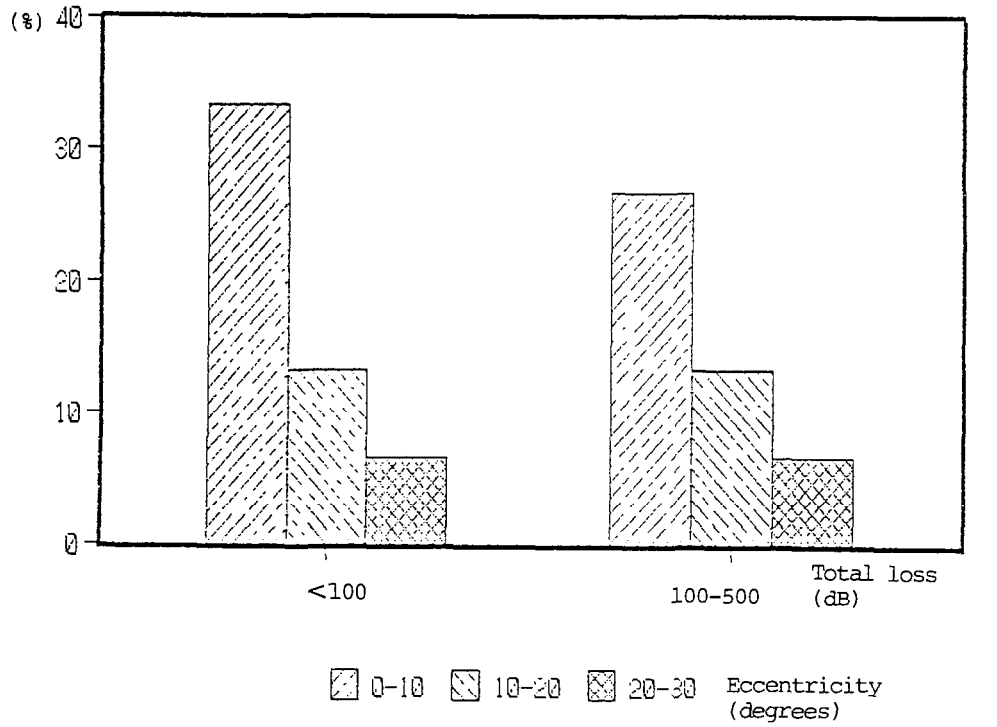

Fig 3 Progression (+).

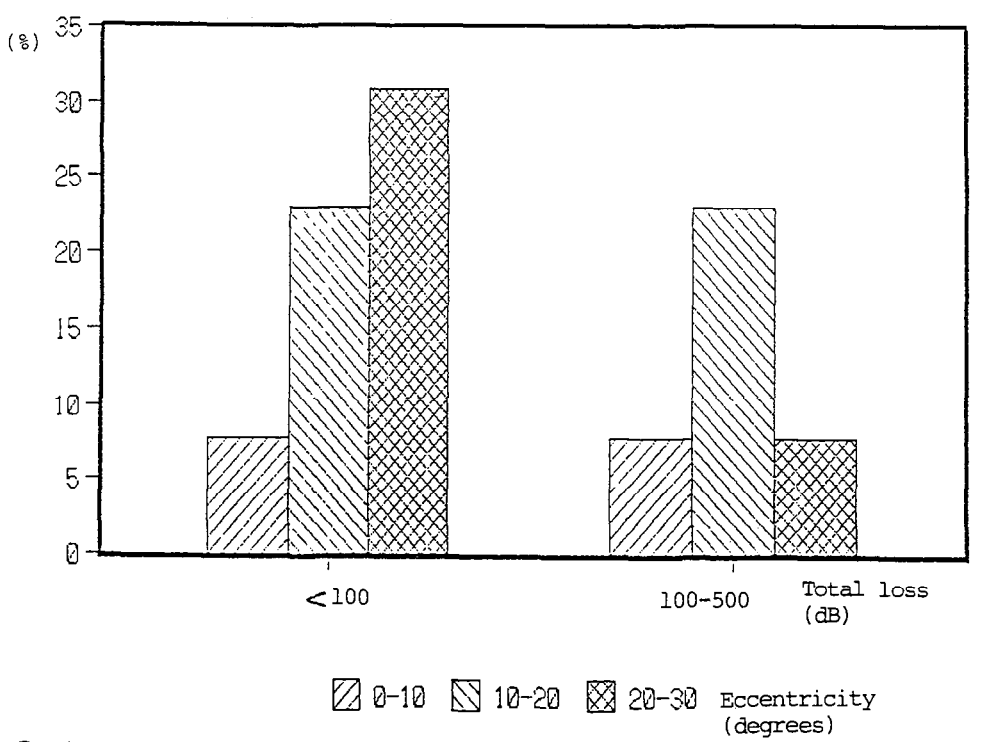

Fig 4 Progression (–).

Table 1

	Number of eyes	*Follow-up period (years)*
Progression (+)	43 (41%)	2.7±1.5
Progression (–)	63 (59%)	2.5±1.2
p (unpaired *t*-test)		NS

Table 2

	Age (years)	*Sex (% female)*
Progression (+)	69 3±8 5	86 7
Progression (–)	66 5±8 5	78 4
p	NS	NS

Table 3

	Max IOP (mmHg)	*Min IOP (mmHg)*	*Mean IOP (mmHg)*	*d-IOP (mmHg)*
Progression (+)	19.1±1 0	12 4±1 9	15 3±1.6	6.7±1.6
Progression (–)	17 0±2 0	12 4+2 0	14.4±2.0	4.6±1.6
p (unpaired *t*-test)	$p<0$ 01	NS	NS	$p<0$ 01

Discussion

The role of IOP in the pathogenesis of LTG is obscured because glaucomatous findings develop despite IOP in the normal range. However, if IOPs were compared between progressive and non-progressive LTG, we might discover the association between IOP and LTG. Our findings that the level of change in IOP and maximum IOP were significantly higher in the group which showed progression of the visual field damage suggested that IOP, although in the normal range, plays at least one of the roles in the pathogenesis of LTG.

We also noted that a dense scotoma of up to ten degrees from fixation was more common in the progressive group, especially in the earlier stages of the disease. The finding that the pattern of visual field defects in progressive LTG differs from that in non-progressive LTG implies a different pathogenesis of optic nerve damage in the two groups.

Although the definition of LTG used is consistent with recently published literature, selection bias may have played a role in producing these findings, because LTG is not exactly defined clinically. Periods of follow-up time and type of perimetry may also have influenced our data.

Our findings suggest that although IOP plays a role in the progression of LTG, some etiological factors in progressive LTG may differ from those in non-progressive LTG. The possible implications in terms of pathogenesis of LTG deserve further study for the understanding of the exact mechanisms in the development of open-angle glaucoma.

References

1. Hitchings RA, Anderson SA: A comparative study of visual field defects seen in patients with low-tension glaucoma and chronic simple glaucoma. Br J Ophthalmol 67:818-821, 1983
2. Caprioli J, Spaeth GL: Comparison of visual field defects in the low-tension glaucomas with those in the high-tension glaucomas Am J Ophthalmol 97:730-737, 1984
3 King D, Drance SM et al: Comparison of visual field defects in normal-tension glaucoma and high-tension glaucoma Am J Ophthalmol 101:204-207, 1986
4 Lewis RA, Hayreh SS, Phelps CD: Optic disc and visual field correlations in primary open-angle and low-tension glaucoma Am J Ophthalmol 96:148-152, 1983

The influence of brovincamine fumarate in low-tension glaucoma

Fumio Furuno, Mie Sakai, Hirotaka Suzumura, Kazuko Yabuki, Takashi Hama and Hiroharu Ohkoshi

Department of Ophthalmology, Tokyo Medical College Hospital, Tokyo, Japan

Abstract

The authors observed changes over time in the visual fields in low-tension glaucoma patients before and after administration of brovincamine fumarate, which has inhibitory action on platelet aggregation and is a Ca^{++} antagonist To evaluate the results obtained with a Humphrey Field Analyzer Central 30-2 program, the amounts of change in the pattern deviation numeric grid and quadrant total were used Improvement in retinal sensitivity of mildly depressed points (-2 to -10 dB) was shown, but no improvement was seen in the areas were sensitivity had greatly increased

Introduction

Studies on the three-dimensional visual field have demonstrated that the visual field defect in LTG differs from that in POAG, which agrees with results of studies investigating other parameters[1]. If the etiology of visual function loss in LTG was due to poor circulation in the optic disc, theoretically one might be able to prevent impairment of the visual field with treatment which improved circulation.

Factors such as the visual field, intraocular pressure, blood pressure, pulse rate and platelet aggregation, were measured in LTG patients before and after administering brovincamine fumarate (BV, Sabromin®), which has an inhibitory action on platelet aggregation[2], is a Ca^{++} antagonist[3], and also improves cerebral circulation and metabolism.

Subjects and methods

A total of 38 eyes of 19 LTG cases under observation at the glaucoma outpatient clinic at Tokyo Medical College Hospital, who were free from ocular diseases other than refractive errors and incipient cataract, were studied.

Their ages ranged from 51 to 81 years (average 66 0±7.8), and they consisted of six males and 13 females (Table 1).

Table 1 Subjects

	Administration of BV	*LTG control*	*Normal control*
Number of patients	19	5	5
Number of eyes	38	10	10
Age (years)	66 0±7 8	61 5±6 9	54 6±13 3
Sex (male/female)	6/13	2/3	2/3

The patients received 60 mg/day BV orally, and drugs in concurrent use consisted of topical pilocarpine hydrochloride in four eyes of two patients and topical β-blockers in ten eyes of five patients. These drugs were continued during oral administration of BV

Intraocular pressure, optic disc, blood pressure and pulse rate in the sitting position, and

Address for correspondence Takashi Hama, Department of Ophthalmology, Tokyo Medical College Hospital, 6-7-1, Nishishinjuku Shinjukuku, Tokyo 160, Japan

Perimetry Update *1990/91*, pp. 517-524
Proceedings of the IXth International Perimetric Society Meeting,
Malmö, Sweden, June 17-20, 1990
edited by Richard P Mills and Anders Heijl

platelet aggregation, were assessed before and one, three and six months after commencement of oral administration of BV.

Examination of the visual field using a central 30-2 program on the Humphrey Field Analyzer and fluorescein fundus angiography (FAG), was performed after continuous oral administration of the drug. To evaluate what changes in the visual field were significant, a similar examination of the visual field, at an interval of six months, was made of ten eyes of five LTG cases who received no oral administration of BV (ages averaging 61.5±6.9 years), and ten eyes of five normal subjects (ages averaging 54.6±13.3 years) served as controls.

To evaluate the results, the amounts of change in (1) pattern deviation numeric plot and (2) quadrant total were used, and a comparison was made among three groups: BV-treated LTG group, non-BV-treated LTG group, and the normal subject group.

Amount of change in pattern deviation

At all test locations, an assessment was made of the relationship in the amount of change in retinal sensitivity before and after oral administration of BV.

Amount of change in quadrant total

The sum per quadrant of the measured threshold values, except for two points occupied by the physiologic blind spot, were divided into six groups of less than 100, 100-199, 200-299, 300-399, 400-499, and more than 500.

Results of the visual field test were reliable as defined by fixation loss of less than 20% and false positive and negative errors of less than 33% each. No difference was observed in the diameter of the pupil before or after oral BV administration.

The subjects were well accustomed to the Goldmann perimeter and Humphrey Field Analyzer and correction for near vision was always used.

Since BV inhibits platelet aggregation, in addition to being a Ca^{++} antagonist, the platelet aggregation induced by ADP was used as an index for judging the effect of the drug. A measurement was made of the maximum aggregation rate after adding ADP in 1×10^{-5} mol to platelet plasma with a platelet count of $30\times10^{4}/\mu l$.

Results

Intraocular pressure

No significant difference was observed during the course of BV treatment (Fig. 1).

Blood pressure and pulse rate

No significant difference was observed during the course of BV treatment (Figs. 2 and 3).

Platelet aggregation

As a result of comparing the maximum aggregation rates (the maximum aggregation value after adding ADP) before and after oral administration of BV, the aggregation rate was significantly inhibited after BV administration (Fig. 4).

Change in visual field

Pattern deviation

The retinal sensitivity before BV administration and amount of change after six months of treatment are shown with regard to all test locations. Eighty percent of the normal control group showed differences within ±2 dB at all test locations (Fig. 5). In the LTG control group, no difference was present and most changes were within ±2 dB (Fig. 6). The LTG group receiving BV showed a trend towards slight improvement at the test locations with retinal sensitivities decreased from 2 to 10 dB (Fig. 7).

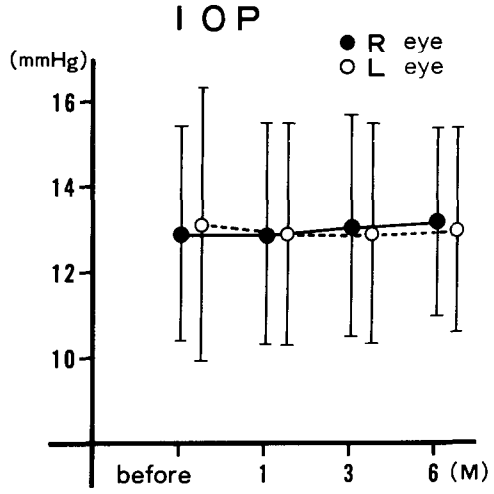

Fig 1. Change in intraocular pressure

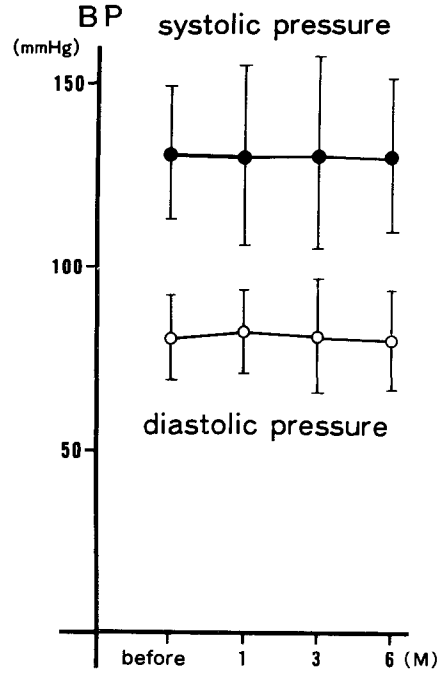

Fig 2 Change in blood pressure

Quadrant total

No change was observed in the normal control group (Fig. 8). The LTG control group showed a decreasing trend to the mean value, except for quadrants initially scoring 300-399, but no statistically significant difference was observed (Fig. 9). The LTG group receiving BV exhibited a trend for the mean to increase, but not for quadrants initially scoring more than 500, after oral administration. A statistically significant difference was observed, particularly in the quadrants initially scoring 300-399 ($p<0.05$) (Fig. 10).

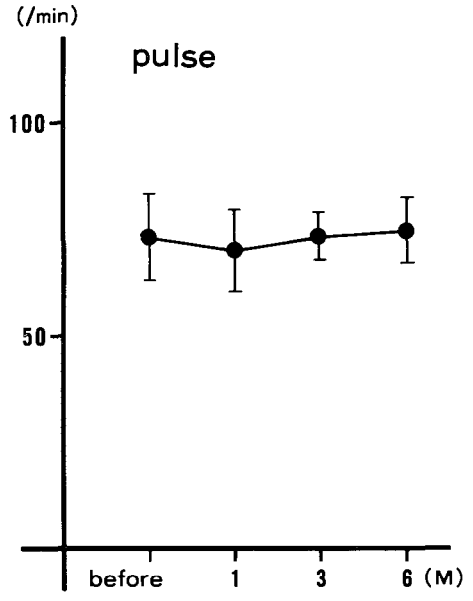

Fig 3 Change in pulse rate

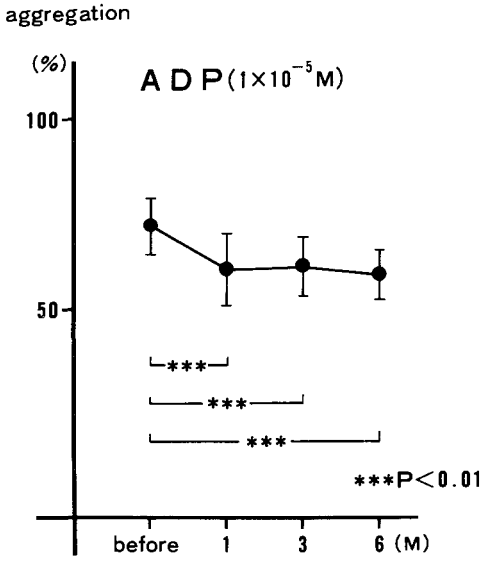

Fig 4 Change in platelet aggregation

Relationship between change in visual field and platelet aggregation

No relationship was observed between the amount of change in the maximum platelet aggregation rate and visual field changes.

Fluorescein fundus angiography

No differences were detectable due to the presence of substantial variance in quality of the angiograms.

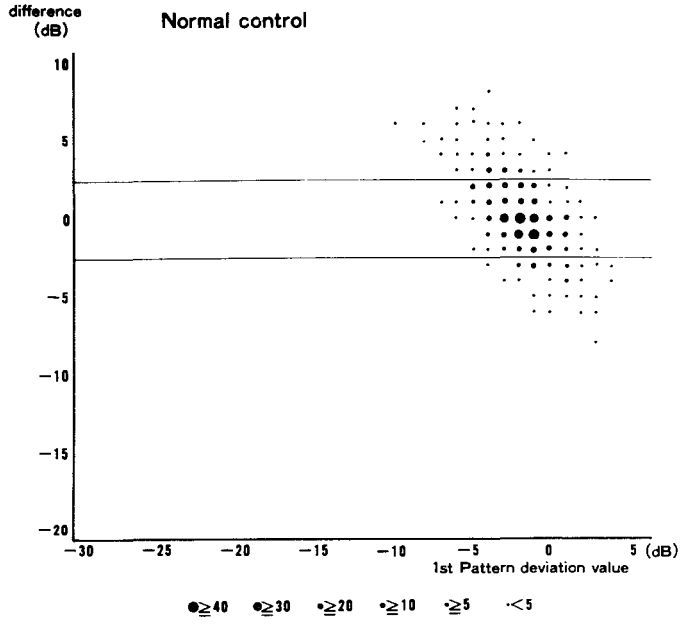

Fig 5 Change in pattern deviation: normal control

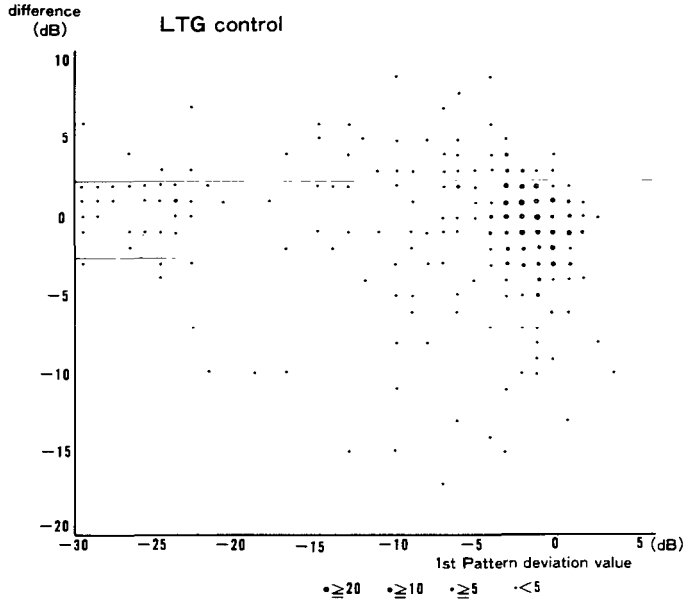

Fig 6 Change in pattern deviation: LTG control

Side effects

Reported side effects of BV include central nervous symptoms such as dizziness, drowsiness and tinnitus, circulatory symptoms such as transient arrhythmia and palpitations, and digestive symptoms such as anorexia, nausea, vomiting and constipation. No side effects were observed in this study except for one case of nausea.

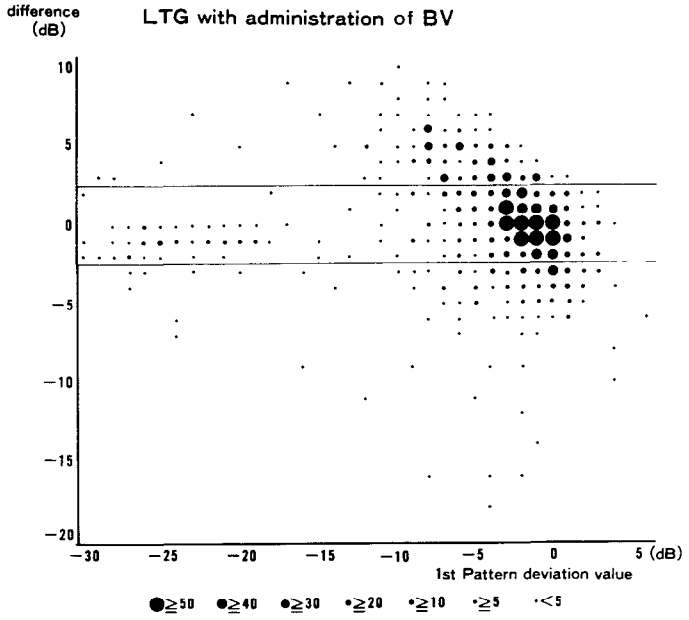

Fig 7 Change in pattern deviation: LTG with administration of BV

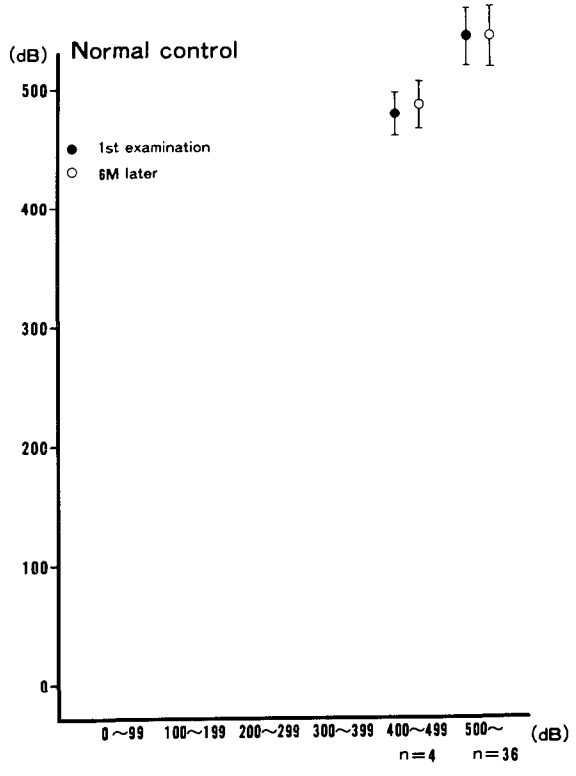

Fig 8 Change in quadrant total: normal control.

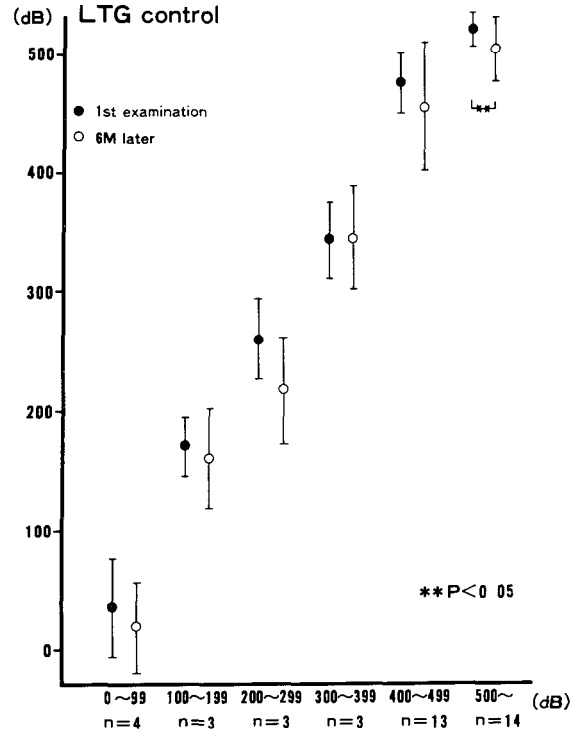

Fig 9 Change in quadrant total: LTG control

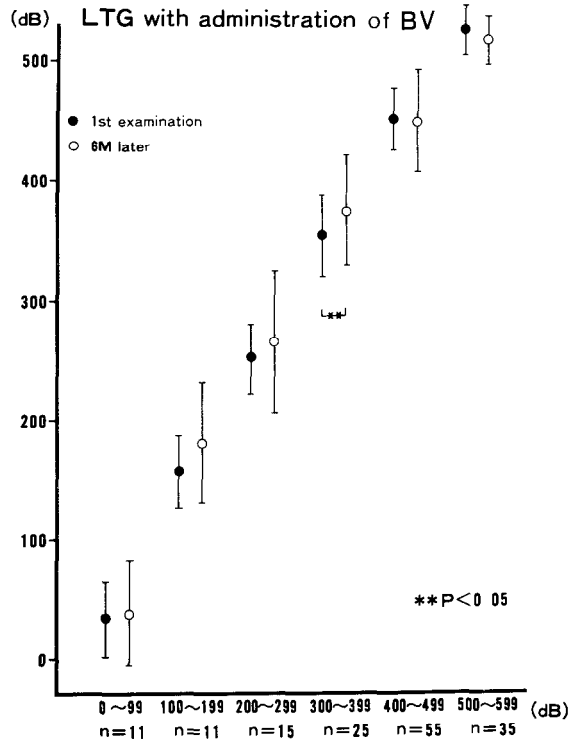

Fig 10 Change in quadrant total: LTG with administration of BV

Discussion

Therapies for reducing ocular tension by drugs or surgery and pharmacotherapy, such as improvement of circulation, were performed as therapeutic procedures for low-tension glaucoma.

It has recently been reported that an improvement of visual field disorder was observed after the administration of a calcium antagonist to patients suffering from this disorder caused by ocular vasospasm. There is also a report that blood viscosity is higher in patients with glaucoma than in those without[4]. Therefore, it is considered that drugs which inhibit platelet aggregation, which reduces blood viscosity, and with calcium-antagonistic activity, are effective against low-tension glaucoma.

It has been reported that mean sensitivity (MS) is useful for judging the effectiveness of drugs[5,6], but judgment of the effect may be difficult because the portion with favorable sensitivity and the exacerbated portion are cancelled out if a comparison is made by MS. A change in the visual field in low-tension glaucoma is characterized by the fact that only the scotomatous portion is exacerbated, whereas the normal portion has the same retinal sensitivity as a normal subject. When the decrease in retinal sensitivity is partially exhibited, as in the case of low-tension glaucoma, we can judge the effectiveness of drugs in relation to the level of decrease in retinal sensitivity, if the degree of the changes is observed at individual points. For this reason it was presumed that the evaluation method by which observation of changes was made at individual points was especially useful for the observation of the change in pattern deviation.

Another report[3] describes an attempt made to judge calcium antagonistic activity with the ice-water loading test, but no such attempt was made in the present study as BV has little effect on capillary dilatation.

The cause for the change in the visual field in low-tension glaucoma is thus known to be circulatory insufficiency, which suggests the possibility of its being due to increased blood viscosity, and therefore it is considered that hope can be entertained of improving the visual field of patients exhibiting a decrease in retinal sensitivity of about -10 dB by oral administration of BV.

References

1 Suzumura H: Volume of the three-dimensional visual field and its objective evaluation by shape coefficient Doc Ophthalmol Proc Ser 42:533-537, 1984
2 Yasunaga K: Inhibitory action of brovincamine on platelet aggregation. Naika Houkan 29/12:699, 1982
3 Kitazawa Y: The effect of Ca^{++} antagonist on visual field in low-tension glaucoma Graefes Arch Clin Exp Ophthalmol 227/5:408-412, 1989
4 Klaver J: Blood and plasma viscosity measurements in patients with glaucoma. Br J Ophthalmol 69:765-770, 1985
5 Flammer J: The effect of a number of glaucoma medications on the differential light threshold Doc Ophthalmol Proc Ser 35:145-148, 1983
6 Flammer J: The effect of acetazolamide on the differential light threshold Arch Ophthalmol 101:1378-1380, 1983

Miscellaneous

Psychophysical studies of the visual fields of monkeys

Ronald S. Harwerth[1], Earl L. Smith, III[1] and Louis DeSantis[2]

[1]*College of Optometry, University of Houston, Houston, TX 77204-6052;* [2]*Alcon Laboratories, Inc., Fort Worth, TX 76134-2099; USA*

Abstract

Psychophysical studies of the visual fields of three normal rhesus monkeys and one monkey with pathological visual field defects were conducted using the Humphrey Field Analyzer With operant control of the position of the animals' eyes and behavioral responses, the visual field data were obtained using the Field Analyzer's standard Central 24-2 threshold program. For each of the normal monkeys, the perimetric reliability tests were well within acceptable limits The Statpac global indices suggested that the monkeys' visual field data were generally consistent with those of "standard" normal human subjects In contrast to the normal fields of the control monkeys, the monkey with retinal lesions had substantially altered fields, with diffuse reductions of sensitivity and dense paracentral scotomas Therefore, the results demonstrate that the thresholding strategies and data analysis protocols of computerized perimetry, which were developed to evaluate visual fields of humans, can also be used to study normal visual fields and the functional alterations produced by experimental models of retinal disease in macaque monkeys

Introduction

Experimental investigations of animal models are critical for clinical and basic research of vision disorders. However, for many of the animal models that are currently available, as well as those that will be developed, the specific model would have greater validity if the functional visual defects that are characteristic of a particular disorder in human patients, were also verified in the animal model For example, research involving laser-induced, experimental glaucoma in monkeys[1] could be expanded considerably, if the characteristic visual field defects associated with glaucoma in humans could be demonstrated in this monkey model. The present study represents the early, initial stages of such an investigation The objectives of this stage of the investigation were to develop the behavioral methodology required to measure the visual fields of macaque monkeys, to collect normative data for monkey subjects, and to determine the utility of behavioral perimetry for measuring pathological visual field defects in the monkey.

Methods

The visual fields of the four monkeys were measured with a modified Humphrey Visual Field Analyzer (Allergan Humphrey, San Leandro, CA) that was attached to a small primate testing cubicle. The modifications to the perimeter, which were made to attain better control of the monkey's behavior during the visual field measurements, did not alter the standard threshold procedures or the data analysis programs. The four major modifications included the following:

1. an LED fixation stimulus was placed in Maxwellian view to control the monkeys' head and eye positions. In about 30% of the session trials, the trial stimulus was a luminance increment of the LED;
2. a microcomputer eye-position monitor (Micromeasurements System 2000, Micromeasurements, Inc., Berkeley, CA), coaxial with the fixation stimulus, was used to interrupt the behavioral paradigm if the monkey moved his eye during a trial;
3. a discrete behavioral response was required after each trial and movement of the perimeter projector was delayed for two seconds following the presentation of the field stimuli;
4. the perimeter response button was controlled through an external computer that controlled the other events of the behavioral procedures. The monkey's behavioral response for "seen"

Perimetry Update 1990/91, pp 527-531
Proceedings of the IXth International Perimetric Society Meeting,
Malmö, Sweden, June 17-20, 1990
edited by Richard P. Mills and Anders Heijl

stimuli was also inverted; they released a response lever to indicate a detected stimulus rather than pressing the response button.

Psychophysical luminance increment-thresholds for the central fixation stimulus and the peripheral visual field stimuli were measured with an adaptation of the criterion, response-time paradigm used in previous psychophysical studies of visual functions of monkeys[2,3]. The specific procedures for visual field studies on monkeys have been described in detail[4]. With this procedure, the monkeys were trained to press and hold down their response lever to initiate a trial and, subsequently, to release the lever in the presence of a visual stimulus. Since the time of the appearance of the stimulus was randomly varied, the lever releases that were closely correlated with the stimulus were operationally defined as true-positive responses and they were rewarded. Alternatively, lever releases not correlated with the visual stimulus were defined as false-negative responses. The visual stimulus in a trial could be either a luminance increment of the central, fixation stimulus, or of a peripheral field stimulus. The location and intensity of the peripheral test stimuli were determined by the specific threshold program of the Humphrey Field Analyzer.

Results

Normal visual fields

Using the behavioral paradigm, perimetry data were collected with standard Humphrey Field Analyzer's full-threshold programs. A typical example of the normal visual fields of the monkeys for the 24-2 program is presented in Fig 1A. In virtually every respect, the visual field data for the monkeys were qualitatively similar to visual field data for human observers.

Several quantitative comparisons between monkey and human observers emphasize this interspecies similarity. Firstly, the perimetry reliability indices for measures of retinal sensitivity across the central visual field were equivalent for the two species, indicating that the threshold values were reliable, valid measures. Secondly, the functions relating the perimetry threshold

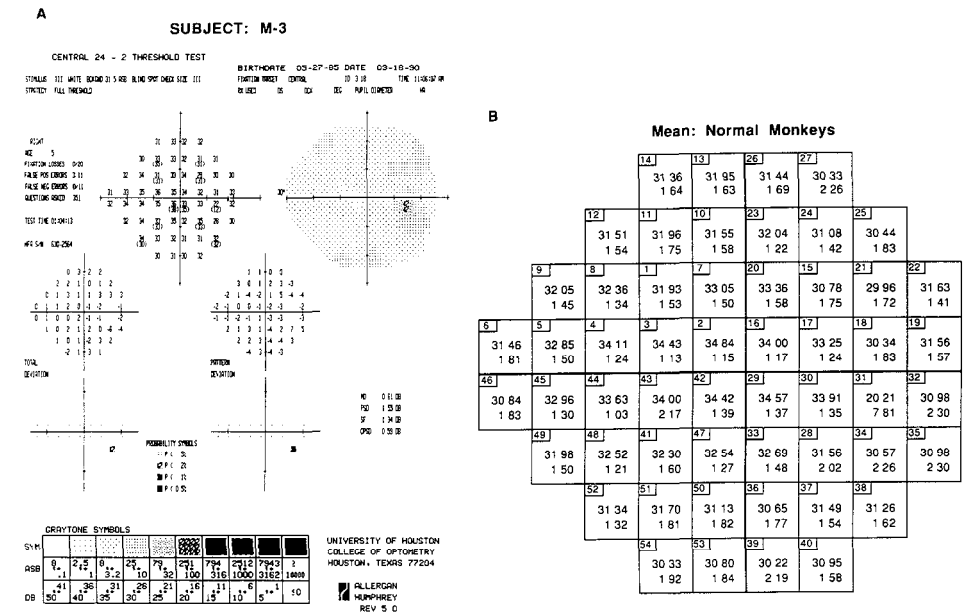

Fig 1 A Visual field plots for the right eye of a normal macaque monkey using the Humphrey Field Analyzer 24-2 full threshold program *B* Visual field data matrix showing the mean (upper value) and standard deviation of the mean (lower value) for each of the field locations measured with the 24-2 program The values were derived from 18 repeated field measurements on each of three normal monkeys

versus stimulus field area for Goldmann stimulus sizes 1-5 were virtually identical for monkeys and humans which indicates that the peripheral stimulus-area integration properties are comparable for these two species. Thirdly, the absolute sensitivity and the shape of the "hill of vision" for normal monkeys were not significantly different from those of the average normal human observer. The perimetry global indices for mean deviation, pattern standard deviation, and short-term fluctuation, calculated via the Statpac analysis of the monkeys' data, were all within the 95% confidence limits of the reference data for humans[5]. Finally, a statistical analysis was performed to test for the equality of the variances of the visual field threshold data (see Fig. 1B). The results of the statistical analysis of the data for monkeys, which were in complete agreement with similar analyses on perimetry data from human observers[6], indicated that the variability of measured thresholds was dependent on eccentricity, with significantly more variability for the more peripheral field locations. Taken together, these studies have clearly demonstrated the general comparability of the performances of monkey and human observers for visual fields tasks and also establish the effectiveness of the behavioral methodology for measurements of visual field data for monkeys.

Pathological field defects

If behavioral perimetry is to be useful for investigations of monkey models of retinal diseases, then the techniques must provide reliable measures for both normal and abnormal visual fields. In order to determine whether the procedures developed for normal monkeys would also be appropriate for studies of pathological field defects, we studied a monkey with reduced visual sensitivity and ophthalmoscopically visible retinal lesions which were produced as a complication associated with intravitreal injections of a neurotransmitter analog, APB (2-amino-4-phosphonobutyric acid)[7]. The effectiveness of the techniques are illustrated by the results of the perimetry measurements on the monkey's right eye (Fig. 2A). The visual field thresholds were elevated at essentially every test location, but the most prominent defects are the dense paracentral scotomas, a relatively large area in the superior nasal visual field and a smaller area in the inferior field. Even though the monkey had some problems with fixation

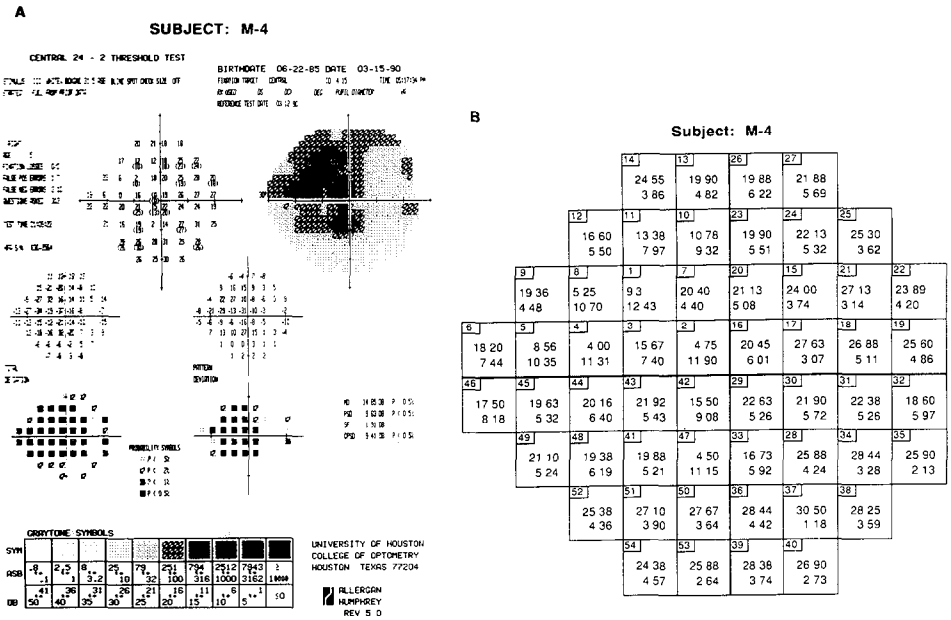

Fig 2 A Visual field plots for the right eye of a macaque monkey with pathological field defects (see text for details) The visual field data were collected using the Humphrey Field Analyzer 24-2 full threshold program. *B* Visual field data matrix, for the same monkey, showing the mean (upper value) and standard deviation of the mean (lower value) for each of the field locations measured with the 24-2 program. The values were derived from eight repeated field measurements

during the procedure, the visual field plots for this animal were qualitatively similar across measurement session.

The perimetry false-positive and false-negative response rates (12.1% ± 0.83% and 1.8% ± 0.53%, respectively) indicated that the data were reliable; the reliability indices for these visual field measurements were similar to those for the normal monkeys. The proportion of fixation losses detected by the external eye position monitor were within a normal range (<10%), however, the proportion of fixation losses (>80%) was very high according to the perimeter's Heijl-Krakau blind spot monitoring technique[8]. The differences in the results of the two techniques of evaluating fixation stability were probably caused by the monkey's reduced foveal vision. The diminished sensitivity for the fixation stimulus apparently affected its ability to reposition its head between trials, although it was able to hold a stable eye position within a given trial. Therefore, in this case, the visual field data were more variable because of the variations in the monkey's head position from trial-to-trial. For instance, the average value for short-term fluctuation was 2.56 dB and flagged as a significant deviation from normal ($p<5\%$) in approximately 50% of the measurements.

The variability of the threshold values across sessions is illustrated by the data matrix shown in Fig. 2B. The data matrix presents both the mean threshold value from eight measurements (upper number) and the standard deviation of the mean (lower number) for each of the test field locations evaluated with the Humphrey 24-2 threshold program. These data may be compared to similar data for the control subjects, presented in Fig. 1B. It is apparent that the threshold values are much more variable for the experimental animal than for the normal animals, especially in the retinal areas with the lowest sensitivity. The threshold variability should not have been due to progressive visual sensitivity changes since the visual field data were collected several months after the intravitreal injection that produced the retinal lesion. In all likelihood, the threshold variability for this monkey, which is comparable to the variability associated with visual field defects in humans[9], was the result of the instability of fixation and/or increased intrinsic noise associated with the retinal lesion.

Although the exact factors that produced the retinal lesion in this animal are not known, for the purposes of the present study the visual field data are sufficient to demonstrate that the procedures for behavioral perimetry in monkeys were adequate to obtain measurements of relatively dense, localized field defects. Therefore, these procedures should also be adequate to follow the development of visual field defects caused by experimentally induced diseases, such as glaucoma, although the sensitivity of the procedure has not yet been determined.

Conclusions

The operant procedures for behavioral perimetry on monkeys provided excellent control of eye position and behavioral responses. The visual field data obtained with a modified Humphrey Field Analyzer were highly reliable; the perimetry reliability indices were similar for monkeys and experienced human subjects.

Comparisons of visual field data for monkeys and humans demonstrated a close agreement in the sensitivities and shapes of the hills of vision of the two species. Therefore, the threshold techniques and statistical analysis of visual field data used in computerized perimetry may be applied to monkey subjects without modification.

Pathological visual field defects were reliably monitored in a monkey with relatively dense paracentral scotomas These measurements demonstrate the utility of behavioral perimetry in investigations of monkey models of retinal diseases, such as glaucoma, and the use of these models in clinical research

Acknowledgements

We thank Christian Kuether for design and construction of the primate testing apparatus, James Rezabek for design and construction of the computer interface system, John Feaster for assistance with the statistical analysis, and Steve Myers and Allergan Humphrey for custom ROM chips for the Humphrey Field Analyzer. This study was supported in part by research funds from Alcon Laboratories, Inc , Forth Worth, TX, and Public Health Service research grants EY-01139 and EY-03611, and core grant EY-07551 from the National Eye Institute, Bethesda, MD

References

1. Quigley HA, Hohman R: Laser energy levels for trabecular meshwork damage in the primate eye. Invest Ophthalmol Vis Sci 24:1305-1307, 1983
2. Harwerth RS, Boltz RL, Smith EL: Psychophysical evidence for sustained and transient channels in the monkey visual system. Vis Res 20:15-22, 1980
3. Harwerth RS, Crawford MLJ, Smith EL, Boltz RL: Behavioral studies of stimulus deprivation amblyopia in monkeys. Vis Res 21:779-789, 1981
4. Harwerth RS, Smith EL, DeSantis L: Behavioral perimetry in monkeys Arch Ophthalmol (submitted for publication)
5. Heijl A, Lindgren G, Olsson J: A package for the statistical analysis of computerized fields. Doc Ophthalmol Proc Ser 49:153-168, 1987
6. Heijl A, Lindgren G, Olsson J: Normal variability of static perimetric threshold values across the central visual field. Arch Ophthalmol 105:1544-1549, 1987
7. Smith EL, Harwerth RS, Crawford MLJ, Duncan GC: Contribution of the retinal ON channels to scotopic and photopic spectral sensitivity. Vis Neurosci 3:225-239, 1989
8. Heijl A, Krakau CET: An automatic perimeter, design and pilot study Acta Ophthalmol 53:293-310, 1975
9 Heijl A, Lindgren A, Lindgren G: Test-retest variability in glaucomatous visual fields. Am J Ophthalmol 108:130-135, 1989

Within and between test learning and fatigue effects in normal perimetric sensitivity

Anne E.T. Searle[1], David E. Shaw[1], John M. Wild[2] and Eamon C. O'Neill[1]

[1]*Department of Ophthalmology (University of Birmingham), Birmingham and Midland Eye Hospital, Church Street, Birmingham B3 2NS;* [2]*Department of Vision Sciences, Aston University, Aston Triangle, Birmingham B4 7GT; United Kingdom*

Abstract

Normal perimetric sensitivity is influenced by a between-examination learning effect and a within-examination fatigue effect for a given eye As yet, the influences of the learning and fatigue effects between eyes at a single visit and the learning effect for a given eye within a single examination are unknown In this study, the effects of phase of examination and order of eye examined over two visits were investigated using a 30-point central threshold program of the Humphrey Field Analyzer Sensitivity decreased in a time related manner, asymmetry being present between the responses of the two eyes at both visits The same effects were found to a similar extent with 105 ms stimulus duration This study demonstrates a time related intra- and inter-test variation in normal automated threshold perimetry which may contribute to the measurement error present in currently used threshold algorithms.

Introduction

The introduction of automated perimetry has permitted a viable technique for the static threshold evaluation of the visual field. The microprocessor-driven thresholding algorithms facilitate controlled and reproducible examination conditions reducing operator involvement to a minimum.

The magnitude of the threshold response is affected by factors such as refractive error[1], pupil size[2], and media opacities[3-5]. The measured threshold at a given test location also varies from one threshold determination to another. The intra-test and inter-test variations in threshold are known as the short-term and long-term fluctuation respectively[6].

A learning effect has been documented in automated static perimetry whereby improvement in the threshold response of a given eye occurs with increasing familiarity of the task. A between-examination learning effect for a given eye over the central field in normal subjects has been shown in retrospective[7,8] and prospective studies and has been found to be eccentricity dependent[9,10]. The within-examination improvement in threshold for a given eye, however, together with the between-eye improvement in threshold at a single patient visit, are unknown

A fatigue effect has also been documented in automatic static perimetry whereby deterioration in the threshold response of a given eye occurs with increasing examination time. A within-examination fatigue effect for a given eye has been described in normal subjects over the time course of a conventional 30° threshold program[11] and also for a given threshold program of extended duration[12]. The between-examination deterioration in threshold for a given eye and the between-eye deterioration in threshold at a single patient visit are unknown.

In this context, it is interesting to note that Brenton *et al.*[13] found interocular differences in sensitivity at pairs of corresponding locations to range from 0 to 9 dB in normal subjects; however Feuer and Anderson[14] suggested, after a study on young normal subjects, that a between-eye difference in mean sensitivity of 2 dB or more at one examination might indicate abnormality.

The purpose of this study was to investigate the influence of the learning effect for a given eye within a single examination and the influences of the learning and fatigue effects between eyes at a single visit. The variation in normal perimetric sensitivity was considered with respect to order of eye examined, phase of the visual field examination and stimulus duration.

Perimetry Update 1990/91, pp 533-537
Proceedings of the IXth International Perimetric Society Meeting,
Malmö, Sweden, June 17-20, 1990
edited by Richard P. Mills and Anders Heijl

Material and methods

Thirty-eight normal volunteers, with a mean age of 45.5 years (SD 8.33) underwent threshold perimetry for the first time. Exclusion criteria included a positive family history of glaucoma, history of eye problems or diabetes mellitus. Inclusion criteria for each eye comprised corrected visual acuity of 6/9 (20/30) or better, refractive error for 33 cm ranging within ±6.00DS and ±2.00DC, intraocular pressures of less than 21 mmHg, normal drainage angles and normal fundal appearance on examination with dilated pupils. To confirm inclusion, ophthalmological examination and conventional visual field examination with program 24-2 were performed on separate occasions after the experimental perimetry had been completed.

A customized program of the Humphrey Field Analyzer 640 (stimulus size III) was utilized, consisting of 30 test locations, situated between 9° and 24° eccentricity. The duration of the customized program was approximately five minutes. All subjects were randomized with respect to order of eye examination (right, $n = 16$), and stimulus duration (105 ms, $n = 20$; 200 ms, $n = 18$). The stimulus duration was selected by software contained in ROM format. A stimulus duration of 100 ms represents a viable alternative to the 200 ms duration and has been used in several other automated perimeters. The 105 ms stimulus duration used in the study represented the shortest duration commensurate within the mechanical requirements of the perimeter shutter assembly. Each subject attended two appointments (visits) separated by approximately two weeks (median eight days; interquartile range 7-18).

At each visit, the randomized first eye underwent three consecutive customized programs, with an interval of up to one minute between each program (phase). Such a protocol was selected to simulate a threshold examination equivalent to the 15 minutes necessary for completion of a conventional 76-point threshold program. The second eye underwent a similar three-phase examination after a five minute interval The mean horizontal pupil diameter measured via the eye monitor (magnification factor 1 .9) was 4.6 mm (SD 0.6) for the first eye and 4.3 mm (SD 0.8) for the second eye.

Mean sensitivity, short-term fluctuation (four double determinations; one in each quadrant), duration of each phase and number of stimulus presentations per phase were analyzed using ANOVA with repeated measures over eye examined, phases and visits. Stimulus duration was considered as a between-subjects factor and age as a covariate.

Ethical approval for this study was obtained from the West Birmingham District Health Authority.

Table 1 Mean values of sensitivity (MS), short-term fluctuation (SF), duration of phase (T) and number of stimulus presentations (Q) for each triple program for 200 ms stimulation duration, with ± standard error in parenthesis

	First eye			*Second eye*		
Phase	*1*	*2*	*3*	*1*	*2*	*3*
First visit						
MS (dB)	27.79	27 64	26 67	28.24	26.03	25 27
	(0 46)	(0 39)	(0.47)	(0 38)	(0.60)	(0 73)
SF (dB)	1 96	2.10	2.11	1 69	2.84	2 40
	(0 26)	(0 24)	(0.20)	(0 19)	(0 38)	(0.25)
T (min)	6.02	5.58	6 04	5.50	5 83	6 04
	(0.22)	(0.18)	(0.23)	(0.19)	(0 18)	(0.21)
Q (no)	203.6	188 9	205 1	189.5	196 0	203.8
	(6 7)	(5.0)	(7 6)	(6 2)	(5 7)	(7.2)
Second visit						
MS (dB)	29 24	27.64	26 96	28 29	26.58	26.09
	(0 31)	(0.51)	(0 55)	(0 51)	(0 65)	(0.65)
SF (dB)	1.62	1.95	1 73	1.44	2 15	1.84
	(0.16)	(0 19)	(0 19)	(0.20)	(0 30)	(0.26)
T (min)	5.35	5 52	5.72	5 42	5.61	5.63
	(0.13)	(0 20)	(0.20)	(0 24)	(0.18)	(0 21)
Q (no)	182 9	189 2	194.4	186 6	190.2	191 9
	(3 9)	(6.5)	(5.9)	(8 0)	(5 6)	(7.0)

Table 2. Significance from ANOVA on the alterations of group mean sensitivity (MS), short-term fluctuation (SF), duration of phase (T), number of stimulus presentations (Q) over phases of tests, eyes and visits

	MS	*SF*	*T*	*Q*
Eye	0.002	NS	NS	NS
Phase	<0.001* (0.019)	<0.001* (0 046)	0.028	NS
Visit	0.029	0.048	0.006	0 015
Eye × phase	0.005* (0.033)	NS	0.039	0 084
Visit × phase	0.001	NS	NS	0 054
Eye × visit	0.006	NS	NS	NS
Eye × visit × phase	0.001	NS	NS	NS

*significant interaction with stimulus duration and p value in parenthesis below

Results

The group mean values for mean sensitivity, short-term fluctuation, duration of phase and number of stimulus presentations as a function of eye examined, phase and visit are shown in Table 1. The significance levels of the main effects together with the interaction terms are shown in Table 2.

The variation of group mean sensitivity for the 200 ms stimulus duration is illustrated graphically in Fig. 1. Group mean sensitivity decreased over each phase of each eye at each visit suggesting an intra-eye fatigue effect. At the first visit, the mean sensitivity of the first eye decreased from the first to the third phases by 1.1 dB and the second eye decreased by 3.0 dB. This asymmetry suggests a greater intra-eye fatigue in the second eye. The mean sensitivity of the first eye for the first phase of the second visit was 1.5 dB higher than at the corresponding phase at the first visit suggesting a between examination learning effect for the first eye. At the second visit, the mean sensitivity of the first eye decreased by 2.3 dB and the second eye by 2.2 dB over the three phases, again suggesting an intra-eye fatigue effect. The initial mean sensitivity of the second eye was less than that of the first eye suggesting inter-eye transfer of fatigue.

The influence of age on mean sensitivity was not statistically significant (p=0.239). Sensitivity recorded with 200 ms stimulus duration was higher than that recorded with the 105 ms duration (p=0.007).

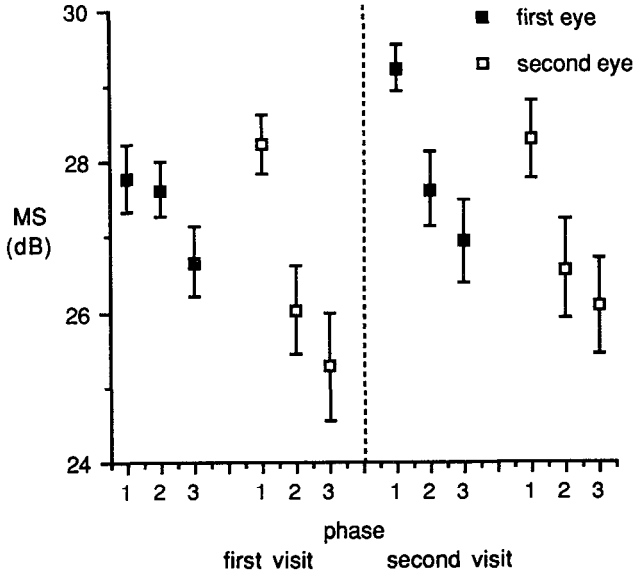

Fig. 1 Mean sensitivity distribution for triple program of both eyes at both visits for 200 ms stimulus duration, with error bars ± 1 standard error

Similar trends were noted for the number of stimulus presentations, the duration of phase and the short-term fluctuation, namely that performance declined in each eye over each of the phases at each visit. The baseline performance levels for both eyes were higher at the first phase of the second visit compared with the first phase of the first visit. The influences of age and of the 105 ms stimulus duration on the magnitudes of short-term fluctuation, number of stimulus presentations and duration of phase were not statistically significant.

Discussion

In this study the depreciation of perimetric sensitivity with time confirmed the results of Heijl who selected six stimulus locations for repeated measurement over 30 minutes in single eyes of both normal and glaucomatous subjects[15,16] and has been attributed to tiredness by Holmin[17], particularly in relative scotomas of visual fields of glaucomatous subjects. It is assumed that repeating a 30-point customized threshold program three times in succession is equivalent to approximately 15 minutes continuous threshold perimetry as required in the 76-point threshold program. Each 30-point program involved the measurement of threshold at four seed points (with double determinations), one in each quadrant and relocation of the blindspot when fixation loss was recorded within the first eight stimulus presentations.

Deterioration in sensitivity occurred after five minutes of threshold perimetry for each eye examined. However, for each 30-point program, the measurement of threshold at four seed points, one in each quadrant, involves up to a third of the duration of phase. If the initial threshold values of these four points are recorded as low due to the timeliness of the algorithm at present incorporated in the software, it can be argued that the starting point for the threshold algorithm at other test locations may be influenced by this fatigue effect and may result in a reduction in sensitivity. A shorter thresholding algorithm such as RIOTS may not produce this effect[18]. With the current software available one questions whether the optimum level of threshold response is recorded within a 15-minute conventional program for each test location.

The time related changes in normal sensitivity for both first and particularly second eyes, illustrated in this study, undoubtedly contribute to the measurement errors of the threshold strategy presently incorporated in the Humphrey Field Analyzer.

Acknowledgements

Anne Searle is supported by the Birmingham Eye Foundation, U K

References

1 Weinreb RN, Perlman JP: The effect of refractive error on automated perimetric thresholds Am J Ophthalmol 101:706-709, 1986
2. Mikelberg FS, Drance SM, Schulzer MD, Wijsman K: The effect of pupil diameter on visual field indices Doc Ophthalmol Proc Ser 49:645-649, 1987
3. Guthauser U, Flammer J, Niesel P: Influence of cataracts on visual fields Doc Ophthalmol Proc Ser 49:39-41, 1987
4 Wood JM, Wild JM, Smerdon DL, Crews SJ: Alterations in the shape of the automated perimetric profile arising from cataract. Graefes Arch Clin Exp Ophthalmol 227:157-161, 1987
5 Dengler-Harles M, Wild JM, Cole MD, O'Neill, Crews SJ: The influence of forward light scatter on the visual field indices in glaucoma Graefes Arch Clin Exp Ophthalmol 228: in press
6. Bebie H, Fankhauser F, Spahr J: Static perimetry: accuracy and fluctuations Acta Ophthalmol 54:339-348, 1976
7. Flammer J, Drance SM, Zulauf M: Differential light threshold: short- and long-term fluctuation in patients with glaucoma, normal controls and patients with suspected glaucoma Arch Ophthalmol 102:704-706, 1984
8. Wilensky JT, Joondeph BC: Variation in visual field measurements with an automated perimeter. Am J Ophthalmol 97:328-331, 1984
9. Wood JM, Hussey MK, Crews SJ: Serial examination of the normal visual field using Octopus automated projection perimetry: evidence for a learning effect Acta Ophthalmol (Copenh) 65:326-333, 1987

10 Heijl A, Lindgren G, Olsson J: The effect of perimetric experience in normal subjects Arch Ophthalmol 107:81-86, 1989
11. Johnson CA, Adams CW, Lewis RA: Fatigue effects in automated perimetry. Appl Optics 27/6:1030-1037, 1988
12. Langerhorst CT, Van Den Berg TJTP, Boersma H, Greve EL: Short-term and long-term fluctuation of thresholds in automated perimetry in normals, ocular hypertensives and glaucoma patients. In: Heijl A (ed) Perimetry Update 1988/1989. Amsterdam/Berkeley/Milano: Kugler & Ghedini Publ 1989
13 Brenton RS, Phelps CD, Rojas P, Woolson RF: Interocular differences of the visual field in normal subjects. Invest Ophthalmol Vis Sci 27:799-805, 1986
14 Feuer WJ, Anderson DR: Static threshold asymmetry in early glaucomatous visual field loss. Ophthalmology 96:1285-1297, 1989
15. Heijl A: Time changes of contrast thresholds during automatic perimetry Acta Ophthalmol 55:696-708, 1977
16. Heijl A, Drance SM: Changes in differential threshold in patients with glaucoma during prolonged perimetry. Br J Ophthalmol 67:512-516, 1983
17. Holmin C, Krakau CET: Variability of glaucomatous visual field defects in computerized perimetry Graefes Arch Clin Exp Ophthalmol 210:235-250, 1979
18. Johnson CA, Shapiro LR: RIOTS (real-time interactive optimized test sequence): a heuristic software test strategy for automated perimetry In Investigative Ophthalmology and Visual Science Annual Meeting. Abstract Issue 31,4:191, 1990

Perimetry and driving licenses

Enrico Gandolfo, Emilio Campos*, Mario Facino and Giovanni Di Lorenzo

*Clinica Oculistica dell'Università di Genova, Ospedale S Martino, Pad IX, Viale Benedetto XV, n. 10, 16132 Genova, *Clinica Oculistica dell'Università di Modena, Via Del Pozzo, 71, 41100 Modena; Italy*

Abstract

A questionnaire on the rules concerning the perimetric capabilities necessary for obtaining a driving license in different countries was sent to all members of the IPS standards and ergoperimetry groups, as well as to the secretaries of the national ophthalmological societies. Of 120 questionnaires distributed, 32 answers were received from 20 countries. Fifteen of these 20 countries had specific rules concerning perimetric damage and driving licenses (in the USA the law varies according to state). Many colleagues recommended the standardization of the perimetric performance necessary for a driving license. Most suggested a threshold-related screening test of the entire visual field (*e g* , Octopus 07, Humphrey 120 point). On the basis of these suggestions and of previous personal experience, the authors performed a large trial employing the more widely used automated instruments and selected the screening programs offered by each perimeter. This study allowed the authors to suggest some visual field programs and evaluation criteria which would be useful for the assessment of driving license fitness, in order to create an international standard in this field.

Introduction

A normal visual field (VF) is one of the requirements currently necessary for a driving license[1,2]. As a consequence, assessment and certification of VF normality are necessary[3,4]. It would therefore seem to be useful to propose some "perimetric rules" in order to standardize the perimetric evaluation and certification criteria[5-7].

Recently, on the initiative of Dr. Gandolfo, chairman of the International Perimetric Society (IPS), Ergoperimetry Study Group, and Prof. Campos, chairman of the IPS Standards Study Group, a questionnaire regarding the VF standards required for a driving license was drawn up (Table 1). This questionnaire was sent to all members of the IPS Standards and Ergoperimetry Groups as well as to the secretaries of the national ophthalmological societies around the world. A total of 120 questionnaires was sent out, and 32 replies were received (from 20 different countries). Fifteen of these countries had rules requiring VF examination before first obtaining a license, as well as for renewal (in the USA, the law varied according to state) (Table 2).

The questionnaire allowed us to obtain suggestions and opinions from ophthalmologists who had dealt with this topic because they had authored reports or were involved in the various international perimetric study groups. Most called for the introduction of rules concerning the smallest VF required for driving license fitness and confirmed the need for international standardization of VF testing under IPS supervision. The use of automated perimeters, of programs evaluating the entire VF and of suprathreshold strategies (threshold-related), were the techniques most commonly recommended for this type of mass VF screening.

On the basis of these suggestions, we investigated the more widely-used perimeters in order to identify the programs and strategies most suitable for the assessment of perimetric driving license fitness.

Address for correspondence. E. Gandolfo, Clinica Oculistica dell'Università di Genova, Ospedale S. Martino, Pad. IX, Viale Benedetto XV, n. 10, 16132 Genova, Italy

Perimetry Update 1990/91, pp 539-544
Proceedings of the IXth International Perimetric Society Meeting,
Malmö, Sweden, June 17-20, 1990
edited by Richard P. Mills and Anders Heijl

Table 1. Questionnaire

1. Is there a law in your country which regulates the degree of visual field integrity necessary to obtain a driver's license? ☐ YES ☐ NO
   If "yes", please indicate the requirements:_____
   If "no", please indicate how this is handled in practice:_____
2. Are the regulations different with regard to high-speed vehicles (airplanes, trains, racing cars and motorcycles) and/or for professional licenses? ☐ YES ☐ NO
   If "yes", please state these requirements:_____
3. What type of assessment do you think should be necessary before granting a driver's license? (indicate the most suitable instrument, program, and strategy):

Type of assessment	Normal vehicle	High-speed vehicle and/or professional license
a. traditional kinetic perimetry		
b. kinetic perimetry with percent quantification of the damage (Esterman grids or analogous systems)		
c automatic static perimetry with supra-threshold program		
d. automatic static threshold perimetry		

Material and methods

We considered the more common automated instruments (Table 3), looking for the programs and strategies that best satisfied our goals. We kept in mind both economical and qualitative requirements, *i e.*, brevity and ease of testing, evaluation of the entire VF with good resolution, comparability between different instruments, etc.

From a practical point of view, we divided the screening programs (Table 4) into three different levels of examination:

Level I. (program Nos. 1, 4, 7 and 9) for subjects with no history or clinical sign of ocular or neurological disease, in whom a simple suprathreshold low-resolution perimetric test was sufficient;

Level II: (program Nos. 2, 5, 8 and 10) for subjects with ocular disorders or systemic or neurologic diseases which might affect the VF, who needed a supraliminal program with a high resolution grid and classification of defects.

Level III (program Nos. 3, 6 and 11) for subjects with ocular and/or neurological disorders usually affecting the VF, in whom a strategy providing precise evaluation of defect depth at all missed points was advisable.

We performed all these programs in a group of normal subjects (50 subjects, 23 males and 27 females, mean age 52±16.2 years) and in a group of subjects with mild VF defects (50 subjects, 28 males and 22 females, mean age 56±15.8 years).

Our goal was to identify perimetric tests which are sufficiently brief (<10 minutes for one eye) but also sensitive enough (<10% false negatives) and easy to perform, both for operator and patient (<5% false positives; not excessively complex management).

Humphrey perimetry[8,9]

For the first level (presumably normal eyes), we selected the "full-field 81-point" (threshold-related strategy) program which evaluates, on the basis of a simple suprathreshold (6 dB) low-resolution strategy, 81 points on the entire VF. Point missed are retested and considered

Table 2 International laws or rules concerning perimetric damage and driver's licenses

	Official law	*Perimetric capability for normal license (binocular people)*	*Perimetric capability for normal or restricted license (monocular people)*	*Perimetric capability for professional or high-speed vehicles license*
Australia	Yes	More than 130° in both eyes (horizontal meridian)	More than 130° (horizontal meridian)	More than 170° in both eyes (horizontal meridian)
Austria	Yes	Normal VF in both eyes	Normal VF	Normal VF in both eyes
Belgium	No	–	–	–
Canada	Yes	More than 120° in both eyes (horizontal meridian)	More than 140° (horizontal meridian)	More than 140° in both eyes (horizontal meridian)
Colombia	No	50% along all meridians in both eyes	Normal VF	Normal VF in both eyes
Czecho-slovakia	Yes	More than 70° (temporal) and more than 20° (nasal) in both eyes	More than 90° (temporal and more than 50° (nasal)	Normal VF in both eyes
Denmark	Yes	Normal VF in both eyes (hand perimetry)	Normal VF (hand perimetry)	Normal VF in both eyes (hand perimetry)
Finland	Yes	Normal VF in both eyes (hand perimetry)	Normal VF (hand perimetry)	Normal VF in both eyes (hand perimetry)
France	No	More than 60° (temporal) and more than 30° (nasal) in both eyes	Normal VF	Normal VF in both eyes
Great Britain	No	At least 120° (horizontal meridian) and 20° (up and down) in both eyes	More than 120° (horizontal meridian), more than 20° (up and down)	Normal VF in both eyes
Hungary	Yes	Normal VF at least in one eye	Normal VF	Normal VF in both eyes
Israel	Yes	More than 140° in binocular vision (horizontal meridian)	More than 130° (horizontal meridian)	Normal VF in both eyes
Italy	Yes	Normal VF in both eyes	Normal VF	Normal VF in both eyes
Japan	No	–	–	–
Luxembourg	Yes	Normal VF at least in one eye	Normal VF	Normal VF in both eyes
Netherlands	Yes	More than 80° (temporal) and more than 60° (nasal) in both eyes	More than 90° (temporal) and more than 60° (nasal)	More than 90° (temporal and more than 60° (nasal) in both eyes
New Zealand	Yes	More than 100° (horizontal meridian) in both eyes	More than 140° (horizontal meridian)	More than 140° (horizontal meridian) in both eyes
Sweden	Yes	VF at least equivalent to that of a normal eye	Normal VF	Normal VF in both eyes
Switzerland	Yes	At least 140° (horizontal meridian) in both eyes	At least 140°	Normal VF in both eyes
USA	Yes	At least 100-140° (horizontal meridian) in both eyes	At least 100-140° (horizontal meridian)	Normal VF in both eyes

pathological if the patient fails to see both exposures.

"Full-field 120-point" with the "3-zone" strategy was chosen for the second level. This program tests 120 points in the central 60 degrees, by means of a threshold-related strategy, and quantifies defects in two steps (relative and absolute), retesting every missed point at the maximum luminance.

Finally, for the third level, we chose the "full-field 120-point" with the "quantify defects" strategy which provides a full-threshold measurement of all missed points.

Octopus perimetry[10]

For the first level, we selected the "short-test" program which measures 59 central and 26 peripheral locations with the "2-level" strategy (phases 1-3). This test uses two questions, one at 6 dB below normal and another at 0 dB (1000 asb) in order to characterize each location as

Table 3 Technical specifications of the perimeters utilized

	Humphrey	*Octopus*	*Peritest*	*Kowa*
Reference threshold	Individual	Age	Individual	Individual
Background luminance	31.5 asb	4 asb	3.5 asb	31.5 asb
Maximal stimulus luminance	10,000 asb	1000 asb	1000 asb	3400 asb
Stimulus duration	0.2 sec.	0 1 sec.	0 2 sec	0.8 sec.
Kind of stimulus	Projection	Projection	LED	LED
Stimulus size	III (4 mm^2)	III (4 mm^2)	III (4 mm^2)	II (1 mm^2)
Bowl radius	33 cm	42 cm	33 cm	30 cm

Table 4

	Perimeter and program	*Strategy*	*Mean duration normal/ pathological eyes*	*% of false positives (normal eyes)*	*% of false negatives (pathological eyes)*	*Management complexity*
1	Humphrey full field 81 point	Threshold-related suprathreshold, without defects classification	4'50"/7'45"	0%	12%	Low
2	Humphrey full field 120 point	Threshold-related suprathreshold, with defects classification (3-zone)	6'41"/9'06"	4%	4%	Medium
3	Humphrey full field 120 point	Threshold-related suprathreshold, with defects quantification (full threshold)	7'02"/10'15"	4%	4%	High
4	Octopus ST (1° and 3° phases) 85 point	Threshold-related suprathreshold, with defects classification (2-level)	6'06"/7'56"	2%	10%	High
5	Octopus 07, 130 point	Threshold-related suprathreshold, with defects classification (2-level)	5'55"/10'26"	2%	2%	Medium
6	Octopus 24, 76 point	Threshold-related suprathreshold with defects quantification (fast threshold)	8'15"/10'50"	4%	8%	High
7	Kowa standard 79 point	Suprathreshold, single level with defects classification (3-level)	6'31"/9'11"	0%	14%	Low
8	Kowa precision 134 point	Suprathreshold single level with defects classification (3-level)	8'20"/12'06"	2%	12%	Low
9	Peritest 1B+periphery 128 point	Threshold-related suprathreshold, without defects classification	6'38"/8'24"	4%	6%	Medium
10	Peritest 1A+periphery 133 point	Threshold-related suprathreshold, with defects classification (3-level)	6'49"/9'12"	2%	6%	Medium
11	Peritest 1A+periphery 206 point	Threshold-related suprathreshold, with defects classification (3-level)	8'40"/11'35"	4%	2%	Medium

normal, or a relative or absolute defect.

For the second level, the "07" program which explores the central 70 degrees with a 130-point grid was chosen. It uses the "2-level" strategy.

The "24" program, which thresholds only the pathological locations (4 dB or more below the norm) of a 15-degree resolution grid within 72 degrees of eccentricity was selected for the third level.

Rodenstock perimetry (Peritest-Perimat)[11]

For the first level, the combination of "1B" and "periphery" programs without defect assessment appeared to be the best choice. It explores 128 points arranged over the entire VF.

The combination of "1A" and "periphery" programs (133 points) with the "3-level" defect quantification which characterizes the VF into four different zones: normal, light (8-12 dB), medium (14-18 dB) and severe (>18 dB) defects, was selected for the second examination level.

For the third level, we chose the combination of "1A", "1B" and "periphery" (206 points) with defect quantification ("3-level" strategy).

Kowa perimetry[12]

For the first level, we chose the "standard" program which evaluated 79 points of the VF, with a "one-level" screening strategy, performing a rough defect quantification as well.

For the second and third levels, the "precision" program, which explores 134 points on the entire VF with the same strategy as the "standard" one, seemed to be the most suitable for our purpose.

Results and comments

Table 4 shows the mean examination times of normal and pathological eyes. Mean test duration was found to be brief enough, particularly in normal subjects, and similar for the different perimeters. Only a few programs exceeded ten minutes' duration in pathological eyes (Nos. 3, 5, 6, 8 and 11).

Performing the various tests was simple and feasible by a well-trained, experienced technician.

The necessary patient cooperation was adequate for the requirements of a mass VF screening test. Only program Nos. 3, 4 and 6 showed a certain management complexity (Table 4). In all cases, the percentages of false positive results was lower than 5% and thus within the established limits.

The percentage of false negative results in pathological eyes was acceptable in many programs. Only programs with low grid resolution (Humphrey full-field 81-point, Octopus short test and program 24, Kowa standard program) resulted in a sensitivity lower than the cut-off point (10%) (Table 4).

Conclusions

Our work stresses that the most common perimeters available today allow good recognition of VF defects which could compromise driving capability, by means of easy and brief supraliminal screening tests.

On the basis of our experience and on the suggestions of ophthalmologists who replied to the questionnaire, we can propose a standard perimetric test for driving licenses consisting of:

- automated examination;
- entire VF exploration (out to at least 60 degrees of eccentricity in the temporal sector; and to at least 40 degrees in the nasal sectors);
- adequate grid resolution (between 100 and 150 points);
- suprathreshold threshold-related strategy with simple defects classification.

For medico-legal data evaluation, we propose the following criteria:

- less than 25% of absolute defects for normal license;
- less than 10% of absolute defects for professional license;
- less than 50% of absolute defects for restricted license.

(Three relative defects = one absolute defect).

References

1. Verriest G, Baily IL, Calabria G, Campos E, Crick RP, Enoch JM, Esterman B, Friedman AC, Hill AR, Ikeda M, Johnson CA, Overington I, Ronchi L, Saida S, Serra A, Villani S, Weale RA, Wolbarsht ML, Zingirian M: The occupational visual field. Doc Ophthalmol Proc Ser 42:281-326, 1985
2. Keltner JH, Johnson CA: Mass visual field screening in a driving population. Ophthalmology 87:785-792, 1980
3. Keltner JH, Johnson CA: Visual function, driving, safety, and the elderly. Ophthalmology 94:1180-1188, 1987
4. Johnson CA, Keltner JH: Incidence of visual field loss in 20,000 eyes and its relationship to driving performance. Arch Ophthalmol 101:371-375, 1983
5. Fonda G: Legal blindness can be compatible with safe driving Ophthalmology 96:1457-1459, 1989
6 Lichter PR: The ophthalmologist's role in licensing drivers (editorial). Ophthalmology 96:1455-1456, 1989
7 Hales RH: Functional ability profiles for drivers licensing: exemplification by visual profile Arch Ophthalmol 100:1780-1783, 1982
8 Heijl A: The Humphrey field analyzer, construction and concepts Doc Ophthalmol Proc Ser 42:77-84, 1985
9 Brenton RS, Phelps CD: The normal visual field on the Humphrey analyzer. Ophthalmologica (Basel) 193:56-74, 1986
10. Bebie H, Fankhauser F, Jenni A, Haberlin H: The new software package First Int Meeting on Automated Perimetry System Octopus, pp 155-177. Schlieren, Switzerland: Interzeag AG 1979
11. Greve EL, Dannheim F, Bakher A: The Peritest, a new automatic and semi-automatic perimeter. Int Ophthalmol 5:201-214, 1982
12. Kowa Automatic Visual Field Plotter AP 340: Operation Manual

A new proposal for classification and quantification of visual disability

E. Gandolfo, M. Zingirian and P. Capris

Clinica Oculistica dell'Università di Genova, Ospedale S Martino, Pad IX, Viale Benedetto XV, n 10, 16132 Genova, Italy

Abstract

The visual disability classification is nowadays mainly based on a well-standardized quantitative evaluation of visual acuity, whereas quantification of visual field damage is often based on arbitrary criteria The authors therefore propose a quantification of perimetric damage parallel to that of visual acuity, in order to obtain five levels of functional loss for both visual acuity and field Visual fields were obtained with a computerized perimetry A binocular suprathreshold strategy testing 100 points and stressing perimetric areas relevant for functional assessment was used. The perimetric results were converted to a percentile score quantifying the residual visual field Combining visual acuity and visual field scores, a decimal index of the overall visual disability, not useful for medico-legal but only for rehabilitative purposes, was obtained.

Introduction

Visual disability depends on loss of visual acuity and/or spatial orientation, in other words, on central and/or peripheral visual damage. The quantification of visual disability is nowadays based on a well-standardized assessment of visual acuity damage, whereas quantification of visual field loss is assessed using arbitrary criteria[1-11].

We therefore propose a quantification of perimetric damage parallel to that almost universally adopted for central visual damage, and thus identifying three levels of low vision and two of blindness for both visual acuity and field. By combining the score assigned to each level of the two residual functions, an index can be obtained which is useful for quantifying the global visual disability, especially for rehabilitative purposes.

Procedure

Quantification of central visual damage

Using the classification accepted by the majority of authors, we have assigned a score from 0 to 5 to every single level of central visual damage, as follows:

Visual acuity	*Central damage level*	*Score*
4/10 or more	none	0
3/10-2/10	slight low vision	1
1/10-3/50	moderate low vision	2
2/50-1/100	severe low vision	3
finger counting-hand movement	relative blindness	4
light perception-no light perception	absolute blindness	5

Considering that the aim of this study was a global functional assessment not for legal but only for rehabilitative purposes, visual acuity was determined under binocular conditions

Address for correspondence E. Gandolfo, Clinica Oculistica dell'Università di Genova, Ospedale S Martino, Pad. IX, Viale Benedetto XV, n. 10, 16132 Genova, Italy

Perimetry Update 1990/91, pp 545-549
Proceedings of the IXth International Perimetric Society Meeting,
Malmö, Sweden, June 17-20, 1990
edited by Richard P Mills and Anders Heijl

Quantification of peripheral visual damage

We began with the following assumptions:

1. Functionally, the most important visual field area for autonomic spatial orientation is that between 5° and 30° eccentricity. The field inside 5° is especially useful for its resolution properties (visual acuity), while that outside 30° is less important for visual orientation, as demonstrated by many patients with peripheral field loss due to photoablation for diabetic retinopathy, surgical encircling procedures for retinal detachment or concentric visual field contraction in retinitis pigmentosa or glaucoma with seemingly normal ability for orientation. Therefore, we assigned a value of 65% to the 5-30° area, 5% to the central 5° area and 30% to the peripheral field outside 30°.
2. The lower half of the visual field is functionally more important than the upper one, as Esterman has established[12-14]. Therefore in each division of the field, 3/5 of the value was assigned to the lower half and 2/5 to the upper half.
3. The evaluation of peripheral visual function should consider not only absolute but also relative loss of sensitivity.
4. The measurement of peripheral sensitivity should be carried out by means of a computerized perimeter, so that the same program can be used and comparable results can be obtained in different ophthalmic centers.
5. Binocular perimetric tests are needed for the assessment of disability caused by visual loss.

As a consequence of the above-mentioned assumptions, the following procedure was adopted:

1. the Perikon PCL90 automatic perimeter (Optikon) was used. Two phases can be distinguished:
   - Phase 1: examination of the central 30 degrees of visual field while the patient was wearing his usual optical correction for refractive error and presbyopia;
   - Phase 2: examination of the peripheral visual field (outside 30°) without any optical correction.
2. In both phases a static supraliminal gradient and an age-related strategy with quantification of defect depth in two levels (absolute and relative) is employed. Target III (4 mm^2) was used. The stimulus was presented at a luminance 6 dB above the theoretical threshold at each location; we considered the following central reference thresholds: 34 dB below 40 years of age; 32 dB between 40 and 60 years of age; 30 dB above 60 years of age. When the stimulus was not perceived, it was presented again at maximum luminance, thus allowing the defect to be classified as relative or absolute.
3. One hundred points were tested. These were arranged so as to favor the functionally most important areas of the field, *i e* , the paracentral area and the lower quadrants. Five points were located inside the central 5°, two in the upper and three in the lower quadrants. Sixty-five points were placed in the area between 5 and 30°, 26 in the upper and 39 in the lower quadrants. Thirty points were distributed in the peripheral visual field, between 30 and 60°, 12 in the upper and 18 in the lower quadrants (Fig. 1).
4. The points seen with a 6 dB supraliminal stimulus were classified as "normal", and a percentage value of "1" was assigned to them. The points seen only with the maximum luminance stimulus (*10,000* asb) were classified as points with "reduced sensitivity" and assigned a value of "0.5". Points not seen, even after two presentations of maximum luminance stimulus, were considered to have absolute defects and assigned a value of "0".
5. Responses corresponding to these three levels (normal, relative and absolute) were represented with three different symbols (Fig. 3). The computer calculated the sum of the relevant values and provided the percentage value of the perimetric residuum and the classification of the peripheral visual damage into six categories:

Residual visual field (%)	*Peripheral damage*	*Score*
70% or more	none	0
69-50%	slight peripheral low vision	1
49-30%	moderate peripheral low vision	2
29-10%	severe peripheral low vision	3
9- 1%	relative peripheral blindness (with residuum)	4
0%	absolute peripheral blindness	5

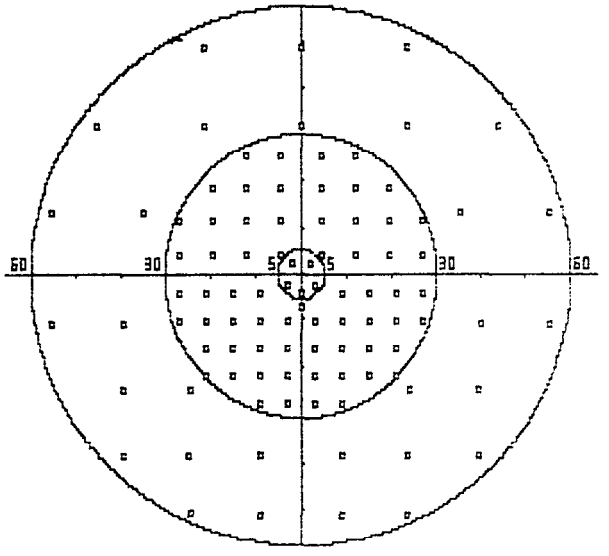

Fig. 1 Arrangement of the 100 points tested

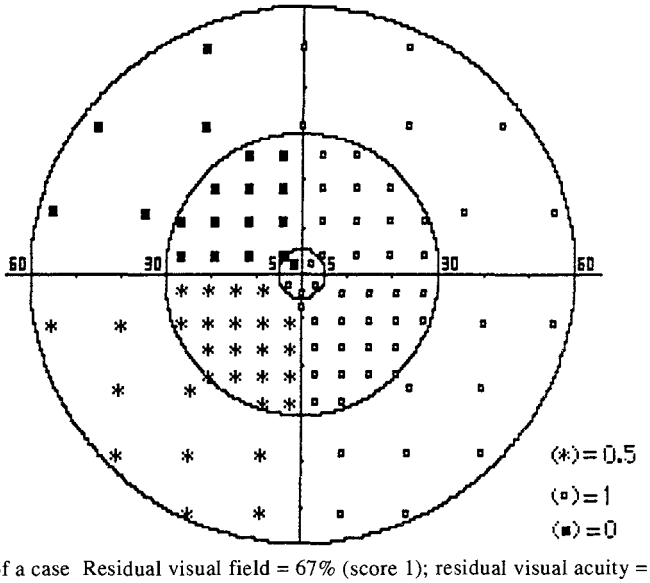

Fig 2 Example of a case Residual visual field = 67% (score 1); residual visual acuity = 3/10 (score 1); global disability = 1+1 = 2 (slight).

Combining the two scores derived from the central and peripheral tests (see example in Fig. 2), an overall score is obtained which identified one of the six levels of global disability:

Global disability	*Score*
none	0
slight	1- 2
moderate	3- 4
severe	5- 6
sub-total	7- 8
total	9-10

Obviously, the two components of visual damage, central and peripheral, can contribute differently to the global disability.

Table 1 shows all the possible combinations of these two components, thus allowing rehabilitative personnel to know how much of the global score is due to each of the two components and, therefore, to choose the most appropriate rehabilitation process.

Table 1 Global visual disability

Degree	*Total score*	*Visual acuity*	*Partial score*	*Visual field*	*Partial score*
Normality	0	4/10 or more	0	70% or more	0
Slight low vision	1-2	4/10 or more	0	30-49%	2
		4/10 or more	0	50-69%	1
		2-3/10	1	50-69%	1
		2-3/10	1	70% or more	0
		3/50-1/10	2	70% or more	0
Moderate low vision	3-4	4/10 or more	0	1-9%	4
		4/10 or more	0	10-29%	3
		2-3/10	1	10-29%	3
		2-3/10	1	30-49%	2
		3/50-1/10	2	30-49%	2
		3/50-1/10	2	50-69%	1
		1/100-2/50	3	50-69%	1
		1/100-2/50	3	70% or more	0
		hand movement-finger counting	4	70% or more	0
Severe low vision	5-6	4/10 or more	0	0%	5
		2-3/10	1	0%	5
		2-3/10	1	1-9%	4
		3/50-1/10	2	1-9%	4
		3/50-1/10	2	10-29%	3
		1/100-2/50	3	10-29%	3
		1/100-2/50	3	30-49%	2
		hand movement-finger counting	4	30-49%	2
		hand movement-finger counting	4	50-69%	1
		abolished light perception	5	50-69%	1
		abolished light perception	5	70% or more	0
Relative blindness	7-8	3/50-1/10	2	0%	5
		1/100-2/50	3	0%	5
		1/100-2/50	3	1-9%	4
		hand movement-finger counting	4	1-9%	4
		hand movement-finger counting	4	10-29%	3
		abolished light perception	5	10-29%	3
		abolished light perception	5	30-49%	2
Absolute blindness	9-10	hand movement-finger counting	4	0%	5
		abolished light perception	5	0%	5
		abolished light perception	5	1-9%	4

Conclusions

The procedure we propose is simple and rapid. Thanks to the use of a computerized perimeter, it required no more than five to eight minutes if the visual acuity has already been determined

Using this procedure, every health professional, if guided by an ophthalmologist, can easily quantify the global visual disability of any patient being sent to a rehabilitation center.

However, for medico-legal and insurance purposes, certain modifications of the procedure are needed:

- each eye should be examined separately;
- the absolute blindness of both central and peripheral vision should be considered as equivalent to a 35% disability in the worst eye and to a 65% disability in the best eye, or other similar values, according to the regulations of medical or insurance associations in each separate country;
- intermediate conditions between the functional levels considered should be taken into account, according to appropriate tables.

References

1. Engelberg AL (ed): American Medical Association Guides to Evaluation of Permanent Impairment, 3rd edn. Chicago: AMA 1984
2. Calabria G, Capris P, Burtolo C: Investigation on space behavior of glaucomatous people with extensive visual field loss Doc Ophthalmol Proc Ser 35:202-210, 1983
3 Capris P, Gandolfo E, Corallo G: Binocular perimetry in detections of simulated visual field defects In: Proceedings 4th World Congress Ergophthalmology Naples: GVA Press 1986
4. Colenbrander MC: Visual acuity, visual field and physical ability: a proposal of a formula Ophthalmologica 171:100-108, 1975
5 Crick RP, Crick JCP, Ripley L: The representation of the visual field Doc Ophthalmol Proc Ser 35:193-203, 1983
6. Gandolfo E, Capris P, Zingirian M: Quantitative evaluation of visual field defects In: Proceedings 4th World Congress Ergophthalmology Naples: GVA Press 1986
7. Gandolfo E: Functional quantification of the visual field: a new scoring method Doc Ophthalmol Proc Ser 49:537-540, 1987
8. Gandolfo E, Rolando M, Zingirian M: Quantificazione funzionale del campo visivo binoculare nel glaucoma Boll Ocul (Suppl) 67/2:283-287, 1988
9 Verriest G: Percentage impairment by visual field defects Doc Ophthalmol Proc Ser 49:505-525, 1986
10. Verriest G et al: The occupational visual field. I Theoretical aspects Doc Ophthalmol Proc Ser 35:165-185, 1983
11. Verriest G et al: The occupational visual field II Practical aspects Doc Ophthalmol Proc Ser 42:281-326, 1985
12. Esterman B: Grids for scoring visual fields I. Tangent screen Arch Ophthalmol 77:780-786, 1967
13. Esterman B: Grids for scoring visual fields II Perimeter Arch Ophthalmol 79:400-406, 1968
14. Esterman B: Functional scoring of the binocular field. Ophthalmology 89:1226-1234, 1982

The differential light threshold as a function of retinal adaptation – the Weber-Fechner/Rose-de-Vries controversy revisited

John G. Flanagan[1], John M. Wild[2] and Jeff K. Hovis[1]

[1]*School of Optometry, University of Waterloo, Waterloo, Ontario, Canada N2L 3G1;* [2]*Aston University, Birmingham, UK B4 7ET*

Abstract

The relationship between the adaptation or background luminance (L) and the minimum detectable stimulus luminance (ΔL), varies as a function of L. In the photopic range the Weber-Fechner law, $\Delta L/L = k$ is generally considered to be the most appropriate. In the low scotopic range, ΔL becomes a constant, independent of L. Within the low photopic and mesopic ranges that are most commonly used in perimetry, the Rose-de-Vries law, $\Delta L/L^{0.5} = k$ is likely to give a more appropriate description. There has been disagreement as to which fraction is most appropriate in clinical perimetry. The aim of this study was to assess the interaction of stimulus size and background luminance on the sensitivity and variability across the visual field. In so doing, it should be possible to establish the suitability of the Weber-Fechner or Rose-de-Vries law for automated perimetry from dark adapted to photopic levels of adaptation. The differential light threshold for the right eye of ten clinically normal age-matched emmetropes was determined using a Humphrey Field Analyzer 630. Stimuli were presented along the 15°-195° meridian for three stimulus sizes (0.108°, 0.431° and 1 724°) over a range of background luminances (0 to 1000 cdm^{-2}) Stimulus luminance and retinal illuminance were calculated for each condition and the values were corrected for the Stiles-Crawford effect. The Rose-de-Vries law was found to be most applicable for luminances up to 100 cdm^{-2} whereas the Weber-Fechner law described the relationship for 10 cdm^{-2} and higher

Introduction

Perimetry may be defined as the measurement of differential light sensitivity as a function of peripheral angle. Differential light sensitivity is usually expressed as ΔL/L where ΔL is the minimum detectable stimulus luminance and L is the adaptation or background luminance. The variation in sensitivity with peripheral angle in the normal eye is influenced by numerous instrument-specific and patient-specific variables. Blair[1] was among the first to realize the importance of this during the examination of the visual field. He recommended a value of 0.01 ml (≅1 asb) for topographic investigation because, at this mesopic level, it was considered that rods and cones were stimulated approximately equally; the ratio of L to ΔL was larger than at photopic levels; the sensitivity curve was relatively flat across the central visual field, thus enabling investigation with a single target; and the effect of ametropia was reduced[2]. Similar observations were subsequently made by Sloan[3], and others[4-7]. Rose[8] agreed that there was an increase in dynamic range with a decrease in adaptation level but only at the expense of increased photon noise giving an increased signal to noise ratio. Fankhauser and Bebie[9] calculated that for a change of background from 31.5 asb to 4 asb the dynamic range at an eccentricity of 50° would increase by 12 dB, whereas the gain would be approximately 3-4 dB at fixation due to reduced spatial summation. However there has been some disagreement as to the relationship between L and ΔL as L is varied. In the photopic range (greater than 100 asb) the Weber-Fechner law, ΔL/L, is generally considered to be the most appropriate. In the low photopic and mesopic range the Rose-de-Vries law $\Delta L/L^{0.5}$ is more appropriate and in the low scotopic range (less than 1 asb), ΔL becomes a constant, independent of L.

Fankhauser[10] has suggested that the Rose-de-Vries law is applicable to the adaptation levels used by all of the currently available perimeters. Other work has considered the Weber-Fechner law to be the most applicable[2,6,11].

Address for correspondence: Dr. J. Flanagan, School of Optometry, University of Waterloo, Waterloo, Ontario, Canada N2L 3G1

Perimetry Update 1990/91, pp. 551-554
Proceedings of the IXth International Perimetric Society Meeting,
Malmö, Sweden, June 17-20, 1990
edited by Richard P. Mills and Anders Heijl

Retinal adaptation will also be affected by pupil size. Pharmacologically induced miosis and mydriasis has been found to produce maximum reduction in central static sensitivity of between 1.4 dB and 2 dB[2,10,12]. Fankhauser[10] found the reduction to be similar between background luminances of 4 asb and 40 asb. Inter-individual pupil size differences have not been found to influence mean sensitivity[13] or the short-term fluctuations measured by automated perimetry[14].

It has been suggested that visual field examination using several levels of adaptation may enhance the detection and differential diagnosis of ocular disease[15-18]. Low levels of adaptation have been proposed for assessment of low vision patients, and retinitis pigmentosa[19]. High adaptation levels have conversely been proposed for early neurological defects[20] and progressive cone dysfunction[21].

The influence of background luminance on threshold variance, across the visual field, is uncertain. Studies have shown an increased variance[5], a decreased variance[22] and no change[2,23], although this may also be influenced by the thresholding strategy.

The two most commonly available luminances used by automated perimeters are the Octopus standard of 4 asb and the Goldmann standard of 31.5 asb. The aim of this study was to assess the interaction of target size and background luminance on the sensitivity and variability across the visual field; and to establish the suitability of the Weber-Fechner or Rose-de-Vries laws for automated perimetry.

Method

The sample comprised of ten clinically normal emmetropes (mean age 23.9, SD 1.91) experienced in making psychophysical observations. Visual acuity was 6/5 or better. The differential light threshold for the visual field of the right eye was determined using the Humphrey Field Analyzer 630. Stimuli were presented along the 15°-195° meridian at eccentricities of 2.5°, 5°, 7.5°, 10°, 12.5°, 15°, 20° and 30° at each of five different background luminances 0, 1 cdm^{-2}, 10 cdm^{-2}, 100 cdm^{-2} and 1000 cdm^{-2}. The foveal threshold was measured at the beginning of each investigation using the foveal threshold option for all except the 0 background as the four LEDs used to guide fixation would affect the desired level of adaptation. Three stimulus sizes of 0.108°, 0.431° and 1.724° were used. The order of the 15 trials was randomized and performed in four sessions of four trials with the first trial of the first session repeated at the end of the final session and discarded to minimize the learning effect. Subjects were dark adapted for 30 minutes prior to testing at zero background luminance and light adapted for five minutes to the other bowl luminances.

At 0 cdm^{-2} background, the fixation LED was reduced in luminance by inserting a two-log unit neutral density filter mounted in a small tube, into the fixation hole at the rear of the bowl. Fixation was constantly monitored using the HFA video camera for all but the 0 cdm^{-2} background To ensure steady fixation with the 1 cdm^{-2} background, a supplementary black and white monitor was connected to the video camera and the contrast and brightness adjusted to give an adequate image of the eye Natural pupils were used and measured throughout. Stimulus luminance was converted from the decibel printout of sensitivity. Both background and stimulus luminance were expressed in trolands by adjusting for pupil area. The results were then compared to the Weber-Fechner and Rose-de-Vries laws. Results at fixation were corrected for the Stiles-Crawford effect using the weighting factors of Wyszecki and Stiles[24].

Results

Fig. 1 illustrates the influence of stimulus size and background luminance upon the differential light sensitivity across the central 30° for the 15°-195° meridian Following calculation of the Weber-Fechner fraction it was found to be approximately constant for bowl luminances between 10 and 1000 cdm^{-2} with target sizes of 0 431° and 1 724°, at all eccentricities.

The Rose-de-Vries fraction was approximately constant for bowl luminances between 1 and 100 cdm^{-2} with target sizes of 0.431° and 1.724°, at all eccentricities. The 0.108° target also approximated a constant over the same range of bowl luminances for all eccentricities other than fixation. However, if the data is corrected for the Stiles-Crawford effect, using the weighting factors of Wyszecki and Stiles[24], it also approximates a constant at fixation (Fig. 2).

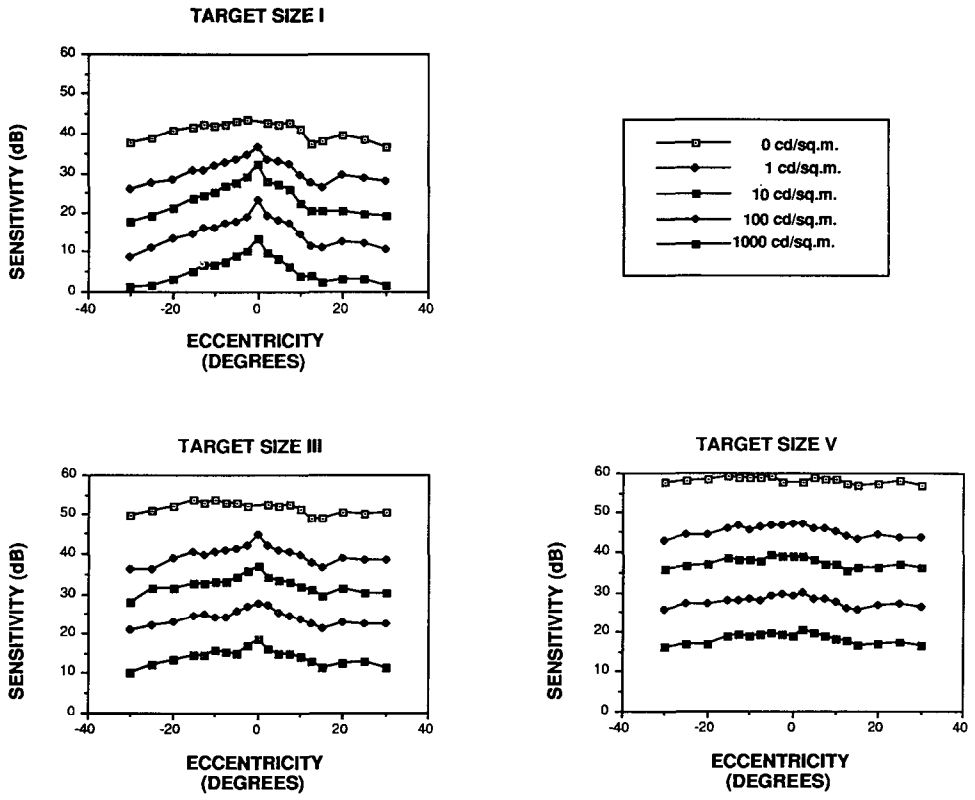

Fig. 1 The influence of stimulus size and background luminance on differential light sensitivity across the central 30° for the 15°-196° meridian

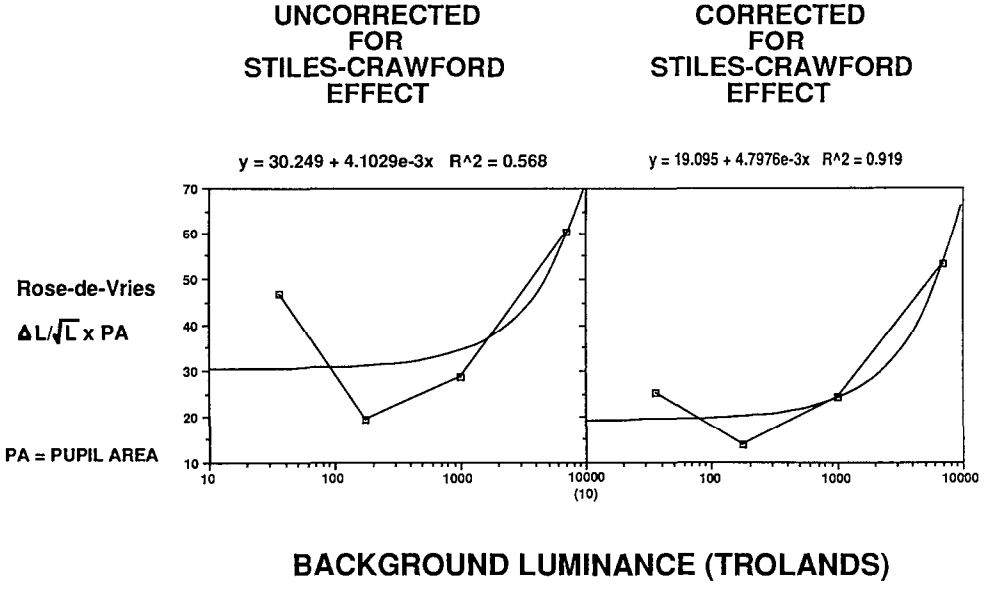

Fig 2 The Rose-de-Vries fraction plotted against background luminance for a 0.108° target at fixation when both uncorrected and corrected for the Stiles-Crawford effect

Discussion

The Weber-Fechner law held true across the central 30 degrees at background luminances of 10 cdm^{-2} or higher, for the two larger stimuli (0.431° and 1.724°) only. The Rose-de-Vries law held true across the central 30 degrees at background luminances of between 1 cdm^{-2} and 100 cdm^{-2} for all three stimuli providing the smallest (0.108°) was corrected for the Stiles-Crawford effect at fixation. In agreement with Fankhauser[10], we conclude that the Rose-de-Vries law is the most applicable, across the central 30 degrees, for the adaptation levels commonly used in perimetry.

Acknowledgements

We thank K. Pratt for assistance in collecting data and gratefully acknowledge the support of computer technologist J. Cassidy. For secretarial support we thank A. Zorian and for graphics services, J. Simpson and A. Lai. This work was supported in part by the Medical Research Council of Canada

References

1 Blair HL: Some fundamental physiologic principles in the study of the visual field. Arch Ophthalmol 24:10-20, 1940
2. Greve EL: Single and multiple stimulus static perimetry in glaucoma: the two phases of visual field examination Doc Ophthalmol 136:1-355, 1973
3. Sloan LL: The threshold gradients of the rods and cones in the dark-adapted and in the partially light-adapted eye Am J Ophthalmol 33:1077-1089, 1950
4. Harms H: Die praktische Bedeuting quantitativer Perimetric Klin Mbl Augenheilk 121:683-692, 1952
5. Aulhorn E, Harms H: Frühe Gesichtsfeld Ausfälle beim Glaukom Glaucoma. Tutzing Symposium Basel: Ed W Leydhecker, S Karger 1967
6. Aulhorn E, Harms H: In: Jameson L, Hurvich LM (eds) Handbook of Sensory Physiology VII Ch 14 Visual Psychophysics, pp 102-145. Berlin: Springer 1972
7 Bedwell CH: Factors affecting the detection of early visual loss. Am J Optom Physiol Opt 49/3:215-226, 1972
8 Rose A: Vision: Human and Electronic New York/London: Plenum Press 1977
9 Fankhauser F, Bebie H: Threshold fluctuations, interpolations and spatial resolution in perimetry. Doc Ophthalmol Proc Ser 19:295-309, 1979
10 Fankhauser F: Problems related to design of automatic perimeters Doc Ophthalmol 47:89-139, 1979
11. Klewin KM, Radius RL: Background illumination and automated perimetry Arch Ophthalmol 104/3:395-397, 1986
12. Bedwell CH, Davies S: The effect of pupil size on multiple static quantitative visual field thresholds. Doc Ophthalmol Proc Ser 14:363-366, 1977
13. Brenton RS, Phelps CD: The normal visual field on the Humphrey Field Analyser Ophthalmology 193:56-74, 1986
14 Flammer J, Drance SM, Fankhauser F, Augustiny L: Differential light threshold in automated static perimetry: factors affecting short-term fluctuation Arch Ophthalmol 102:876-879, 1984
15 Jayle GE, Aubert L: Le champ visuel mésopique en pathologie oculaire In: Actualités Latines d'Ophtalmologie, pp 50-115 Paris: Masson 1958
16 Greve EL, Bos PJM, Bakker D: Photopic and mesopic central static perimetry in maculopathies and central neuropathies Doc Ophthalmol Proc Ser 14:243-250, 1976
17. Nara T: Visual field changes in mesopic and scotopic conditions using Friedmann Visual Field Analyser Doc Ophthalmol Proc Ser 19:403-407, 1979
18 Flanagan JG, Wild JM, Barnes DA, Gilmartin BA, Good PA Crews SJ: The qualitative comparative analysis of the visual field using computer assisted, semi-automated and manual instrumentation: III. Clinical analysis Doc Ophthalmol 58:341-350, 1984
19 Marmor MF, Aquirre G, Arden G, Berson E, Birsch DG: Retinitis pigmentosa: a symposium on terminology and methods of examination Ophthalmology 90:126-131, 1983
20. Page GD: Effect of increased background luminance on static threshold perimetry Invest Ophthalmol Vis Sci (Suppl) 26:226, 1985
21. Elenius V, Leinonen M: Photopic tangential perimetry Acta Ophthalmol (Copenh) 64/2:134-137, 1986
22. Jayle GE, Vola J, Aubert L, Braccini G: Etudes des seuils différentiels en périmétrie statique sur le méridien nasal inférieur Arch Ophtalmol (Paris) 25:65-78, 1965
23. Fankhauser F, Schmidt TH: Die optimalen Bedingungen für die Untersuchung der räumlichen Summation mit stehender Reizmarke nach der Methode der quantitativen Lichtsinnperimetrie. Ophthalmologica 139:409-423, 1960
24. Wyszecki G, Stiles WS: Color Science – Concepts and Methods, Quantitative Data and Formulas, p 427. New York: John Wiley and Sons 1967

The frequency-of-seeing curve under perimetric conditions

Stefan Rau and Jörg Weber

Department of Ophthalmology, University of Cologne, Cologne, Germany

The frequency-of-seeing curve is the fundamental function which describes the patient's response behavior to liminal light stimuli. It reveals the threshold as a transient zone where the frequency of seeing increases in an s-shaped manner from nearly 0% to nearly 100%. The threshold and the short-term fluctuation, which are recorded by means of common staircase procedures in automated perimetry, are only dependent phenomena of this function and are often biased. To gather knowledge on the basic relationship between stimulus intensity and response, we determined the frequency-of-seeing curves at several test locations in 14 normal and seven pathological glaucomatous eyes using stimuli according to standardized perimetric conditions.

Eleven normal eyes were tested at four central locations (maximum eccentricity 21°). Seven eyes with confirmed visual field defects were tested at four different central visual field locations (maximum eccentricity 26°). The locations were chosen according to the previous field results to furnish normal points, relative and absolute defects. Six normal eyes (three of them overlapping with the first group) were tested at four peripheral locations (minimum eccentricity 29±, maximum eccentricity 51°).

The measurement procedure to determine frequency-of-seeing curves is the "method of constant stimuli". In each of the four test locations, ten constant, predetermined stimulus intensities were offered 50 times each in the first group and 25 times each in the other groups. Both stimulus intensities and test point locations were presented in random order. The stimulus projection was performed using a modified Humphrey Field Analyzer 620. The physical dimensions of the stimuli were standard: background luminance 10 cd/m^2, stimulus size Goldmann III (0.43°), stimulus color white, stimulus duration 200 ms. The test sequence, control and data storage were entirely managed by an external PC. For this purpose, the modified Humphrey Field Analyzer was switched into a "slave mode" during which it only reacted to commands from the external PC. The program on the PC was written by one of the authors.

Ninety-six frequency-of-seeing curves were obtained. Two curves could not be evaluated because the predetermined intensity levels failed to include the 50% level (threshold) At central points of normal sensitivity, the frequency-of-seeing curve of perimetric stimuli is regular, steep and s-shaped. At peripheral points of normal but low sensitivity, as well as at central locations of reduced sensitivity, the response function shows irregularity, flattening and deviations from the typical s-shape. The threshold coefficient is highly dependent on the threshold level. At low threshold levels (equivalent to high sensitivity), it ranges between 1 and 2 dB. At high levels (equivalent to low sensitivity), it reaches values of up to 12.6 dB.

Because the frequency-of-seeing curve is the basis for all theoretical considerations of staircase methods, these facts should have consequences for measurement procedures in automated perimetry. A rigid strategy using fixed steps of 4 dB or 2 dB, respectively, does not seem to be optimal for all possible threshold levels. The use of dynamic step sizes which adapt to the expected threshold level is better suited to the optimal methods predicted by theoretical models of measurement strategies.

The full article will be published elsewhere.

Address for correspondence Dr J Weber, Universitäts-Augenklinik, Joseph-Stelzmann-Strasse 9, D-5000 Köln 41, Germany

Perimetry Update 1990/91, p. 555
Proceedings of the IXth International Perimetric Society Meeting,
Malmö, Sweden, June 17-20, 1990
edited by Richard P. Mills and Anders Heijl

Functional alterations predictive of diabetic retinopathy: visual field, macular recovery and chromatic sense

A. Polizzi, M. Bovero, R. Gesi, C. Orione, C.P. Camoriano and E. Gandolfo

University Eye Clinic, Genoa, Italy

Abstract

Long-term evaluation of the visual field (Octopus 2000, program 32), macular recovery after photostress (Goldmann-Weekers adaptometer) and chromatic sense (Farnsworth 100 Hue and Panel D15 desaturated) were performed on diabetic patients without ophthalmoscopic or fluorescein angiographic evidence of retinopathy. After a five-year follow-up it was found that those patients who had initial alterations (even non-significant ones) on all three tests were more likely to develop retinopathy than were those who had alterations in none or only one or two of the tests.

Introduction

The aim of this study was to detect the predisposition to develop retinopathy in those diabetics in whom ophthalmoscopic and fluorescein angiographic examinations were negative. Therefore, at the University of Genoa Eye Clinic, we studied the visual functional alterations in diabetes mellitus by means of perimetry, macular recovery test and chromatic sense examination.

Patients and methods

Forty eyes of 20 long-standing type I diabetics (IDDM), average age 38.3 years (range 21-54), affected by IDDM for an average of 20.7 years (range 11-30), were studied. Their diabetic control was adequate (blood glucose 130-180 mg/dl, HbA1c 5-8 mg/dl, no glycosuria). The patients were chosen from a larger population enrolled in a five-year longitudinal morphological and functional study, based on the following criteria:

- corrected visual acuity of at least 20/20 in each eye;
- emmetropia or ametropia of less than 3D, with astigmatism of not greater than 1D;
- no congenital alteration of chromatic sense;
- absence of ocular or systemic disease which could alter visual field;
- absence of ophthalmoscopic and fluorescein angiographic abnormalities at the time of the first observation.

Visual fields were examined using an Octopus 2000 perimeter (program 32) with proper correction.

All patients had previously undergone several perimetric examinations so as to exclude learning phenomena. The perimetric results were considered as pathological when SF was greater than 2.5 dB or when localized defects were found with more than six points with a deviation from the normal of between 5 and 9 dB, or with more than three points with a deviation greater than 9 dB.

The macular recovery test was executed using a Goldmann-Weekers adaptometer, according to an optimized method proposed by Zingirian *et al* [1]. This method analyzes the reading time of an optotype plate in photopic light (2.5 lux) before and after macular glare, for one minute, using the projector of the Goldmann perimeter (target V4e).

Chromatic sense examination, after excluding congenital color deficiency with the Ishihara plates, was performed using the Farnsworth-Munsell 100 Hue and Lanthony desaturated D15

Perimetry Update 1990/91, pp 557-559
Proceedings of the IXth International Perimetric Society Meeting,
Malmö, Sweden, June 17-20, 1990
edited by Richard P. Mills and Anders Heijl

Panel, in monocular vision and under the prescribed lighting conditions (450 lux Macbeth lamp)[2].

Results

During the five-year observation period, 24 eyes developed ophthalmoscopic and fluorescein angiographic signs of retinopathy (background retinopathy in 16, ischemic alteration in eight).

Group 1. Patients developing retinopathy

In these eyes, the tests at the first observation were altered as follows:
- twelve eyes (50%) had all three tests altered;
- six eyes (25%) had two tests altered;
- six eyes (25%) had only one test altered

Group 2 Patients not developing retinopathy

- twelve eyes (75%) had no alteration in the three tests;
- two eyes (12.5%) had two tests altered;
- two eyes (12.5%) had one test altered

Perimetry

Of the 24 eyes developing retinopathy, 20 had perimetric alterations at the first observation (12 with paracentral defects, four with pathological SF and four with both defects and altered SF) Only four eyes had normal results.

Of the 16 eyes not developing retinopathy, only one had mild paracentral defects with a normal SF.

Macular recovery

As proposed in a previous paper[1], we considered 131.48 sec to be the discriminant value between normal patients and those destined to develop retinopathy. Of the 24 eyes in this series developing retinopathy (average macular recovery time 151.25 sec, SD 29.49), 20 had recovery times above this value and four below Of the patients not developing retinopathy (average macular recovery time 104 38 sec, SD 22.49), five had times above this value and 11 below.

Chromatic sense

Of the 24 eyes developing retinopathy (Farnsworth 100 Hue, total score average 127, SD 15.8), 12 presented a tritan axis and 12 were normal. Of the 16 eyes not developing retinopathy (Farnsworth 100 Hue, total score average 87, SD 17 4), two presented tritan axis dichromatism and 14 were normal.

The desaturated Panel D15 confirmed the prevalent tritan axis of the dichromatism.

Discussion

The need for early diagnosis of diabetic retinopathy fuels the search for methods able to recognize the first signs of retinal damage caused by the disease. Presently, much interest has been aroused by tests which analyze retinal function, as they may indicate the existence of damage before fluorescein angiographic and fluorophotometric alterations appear Quantitative kinetic perimetry studies have shown, in the absence of or with incipient retinopathy, the presence of small scotoma within the central paracentral area and partial restriction of the central isopters[3]. Static perimetry revealed depression of central sensitivity and the presence of localized sieve-like defects in the paracentral area[4]. Macular recovery after glare, measured using nyctometry, was found to be altered in 55% of non-retinopathic diabetics[5]. Frost Larsen and

Larsen[6] and Lauritzen *et al.*[7] demonstrated the predictive value of nyctometry with regard to the later development of proliferative retinopathy in insulin-dependent diabetics, and showed the favorable effect of good metabolic control on macular recovery after glare in diabetics with early retinopathy. A mild dichromatism of the tritan axis has been found in diabetics with and without retinopathy by several authors[8-11].

Conclusions

The tests of macular function studied by us have the advantage of being non-invasive, economical and well accepted by the patient These tests allow the identification, even if with a certain degree of error, of those diabetics at risk for developing retinopathy. Particularly at risk are those diabetics who, even in the absence of fluorescein angiographic lesions, have altered results on all or most of the tests. In fact, the concomitance of perimetric alteration, a macular recovery time greater than normal and a tritan dichromatism, can be considered indicative of initial retinal damage, even before the appearance of morphological changes This study showed that, after a five-year follow-up, patients who initially had perimetric, macular recovery and chromatic sense abnormalities, had a greater likelihood of developing retinopathy compared to those who had no, or only one or two tests altered.

References

1. Zingirian M, Polizzi A, Mosci C, Capris P, Grillo N, Rovida S: Optimized macular recovery test for the early diagnosis and risk prediction of retinopathy in diabetics Acta Diabetol 24:311-316, 1987
2. Lanthony P: Evaluation du Panel D15 desaturé. J Fr Ophtalmol 579-585, 1987
3. Caird RI, Piris A, Ramsell IG: In: *Diabetes and the Eye*, pp 27-29 Oxford/Edinburgh: Blakewell Scientific 1969
4. Gandolfo E, Polizzi A, Zingirian M: Functional alteration in diabetic retinopathy: visual field and macular recovery In: Microvascular and Neurological Complications of Diabetes, Fidia Res Ser 10:53-59, 1987
5 Gliem H, Schulze DP: Sofortadaptation, Blendungsempfindlichkeit und diabetische Retinopathie Klin Mbl Augenheilk 166:766-769, 1975
6 Frost Larsen K, Larsen HN: Macular recovery time recorded by nyctometry: a screening method for selection of patients who are at risk of developing proliferative diabetic retinopathy: result of a 5-year follow-up. Acta Ophthalmol 63:39-47, 1985
7 Lauritzen T, Larsen KF, Larsen HW, Deckert T, Steno Study Group: Effect of 1 year of near normal blood glucose levels on retinopathy in insulin dependent diabetics Lancet 200, 1983
8. Kinnear PR, Aspinall PA, Lakowski R: The diabetic eye and colour vision Trans Ophthalmol Soc UK 92:69-78, 1972
9. Salagnac J, Briedel R, Roth A, Royer J: Atteinte functionelle au cours de la rétinopathie diabétique débutante Bull Soc Ophtalmol Fr 76:855-857, 1976
10 Saracco JB, Gastaud P, Estachy G, Trani JC, Leid J: Intérêt du Panel D15 désaturé dans le dépistage de la rétinopathie diabétique Bull Soc Ophtalmol Fr 10:969-973, 1980
11 Leid J, Gastaud P, Vola J: Résultats de examens de la vision colorée chez les diabétiques avec ou sans rétinopathie Bull Soc Ophtalmol Fr 3:351, 1982

Automated perimetry of photopic and mesopic adapted visual fields in the evaluation of retinitis pigmentosa

Hirotaka Suzumura, Takahisa Nonaka, Yong-Mi Ko, Saori Wakasugi, Tetsuro Ogawa and Harutake Matsuo

Department of Ophthalmology, Tokyo Medical College, 6-7-1, Nishishinjuku, Shinjukuku, Tokyo 160, Japan

Abstract

The nocturnal activity of patients with retinitis pigmentosa (RP) is restricted by visual field defects and nyctalopia. The relationship between differences of retinal sensitivities under photopic and mesopic adaptations and the dark adaptation curve was analyzed in 17 RP patients. The visual fields were measured with the Humphrey Field Analyzer under photopic and mesopic adaptations. The dark adaptation curve was measured with the Goldmann-Weekers adaptometer. In some cases the increases in retinal sensitivity were greater when the threshold of dark adaptation was less than -3 than when the threshold was more than -3. However, there was no significant relationship between the increases in retinal sensitivity under mesopic adaptation and the threshold of dark adaptation Thus, the visual fields of RP patients should be analyzed individually and, when measured under photopic and mesopic adaptations, can yield useful information regarding the degree of nyctalopia, which is useful in assessing the level of visual disability in RP patients

Introduction

The nocturnal activities of patients with retinitis pigmentosa (RP) are restricted by nyctalopia and visual field defects. Therefore, the measurement of thresholds of dark adaptation and visual fields provides important information. However, measurements by changing adaptive conditions and using color visual targets are only at the experimental stage[1-5].

Repeated measurements of the visual field by changing the color of the visual target impose a considerable burden on the patient. On the other hand, human eyes at night are usually in a state of mesopic adaptation, and thus measurement of the visual field under mesopic adaptation would enable us to determine the patient's visual condition at night and would also reduce the testing burden on patients Therefore, an assessment has been made regarding the relationship of changes between photopic and mesopic adaptation in the retinal sensitivity of the visual field

Material and methods

Twenty-one eyes of 11 cases of typical RP and 12 eyes of six cases of non-pigmentary RP, without abnormality in the anterior segment and ocular media, were studied Ten eyes of five normal subjects were used as controls: the visual fields were measured under photopic and mesopic adaptation to compare the results with the visual fields of RP patients. The ages of the RP patients ranged from 15 to 76 years with an average of 31.5±16.7 years, and those in the control group ranged from 26 to 37 years with an average of 31.5±3.1 years The visual field was measured within the central 30° under photopic and mesopic adaptation using the Humphrey Field Analyzer. Measurement was first made under photopic adaptation with a background luminance of 31.5 asb, and then after dark adaptation for 20 minutes under mesopic adaptation with a background luminance of 0.04 asb The fixation target of the Humphrey Field Analyzer was yellow instead of red. Quantitative kinetic perimetry was also performed with the Goldmann perimeter (GP). The dark adaptation curve was measured using the Goldmann-Weekers adaptometer with a visual target of 10°.

Perimetry Update 1990/91, pp 561-566
Proceedings of the IXth International Perimetric Society Meeting,
Malmö, Sweden, June 17-20, 1990
edited by Richard P Mills and Anders Heijl

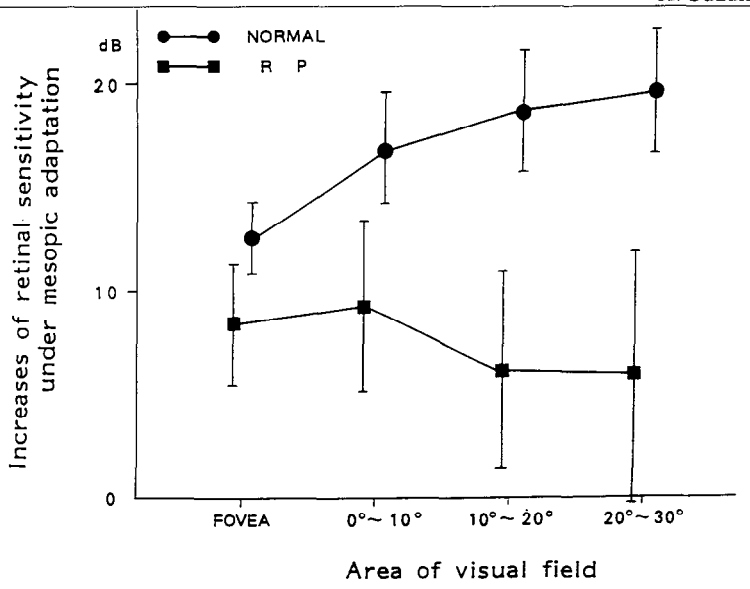

Fig 1 Differences in retinal sensitivity under photopic and mesopic adaptation in normal subjects and RP patients

Results

Differences in retinal sensitivity under photopic and mesopic adaptation

In normal subjects, the increases in retinal sensitivity under mesopic adaptation increased towards the peripheral area, and the visual field profile in mesopic adaptation became flat. In RP patients, these increases were largest in the area of 0 to 10° eccentricity and there was a significant difference between the increases of retinal sensitivity in the areas within 10° and outside 10° (Fig. 1)

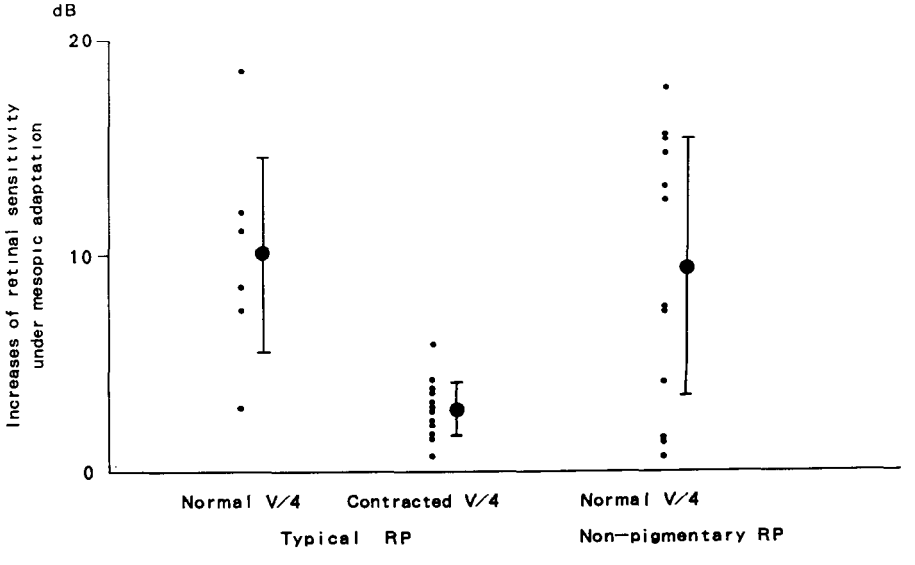

Fig 2 Differences in increases of retinal sensitivity under mesopic adaptation between typical RP and non-pigmentary RP

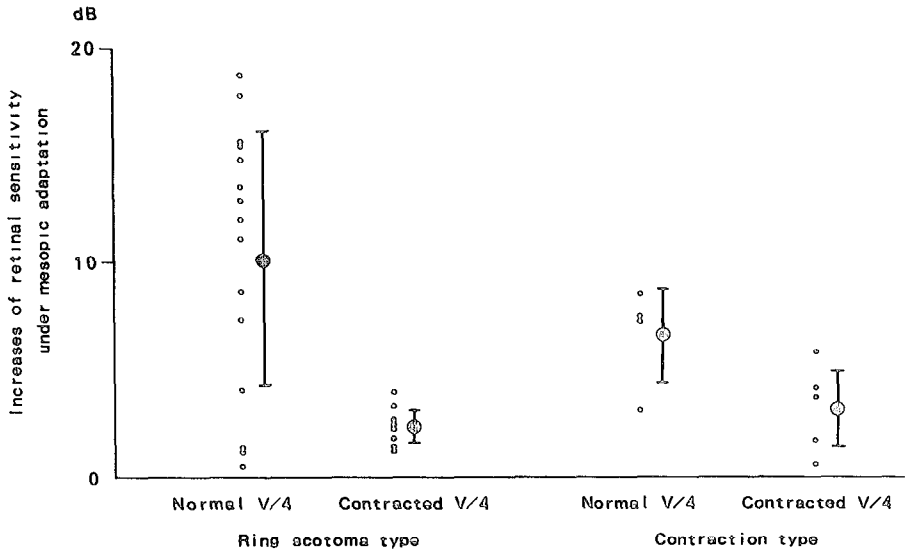

Fig 3 Differences in the increases of retinal sensitivity under mesopic adaptation between RP patients with a normal V/4 area and those with a contracted V/4 area

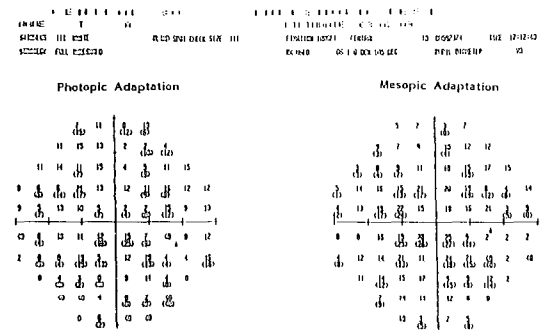

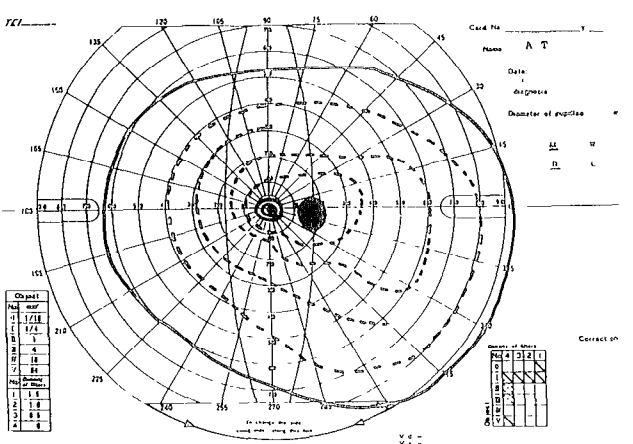

Fig 4a Typical RP: this case showed increases in retinal sensitivity of less than 10 dB under mesopic adaptation and had a visual field with a contraction of the inner isopters and a normal V/4 area on Goldmann kinetic perimetry

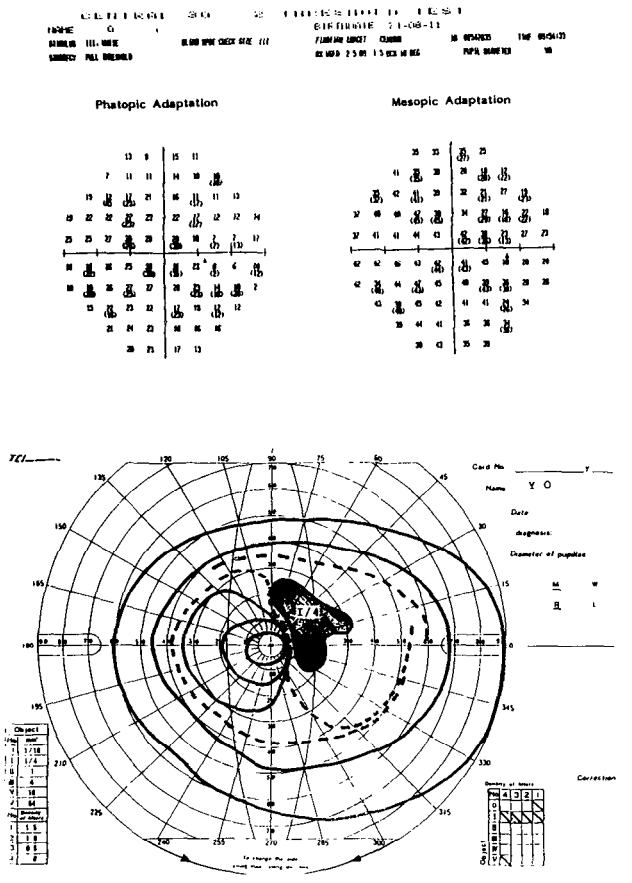

Fig 4b Non-pigmentary RP: this case showed increases in retinal sensitivity of more than 10 dB under mesopic adaptation and had a visual field with a ring scotoma and a normal V/4 area on Goldmann kinetic perimetry

Difference in increases of retinal sensitivity under mesopic adaptation between typical RP and non-pigmentary RP

In cases with a normal V/4 area, there was no significant difference in the increase of retinal sensitivity under mesopic adaptation between typical and non-pigmentary RP. In pigmentary RP cases with a contracted V/4 area, the increases of retinal sensitivity under mesopic adaptation were markedly less than in cases with a normal V/4 area. There was no non-pigmentary RP case with a contracted V/4 area, so that a similar comparison in these cases was not possible (Fig. 2).

Difference in increases of retinal sensitivity under mesopic adaptation between RP patients with a normal V/4 area and those with a contracted V/4 area

In cases with a normal V/4 area, the increase in retinal sensitivity under mesopic adaptation in visual fields with a ring scotoma tended to be greater than in contracted visual fields without a scotoma. However, there was no statistical significance.

All cases with increases in retinal sensitivity of more than 10 dB had a visual field with a ring scotoma and a normal V/4 area. In contrast, all cases with a contracted visual field without a scotoma and with a normal V/4 area showed increases of less than 10 dB under mesopic adaptation.

In cases with a contracted V/4 area, there was no significant difference in the increases of retinal sensitivity under mesopic adaptation between RP patients with visual fields of the ring scotoma type and those of the contraction type (Fig. 3). Fig. 4 shows typical cases of the ring scotoma type with a normal V/4 area and of the contraction type with a normal V/4 area.

Relationship between increases in retinal sensitivity under mesopic adaptation and the threshold of the dark adaptation curve

In some cases the increases of retinal sensitivity were greater when the threshold of dark adaptation was less than -3 than when the threshold was more than -3. However, the relationship between the threshold of dark adaptation and the increases in retinal sensitivity under mesopic adaptation showed great individual variation (Fig. 5).

Discussion

In normal subjects, the increases in retinal sensitivity under mesopic adaptation were larger towards the peripheral visual field, and the shape of the normal visual field became flat under mesopic adaptation. In RP patients, the increases in retinal sensitivity in the visual field of between 10 and 30° eccentricity, where retinal distribution of rods was the greatest, were less than those in the visual field of 0 to 10°. These findings suggested that RP mainly involved disturbed rod function and comparison of the visual fields under photopic and mesopic adaptation might permit evaluation of the nyctalopia, which was one of the chief complaints of RP patients.

There was no significant difference in the increases of retinal sensitivity under mesopic adaptation between typical RP and non-pigmentary RP or between RP cases with ring scotomas and those with concentric contraction alone However, all cases showing an increase of more than 10 dB in retinal sensitivity under mesopic adaptation were of the ring scotoma type and no case that showed an increase of more than 10 dB was of the contraction type These findings suggested that the ring scotoma type might keep relatively good function in the retina, except for the disturbed area, while the contraction type of RP might have diffuse disturbed retinal function The latter may correspond to RP with diffuse disturbed rod function and the former

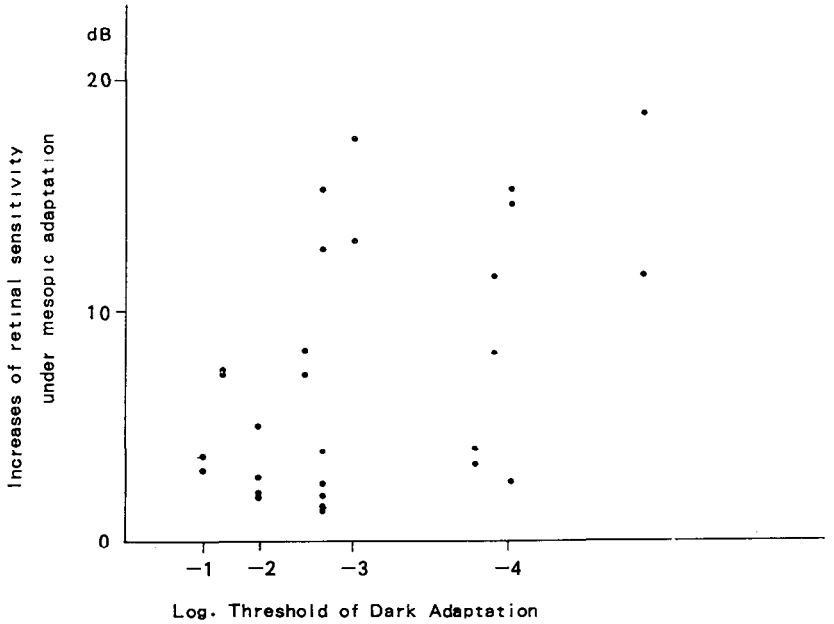

Fig 5 Relationship between the increases in retinal sensitivity under mesopic adaptation and the threshold of dark adaptation curve There was no significant correlation between them

may correspond to RP with regional abnormality of rod function, as reported by Lyness *et al* [5].

The threshold of dark adaptation curve is usually measured in order to determine the degree of nyctalopia[7]. There was no correlation between the increase in retinal sensitivity under mesopic adaptation and the threshold of dark adaptation curve. Therefore, the threshold of dark adaptation curve alone is not enough to evaluate retinal function during night conditions. Thus, the visual fields of RP patients should be analyzed individually.

It was not possible to evaluate the function of both cones and rods from the results obtained by us, but the visual fields of RP patients, when measured under photopic and mesopic adaptation, can yield useful information regarding the degree of nyctalopia, which is useful in assessing the level of visual disability in RP patients. This comparison can be made with only a slight modification of the Humphrey automated perimeter, and the burden imposed on the patient undergoing the test is lessened.

References

1 Sunga RN, Sloan LL: Pigmentary degeneration of the retina: early diagnosis and natural history Invest Ophthalmol 6:309-325, 1967
2 Mitsuya M, Yoshimura N, Shirakawa H: Absolute sensitivity in retinitis pigmentosa Folia Ophthalmol Jpn 31:1460-1465, 1980
3 Matsuo H, Endo N, Suzuki K, Tasaka S: Quantitative visual field in retinitis pigmentosa Jpn J Ophthalmol 22:281-292, 1968
4 Hara T: Visual field changes in mesopic and scotopic conditions using Friedmann visual field analyzer II. Pigmentary retinal degeneration and congenital stationary night blindness Acta Soc Ophthalmol Jpn 83:485-494, 1979
5 Lyness AL, Ernest W, Quinlan MP, Clover GM, Arden GB, Carter RM, Bird AC, Parker JA: A clinical, psychophysical, and electroretinographic survey of patients with autosomal dominant retinitis pigmentosa. Br J Ophthalmol 69:326-339, 1985
6 Jacobson SG, Voigt WJ, Parel JM, Apathy PP, Nghiem-phu L, Myers SW, Patekka VM: Automated light- and dark-adapted perimetry for evaluating retinitis pigmentosa Ophthalmology 93:1604-1611, 1986
7 Marmor MF, Aguirre G, Arden G et al: Retinitis pigmentosa: a symposium on terminology and methods of examination Ophthalmology 90:126-131, 1983

Influence of learning on the peripheral field as assessed by automated perimetry

N.M. Guttridge[1], P.M. Allen[1], A.R. Rudnicka[1], D.F. Edgar[1] and A.E. Renshaw[2]

[1]*Applied Vision Research Centre and* [2]*School of Mathematics, Actuarial Science and Statistics, City University, Northampton Square, London EC1V 0HB, UK*

Abstract

The effect of learning on the peripheral field following repeated automated perimetry was investigated in 12 eyes of 12 normal subjects with no previous experience of automated perimetry. Peripheral full threshold fields were obtained using the peripheral 30/60-2 program of the Humphrey Field Analyzer Each subject attended for five sessions, at least five days apart and one field was plotted at each session There was considerable inter-subject variation in learning in the peripheral field Learning effects were demonstrated by six subjects (Group 1) and the remainder (Group 2) revealed no tendency to learn. The average mean sensitivity was 1.40 dB lower at session 1 in Group 1 than in Group 2 suggesting that non-learners are already operating at or close to their peak performance from session 1 whilst learners reach their peak over time Based on a computation of the number of questions asked per threshold determined there was no link between learning and the ease with which subjects determined threshold There were no obvious differences in learning between superior and inferior hemifields nor was there evidence to suggest increasing learning with eccentricity Amongst Group 1 subjects learning effects were greater in the nasal than the temporal hemifield A statistical model with two-factor structure incorporating an interaction term was used to test for interactions between location and session The interaction term failed to reach significance for any subject with the field divided into either quadrants or concentric shells For many subjects learning is a major factor in the peripheral field and allowance must be made when recording serial fields

Introduction

The effects of prior perimetric experience on the results of serial visual field examination by automated perimetry have been investigated in a number of recent studies Wood *et al* [1] identified three categories of subject amongst an untrained sample of 10 young normals: a category in which most learning took place between the first and second sessions followed by a learning plateau, a second category in which learning continued throughout the study period and a third category in which no learning affect was exhibited. The full field was investigated using the Octopus program 21. Heijl *et al* [2], using the Central 30-2 program of the Humphrey Field Analyzer (HFA) found clear evidence for a learning effect in two groups of normal subjects, one a group of 74 subjects who underwent perimetry in both eyes over three sessions and the second a group of 10 subjects who attended on 10 occasions at one week intervals. In both groups some learning took place after the second session Both studies stress the considerable inter-individual variation associated with the learning process

The purpose of this study was to investigate the effects of prior perimetric exposure on the results of serial peripheral field examination by automated static threshold perimetry.

Material and methods

Subjects

A group of 12 clinically normal young subjects with a mean age of 20.4 years (SD 1.9 years) were selected. Of these, eight were emmetropic and four were low myopes with equivalent spherical error not greater than 3D. All had corrected visual acuities of 6/6 or better. The subjects had no prior experience of automated perimetry and were naive to the purpose of the study.

Perimetry Update 1990/91, pp 567-575
Proceedings of the IXth International Perimetric Society Meeting,
Malmö, Sweden, June 17-20, 1990
edited by Richard P. Mills and Anders Heijl

Method of testing

Full-threshold static perimetry was performed using program 30/60-2 of the Humphrey Field Analyzer. This program measured the increment threshold at 68 points of the field between 30° and 60° from fixation with an inter-stimulus separation of 12°. The visual field was investigated at roughly the same time of day on five occasions not less than five days and not more than 14 days apart.

Analysis

Analysis based on mean sensitivity

Changes in mean sensitivity were computed for the full field tested and for the following configurations:

1. hemifields
2. shells comprising inner, middle and outer annuli
3. quadrants

Statistical analysis

The threshold Y_{ijk} at any location in the visual field may be expressed as $Y_{ijk} = M_{ijk} + \in_{ijk}$, where M_{ijk} represents the actual physiological component of threshold and $\in_{ijk}$ is an error term The symbol *i* defines the position of the location in the field, *j* defines the session and *k* the number of replications or measurements at a given location during a specific session.

It is assumed that Y_{ijk} has an independent normal distribution with mean given by $m_{ijk} = \mu + \alpha_i + \beta_j + (\alpha\beta)_{ij}$ and constant variance σ^2. It also follows that the error term $\in_{ijk}$ has an independent normal distribution with mean o and variance σ^2.

This model has an additive two factor structure involving location and session with an interaction term. It has been used by a number of authors including Hirsch[3] and Flammer *et al.*[4]

The validity of such a normal or Gaussian distribution to accurately represent the visual fields has been challenged by Heijl et al.[5] who found that inter-test point-wise variation did not follow a normal distribution using the 30-2 program of the Humphrey Field Analyzer. The Gaussian distribution became less valid as the distance from fixation increased.

Our model was tested by the standard procedure of an examination of residual plots using the GLIM statistical package. It was also used to test for interactions between location and session.

Results

Individual variations of mean sensitivity with session

Full peripheral field

The variations in mean sensitivity from the first session were calculated and plotted for each subject. It was assumed that an increase in mean sensitivity is indicative of a learning effect By inspection, subjects were initially divided into those who showed learning effects and those who failed to learn. A further subdivision of the learning group was possible leading to the following classification:

- Group 1
  - Type 1 (Fig. 1) exhibited a sustained learning effect over at least the first three sessions (four subjects);
  - Type 2 (Fig. 2) demonstrated a learning effect delayed until after the second session (two subjects);
- Group 2 (Figs 3a and b) showed no learning effect.

Configurations

The percentage change in mean sensitivity between sessions 1 and 5 was computed for each configuration.

Hemifields (Table 1)

- Group 1 showed;
  - no obvious differences between superior and inferior hemifields;
  - greater learning in the nasal than in the temporal hemifields (5/6).

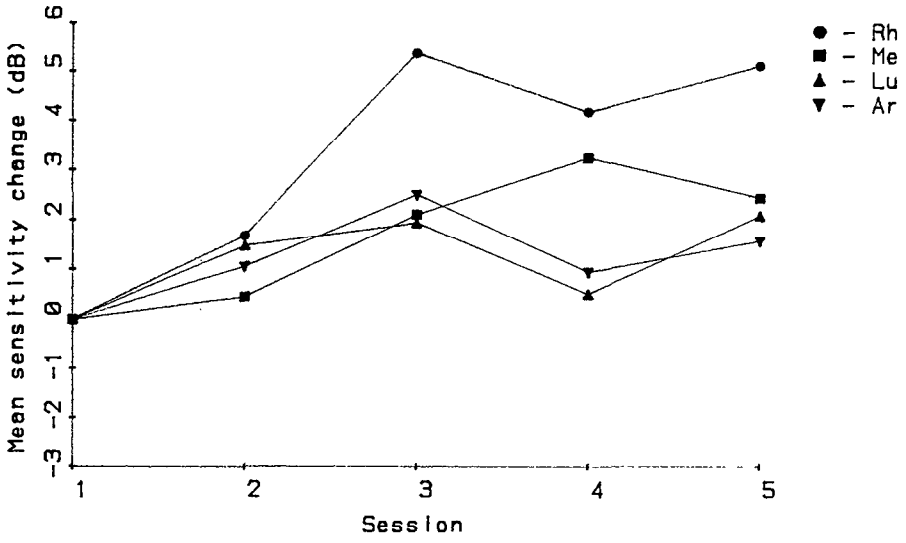

Fig 1 Change in mean sensitivity for group 1, type 1 subjects

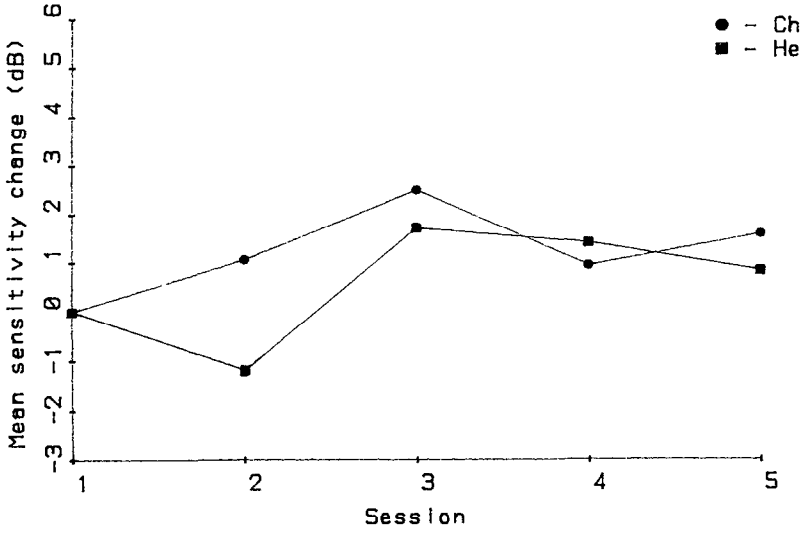

Fig 2 Change in mean sensitivity for group 1, type 2 subjects

- Group 2 showed:
  - no obvious differences between superior and inferior hemifields;
  - a reduction in mean sensitivity in the nasal compared with the temporal hemifield (5/6).

Shells (Table 2)

In the inner shell, all subjects showed a mild learning effect or remained effectively unchanged. Results are considerably less stable in the middle and outer shells.

In Group 1 there was little evidence to suggest increased learning with increasing eccentricity, despite the spectacular performance of one subject (Rh).

Among Group 2 subjects there was a consistent decrease (6/6) in mean sensitivity in the outer shell between sessions 1 and 5.

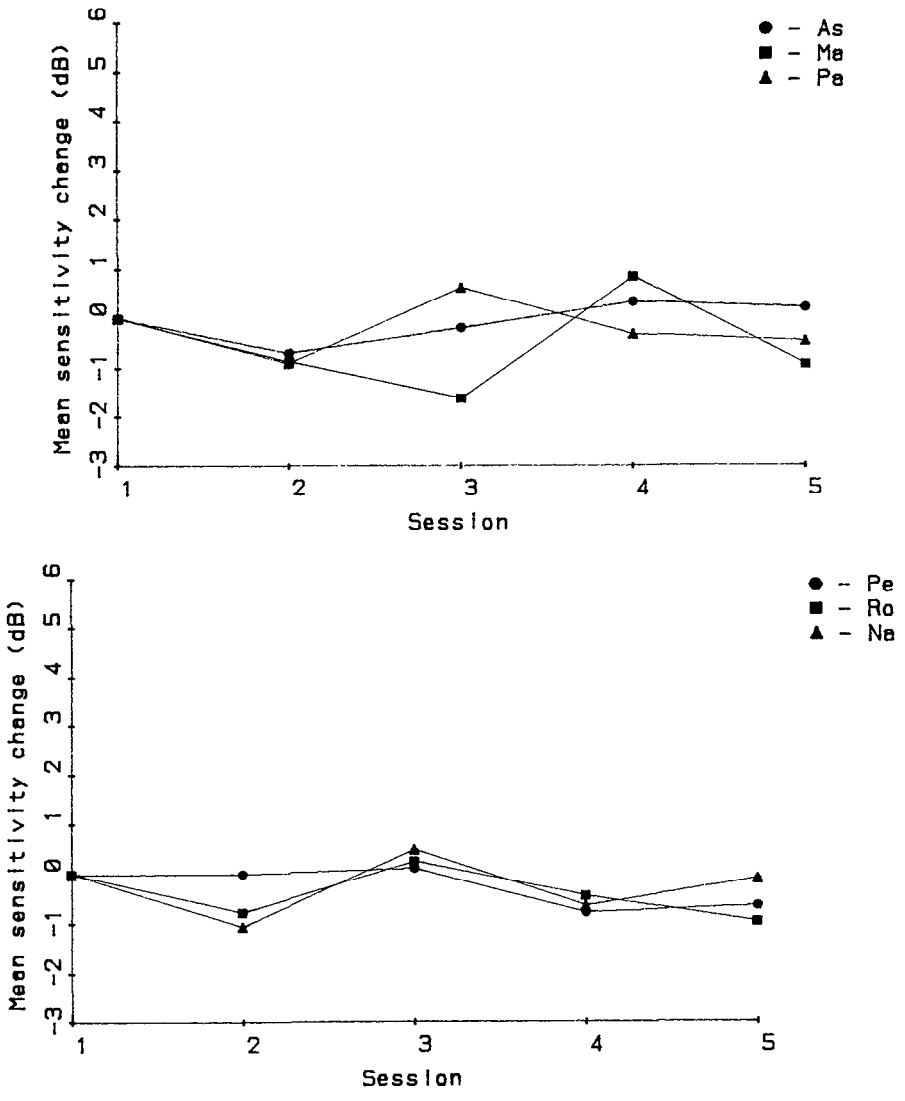

Fig 3a and b Change in mean sensitivity for group 2 subjects

Quadrants (Table 3)

There were no obvious differences between either the lower and upper nasal quadrants or the lower and upper temporal quadrants for either group.

The learning peak was attained at session 3. The above observations apply equally to a comparison between sessions 1 and 3, apart from the reduction in mean sensitivity in the nasal hemifield compared with the temporal, which was not present between sessions 1 and 3.

Statistical analysis

Residual plots for a typical subject are shown in Figs. 4a,b and 5a,b. The departures from a classic residual distribution are concentrated in locations at the extremes of the nasal field both superiorly and inferiorly (Fig. 5a,b). Excluding those locations missed or seen only at maximum intensity leads to a marked improvement in the residual plots (Figs. 4c,d and 5c,d). This supports the view that the Gaussian model tends to break down in the periphery of the field[5].

Table 1 Percentage change in mean sensitivity for hemifields between sessions 1 and 5

	Change in mean sensitivity (%)			
Subject	*Superior*	*Inferior*	*Nasal*	*Temporal*
Group 1				
Type 1				
Rh	26 0	29.8	51 3	14 5
Me	24 2	8.9	11 8	17 4
Lu	23 0	3 7	34.6	−1 8
Ar	6 4	12 2	12 5	7 9
Type 2				
Ch	−9.9	2.9	5 4	−7 2
He	−3.7	11.9	11 6	0 8
Group 2				
Ma	−12.0	1.3	−9.6	−1 5
Pe	−0.2	−6.7	0.0	−5 7
Ro	−23 2	−0 3	−9 5	−6 0
Na	1 8	−2 7	−5 5	3 6
Pa	−3 4	−1 3	−10 0	3 3
As	4 8	−1 5	−10 5	9 5

Table 2 Percentage change in mean sensitivity for shells between sessions 1 and 5

	Change in mean sensitivity (%)		
Subject	*Inner*	*Outer*	*Middle*
Group 1			
Type 1			
Rh	9 1	62 0	32.4
Me	18 2	12 6	19 9
Lu	6 1	12 2	16 9
Ar	9.5	13 5	7 8
Type 2			
Ch	1 4	−5 3	−5 3
He	4 3	4 1	6 1
Group 2			
Ma	−0 9	−6 3	−7 9
Pe	2.8	−25 0	1 0
Ro	−12 8	−18.9	8 1
Na	1.1	−11 6	2 7
Pa	0 2	−7 2	−1 8
As	4 0	−1 3	−0 2

Table 3 Percentage change in mean sensitivity for quadrants between sessions 1 and 5

	Change in mean sensitivity (%)			
Subject	*Lower temporal*	*Lower nasal*	*Upper temporal*	*Upper nasal*
Group 1				
Type 1				
Rh	13 3	55 9	15 5	44.9
Me	9 5	8 3	29 9	15 2
Lu	−7.7	21.3	6 0	59 0
Ar	5.8	26 9	10 6	0 0
Type 2				
Ch	0.8	6 1	−18 9	4 2
He	6.1	21 2	−5 9	0 0
Group 2				
Ma	1 6	1.2	−4.8	−22 1
Pe	−6 8	−7 0	−4 2	7 1
Ro	4 6	−9 1	−24 5	−12 5
Na	2 6	−9 7	5 0	−1 0
Pa	3 3	−7 1	3.5	−14 6
As	6 6	−12 8	13 6	−8 2

a)

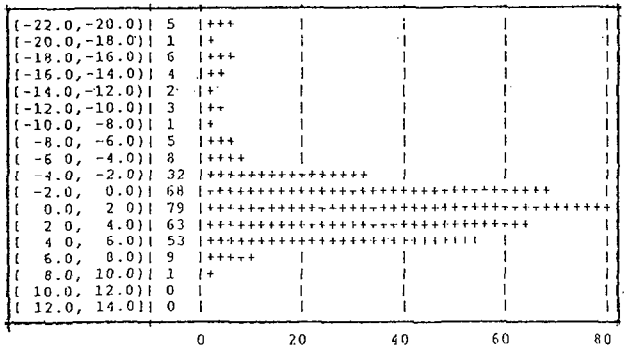

Residual histogram.

b)

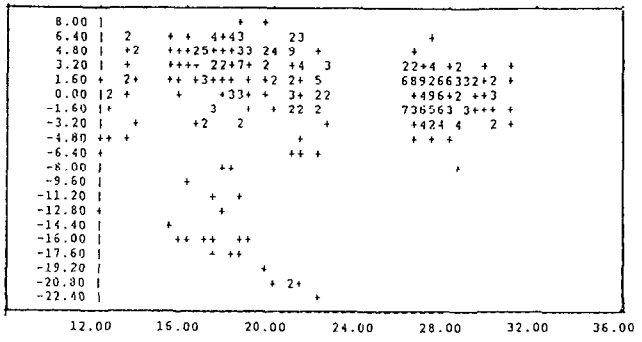

Residuals vs. fitted values.

c)

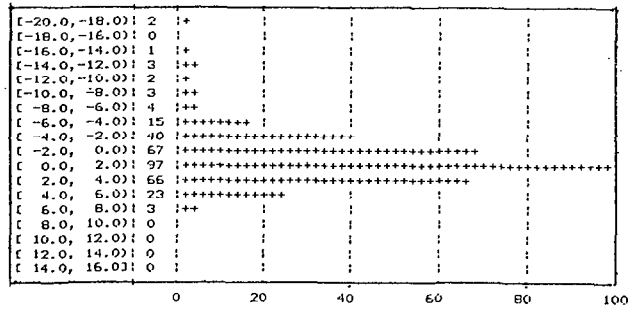

Residual histogram.

d)

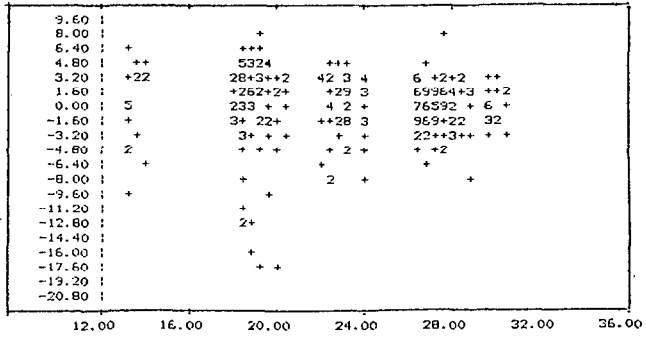

Residuals vs. fitted values.

Fig. 4. Residual plots (a and b) for all locations in a typical subject. Excluding points missed or seen only at maximum intensity (c and d) leads to a marked improvement in the plots.

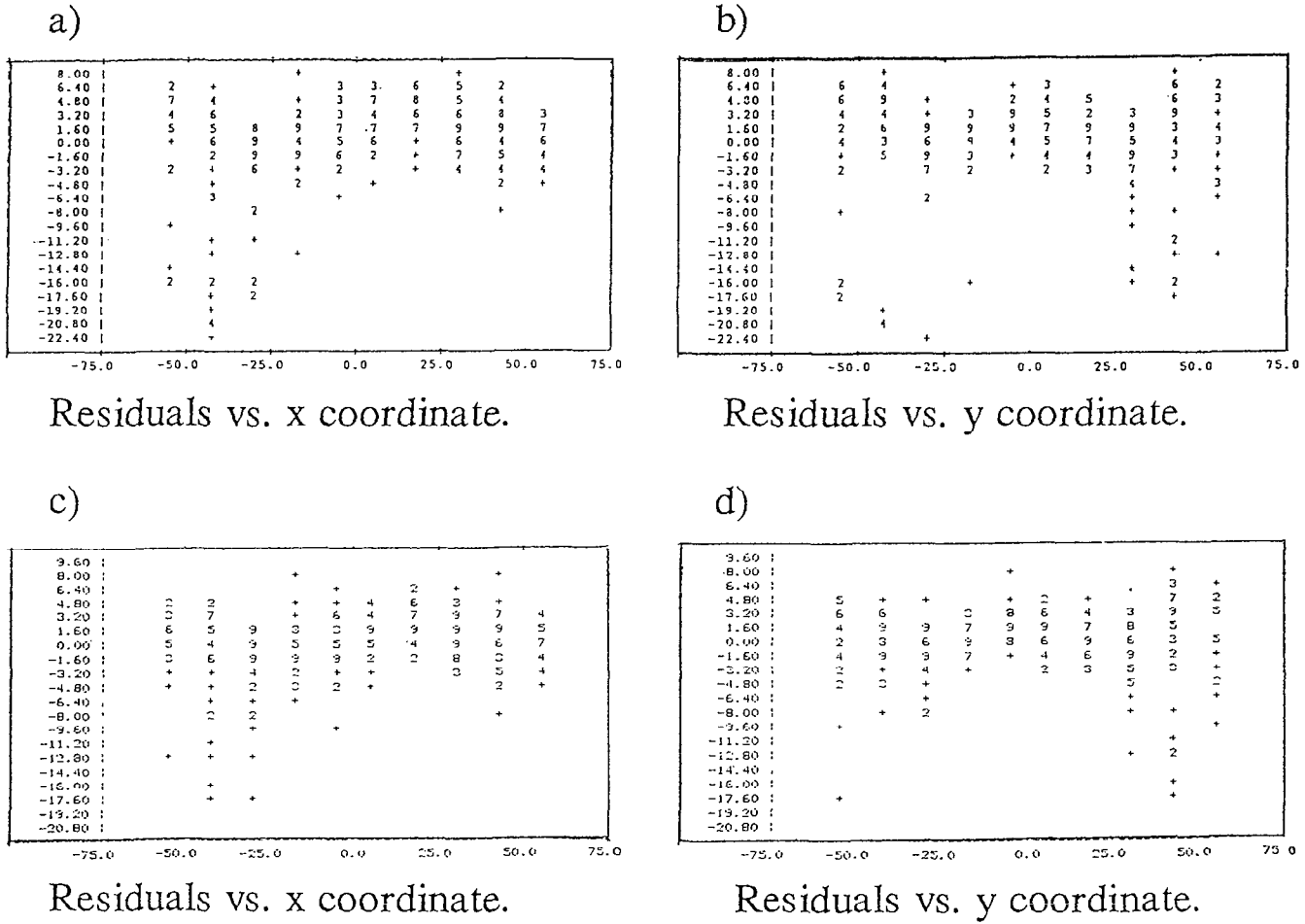

Fig. 5 Residuals plotted against x and y coordinates (a and b) for all locations. Departures from a classical distribution are concentrated in the extreme nasal hemifield. Excluding points missed or seen only at maximum intensity (c and d) leads to a marked improvement in the plots.

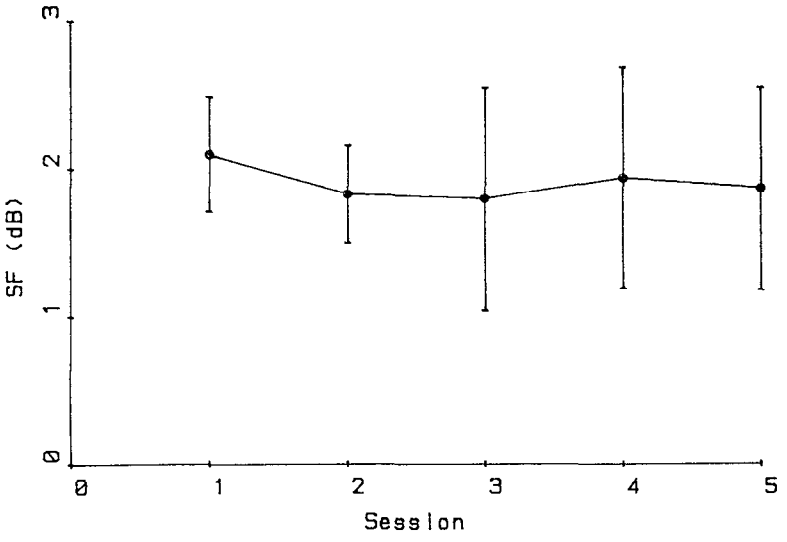

Fig 6 Mean SF for all subjects plotted against session

The validity of the model was accepted whilst acknowledging its weaknesses.

The model was used to test each subject for interactions between location and session. Two configurations were tested with the field divided into either quadrants or three shells.

There was no significant interaction effect for any subject for either configuration with F values ranging from 0.14 to 0.59 for quadrants and from 0.05 to 0.41 for shells.

Short-term fluctuation (SF)

The mean changes in SF with session for all subjects are shown in Fig. 6. There was a marked reduction in SF between sessions 1 and 2, as found by other authors[1,2], which continued through session 3 before a slight increase at sessions 4 and 5

Variability of threshold with location

The coefficient of variation was calculated for each quadrant for each subject (Table 4). The variation of threshold is not a constant across the field, a finding in accord with Heijl *et al* [5]. Greatest variability occurred in the upper nasal quadrant with least in the lower temporal quadrant.

Table 4 Means and SD of coefficient of variation for each quadrant

	Coefficient of variation			
	Lower temporal	*Lower nasal*	*Upper temporal*	*Upper nasal*
Mean	2 8	8 6	8 8	11 4
SD	1 2	4 0	5 3	6 1

Reliability parameters

False positive errors, false negative errors and fixation losses were plotted against session but no trends emerged. The questions asked were plotted against session for each group and between sessions 1 and 5 the mean for Group 1 fell from 445.3 (SD 31.5) to 421.7 (SD 27.8) and for Group 2 from 460.2 (SD 42.3) to 440.5 (SD 35.8). These figures are influenced by the number of repetitions. By dividing the questions asked by the number of repetitions plus 68, the mean number of questions asked per threshold determination can be computed. In Group

1 this figure fell from 4 93 (SD 0.25) to 4.80 (SD 0.33) and in Group 2 from 5.08 (SD 0.40) to 4.73 (SD 0.32). The number of questions asked per threshold determination may vary in different regions of the peripheral field, however this was not investigated in this study

Discussion

There is considerable inter-subject variation in perimetric learning in the peripheral field.

Six out of 12 subjects showed learning effects. The remainder revealed no tendency to learn. At session 1 the average mean sensitivity for Group 1 was 17 12 dB (SD 0 93) while for Group 2 it was 18.52 dB (SD 3 27). This supports the possible explanation reported elsewhere[1,2] that non-learners are already operating at or close to their peak performance from session 1, while learners reach their peak over time.

A reduction in questions asked may reflect an improvement in the subject's appreciation of the differential light threshold or increasing confidence in their abilities to judge the threshold. Based on our computation of the number of questions asked per threshold determination, there was no link between learning and the ease with which subjects determined threshold.

There were no obvious differences in learning between the superior and inferior hemifield Nor was there convincing evidence to suggest increased learning with eccentricity These findings conflict with those from other studies[1,2].

Among Group 1 subjects, learning effects were greater in the nasal than the temporal hemifield The distribution of stimuli was symmetrical within each quadrant of the 30/60-2 program As a result, a greater proportion of the locations lies closer to the limits of the nasal field than the temporal. Thus, the increased learning in the nasal hemifield is consistent with the concept of the periphery as an unpracticed area[6]. However, there was nothing to suggest a similar phenomenon amongst non-learners

The failure of the interaction term to reach significance for any subject for either quadrants or shells was noteworthy. A significant interaction term could indicate for example that some sectors of the field have stable thresholds over five sessions whilst others have thresholds which increase or decrease with session There is no statistical evidence that such effects occur.

For many subjects learning is a major factor in the peripheral field and allowance must be made when recording serial fields

Acknowledgement

Ms. N.M Guttridge receives a scholarship from the British College of Optometrists

References

1 Wood J, Wild JM, Hussey MK, Crews SJ: Serial examination of the normal visual field using Octopus automated perimetry: evidence for a learning effect Acta Ophthalmol 65:326-333, 1987
2 Heijl A, Lindgren G, Olsson J: The effect of perimetric experience in normal subjects Arch Ophthalmol 107:81-86, 1989
3 Hirsch J: Statistical analysis in computerized perimetry. In: Whalen WR, Spaeth GL (eds) Computerized Visual Fields, pp 309-342 Thorofare, NJ: Slack Inc 1985
4 Flammer J, Drance SM, Schulzer M: The estimation and testing of the components of long-term fluctuation of the differential light threshold Doc Ophthalmol Proc Ser 35:383-389, 1983
5 Heijl A, Lindgren G, Olsson J: Normal variability of static perimetric threshold values across the central visual field Arch Ophthalmol 105:1544-1549, 1987
6 Low F: Some characteristics of peripheral visual performance Am J Physiol 146:573-584, 1946

The relationship between backward and forward intraocular light scatter

Maria Dengler-Harles[1], John M. Wild[1], Anne E.T. Searle[2] and S. James Crews[2]

[1]*Department of Vision Sciences, Aston University,* [2]*Birmingham and Midland Eye Hospital, Birmingham, UK*

Abstract

Media opacities lead to visual disability through increased intraocular light scattering and confound the interpretation and analysis of automated perimetric data Previous studies have related perimetric attenuation, arising from media opacities, to measurements of either backward or forward intraocular light scatter This study determined the clinical relationship between backward and forward intraocular light scatter. The objective measurement of back scatter may underestimate the full extent of forward light scatter, particularly in cases of posterior subcapsular opacities, and thus the visual field alteration due to the opacity.

Introduction

The automation of perimetry has revolutionized the role of visual field examination in the detection and diagnosis of abnormality, facilitating the rapid and comprehensive assessment of the differential light threshold relatively free from examiner bias. The presence of media opacities, however, confounds the interpretation and analysis of automated perimetric data. It is necessary to separate perimetric attenuation arising from optical degradation from that due to neural dysfunction.

Media opacities lead to optical degradation through light scattering, absorption and image distortion. It is generally accepted that an increase in intraocular light scattering is the main cause of visual disability[1-3]. Indeed, from studies on the point spread function of the eye, Van den Berg[4] has predicted considerable changes in the visual field due to increased intraocular light scattering arising from relatively mildly disturbed media.

Scattering of light by the media may occur at any angle. Light scattered at angles of greater than 90° to the incident source is termed back scatter; light scattered at angles of less than 90° to the incident source is termed forward scatter The distinction between forward and back scattered light is illustrated in Fig 1 It is frequently assumed that light back-scattered by the crystalline lens is related to light scattered forwards towards the retina and that measurements of back scattered light represent image degradation[5,6]. The exact form of the relationship between forward and back-scattered light is unknown

Objective tests are used to evaluate back light scatter such as slit-lamp and photographic techniques Recently a commercially available device, the Opacity Lensmeter 701 (OLM), has been described by Flammer and Bebie[7]. This instrument measures stray light back scattered from the crystalline lens. A beam of light 1.5 mm in diameter of wavelength 700 nm is used to produce scattered light along the optic axis of the lens. The back scattered light is detected at an angle of 27° to the incident beam, converted into an electrical impulse and displayed on an arbitrary scale of 0-99. Subjective methods are used to evaluate forward intraocular light scatter; clinical tests are based on the depression of visual function in the presence of glare light, which is greater in patients with disturbed media than in those with clear media.

Previous studies have determined the influence of media opacities on the outcome of automated perimetry by relating perimetric attenuation in the presence of the opacity to measurements of both backward[8-11] and forward[12-17] intraocular light scatter. The aim of this study was

Address for correspondence J.M Wild, Department of Vision Sciences, Aston University, Aston Triangle, Birmingham B4 7ET, UK

Perimetry Update 1990/91, pp 577-582
Proceedings of the IXth International Perimetric Society Meeting,
Malmö, Sweden, June 17-20, 1990
edited by Richard P. Mills and Anders Heijl

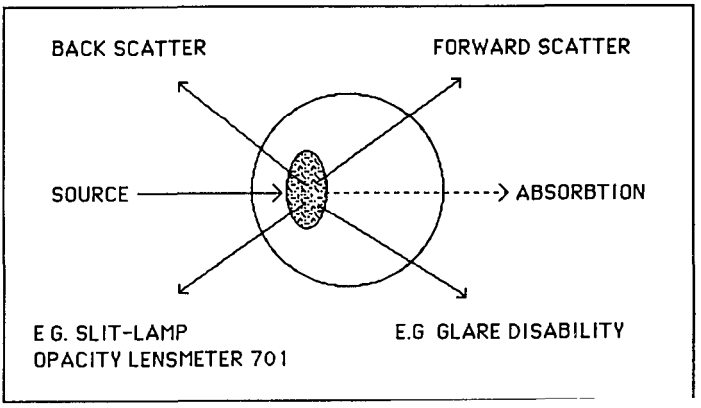

Fig 1 Difference between back and forward intraocular light scatter

to determine the clinical relationship between backward and forward intraocular light scatter. Measurements of back light scatter evaluated using the commercially available OLM were compared with forward light scatter, assessed using glare disability, in a sample of patients with varying levels of cataract.

Material and methods

The sample consisted of 60 patients (mean age 65.5 years; SD 17.0). Exclusion criteria comprised a history of diabetes and other systemic conditions with ocular complications, corneal disorders or contact lens wearers, glaucoma and ocular hypertension, previous intraocular surgery, vitreous floaters and retinal disorders Inclusion criteria comprised the presence of lens opacities but absence of other ocular pathology

Each subject underwent assessment of Snellen VA, a detailed slit-lamp examination of the anterior segment and crystalline lens together with ophthalmoscopy using white and red-free light. The media of one eye of each subject were classified on the basis of these examinations. Normal media were defined as those in which the VA was better than or equal to 6/9, retinal nerve fibers could be seen by ophthalmoscopy with red-free light and no lens opacity was visible within the pupillary area by ophthalmoscopy or slit-lamp examination (n=14; mean age 46 5 years, SD 16 2). Cataractous media were divided into those with primarily anterior cortical opacities (n=26; mean age 73 8 years, SD 7 7), those with nuclear sclerosis (n=9; mean age 76.8 years, SD 6.8) and those with posterior sub-capsular opacities (n=11; mean age 60.7 years. SD 17.9)

Back scatter was taken as the mean of five OLM readings. As recommended by the manufacturer, a pupil size greater than 4 mm was ensured for all readings; where necessary this was achieved by reducing the ambient illumination of the OLM

Forward light scatter was assessed by measuring contrast sensitivity with the Nicolet CS2000 system, in the presence and absence of both narrow- and wide-angle circular glare sources. This method was developed by Griffiths *et al* [18], and utilized by Wood *et al* [13,14] and Dengler-Harles *et al* [17] in relation to automated perimetry Vertical sine-wave gratings of spatial frequency 1 c/deg, counter-phased at 2 Hz to avoid the production of after-images, were generated on the monitor which was surrounded by a circular diffusing screen. A low spatial frequency was chosen for several reasons: optical attenuation due to blur is avoided[19], threshold determinations are less variable[20], low spatial frequencies are relatively unaffected by cataract[23] and are more susceptible to glare compared with high and intermediate spatial frequencies[24,25] A low temporal frequency was chosen since phase alternating stimuli produce more reliable responses in elderly patients[20] In addition, the normal age-related depression of contrast sensitivity is greatest at higher spatial and temporal frequencies[21,22]. Contrast sensitivity was measured using the method of increasing contrast, and an average of six contrast determinations taken The monitor was 3 m from the observer and the screen 22.5 cm in diameter. The screen luminance was 101 25 cd/m^2 and was calibrated before each examination. The illuminance

of the narrow (3.5°) and wide (30°) angle glare sources at the eye were 63 6 lux and 1272.4 lux, respectively. Patients wore their distance optical correction for threshold determinations Á recovery time of five minutes was allowed between exposure to each of the glare sources[26].

A forward light scattering factor (LSF) was calculated for each patient for both wide and narrow-angle glare light using the equation of Paulsson and Sjostrand[24]:

$$LSF = L/E(M_2/M_1 - 1)$$

where L = screen luminance; E = illuminance of the glare source at the eye and M_2 and M_1 are the contrast thresholds in the presence and absence of glare light respectively. Natural pupils were used throughout as the procedure was intended for clinical application. Patients were trained in the psychophysical technique until the contrast threshold without glare light reached a plateau

Results

Back light scatter was found to increase with increasing age for the 14 patients with clear media. This relationship was fitted using linear regression (adjusted $R^2 = 0.84$). Non-linear regression using a second order polynomial resulted in a marginal improvement over the linear

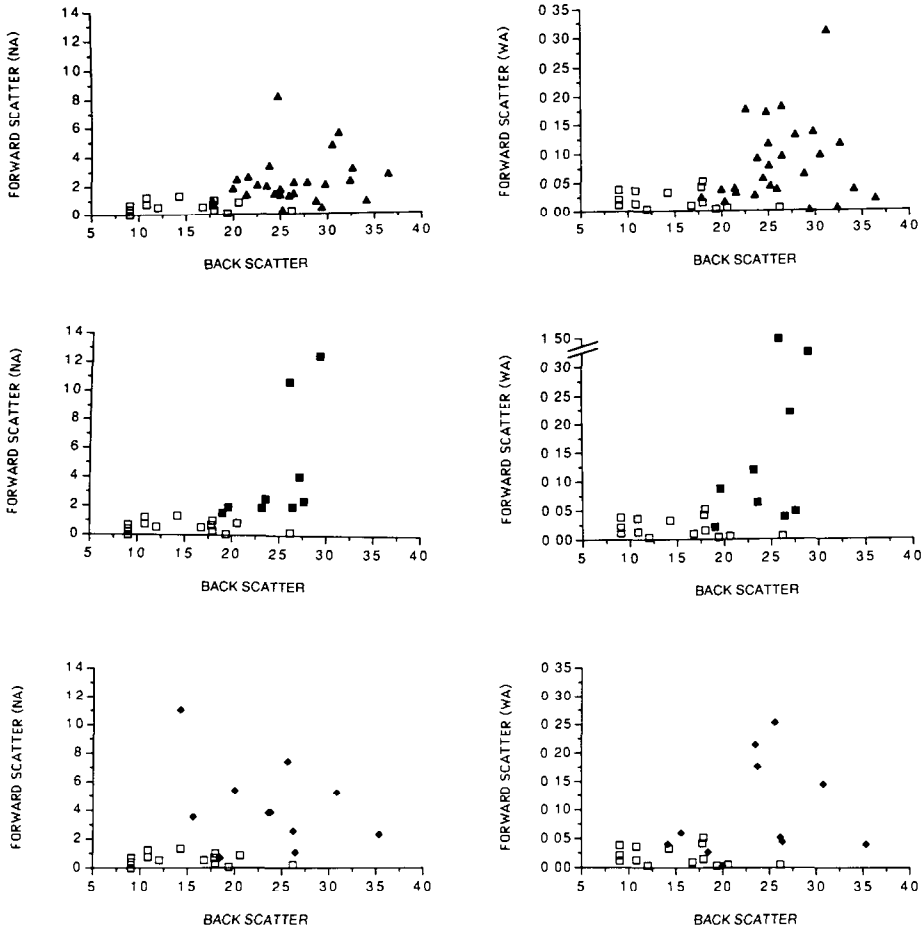

Fig 2 The relationship between forward and back scatter for anterior cortical (top: filled triangles), nuclear sclerosis (middle: filled squares) and posterior subcapsular (bottom: filled diamonds) opacities for both narrow-angle (left) and wide-angle (right) forward scatter Data for normal clear media (open squares) is included on each graph for comparative purposes

fit. There was no correlation between the forward LSF and age (for narrow-angle glare R^2 = 0.01; for wide-angle glare R^2 = 0.09).

The relationship between back and forward intraocular light scatter is shown in Fig. 2 for anterior cortical opacities, nuclear sclerosis and posterior sub-capsular opacities respectively. Data for normal clear media is included on each graph for comparative purposes (open squares). The relationships between both back and forward light scatter and the minimum angle of resolution were not statistically significant.

The standard deviations of the five back scatter measurements were noted to be higher for anterior opacities than for nuclear or posterior opacities, although this difference was not statistically significant. The standard deviations of the contrast threshold determinations were similar for all opacity types.

Discussion

A good correlation exists between back scattered light measured with the OLM and age in the small sample of patients with clear media. This is in agreement with previous work[27-31]. The difference between linear and non-linear regression of the data would possibly be greater if there had been more patients over the age of 65 years, since De Natale *et al.*[27] found the relationship between back scatter and age to be linear up to the age of 65. When subjects over the age of 65 were included, the relationship was best fitted by a quadratic function.

Generalizations regarding a cataractous sample are difficult since every cataract is a separate clinical entity[32]. From Fig 2 it can be seen that forward light scatter increases with increasing back light scatter factor. The data, however, could not be fitted by linear or curvilinear functions. For anterior cortical opacities a particular forward light scattering factor is associated with a wide range of OLM readings whilst at higher levels of back scatter, there is increased spread of the forward scatter data. The former could be due to the higher resolution of back scatter measurements compared with forward scatter techniques but this explanation is unlikely since an adequate forward scatter resolution is present for other opacity types. Alternatively, the anterior cortical opacities in the sample may not produce marked forward scatter. In cases of nuclear sclerosis and posterior subcapsular opacities, measurement of back light scatter appears to underestimate the glare sensitivity experienced by the patient as assessed by forward scatter This under-estimation could result from the greater absorption characteristics of these opacities Alternatively it could imply that the OLM is less efficient at detecting light scattered from more posteriorly located opacities and the necessity of pupil dilation for OLM reading, as advocated by Wegener and Hockwin[28], may be greater for this type of opacity. Posteriorly located opacities scatter light in an irregular fashion (*i e* , at all angles) compared with nuclear opacities; since the OLM only detects light scattered from the central lens area at one particular angle this could also lead to an underestimation of backward intraocular light scatter. In addition, light of wavelength 700 nm is used Since Rayleigh scattering is inversely proportional to the fourth power of the wavelength, this would also lead to a lower estimation of back scattered light than if white light were used. Our data is in agreement with that of Elliott and Hurst[30], who found that the relationship between glare sensitivity and OLM reading was not significant in cataract patients, and implies that a direct relationship between forward and backward intraocular light scatter[5,6] cannot be assumed *in vivo*.

Pupil size has a great effect on the visual capacity of cataract patients, especially those with posterior subcapsular cataracts[23 33]. It could be argued that change in pupil size due to the glare source during measurement of contrast sensitivity would affect determination of the forward LSF. Indeed, a miotic pupil has been shown to improve contrast sensitivity in elderly patients[34] and thus an underestimation of the LSF would result. However, Abrahamsson and Sjostrand[35] utilized an empirically determined correction factor of only 1.2 to account for a reduction in pupil size of 3-4 mm in the presence of a glare source of luminance 21,000 cd/m^2 (65,973 lux) and Vos[36] showed that pupil size did not significantly alter the results of his glare experiments. Furthermore, variation in pupil size has been shown to have little effect on contrast sensitivity at all spatial frequencies[19] and the pupil has been shown to adopt a diameter that optimizes resolution over a wide range of ambient luminances[37] and contrast levels[38].

Although a pupil diameter greater than 4 mm was ensured for measurement of back scatter, the highest OLM reading obtained was 36 4 Our readings seem relatively low considering the

recommended levels of abnormality (cited in[28]). This could indicate the necessity of pupil dilation for OLM readings, even if the pupil size is greater than 4 mm. Indeed, Wegener and Hockwin[28] found differences of 2-4 units in normals and larger differences in cataract patients following mydriasis, although the undilated pupil was greater than 4 mm. Conversely, Elliott and Hurst[30] found an average increase in OLM reading post-dilation of 3.8 units for pupils smaller than 4 mm pre-dilation in normal subjects. For pupils larger than 4 mm pre-dilation, no further increase in score occurred These authors do not mention the effect of dilation on the OLM score in patients with disturbed media. Natural pupils were used in our study since perimetry would not be carried out with a dilated pupil.

The relationship between back scatter and the minimum angle of resolution is in agreement with previous studies supporting the concept that visual acuity is not related to back scattered light[5,6]. Similarly, forward light scatter is not related to visual acuity since the effects of intraocular light scatter cannot be modelled by defocus[39,40]

Although good agreement has been found between backward intraocular light scatter and perimetric attenuation[11] and forward intraocular light scatter and perimetric attenuation[13,14,16,17], this study indicates that measurement of back scatter would lead to an assumption of forward intraocular light scattering that is an underestimation of the true value The visual disability experienced by the patient and the extent of perimetric attenuation due to the media opacities would therefore be underestimated

Acknowledgements

We acknowledge the Royal National Institute for the Blind for the provision of a research studentship to Maria Dengler-Harles

References

1. Philipson B: Light scattering in lenses with experimental cataract. Acta Ophthalmol 47:1089-1101, 1969
2. Zuckerman JL, Miller D, Dyes W, Keller M: Degradation of vision through a simulated cataract. Invest Ophthalmol 12:213-242, 1973
3 Bettelheim FA, Ali S: Light scattering of normal human lens Relationship between forward and back scatter of whole excised lenses Exp Eye Res 41:1-9, 1985
4 Van den Berg TJTP: Relation between media disturbances and the visual field Doc Ophthalmol Proc Ser 49:33-38, 1987
5. Allen MJ, Vos JJ: Ocular scattered light and visual performance as a function of age Am J Optom Arch Am Acad Optom 44:717-727, 1967
6. Sigelman J, Trokel SL, Spector A: Quantitative biomicroscopy of lens light back scatter. Arch Ophthalmol 92:437-442, 1974
7. Flammer J, Bebie H: Lens opacity meter: a new instrument to quantify lens opacity Ophthalmologica 195:69-72, 1987
8. Guthauser U, Flammer J, Lotmar W, Niesel P: Einfluss der Katarakt auf das Gesichtsfeld Klin Mbl Augenheilk 188:409-411, 1986
9. Guthauser U, Flammer J, Niesel P: Relationship between cataract density and visual field damage Doc Ophthalmol Proc Ser 49:39-41, 1987
10. Guthauser U, Flammer J: Quantifying the visual field damage caused by cataract Am J Ophthalmol 106:480-484, 1988
11. De Natale R, Flammer J: The relationship between the lens opacity meter 701 readings and the visual field. In: Heijl A (ed) Perimetry Update 1988/1989, pp 455-457 Amsterdam/Berkeley/Milano: Kugler & Ghedini Publ 1989
12 Heuer DK, Anderson DR, Feuer WJ, Knighton RW, Gressel MG, Fantes FE: The influence of simulated media opacities on threshold measurements. Doc Ophthalmol Proc Ser 49:15-22, 1987
13. Wood JM, Wild JM, Crews SJ: Induced intraocular light scatter and the sensitivity gradient of the normal visual field Graefes Arch Clin Exp Ophthalmol 225:369-373, 1987
14. Wood JM, Wild JM, Smerdon DL, Crews SJ: The role of intraocular light scatter in the attenuation of the perimetric response. Doc Ophthalmol Proc Ser 49:51-59, 1987
15. Heuer DK, Anderson DR, Feuer WJ, Knighton RW, Gressel MG: The influence of simulated light scattering on automated perimetric threshold measurements Arch Ophthalmol 106:1247-1251, 1988
16. Wood JM, Wild JM, Smerdon DL, Crews SJ: Alterations in the shape of the automated perimetric profile arising from cataract Graefes Arch Clin Exp Ophthalmol 227:157-161, 1989

17. Dengler-Harles M, Wild JM, Cole MD, O'Neill E, Crews SJ: The influence of forward light scatter on the visual field indices in glaucoma Graefes Arch Clin Exp Ophthalmol 228:326-331, 1990
18 Griffiths SN, Drasdo N, Barnes DA, Sabell AG: Effect of epithelial and stromal oedema on the light scattering properties of the cornea Am J Optom Physiol Opt 63:888-894, 1986
19 Campbell FW, Green DG: Optical and neural factors affecting resolution J Physiol 181:576-593, 1965
20 Vaegan, Halliday BL: A forced choice test improves clinical contrast sensitivity testing Br J Ophthalmol 66:477-491, 1982
21 Owsley C, Sekuler R, Siemson D: Contrast sensitivity throughout adulthood Vis Res 23:689-699, 1983
22 Wright C, Drasdo N: The influence of age on the spatial and temporal contrast sensitivity function Doc Ophthalmol 59:385-395, 1985
23 Elliott DB, Gilchrist J, Whitaker D: Contrast sensitivity and glare sensitivity changes with three types of cataract morphology: are these techniques necessary in a clinical evaluation of cataract? Ophthalm Physiol Opt 9:25-30, 1989
24 Paulsson LE, Sjostrand J: Contrast sensitivity in the presence of a glare light Invest Ophthalmol Vis Sci 19:401-406, 1980
25 Elliott DB: Contrast sensitivity decline with ageing: A neural or optical phenomenon? Ophthalm Physiol Opt 7:415-419, 1987
26 Collins M: The onset of prolonged glare recovery with age Ophthalm Physiol Opt 9:368-371, 1989
27 De Natale R, Flammer J, Zulauf M, Bebie H: Influence of age on the transparency of the lens in normals: a population study with help of the lens opacity meter 701 Ophthalmologica 197:14-18, 1988
28 Wegener A, Hockwin O: First experiences with the lens opacity meter in measuring normal and cataractous lens Lens Res 5:183-190, 1988
29 Costagliola C, Iuliano G, Rinaldi E, Trapanese A, Russo V, Camera A, Scibelli G: In vivo measurement of human lens aging using the lens opacity meter Ophthalmologica 199:158-161, 1989
30 Elliott DB, Hurst MA: Assessing the effect of cataract: a clinical evaluation of the opacity lens meter 701 Optom Vis Sci 66:257-263, 1989
31 Tuft SJ, Fitzke FW, Lawrenson J, Silver J, Marshall J: Quantification of lens opacification with a commercially available lensmeter Br J Ophthalmol 74:78-81, 1990
32 Siew EL, Bettelheim FA, Chylack LT, Tung WH: Studies on human cataracts: correlation between the clinical description and the light-scattering parameters of human cataracts Invest Ophthalmol Vis Sci 20:334-347, 1981
33 Rubin ML: The little point that isn't there Surv Ophthalmol 17:52-53, 1972
34 Sloane ME, Owsley C, Alvarez SL: Aging, senile miosis and spatial contrast sensitivity at low luminance Vis Res 28:1235-1246, 1988
35 Abrahamsson M, Sjostrand J: Impairment of contrast sensitivity function as a measurement of disability glare Invest Ophthalmol Vis Sci 27:1131-1136, 1986
36 Vos JJ: Describing glare at tunnel entrances (1983) Cited in: Van der Heide GL, Weber J, Boukes R: Effects of stray light on visual acuity in pseudophakia Doc Ophthalmol 59:81-84, 1985
37 Campbell FW, Gregory AH: Effect of pupil size on visual acuity Nature 187:1121-1123, 1960
38 Woodhouse JM: The effect of pupil size on grating detection at various contrast levels Vis Res 15:645-648, 1975
39 Hess RF, Garner LF: The effect of corneal oedema on visual function Invest Ophthalmol Vis Sci 16:5-13, 1977
40 Hess RF, Woo G: Vision through cataracts Invest Ophthalmol 17:428-435, 1978

Index of authors

ACKNOWLEDGEMENT

The following Main Sponsors have contributed significally to the IXth International Perimetric Society Meeting. Their generous support is gratefully acknowledged.

Alcon International
Fort Worth, Texas

Allergan Humphrey
San Leandro, California

Chibret International
Rahway, New Jersey

HighTech Vision
Malmö, Sweden

Interzeag AG
Schlieren - Zürich, Switzerland

MSD Sweden AB
Bromma, Sweden